



<https://theses.gla.ac.uk/>

Theses Digitisation:

<https://www.gla.ac.uk/myglasgow/research/enlighten/theses/digitisation/>

This is a digitised version of the original print thesis.

Copyright and moral rights for this work are retained by the author

A copy can be downloaded for personal non-commercial research or study,
without prior permission or charge

This work cannot be reproduced or quoted extensively from without first
obtaining permission in writing from the author

The content must not be changed in any way or sold commercially in any
format or medium without the formal permission of the author

When referring to this work, full bibliographic details including the author,
title, awarding institution and date of the thesis must be given

Enlighten: Theses

<https://theses.gla.ac.uk/>
research-enlighten@glasgow.ac.uk

**PETROLOGY AND SEDIMENTATION OF THE CAMBRO-ORDOVICIAN
SAQ SANDSTONE - SAUDI ARABIA**

By

OMAR ASSAF ABBAS AL-HARBI (M.Sc.)

A thesis submitted in fulfilment of the degree of Doctor of
Philosophy (by research) in the Faculty of Science,
Department of Geology and Applied Geology,
University of Glasgow

Department of Geology and Applied Geology

University of Glasgow

Scotland

March, 1991

ProQuest Number: 11007970

All rights reserved

INFORMATION TO ALL USERS

The quality of this reproduction is dependent upon the quality of the copy submitted.

In the unlikely event that the author did not send a complete manuscript and there are missing pages, these will be noted. Also, if material had to be removed, a note will indicate the deletion.



ProQuest 11007970

Published by ProQuest LLC (2018). Copyright of the Dissertation is held by the Author.

All rights reserved.

This work is protected against unauthorized copying under Title 17, United States Code
Microform Edition © ProQuest LLC.

ProQuest LLC.
789 East Eisenhower Parkway
P.O. Box 1346
Ann Arbor, MI 48106 – 1346



JABAL SAQ (SAQ MOUNTAIN)

ACKNOWLEDGEMENT

I particularly deeply wish to thank my supervisor Professor Brain J. Bluck for his continuous help, patience, encouragement and constant advice.

I am grateful to Professor B. E. Leake for use the facilities in the Department of Geology and Applied Geology.

Thanks are also extended to Dr. C. M. Farrow for his help with XRF and computer facilities.

I would also like to express my thanks to Mr R. Morrison, Chief Technician, Mr D. McLean for photography and the technical staff of the Department of Geology and Applied Geology for their help.

I gratefully acknowledge Saudi Arabia Government Scholarship from King Abdulaziz City for Science and Technology (KACST) which funds this research project.

Finally, I wish to sincerely thank my parents, my wife, my two children and all my family for the help support and encouragement they have given me.

ABSTRACT

The Saq Sandstone is 600m thick and of Cambro-Ordovician age (?). It is vertically and laterally uniform succession, >90% of which cross-stratified. It is a texturally and mineralogically mature, fine to coarse-grained quartz arenite, with subordinate shale, siltstone, breccia and conglomerate.

The Saq Sandstone comprises an upward maturing and fining sequence. It was largely derived from a craton interior made up of pre-existing and multi-cycle sedimentary rocks. A new formation (The Idwah Formation) overlying the Precambrian-Cambrian basement and older than the Saq Sandstone has been defined. This is a remnant of an earlier extensive cover over the peneplained Precambrian-Cambrian surface.

The sandstone was partly or totally deposited in a tide-dominated shallow-shelf marine environment. Six Facies Associations have been recognized: (1) Facies Association A (Bar areas); (2) Facies Association B (Inter-Bar); (3) Facies Association C (Inner-shelf); (4) Facies Association D (Shoreline) and (5) Facies Association E (Scree).

The Saq Sandstone was deposited initially during a transgression (Lower and Middle) and then during a regression (Upper) cycle. The regression producing a laterally extensive sheet of beach sandstone.

The palaeocurrent pattern throughout Saq Sandstone is unidirectional (NE). This together with the orientation of the beach lamination, suggest that the source lay S to SW of the Saq Basin, although it is difficult to reconstruct a palaeoslope from tidally induced flows.

The dominance of a single palaeoflow suggest a strongly asymmetrical tidal system.

DEDECATION

**This thesis is dedicated to my parents,
my wife, my son Osama and
to my daughter Ebtehal**

DECLARATION

STATEMENT

BY THE AUTHOR

OF THE

THESIS

ENTITLED

...

DECLARATION

The material presented herein is the result of independent research by the author undertaken from October, 1987 to February, 1991 at the department of Geology and Applied Geology, University of Glasgow. Any published or unpublished data of other workers has been given full acknowledgement in the text.

Omar Al-harbi

LIST OF CONTENTS

Page No.

ACKNOWLEDGEMENTS

ABSTRACT

DEDICATION

DECLARATION

LIST OF CONTENTS.....	I
LIST OF FIGURES.....	VI
LIST OF TABLES.....	XII
LIST OF PLATES.....	XIV

CHAPTER ONE: INTRODUCTION..... 1

1.1	General geology of Saudi Arabia.....	1
1.2	The evolution of The Arabian Shield.....	1
1.3	The tectonic framework of the Arabian Peninsula.....	3
1.4	The Palaeozoic of Saudi Arabia.....	3
1.5	Cambro-Ordovician Saq Sandstone.....	4
1.6	Correlation of the Paleozoic units in some neighbouring countries.....	6
1.7	Previous work.....	6
1.8	Location and sampling.....	6
1.9	Aims and scope of the study.....	7

CHAPTER TWO: STRATIGRAPHY & FACIES OF SAQ THE SANDSTONE

2.1	Introduction.....	19
2.2	Stratigraphic setting.....	19
2.3	Shallow marine environment.....	22
2.4	Tide-domineated shelf.....	23
2.4.1	Tidal currents and unidirectional flow.....	24
2.4.2	Ebb or Flood.....	26
2.5	Facies description and interpretations.....	26
2.5.1	Facies 1: Small-Medium scale grouped cross-stratified sandstone.....	27
2.5.1.1	Subfacies 1a: Sand sheets with inclined boundaries : Top-sets.....	27
2.5.1.2	Subfacies 1b: Interbedded cross-stratified sand sheets and Shale.....	29
2.5.1.3	Subfacies 1c: Sand sheets with flat boundaries	30
2.5.2	Facies 2: Large-scale hetroegenous cross-stratified sandstone.....	31
2.5.3	Facies 3; Down-foreset dipping cross-stratified sandstone.....	34

II

2.5.4	Facies 4: Bottomsets.....	35
2.5.5	Facies 5: <i>Cruziana</i> facies.....	36
2.5.6	Facies 6: Interbedded fine sandstone and siltstone.....	37
2.5.7	Facies 7: Planar to gently dipping stratified sandstone.....	38
2.5.8	Facies 8: Large scale high angle cross-stratified sandstone	38
2.5.9	Facies 9: Conglomerates and breccias.....	39
2.5.9.1	Subfacies 9a: Basal breccia.....	39
2.5.9.2	Subfacies 9b: Fine conglomerate.....	39
2.5.9.3	Subfacies 9c: Bioclastic conglomerate.....	40
2.5.9.4	Subfacies 9d: Basal breccia and conglomerate.....	41
2.5.10	Facies 10: Flat-stratified red sandstone.....	41
2.6	FACIES ASSOCIATIONS.....	41
2.6.1	Facies Association A.....	42
2.6.2	Facies Association B.....	42
2.6.3	Facies Association C.....	43
2.6.4	Facies Association D.....	43
2.6.5	Facies Association E.....	43
2.6.6	Facies Association F.....	44
2.7	Process of formation of tidal bars.....	44
2.7.1	Overtaking mechanism.....	44
2.7.2	Stacking of wedges mechanism.....	45
2.7.3	Scour and reactivation mechanism.....	45
CHAPTER THREE: PETROGRAPHY OF THE SAQ SANDSTONE.....		107
3.1	Introduction.....	107
3.2	Mineralogical classification.....	108
3.3	Framework grain composition.....	109
3.4	Description of the mineralogy.....	110
3.4.1	Quartz:.....	110
	Non-undulatory monocrystalline.....	112
	Undulatory monocrystalline.....	112
	Polycrystalline quartz.....	113
3.4.2	Feldspar.....	115
3.4.3	Lithic fragments.....	115
3.4.4	Heavy minerals.....	115
	Opaque minerals.....	116
	Non-opaque minerals.....	116

	Zircon.....	117
	Tourmaline.....	117
	Rutile.....	118
	Sphene.....	118
3.4.5	Mica.....	119
3.4.6	Clay minerals.....	119
	1- X-ray diffraction (XRD).....	120
	2- Scanning electron microscope (SEM).....	121
3.5	Ferricrete.....	122
3.6	Diagenesis of Saq the Sandstone.....	123
3.6.1	Compaction.....	123
3.6.2	Cementation.....	124
	1. Secondary quartz.....	124
	2. Carbonate.....	125
	3. Iron Oxide.....	126
	4. Kaolinite.....	126
3.7	Cathodoluminescence petrography.....	127
3.8	Maturity of the Saq Sandstone.....	127
3.8.1	Reworking of sediment during the phase of deposition.....	128
3.8.2	Reworking of sediment belonging to an older phase of deposition.....	128
3.8.3	Reworking of sediment belonging to an older cycle.....	128
3.8.4	Reworking directly from the basement.....	129
3.7	Conclusions.....	130
CHAPTER FOUR: GEOCHEMISTRY OF THE SAQ SANDSTONE.....		166
4.1	Introduction.....	166
4.2	Analytical methods.....	167
4.2.1	X-ray fluorescence spectrometer (XRF).....	167
4.2.2	Wet chemical analysis.....	167
4.3	Niggli number.....	168
4.4	Geochemistry of major elements	169
4.4.1	SiO ₂	169
4.4.2	Al ₂ O ₃	169
4.4.3	TiO ₂	170
4.4.4	FeO and Fe ₂ O ₃	170
4.4.5	CaO.....	171
4.4.6	Na ₂ O.....	171

4.4.7	K ₂ O.....	171
4.5	Geochemistry of trace elements.....	172
4.5.1	Niggli al-alk versus trace elements.....	172
4.5.2	K ₂ O versus trace elements.....	173
4.5.3	Zr versus Th and U.....	173
4.5.4	Y+La+Ce versus Ni+Cr versus Sr.....	173
4.6	Discrimination function analysis and tectonic setting.....	174
4.6.1	Bhatia (1983), Bhatia <i>et al.</i> , (1986) discrimination analysis.....	174
4.6.2	Roser & Korsch (1986) discrimination analysis.....	175
4.7	Relation of grain-size and chemical composition.....	176
4.8	Conclusion.....	176
 CHAPTER FIVE: GRAIN-SIZE ANALYSES OF THE SAQ SANDSTONE.		201
5.1	Introduction.....	201
5.2	Method.....	201
5.3	Presentation of grain-size analysis data.....	202
5.3.1	Cumulative curves.....	202
5.3.2	Histogram.....	204
5.4	Grain-size parameters.....	204
5.4.1	Median size (Md).....	205
5.4.3	Graphic mean-size (Mz).....	205
5.4.3	Inclusive graphic standard deviation.....	206
5.4.4	Inclusive graphic skewness.....	207
5.4.5	Graphic kurtosis.....	208
5.5	Multivariate test.....	209
5.5.1	Bivariate discriminate plots.....	209
5.5.1.1	Median size vs Skewness & Median size vs Standard deviation.....	209
5.5.1.2	Standard deviation vs. Mean-size.....	210
5.5.1.3	Mean-size vs. Skewness.....	210
5.5.1.4	Standard deviation vs. Skewness.....	210
5.5.2	Linear discrimination function.....	211
5.5.2.1	The discrimination function of Sahu (1964).....	211
5.5.2.2	The discrimination function of Sevon (1966).....	213
5.6	The grain-size image (CM Diagram).....	214
5.7	Discussion	215

CHAPTER SIX: DEPOSITIONAL ENVIRONMENT AND PALAEO- GEOGRAPHIC SETTING OF THE SAQ SANDSTONE.....	243
6.1 Introduction.....	243
6.2 Facies association and tidal current path.....	244
6.3 Depositional history of the Saq Sandstone.....	245
6.4 Palaeogeographic setting.....	246
CHAPTER SEVEN: CONCLUSIONS.....	260
APPENDIX A.....	263
APPENDIX B.....	279
APPENDIX C.....	299
REFERENCES.....	316

LIST OF FIGURES

	<u>Page No.</u>
FIGURE 1.1 Simplified geological map of Saudi Arabia.....	9
1.2 The evolution of the Arabian Shield.....	10
1.3 Tectonic framework map of the Arabian Peninsula.....	11
1.4 General lithostratigraphy scheme of centre Saudi Arabia.....	12
1.5 Geological map of the study area.....	13
1.6 Isopach map of the Cambro-Ordovician Saq Sandstones.....	14
1.7 Outcrop and sub-surface extent of the Saq Sandstone in Saudi Arabia.....	15
1.8 General columnar section of the Saq Sandstones.....	16
1.9 Correlation chart of Palaeozoic exposures in Saudi Arabia, Jordan, SW Sinai (Egypt), Libya and Algeria.....	17
1.10 Location map of the Saq Sandstones showing sample locations.....	18
 FIGURE 2.1 Columnar section of pre-Saq sediment and basal the Saq Sandstones (Idwah Formation).....	 53
2.2 Generalized columnar stratigraphic section of Lower Saq Sandstone.....	54
2.3 Distribution of average grain-size of the Saq Sandstones.....	55
2.4 Distribution of cross-strata thickness of the Saq Sandstones.....	56
2.5 Generalized columnar stratigraphic section of Middle Saq Sandstone.....	57
2.6 Generalized columnar stratigraphic section of Upper Saq Sandstone.....	58
2.7 Palaeocurrent directions of the Saq Sandstones.....	59
2.8 Circulation of tidal current of the Cambro-Ordovician Saq Sandstone Basin and zone of accumulation of fine sediments.....	 60
2.9 Facies and subfacies distribution of the Saq Sandstones.....	61
2.10 Distribution of cross-strata thickness of subfacies 1a	62
2.11 Distribution of average grain-size of subfacies 1a	63
2.12 Palaeocurrent directions of subfacies 1a of Lower Saq Sandstone.....	64
2.13 Palaeocurrent directions of subfacies 1a of Middle Saq Sandstone.....	65
2.14 Palaeocurrent directions of subfacies 1a of Upper Saq Sandstone.....	66
2.15 Relationship between thickness of large scale cross-strata (Facies 2) and average thickness of sand sheets with inclined boundaries (Subfacies 1a). 67	 67
2.16 Distribution of cross-strata thickness of subfacies 1b	68
2.17 Distribution of average grain-size of subfacies 1b	69
2.18 Diagrammatic model showing the depositional environment of inter- bedded cross-stratified sandstone and shale (Subfacies 1b).....	 70

VII

2.19 Diagrammatic model showing the depositional environment of inter-bedded cross-stratified sandstone and shale (Subfacies 1b).....	71
2.20 Palaeocurrent directions of subfacies 1b of the Lower Saq Sandstone.....	72
2.21 Palaeocurrent directions of subfacies 1b of the Middle Saq Sandstone.....	73
2.22 Palaeocurrent directions of subfacies 1b of the Upper Saq Sandstone.....	74
2.23 Distribution of cross-strata thicknesses of subfacies 1c.....	75
2.24 Distribution of average grain-size of subfacies 1c of the Saq Sandstone...	76
2.25 Diagrammatic model showing the depositional environment of subfacies 1c.....	77
2.26 Palaeocurrent directions of subfacies 1c of the Lower Saq Sandstone.....	78
2.27 Palaeocurrent directions of subfacies 1c of the Middle Saq Sandstone.....	79
2.28 Palaeocurrent directions of subfacies 1c of the Upper Saq Sandstone.....	80
2.29 Distribution of cross-strata thicknesses of large scale cross-stratified sandstone (Facies 2) of the Saq Sandstone.....	81
2.30 Distribution of average grain-size of facies 2.....	82
2.31 Palaeocurrent directions of large scale cross-stratified sandstone (Facies 2) of the Lower Saq Sandstone.....	83
2.32 Palaeocurrent directions of large scale cross-stratified sandstone (Facies 2) of the Middle Saq Sandstone.....	84
2.33 Palaeocurrent directions of large scale cross-stratified sandstone (Facies 2) of the Upper Saq Sandstone.....	85
2.34 Diagrammatic model showing the formation of large scale foresets (Facies 2).....	86
2.35 Evolution stages of down-foreset dipping cross-stratified sandstone (Facies 3).....	87
2.36 Diagrammatic model showing the formation of Co-flow and back-flow strata.....	88
2.37 Facies Associations of the Saq Sandstones and Idwah Formation.....	89
2.38 Diagrammatic model showing the evolution of tidal sand bar by overtaking mechanism.....	90
2.39 Cross-section of tidal sand bar (Location K-16, Middle Saq Sandstone)..	91
2.40 Diagrammatic model showing the growth of bar by stacking of wedges (Fixed tip of the wedge).....	92
2.41 Diagrammatic model showing the growth of bar by stacking of wedges mechanism (Migrating tip of the wedge for small rate).....	93
2.42 Diagrammatic model showing the growth of bar by scour and reactivation mechanism.....	94

VIII

FIGURE	3.1	Reference diagrams for petrographic data.....	132
	3.2	QFL diagrams showing the composition of the Saq Sandstones.....	133
	3.3	QFL diagrams to decipher the provenance of the Saq Sandstones.....	134
	3.4	QmFLt diagrams to decipher the provenance of the Saq Sandstones.....	135
	3.5	Plot of polycrystalline abundance and grain-size.....	136
	3.6	Vertical variation of grain-size and type of quartz (Qm, Qp).....	137
	3.7	Flow diagram for determination of stable and unstable polycrystalline quartz.....	138
	3.8	Instability index vs. polycrystalline index to discriminate provenance of detrital polycrystalline quartz.....	139
	3.9	Distribution of averages of heavy minerals of the Saq Sandstones (3 phi).	140
	3.10	Distribution of averages of heavy minerals of the Saq Sandstones (4 phi).	141
	3.11	Variation of FeO and MgO content of detrital tourmalines.....	142
	3.12	X-ray diffractogram of the oriented clay fraction (< 2 micron) - Upper Saq Sandstone.....	143
	3.13	X-ray diffractogram of the oriented clay fraction (< 2 micron) - Middle Saq Sandstone.....	144
	3.14	X-ray diffractogram of the oriented clay fraction (< 2 micron) - Lower Saq Sandstone.....	145
	3.15	X-ray diffractogram of the oriented clay fraction (< 2 micron) - from mud-clasts of Saq Sandstone.....	146
	3.16	Diagram showing the two stages of formation of ferricrete.....	147
	3.17	Diagrammatic model showing the diagenesis stages of the Saq Sandstone	148
	3.18	Diagram showing the various processes which are thought to control the maturity of the Saq Sandstones.....	149
	3.19	Model for different sources of the Saq Sandstones.....	150
	3.20	Diagrammatic model showing the percentage input of each process of maturing the Saq Sandstones.....	152
	3.21	Energy dispersive spectrum of ferricrete- Upper Saq Sandstone.....	160
	3.22	Energy dispersive spectrum of broken shell- Upper Saq Sandstone.....	161
FIGURE	4.1	SiO ₂ vs Al ₂ O ₃	180
	4.2	Al ₂ O ₃ vs.K ₂ O.....	180
	4.3	SiO ₂ vs.TiO ₂	181
	4.4	al-alk vs.TiO ₂	181
	4.5	Al ₂ O ₃ vs.Fe* ₂ O ₃	182
	4.6	SiO ₂ vs.CaO.....	182

IX

4.7	CaO vs.CO ₂	183
4.8	CaO vs.P ₂ O ₅	183
4.9	SiO ₂ vs.Na ₂ O.....	184
4.10	al-alk vs.K [^]	184
4.11	al-alk vs.Ba.....	185
4.12	al-alk vs.Ce.....	185
4.13	al-alk vs.Cr.....	186
4.14	al-alk vs.Cu.....	186
4.15	al-alk vs.Ga.....	187
4.16	al-alk vs.La.....	187
4.17	al-alk vs.Ni.....	188
4.18	al-alk vs.Pb.....	188
4.19	al-alk vs.Rb.....	189
4.20	al-alk vs.Sr.....	189
4.21	al-alk vs.Th.....	190
4.22	al-alk vs.U.....	190
4.23	al-alk vs.Y.....	191
4.24	al-alk vs.Zn.....	191
4.25	K ₂ O vs.Ce.....	192
4.26	K ₂ O vs.La.....	192
4.27	K ₂ O vs.Rb.....	193
4.28	Zr vs.Zr.....	193
4.29	Zr vs.U.....	194
4.30	Plot of Ni+Cr versus Y+La+Ce versus Sr.....	195
4.31	Plot of Discriminate Function I versus Discriminate Function II.....	196
4.32	Plot of Fe ₂ *O ₃ +MgO versus TiO ₂	197
4.33	Plot of Fe ₂ *O ₃ +MgO versus Al ₂ O ₃ /SiO ₂	197
4.34	Plot of Fe ₂ *O ₃ +MgO versus Al ₂ O ₃ (CaO+Na ₂ O).....	198
4.35	Plot of SiO ₂ versus K ₂ O/Na ₂ O.....	199
4.36	Grain-size vs. K ₂ O.....	200
4.37	Grain-size vs. SiO ₂	200
FIGURE 5.1	Cumulative-frequency curves of grain-size of Lower Saq Sandstone.....	219
5.2	Cumulative-frequency curves of grain-size of Lower Saq Sandstone.....	220
5.3	Cumulative-frequency curves of grain-size of Middle (A) and Lower (B) Saq Sandstone.....	221
5.4	Cumulative-frequency curves of grain-size of Middle Saq Sandstone.....	222

5.5	Cumulative-frequency curves of grain-size of Middle Saq Sandstone.....	223
5.6	Cumulative-frequency curves of grain-size of Middle Saq Sandstone.....	224
5.7	Cumulative-frequency curves of grain-size of Upper Saq Sandstone.....	225
5.8	Cumulative-frequency curves of grain-size of Upper Saq Sandstone.....	226
5.9	Cumulative-frequency curves of grain-size of average Saq Sandstone.....	227
5.10	Relation of sediment transport dynamics to populations and truncation point in grain-size distribution.....	228
5.11	Histograms, showing grain-size distribution of Lower Saq Sandstone....	229
5.12	Histograms, showing grain-size distribution of Middle Saq Sandstone....	230
5.13	Histograms, showing grain-size distribution of Upper Saq Sandstone....	231
5.14	Vertical variation of grain-size parameters in vertical sequence of Saq Sandstone.....	232
5.15	Histograms, showing the average standard deviation (sorting) of the Saq Sandstones.....	233
5.16	Histograms, showing the average skewness distribution of the Saq Sandstones.....	234
5.17	Histograms, showing average of Kurtosis distribution of the Saq Sandstones.....	235
5.18	Bivariant plot of median diameter vs. skewness.....	236
5.19	Bivariant plot of median diameter vs. standard deviation.....	236
5.20	Bivariant plot of mean-size vs. standard deviation.....	237
5.21	Bivariant plot of mean-size vs. skewness.....	238
5.22	Bivariant plot of standard deviation vs. skewness.....	239
5.23	Bivariant plot of C (1st phi percentile) vs. M (Median diameter).....	240
5.24	Diagrammatic model showing the effect of the drainage distance on the grain-size.....	241
5.25	Diagrammatic model showing the relationship between grain-size and type of sediment source.....	242
FIGURE 6.1	Diagrammatic model illustrating major sedimentary facies of Saq Sandstone.....	249
6.2	Dispersal of sand around the British coast with sketch showing typical changes observed in a downcurrent direction.....	250
6.3	Diagrammatic model of Lower Saq Sandstone depositional environment..	251
6.4	Diagrammatic model of Middle Saq Sandstone depositional environment.	252
6.5	Diagrammatic model of Upper Saq Sandstone depositional environment..	253
6.6	Diagrammatic model showing depositional environment of the most Upper	

LIST OF TABLES

	<u>Page No</u>
TABLE 1.1	Summary of Precambrian stratigraphy, tectonism, plutonism and volcanism of the Arabian Shield..... 8
TABLE 2.1	Facies and subfacies of the Saq Sandstone and pre-Saq sediment (Idwah Formation)..... 46
2.2	Statistical parameters of palaeocurrent data of subfacies 1a..... 47
2.3	Statistical data of cross-strata thickness of subfacies 1b..... 48
2.4	Statistical parameters of palaeocurrent data of subfacies 1b..... 49
2.5	Statistical data of cross-strata thickness of subfacies 1c..... 50
2.6	Statistical parameters of palaeocurrent data of subfacies 1c..... 51
2.6	Statistical parameters of palaeocurrent data of facies 2..... 52
TABLE 3.1	Mineralogy of the Lower Saq Sandstone..... 264
3.2	Mineralogy of the Middle Saq Sandstone..... 266
3.3	Mineralogy of the Upper Saq Sandstone..... 270
3.4	Average mineralogy of the Saq Sandstone..... 131
3.5	Tourmaline analysis..... 272
3.6	Muscovite analysis..... 276
TABLE 4.1	Chemical analyses (Major & Trace elements) of the Lower Saq Sandstone. 277
4.2	Chemical analyses (Major & Trace elements) of the Middle Saq Sandstone 285
4.3	Chemical analyses (Major & Trace elements) of the Upper Saq Sandstone. 291
4.4	Average chemical composition of quartz arenite of Saq Sandstone..... 178
4.5	Average of trace elements of Saq Sandstone..... 179
4.6	Unstandardised discriminant function coefficient used to calculate discriminant scores for the Saq Sandstone..... 295
4.7	discriminant scores of Lower Saq Sandstone..... 296
4.8	discriminant scores of Middle Saq Sandstone..... 297
4.9	discriminant scores of Upper Saq Sandstone..... 298
TABLE 5.1	Seven percentile of grain-size analyses - Lower Saq Sandstone..... 300
5.2	Seven percentile of grain-size analyses - Middle Saq Sandstone..... 301
5.3	Seven percentile of grain-size analyses - Upper Saq Sandstone..... 302
5.4	Summary of grain-size analyses of Lower Saq Sandstone..... 303
5.5	Summary of grain-size analyses of Middle Saq Sandstone..... 305

5.6 Summary of grain-size analyses of Upper Saq Sandstone..... 307

5.7 Summary of Sahu's parameters of Lower Saq Sandstone..... 308

5.8 Summary of Sahu's parameters of Middle Saq Sandstone..... 310

5.9 Summary of Sahu's parameters of Upper Saq Sandstone..... 312

5.10 Summary of average of Sahu's parameters of the Saq Sandstone..... 217

5.11 Summary of Sevon's parameters of Lower Saq Sandstone..... 313

5.12 Summary of Sevon's parameters of Middle Saq Sandstone..... 314

5.13 Summary of Sevon's parameters of Upper Saq Sandstone..... 315

5.14 Summary of average of Sevon's parameters of the Saq Sandstone..... 218

8 Identification of the large-scale structure of the Saq Sandstone (Figure 2) - Middle Saq Sandstone..... 217

9 Detailed description of the large-scale structure of the Saq Sandstone (Figure 3) - Middle Saq Sandstone..... 217

10 Detailed description of the large-scale structure of the Saq Sandstone (Figure 4) - Lower Saq Sandstone..... 217

11 Detailed description of the large-scale structure of the Saq Sandstone (Figure 5) - Upper Saq Sandstone..... 217

12 Detailed description of the large-scale structure of the Saq Sandstone (Figure 6) - Middle Saq Sandstone..... 217

13 Detailed description of the large-scale structure of the Saq Sandstone (Figure 7) - Lower Saq Sandstone..... 217

14 Detailed description of the large-scale structure of the Saq Sandstone (Figure 8) - Upper Saq Sandstone..... 217

15 Detailed description of the large-scale structure of the Saq Sandstone (Figure 9) - Middle Saq Sandstone..... 217

16 Detailed description of the large-scale structure of the Saq Sandstone (Figure 10) - Lower Saq Sandstone..... 217

17 Detailed description of the large-scale structure of the Saq Sandstone (Figure 11) - Upper Saq Sandstone..... 217

18 Detailed description of the large-scale structure of the Saq Sandstone (Figure 12) - Middle Saq Sandstone..... 217

19 Detailed description of the large-scale structure of the Saq Sandstone (Figure 13) - Lower Saq Sandstone..... 217

20 Detailed description of the large-scale structure of the Saq Sandstone (Figure 14) - Upper Saq Sandstone..... 217

LIST OF PLATES

	<u>Page No.</u>
PLATE 2.1 Sand sheets with inclined boundaries (Subfacies 1a) Middle Saq Sandstone.....	95
2.2 Interbedded sandstone and shale subfacies (1b).- Middle Saq Sandstone...	95
2.3 Large scale cross-stratified sandstone (Facies 2) - Middle Saq Sandstone.....	96
2.4 Mud-clast - Middle Saq Sandstone.....	96
2.5 Massive and normal grading - Middle Saq Sandstone.....	97
2.6 Deformation of large scale cross-stratified sandstone (Facies 2) - Middle Saq Sandstone.....	97
2.7 Vertical burrows in large scale cross-stratified sandstone (Facies 2) - Middle Saq Sandstone.....	98
2.8 Reactivation surface - large scale cross-stratified sandstone (Facies 2) - Middle Saq Sandstone.....	98
2.9 Down-foreset dipping cross-stratified sandstone (Facies 3) - Middle Saq Sandstone.....	99
2.10 Bottomset facies (4) - Middle Saq Sandstone.....	99
2.11 <i>Cruziana</i> facies (5) - Middle Saq Sandstone.....	100
2.12 Brachiopod shells (Facies 6) - Upper Saq Sandstone.....	100
2.13 Planar to gently dipping stratified sandstone (Facies 7) - Upper Saq Sandstone.....	101
2.14 Heavy mineral bands and vertical burrow (Facies 7) - Upper Saq Sandstone.....	101
2.15 Large scale High angle cross-stratified sandstone (Facies 8) Upper Saq Sandstone.....	102
2.16 Inter-tidal zone - Welsh Beach.....	102
2.17 Basal breccia (Subfacies 9a) - Pre-Saq sediment - Idwah Formation.....	103
2.18 Fine conglomerate (subfacies 9b) - Middle Saq Sandstone.....	103
2.19 Bioclastic conglomerate (subfacies 9c) - Upper Saq Sandstone.....	104
2.20 Basal breccia and conglomerate (subfacies 9d) - Lower Saq Sandstone.....	104
2.21 Planar-stratified red sandstone (facies 10) - Idwah Formation.....	105
2.22 Overtaking mechanism - Middle Saq Sandstone.....	105
2.23 Wedge mechanism - Middle Saq Sandstone.....	106

PLATE 3.1	Photomicrograph showing two generations of quartz overgrowths - Lower Saq Sandstone.....	152
3.2	Photomicrograph showing more than three generations of quartz overgrowths and euhedral quartz overgrowth - Middle Saq Sandstone.....	152
3.3	Photomicrograph showing inherited well rounded overgrowth - Middle Saq Sandstone.....	153
3.4	Photomicrograph showing undulose polycrystalline quartz grain breaking down to monocrystalline quartz - Lower Saq Sandstone.....	153
3.5	Photomicrograph showing undulose monocrystalline quartz grain breaking down to non-undulose monocrystalline grains - Lower Saq Sandstone.....	154
3.6	Photomicrograph showing metamorphic polycrystalline quartz rich rock fragment - Lower Saq Sandstone.....	154
3.7	Photomicrograph showing well rounded polycrystalline quartz grain - Lower Saq Sandstone.....	155
3.8	Photomicrograph showing altered feldspar grain - Lower Saq Sandstone..	155
3.9	Photomicrograph showing sedimentary rock fragment - Lower Saq Sandstone.....	156
3.10	Photomicrograph showing sedimentary rock fragment (sandstone) - Lower Saq Sandstone.....	156
3.11	Photomicrograph showing well rounded heavy minerals - Upper Saq Sandstone.....	157
3.12	Photomicrograph showing heavy minerals - Middle Saq Sandstone.....	157
3.13	Photomicrograph showing the effect of mechanical deformation on flake of muscovite - Lower Saq Sandstone.....	158
3.14	Photomicrograph showing detrital muscovite altered to kaolinite Middle Saq Sandstone.....	158
3.15	SEM photomicrograph showing authigenic kaolinite consisting of stacked pseudo-hexagonal platy crystals (books) - Middle Saq Sandstone.....	159
3.16	Back-scattered electron images showing ferricrete coating quartz grains Upper Saq Sandstone.....	160
3.17	Back-scattered electron images showing ferricrete coating broken shell - Upper Saq Sandstone.....	161
3.18	SEM micrograph (left) and SEM luminescence (right) showing the effect of quartz overgrowth on the nature of quartz grains - Middle Saq Sandstone.....	162
3.19	Photomicrograph showing convex-concave contact between quartz grains as result of pressure dissolution - Middle Saq Sandstone.....	162

3.20 Photomicrograph showing the different stage of cementation - Middle Saq Sandstone..... 163

3.21 SEM micrograph showing euhedral quartz overgrowths - Middle Saq Sandstone. 163

3.22 Photomicrograph showing carbonate cement framing chert grain - Middle Saq Sandstone.....164

3.23 Photomicrograph showing hematite coating sand grain, note the hematite is present where grains are in contact - Lower Saq Sandstone..... 164

3.24 Photomicrograph showing luminescence of quartz (Blue, dull red and black (overgrowth) and also carbonate (Brilliant orange) Lower Saq Sandstone..... 165

CHAPTER ONE

INTRODUCTION

1.1 General geology of Saudi Arabia

The surface geology of Saudi Arabia (Fig. 1.1) is divided into two geological regions:(1) An extensive and broad area of Precambrian-Cambrian igneous and metamorphic rocks crops-out in the west. This is over 1100 km long and up to 640 km wide. It is partly overlain by Cenozoic extrusive volcanics in its western part. The shield is separated by the Red Sea from similar rocks in Egypt and Sudan, referred to as the Nubian Shield.(2) The second region is an elongate arc flanking shield outcrops to the east and involving successive bands of Palaeozoic, Mesozoic and Cenozoic sedimentary rocks. These outcrops dip eastwards towards the Arabian Gulf (Fig. 1.1).

The basement and the overlying sediments dip gently and regularly towards the east. The age of the rocks exposed at the surface becomes progressively younger in the same direction. In the vicinity of the Arabian Gulf the sedimentary sequence may reach thickness in excess of 10000 m.

1.2 The evolution of the Arabian Shield

The evolution of the Arabian Shield has been discussed by many writers, including, Brown, (1970); Greenwood *et al.*, (1976); Gass, (1977); Fleck *et al.*, (1980); Greenwood *et al.*, (1980); Stacy & Hedge,(1984); Nassief *et al.*, (1984); White, (1985); Stoeser & Camp, (1985); Agar, (1985); Bentor, (1985) and others.

Stoeser & Camp, (1985) recognized five main phases of evolution for the Arabian Shield, (Fig. 1.2): (1) rifting of the African Craton (1200-950 Ma), (2) ensimatic island-arc development (~ 950-715 Ma), (3) formation of the Arabian-Nubian neocraton by microplate accretion and continental collision (715-640 Ma), (4) collision-related

intracratonic magmatism and tectonism (640-550 Ma) and (5) epicontinental subsidence (<550 Ma).

The stratigraphy of the Arabian Shield was classified into two principal series by Karpoff, (1957a, 1957b, 1960) and was considerably improved upon by many writers. Schmidt *et al.*, (1973); Greenwood *et al.*, (1976); Greenwood *et al.*, (1980); Fleck *et al.*, (1980); Hadley & Schmidt, (1980) and others, recognized eight stratigraphic units exclusive of plutonics. A summary of the Arabian Shield rock units, tectonism, plutonism, and volcanism are shown in Table 1.1.

The pre-Idwah Formation Palaeozoic sediments are represented by the strongly folded and unmetamorphosed conglomerates, limestone, sandstone and andesitic and basaltic lavas and pyroclastics of the Jubaylah Group (Delfour, 1970). Radiometric dating of the Jubaylah andesite gives a Cambrian age (Hadley, 1975) between 520-500 Ma (Delfour, 1982). Basahal *et al.*, (1984) reported the presence of *archaeocyathid* fossils in the Fatima Formation which is equivalent to the Jubaylah Group and dated them as Cambrian, confirming the age for at least a portion of the formation. According to the faunas and the radiometric dates (Gettings and Stoesser 1981) the youngest rocks in the Arabian Shield are about $530 \pm$ Ma (Greenwood *et al.*, 1980; based on a whole-rock K-Ar date) which is, according to the time scale of Harland *et al.*, (1989), near the Middle Cambrian.

The age of the basal Saq Sandstone is not known, but if a Middle Cambrian (\approx 540 Ma) - Early Ordovician (\approx 500 Ma ; Harland *et al.*, 1989) age is accepted for the Saq Sandstone then there is little time to create the peneplaned surface upon which the Idwah Formation and the Saq were laid down.

So, the age of the Saq Sandstone is uncertain, but if the present correlations are accepted then it is Middle Cambrian to Early Ordovician.

1.3 The tectonic framework of the Arabian Peninsula

There are three main tectonic elements making up the Arabian Peninsula (Fig. 1.3).

1- The Arabian Shield occupies the greater part of the Peninsula, consisting of crystalline basement, lies to the west. 2- The Arabian Shelf, which is located north and northeast of the Shield, is characterized by a sequence of shallow water and continental sedimentary rocks of Palaeozoic-Cenozoic age. This shelf can be divided into three natural and distinct structural provinces: the interior homocline, interior platform, and several basin areas. 3- The mobile belt north and east of the shelf, include the Zagros belt and Oman Mountains which became mobile zones during the Late Cretaceous.

Several unconformities can be recognized in the Palaeozoic rocks of the Arabian Peninsula. These are related to gentle epeirogenic events, the most important of which occurred during the Late Cambrian, Early Devonian, and Early Carboniferous (Murriss, 1980). Central and southern Saudi Arabia shows the effects of the Hercynian orogeny on Devonian to Permian sediments (Saint-Marc, 1978). The main phase of the Hercynian orogeny occurred during the Carboniferous. This event is reflected in regional uplift and a renewed peneplanation that cut through the developing platform, eroding as deep as the Precambrian (Murriss, 1980).

1.4 The Palaeozoic of Saudi Arabia

Following its stabilization the Arabian Shield was reduced to a peneplaned surface made up of igneous and metamorphic rocks. Epicontinental seas moved back and forth across parts or most of this stable basement core and deposited a comparatively thin succession of almost flat-lying strata on it. The epicontinental seas were in turn flanked on the north and east by a great sedimentary basin-the Tethyan trough-that occupied a relatively constant area in Turkey, northern Iraq and southwestern Iran. The trough remained a negative feature throughout most of the Palaeozoic and Mesozoic and many thousands of meters of sediments accumulated in it.

The Palaeozoic sedimentary successions are continuously exposed in the western part of the Arabian Peninsula. These rocks dip off the eastern edge of the shield, and extend from southern Jordan in the north to the Asir-Yemen region in the south. The whole cycle was initiated by deposition of the Cambrian Idwah Formation thin followed by the Cambro-Ordovician Saq Sandstone (+600m); followed by the Upper Ordovician to Silurian Tabuk Formation (1072m), consisting of alternating shales and micaceous sandstones, and the Devonian to late Lower Permian Jauf Formation (299m), consisting of shales with subordinate sandstones, (Fig. 1.4), Steineke *et al.*, (1958); Powers *et al.*, (1966).

Towards the south end of the Arabian Peninsula late Permian erosion has progressively eliminated most of these Palaeozoic rocks, so that eventually upper Permian rocks overstep the Palaeozoic to rest on the basement (Powers *et al.*, 1966).

1.5 Cambro-Ordovician Saq Sandstone

The Cambro-Ordovician Saq Sandstone, defined by Steineke *et al.*, (1958), is described by Powers *et al.*, (1966), and Powers, (1968), as a vertically and laterally uniform succession of white, gray, and brown, cross-bedded sandstone. It is named after the type section at Jabal Saq (lat. 26°16'02"N, long 43°18'37" E), (Fig. 1.5). The Saq Sandstone is at least 600m thick at the type section at Jabal Saq, increasing to about 750 m at Al-Quwayrah. To the south in the As Sirr area the thickness decreases gradually because of erosion beneath the Permian Khuff Formation but in the Tabuk region the unit is as much as 1000 m. Figure 1.6 shows the variation in thickness of the Saq Sandstone, and the extent of the Saq Sandstone in the sub-surface is shown in Figure 1.7.

Powers *et al.*, (1966) regarded the Saq Sandstone as being Cambro-Ordovician in age. This was based on correlating the lower part of the unit with a Middle Cambrian trilobite bearing sequence in Jordan, and on the presence of *Cruziana* spp. which

indicated an early Ordovician (Tremadocian-Arenigian) age in the upper part. Thus the Saq sandstone may record Middle Cambrian to Early Ordovician sedimentation.

Helal, (1964a, 1965) excluded rocks containing traces of organisms, "the *Cruziana* series", from the upper part of the Saq Sandstone in the Tabuk region. Selly, (1970, 1972), in his studies of the Cambrian and Ordovician rocks of Jordan, recognized two members in an equivalent series to the Saq Sandstone. In this research project three members have been recognized, Lower, Middle, and Upper Saq sandstone.

The Saq Sandstone is often red-brown on the surface, but when fresh is a gray and white quartz arenite. It is abundantly cross-stratified, moderately sorted in the Lower and middle parts and moderately well sorted to well sorted in its upper part. It is composed of medium to coarse sandstone in Lower and Middle Saq and fine to very fine sandstone in the Upper Saq. It has mainly monocrystalline grains, which range from sub-angular to sub-rounded in Lower Saq Sandstone and sub-rounded to rounded in Middle and Upper Saq Sandstone. The dominant cement in the Lower Saq Sandstone is iron oxide, with some carbonate and silica cement, while in Middle and Upper Saq Sandstone carbonate and silica are dominant (Fig. 1.8).

The contact between the Saq Sandstone and the underlying rocks, varying from pre-existing sandstone (Idwah Formation; Location K-26) to Precambrian-Cambrian basement rocks, is observed in numerous localities. It is marked by a planar surface overlain by the basal Saq Sandstone which comprises a thin veneer of sandstone, conglomerate and breccia derived from the underlying basement. The upper contact coincides with a sharp lithological and topographical break between the Upper Saq Sandstone and the Hanader Shale (Tabuk Formation).

In the course of this study a sequence of red sandstone and breccia was discovered below the Saq Sandstone. Although these strata are still uncertain, the rocks are regarded as belonging to an older formation - the Idwah Formation which is named after a village near the type section.

1.6 Correlation of the Palaeozoic units in some neighbouring countries.

Correlation of the Palaeozoic Formations of Saudi Arabia with the Palaeozoic rocks cropping out in some neighbouring countries (Jordan, Egypt, Libya and Algeria), is illustrated in Fig.1.9.

The Cambro-Ordovician Saq Sandstone correlates most easily with the Jordanian Quweira Sandstone, Ram and Umm Sahm Sandstones (Quennell, 1951; Bender, 1975); with the Cambro-Ordovician Hassaouna-Memouniat Formations of the Kufrah basin, Libya (Billani & Massa, 1980), and with the Cambro-Ordovician of Sarabit El-Khadim, Abu Hamata, Nasib, and Adedia Formations of SW Sinai -Egypt (Kora, 1984) and with Cambro-Ordovician Ajjer Formation of Algeria (Bennacef *et al.*,1971).

1.7 Previous work

Blackenhorn, (1914) was the first who mentioned the presence of the Lower Palaeozoic in Saudi Arabia. The most comprehensive accounts covering Saudi Arabia in general appear in the publications of Arkell, (1952), Henson, (1951), Steinke *et al.*, (1958), Bramkamp *et al.*, (1958), Powers *et al.*, (1966), and Powers, (1968).

Helal, (1964a, 1964b, 1965, 1968); Hemer, (1965); Hemer & Nygreen (1967a,1967b); Delfour, (1967, 1970); McClure, (1978); Bigot & Lafoy, (1970); Bigot, (1970); Brown, (1970); Hadley, (1973); Cloud *et al.*, (1979); Clark-Lowes, (1980); El-Khayal *et al.*, (1980); Bahafzallah *et al.*, (1981); Sharief, (1982); Delfour *et al.*, (1982); Vaslet *et al.*, (1982); Al-laboun, (1982, 1986); El-Khayal & Romano, (1988); Hussein, (1991) all contributed valuable information on the Palaeozoic of Saudi Arabia in general.

There are very little previous work concerning the Cambro-Ordovician Saq Sandstone, and most of the studies lack detail.

1.8 Location and sampling

The area of study lies between latitudes $26^{\circ}30'$ to $28^{\circ}00'$ and longitude $42^{\circ}00'$ to $43^{\circ}30'$, exposed between Precambrian-Cambrian basement rocks and a cuesta formed by

the Hanader shale of the Tabuk Formation. It forms a fairly flat surface where there are numerous exposures, but few deep sections. Only in a few instances do inselberges like Jabal Al Ghumayq (K-20), rise more than 55m above surrounding landscape to give good sections through part of the formation.

36 outcrops have been sedimentologically and stratigraphically examined and sampled throughout the study area (Fig. 1.10).

1.9 Aims and scope of the study

The aims of this research project are to examine in detail the sedimentary history of Cambro-Ordovician Saq Sandstone. They include the following:

1. A detailed study of facies and stratigraphy of the Saq Sandstone
2. Detailed study of sedimentary structures especially cross-stratification in order to establish the dispersal system and changes in dispersal through time in the Saq Sandstone.
3. Petrography and mineralogical investigations to identify the mineralogical composition of the formation and its vertical and lateral variation. From these data to decipher the provenance of the sediments and evaluate current views on the genesis of quartz arenite.
4. Geochemical study of major and trace elements has been done in order to relate geochemistry to petrographic composition, and to aid in the identification of the source.
5. Grain-size analysis has been done to determine textural variation and to give a clear picture of depositional environments and the nature of the transporting agents of the sediments.
6. The examination of lithological sequences, sedimentary structures, and grain-size analysis will allow the establishment of the depositional environment.
7. From the study of environment through time to deduce the effects of changes in sea-level, subsidence and sediment supply on the history of the basin margin.

ASSEMBLAGES	UNITS	MAJOR ROCK TYPES	TECTONISM EPISODES	PLUTONISM	AGES (m.y.)	
Non-metamorphosed	Jubaylah Group	Clastic rocks, minor volcanic rocks, and marine limestone	Najd faulting: Northwest-trending left-lateral wrench faulting	Granite to granodiorite	530	
	Shammar Group	Rhyolite, trachyte, and minor clastics	- ? -	Granite to granodiorite	570 (?)	
Meta-andesitic	Murdama Group	Conglomerate and graywacke, minor andesite and rhyolite, locally thick marble	Bishah orogeny: Folds and faults, north trends; greenschists metamorphism	Quartz monzonite, subordinate diorite, gabbro, granite	550-570	
	Halaban Group	Andesite to rhyolite, volcanic and pyroclastic rocks and volcaniclastic sediments	Yafikh orogeny: Folds and faults, north; greenschist metamorphism	Quartz monzonite, subordinate diorite, gabbro, granite	600-650	
	Ablah Group	Basalt to rhyodacite, volcanic and pyroclastic rocks and volcaniclastic rocks, locally thick marble	TECTONIC CYCLE	Granodiorite gneiss second diorite series; gabbro; gabbro to iron-diorite, mainly diorite and quartz diorite	750-835	
	Jiddah Group	Basalt and dacite volcanic pyroclastic, and volcaniclastic rocks, minor rhyodacite	TECTONIC CYCLE	First diorite series; gabbro to iron-diorite mainly diorite and quartz diorite	890	
	Meta-basalt-graywacke-chert	Bahah Group	Graywacke, chert, minor marble and tuff, all locally graphitic, and minor basalt			
		Baish Group	Mafic volcanic rocks, mafic tuff, graywacke, and minor chert and marble		Quartz porphyry orthoschist, diabase	1165

Table 1.1 Summary of Precambrian stratigraphy, Tectonism, Plutonism and Volcanism of the Arabian Shield (adapted from Greenwood et al, 1980; Beydoun, 1988).

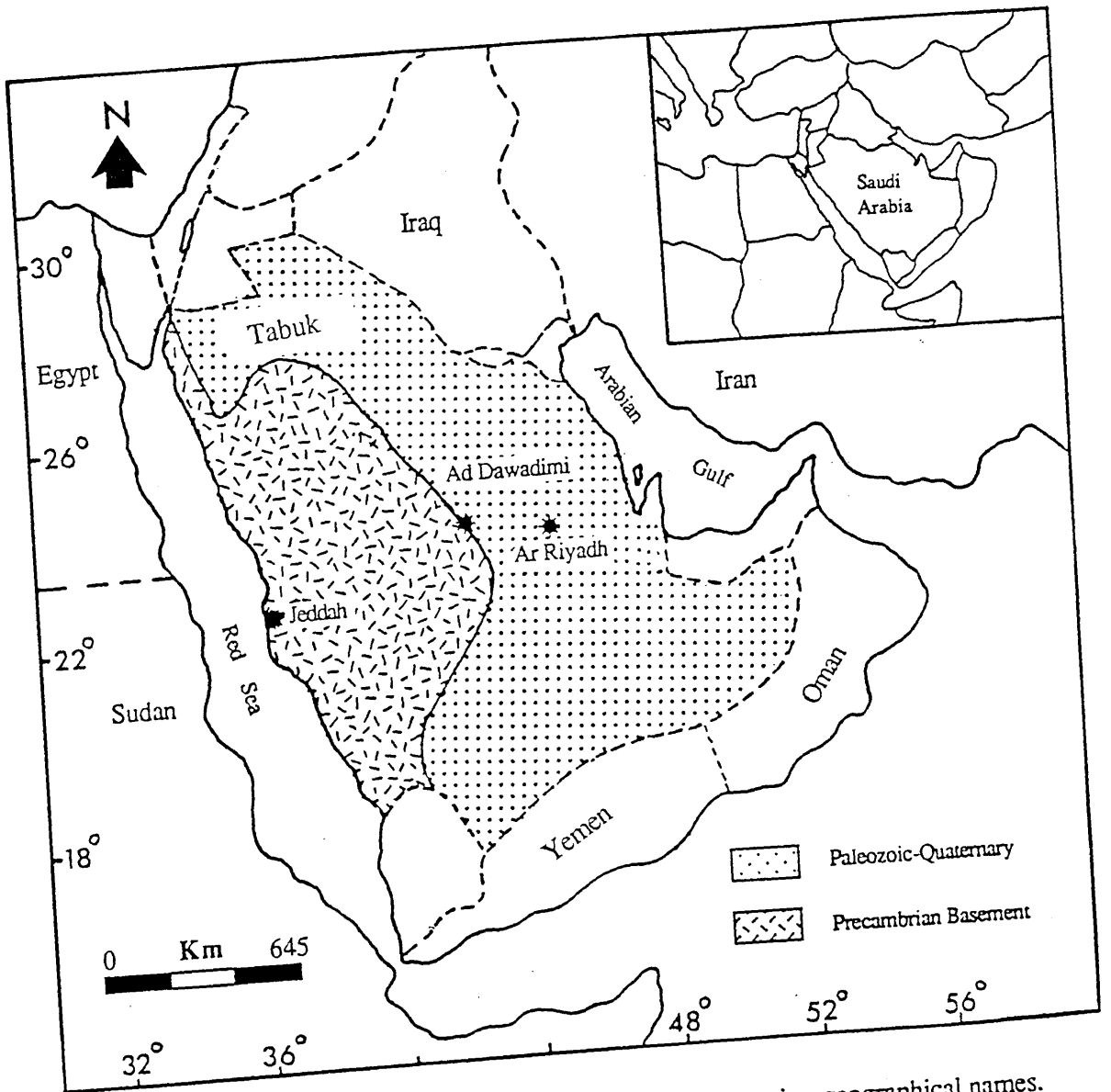


Fig. 1.1 Simplified geological map of Saudi Arabia, showing geographical names.

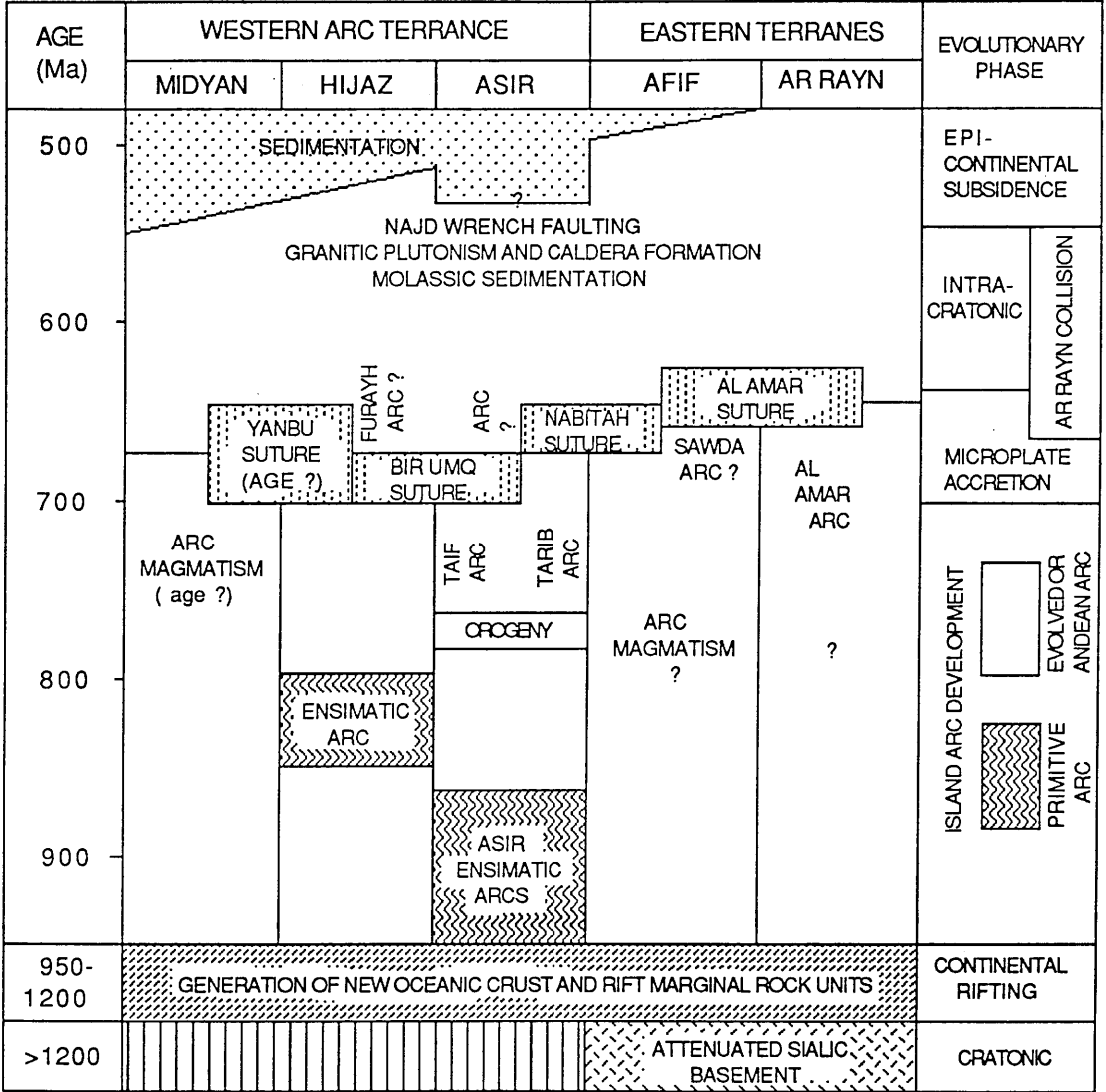


Fig. 1.2 Showing the evolution of the Arabian Shield (Adapted from Stoesser & Camp, 1985).

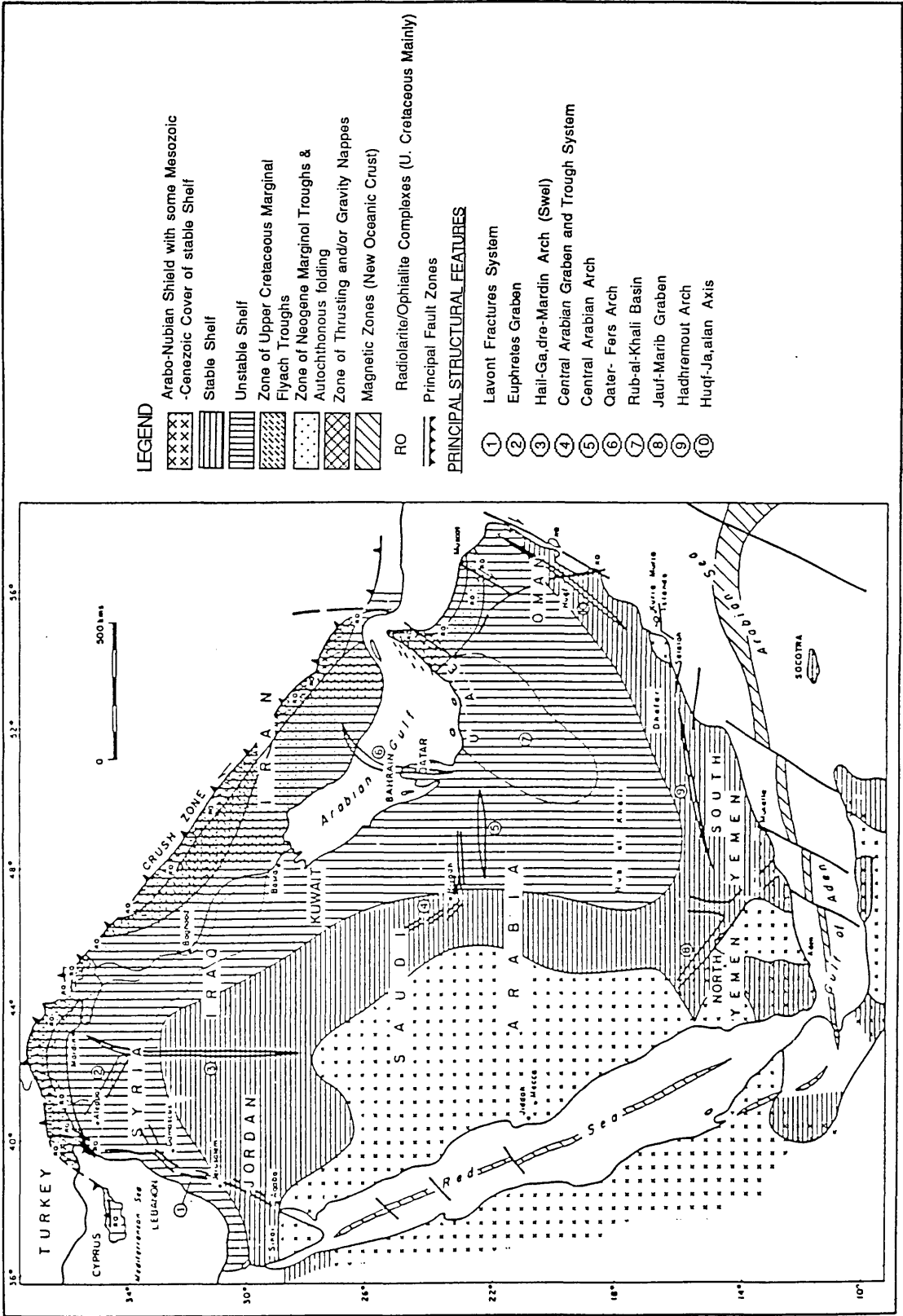


Fig. 1.3 Tectonic framework map the Arabian Peninsula (Adapted from Henson, 1951; Beydoun, 1988).

ERA	PERIOD		FORMATION	MEMBER	THICKNESS (m)	LOG	LITHOLOGY	
Mesozoic	Triassic	Liassic	Minjur				Sandstone ; poorly sorted, reddish Shale	
		Middle	Jilh				Dolomite ; limestone ; shale gypsum ; sandstone	
		Early	Sudair				Shale , red , green ; sandstone ; dolomite ; gypsum	
Palaeozoic	Permian	Early To Late	Khuff	Khartm			Limestone , aphanitic ; dolomite ; calcareneite	
				Midhnab			Clay ; gypsum	
				Duhaysan Huoyaf			Limestone ; dolomite ; clay	
				Unayzah			Sandstone, fine-grained ; shale ; claystone	
	Carboniferous	Westphal. Tournais.	Berwath				Sandstone , fine to coarse-grained, argillaceous ; shale ; siltstone	
							Sandstone ; siltstone ; shale ; lightite	
	Silurian	Emsian	Jauf	U.Sandstone			Sandstone ; siltstone ; shale ; lightite	
				Hamamiyat			Limestone ; calcareous shale	
				Subbat			Shale , silty , gray , red	
				Shaiba			Shale ; sandstone	
		Siegenian		Tabuk	Tawil			Sandstone , medium to coarse-grained clay , red ; siltstone
		Late Ludlovian	Middle Ludlovian	Early - Ludlovian To Wenlockian	Sharawrah			Siltstone , fine-grained, micaceous
					Qusaiba			Shale , gray , green Shale silty
					Sarah			Sandstone , fine-grained, red, brown green ; shale, micaceous ; diamictites
					Middle Sandstone			Sandstone, clayed, gray shale, micaceous
Ordovician		Llandelian To Llanvirnian	Arenigian	Raan			Shale, micaceous, gray ; siltstone	
	Lower Sandstone					Sandstone, medium to coarse-grained clay, gray sandstone, medium grained, micaceous.		
	Hanadir					Clay, grey ; shale ; siltstone .		
Cambrian			Saq Sandstone				Sandstone, fine to medium-grained white, yellow brown.	
					Sandstone, arenaceous, poorly cemented medium to fine-grained, cross-bedded or massive, variegated reddish-brown, black or maroon.			
					Sandstone, coarse-grained			
					sandstone, fine to coarse-grained bedded or cross-bedded, red and yellow			
							Local conglomerate	
							Basal conglomerate	
Pre-Cambrian							Basement rocks	

Fig. 1.4 General lithostratigraphy scheme of central Saudi Arabia.

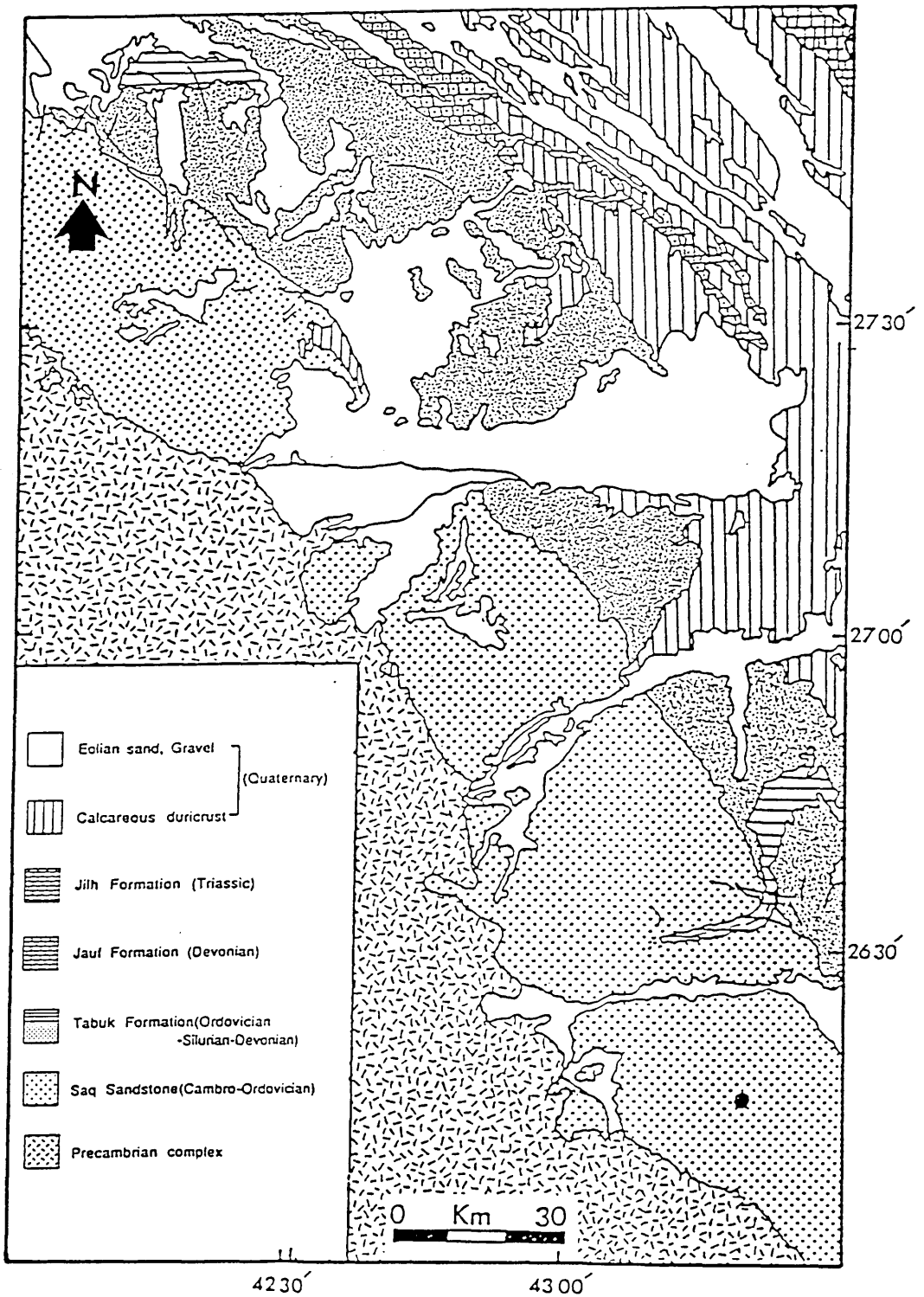


Fig. 1.5 Geological map of the study area (Bramkamp et al., 1963)

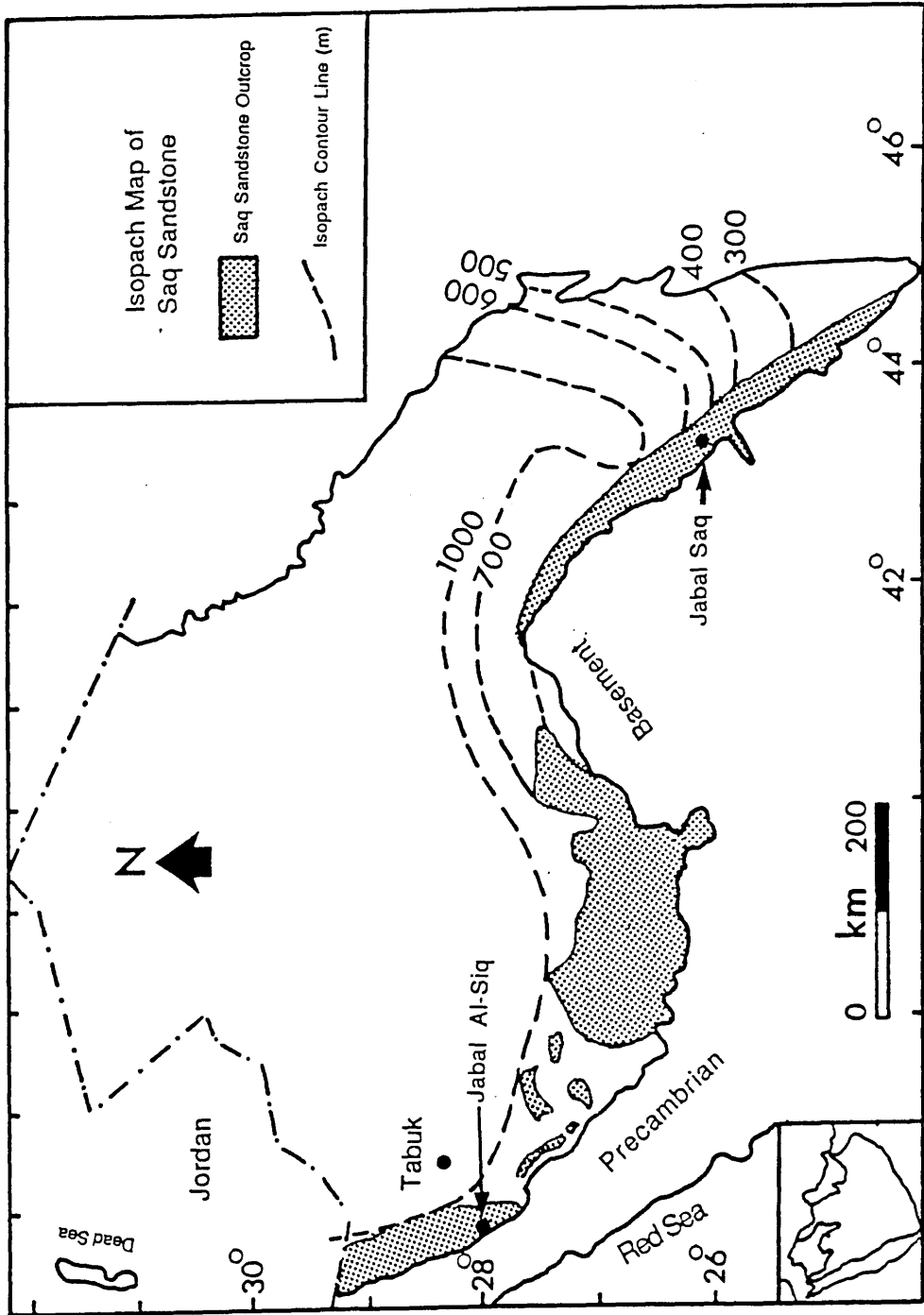


Fig. 1.6 Isopach map of Cambro-Ordovician Saq Sandstone.

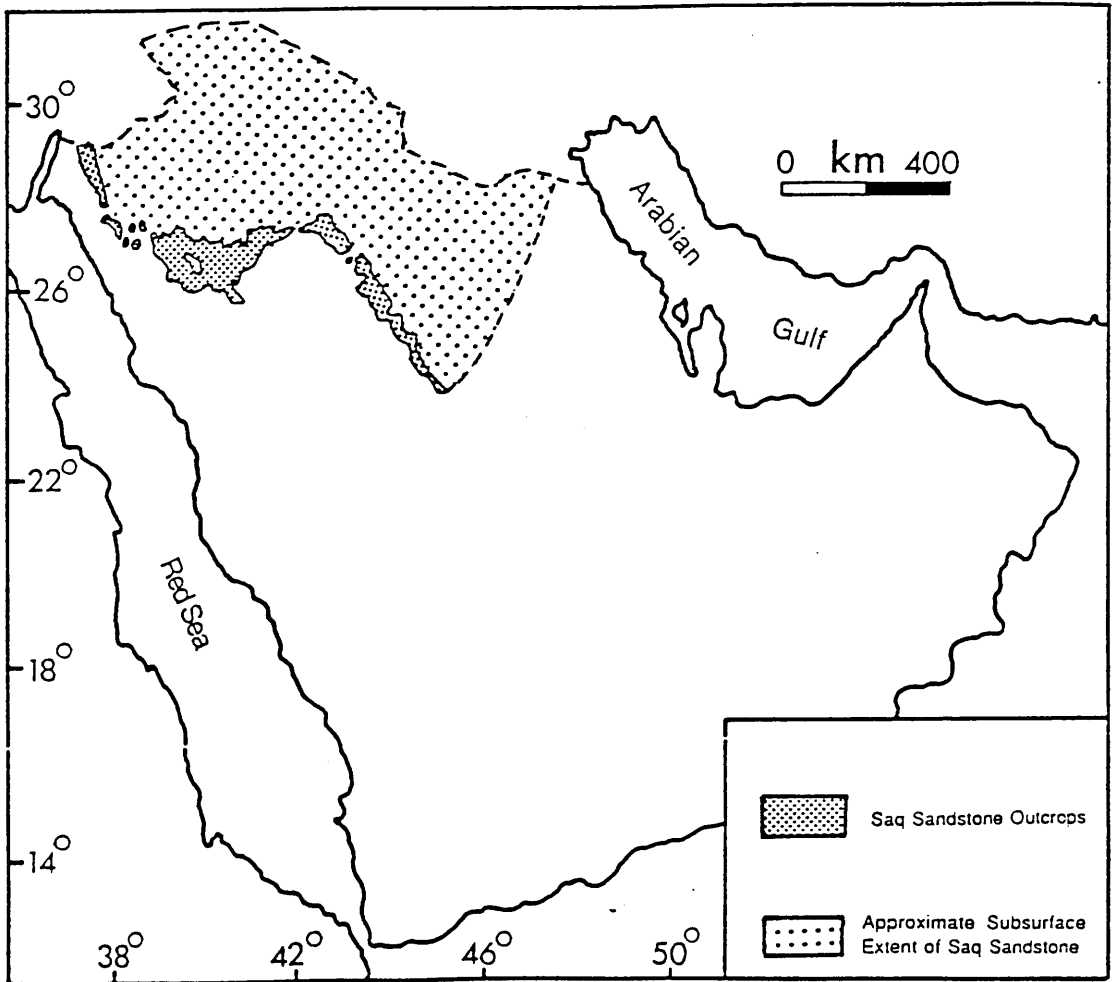


Fig. 1.7 Showing outcrop and sub-surface extent of the Saq Sandstone in Saudi Arabia.

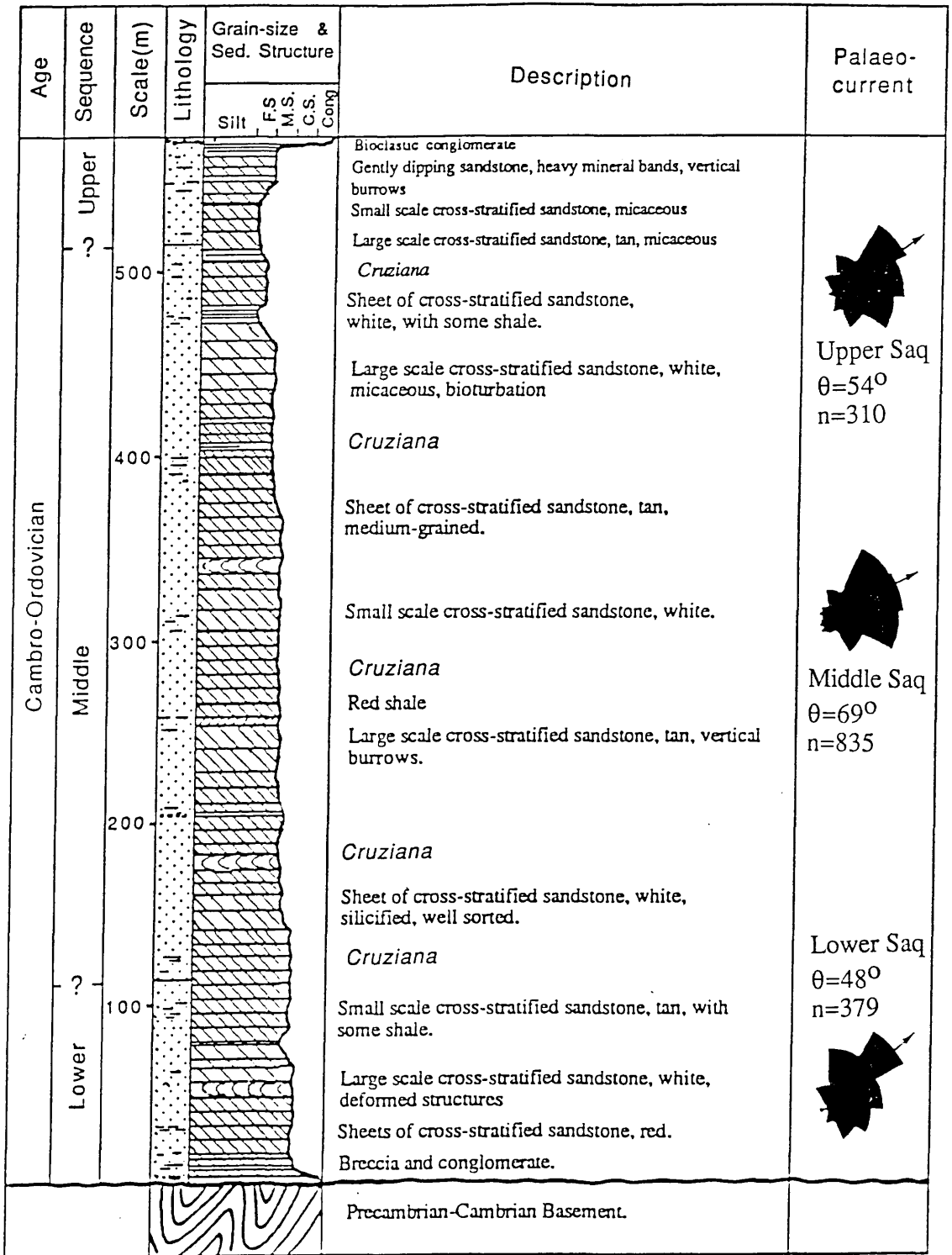


Fig. 1.8 General columnar section of the Saq Sandstones.

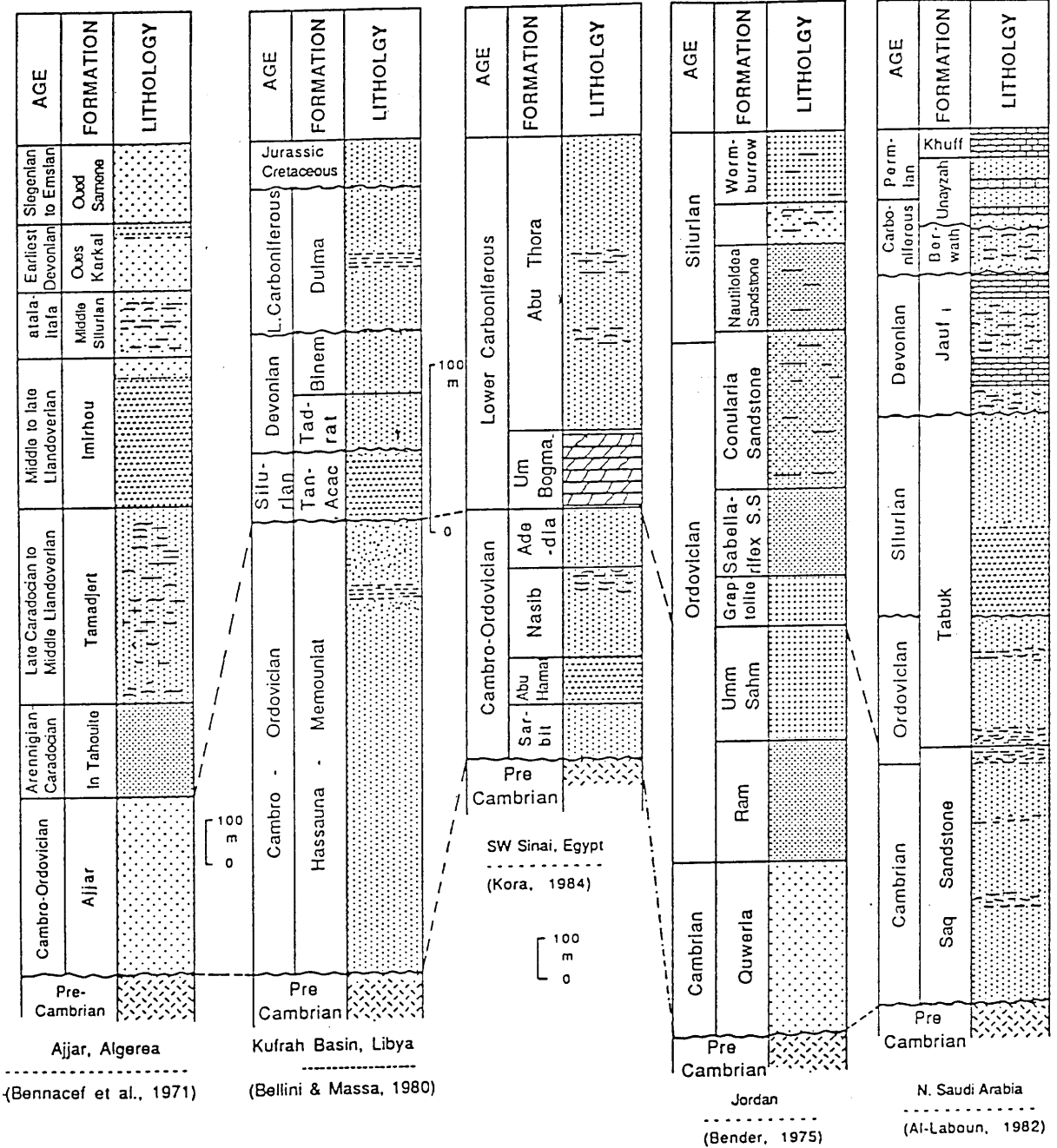


Fig. 1.9 Correlation chart of Palaeozoic exposures in Saudi Arabia, Jordan, SW Sinai (Egypt), Libya and Algeria (adapted and modified from Kora, 1984).

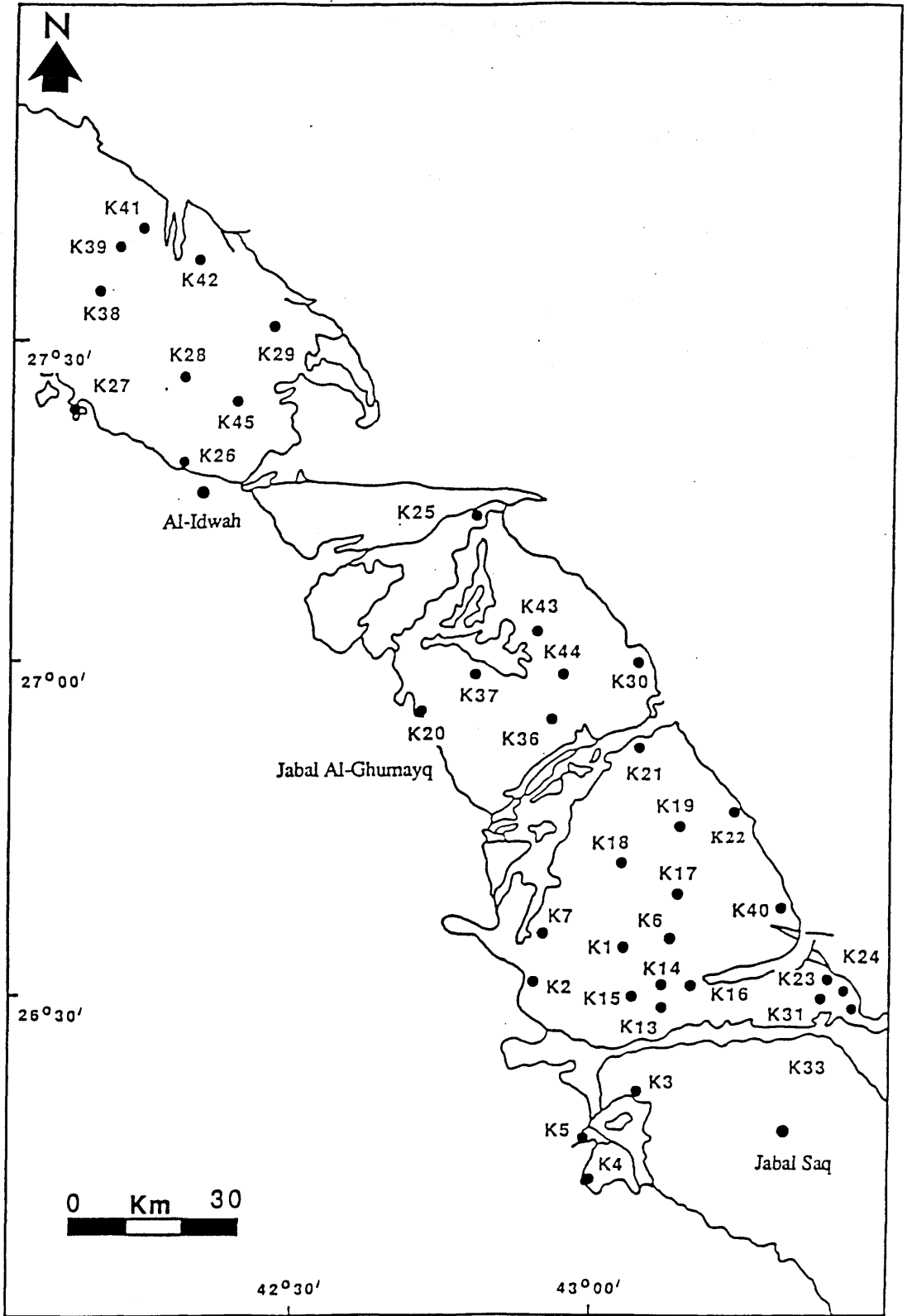


Fig. 1.10 Location map of the Saq Sandstones showing sample locations.

CHAPTER TWO

STRATIGRAPHY AND FACIES OF THE SAQ SANDSTONE

2.1 Introduction

The Cambro-Ordovician Saq Sandstone, consists of at least 600m of mineralogically and texturally mature sandstone (up to 95%) with subordinate shale, siltstone, breccia and conglomerate. The area of study is more than 8000 Km², forming a flat surface with small hills up to 20m high, but in some instance rising up to 50m (Jabal Al-Ghumayq, K-20; see Fig. 1.10).

With the dip of the beds being $\approx 1^{\circ}$ and with no long continuous sections it is difficult to established the precise stratigraphic position of individual outcrops on the rough, stony desert, but this could be easily established where the upper contact with the Hanader shale (Tabuk Formation) or the basal contact with the Precambrian-Cambrian basement and Idwah Formation was exposed. The approximate stratigraphic positions within the known outcrop belt were established using the exposure elevation, and assuming a constant regional dip of one degree toward the northeast.

The objectives of this chapter are (1) To record the general stratigraphy of the Saq Sandstone, (2) To provide detailed descriptions and interpretations of the component facies (3) To discuss the nature of the processes controlling bed form migration in a shallow marine environment.

2.2 Stratigraphic setting

The Saq Sandstone defined formally by Steineke *et al.*, (1958) and originally described by Powers *et al.*, (1966) and Powers, (1968) as a uniform formation of white, red, gray or brown cross-stratified sandstone. Delfour *et al.*, (1982), Vaslet *et al.*, (1985) and Williams *et al.*, (1986) have divided the Saq Sandstone into two members (1)

a lower Risha member of coarse-grained and conglomeratic sandstone and (2) an upper Sajir member of white fine-grained sandstone with silty layers and traces of organisms.

Al-laboun, (1982 and 1986), using sub-surface data, also divided the Saq Sandstone into two members (1) a Lower fluvial facies and (2) an Upper littoral to shallow marine facies.

In this study the stratigraphy of the Saq Sandstone is divided into three members (Lower, Middle and Upper). The precise positions of the boundaries are not identified, but the general differentiations between these members are based mainly on the change of the assemblage of grain-size, sedimentary structures, thickness of the beds, presence and abundance of trace fossils and colour. The Saq Sandstone generally fines and matures upward.

Stratigraphically below the Saq Sandstone and well exposed in the area near the village of Al-Idwah (Location K-26, see Fig. 1.10), is a red coloured group of rocks referred to here as the Idwah Formation. Outcrops of this formation occur scattered either as outliers within the Precambrian-Cambrian basement or as inliers beneath the base of the Saq Sandstone.

The Idwah Formation comprises a flat-stratified red sandstone (up to 110cm) and thick sequence of breccia (up to 75 cm thick), which most likely was derived from underlying rocks. The sandstone is fine to medium-grained quartz arenite, moderately well sorted. The breccia is composed predominantly of angular to sub-angular quartz clasts with some metamorphic clasts up to 12cm in diameter. The matrix is poorly sorted fine to very coarse-grained sand (Fig. 2.1).

The Lower Saq Sandstone is up to 110m thick, and lies unconformably on the Precambrian-Cambrian basement and pre-Saq sediment (Fig. 2.2). The surface of unconformity is typically flat. The sequence begins with a basal conglomerate and breccia (<1 m thick) composed of mainly angular to sub-rounded quartz pebbles, most of which came from the underlying pre-Saq sediments and basement.

Most of the Lower Saq Sandstone consists of medium to coarse-grained, pebbly red quartz arenite (Fig. 2.3). Less common lithologies consist of red and black shale, conglomerate and breccia. The sediments are moderately well sorted.

Sedimentary structures are dominated by tabular planar cross-strata, and some trough cross-strata, ranging in thickness between 0.1 to 4m (Fig. 2.4). Deformed cross-strata are common in the lower part of the sequence, the style of deformation ranging from overturned to convoluted foresets. The foreset dip angles average 21° . Most of the cross-strata exhibit sharp bases with truncated tops. The Lower Saq Sandstone has not yet yielded any body or trace fossils.

The Middle Saq Sandstone (up to 420m) is characterized by medium-grained quartz arenite with subordinate fine conglomerate, siltstone and shale occurring throughout the sequence (Fig. 2.5). The sandstone is medium to coarse-grained, moderately well sorted (Fig. 2.3). Tabular planar cross-strata are the dominant sedimentary structures throughout the sequence, ranging in thickness between 0.1 to 6.5m with an average of 1.63m (Fig. 2.4). In the Middle Saq Sandstone the first best developed tidal sand bars appear, especially in the middle of the sequence (Location K-16) where the thickness of the bar is up to 7m. *Cruziana* occurs in more than 5 levels of the stratigraphic sequence.

The Upper Saq Sandstone, which consists of 55m of stratigraphic sequence is dominated by cross-stratified micaceous quartz arenite, with subordinate shale and siltstone (Fig. 2.6). The sandstone is fine to medium-grained, well sorted to very well sorted (Fig. 2.3). Thicknesses of cross-strata range between 0.1 to 3.5m with an average of 0.87m (Fig. 2.4). Most of the cross-strata foresets exhibit sharp bases with truncated tops. The fine sediments (shale and siltstone) are more abundant than in either the Middle or the Lower Saq Sandstone. *Cruziana* trace fossils of trilobites and body fossils, mainly brachiopods, also occur. The fossils are sometimes in thick concentrated shell beds where they are often very broken-up.

The upper part of the sequence represents progradational beach-shoreface deposits.

More than 1500 palaeocurrent readings from the Lower, Middle and Upper Saq Sandstones, were measured. As the Saq Sandstone are nearly flat-lying ($< 1^{\circ}$) no correction for tectonic tilting was required. The palaeocurrent directions are generally unidirectionals, towards the northeast (Fig. 2.7).

2.3. Shallow marine environment

A shallow marine environment is envisaged for part or all of the Saq Sandstone, for the following reasons :

- (1) The presence of brachiopod shells in the Upper Saq Sandstone.
- (2) Abundance of trace fossils (*Cruziana*) at more than five levels throughout the Saq Sandstone. These trails were produced by trilobites, which were exclusively marine organisms and their tracks can be considered to be direct evidence of marine conditions (Sielacher, 1970; Selly, 1970; Goldring, 1985).
- (3) The presence of beach deposits, comprising low-angle cross-strata dipping northeast, with many heavy mineral bands characteristic of upper foreshore beach deposits (Thompson, 1937; Clifton, 1981).
- (4) The highly maturity of the sandstones which could reflect inheritance from a pre-existing mature sandstone. The consistent maturity of sandstone in these deposits suggests that the environment was too energetic to allow first cycle sand from the basement to be present.
- (5) The high abundance of cross-stratification in the Saq Sandstone. Many Late Precambrian and Early Cambrian offshore shallow marine successions are characterized by abundant of cross-stratification (*e.g.* Pryor & Amaral, 1971; Sweet & Smitt, 1972; Hereford, 1977).

So, with absence of any evidence of subaerial exposure in the Saq Sandstone; the absence of channelling and fining-upward sequences which characterize alluvial deposits,

along with features which have been listed previously, the Saq Sandstone is interpreted as shallow subtidal marine shelf deposits.

2.4 Tide-dominated shelf

Tidal currents are thought to have deposited part or all of the Saq Sandstone. The Saq Sandstone is thought to have been deposited on a tidally dominated shallow shelf for the following reasons :

- (A) Large scale sand waves (bars) associated with marine trace fossils (*Cruziana*) have been found throughout the Saq Sandstone. These are not found as active features in tideless seas (Narayan, 1971; McCave, 1973; Anderton., 1976; Nio *et al.*, 1983; Smith & Smith, 1988, Allen & Homewood, 1984; Houbolt, 1982).
- (b) Unimodal palaeocurrent cross-strata associated with reactivation surfaces. Reactivation surfaces could have been formed when the tidal current was asymmetric (ebb dominant), with the bed-form migrating in response to the stronger tidal current. The subordinate current (flood) was in some instances strong enough to erode the crest and the lee face of large sand waves to create reactivation surfaces (Level, 1980; Driese *et al* , 1981).
- (c) The abundance of cross-stratification. Many ancient tidal offshore shallow marine sandstones are reported to be abundantly cross-stratified (Pryor & Amaral, 1971; Sweet & Smett, 1972; Dott & Batten, 1971; Hereford, 1977; Banks, 1973; Soegaard & Eriksson, 1985).
- (d) Mud-clasts are not entirely a diagnostic feature of tidal deposits, but in association with other features could indicate tidal current activity. Mud-clasts could be formed by break-up mud drapes which were deposited during slack periods of tidal currents (Terwindt, 1971; Allen, 1980).
- (e) The large volume of sand and the high ratio of sandstone : shale. These criteria along with other features suggest that tidal currents are the only mechanism capable of transporting a large volumes of sand offshore. There is little fine sediment,

suggesting that the tidal processes were active over much of the shelf. Storm-generated currents are capable of moving large quantity of sand offshore, but storm deposits have not recognized anywhere in the Saq Sandstone and the cross-strata are far too thick for storm deposition.

- (f) Association with beaches.

In summary, the Saq Sandstone is thought to have formed in an extensive tide-dominated shallow shelf environment and included some near-shore beach deposits. There are few if any deposits which may be clearly interpreted as being the result of storm deposition.

2.4.1 Tidal currents and unidirectional flow

Palaeoflow throughout the Saq Sandstone is unidirectional in a north-northeasterly direction, except in few localities (*e. g.* K-16, K5, K4) the cross-strata dips are bipolar-bimodal distributions. The consistency and similarity of the palaeoflow orientation of the sand sheets and bar fields suggests a very uniform dispersal system throughout the basin of deposition.

Many workers have reported unidirectional palaeocurrents from sandstones that are interpreted as shallow marine tidal deposits (Narayan, 1971; Banks, 1973; McCave, 1973; Anderton, 1976; Nio, 1976; Level, 1980; Allen and Homewood, 1984; Santisteban & Taberner, 1988).

Levell, (1980) has attributed the unidirectional palaeocurrents in the Lower Sandfjord Formation in north Norway to three mechanisms, operating in shallow marine environments:

- (1) Regional transport dominance.

Stride, (1963), Belderson & Stride, (1969) and Kenyon & Stride, (1970) have documented persistent transport dominance over several hundreds of square kilometres of seafloor which results in unidirectional transport paths. This arises because sediment transport during one tidal phase systematically exceeds that

during the other. This asymmetry of the tidal ellipse is caused by the way in which the tidal wave is propagated into the basin as a whole, and thus depends upon the shape of the basin (Johnson & Belderson, 1969 ; Mofjeld, 1976). When the subordinate current is below threshold, or the volumes of sediment it transports are small the structures produced by reversing currents are obliterated, and the dominant current is left as the sole record and is represented in the larger types of bedforms. A unidirectional cross-stratification then results.

(2) Local transport dominance.

On a smaller scale than (1), this is likewise due to the deformation of the tidal wave by bottom friction, reflection shielding (Postama, 1967) and can result in transport dominance capable of producing unidirectional cross-stratification (Terwindt, 1971).

(3) Preservational considerations.

(A) Large bed forms commonly display partial reversal when the subordinate tidal current produces a cut-back form (Van Venn, 1935; McCave, 1971)

(B) The lateral migration postulated for large subtidal sand bars (Houbolt, 1968; Caston, 1972) is extremely regular, and may lead to the preferred preservation of only one element of the ebb/flood circulation system, and hence to unidirectional cross-stratification.

Levell, (1980) argued that these mechanisms cannot be used to explain unimodal palaeocurrent patterns in tidal sandstones that are hundreds of meters thick, simply because a series of bar and inter-bar deposits affected by different dominant current directions would be expected.

Although all these processes could contribute to unidirectional palaeocurrent patterns, reinforcement of the tidal current by other unidirectional basinal currents, such as wind-driven and oceanic currents is the best explanation for unimodal palaeocurrent

patterns throughout a thick tidal shelf sandstone (Johnson & Stride, 1963; Levell, 1980; Anderton, 1976; Johnson & Baldwin, 1986).

In the absence of any evidence to the contrary, most of the unidirectional palaeocurrents of the Saq Sandstone are assigned to strong asymmetrical tidal currents

2.4.2 Ebb or flood

The tidal currents are thought to be ebb for the following reasons:

- (1) From a consideration of the Cambro-Ordovician palaeogeography (Fig. 6.3) it is evident that the Afro-Arabian shield existed to the west and the Cambro-Ordovician deeper water, fine-grained sediment occur in east and northeast.
- (2) The strike of the beach deposits. The beach sediments comprise shallow dipping, upper foreshore strata which consistently strike roughly N-S and dip to the E. This indicated that during regression the coastline built East into the basin.

In addition to this two factors, facies distributions and palaeoflow pattern (NE) indicate that the Cambro-Ordovician shelf sloped gently to the north-northeast, where tidal current circulating the shelf (rotary tidal current ?). Also the area of study (8000 Km²) formed a small part of a larger shelf, which could record only one direction of tidal current (Ebb), where a stratigraphic horizon may show unimodal but opposed to flow patterns in different places due to non-correspondence of ebb and flood current pattern (Rust, 1977).

A possible explanation for ebb-dominated shallow shelf is illustrated in figure 2.8, where a large scaled rotary tidal regime is postulated.

2.5 Facies description and interpretations

The sediments of the Idwah Formation and the Saq Sandstone can be divided into 15 sedimentary facies and subfacies based on lithology, grain-size, sedimentary structures, thickness of the beds and presence or absence of trace fossils. Facies were

first defined at type locality and then identified in other outcrops. Distributions of facies and subfacies are shown in Figure 2.9 and Table 2.1.

In course of the study of the Saq Sandstone two terms (megaripple and sand wave) have been used to describe the bedforms, which are thought to have generated the cross-strata. A megaripple is a bedform, which deposits a single unit of cross-strata with a thickness less than or equal to 70 cm. A sand wave is used to describe bedform which deposited a single unit of large scale cross-strata with thickness more than 70 cm.

2.5.1 Facies 1: Small-Medium scale grouped cross-stratified sandstone

This facies is volumetrically the most abundant throughout the Saq Sandstone (more than 56% of total Saq Sandstone sequence). It comprises variable thicknesses of small-medium scale cross-strata, ranging from 8 to 70cm thick. This facies can be subdivided into three subfacies.

2.5.1.1 Subfacies 1a: Sand sheets with inclined boundaries: Top-sets

This subfacies is dominated by small scale tabular cross-strata, ranging in thickness from 8 to 70cm (Fig. 2.10), with high angle foresets (18° - 26°). It rests sharply or, less frequently tangentially, on the underlying sediments. The upper contacts are generally truncated, where the boundaries are climbing down-dip (Plate 2.1). It is composed of medium to coarse grained sandstone, with some pebbles, showing moderate to good sorting in the Lower and Middle Saq Sandstones, and fine-grained sandstone in Upper Saq Sandstone (Fig 2.11). The small scale cross-stratified sets may increase in thickness down dip (in the palaeoflow direction) to become large foresets (Facies 2). This subfacies occurs most commonly on the top of large scale cross-stratified units (Facies 2), where it may form cosets overlying these larger bed forms.

The sand sheets with inclined boundaries subfacies (1a) form 15% of the whole Saq Sandstone sequence, but are more abundant in the Middle Saq Sandstone where they

form 19% of the sequence forming 14% and 10% respectively in Lower and Upper Saq Sandstone .

More than 400 dip orientation directions of planar tabular cross-stratified sandstone have been measured from the whole Saq Sandstone sequence and plotted as rose diagrams (Figs 2.12 to 2.14). The statistical parameters are summarized in Table 2.2. A unidirectional palaeocurrent pattern toward the north to northeast is the dominant pattern, except in locations K5, K14 and K16 where the palaeocurrent is bidirectional.

Process interpretation

The deposits of the top-set subfacies (1a) developed in response to migration of superimposed straight crested megaripples on the crest and stoss (landward) side of submarine bars (sand waves). Because the landward side of the bar received the dominant ebb tidal current, the cumulative effect of the tidal current was to transport the finer sediment at a faster rate than the coarser fraction which is transported as bedload. This coarse sediment is retained within the megaripples which built the cross-strata. The fine sand which by-passed the megaripple field or was directly transported from the landward side was deposited down-current on the lee (seaward) slopes in facies 2 and facies 4. Subfacies 1a may merge or intertongue with the underlying large scale cross-stratified sandstone (Facies 2). This intertonguing is produced when megaripples migrate up the stoss side of larger bed-forms and over the crest to deposit sediment on the lee face. This is typical of modern shallow marine environments where small megaripples (Subfacies 1a) are developed on the surfaces of large sand waves (Belderson et al., 1982).

There is a weak positive relationship between the thickness of adjacent small scale cross-stratified sandstone units (Subfacies 1a) and large scale cross-stratified sandstone units (Facies 2). This correlation is clearer in the Middle Saq Sandstone where the bars are better developed (Fig. 2.15).

The correlation between the thickness of this subfacies and that of the underlying large scale cross-stratified sandstone (Facies 2) may illustrate the effect of scale : larger foresets have larger top-sets.

The unidirectional palaeocurrent pattern is a result of migration of megaripple bed forms within an asymmetric ebb-dominant tidal current. The bidirectional pattern in locations K5, K14 and K16 is attributed to the tidal current where the flood current was strong enough to transport sediment and generate cross-beds with reverse directions of flow.

This may be also due to the deflection of the tidal path by the topography of the sub-marine dune field, it may also be the result of a complex mixing of more than one tidal current. However since there is a consistency in the palaeocurrent pattern throughout the Saq Sandstone, the former explanation is more probable.

2.5.1.2 Subfacies 1b: Interbedded cross-stratified sand sheets and shale

This subfacies is characterized by alternating sheets of cross-stratified sandstone and shale. It is usually seen to occur between the big bars (*e.g.* bar at location K16). The sandstone units form more than 85% of this subfacies. The cross-strata range between 10 to 70cm thick (Fig. 2.16; Table 2.3), with nearly-horizontal bounding surfaces (Plate 2.2). The sandstone is fine to medium-grained quartz arenite, moderately well sorted (Fig. 2.17). Foresets usually have both a sharp base and tops. The shale may occur as lenses in sand sheets (Fig. 2.18) or as interbedded shale and sand sheets (Fig. 2.19). The shale is a red weathering black shale, with thin parallel-laminated sand strata. The palaeocurrent pattern for this subfacies is unidirectional northeasterly (Fig. 2.20 to 2.22) and the statistical parameters are summarized in Table 2.4.

Process interpretation

The interbedding of sheet of cross-stratified sandstone and shale implies that this facies was deposited in a region of the shelf characterized by fluctuating current strength.

The cross-stratified sheets of sandstones were deposited by migration of straight crested megaripples in response to an asymmetric tidal current. This subfacies may have been formed by tidal currents entering between the offshore bars (Kumar & Sanders, 1974; Barwis & Makurath, 1978; MacCarthy, 1987).

During the intervals between deposition of sand sheets there little or no current activity and mainly muds were laid down from sediment in suspension, giving rise to the shale interbeds (Banks, 1973). It seems probable that the shale could be deposited in at least three ways (1) directly from suspension during the subordinate tidal flow (flood); (2) as an end member of tidal sand paths (Anderton, 1976) and (3) as sediment accumulating to the side of net sand transport paths (Stride *et al.*, 1982).

However, during the periods of dominant flow (ebb) the cross-stratified sandstone was deposited by the migration of megaripples.

2.5.1.3 Subfacies 1c: Sand sheets with flat boundaries

This subfacies consists of sheets of small scale cross-stratified sandstone ranging in thickness from 10 to 70cm (Fig. 2.23). The sandstones are fine to medium-grained quartz arenite, moderately well sorted (Fig. 2.24). The subfacies forms a high topography (Fig. 2.25), where it comprises the most extensive subfacies throughout the Saq Sandstone (32% of the total Saq Sandstone sequence). The majority of the cross-strata are tabular sometimes as planar sheets and sometimes as wedges, with nearly horizontal boundary surfaces. Trough cross-strata are present. The cross-strata foresets exhibit sharp bases, with no evidence of erosion, and truncated tops.

Observations on these sheets shows that this subfacies is characterized mostly by uniform cross-strata thicknesses with small range of standard deviation (Table 2.5).

The palaeocurrent pattern is generally unidirectional to the northeast (Figs 2.26 to 2.28), and the statistical parameters are summarized in Table 2.6.

Process interpretation

The cross-stratified sheets of sandstone were deposited by migration of straight crested megaripples in response to asymmetric tidal currents.

This subfacies may have been an early stage of formation of marine bars.

2.5.2 Facies 2: Large-scale heterogenous cross-stratified sandstone

This facies comprises large scale cross-strata, and is the most important facies, forming 28% of the whole Saq Sandstone sequence. It is particularly abundant in the Middle Saq sandstone where it forms 36% of the sequence; and is less common in the Lower Saq where it is only 19% and the Upper Saq Sandstone where it forms 8%.

The large scale heterogenous cross-stratified sandstone facies (Plate 2.3) is dominated by large foresets which in some cases persist for more than 70m laterally, and range in thickness from 1.3 to 6.5m (Fig. 2.29). It is generally in medium to coarse-grained sandstone in the Lower and Middle Saq Sandstone and in fine-grained sandstone in the Upper Saq Sandstone (Fig. 2.30). It contains some well rounded quartz pebbles and rare mud-clasts, none of which exceeds 7cm in diameter (Plate 2.4). The sandstones of this facies are moderately well sorted to well sorted based on grain-size analysis. Foreset beds are 1 to 9cm thick and display changes in grain-size and structure when traced along the length of the bar. In the upstream section the strata are massive and ungraded but they are normally graded in the downstream regions (Plate 2.5). They range from coarse-grained strata to fine in a downcurrent direction. They are either gradational upward into top-sets (Subfacies 1a) or more commonly truncated by erosional surfaces overlain by small scale cross-stratified. The lower boundaries of the cross-strata are usually sharp, and in only some instances are tangential. The angle of foreset dip ranges between 19° to 28° and this value decreases down-current, presumably indicating a strengthening current (Stride *et al.*, 1982). A single cross-stratum may, along its length, change from tabular-planar foresets near the crest to tabular-tangential foresets near the base.

Soft-sediment deformation like convoluted and overturned foresets are rare in the Lower and Middle Saq Sandstone (Plate 2.6), sparse examples of vertical burrow tubes occur within the large foresets (Plate 2.7). There are few reactivation surfaces in this facies and these dip at low angles (Plate 2.8).

Over 500 measurements of direction of dip of cross-strata were made from this facies. The palaeocurrent directions of large scale planar cross-stratified sandstone facies are unidirectional at any one locality. A general north to northeasterly trend is indicated by the regional palaeocurrent pattern which remained fairly constant throughout the Saq Sandstone (Figs. 2.31 to 2.33). The statistical parameters of the palaeocurrent directions are summarized in Table 2.7.

Process interpretation

Large scale cross-stratified sandstones have been reported in several environments; large rivers, deltas, estuaries, aeolian sand seas and shallow marine shelves. The Saq Sandstone lacks any fluvial and deltaic characteristics such as channel forms; lenticular sand body geometry; lenticular cosets with scour surfaces at the bases; overbank deposits, or any evidence of subaerial exposure. Characteristics of an aeolian environment such as climbing translent strata or sandflow toes (Hunter, 1977, 1981; Kocurek, 1981; Blakey, 1984) are also absent. The presence of *Cruziana* trails (Plate 2.11), body fossils and the association with beaches all point to an origin in a marine environment. The abundance of cross-stratification and the absence of storm layered deposits or hummocky cross-strata favour a high energy, shallow marine, tidal environment.

The large scale cross-stratified sandstone facies was deposited in a strong, time-velocity asymmetric, tidal current regime by the migration of relatively straight crested sand waves (Dalrymple *et al.*, 1978; Allen, 1980).

The repetitive foresets without mud-drapes are similar to features described by Boersma & Terwindt, (1981), Allen & Homewood, (1984), Dalrymple, (1984) and Harris & Erikson, (1990).

The small scale cross-stratified sandstones (Subfacies 1a) which are superimposed on the large scale cross-stratified sandstones (and which erodes the tops of the large ones) were formed by migration of straight transverse crested megaripples which fed the slip-faces of the sand waves by avalanching. Avalanching down the lee side of the sand waves takes place in response to oversteepening produced by deposition of bedload at the brinkpoint of the sand wave (Allen, 1968; Allen & Homewood, 1984).

In strong tidal regimes flow separation develops on the lee side of sand waves under conditions of time-velocity asymmetry. The resulting unidirectional currents produce steep avalanche foresets migrating in the dominant flow direction (ebb). The large scale cross-stratified facies resulted from north-northeasterly migration of large scale sand-waves in response to extreme time-velocity asymmetry of tidal current (ebb-dominant). Reference to Allen's diagram (1968, Fig. 6.4) showing the correlation between water depth and sand wave height shows that 6.5m high sand waves are likely to occur in 40-45m of water.

The reason why this facies is not characterized by abundant reactivation surfaces is that the subordinate currents (Flood currents) were mostly too weak to erode and transport even a small quantity of sand. However occasionally they were strong enough to create some low angle reactivation surfaces (Mowbray & Visser, 1984; Boersma & Terwindt, 1981; Houthys & Gullentops, 1988).

The mud-clasts deposited on the large foresets are thought to have been produced from the break-up of thin mud drapes formed on the large foresets during periods of low sediment transport. The mud could be ripped up during strong ebb-tidal currents to form mud-clasts, and redepositing as intraformational conglomerates.

On the basis of numerous observations on partially exposed structures comprising large scale cross-strata the evolution of structure of the large scale foresets could be

organized in two stages: **stage A** beginning with the formation of small scale cross-strata (subfacies 1a), characterized by massive ungraded avalanching foresets with coarsening grains, and **stage B** late stage of growing of the larger fine to medium graded foresets (Fig. 2.34). Graded foresets have been attributed to avalanching of sediment previously sorted by smaller bed forms, superimposed on the stoss side of the large sand waves (Hooke, 1968; Smith, 1972).

Overtuned and convoluted foresets are attributed to the action of rapid sedimentation on inclined surfaces during the ebb-dominant tidal current which cause overloading that resulted in differential liquefaction and hydroplastic flowing of sediment (Allen & Banks, 1972; Reineck & Singh, 1973). Similar deformation structures have been reported from many shallow marine sandstones (Banks, 1973; Anderton, 1976; Johnson, 1977 and Swift *et al.*, 1987).

2.5.3 Facies 3: Down-foreset dipping cross-stratified sandstone

This facies comprises cross-strata (5 to 20 cm thick) which have bounding surfaces dipping in the direction of foreset dip. The bounding surfaces are convex-up and are often seen to form at the early stage of bar growth. The cross-strata can be traced up-current into the top-set facies (Subfacies 1a) and down current i.e. down the foresets, they break-down into single foreset beds (Plate 2.9). The foresets of the cross-strata are tangential to the base. The sandstones are generally medium-grained quartz arenite, moderately well sorted. This facies has been noticed in two localities throughout the Saq Sandstone. Unidirectional palaeocurrents are towards the northeast, and always in the direction of dip of the larger forests which they form.

Process interpretation

This facies is generated by the migration of bed-forms over the crest of the bar and down the bar lee face. The cross-strata can be traced down the foresets to a point where they lose their structure and avalanche down as a mass-flow. In order for these cross-

strata to retain their structure the crest region has to have a fairly low slope and may be a reactivation surface. Figure 2.35 illustrates the possible formation of this facies.

Low-angle reactivation surfaces could be formed either in unidirectional or bidirectional tidal currents.

Under steady uniform and unidirectional flow conditions bed forms interact with the flow producing local velocity fluctuations. Large bed-form have smaller megaripples superimposed on them. The small megaripples migrate faster than larger and, as they approach the crest of the larger one, their lee-side vortex starts to erode it. The resulting erosion surface (reactivation surface) is then rapidly buried by deposition of smaller size megaripples, migrating on top of it (McCabe & Jones, 1977; Mowbray & Visser, 1984).

Formation of reactivation surfaces in tidal regimes could be related to (1) unsteady flow (Boersma & Terwindt, 1981); (2) reworking of bedforms by reversed subordinate-strength currents (Klein, 1970) and (3) migration of superimposed bedforms (McCabe and Jones, 1977).

Asymmetrical tidal currents (ebb-dominant) were the main flows responsible for the unidirectional palaeocurrents of this facies.

2.5.4 Facies 4: Bottomsets

The large scale cross-stratified sandstone facies (Facies 2) grades laterally and downwards into bottomsets, which are tangential to the lower set boundary (Plate 2.10). Bottomsets are much thinner than the large foresets which immediately overlie them. They comprise relatively well sorted fine-grained quartz and sometimes mica-rich arenite which ranges in thickness from 5 to 40cm. They are generally plane-parallel laminated, with some co-flow rippled stratification.

This facies has been observed in a few intervals in the Middle Saq Sandstone where the processes which caused the accretion of the large foresets did not erode the surface over which the latter migrated, instead the surface is covered by relatively thick and gradational bottomsets. Bottomsets comprise less than 1% of the total sequence. The

rare occurrence of this facies could be due to the fact that in most cases the base of the large scale cross-stratified sandstone (Facies 2) is not exposed, being at the base of cliff sections and often covered with scree.

Process interpretation

The deposition of this facies may have occurred by the accretion of sediment on the lee slope of the large scale cross-stratified units (Facies 2), which had ceased to migrate by foreset avalanching. It represents fall-out from a density layer of suspended fine sand which flowed over the lee sand wave side.

The co-flow strata are produced by traction which remains in contact with the bed: there is no evidence for flow detachment in this instance. Flow detachment would result in back-flow strata which are not seen in the Saq Sandstone (Fig. 2.36). The general absence of back-flow cross-strata is not understood.

2.5.5 Facies 5: *Cruziana* facies

Beds belonging to this facies are mainly siltstone and fine-grained sandstone. They are often intensely covered by trace fossils (Plate 2.11) which show many phases of reworking of the sediment. This facies often occurs as a drape on the tops of bars. The beds may overlie the cross-strata of the top-sets (Subfacies 1a) or may directly overlie large foresets (Facies 2).

Process interpretation

This facies represents the abandonment of the bars and their subsequent covering by fine suspended sediment. Animal traces may then remain in the sediment without being destroyed by reworking. Abandonment may occur in at least 3 ways :

- (1) As result of strong ebb-dominated tidal currents bars may migrate away from the shore regions into deeper water where there may be less tidal influence and a more restricted supply of sand.

- (2) Bars may migrate laterally out of the path of a dominant tidal current so that they may therefore lie away from the main sand supply.
- (3) During a rapid transgression, bars which were active at the deepest edge of the zone of current activity may be abandoned as water depth increases and become moribund. In all these instances the fine sediment deposited from suspension will drape over the bar surfaces and form beds which not only contain more nutrients for the faunas but also provide ideal conditions for their preservation. It is possible that Trilobites lived amongst the active sand bars but preservation of their tracks was not likely in loose sand and in any case these would be destroyed by constant movement of the sand there.

2.5.6 Facies 6: Interbedded fine sandstone and siltstone

This facies is characterized by parallel laminated sandstone which laminae are defined by concentration of muscovite flakes and bedded siltstone. The interbedded sandstone is a fine to very fine-grained micaceous quartz arenite, well sorted and friable. Ripples and bioturbation are rarely observed in this facies. The lower part of this facies is characterized by lags of broken brachiopod shells (Plate 2.12).

Process interpretation

This facies was deposited in an environment deeper than the one represented by facies 8 and is characterized by fluctuations in the energy of the depositing current. The concentration of muscovite flakes possibly resulted from differential settling of quartz and mica from turbulent suspensions generated by passing waves (Clifton, 1981). The upper shoreface is the possible depositional environment for this facies.

This facies, along with the lags of broken shells, could represent the transition zone between the prograding beach deposit and the small offshore bars, but the erosion surfaces (see Clifton, 1981) which normally characterize this zone have not been recognized.

2.5.7 Facies 7: Planar to gently dipping stratified sandstone

This facies is characterized by planar to gently dipping stratified sandstones (Plate 2.13). It generally a fine to medium-grained quartz arenite. The planar laminations are defined by concentrations of heavy minerals bands, which are up to 0.4cm thick. In some beds the lamination clearly forms gently inclined beds, which show a consistent dip in an easterly direction. Nearly vertical burrows 0.5 cm diameter occur (Plate 2.14).

Process interpretation

This facies contains many features indicative of beach upper foreshore deposits (Clifton, 1975, 1981). Planar lamination gently dipping in a seawards direction is a classic characteristic of the upper foreshore (Thompson, 1937). The concentration of heavy minerals commonly occurs in the upper foreshore of modern beaches. The laminations are attributed to grain segregation under condition of plane bed sediment transport during swash-backwash flow (Clifton, 1969).

2.5.8 Facies 8: Large-scale high angle cross-stratified sandstone

This facies is characterized by high angle large scale cross-stratified sandstone up to 110 cm thick. This is a fine to medium grained quartz arenite, well sorted with some ripples on the top of the unit (Plate 2.15). Palaeocurrents are unidirectional towards the north (Parallel to the postulated shoreline).

Process interpretation

The large-scale high angle cross-stratified sandstone could be interpreted as the product of deposition of a shallow subtidal to low intertidal migrated bar (Clifton *et al.*, 1971). Similar large megaripples are formed on a macrotidal beach in Wales (Plate 16). The shore-parallel palaeocurrent may have been initiated by tidally induced longshore flow (Seymour, 1980; Wright, 1981).

2.5.9 Facies 9: Conglomerates and breccias

This facies comprises the coarser grain-size throughout the sequence. It has been subdivided into four subfacies: (1) Basal breccia (Subfacies 9a); (2) Fine conglomerate (Subfacies 9b); (3) Bioclastic conglomerate (Subfacies 9c) and (4) Basal breccia and conglomerate (Subfacies 9d).

2.5.9.1 Subfacies 9a: Basal Breccia

A thick breccia is exposed at the base of the section in locality K-26. It is up to 75 cm thick, has a sharp top and is composed of very angular clasts. Clasts are up to 12 cm in diameter, have no preferred orientation, and are very poorly sorted. The matrix is a poorly sorted fine to coarse-grained red sandstone (Plate 2.17).

Process interpretation

The basal breccia subfacies is interpreted as the patchy remnants of talus-slope deposits that accumulated adjacent to low hills. The high angularity, coarseness and poorly sorted character of the breccia indicate that the clasts were not transported any appreciable distance (Ware & Hiscot, 1985).

2.5.9.2 Subfacies 9b: Fine conglomerate

The fine conglomerate subfacies (Plate 2.18) is usually associated with bars (inter-bar areas) and/or with flat-bounded sand sheets (Subfacies 1c). It comprises a lag of rounded to well rounded quartz pebbles, up to 1cm diameter, and is moderately sorted.

Process interpretation

This subfacies may be the result of winnowing of sand from coarser material in situ, during periods of accelerated sheet-like erosion or reduced sand supply (Richards, 1986). Alternatively it may represent lags produced by traction-clogging in megaripple scour pits (Levell, 1980).

Similar lag deposits have been described and interpreted as the product of winnowing in a shallow marine setting (McCave, 1973; Brenner and Davies, 1973; Berg, 1975; Anderton, 1976; Spearing, 1976; Johnson, 1977; levell, 1980; Richards, 1986).

2.5.9.3 Subfacies 9c: Bioclastic conglomerate

The upper contact of the Saq Sandstone with the overlying Hanader Shale (Tabuk Formation) represents a regional unconformity, commonly marked by a relatively thick unit (up to 35 cm thick) of bioclastic conglomerate (Plate 2.19). This contains sandstone and quartz pebbles up to 2cm in diameter which are coated by iron cement. These clasts are thought to have been derived from a ferricrete palaeosol. Other clasts include angular fragments of debris of phosphatic shells. This subfacies contains some of the coarsest sediments in the Saq Sandstone and certainly the coarsest sediment in the Saq Sandstone above the basal breccia and conglomerate.

Process interpretation

The grain-size of this unit stands in great contrast to the grain-size of the surrounding sediments, all of which are fine to medium-grained sandstone. This coarse sediment is therefore seen as lag-sheet left after a considerable amount of reworking of the sediment. The iron oxide coatings on quartz clasts; and the abundance of iron oxide cemented sandstone clasts points to the presence of ferricrete (Palaeosol) in deposits being reworked by a transgressive sea. As ferricrete is of subaerial origin, the intensive reworking which has resulted in this conglomerate is thought to have taken place at the strand line. This is supported by the abundance of broken *Lingula* shells in the conglomerate, and the position of the conglomerate just above the supposed beach.

A probable explanation of this subfacies is given in figure 3.16 (Chapter 3).

2.5.9.4 Subfacies 9d: Basal breccia and conglomerate

The basal breccia and conglomerate subfacies occurs along the length of the Saq Sandstone outcrops, above the unconformity and ranges from 20 to 60cm in thickness. It is composed mainly of sub-angular to rounded quartz pebbles 2 to 8cm diameter (Plate 2.20).

Process interpretation

This subfacies was evidently the initial product of transgression of the Cambrian sea, left behind as the sea advanced over the Arabian Shield. Clasts too large to be significantly engaged in transport are concentrated on the erosional surface as the sea transgresses (Clifton, 1981). The composition suggests that the majority of the breccia must be derived from the immediately underlying Precambrian-Cambrian basement, but the well rounded conglomerate was from another source.

2.5.10 Facies 10: Flat-stratified red sandstone

This facies consists primarily of flat-stratified red sandstones with interbedded cross-stratified units (Plate 2.21). It can attain a thickness up to 110cm, which are laterally traceable for several meters. The upper and lower boundaries of this facies are sharp. The sandstone is a fine to medium-grained quartz arenite, moderately well sorted.

Process interpretation

There is no complete outcrop to assign the precise depositional system for this facies, but in association with subfacies 8a (basal breccia) it could be interpreted as having been deposited by sheet-floods, on an alluvial braidplain.

2.6 FACIES ASSOCIATIONS

The facies and subfacies which have been recognized in the Saq Sandstone and pre-Saq sediments (Idwah Formation) are grouped into six main Facies Associations (A to F)

on the basis of occurrence of the assemblages. These Facies Associations are: (1) Association A (Facies 2, 3, 4 and subfacies 1a); (2) Association B (Subfacies 1b, 9b and Facies 5); (3) Association C (Subfacies 1c and facies 5); (4) Association D (Facies 6, 7, 8 and subfacies 9c); (5) Association E (subfacies 9d); (6) Association F (Facies 10 and subfacies 9a) - (see Table 2.1).

2.6.1 Facies Association A (Bar areas)

This association comprises facies 2, 3, 4 and subfacies 1a which are combined to form a complete bar structure with subfacies 1a being the top-set; 2, the top-set grading down into the foresets (3) and 4 the bottomsets (Fig. 2.37). For reasons given in paragraph 2.3 these bars are considered to be of tidal origin and to range in thickness from 1.3 to 6.3 m high.

Numerous observations of the orientation of bar axes and palaeoflow pattern (NE) of the Lower, Middle and Upper Saq Sandstones, suggest that the bars were elongate parallel to the tidal current (Normal to the shoreline).

2.6.2 Facies Association B (Inter-bars)

This facies association occurs between facies association A (Fig. 2.37). It comprises subfacies 1b (Interbedded cross-stratified sand sheets and shale), 5 (*Cruziana*) and fine conglomerate (subfacies 9b). On large-scale outcrops rocks of this association can be found between major bars (Facies Association A). This facies association can be well seen at location K16 (Middle Saq Sandstone). The cross-strata sand sheets are thought to have been generated during periods where strong ebb tides migrated between the larger bar. These currents were sometimes so strong that they produced fine conglomerate lag sheets (9a) - or so weak to permit the development of mud with *Cruziana* (5)

2.6.3 Facies Association C (Inner Shelf)

Facies association C represents the transition zone between beach deposits (Facies association D) and offshore bar area (Facies association A). It consists of two subfacies (1) Sand sheet with flat boundaries (subfacies 1c) and (2) *Cruziana* (facies 5).

Sand sheets subfacies (1c) is thought to have been generated by migration of megaripples in response to strong asymmetrical tidal currents (Ebb), but in low areas surrounding sand sheets where tidal currents are weak, mud is deposited from suspension (5). In these area trilobites were able to feed on the muds.

2.6.4 Facies Association D (Shoreline)

This facies association predominates in the top part of the Saq Sandstone, immediately below the Hanader shale (Tabuk Formation) and represents the final marine-marginal beach progradation sequence. It has been divided into: (1) interbedded fine sandstone and siltstone deposited in upper shoreface (facies 6); (2) planar to gently dipping plane bedded sandstone, which were deposited on the beach upper foreshore (facies 7); (3) large scale high-angle cross-stratified sandstone (facies 8), which is the product of deposition of a shallow subtidal to low intertidal migrating bars; and Bioclastic conglomerate (subfacies 9c), which is product of ferricrete palaeosole reworked by marine processes (Fig. 2.37).

2.6.5 Facies Association E (Scree)

The facies association E is mostly occurs at the base of the Saq Sandstone sequence where it consists of a single subfacies (Basal breccia and conglomerate - 9d). It occur along the length of the Saq Sandstone outcrops, and represent the initial product of transgression of the Cambrian sea left behind as the sea advanced over the Arabian Shield (Fig. 2.37).

2.6.6 Facies Association F (Pre-Saq sediment)

This facies association is restricted to pre-Saq sediment and has been interpreted as the product of shallow braided rivers or sheet-wash, where it occurs as small patchy remnants as a result of reworking of Idwah Formation by Saq Sandstone Sea (Fig. 2.37). It comprises flat-stratified red sandstone (facies 10), and basal breccia (subfacies 9a).

2.7 Process of formation of tidal bars

Many studies of modern and ancient offshore sediments have developed a good understanding of the formation of offshore bars (Stride, 1963; Houbolt, 1968, 1982; MaCave, 1971; Stride & Chesterman, 1973; Freeman & Visser, 1975; Nio, 1976; Johnson, 1977; Hobday & Tankard, 1978; Banerjee, 1980; Levell, 1980; Fon, 1981; Hobson *et al.*, 1982; Boyles & Scott, 1982; Fruit & Elmore, 1988; Smith & Smith, 1988; Brenner & Martinseno, 1990).

There are three mechanisms to build up tidal sand bars that have been recognized in the Saq Sandstone: (1) overtaking, (2) stacking of sand wedges (3) scour and reactivation.

2.7.1 Overtaking mechanism

The bars commonly begin as a sheet of megaripples which, by overtaking each other, build up foresets that increase in thickness in the growth direction (Plate 2.22). Bluck, (1971, 1979) deduced this process in alluvial sediments and such a process is thought to be operating here.

In the initial stage of transgression and during the dominant current (tidal ebb) a small scale sand wave will be developed wherever there is a sufficient sand supply, water depth and currents capable of transporting bed sediments (Harris, 1988). By protracted transgression and/or increasing sand supply small megaripples will be superimposed on the stoss side of the small sand waves. The superimposed megaripples will migrate faster than the underlying small sand waves, until they reach the brinkline and then avalanche to feed the slip-face to create the larger bed form (Fig. 2.38).

The overtaking mechanism is thought to be the main process responsible for the evolution and growth of the majority of bars especially in the Middle Saq Sandstone, where the bar reach a maximum growth (*e.g.* bar at location K-16). The bar at location K-16 attained maximum thickness up to 7m and length up to 90m parallel to the palaeoflow. Grain-size decreases down-flow from medium to coarse-grained sandstone at the head of the bar to fine to medium-grained sandstone at the tail of the bar (Fig. 2.39).

2.7.2 Stacking of sand wedges mechanism

Wedge-shaped foresets are the result of a decrease in sediment supply down the foresets. Sheet of cross-stratified sandstone wedging out and thinning in the direction of the ebb-dominant tidal current create a steep slip-face where the next migrating bed form will be avalanching to form the large foresets of the bar (Plate 2.23). Wedges best form when the tip of the wedge (P) is fixed or migrates downstream at a small rate (Figs. 2.40 and 2.41).

2.7.3 Scour and reactivation mechanism

This mechanism is developed in three successive stages: (1) formation of sand sheets (2) scour and (3) reactivation.

In the first stage the bars begin as a field of sand sheets of different sizes which form by migration of straight crest megaripples in response to asymmetrical tidal currents. In the second stage the field of sand sheets stops developing and starts to scour by reversal of tidal flow (Flood). This occasionally modifies the slip face, eroding some previously deposited foresets and creating a low gently dipping erosion surface. The subsequent flow of the predominant current (ebb) in the third stage will builds large foresets over the erosion surface (Fig. 2.42).

Table 2.1 Facies and subfacies of the Saq Sandstone and pre-Saq sediment

FACIES	SUB-FACIES	TITLE
1		Small-Medium scale grouped cross-stratified sandstone
	1a	Sand sheets with Inclined boundaries
	1b	Interbedded cross-stratified sandstone and shale
	1c	Sand sheets with Flat boundaries
2		Large scale heterogenous cross-stratified sandstone
3		Down-foresets dipping cross-stratified sandstone
4		Bottomsets
5		<i>Cruziana</i>
6		Interbedded fine sandstone and siltstone
7		Planar to gently dipping stratified sandstone
8		Large scale high angle cross-stratified sandstone
9		Conglomerates & Breccias
	9a	Basal breccia
	9b	Fine conglomerate
	9c	Bioclastic conglomerate
	9d	Breccia and conglomerate
10		Flat-stratified red sandstone
FACIES ASSOCIATION A (Bar areas)		1a+2+3+4
FACIES ASSOCIATION B (Inter-bars)		1b+5+9b
FACIES ASSOCIATION C (Inner-shelf)		1c+5
FACIES ASSOCIATION D (Shoreline)		6+7+8+9c
FACIES ASSOCIATION E (Scree)		9d
FACIES ASSOCIATION F (Pre-Saq sediment; Fluvial)		9a+10

Table 2.2 Statistical parameters of palaeocurrent data of subfacies 1a

Location	n	$\Theta(^{\circ})$	R	L(%)	SD	V
K1	23	74	21.29	92.59	22.04	486.03
K2	7	15	4	100	0	0
K3	21	102 30	19.26	91.73	23.29	542.5
K4	15	29 30	13.97	93.15	21.21	450.1
K5	14	121 22	4.57	32.68	66.48	4420
K6	9	84 53	8.73	96.98	14.08	198.47
K7	10	27 16	9.411	94.11	19.66	386.63
K13	24	91 30	18.93	78.92	37.21	1384.5
K14	15	48 41	13.45	89.71	25.99	675.77
K17	11	38 58	9.52	86.52	29.75	885.29
K18	16	31 22	13.71	85.73	30.61	937.1
K19	7	45	5.46	78.06	37.95	1440.59
k20	9	32 13	8.44	93.79	20.19	407.78
k21	8	45	7.73	96.65	14.82	219.91
k25	9	27 46	8.44	93.79	20.19	407.87
k28	30	62 59	25.79	85.96	30.36	922.04
k29	15	62 56	12.43	82.89	33.51	1122.85
k30	7	49 9	6.88	98.35	10.42	108.61
k31	25	64 10	23.95	95.81	16.58	275.03
k36	19	54 11	17.92	94.35	19.25	370.87
k37	18	69 48	16.59	92.19	22.64	512.76
k38	8	52 37	7.53	94.13	19.62	385.08
k39	18	60 27	14.86	82.60	33.79	1142.3
k40	13	21 21	11.13	85.61	30.72	944.14
k41	9	60	7.21	80.10	36.13	1305.9
k42	7	36 33	6.80	97.22	13.49	182.03
k43	11	55 36	10.13	92.16	22.69	514.91
k44	11	61 2	10.36	94.25	19.42	377.16
k45	7	47.20	6.61	94.53	18.95	359.23

n=number of readings ; Θ =vector mean ; R=the magnitude or length of the resultant vector; L=the magnitude or length of the resultant vector in terms of per cent; SD=st.deviation; V= Variance

Table 2.3 Statistical data of cross-strata thickness of subfacies 1b.

Location	n	\bar{x} (Cm.)	SD	V
K41	13	28.08	12.63	159.76
K42	13	25.76	9.97	99.41
K31	12	29.16	12.55	157.63
K38	20	37.50	18.13	328.75
K18	23	37.60	14.80	219.28
K17	9	37.22	7.85	61.72
K19	18	30.00	15.72	247.22
K14	11	28.63	17.72	314.04
K13	14	40.71	20.25	410.2
K15	16	40.00	18.02	325.00
K20	17	26.17	11.31	128.02
K5	13	29.61	14.99	224.85

n=number of readings; \bar{x} =average; SD=standard deviation;
v=variance

Table 2.4 Statistical parameters of palaeocurrent data of subfacies 1b

Location	n	$\Theta(^{\circ})$	R	L(%)	SD	V
K1	18	57.59	16.17	89.84	25.82	666.80
K5	11	50.36	10.24	93.13	21.22	450.59
K18	8	72.2	7.10	88.84	27.06	732.47
K13	17	49.5	14.57	85.75	30.58	935.23
K14	17	46.25	14.76	86.84	29.39	864.00
K15	27	77.38	24.65	91.29	23.9	571.31
K17	21	48.34	18.19	86.64	29.61	876.78
K19	20	37.19	17.72	88.60	27.35	748.20
K20	19	47.11	16.57	87.23	28.95	838.21
K31	16	73.55	14.19	88.74	27.18	739.17
K38	15	61.3	13.97	93.15	21.19	449.24
K41	8	49.9	6.88	86.05	30.26	915.73
K42	8	38.10	7.28	91.04	24.24	587.85

n=number of readings; Θ =vector mean; R=the magnitude or length of the resultant vector; L=the magnitude or length of the resultant vector in terms of per cent; SD=St.Deviation; V= Variance

Table 2.5 Statistical data of cross-strata thickness of subfacies 1c.

Location	n	\bar{x} (Cm.)	SD	V
K25	16	23.12	7.26	52.73
K39	10	42.00	7.81	60.99
K45	14	32.14	6.99	48.97
K44	7	43.57	6.38	40.81
K43	9	39.44	6.849	46.91
K37	11	38.63	7.71	59.50
K6	15	31.00	8.00	64.00
K7	13	33.46	5.32	28.40
K4	23	32.82	6.56	43.10
K2	28	28.92	8.99	80.99

n=number of readings; \bar{x} =average ; SD=standard deviation ;
v=variance

Table 2.6 Statistical parameters of palaeocurrent data of subfacies 1c

Location	n	Θ (°)	R	L(%)	SD	V
K2	16	15	15.19	94.97	18.16	329.85
K4	18	36.47	17.50	97.27	13.37	178.90
K6	9	25.12	8.46	94.04	19.77	390.94
K7	10	33.4	9.67	96.73	14.64	214.61
K25	9	64.29	7.49	83.24	33.17	1100.38
K37	25	50.55	24.19	96.76	14.56	212.27
K39	16	60.00	15.45	96.59	14.95	223.71
K43	7	23.15	6.02	86.09	30.21	912.91
K44	9	65.6	7.94	88.31	27.69	767.16
K45	8	52.37	7.53	94.13	19.62	385.08

n=number of readings ; Θ =vector mean; R=the magnitude or length of the resultant vector; L=the magnitude or length of the resultant vector in terms of per cent; SD=St.Deviation; V= Variance

Table 2.7 Statistical parameters of palaeocurrent data of facies 2

Location	n	Θ (°)	R	L(%)	SD	V
K21	14	27 59	12.75	91.10	24.16	584.15
K31	39	77 09	36.24	92.94	21.52	463.26
K23	25	87 2	23.39	93.58	20.51	421.01
K25	6	39 53	5.62	93.67	20.38	415.42
K29	26	48 16	21.56	82.92	33.47	1120.82
K30	27	56 39	22.25	82.42	33.97	1154.10
K41	15	29 12	13.71	91.42	23.72	563.00
K42	18	40 36	16.11	89.49	26.26	689.62
K40	12	72.24	11.07	92.23	22.51	506.93
K1	22	58 54	19.83	90.10	25.39	644.69
K6	22	85 49	21.30	96.85	14.38	206.80
K13	14	53 26	13.61	97.22	13.49	182.03
K14	28	67 29	24.73	88.35	27.65	764.61
K15	7	53 47	6.54	93.44	20.79	430.52
K17	13	38 24	11.90	91.60	23.47	551.14
K18	17	33 05	15.66	92.16	22.68	514.77
K19	9	14 59	8.19	91.06	24.21	586.41
K28	25	52 26	21.11	84.42	31.97	1022.71
K36	25	54 35	25.99	95.98	16.23	263.67
K37	16	71 14	15.22	95.18	17.78	316.37
K38	16	54 25	15.26	95.42	17.32	300.27
K39	22	47 4	20.95	95.23	17.68	312.73
K43	13	39 46	10.97	84.41	31.98	1023.29
K44	13	53.35	11.59	89.18	26.64	709.99
K45	14	47 14	12.80	91.45	23.68	560.89
K20	25	31	22.59	90.39	25.11	630.63
K2	14	23 47	13.08	93.44	20.75	430.52
K3	58	85 39	44.14	76.12	39.61	1568.5
K4	15	6 58	14.33	95.57	17.04	290.48
K5	14	36 24	11.59	82.81	33.58	1128.25
K7	48	33 28	44.89	93.53	20.61	424.79

n=number of readings ; Θ =vector mean; R=the magnitude or length of the resultant vector; L=the magnitude or length of the resultant vector in terms of per cent; SD=St.Deviation; V= Variance

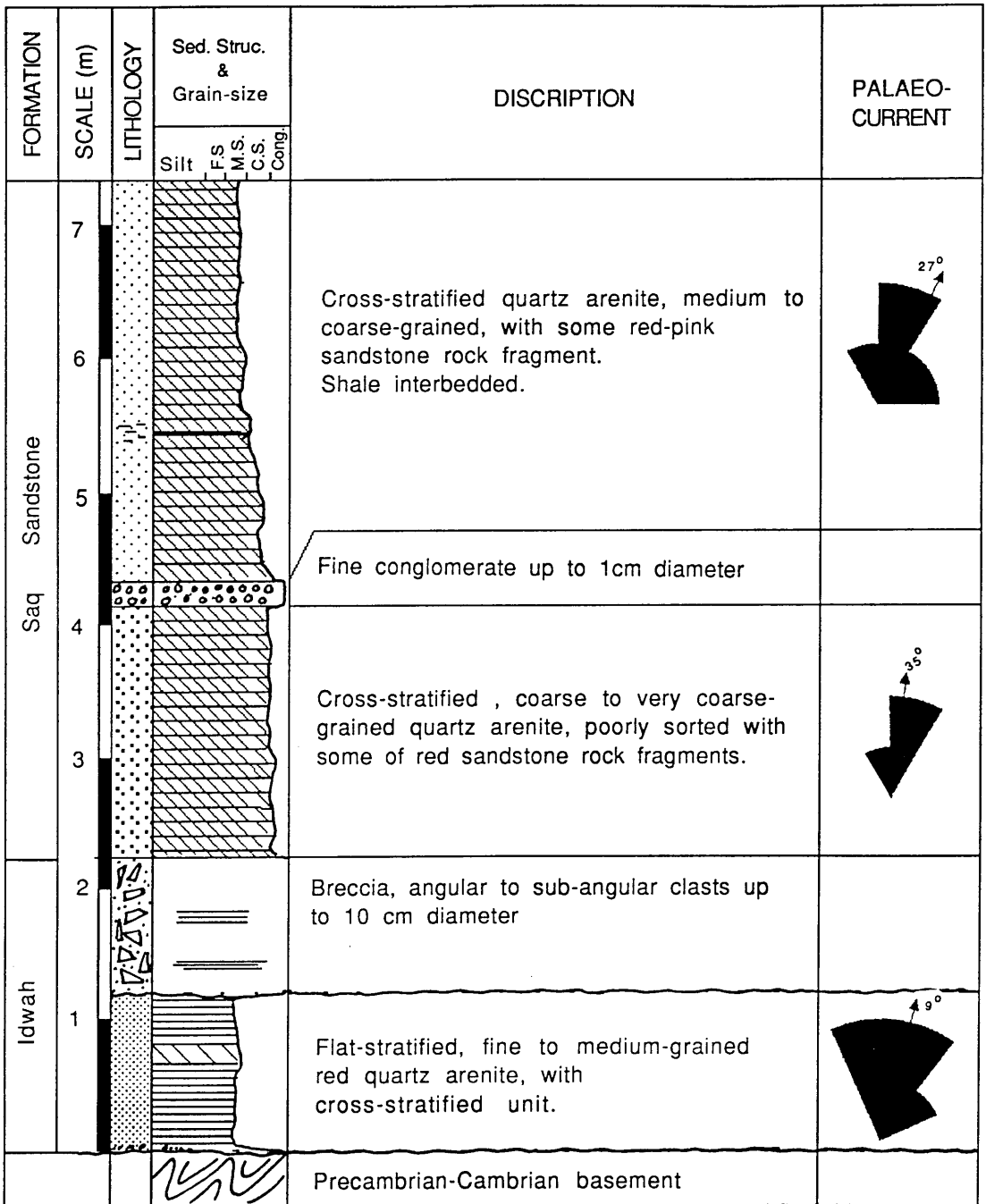


Fig. 2.1 Columnar section of pre-Saq sediment and basal Saq Sandstone (Location K-26).

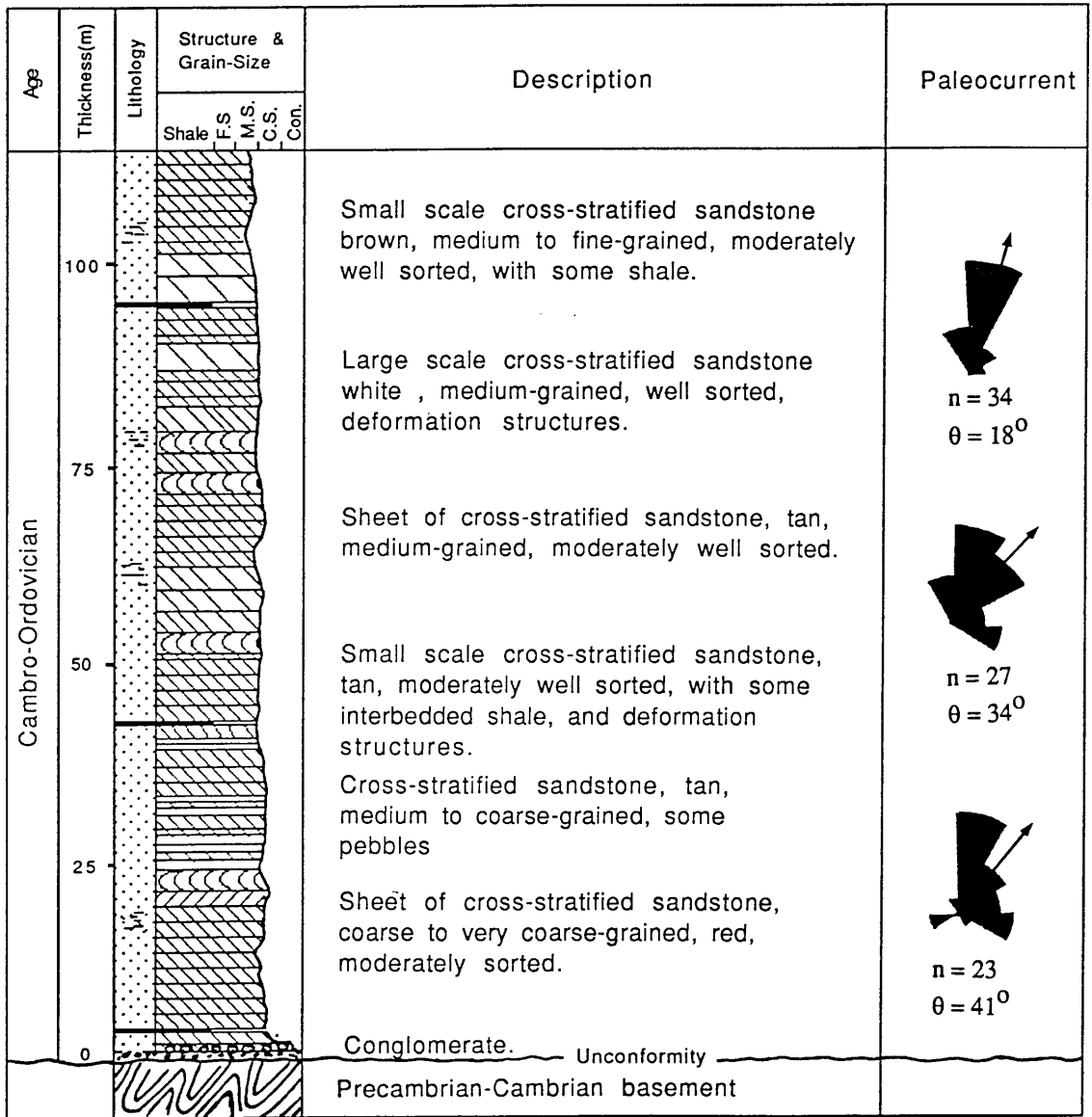


Fig. 2.2 Generalized columnar stratigraphic section of Lower Saq Sandstone.

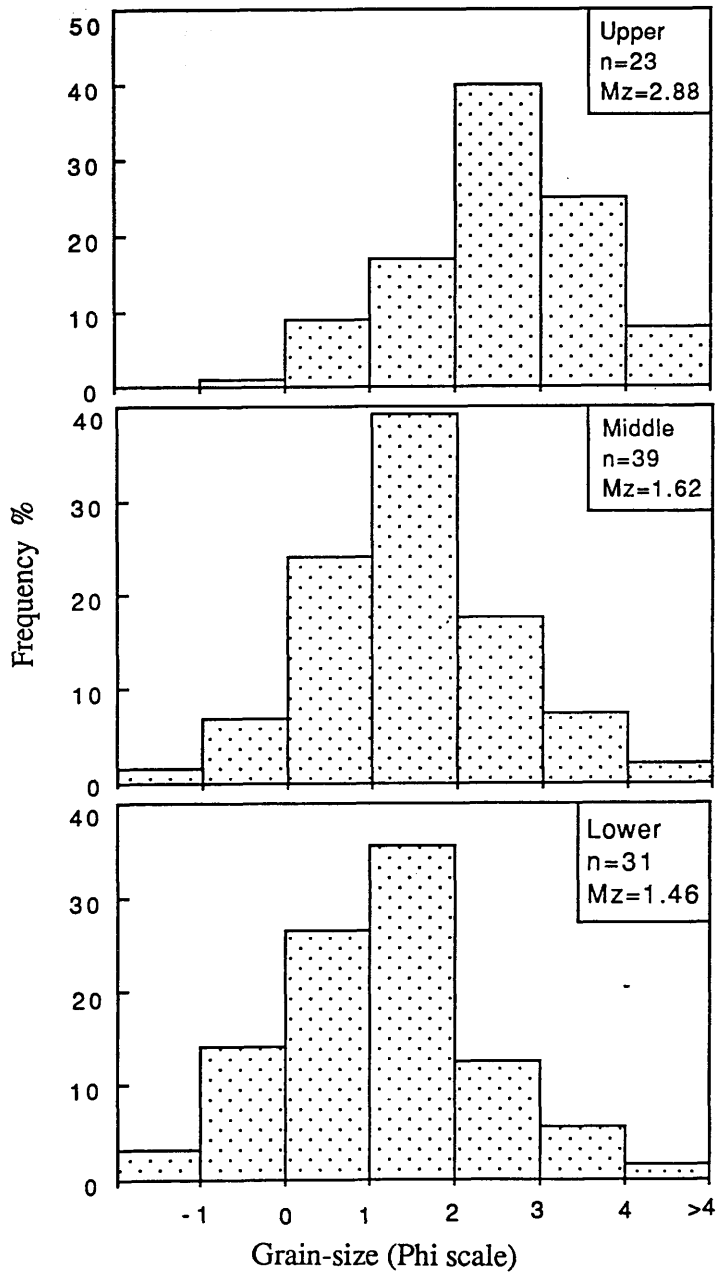


Fig. 2.3 Distribution of average of grain-size of the Saq Sandstones.

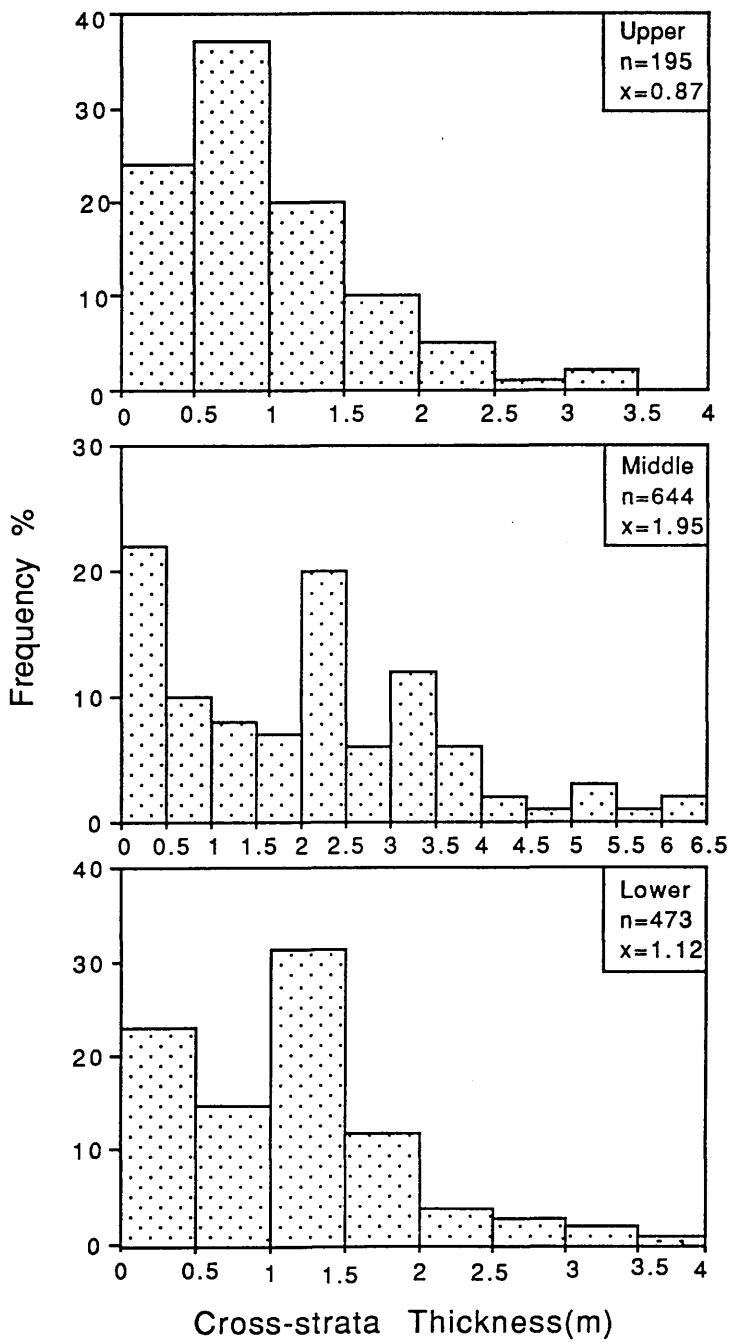


Fig. 2.4 Distribution of cross-strata thickness of the Saq Sandstones.

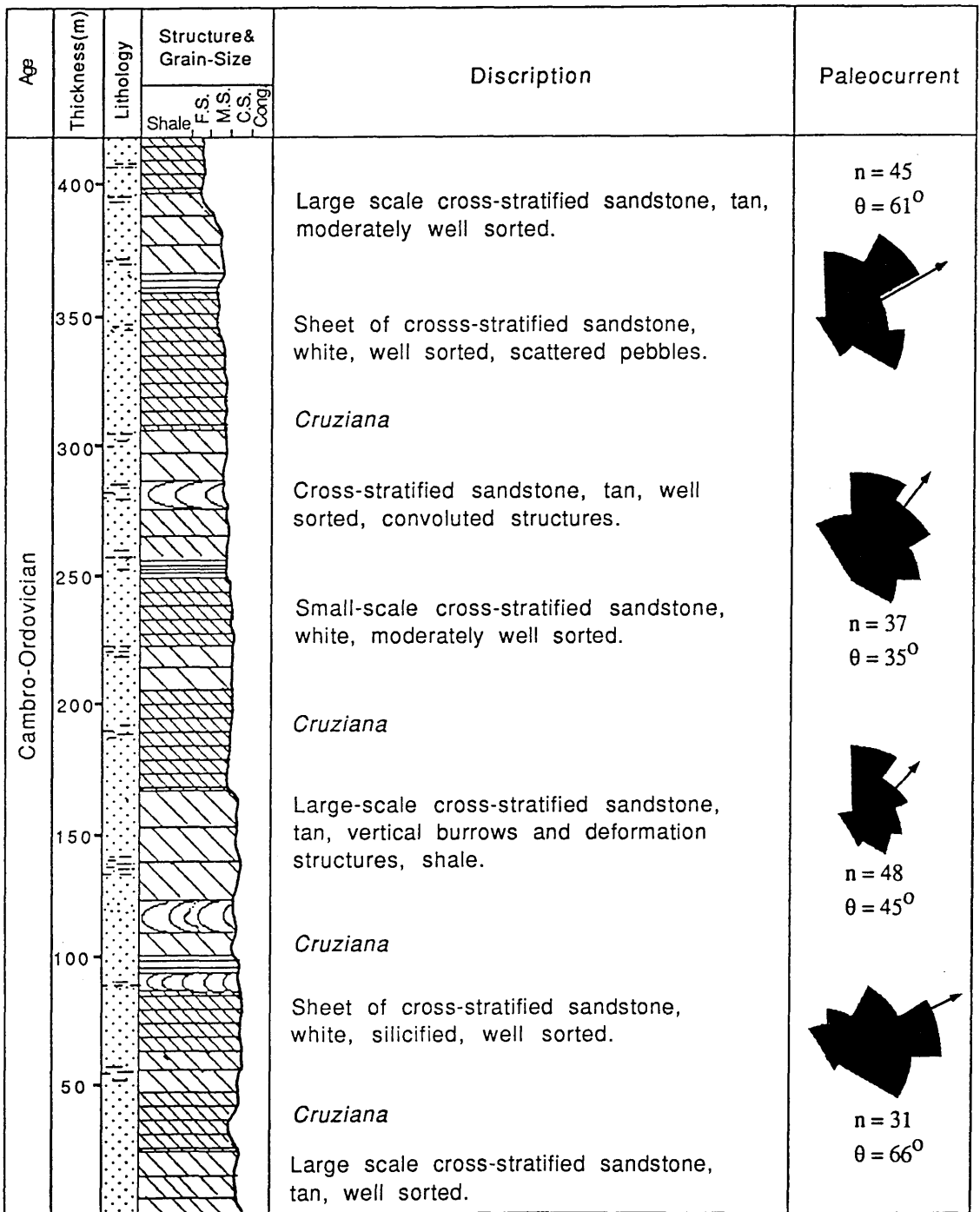


Fig. 2.5 Generalized columnar stratigraphic section of Middle Saq Sandstone.

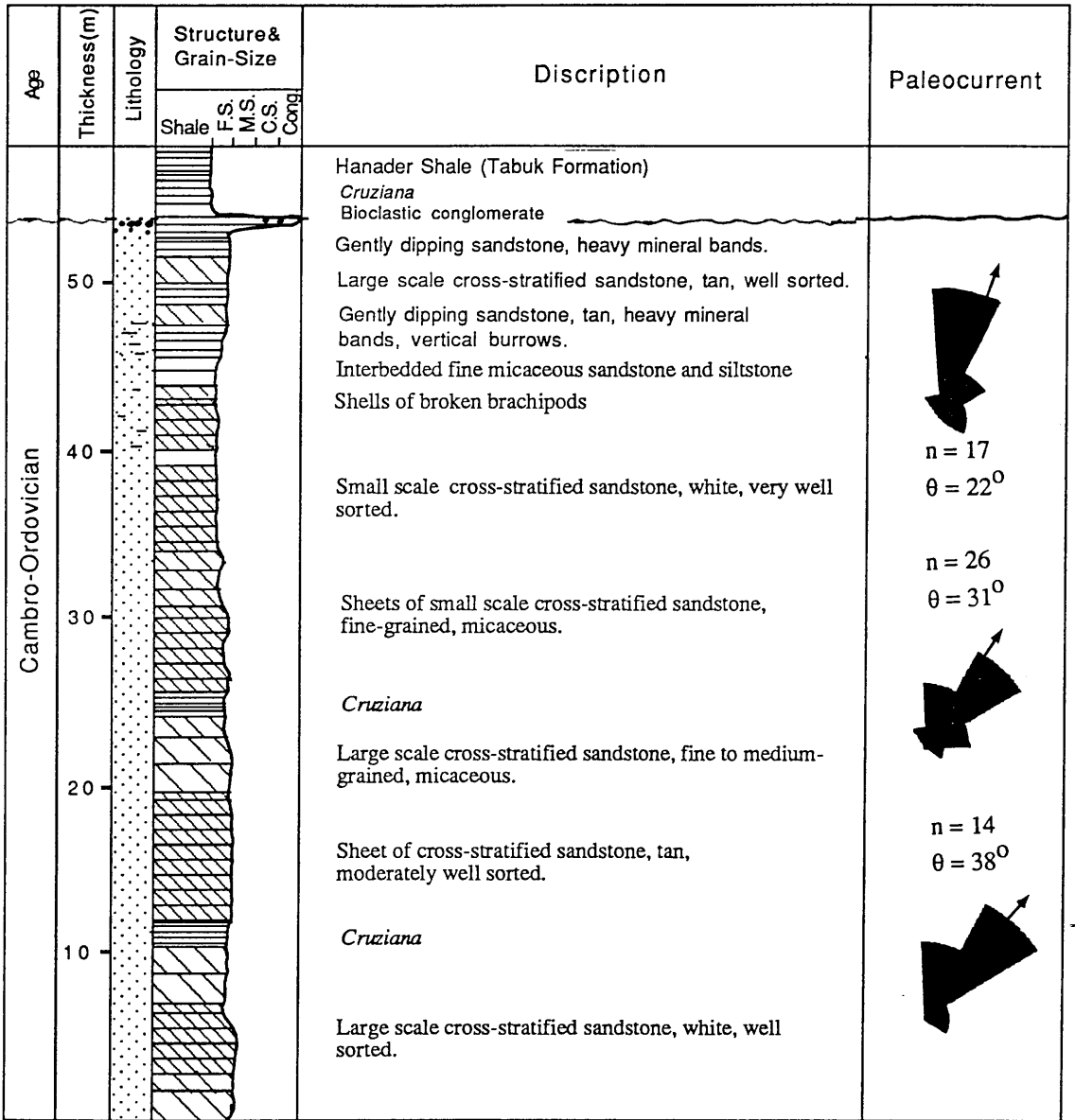


Fig. 2.6 Generalized columnar stratigraphic section of Upper Saq Sandstone.

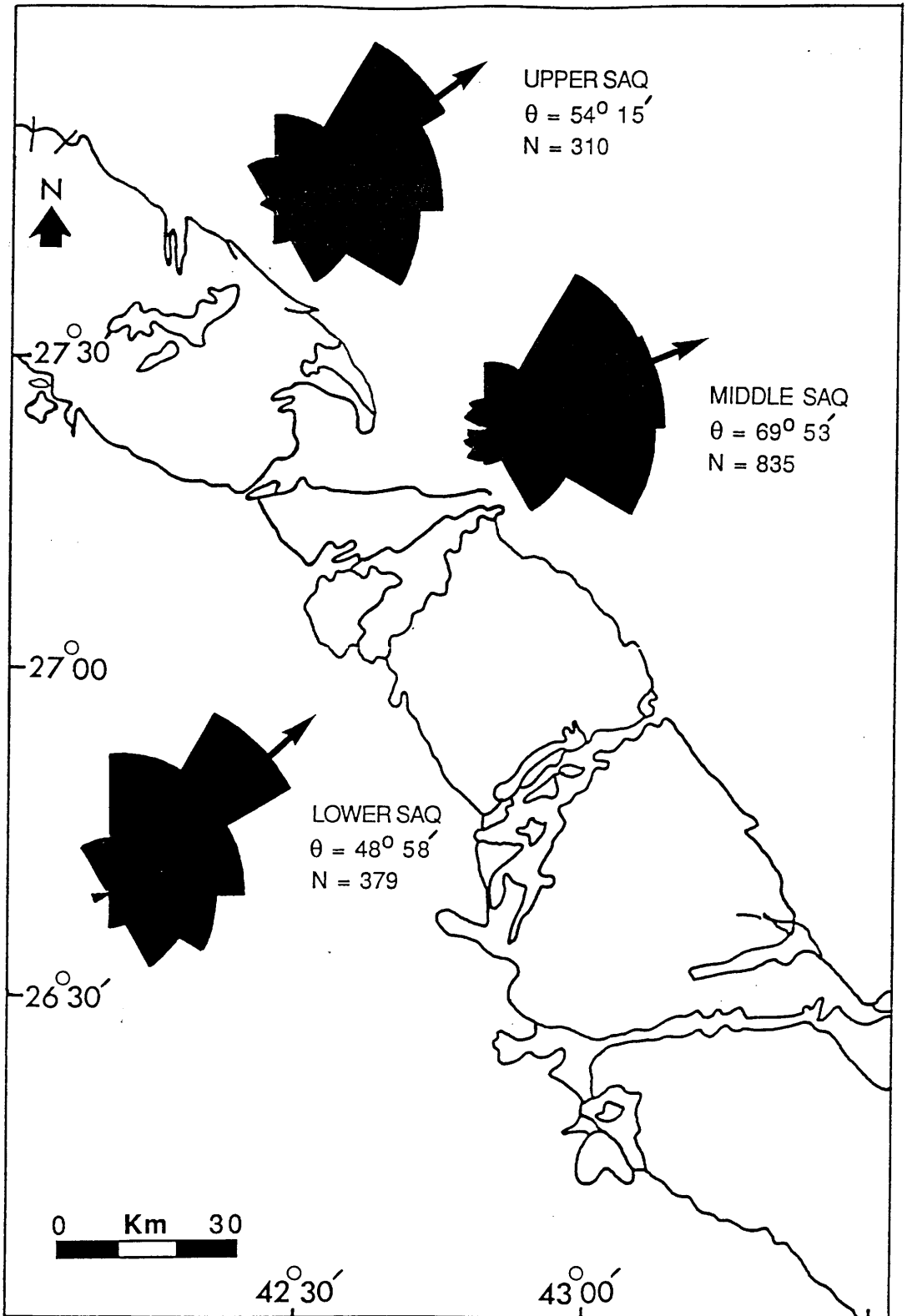


Fig. 2.7 Palaeocurrent directions of the Saq Sandstones.

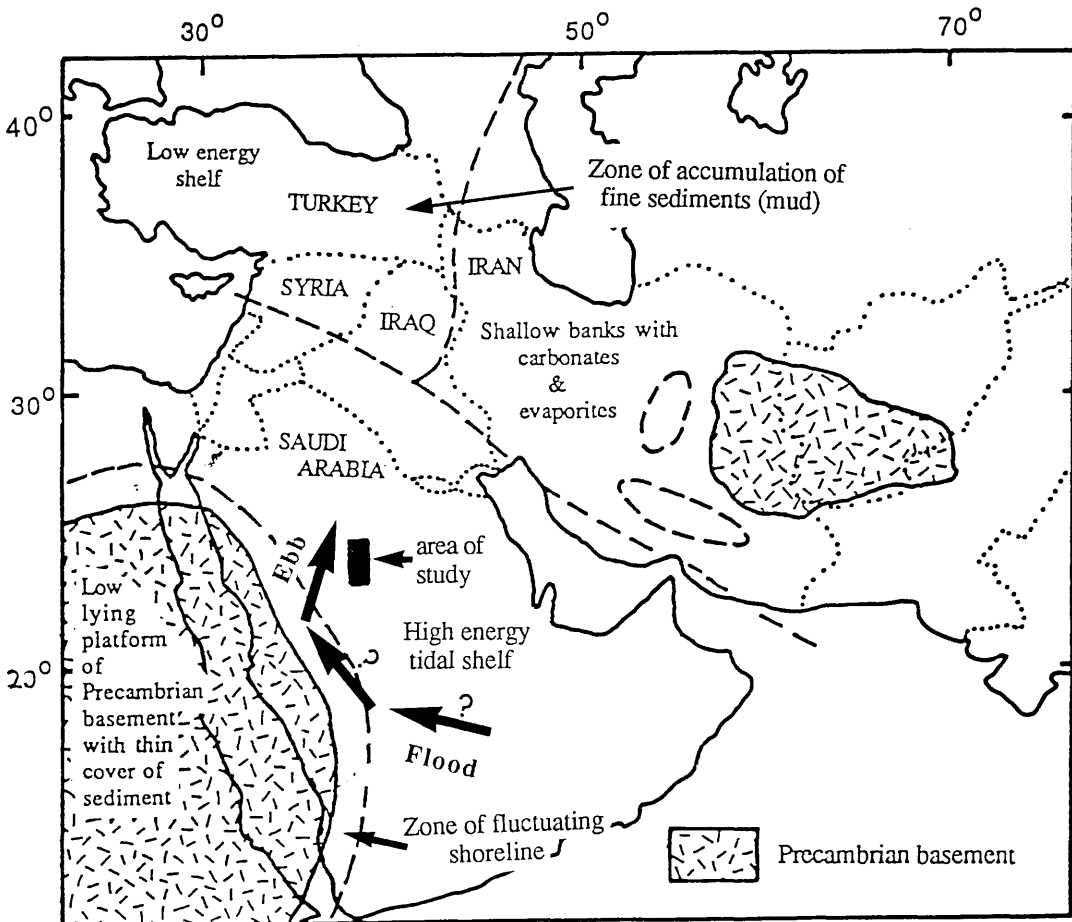


Fig. 2.8 Circulation of tidal current of the Cambro-Ordovician Saq Sandstone Basin and zone of accumulation of fine sediments (adapted and modified from Wolfart, 1981).

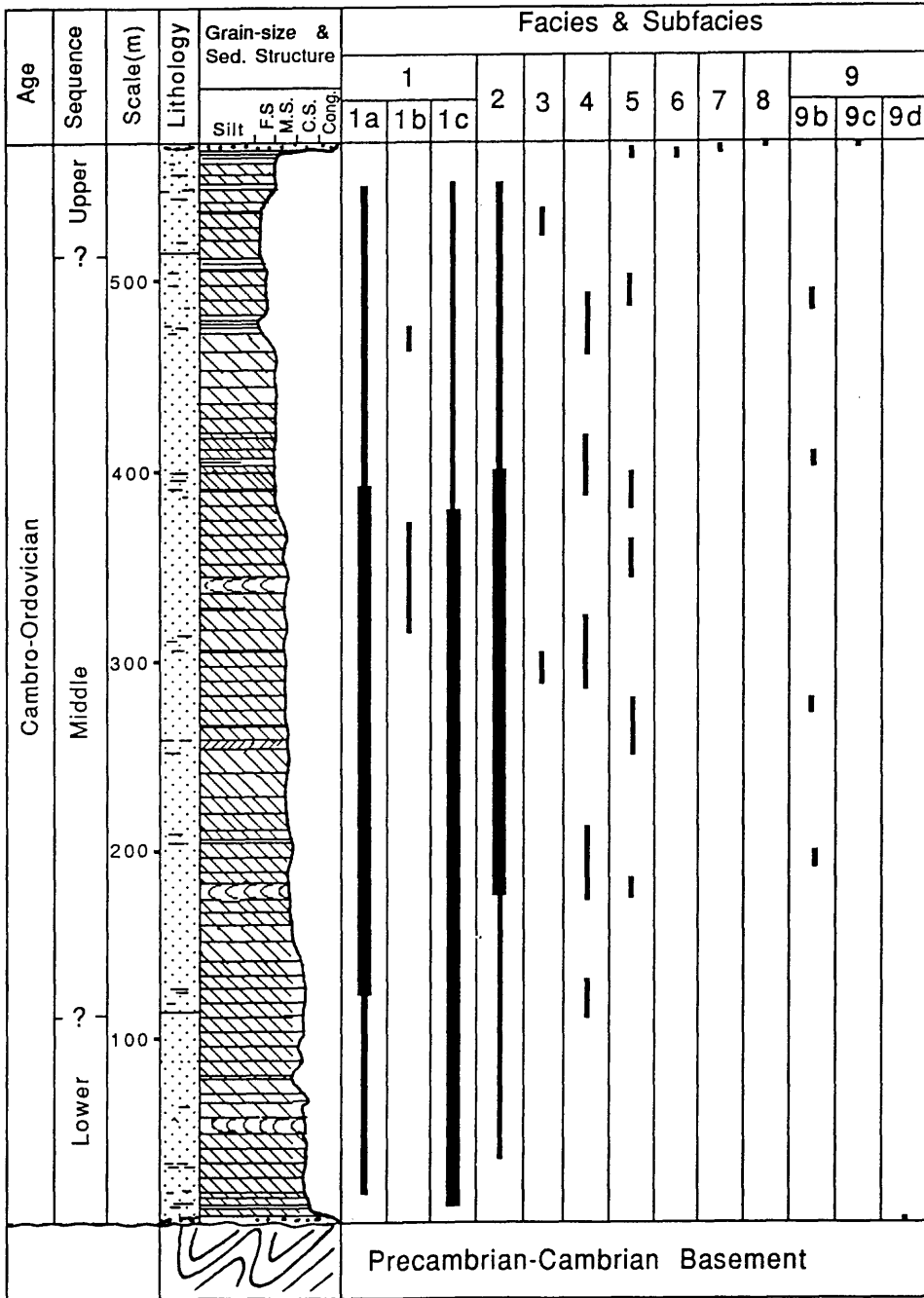


Fig. 2.9 Facies and subfacies distribution of the Saq Sandstones.

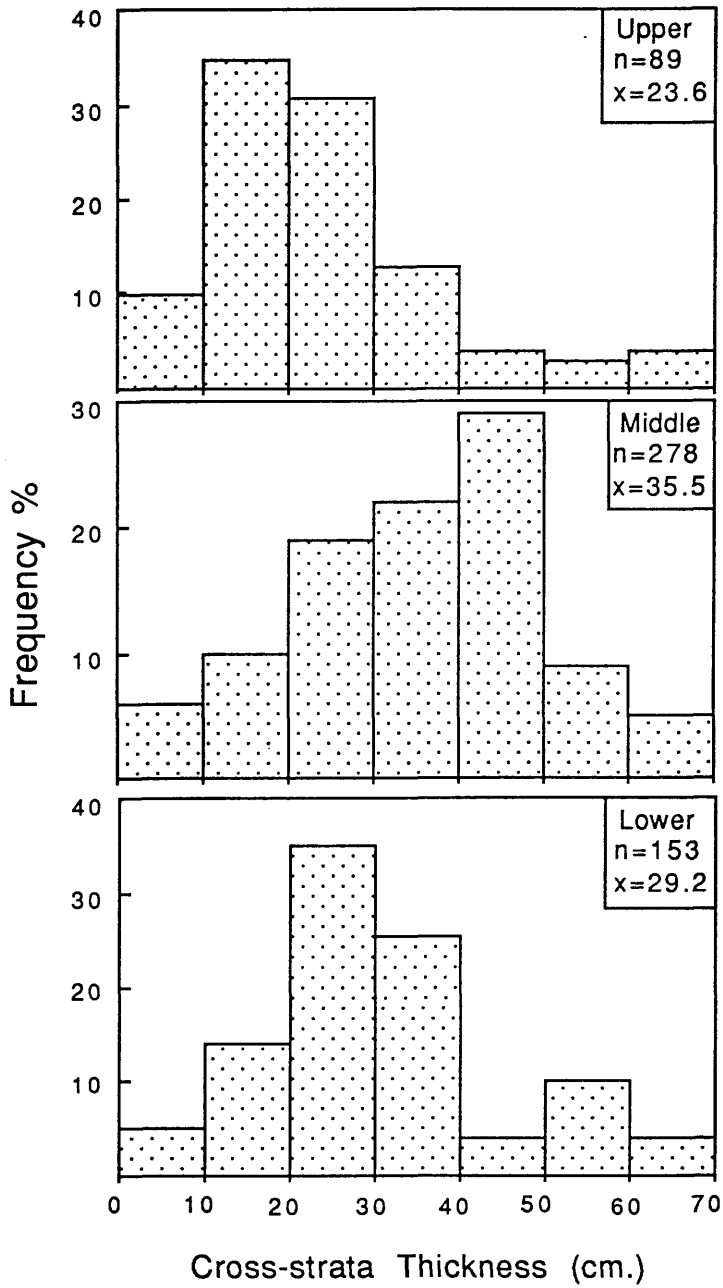


Fig. 2.10 Distribution of cross-strata thickness of subfacies 1a.

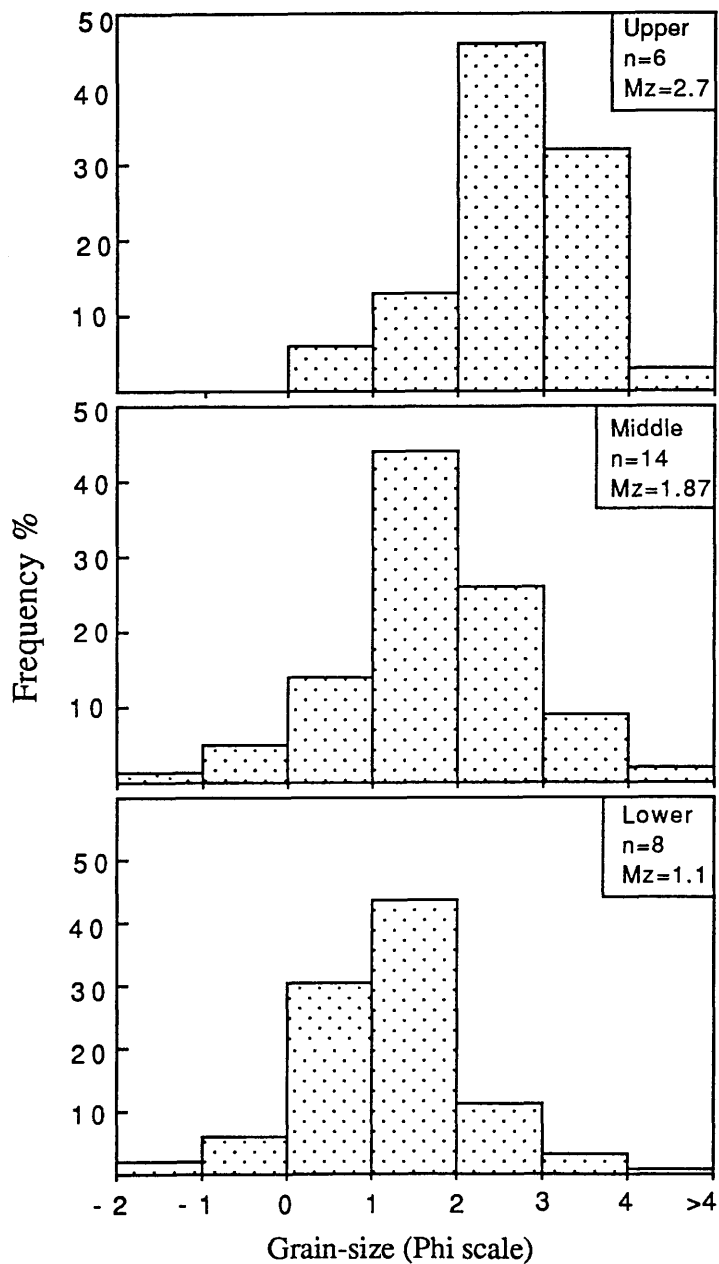


Fig. 2.11 Distribution of average grain-size of subfacies 1a.

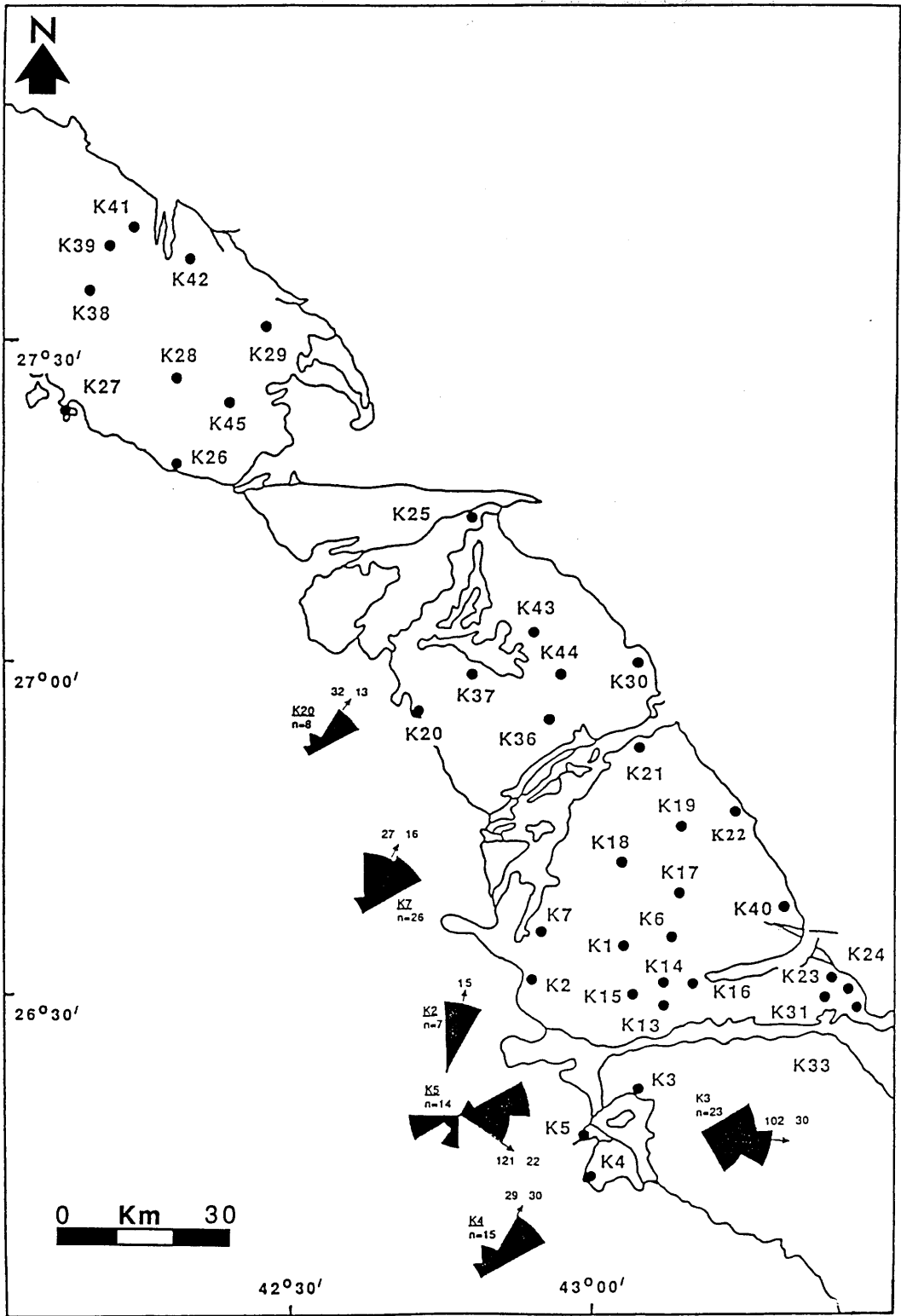
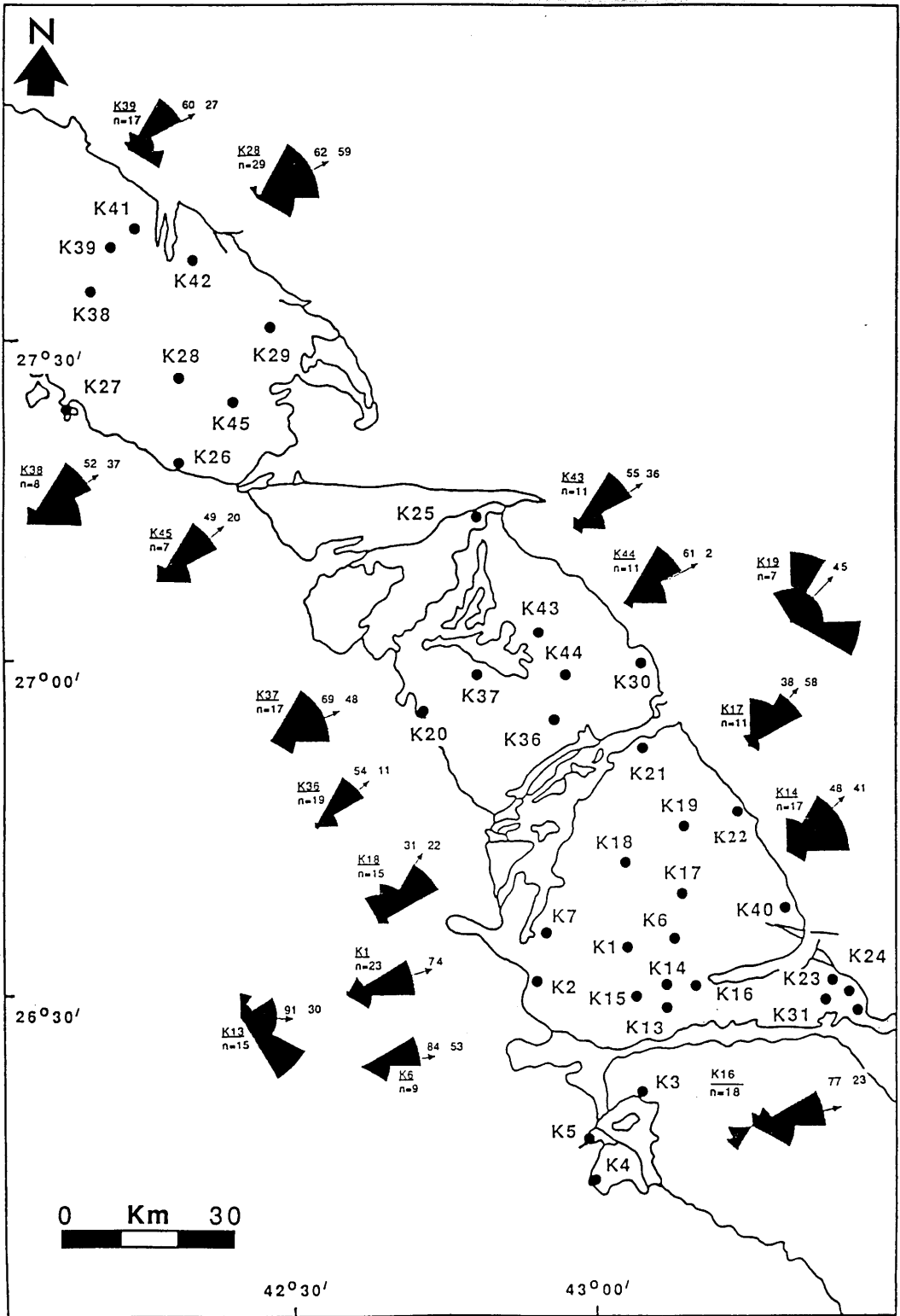


Fig. 2.12 Palaeocurrent directions of subfacies 1a of the Lower Saq Sandstone.



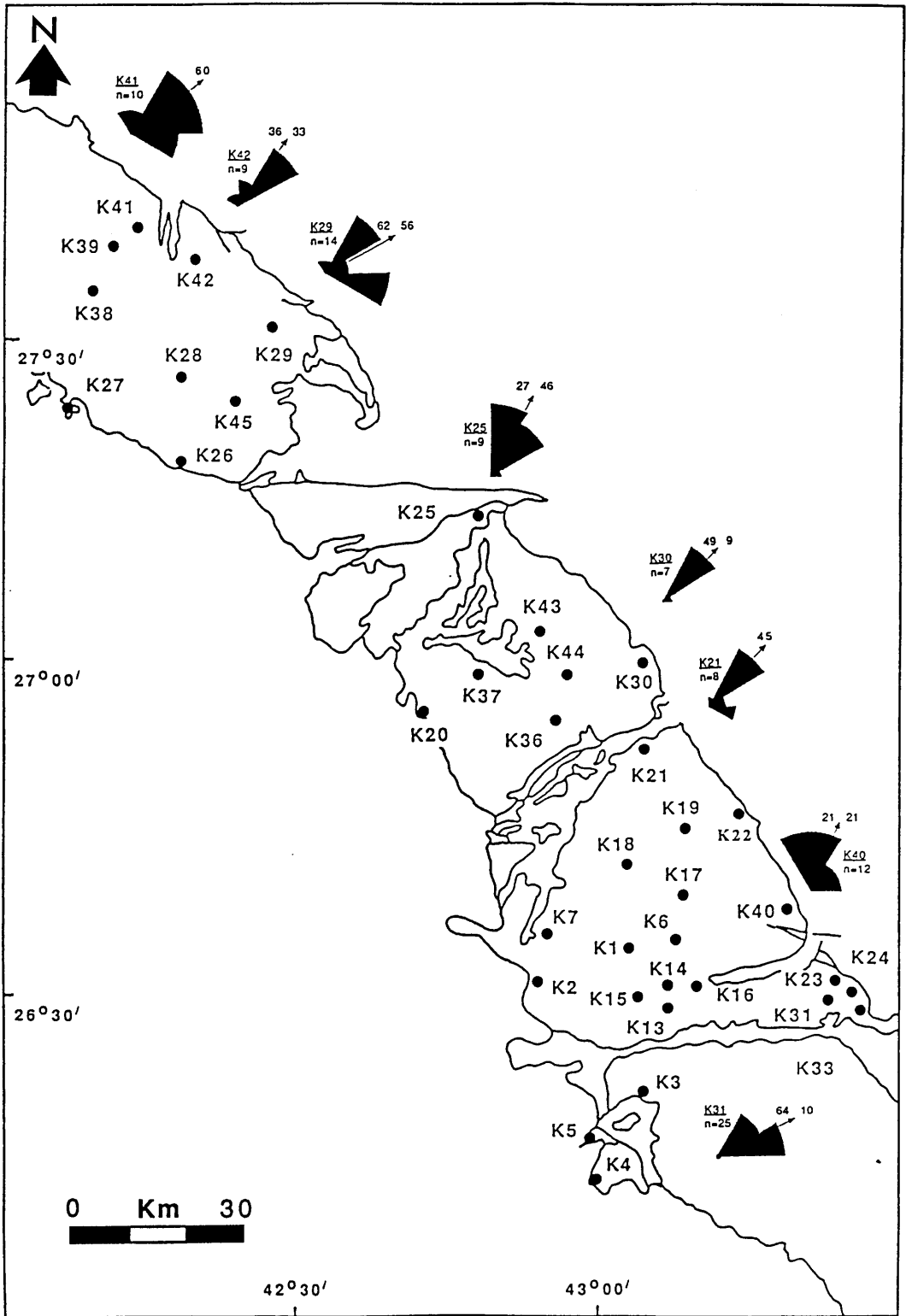


Fig. 2.14 Palaeocurrent directions of subfacies 1a of the Upper Saq Sandstone.

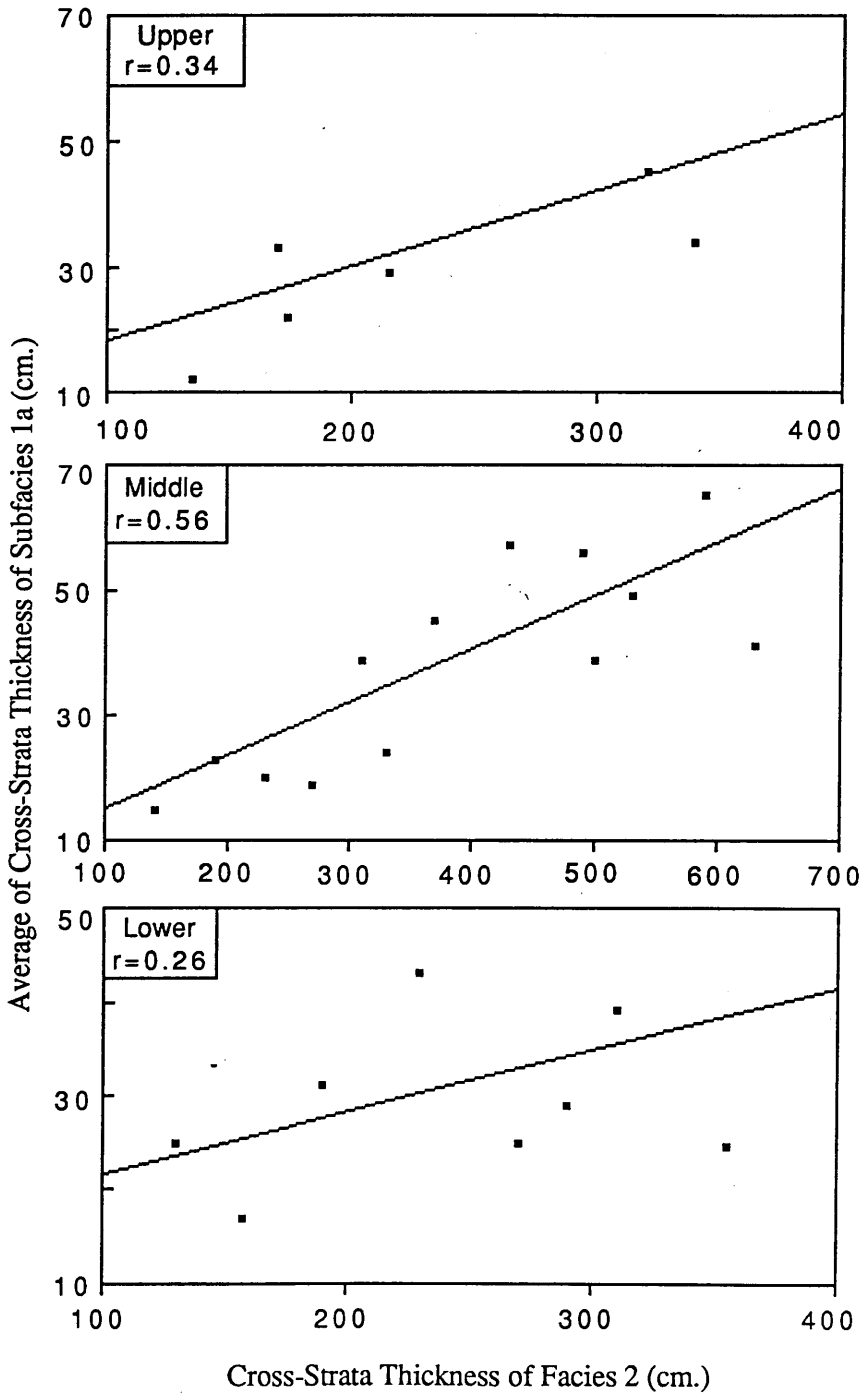


Fig. 2.15 Relationship between thickness of large scale cross-strata (Facies 2) and average thickness of sand sheets with inclined boundaries (Subfacies 1a).

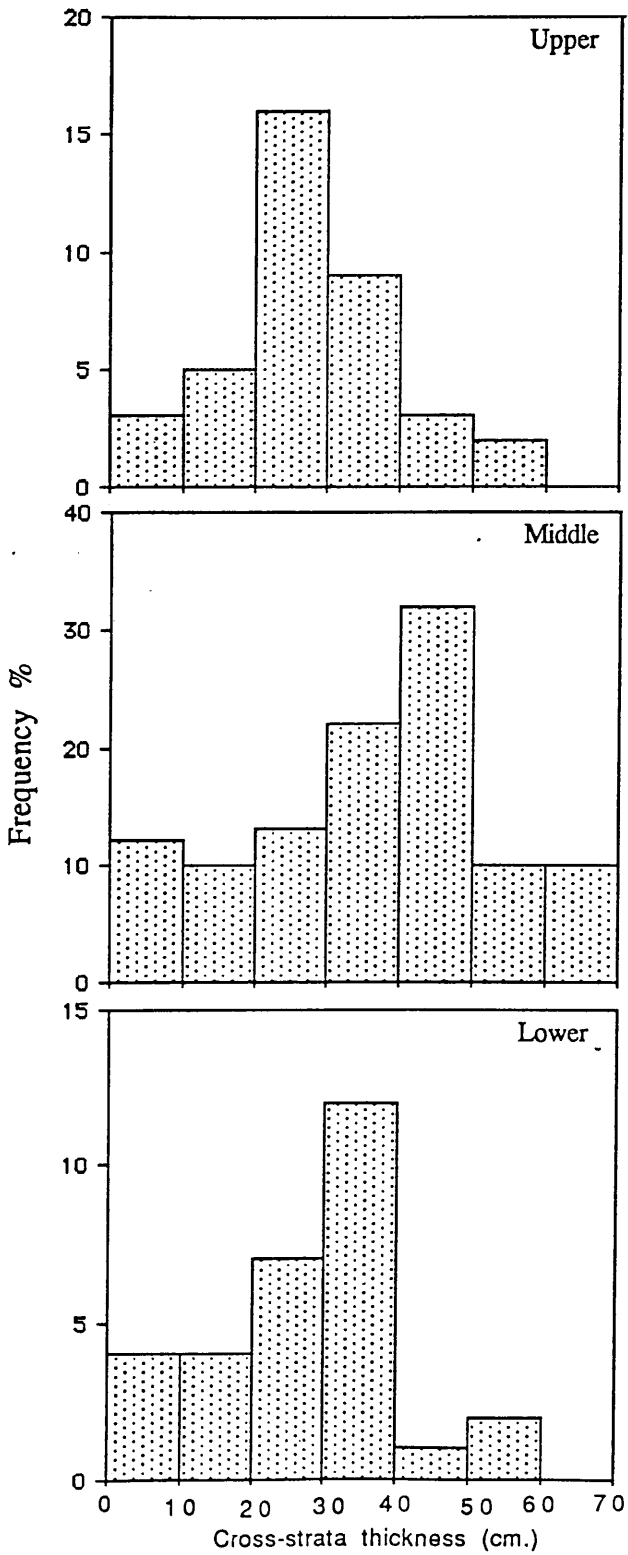


Fig. 2.16 Distribution of cross-strata thickness of subfacies 1b.

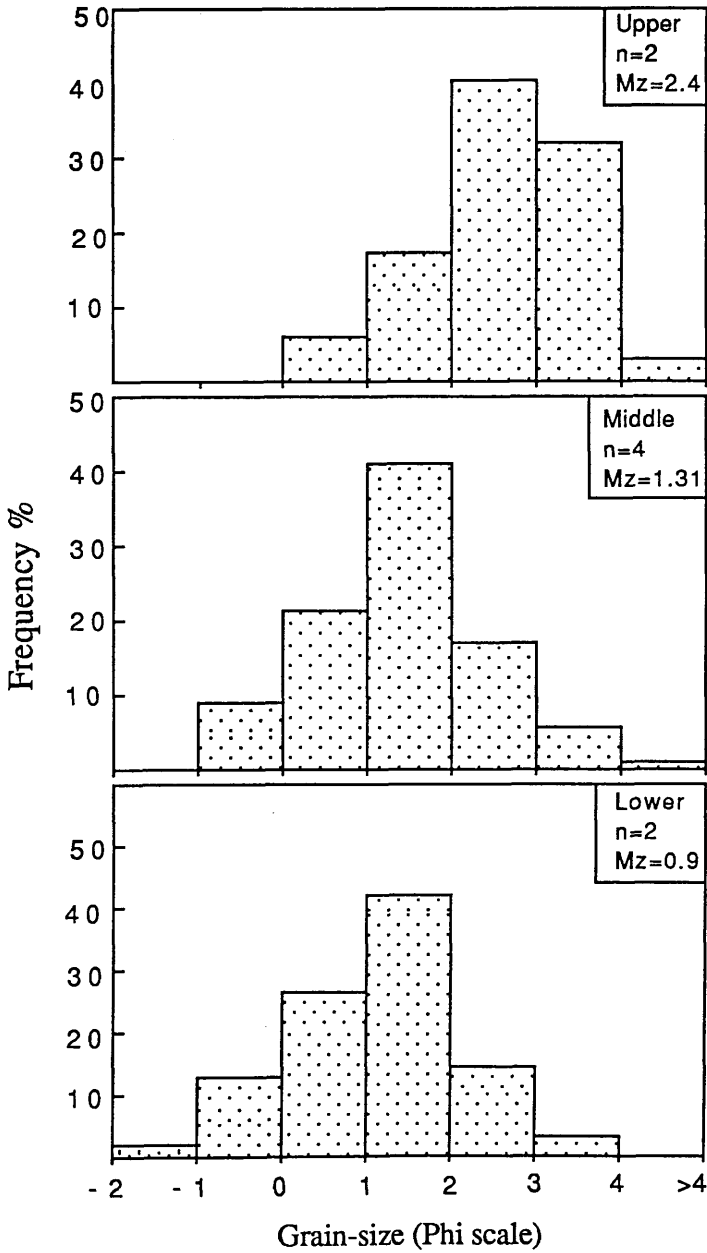


Fig. 2.17 Distribution of average grain-size of subfacies 1b.

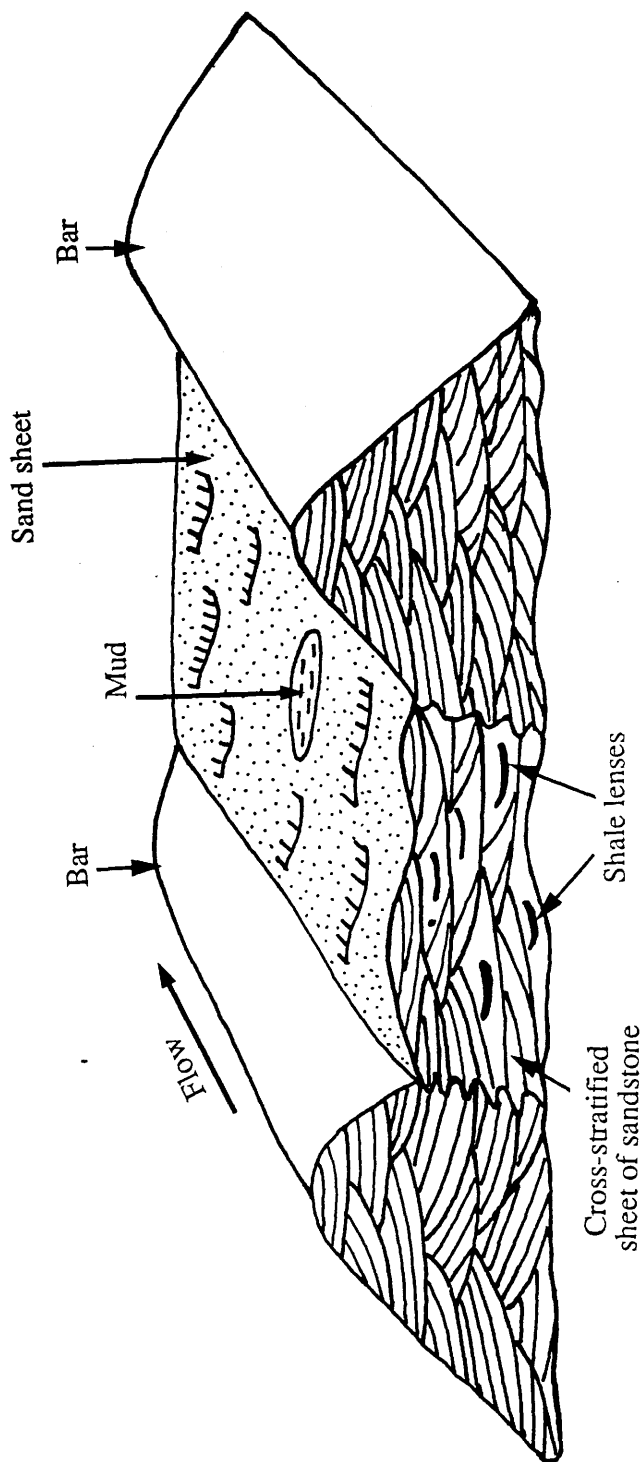


Fig. 2.18 Diagrammatic model showing the depositional environment of interbedded cross-stratified sandstone forming longitudinal sand waves and shale (Subfacies 1b). Here we have a fairly active current system between the sand bars, but there are times when the current activity is low- but the whole regime is active. The short periods of low current activity produces small areas of shale (mud).

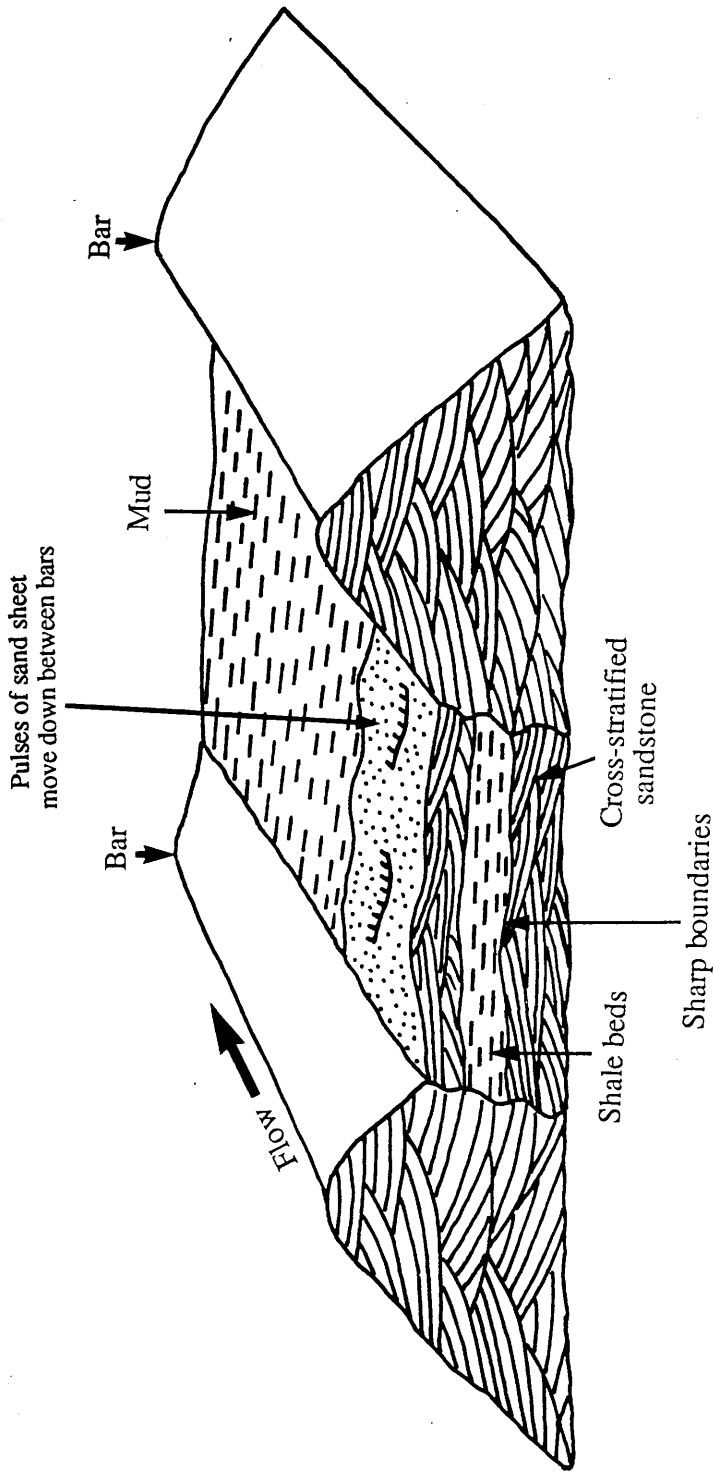


Fig. 2.19 Diagrammatic model showing the depositional environment of interbedded cross-stratified sandstone forming longitudinal sand waves and shale (Subfacies 1b). Here the whole area of bars has been abandoned, with main current activity affecting only the tops of the longitudinal sand bars. These phases of renewed current activity bring sand sheets between the bars and reactivate the large longitudinal sand bars.

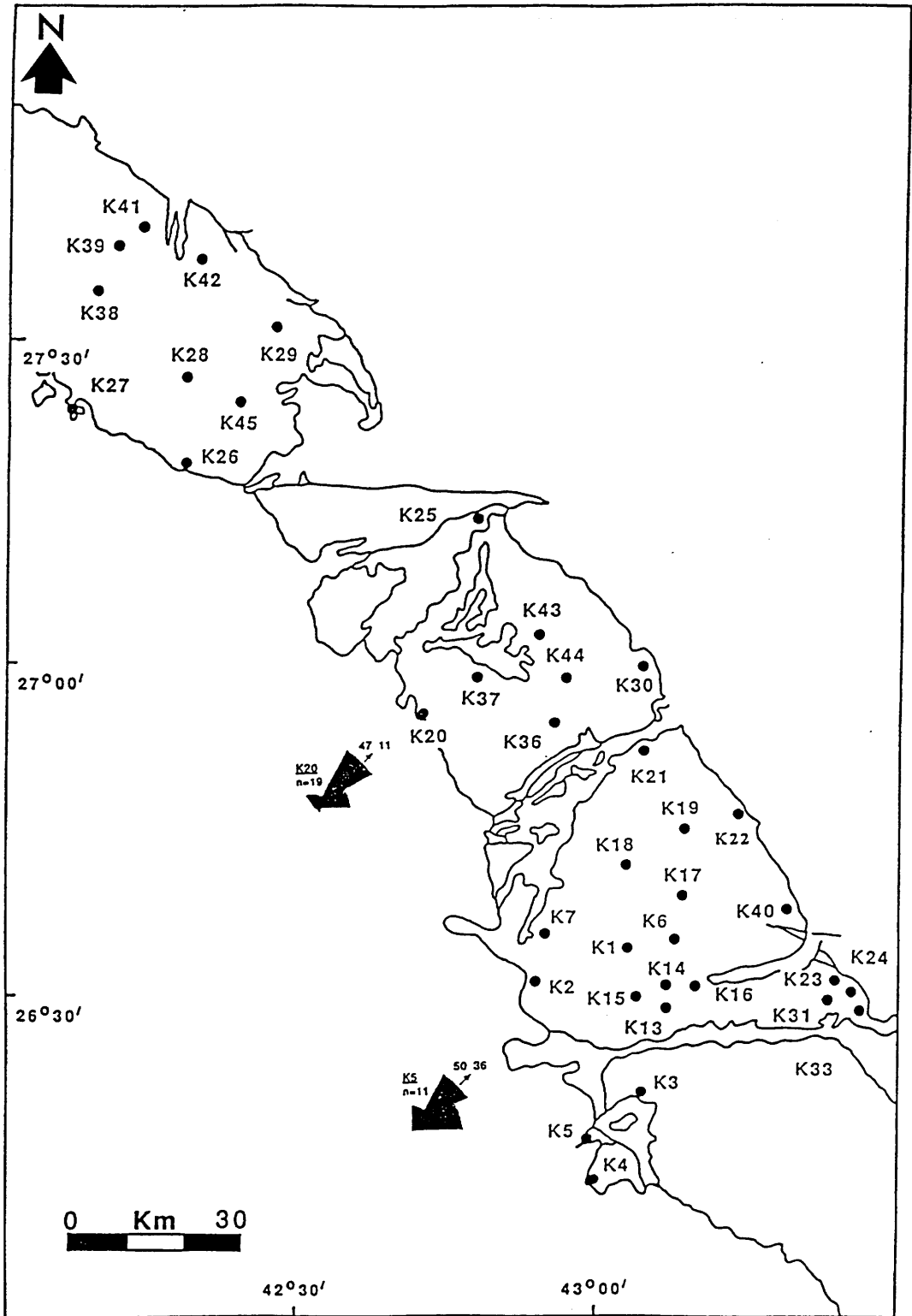


Fig. 2. 20 Palaeocurrent directions of subfacies 1b of the Lower Saq Sandstone.

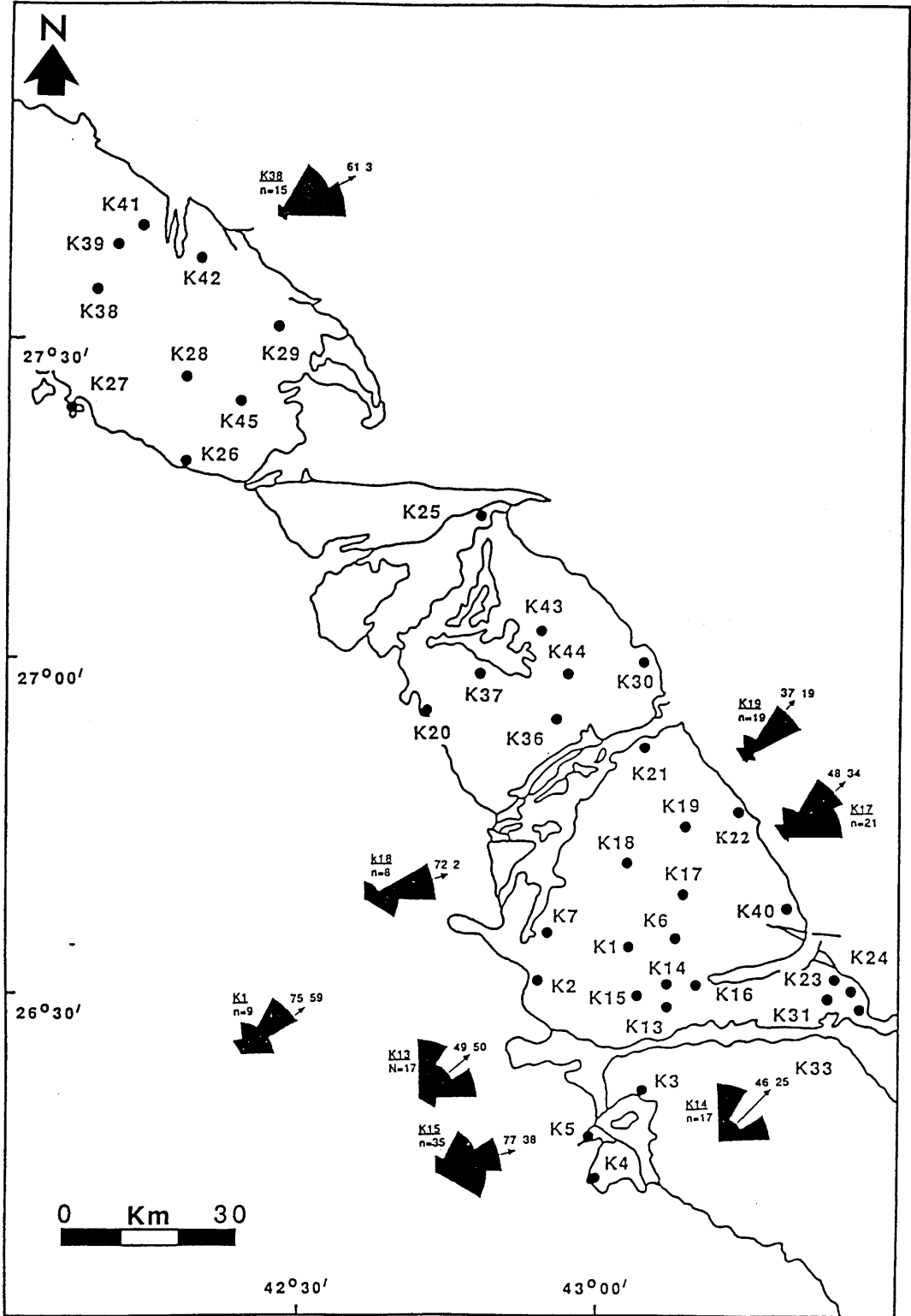


Fig. 2. 21 Palaeocurrent directions of subfacies 1b of the Middle Saq Sandstone.

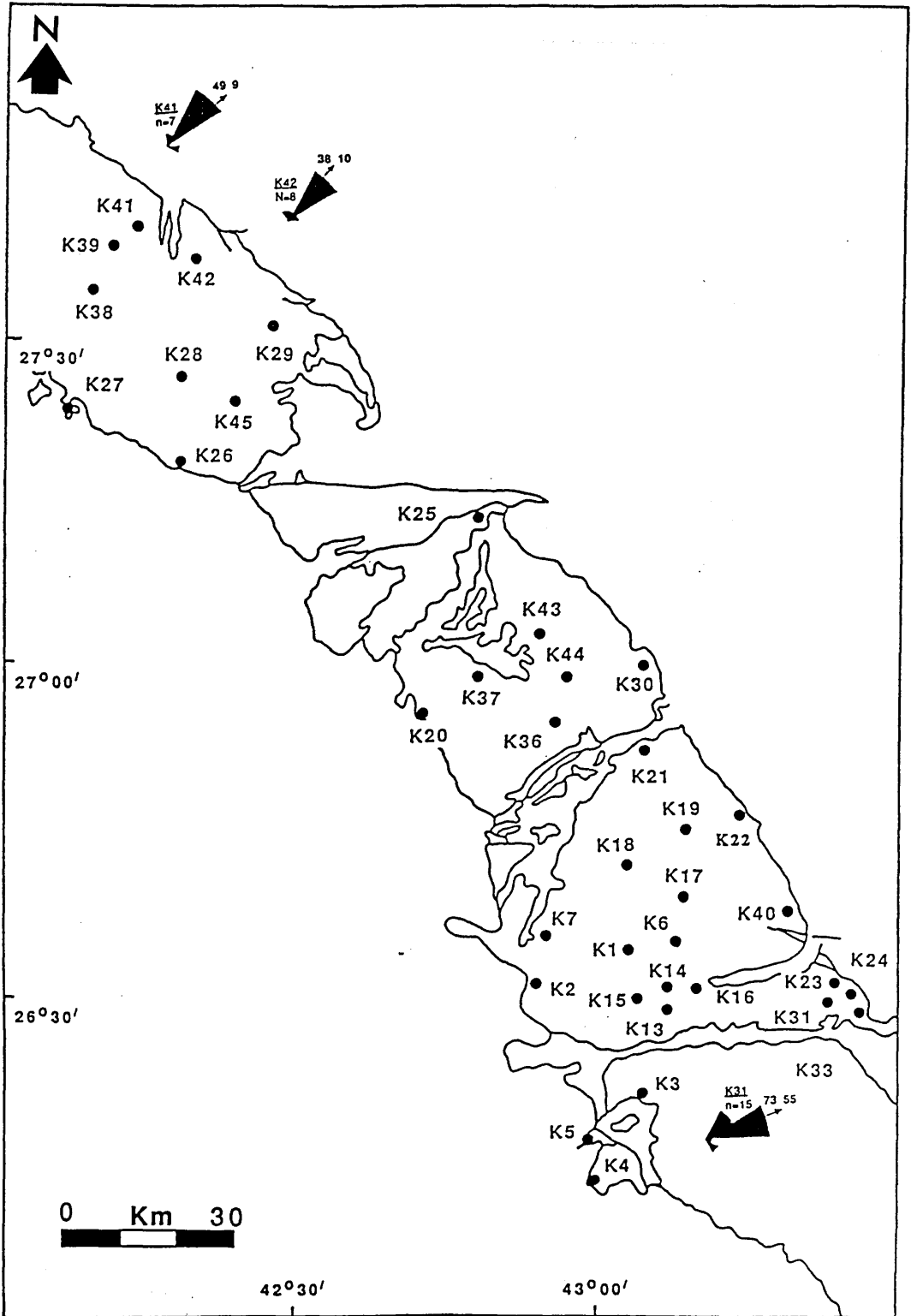


Fig. 2. 22 Palaeocurrent directions of subfacies 1b of the Upper Saq Sandstone.

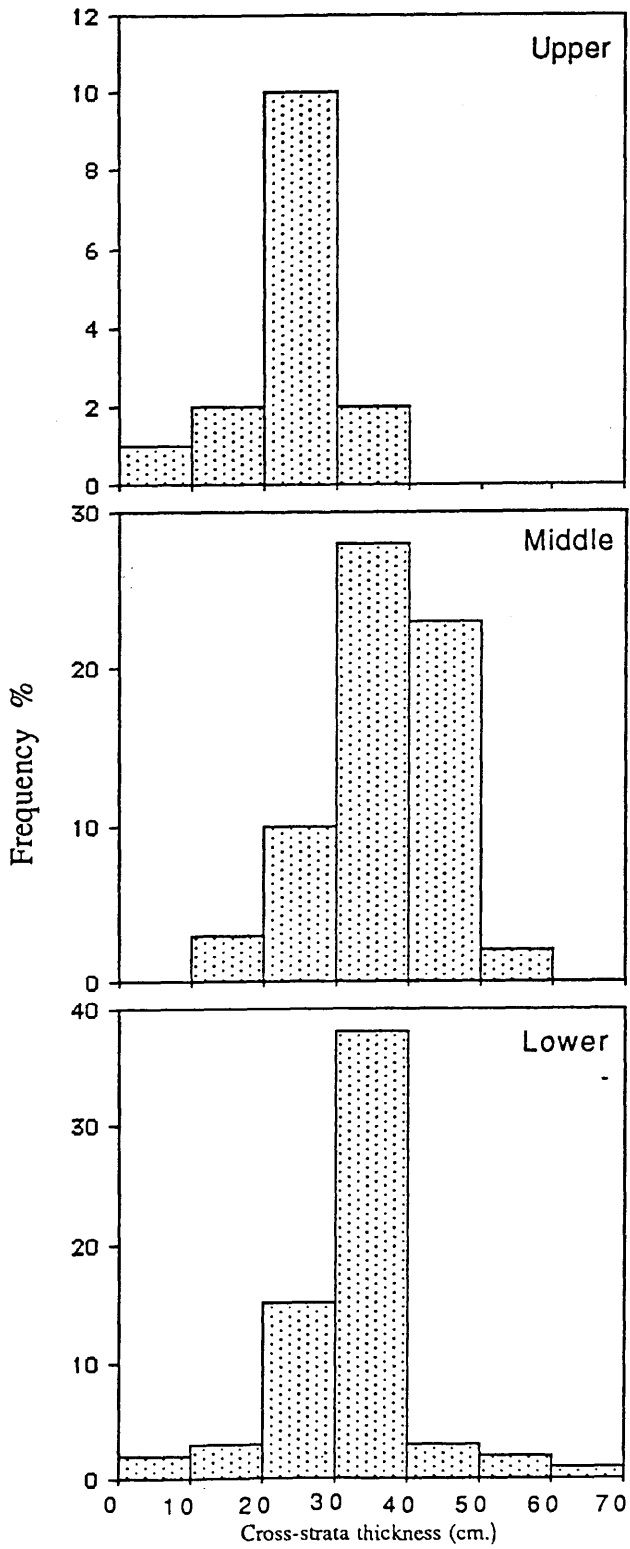


Fig. 2.23 Distribution of cross-strata thicknesses of subfacies 1c.

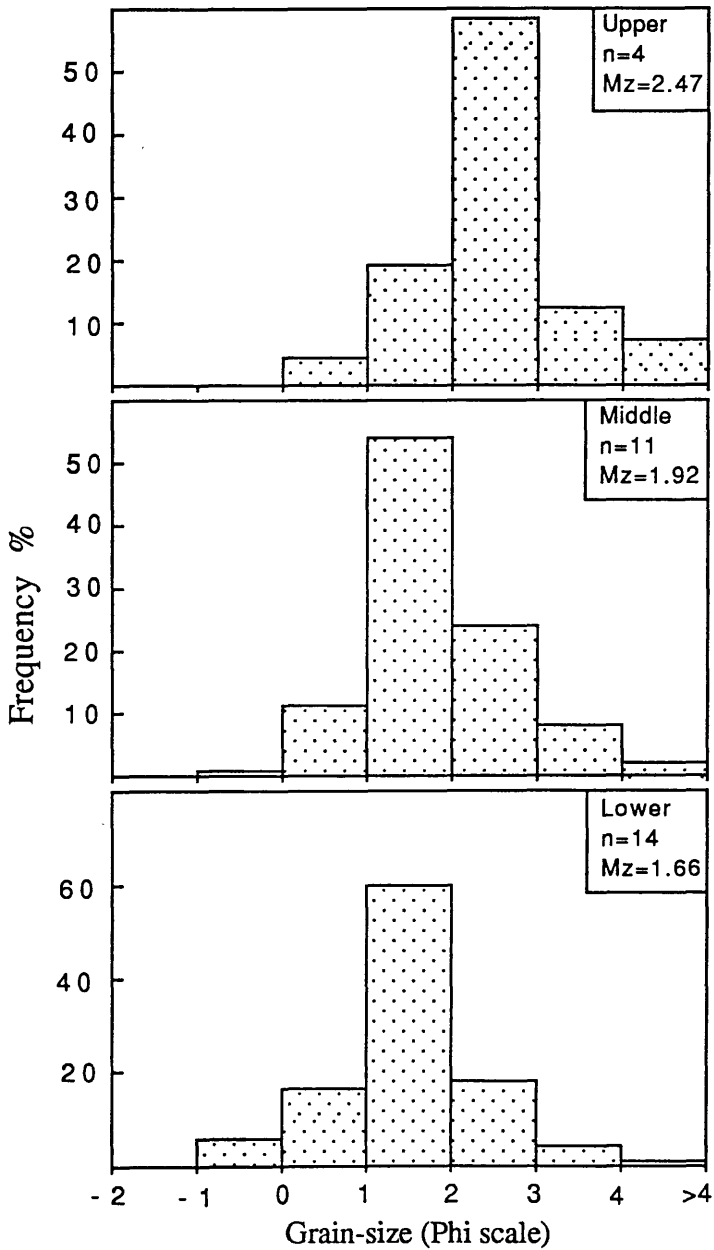


Fig. 2.24 Distribution of average grain-size of subfacies 1c of the Saq Sandstone.

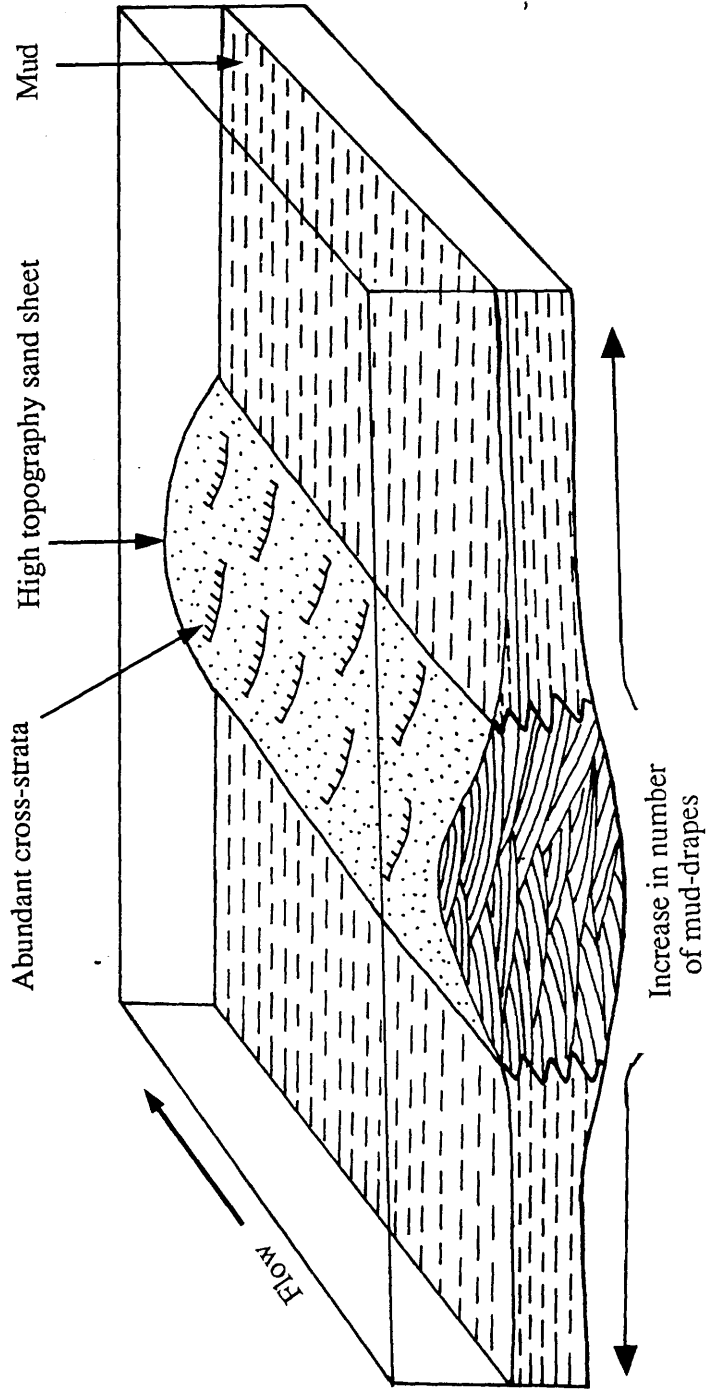


Fig. 2.25 Diagrammatic model showing the depositional environment of subfacies 1c.

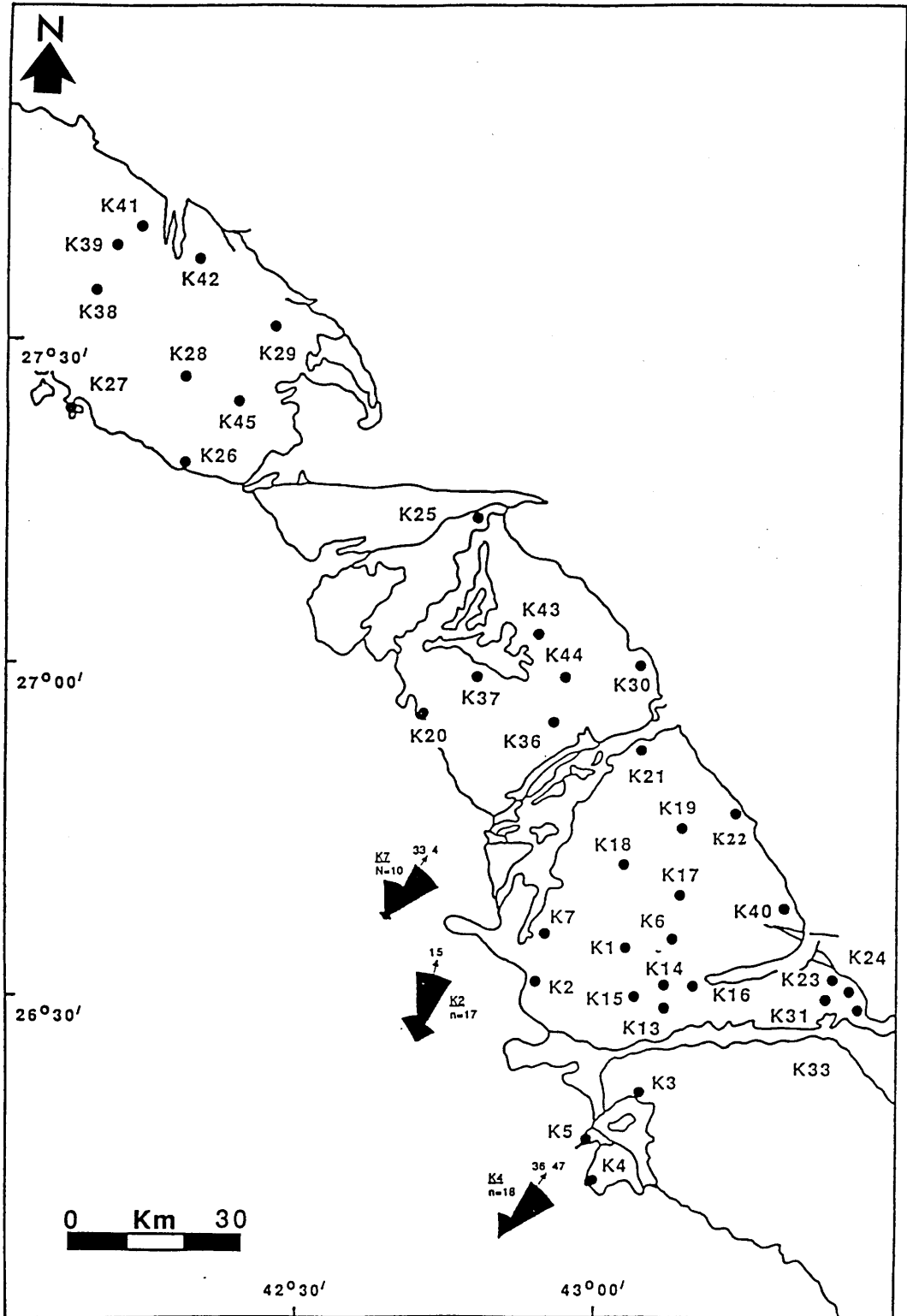


Fig. 2.26 Palaeocurrent directions of subfacies 1c of the Lower Saq Sandstone.

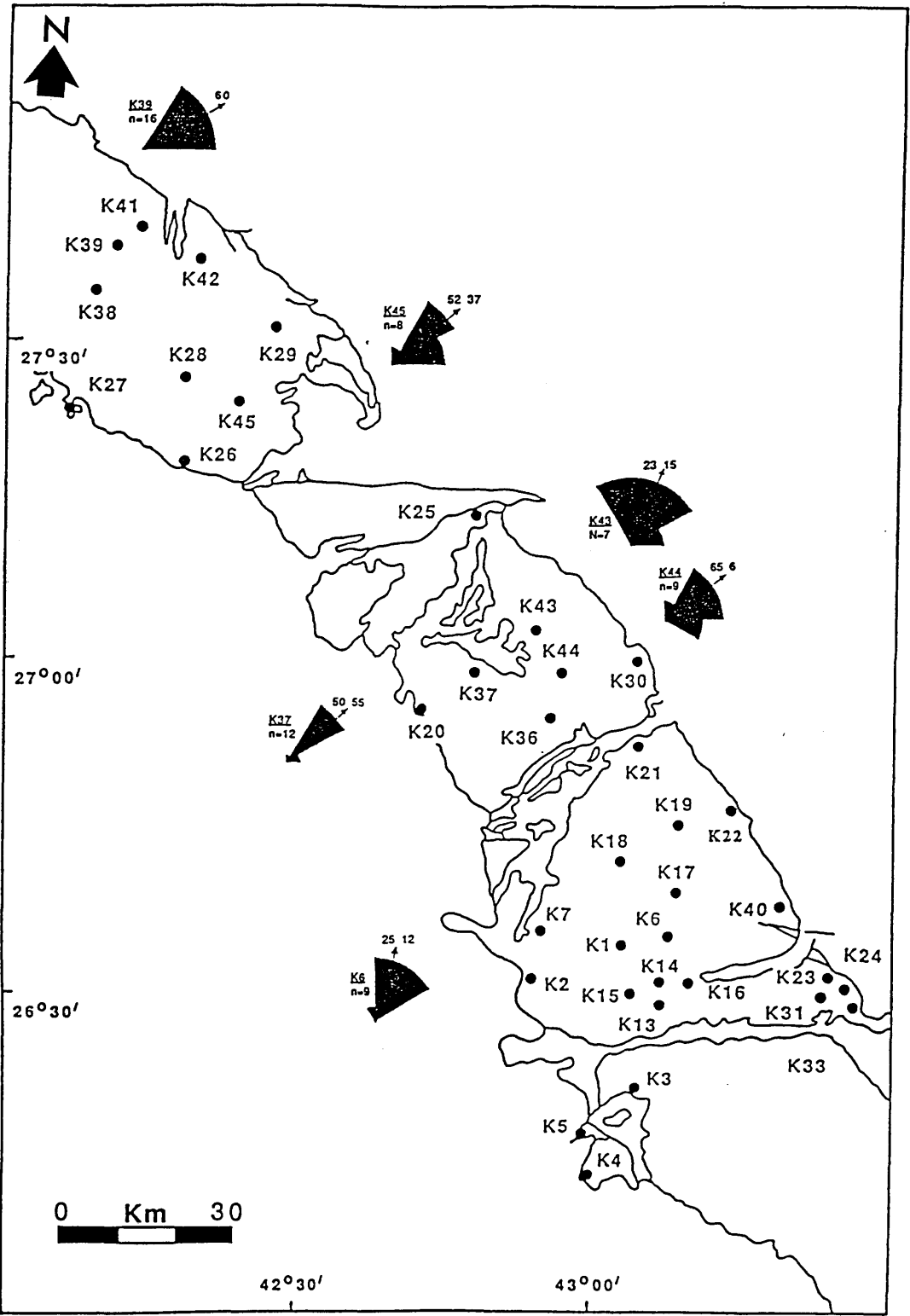


Fig. 2.27 Palaeocurrent directions of subfacies 1c of the Middle Saq Sandstone.

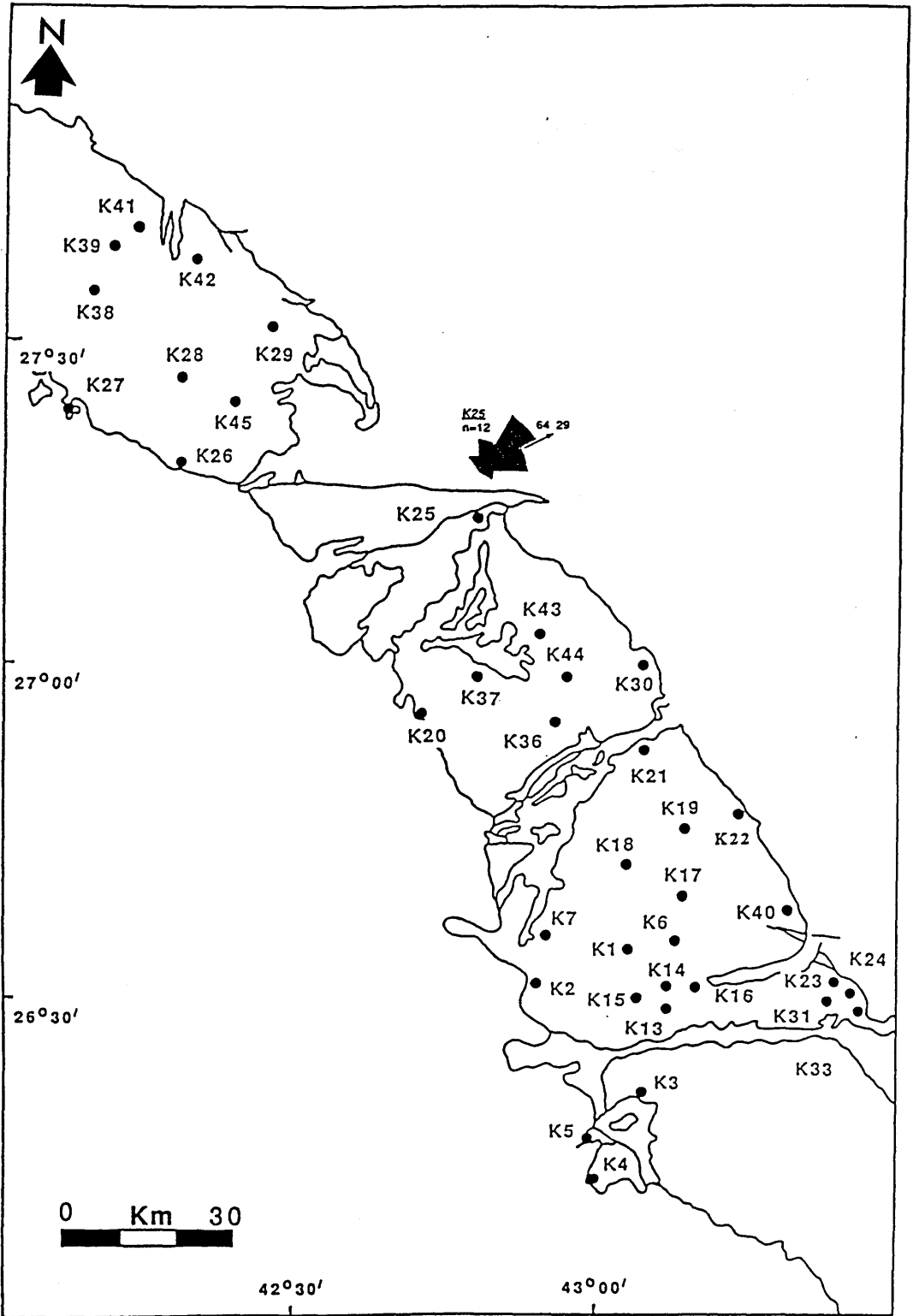


Fig. 2.28 Palaeocurrent directions of subfacies 1c of the Upper Saq Sandstone.

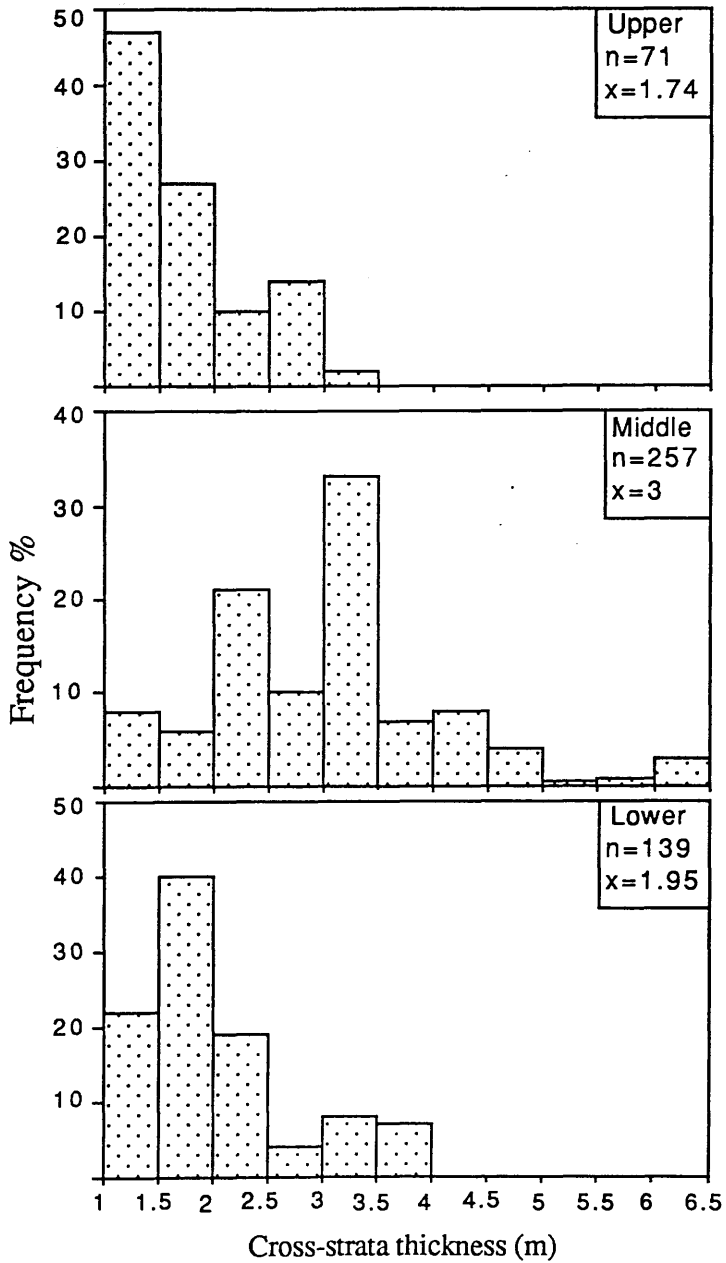


Fig. 2.29 Distribution of cross-strata thicknesses of large scale cross-stratified sandstones (Facies 2) of the Saq Sandstone.

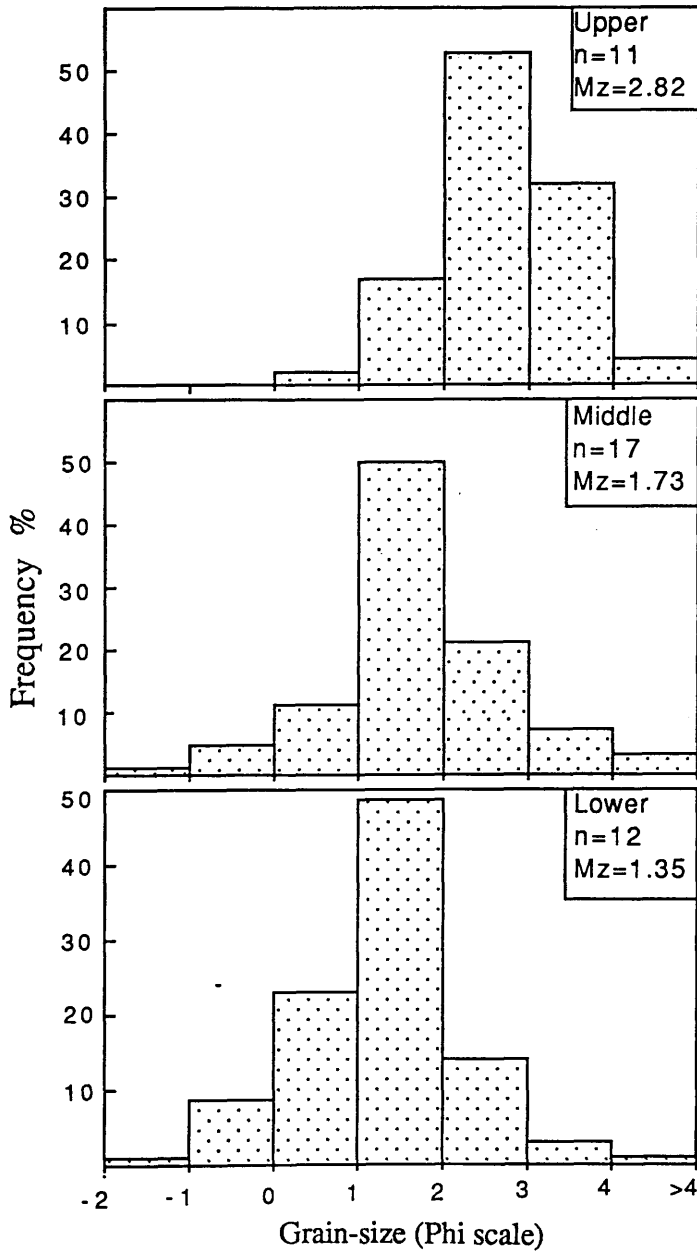


Fig. 2.30 Distribution of average grain-size of facies 2

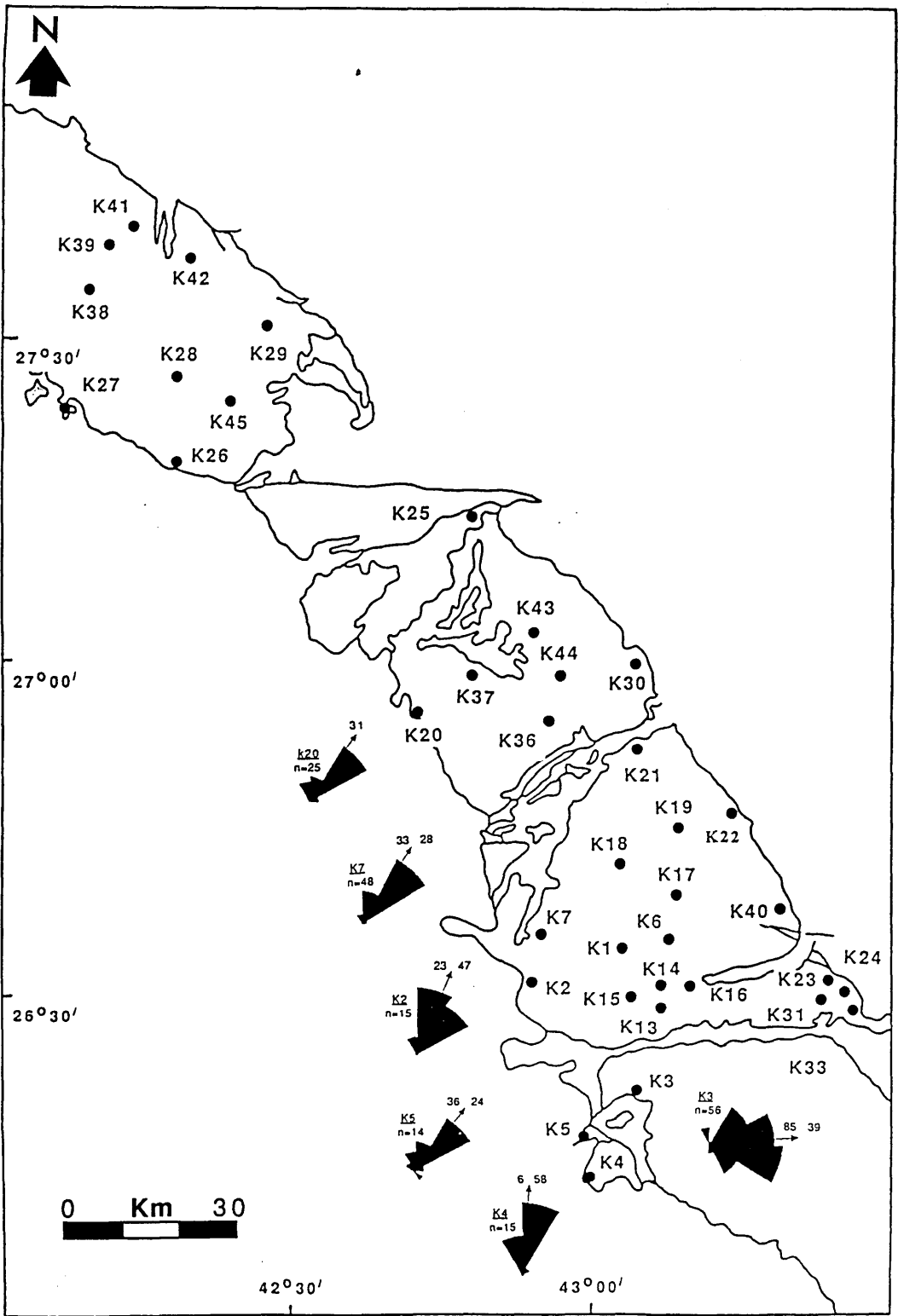


Fig. 2.31 Palaeocurrent directions of large scale cross-stratified sandstones (Facies 2) of the Lower Saq Sandstone.

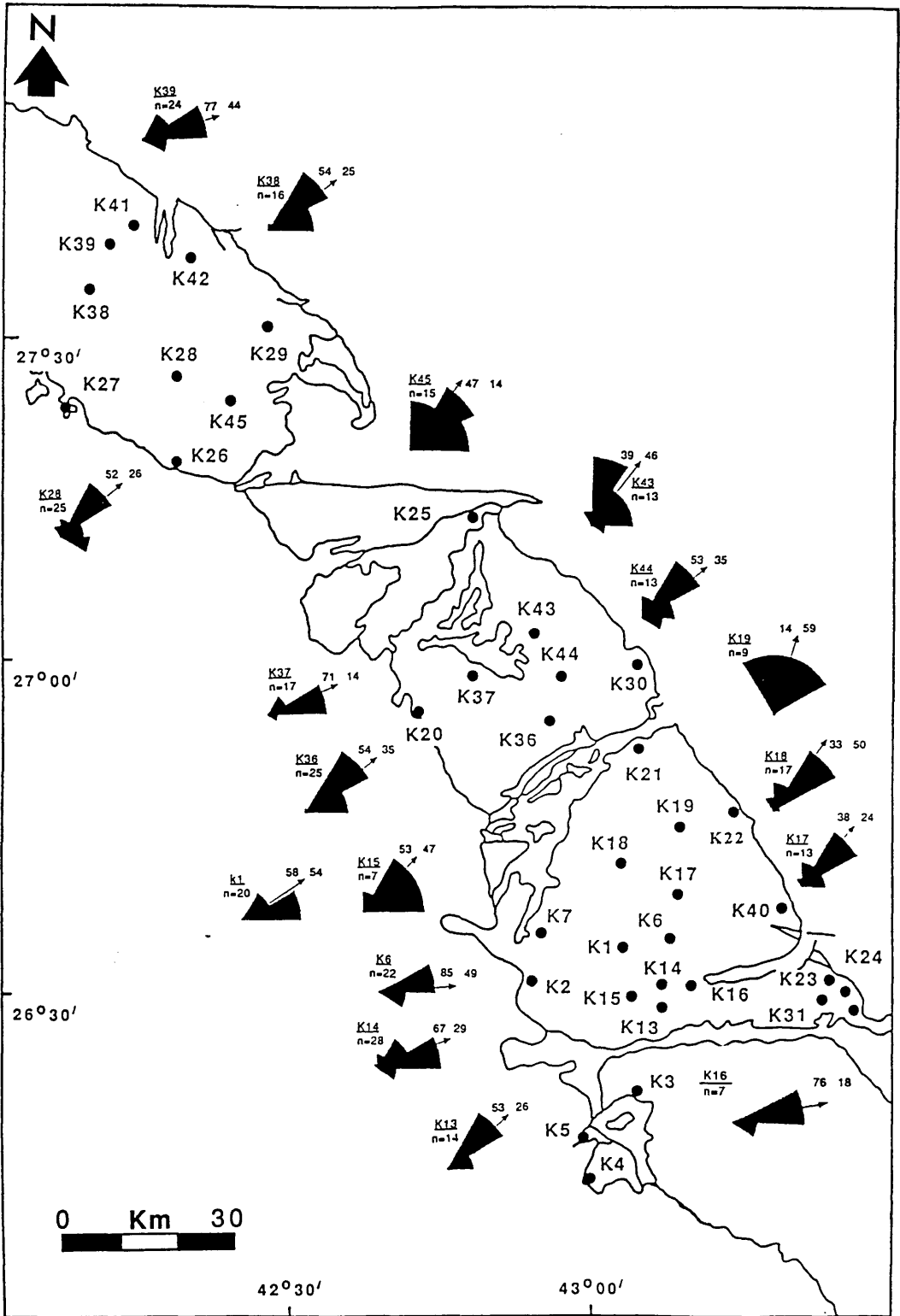


Fig. 2.32 Palaeocurrent directions of large scale cross-stratified sandstones (Facies 2) of the Middle Saq Sandstone.

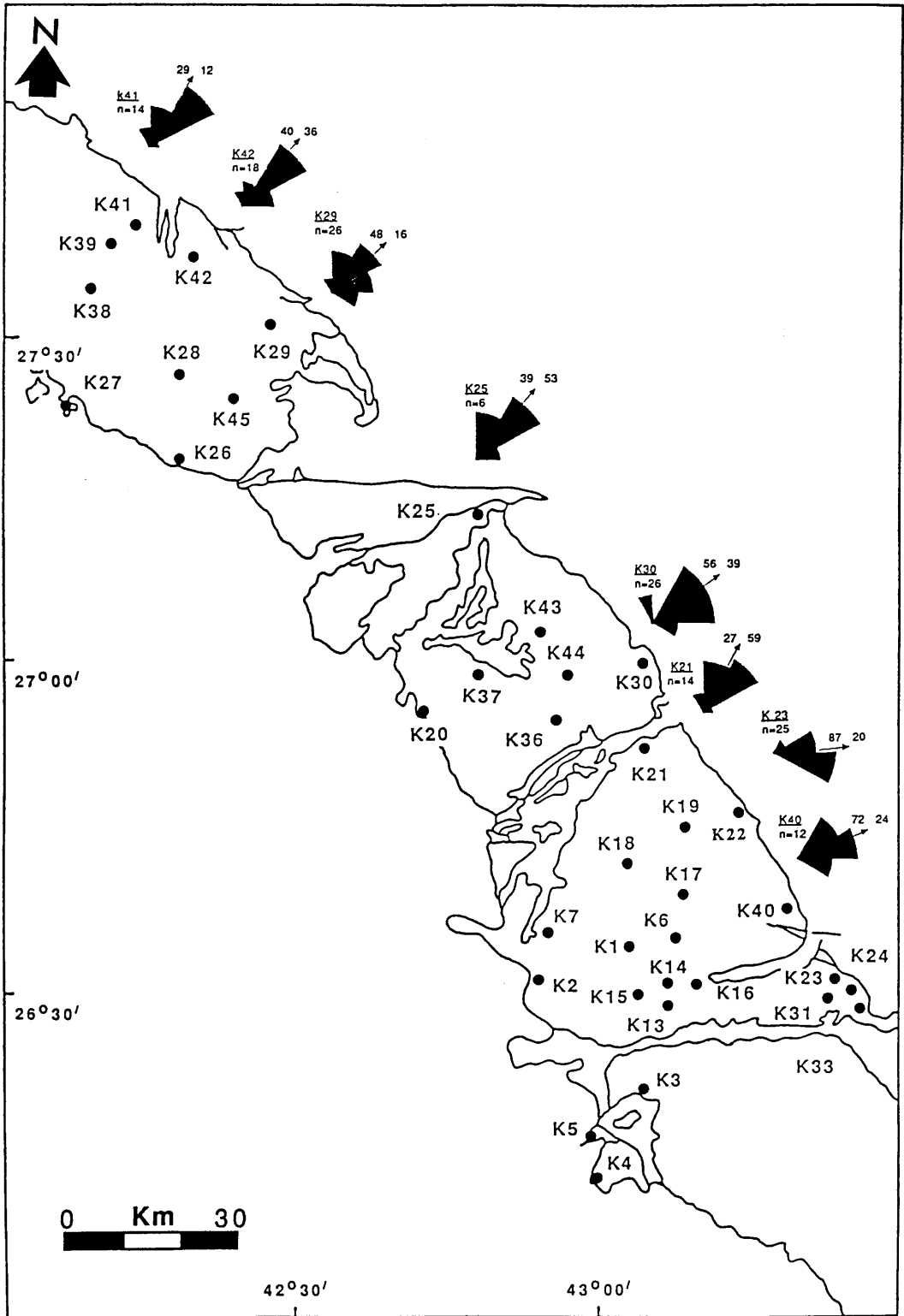


Fig. 2.33 Palaeocurrent directions of large scale cross-stratified sandstones (Facies 2) of the Upper Saq Sandstone.

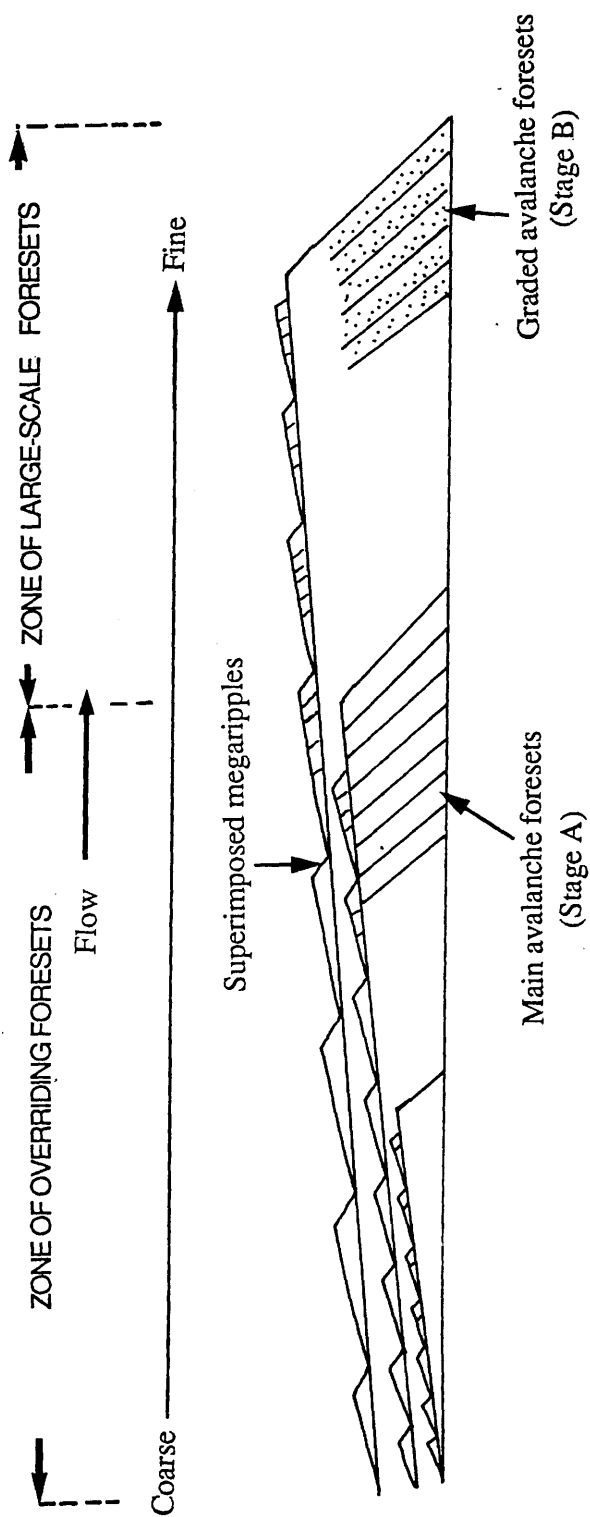


Fig. 2.34 Diagrammatic model showing the formation of large scale foresets (Facies 2).

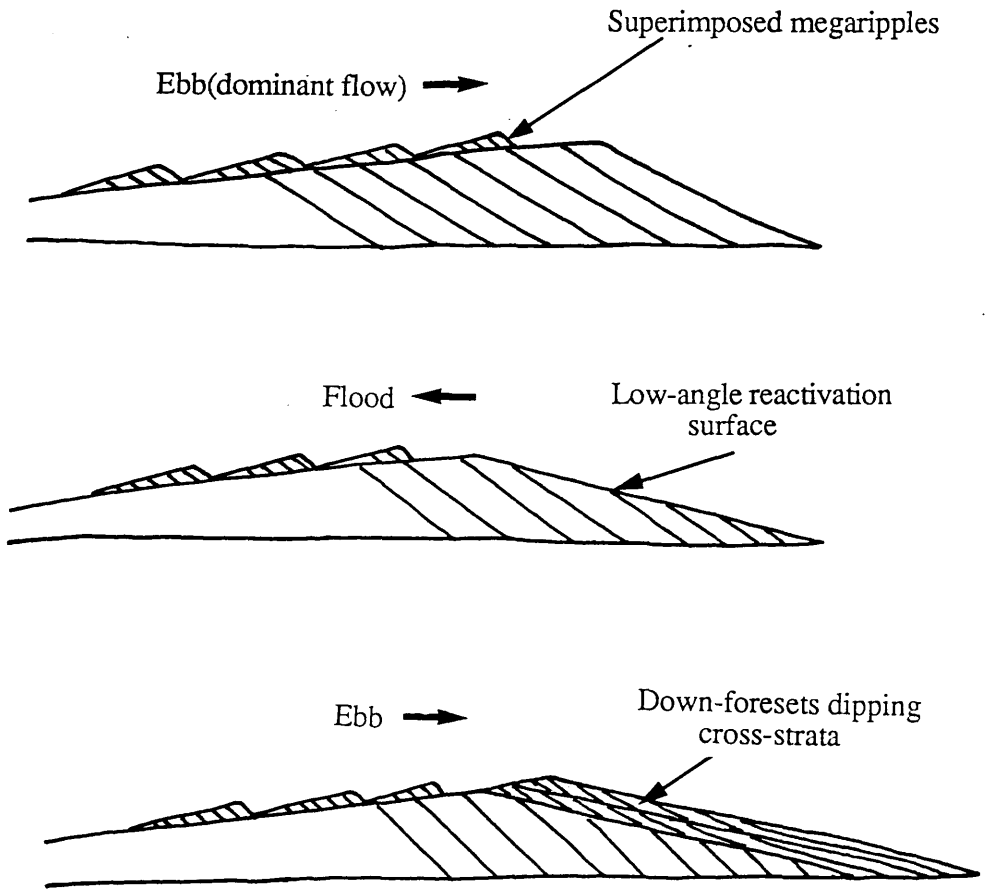


Fig. 2.35 Evolution stages of down-foreset dipping cross-stratified sandstone (Facies 3).

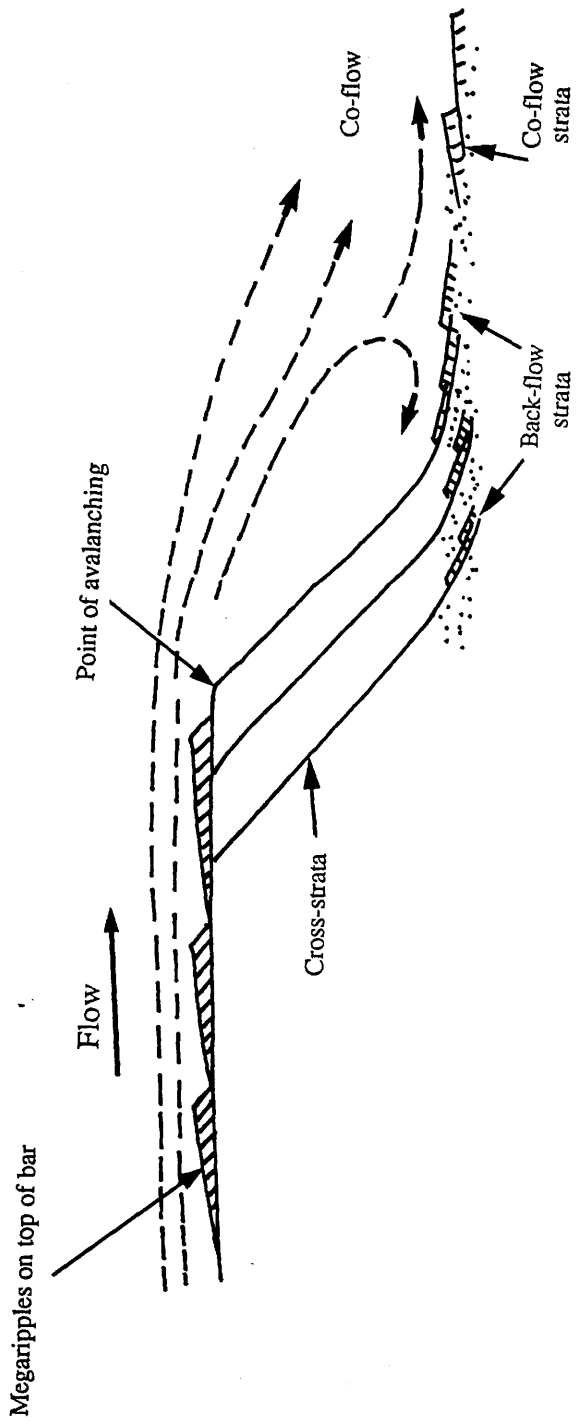
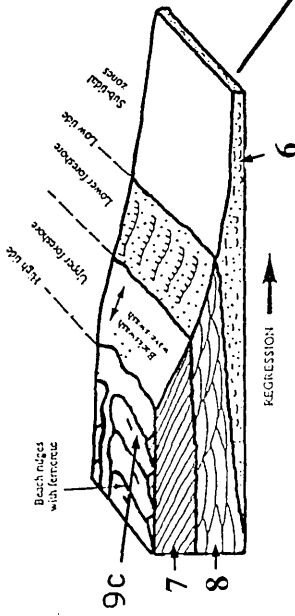
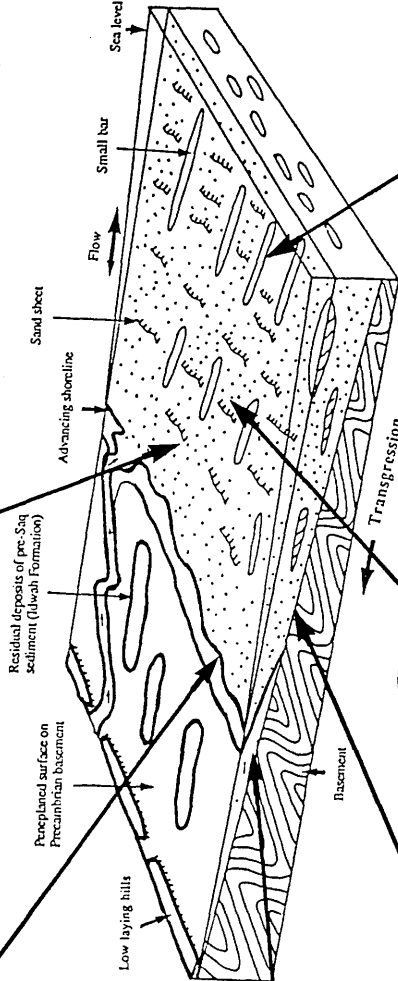
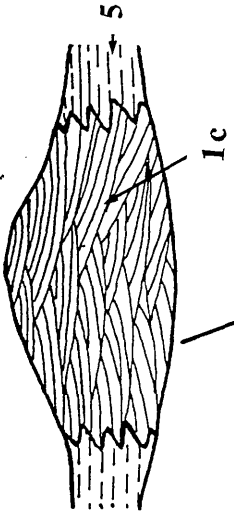


Fig. 2.36 Diagrammatic model showing the formation of Co-flow and back-flow strata.

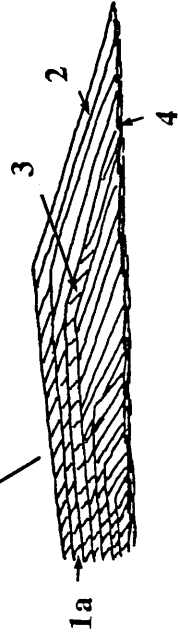
Facies Association D



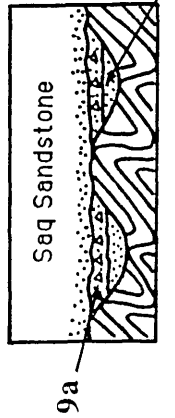
Facies Association C



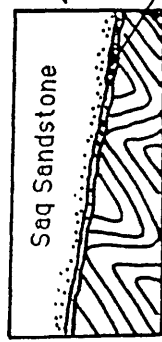
Facies Association A



Facies Association F



Facies Association E



Facies Association B

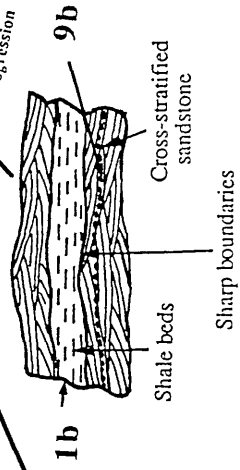


Fig.2.37 Facies Associations of the Saq Sandstones and Idwah Formation.

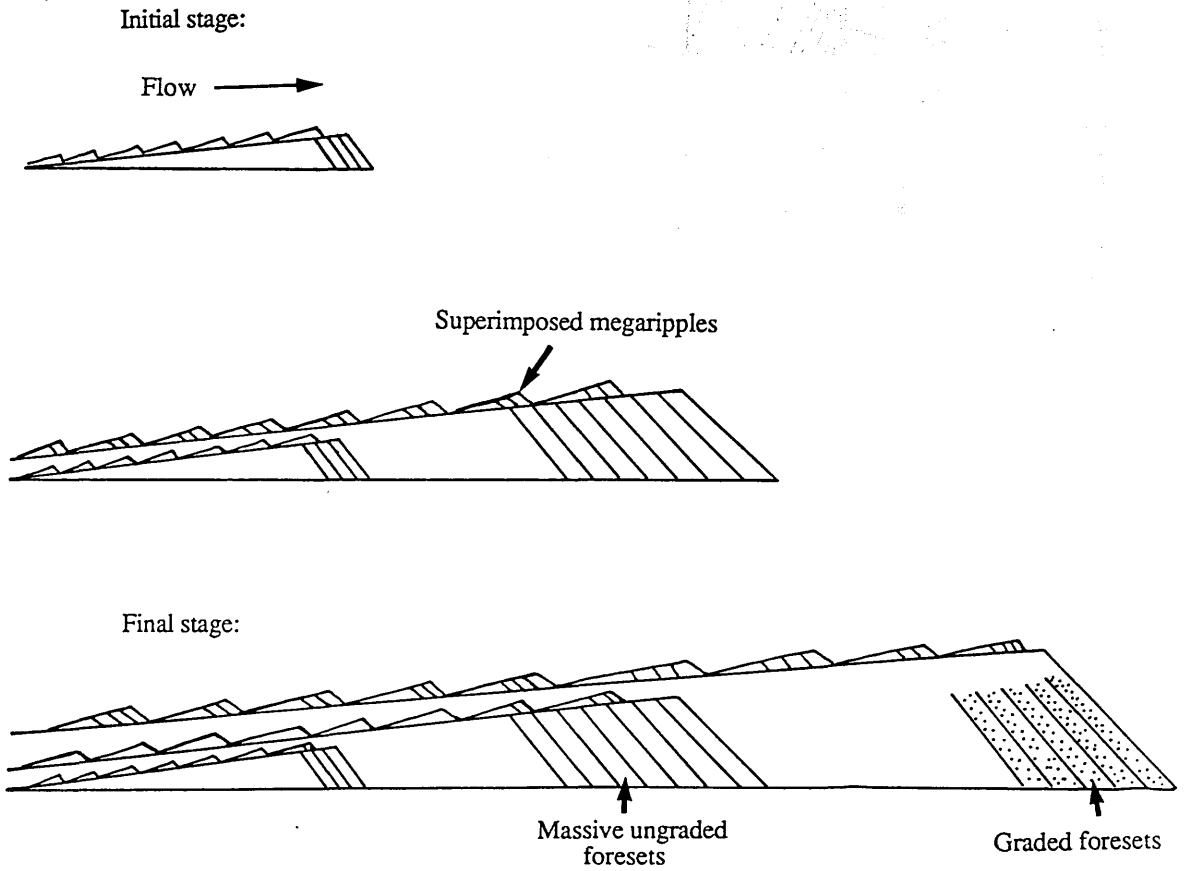


Fig. 2.38 Diagrammatic model showing the evolution of tidal sand bar by overtaking mechanism.

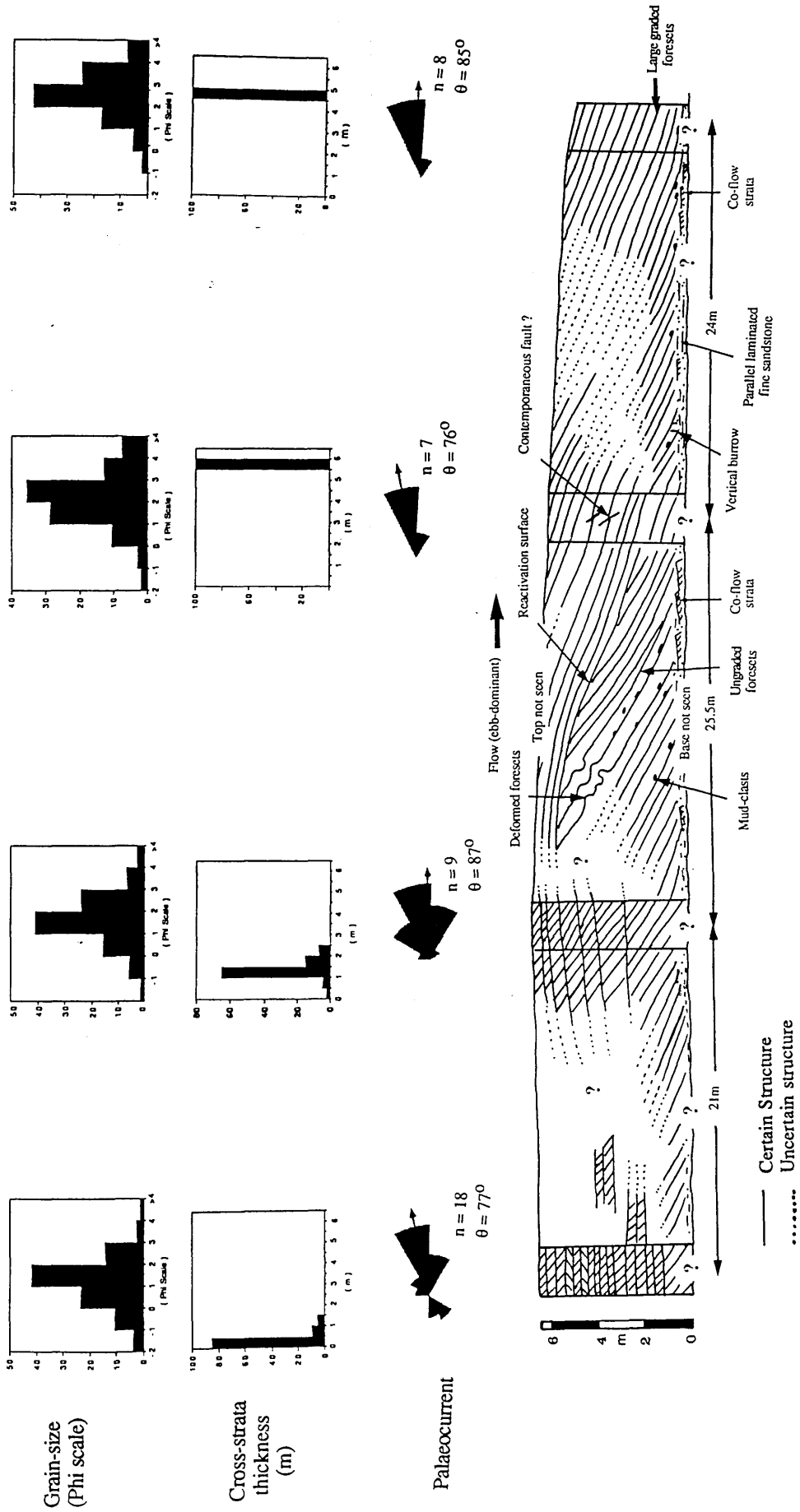


Fig. 2.39 Cross-section of tidal sand bar (Location K-16, Middle Saq Sandstone).

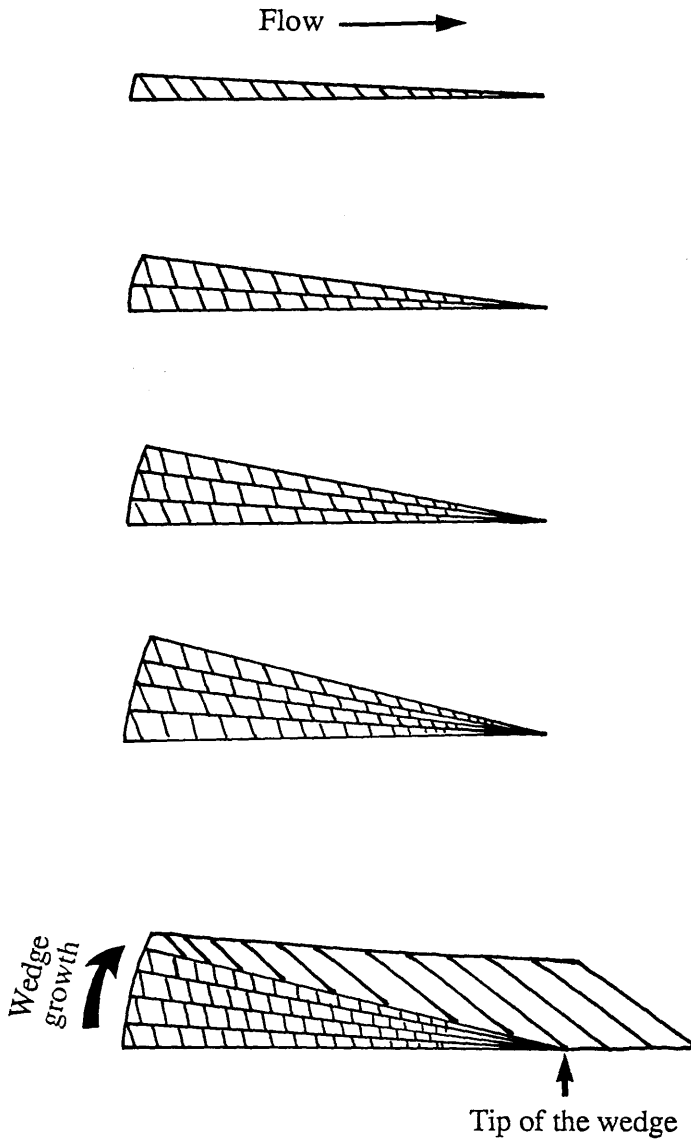


Fig. 2.40 Diagrammatic model showing the growth of bar by stacking of wedges mechanism (Fixed tip of the wedge).

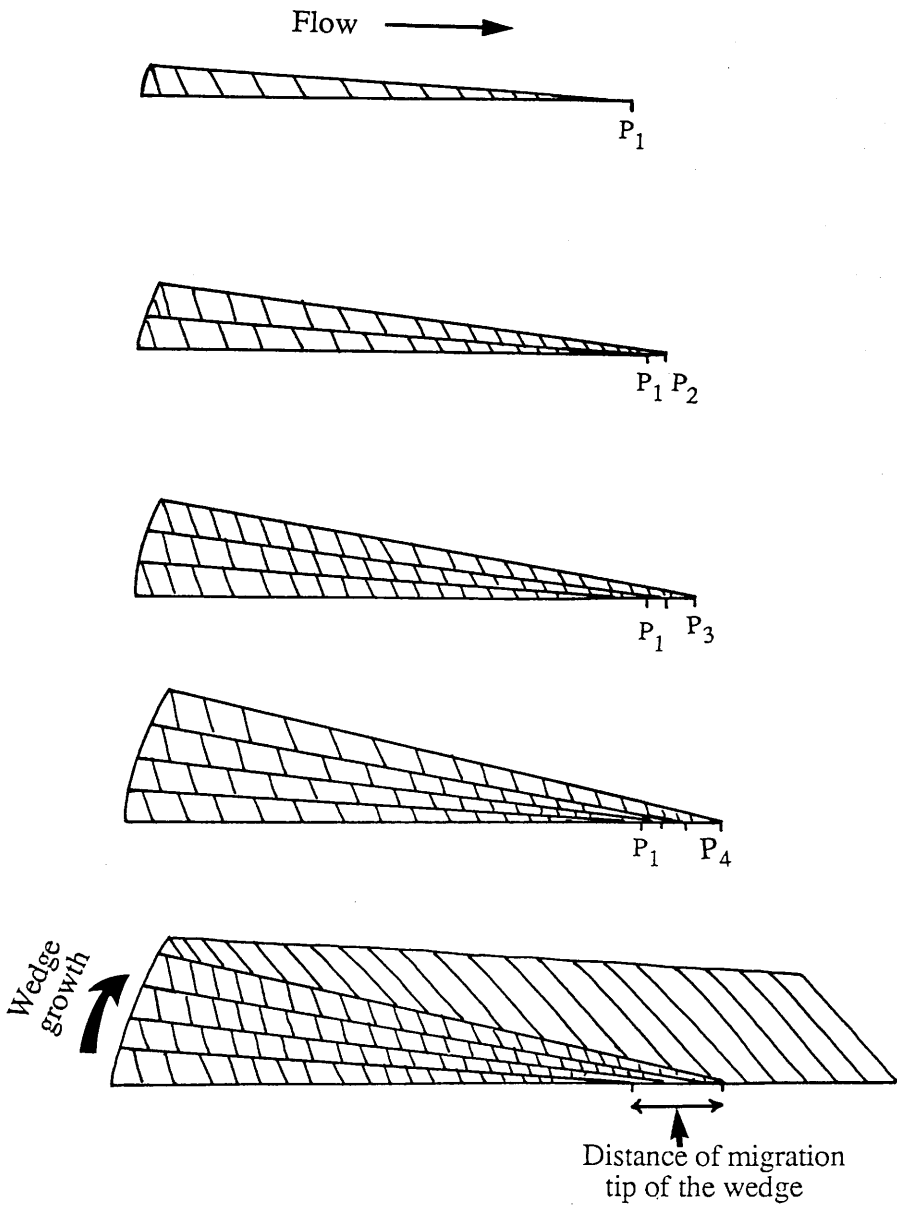


Fig. 2.41 Diagrammatic model showing the growth of bar by stacking of wedges mechanism (Migrating tip of the wedge for small rate).

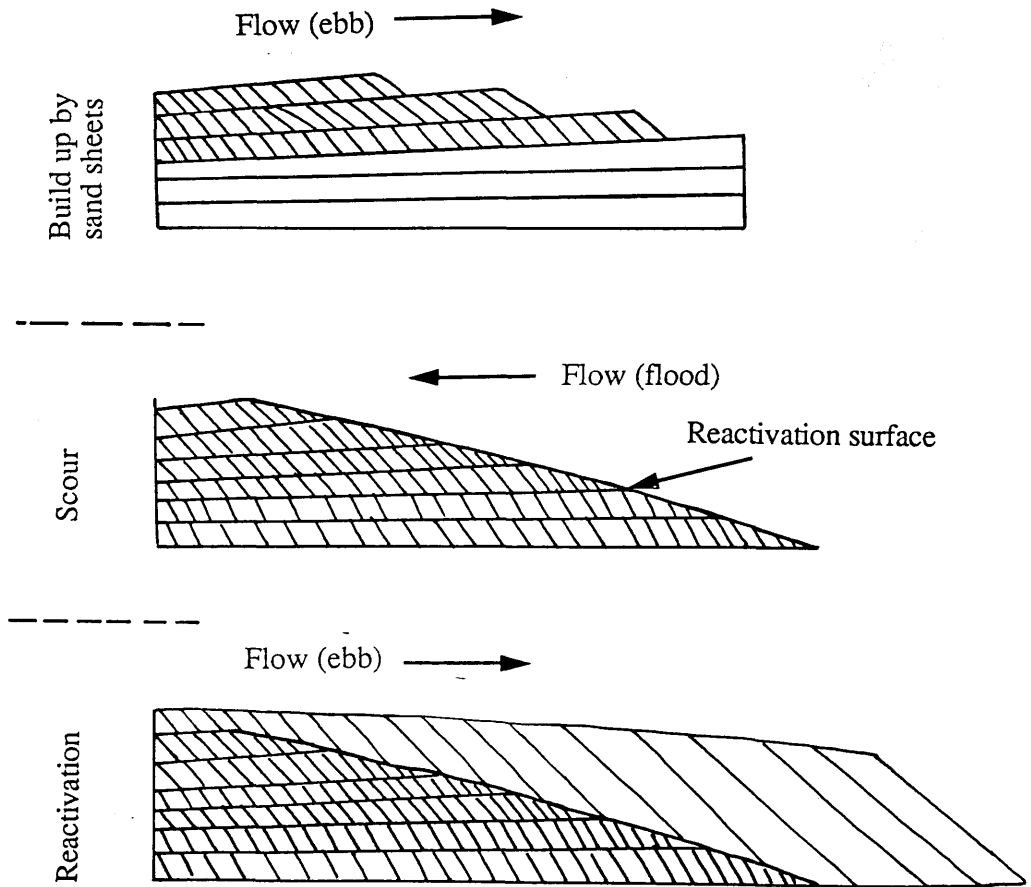


Fig. 2.42 Diagrammatic model showing the growth of bar by scour and reactivation mechanism.



Plate 2.1 Sand sheets with inclined boundaries (Subfacies 1a) Middle Saq Sandstone



Plate 2.2 Interbedded sandstone and shale subfacies (1b).- Middle Saq Sandstone.



Plate 2.3 Large scale cross-stratified sandstone (Facies 2) - Middle Saq Sandstone.



Plate 2.4 Mud-clast - Middle Saq Sandstone.



Plate 2.5 Massive and normal grading foresets (Facies 2).- Middle Saq Sandstone.



Plate 2.6 Deformation of large scale cross-stratified sandstone (Facies 2) - Middle Saq Sandstone.

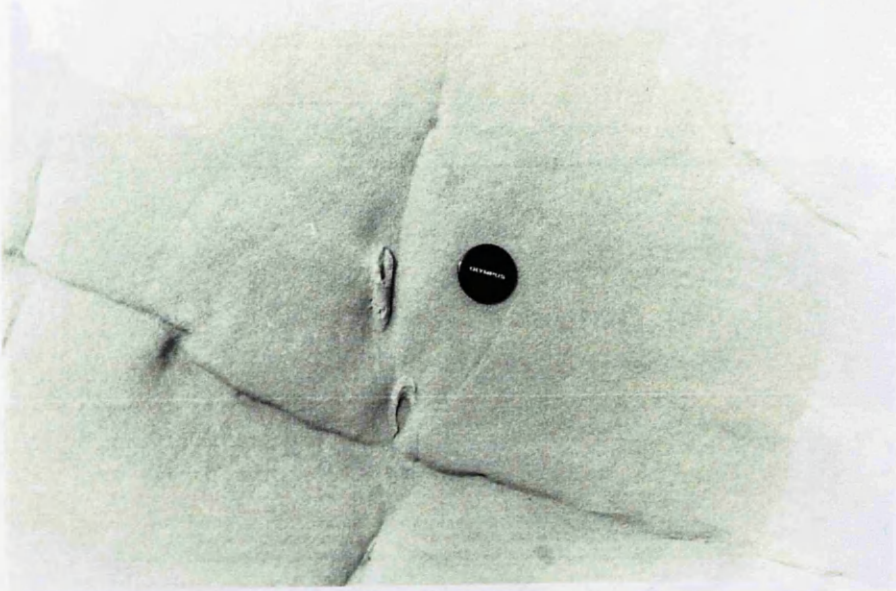


Plate 2.7 Vertical burrows in large scale cross-stratified sandstone (Facies 2) - Middle Saq Sandstone.



Plate 2.8 Reactivation surface (arrow) - large scale cross-stratified sandstone (Facies 2) - Middle Saq Sandstone.



Plate 2.9 Down-foreset dipping cross-stratified sandstone facies (arrow) - Middle Saq Sandstone.



Plate 2.10 Bottomset facies (4) - Middle Saq Sandstone.



Plate 2.11 *Cruziana* facies (5) - Middle Saq Sandstone.



Plate 2.12 Brachiopod shells (Facies 6) - Upper Saq Sandstone.



Plate 2.13 Planar to gently dipping stratified sandstone (Facies 7) - Upper Saq Sandstone.

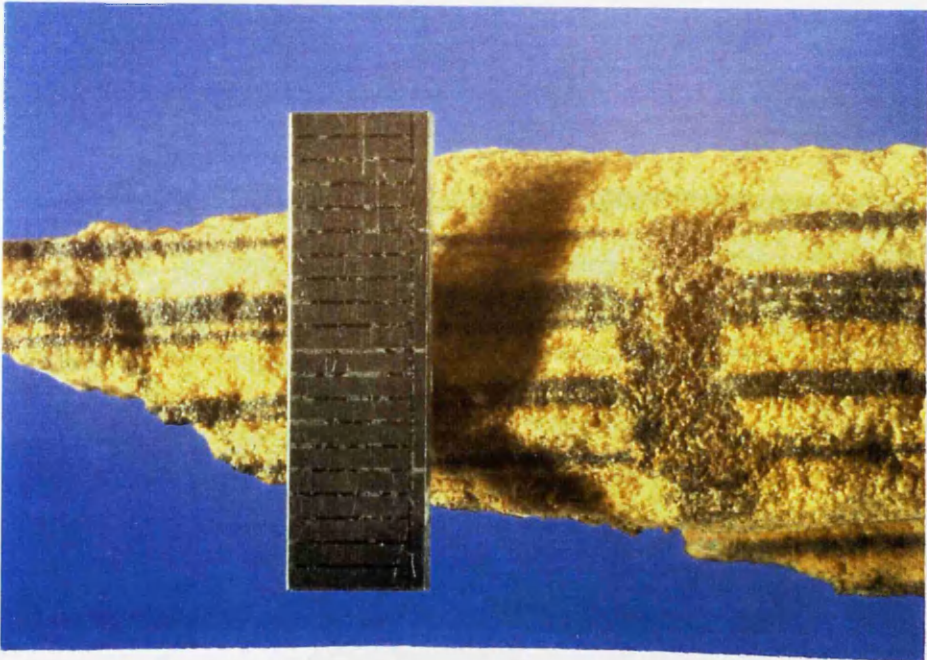


Plate 2.14 Heavy mineral bands and vertical burrow (Facies 7) - Upper Saq Sandstone (Bar for scale = 2cm).



Plate 2.15 Large-scale High angle cross-stratified sandstone (Facies 8)
Upper Saq Sandstone.



Plate 2.16 Inter-tidal zone - Welsh beach - U.K (Photo from Prof. B.J. Bluck).



Plate 2.17 Basal breccia (Subfacies 9a) - Pre-Saq sediment - Idwah Formation.



Plate 2.18 Fine conglomerate (Subfacies 9b) - Middle Saq Sandstone,
(Bar for scale = 2cm)

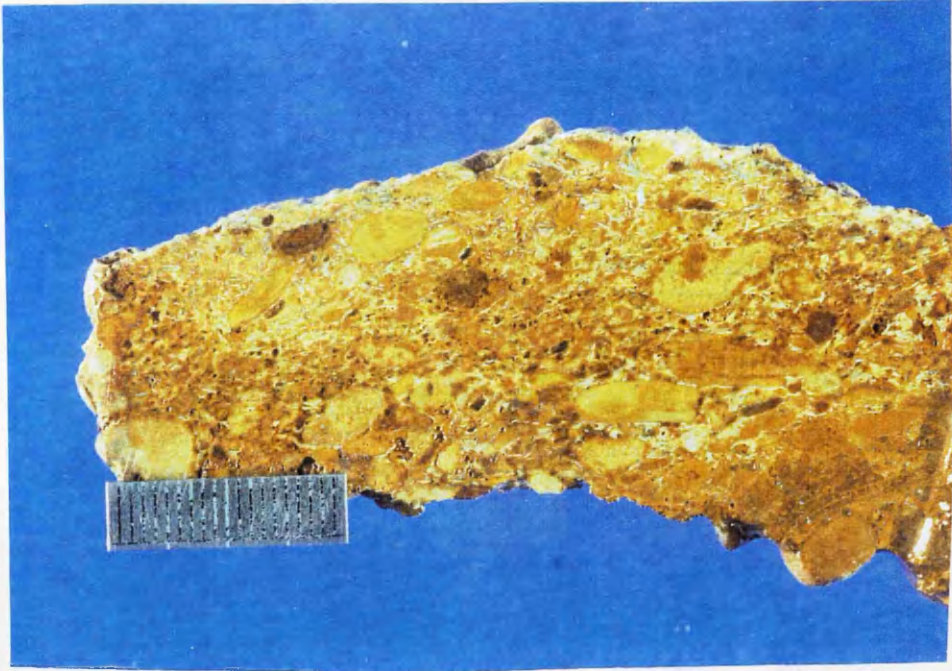


Plate 2.19 Bioclastic conglomerate (subfacies 9c) - Upper Saq Sandstone
(Bar for scale = 2cm).



Plate 2.20 Basal breccia and conglomerate (Subfacies 9d) - Lower Saq Sandstone.

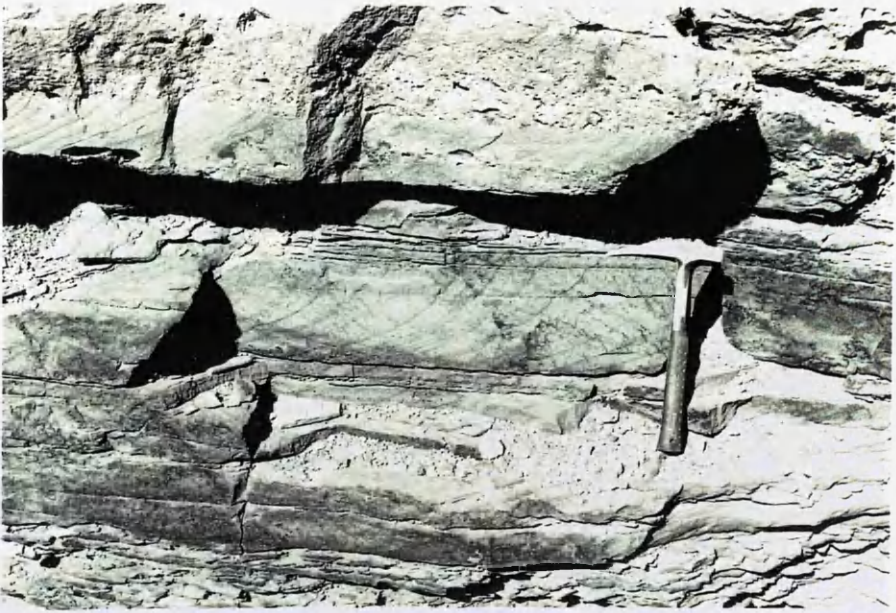


Plate 2.21 Flat-stratified red sandstone (facies 10) - Idwah Formation.



Plate 2.22 Overtaking mechanism (arrow) - Middle Saq Sandstone

CHAPTER THREE

PETROGRAPHY OF THE SAQ SANDSTONE



Plate 2.23 Wedge Mechanism - Middle Saq Sandstone.

The Saq Formation in central and northern Saudi Arabia is entirely clastic. It consists of a vertically and laterally uniform succession of white, gray, red and brown coarse-grained quartz arenites, with subordinate shales, conglomerate and breccia.

The aims of these petrographical studies are:

1. To identify the petrographical composition of the Saq Sandstone
2. To record any vertical or lateral variation throughout the formation
3. To provide information about the provenance of the sediments & the tectonic regimes of this formation

CHAPTER THREE

PETROGRAPHY OF THE SAQ SANDSTONE

3.1 Introduction:

The detrital composition of sandstones is influenced by several factors including provenance, weathering processes, transportation to the depositional basin and diagenesis. Following the work of Crook, (1974) and Schwab, (1975), there has been a resurgence of interest in the relationship between sandstone compositions and the plate tectonic setting of the depositional basin (Dickinson & Suczek, 1979; Moore, 1979; Dickinson & Valloni, 1980; Valloni & Maynard, 1981; Schwab, 1981; Franzinelli & Potter, 1983; Dorsey, 1988; Dickinson *et al.*, 1988; Cavazza, 1989; Johnsson, 1990).

The nature of source rocks near to sedimentary basins and the impact that the sedimentary process acting in a receiving basin have on the sediments are considered a guide to the general tectonic regime in which sediments accumulate. In addition, framework mineralogy is an indicator of both the subsidence history of a basin and uplift history of a source. Continual reworking eliminates unstable grains and concentrates the more stable, such as quartz.

The Saq Formation in central and northern Saudi Arabia is entirely clastic. It consists of a vertically and laterally uniform succession of white, gray, red and brown cross-stratified quartz arenites, with subordinate shale, conglomerate and breccia.

The aims of these petrographical studies are:

- 1- To identify the petrographical composition of the Saq Sandstone
- 2- To record any vertical or lateral variation throughout the formation
- 3- To provide information about the provenance of the sediments & the tectonic regime of this formation

4- To evaluate current views on the genesis of quartz arenite.

The Saq Sandstone was examined by a number of standard petrographic methods. Optical microscopy, X-ray diffraction (XRD), scanning electron microscopy (SEM), and cathodoluminescence microscopy were done when appropriate.

For more than 180 thin sections framework composition was determined on the basis of 400-grain counts per thin section using a petrographic microscope fitted with a Swift automatic point counter. The technique described by Galehouse (in Carver, 1971), was used where grid spacing slightly exceeded the average grain-size so that in most cases individual grains were not counted more than once.

3.2 Mineralogical classification

There are many classifications concerned mainly with the mineralogy and texture of sandstone (*e.g.* Pettijohn, 1975 ;McBride, 1963; Pettijohn *et al.*, 1984; Folk, 1974 and others).

McBride, (1963) proposed the classification which has been used in this study, which depends on the following framework mineral groups (Fig. 3.1) :

- **Q** - Total quartzose grains of both poly-and monocrystalline varieties, chert, orthoquartzite and metaquartzite lithic fragments are included here.
- F** - Monocrystalline feldspar grains.
- L** - Lithic fragments of igneous, metamorphic or sedimentary varieties.

These framework minerals are recalculated to 100% and are plotted in a ternary diagrams. All the samples from the Lower, Middle and Upper Saq Sandstone fall in the quartz arenite field (Fig. 3.2) according to terminology of McBride (1963). Compositionally the sandstone sample population is quite homogeneous. This can be seen in Figure 3.2, where virtually all the samples plot in a small area of the standard QFL triangular diagram.

Dickinson, (1970), along with many other workers has observed that concentration towards the Q apex usually indicates maturity, and as all of the Saq Sandstone samples plot very close to the Q apex, they are therefore defined as mature.

3.3 Framework grain composition

The Saq Sandstone is petrographically homogenous and texturally and mineralogically mature; the sandstone is mainly a quartz arenite over the entire area. The main constituent mineral is quartz which is up to 90.97%, 94.29% and 95.66% of total volume of the rock in the Lower, Middle and Upper Saq Sandstones respectively. Most of the quartz occurs as mono or polycrystalline grains but quartz also present in authigenic form as quartz overgrowths. Some of the quartz grains are polycyclic, as indicated by worn overgrowths, and also some grains have double overgrowths, which are the result of two (or more) generations of recycled sediments (Plates 3.1, 3.2). The remaining detrital grains include feldspar, chert, mica, rock fragments and stable heavy minerals (Tables 3.1 to 3.3 - Appendix A). The average of the Saq Sandstone mineralogy is shown in Table 3.4.

The relationship between sandstone composition and plate tectonics has been the subject of intensive research and discussion by many workers (Dickinson & Suczek, 1979; Ingersoll & Suczek, 1979; Dickinson & Valloni, 1980; Valloni & Mezzadri, 1984; Aalto, 1989), and this approach has contributed to our ability to predict the tectonic setting of a source terrane from framework compositional modes (Dorsey, 1988).

Limitation of this approach include such problems as temporal variations related to depositional environment and climate (Suttner, 1974 ; Mack, 1984) and large-scale lateral transport of sand from regions tectonically unrelated to the basin of deposition (Velbel, 1985). In spite of these problems, recent workers have been able to recognize unique lithic fragment detrital modes in sands and sandstones that are derived from uplifted zones of continental collision, or suture belts (Graham *et al.*, 1976; Ingersoll & Suczek, 1979;

Korsch, 1984; Suczek & Ingersoll, 1985; Lash, 1986; Jett & Heller, 1988; Dorsey, 1988).

Two ternary diagrams are especially useful for identifying the provenance of the sandstone QFL and QmFLt (Fig. 3.1) in which :

$Q = Q_m + Q_p$	where	Q=total quartzose grains.
		Q_m =monocrystalline quartz grains.
		Q_p =polycrystalline quartz grains.
$F=K$	where	F=total feldspar grains.
		K=potassium feldspar grains.
$L_t=L+Q_p$	Where	L_t =total aphanitic lithic grains.
		L=total unstable aphanitic lithic grains.

Dickinson & Suczek, (1979) showed that the mean composition of sandstone suites derived from different kinds of provenance terranes controlled by plate tectonics tend to lie within discrete and separate fields on QFL and QmFLt diagrams (Dickinson *et al.*, 1983).

The results of the point count analyses are plotted on QFL and QmFLt provenance-discrimination diagrams of Dickinson *et al.*, (1983). In this illustration the Lower, Middle and Upper Saq Sandstone originated mostly or exclusively from the craton interior and recycled orogenic sources (Figs. 3.3 and 3.4).

3.4 Description of the mineralogy

3.4.1 Quartz

Quartz is the most stable and common component present in sandstone, it has a source in many igneous, metamorphic and pre-existing sedimentary rocks, and attempts were made long time ago to characterize the quartz grains produced from the various source rocks. The usefulness of quartz as an indicator of provenance has been much

professed in the literature. The presence or absence of undulatory extinction and the polycrystallinity of detrital grains are the most used criteria for provenance determinations (Bokman, 1952; Blatt & Christie, 1963; Blatt, 1967; Basu *et al.*, 1975; Young, 1976; Mack *et al.*, 1981; Mack *et al.*, 1983; Tortosa *et al.*, 1991). However, it was the pioneering work of Blatt & Christie, (1963) which demonstrated that the relative abundance of mono-polycrystalline quartz was a key to determine both the provenance and the maturity of sandstone.

There are several constraints on the use of the type of quartz as a provenance indicator :-

1. The abundance of monocrystalline quartz is partly related to grain size (Blatt & Christie, 1963; Blatt *et al.*, 1980 ; Basu *et al.*, 1975). As the grain size of the rock increases so the abundance of monocrystalline quartz decreases. The investigation of Blatt, (1967) showed that the number of crystal components in polycrystalline grains increases with increasing size (Fig. 3.5).
2. Polycrystalline quartz is less stable than monocrystalline quartz and also undulatory monocrystalline quartz is less stable than non-undulatory quartz (Blatt & Christie, 1963; Basu *et al.*, 1975).

The average concentrations of quartz in Lower, Middle and Upper Saq Sandstone are 90.97%, 94.29% and 95.66% respectively of the total volume of the rock. Quartz grains in the Saq Sandstone show slight to strong undulatory extinction, with a high proportion of the grains showing single outgrowth enlargements (Plate 3.2). Grain margins sometimes exhibit a corroded interpenetrations with clay minerals or carbonate.

The grains in the Saq sandstone are sub-angular to sub-rounded, moderately sorted, as a result of processes such as pressure solution and grain intergrowth. Hematite and clay coatings on grains show the original grains were rounded to well-rounded (Plate 3.3).

A large variety of detrital quartz grain types can be recognized in the Saq Sandstone and can be sub-divided into three classes: non-undulatory (unstrained), undulatory (strained) monocrystalline and polycrystalline, as defined by Blatt & Christie, (1963).

Non-undulatory monocrystalline

Non-undulatory monocrystalline grains are defined as a grains of quartz consisting of single crystal units which are completely extinguished upon very slight (less than one degree) rotation of the microscope stage (Blatt & Christie, 1963). They are characteristically produced from igneous and high grade metamorphic rocks but are also the end products of the breakdown of polycrystalline quartz and undulose monocrystalline quartz grains (Plates 3.4 and 3.5).

The average percentages of non-undulatory quartz of the total of monocrystalline grains are 43%, 58%, and 67% in Lower, Middle and Upper Saq Sandstones respectively. Since most of the Saq Sandstone fall within the medium sandstone grain size (up to 90%), the effect of grain-size on the relative abundance of quartz types is thought to be minimal. The slightly high abundance of non-undulatory quartz is therefore thought to be a consequence of either a source dominated by igneous rocks or the maturing of a metamorphic source which had few low grade metamorphic rocks.

Undulatory monocrystalline

Undulatory monocrystalline quartz is any single quartz crystal which is not completely extinguished upon a very slight rotation of the microscope stage. Quartz which has been subjected to considerable pressure shows strain shadows or undulatory extinction. The average proportion of undulatory quartz of the total of monocrystalline grains in Lower, Middle and Upper Saq Sandstone is 57%, 42%, and 33% respectively.

The quartz of Saq Sandstone is largely monocrystalline quartz, the polycrystalline grains seem less stable and tend to be eliminated (Blatt, 1967). Also, the proportion of

quartz with undulatory extinction tends to be lower for the same reasons (Blatt & Christie, 1963).

Blatt & Christie, (1963) observed that polycrystalline undulose quartz is not stable when it is transported and soon breaks-down to monocrystalline grains with undulatory extinction (Plate 3.4).

Polycrystalline quartz

Polycrystalline grains are those composed of two or more distinct crystals with different optical orientation (Plates 3.6 and 3.7). The boundaries between crystal may be either planar, curved, or sutured, Blatt, (1967).

The average proportions of the total framework of polycrystalline quartz in Lower, Middle, and Upper Saq Sandstone are 7.5%, 4.2%, and 2.6% respectively. There is a positive relationship between the grain-size of the sediments and the abundance of polycrystalline quartz (Figs. 3.5 and 3.6).

Many attempts have been made to utilise polycrystalline quartz grains as a guide to provenance, (Blatt & Christie, 1963; Blatt, 1967; Folk, 1974; Basu *et al.*, 1975; Young, 1976; Mack *et al.*, 1981; Mack *et al.*, 1983).

Young, (1976) used petrographic textures in detrital quartz grains as an aid to interpretation of composition of crystalline source rocks. He devised a polycrystalline quartz provenance diagram in which it was claimed, quartz populations with different provenance occupy different zones. Mack *et al.*, (1981) revised the classification but retained the three original stability fields: low grade metamorphic; high grade metamorphic; and plutonic polycrystalline quartz.

The classification of polycrystalline quartz grains into stable and unstable varieties was made using the methods of Young, (1976), who recognized a number of characteristics of quartz grains which he saw as indications of their possible stability. These include (1) the nature of contacts between crystals of polycrystalline grains (sutured contacts are unstable ; smooth contacts are more stable); (2) the type of extinction

(deformation bands are unstable ; grains with non-undulose extinctions are stable; and (3) crystal size (uniform size grains are more stable). These methods have been summarised as a flow diagram in Figure 3.7

According to these criteria, the majority of polycrystalline quartz grains in the Saq Sandstone are unstable (more than 80%), yet there are very few polycrystalline grains present (less than 8%).

This may be explained by (1) there being a source with abundant igneous rock and few low grade metamorphic rocks to yield the unstable polycrystalline grains (2) by the bulk of the sandstone being derived from a pre-existing sandstone formation and with there being a small additional amount being added by the basement.

The second alternative is accepted for the following reasons:

- (1) The bulk of the sandstone is seen from petrographic studies to comprise sub-rounded to rounded grains which suggest that the sands have been subjected to much reworking. This may have taken place within the environment of deposition, or by reworking of a pre-existing sandstone.
- (2) The presence of very well rounded overgrowths indicate clearly that there has been recycling of pre-existing sandstone.

The modified scheme employed by Mack *et al.*, (1981) involves a plot of polycrystallinity index versus instability index. The polycrystallinity index is the ratio of polycrystalline quartz to total quartz. The instability index is the ratio of unstable to total polycrystalline quartz. All Saq Sandstone samples are characterized by quartz populations with a high instability index and a low polycrystallinity index (Fig. 3.8). A high instability index is commonly related to low-grade metamorphic source rocks, which provide a large amount of unstable polycrystalline quartz (Young, 1976). A low polycrystallinity index is the result of the dilution of the quartz population with monocrystalline quartz from sedimentary source rocks, especially sandstones. Mack *et al.*, (1981) demonstrated that well sorted sandstones supply monocrystalline quartz in

amounts disproportionate to the surface area occupied by the sandstones in the source area (Mack *et al.*, 1983).

3.4.2 Feldspar

Feldspar is a minor constituent of the Saq Sandstone which rarely exceeds 1% of the total rock volume. Most of feldspar is generally weathered or more less replaced by clay (kaolinite), kaolinitization is common (Plate 3.8).

The average abundances of total (altered and unaltered) feldspars are 0.92%, 0.63%, and 0.53% in Lower, Middle, and Upper Saq Sandstone respectively.

3.4.3 Lithic fragments

Fragments of sedimentary rocks are the principle types present in Saq Sandstone which include fragment of sandstone and shale, some very few of metamorphic and igneous rock fragments (Plates 3.9 and 3.10).

The averages rock fragments in Upper, Middle, and Lower Saq Sandstone are 0.29%, 0.41%, and 0.74% respectively.

A qualitative estimate of the relative abundance of sedimentary and metamorphic source rocks is defined by the percentages of sedimentary rock fragment and metamorphic rocks fragments. The Saq sandstone is characterized by higher percentages of sedimentary rock fragment (90% of the total rock fragments) than metamorphic rock fragments, which indicates that the source area was dominated by sedimentary rocks.

3.4.4 Heavy minerals

Heavy mineral analyses is a proven method to decipher provenance of sand and sandstone (Morton, 1985, 1991). It has been valuable in paleogeographic reconstruction and for determining the setting of clastic rock sequences within an orogenic cycle (Krynine, 1942; Van Andel, 1959), provided that diagenetic alteration is limited (Pettijohn, 1941; McBride, 1985).

Accessory heavy minerals are usually scattered throughout the Saq sandstone and may also occur as distinctive laminae in some deposits such as beach deposits. Heavy minerals rarely exceed one percent and commonly form less than 1 percent of the rock constituents.

Following disaggregation of sandstone samples, heavy minerals from more than sixty samples were separated from the 3 ϕ and 4 ϕ fractions of each samples using gravity-settling in bromoform (sp. gr. 2.81). The resulting separations were mounted and examined under the petrographic microscope with heavy minerals being estimated by counting an average of 100 grains of each fraction.

The heavy mineral assemblage of the Saq Sandstone consists of both opaques and nonopaques. The opaques which are volumetrically more abundant (36.04%) include ilmenite and magnetite and some hematite, the nonopaques include zircon (24.14%), tourmaline (27.20%), rutile (12.34%) and sphene (0.12%), Figs. 3.9 and 3.10.

The Saq Sandstone is characterized by an assemblage of very rounded stable heavy minerals such as opaque, zircon, tourmaline, rutile and sphene (Plates 3.11 and 3.12).

Opaque minerals

Opaque heavy minerals are common in all the examined samples. They are mostly composed of magnetite and ilmenite with less hematite. They occur as rounded to well rounded grains. Opaque minerals are more abundant in the 3 ϕ fraction than the 4 ϕ fraction.

The average percentages in the Lower, Middle, and Upper Saq Sandstone are 44.30%, 33.41%, and 30.76% respectively.

Non-opaque minerals

Zircon, tourmaline, rutile and sphene are the only abundant non-opaques heavy minerals in the Saq Sandstone.

Zircon

Zircon is an ultra-stable mineral, it is very hard, inert and can survive much recycling (Folk, 1974). Zircon crystals initially by crystallisation from a magma and they develop typically as euhedral or subhedral, sharply-faceted crystals. Weathering of igneous rocks normally causes little or no change in the morphology of zircons. However, when subjected to aqueous transport, such zircons become rounded to varying degrees due to attrition.

Zircon is generally considered to be primarily of igneous origin but may be produced in very high grade metamorphic rocks (Deer *et al.*, 1983). However, a purely magmatic origin for zircon has been questioned in a controversial paper by Saxena, (1966). He suggests that authigenesis and low-grade metamorphism may not only generate outgrowths, but in suitable environments, can form zircon by authigenesis (see also Goold, 1986).

The mean average percentage of zircon in the 4 ϕ fraction is more than in the 3 ϕ fraction. This due to the small size of the zircons, which tend to accumulate in the very fine fractions.

The zircon grains recognized in the Saq Sandstone are mainly well rounded to subrounded with few subhedral grains. They are colourless, commonly worn and contain a variety of minute inclusions. This suggests that most of the Saq Sandstone zircons are likely either to have undergone weathering and abrasion for long periods or they are recycled and derived from pre-existing sedimentary sources. A very few zircons may be first cycle grains, having been derived from plutonic source.

Tourmaline

Tourmaline is one of the most widespread of the nonopaque heavy minerals in sediments.

The mean average percentages of tourmaline in the Lower, Middle, and Upper Saq Sandstone are 24.20%, 32.39%, and 25.03% respectively. It occurs in a variety of

colour. Brown predominates, in shades ranging from red-brown, through yellow-brown. Brown and yellow-brown varieties are the most common and probably derive from a metamorphic source (Blatt *et al.*, 1980).

Tourmaline is a relatively complex silicate mineral. It is typically a mineral of granite pegmatite, pneumatolytic veins, and of some granites, and is also commonly found in metamorphic rocks. Phillips & Griffen, (1981); Deer *et al.*, (1983); Morton, (1991) reported that in granites or pegmatic rocks tourmaline is usually Fe-rich schorl or elbaite while dravite and uvite which are usually Mg-rich are typically metamorphic or metasomatic origin.

Electron microprobe analyses were carried out on few grains of tourmaline from the Saq Sandstone (Table 3.5, Appendix A).

Morton, (1991) used MgO and FeO variation in tourmaline to discriminate between tourmalines from granites, pegmatic, metamorphic or metasomatic rocks. The same technique used for samples from the Saq Sandstone.

The majority of the tourmaline grains fall in the dravite field which indicates a metamorphic origin. A few grains are schorl (Fig. 3.11).

Rutile

This mineral is common in all studied samples but less abundant than zircon and tourmaline. The averages of rutile in the Saq Sandstone are 11%, 11.20%, and 14.82% in Lower, Middle, and Upper respectively. Rutile grains range in shape from sub-rounded to rounded, with a few elongated grains. They are mainly reddish-brown to dark red coloured. Rounded rutile grains are more abundant (97%) than euhedral grains.

Sphene

The average of sphene in the Lower, Middle and Upper Saq Sandstone is 1.82%, 1.2% and 0.92% respectively. It forms colourless, rounded to sub-rounded grains.

3.4.5 Mica

Muscovite is more abundant in fine sandstone of the Upper Saq Sandstone, than Lower and Middle units. The averages are 0.26%, 0.28%, and 0.83% in Lower, Middle, and Upper Saq Sandstone respectively. Because of their thin sheet like shape and consequent lower settling velocity, they are associated with fine grained quartz. Clear fresh grains of muscovite occur throughout the formation and may be parallel with bedding or, in more compressed samples, considerably bent around the enclosing quartz grains (Plate 3.13). When suffering alteration they expand and are replaced by kaolinite (Plate. 3.14).

A few detrital muscovites were analyzed with electron microprobe. They are rich in K_2O (about 10%) and low in MgO , Na_2O , and TiO_2 (Table 3.6 - Appendix A).

Muscovite is one of the most common of the micas and occurs in a wide variety of rocks. It occurs in a wide range of regionally metamorphosed sediments. In low grade metamorphism it is found in albite-chlorite-sericite schists or in sericite phyllites where the original sediments were rich in aluminium. At the highest grades of metamorphism muscovite is commonly dissociated to form potassium feldspar and sillimanite. Muscovite is less common in igneous rocks, and is generally found in muscovite-biotite granites (Deer *et al.*, 1983).

By comparing the muscovite analyses from the Saq Sandstone with other muscovite analyses from different localities reported by Deer *et al.*, (1983); Millar *et al.*, (1981); Pigge, (1982) it seems that the muscovite from the Saq Sandstone could have been derived from low grade metamorphic rocks.

3.4.6 Clay minerals

Clay minerals are finely crystalline hydrous silicates of aluminium, iron, and magnesium. They are represented by kaolinite, smectite (montmorillonite), illite and vermiculite. Clay forms 25%- 35% of the terrigenous fraction of sedimentary rocks (Folk, 1974).

The average content of clay minerals in Lower, Middle and Upper Saq Sandstone is 1.32%, 1.06% and 0.77% respectively.

There are three ways in which clay minerals can originate in sandstones:(1) as detrital particles or aggregates brought into the basin of deposition through erosion and redistribution of previously existing rocks, including soils, (2) by in situ alteration of unstable detritus (feldspars, micas, etc) subsequent to deposition, and possibly burial, (3) by deposition from solutions in the intergranular pores of sediments during diagenesis as an interstitial cement (Carrigy & Mellon, 1964).

The study of clay minerals has been and still is, for that mater, greatly hampered by the innate character of material which , by its definition is of small particle size. Particles of this size-range are easier to study by x-ray diffraction (XRD) or scanning electron microscope (SEM).

1 X-ray diffraction (XRD)

The x-ray diffractogram consists of an x-y plot of diffraction angle versus intensity of diffracted radiation. The angles 2θ must be converted into molecular plane repeat distances (d-spacings) in Angstrom (\AA) units. This conversion is based on the Bragg equation.

$$n \lambda = 2d \sin \theta$$

Where :

$$n = 2 d \sin \theta$$

d = distance

λ = wavelength

n = multiplan of x-ray

In actual practice the Bragg calculation is rarely made; prepared tables of 2θ angle versus d-spacing are available for all the common x-ray wavelengths, (Grim & Johns, 1954; Grim, 1962; Carroll, 1970; Chen, 1977).

Method

The less than 2 μm fraction was analyzed in 73 samples. The samples were first disaggregated and dry sieved to 62 μm to obtain the silt and clay fraction. The silt and clay were ultrasonically agitated then the less than 2 μm fraction was obtained by centrifugal sedimentation in distilled water.

An oriented specimen was prepared for x-ray diffraction analysis (XRD) by smearing a paste of material onto a glass slide, and allowing the clay-water suspension to dry on the glass overnight. Diffraction patterns were obtained for three preparations: air dried, ethylene-glycol saturated, and heated to 450-550°C for one hour. XRD analyses were run on a Phillips x-ray diffractometer using Ni-filtered Cu-K α radiation. Scans were run at a goniometer speed of 2° per minute.

Clay minerals can be identified more easily by diffraction analysis of their basal (001) crystallographic planes, so the oriented aggregates prepared as indicated above give the best possible diffraction data.

After comparing d-spacing (\AA) values with standard clay minerals tables, kaolinite is the only clay mineral found in all the samples of Saq Sandstone. It is characterized by a series of basal x-ray diffraction peaks at about 14 \AA , and 7 \AA , which remain unchanged upon glycolation or thermal heating to 450°C, but the structure collapses to an x-ray amorphous mineral on heating to 550°C (Figs 3.12 to 3.14).

A few mud-clasts from the Saq Sandstone also have been analysed by x-ray diffraction. Kaolinite is the mainly clay mineral found, with some illite (Fig. 3.15).

2 Scanning electron microscope (SEM)

Many workers have used the scanning electronic microscope (SEM) to identify the type and origin of clay minerals (Hayes, 1970; Pittman, 1974; Kantorowicz, 1984).

In order to identify the clay minerals in the Saq Sandstone 27 samples have been examined using Cambridge Instruments S360 Scanning Electron Microscope with

integrated Link analytical A N 10,000 series EDX, system. Samples were coated with a gold palladium alloy.

Kaolinite is the only clay mineral to have been found from all the samples of the Saq Sandstone, (Plates 3.15)

Kaolinite is the common authigenic clay in the Saq Sandstone. It is generally present as pseudo-hexagonal stacked plates (books). The kaolinite may completely fill pore spaces or may occur as small books growing into pore spaces from detrital grains. The following criteria suggest that the kaolinite is of authigenic origin (Shelton, 1964; Wilson & Pittman, 1977):

1. Delicate crystal form and relatively large size
2. Presence within well sorted sandstones.
3. Absence of kaolinite at grain to grain contact.
4. Scattered and sporadic distribution in the sandstone.

3.5 Ferricrete

Fragments from a ferricrete palaeosol have been recognized in the bioclastic conglomerate of the Upper Saq Sandstone, (Subfacies 9c - Chapter 2). These represent a regional unconformity between the Saq Sandstone and Hanader Shale (Tabuk Formation).

The palaeosol is characterized by iron cemented rounded clasts up to 2cm diameter, which comprise a thick iron coatings on clasts containing sandstone and quartz grains (Plate 3.16, Fig. 3.21) and also inarticulate brachiopod shells (Plate 3.17, Fig. 3.22). The rounded clasts are clearly eroded from an earlier deposit where these iron cemented sands occurred (McBride, 1974; Elston, 1976; Meyer, 1976).

There are no clasts of sandstone present without iron cement i.e. there is no evidence of any other mechanism of cementation such as might be produced during deep burial. On this basis it is thought likely that the source was made of sand and iron oxide

cemented sand ; the sand was reworked into the new deposit and the iron cemented sand was broken down into fragments and then rounded into pebbles. The source of ferricrete was possibly a marine sand sequence slightly older than the sequence containing the clasts (Fig. 3.16). The ferricrete probably formed along porous shell beds in the older formation, since a high proportion of brachiopods shells have been coated by the iron.

3.6 Diagenesis of the Saq Sandstone

Diagenetic processes can cause significant changes in sandstone composition. The most common diagenetic alterations are complete or partial dissolution or replacement of chemically unstable detrital grains and introduction of pore-filling cement.

Texture, chemical composition, compaction of the sediments, type and movement of pore water, regional properties such as the burial depth of the sandstone, and biological activity are the main parameters which control diagenetic processes in sediments.

The Saq Sandstone displays a variety of diagenetic features, indicative of both mechanical and chemical diagenesis, which reflect alteration by two diagenetic processes. These are compaction and cementation. The broad relative order of diagenetic processes can be determined by examining the textural relationships between the authigenic minerals and the detrital framework grains (Fig. 3.17).

3.6.1 Compaction

The degree of compaction varies considerably, ranging from nearly uncompacted to strongly compacted sandstone, the observed features are due two processes: mechanical and chemical compaction. Compaction by mechanical processes involves movement by slippage between grains and the breaking, or fracture. Chemical compaction or pressure solution is indicated by dissolution at grain to grain contact in an uncemented sediment or within a cemented sediment, by dissolution being concentrated along a particular surface, usually irregular, termed a stylolite (Harwood, 1988).

Mechanical compaction effects in the Saq Sandstone are more clearly shown in the detrital micas, which are slightly to strong bent. Micas show increasing bending in progressively deeper-buried sandstones (Plate 3.13). Some metamorphic rock fragments may be bent or crushed in deeply buried samples (Plate 3.6).

Convex-concave (Plates 3.19, 3.23) and sutured contacts between quartz grains are less common in the Saq Sandstone. These two kinds of interlocking grain boundaries generally may be taken as evidence of chemical compaction or pressure dissolution, but studies by luminescence petrography show that interlocking crystal of overgrowth cement can also produce sutured contacts (Sippel, 1968; Sibley & Blatt, 1976).

The following petrographic and luminescence evidence indicates that consertal quartz in the Saq Sandstone is not all due to pressure solution, but the majority is more likely to result from overgrowth cementation (Plate 3.18). In only a few thin sections from the Saq Sandstone has a chemical or pressure solution been observed (Plate 3.18, 3.19).

3.6.2 Cementation

Cementation of the Saq Sandstone is variable, consisting of iron oxide, carbonate, silica, and authigenic kaolinite. Based primarily on microtextural (fabric) relationships, the sequence of cement was secondary quartz, early calcite, iron oxide, late calcite, and authigenic kaolinite (Plate 3.20)

1. Secondary quartz

Secondary quartz usually forms optically continuous overgrowths on detrital quartz grains. The quartz cement is normally separated from the detrital grains by rings of iron oxide or clay minerals, but in few cases it is inclusion-free. A mosaic texture develops where secondary quartz overgrowths are abundant.

The maximum degree of quartz overgrowths is present in medium to coarse sandstones, which possess the highest porosity and was rapidly compacted during the

early burial of the sandstone. The overgrowths had sufficient space in which to develop perfect euhedral forms (Plate 3.21).

The Lower and Middle Saq Sandstone composed mainly of medium to coarse sand size grain, contains the highest proportion of quartz overgrowth, while the Upper Saq Sandstone is composed mainly of fine to very fine sand sized grain which has less quartz overgrowths

Siever, (1962); Buck & Mankin, (1971), published evidence suggesting that quartz overgrowths are the first diagenetic precipitate and characterize early burial.

The sources of silica may be internal (intergranular pressure solution, stylolitization, dissolution of siliceous framework grains) or external (weathering products carried in meteoric water, derived from clay mineral diagenesis and/or dissolution of siliceous skeletons in associated mudstones) to the sandstone formation (Houseknecht, 1988). In this study the major source of silica is not clear but dissolution of siliceous framework grains such as feldspar is considered as the principal source in the Saq Sandstone with some contribution from intergranular pressure solution.

2. Carbonate

The distribution of calcite cement is different throughout the Saq Sandstone and calcite was introduced to the formation at various stages. The calcite is mostly poikilotopic, occurring as large crystals of up 1mm diameter and enclosing grains of quartz and feldspar. Sometimes it occurs as imperfect rhombs that fringe detrital grains (Plate 3.22). The average amounts of carbonate cement in Lower, Middle, and Upper Saq Sandstone are 1.42%, 1.16%, and 1% respectively.

Dapples, (1971) interpreted poikilotopic calcite cements in sandstones to as products of slow precipitation from dilute solutions. Folk, (1974) stated that poikilotopic calcite precipitates at a slow rate from fluids deficient in magnesium.

Conditions necessary for precipitation of calcium carbonate include increasing the (Ca^{2+}) (CO_3^{2-}) product in pore waters by an increase in the pH of the environment,

probably due to an increase in temperature (Buck & Mankin, 1971). The ease of precipitation of calcite cement in sandstones increases with burial depth because calcite solubility decreases with increasing temperature (Siever, 1962).

3. Iron oxide

The averages of iron oxide cement in Lower, Middle, and Upper Saq Sandstones are 2.63%, 0.57%, and 0.16% respectively. It is present as a pore filling and is generally associated with clays, sometime coating secondary growths and detrital grains. Hematite is the dominant ferruginous cement. It is generally accepted that the red pigment in red beds may be to the transformation of ferric hydroxide into hematite under high Eh and pH conditions (oxygenated environment), or to the presence of original red pigment derived from pre-existing red beds.

The origin of red beds has been controversial for many years. Dunbar & Rodgers, (1957); Van Houten, (1961, 1964, 1968, 1973) and Glennie, (1970) have reviewed the problem in some detail.

The major source of iron oxide is not clear, but the observed evidences indicate that the colour red beds has at least two origins. Sediments derived from pre-existing sandstones are in part red, and some of the red colour is thus primary and reflects red clastic detritus, (Plates 3.23). Secondly, iron-bearing minerals were altered by intrastratal solutions, providing some additional red colour.

4. Kaolinite

The final step in the diagenetic sequence interpreted for the Saq Sandstone is the development of authigenic kaolinite, partially filling pore spaces and in a few cases replacing some feldspar or mica grains. Kaolinite is generally precipitated under acidic conditions (Garrels & Christ, 1965; Karen & Weimer, 1982).

3.7 Cathodoluminescence petrography

The cathodoluminoscope has evolved as a powerful petrographic tool in carbonate studies since its development 20 years ago. Smith & Stenstrom, 1965; Sippel, 1968; Sibley & Blatt, 1976; Zinkernagel, 1978; Ramseyer *et al.*, 1988, have applied the cathodoluminoscope in studies of silica authigenesis

The most common colour of quartz luminescence is dull red which may indicate a low temperature igneous or sedimentary origin. Some quartz luminesces blue and this is produced at high temperatures. Authigenic quartz is commonly non-luminescent (Smith & Stenstrom, 1965).

Generally most of the quartz grains from the Saq Sandstone luminesce dull red (> 75%), with fewer grains showing blue luminescence (Plate 3.24).

Luminescence has been used here to identify the original roundness of quartz grains to compare this with Pettijohn's roundness grades (Pettijohn, 1975). Most of the grains were sub-rounded to rounded- p (ρ) = 0.315 to 0.50 (Plate 3.18).

3.8 Maturity of the Saq Sandstone

Major sand bodies composed of quartz arenite are found in many parts of the geological record, but they are particularly common in Cambro-Ordovician sequences. There has been a good deal of discussion over the ways in which quartz rich sands can be generated (Krynine, 1941; Suttner *et al.*, 1981; Pettijohn *et al.*, 1984; Suttner & Dutta, 1986; Chandler, 1988; Johnsson *et al.*, 1988; Schieber, 1989; Soegaard & Eriksson, 1989).

For the Saq Sandstone four possible origins are envisaged: (1) Reworking of sediments during deposition; (2). Reworking of sediments belonging to an older phase of deposition; (3). Reworking of sediments belonging to an older cycle (*i.e.* a pre-Saq cycle of deposition) and (4) Reworking directly from the basement. These are summarized in Figs. 3.18. and 3.19.

3.8.1 Reworking of sediment during deposition

This occurs during the depositional process where sands in megaripples or bars are reworked out of one form to another; or where megaripple sheets or bars, which had been abandoned by a change in tidal path, were subsequently reworked to be incorporated into new bed-forms. Evidence for this type of reworking may be seen in broken shell-beds and in beds with rounded mud clasts within the Saq Sandstone.

3.8.2 Reworking of sediments belonging to an older phase of deposition

This type reworking involves the erosion and deposition of sediments which were buried or laid down under one set of conditions (e.g. during a given tectonic regime or a given sea-level) and were then re-eroded when these condition changed. In this way sediments at the basin edge such as former beaches or coastal deposits, may be reworked into the new cycle. Tidal scour may also could reach deep enough into the shelf to erode sediments belonging to an earlier stage of sedimentation (but which was still part of the Saq cycle).

Evidence for this type of reworking comes from the clasts of ferricrete. These are thought to have formed in palaeosols which developed on older Saq sediments which were otherwise uncemented. Such palaeosols developed on the margins to the Saq basin and were reworked during transgression of the sea.

3.8.3 Reworking of sediments belonging to an older cycle

In this instance, a source in a sediment which did not belong to the Saq cycle is envisaged. This might occur if the Precambrian-Cambrian basement was covered by a sedimentary formation which was lithified and then eroded to provide the source for sediments accumulating during the new transgression. In this instance, the Red bed deposits the newly defined Idwah Formation, which rest unconformably upon the basement (Location K-26), may be that earlier formation. These beds were reworked into the Saq Sandstone, during a second phase in which subsidence affected the basement.

At the base of the Saq Sandstone the red beds are sometime overlain by quartz rich Saq beds which have a pink-red colour and may have been derived from these older deposits.

Petrographic features suggest that at least some of the Saq Sandstone was derived from pre-existing sandstones. Sedimentary rock fragments (Red sandstone), quartz grains with abraded overgrowths, double rounded overgrowths and a stable very well rounded heavy mineral assemblage (opaque, zircon, tourmaline, rutile and sphene) are all features that suggest contributions from pre-existing sandstone sources.

3.8.4 Reworking directly from the basement

Sediments reworked directly from the basement into the overlying Saq, can be seen at many places just above the unconformity. In these areas angular blocks of basement rock occur in breccias which may be as much as 1m thick. These breccias have within their matrices sand grains, some of which are angular and some well rounded. The angular grains have come directly from the basement rocks while the rounded grains clearly belong to an older sandstone.

It is very clear that the input directly from the basement is negligible. The sandstones, often resting directly on a granitic basement are quartz arenites- and this can only be explained by the sands having been derived from an entirely different source.

From these data and the reasoning already expressed, an estimate of the relative importance of the four process is given in Figure 3.20. Derivation from older formation is thought to be the biggest single factor which enhanced the maturity of the sandstone. Derivation directly from the basement is not thought to be important

3.9 Conclusions

From the foregoing data the following conclusions are drawn:

- (1) The Sandstone from Upper, Middle, and Lower Saq Sandstone are quartz arenite in composition.
- (2) Texturally the Saq Sandstone is mature sediments, and display an upward increasing in the maturity.
- (3) Monocrystalline quartz is the most abundant detrital minerals in the Saq Sandstone.
- (4) Most of quartz grains in the Saq Sandstone was originally well rounded but have been altered by the effect of overgrowths.
- (5) Saq Sandstone characterized by very restricted heavy minerals assemblage which include zircon, tourmaline, rutile, sphene and opaque minerals.
- (6) Kaolonite is the only authigenec clay minerals in the Saq Sandstone, and mostly originate either directly from dissolution of feldspar or muscovite or through flush the formation by fresh water during the progradations.
- (7) The framework mineralogy indicate that the Saq Sandstone was derived largely from a craton interior possessing pre-existing and recycled sedimentary rocks.
- (8) Studies of polycrystalline quartz suggest mixed source for the Saq Sandstone which include low grade metamorphic and pre-existing sedimentary rocks sources which would have yielded sediments faster than the basement.
- (9) There is however a sediments yield from the basement and this is recognised in the Lower Saq Sandstone as a thick breccia (up to 1m) and red coloured sandstones rich in rock fragments, and also in the presence of unstable polycrystalline grains in rest of the Lower Saq sequence.

Table 3.4 Average mineralogy of the Saq Sandstone

	Quartz				Feldspar	Rock Frag.	Micas	Cement				Heavy Mineral
	Mono.		Poly.	Chert				Kaolinite	Carbo- nate	Iron	Silica	
	Undu.	Non- und.										
Upper n=42	92.48		2.6	0.58	0.53	0.29	0.83	0.77	1.00	0.36	0.16	0.40
	33	67										
Middle n=94	89.17		4.2	0.92	0.63	0.41	0.28	1.06	1.16	0.57	0.39	0.35
	42	58										
Lower n=48	82.51		7.5	1.54	0.92	0.74	0.26	1.32	1.82	2.63	0.13	0.61
	57	43										

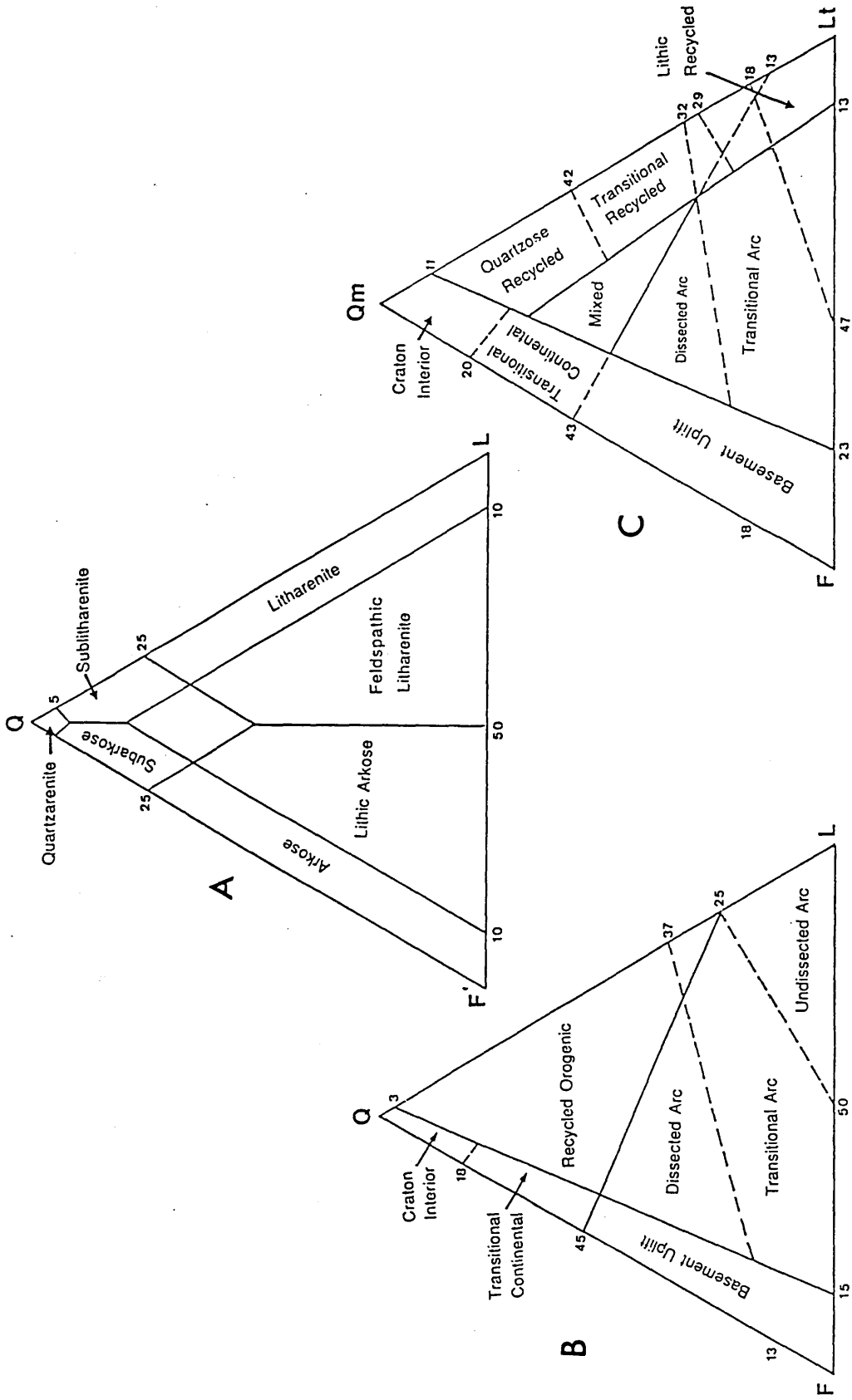


Fig. 3.1 Reference diagrams for petrographic data. (A) QFL diagram (after McBride, 1963) for classification of sandstone; (B) QFL; (C) QmFLt (after Dickinson et al., 1983) to decipher provenance.

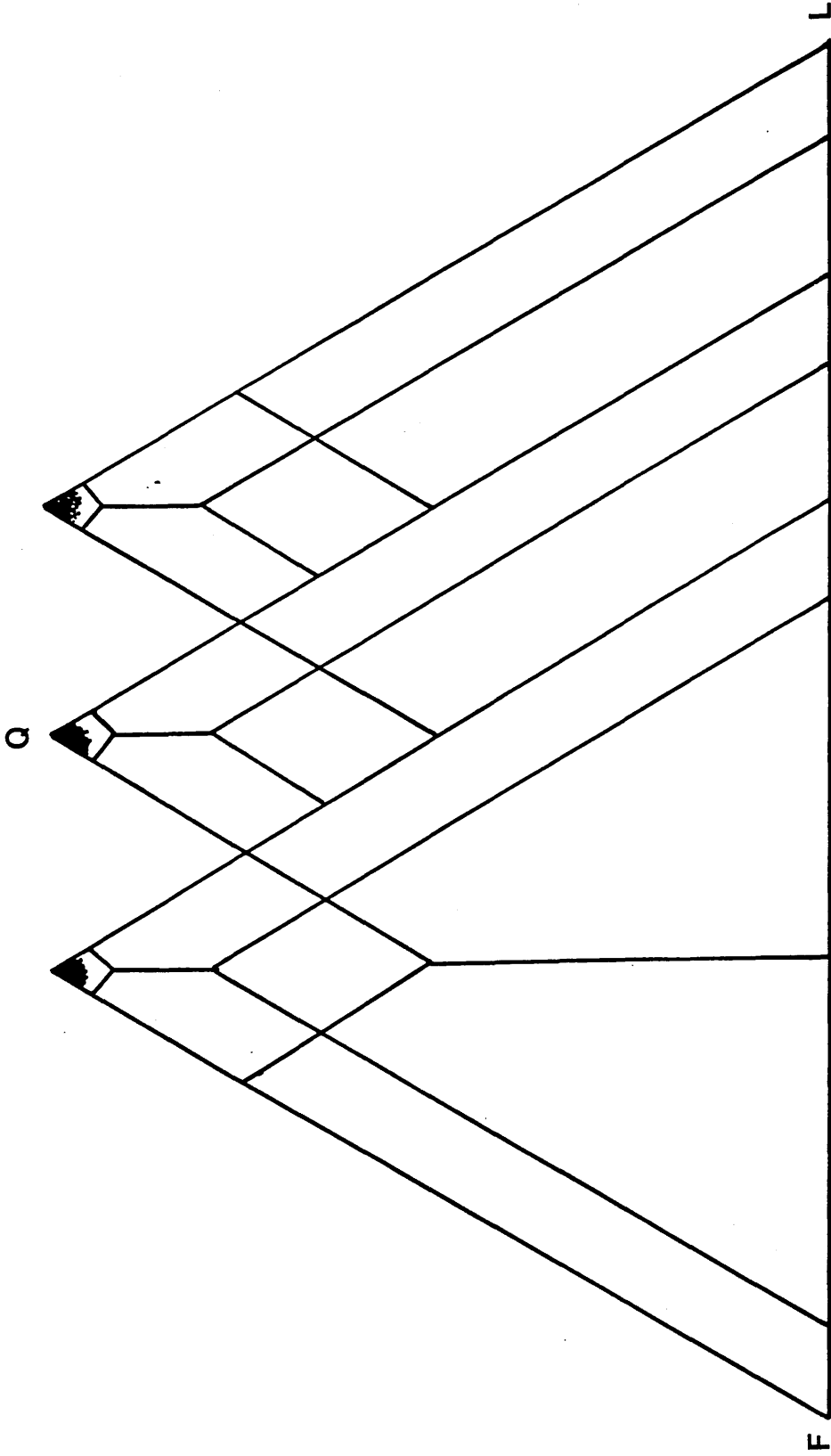


Fig. 3.2 QFL diagrams showing the composition of the Saq Sandstone.

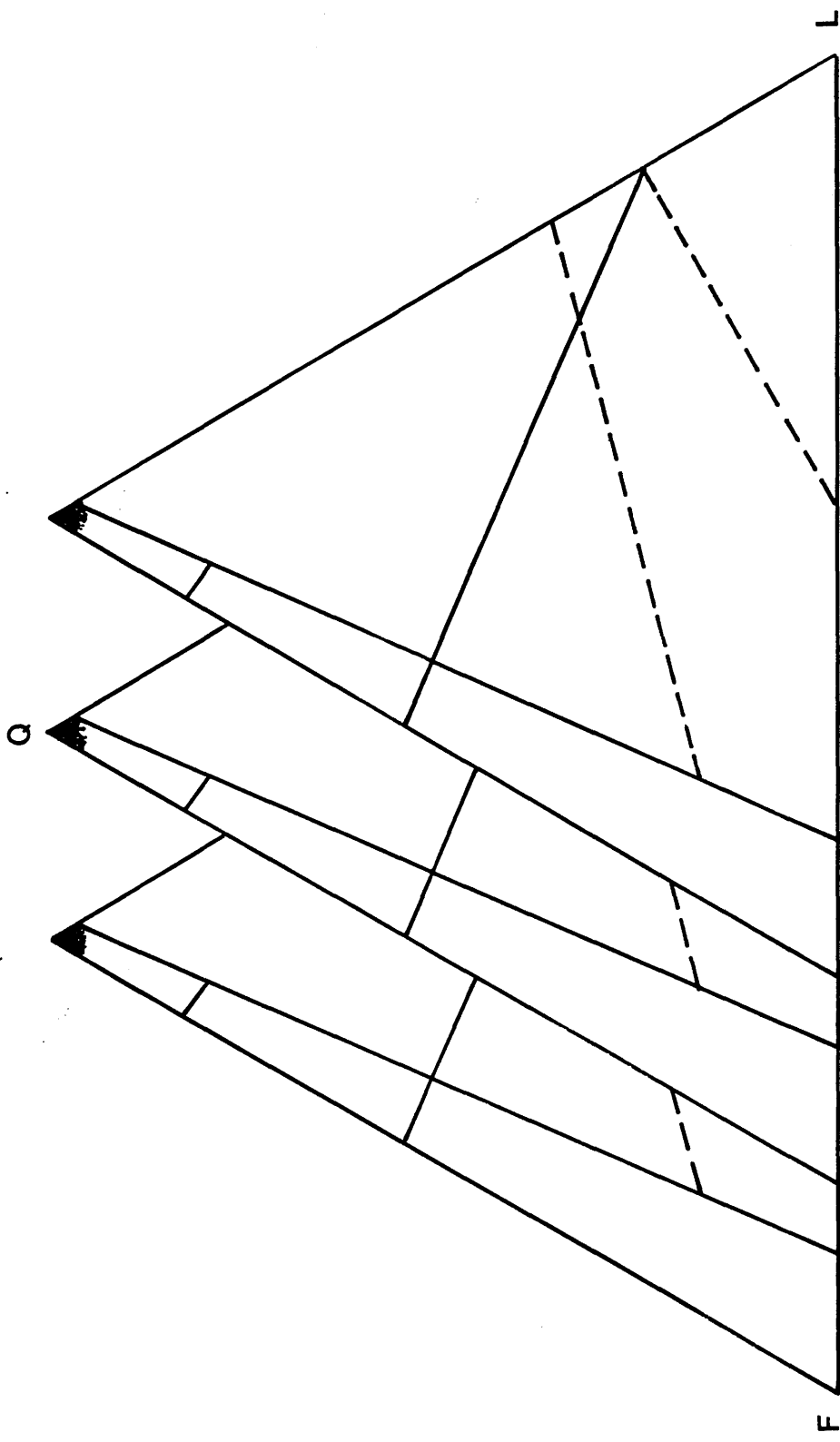


Fig. 3.3 QFL diagrams to decipher the provenance of the Saq Sandstone.

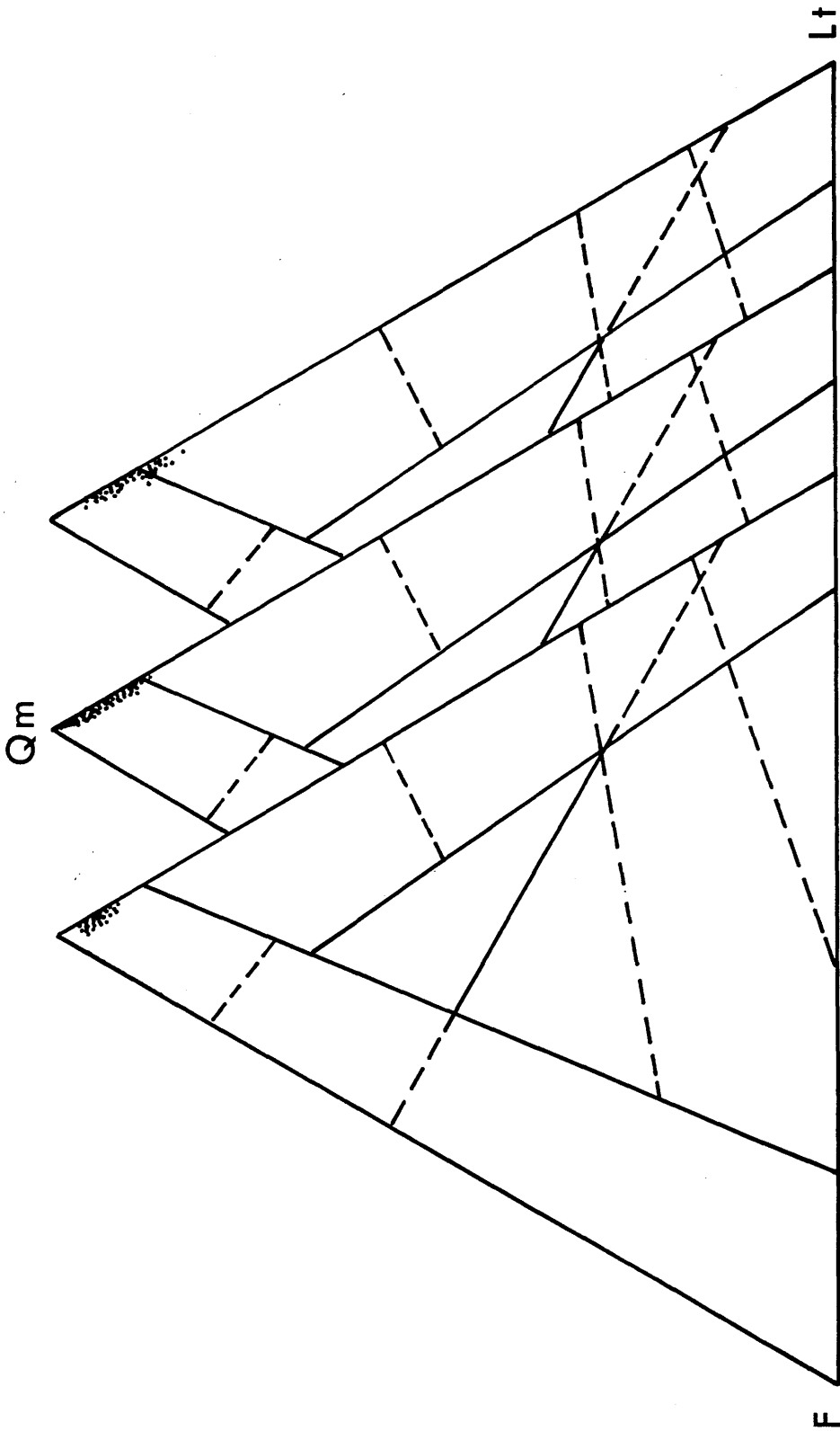


Fig. 3.4 QmFLt diagrams to decipher the provenance of the Saq Sandstone.

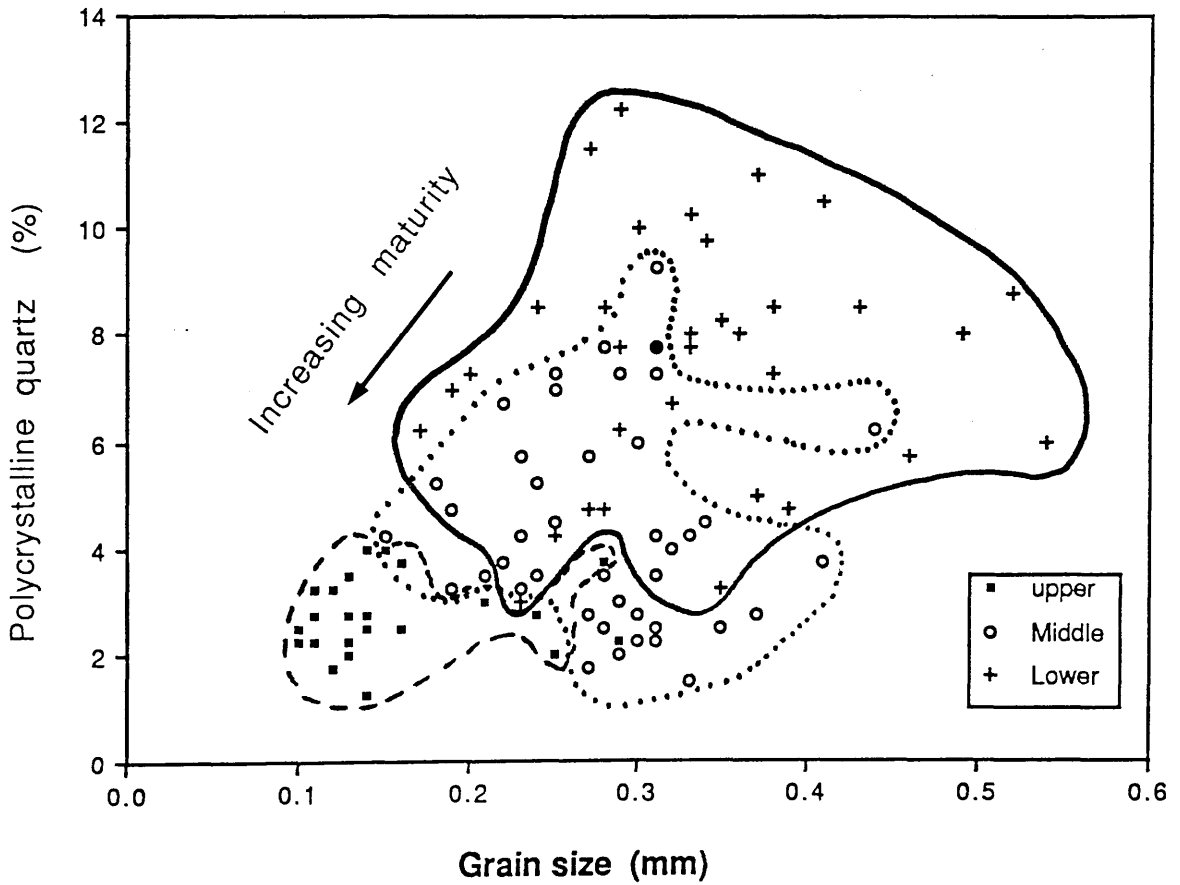


Fig. 3.5 Plot of polycrystalline abundance and grain-size (mm) which shows positive correlation.

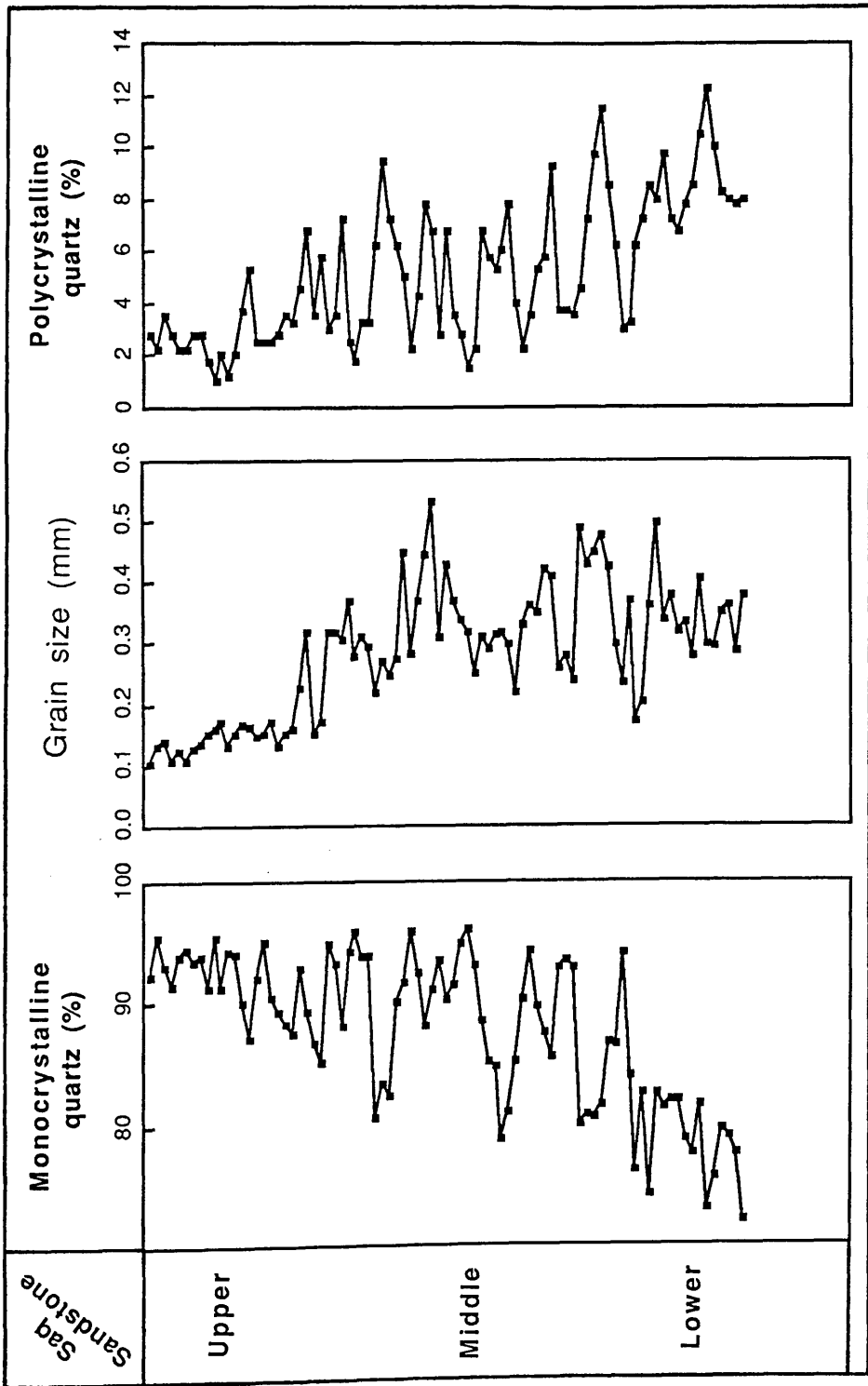


Fig. 3.6 Vertical variation of grain-size and type of quartz (Qm, Qp).

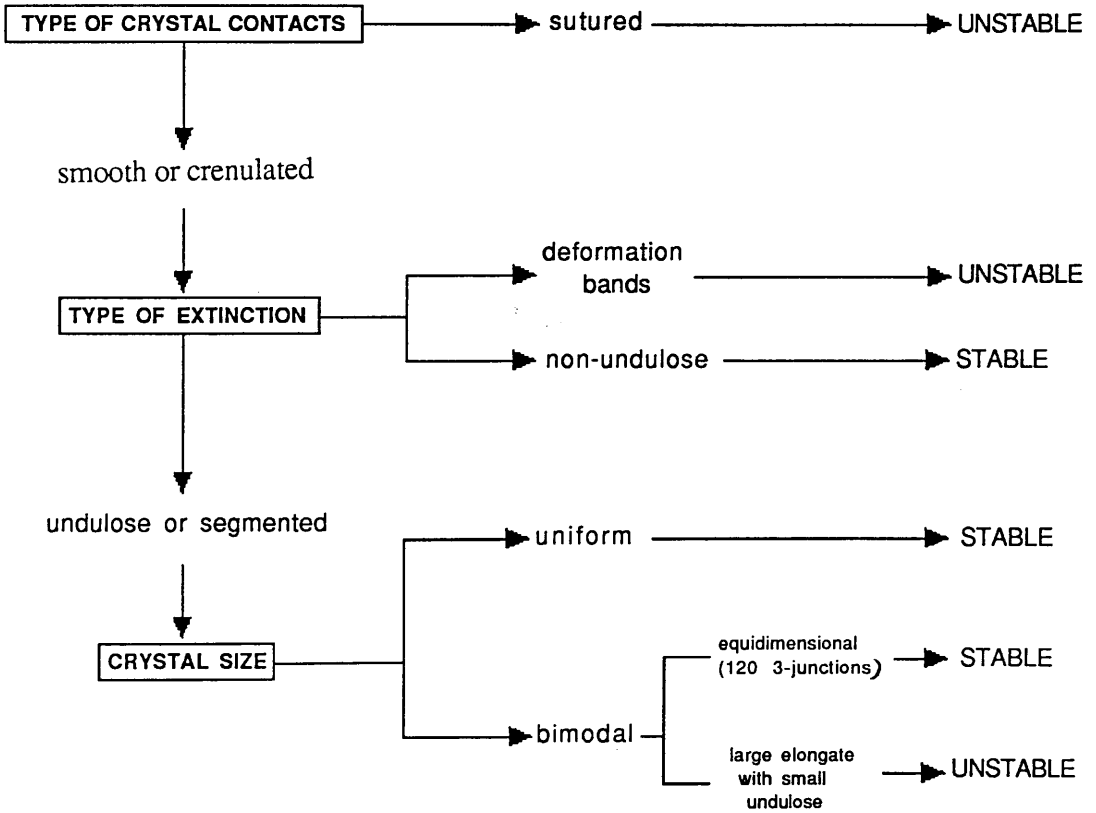


Fig. 3.7 Flow diagram for determination of stable and unstable polycrystalline quartz (adapted from Young, 1976; Goold, 1986).

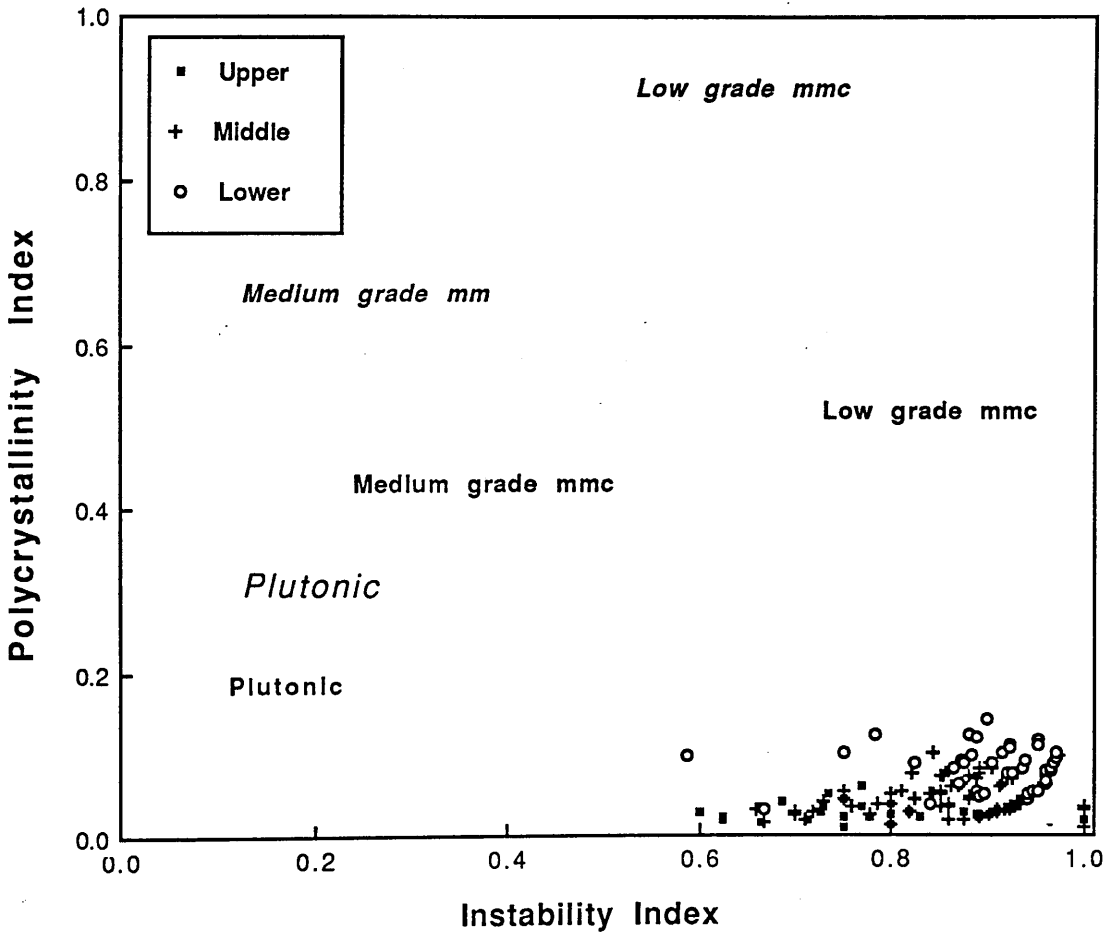


Fig. 3.8 Instability index vs. polycrystalline index to discriminate provenance of detrital polycrystalline quartz (Mack et al 1981 (Normal print) and Mack et al., 1983 (Italic print), Young, 1976; Goold, 1986).

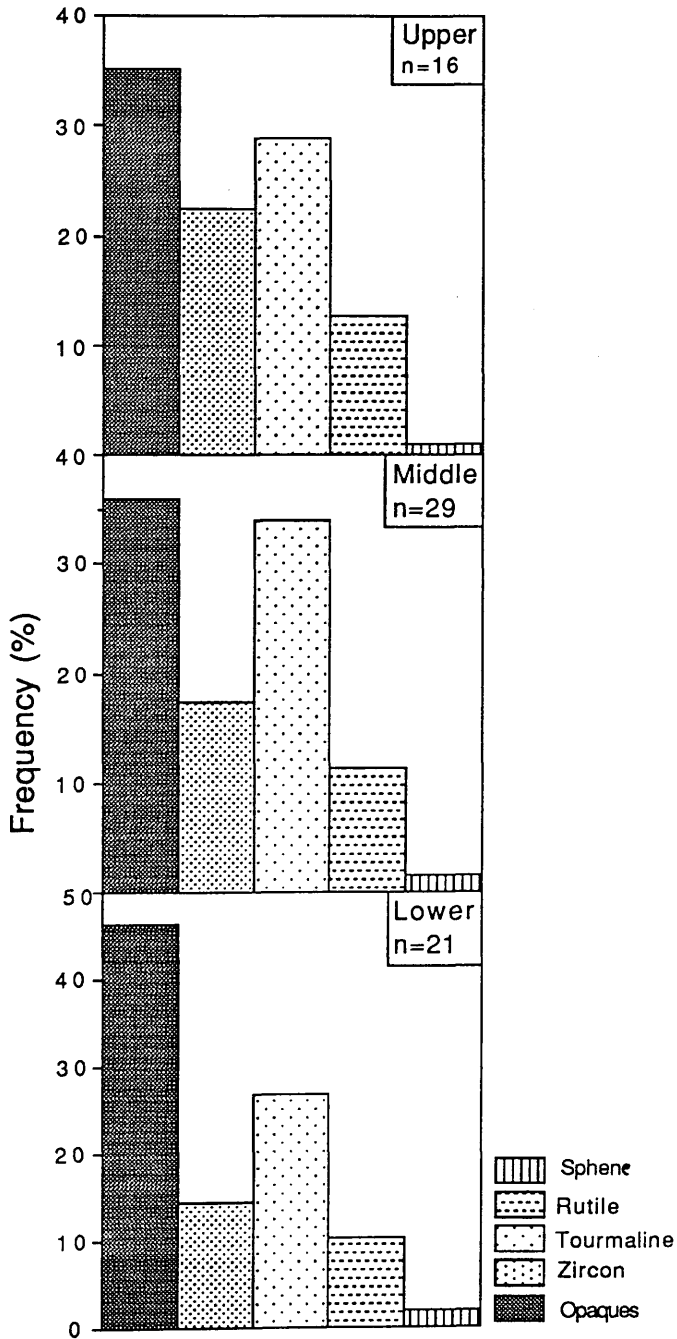


Fig. 3.9 Distribution of averages of heavy minerals of the Saq Sandstone (3 phi).

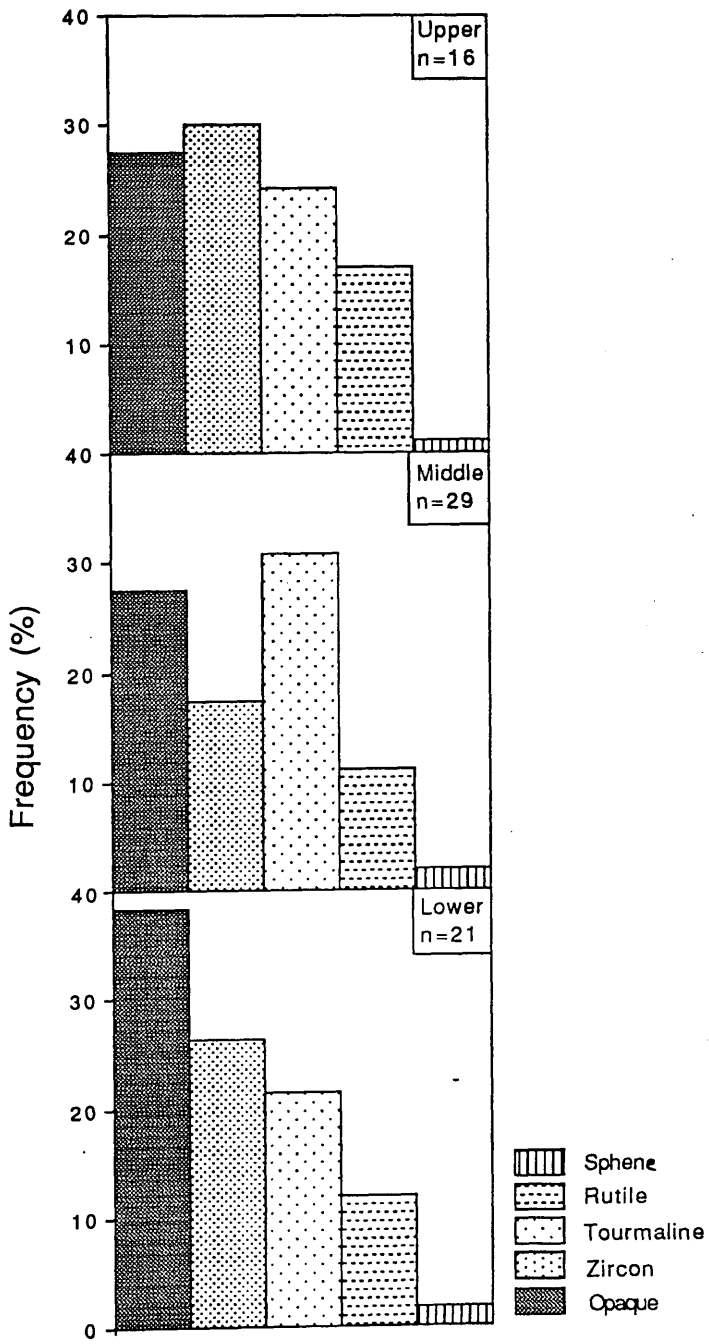


Fig. 3.10 Distribution of averages of heavy minerals of the Saq Sandstone (4 phi).

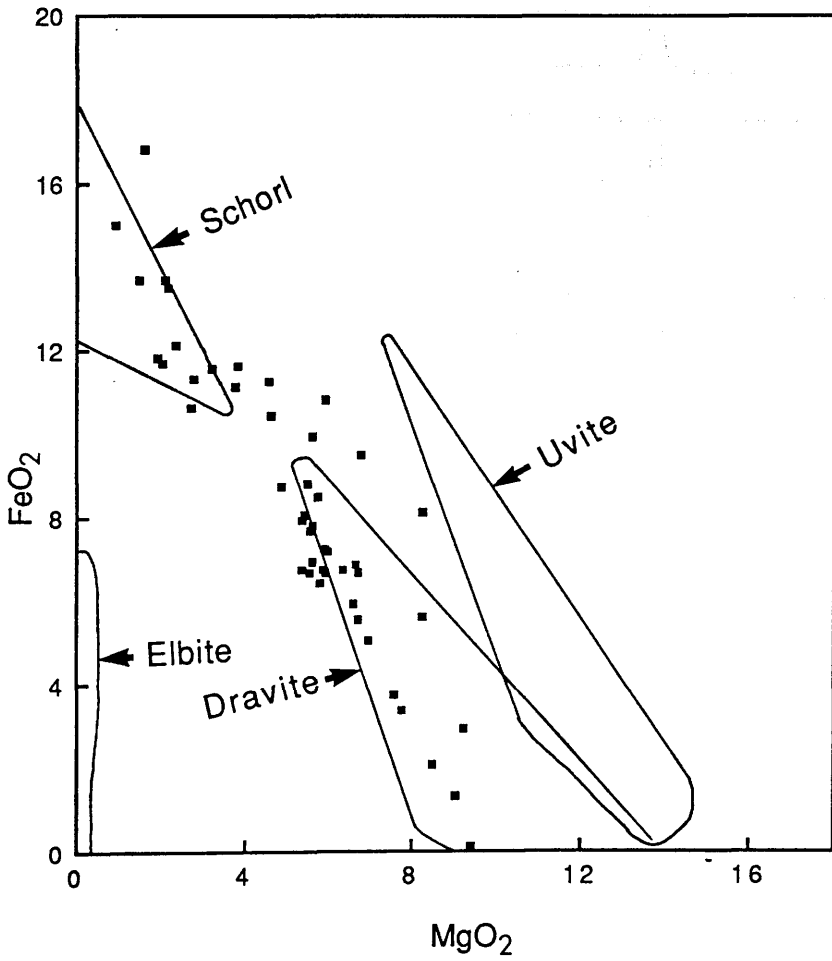


Fig. 3.11 Variation of FeO and MgO contents of detrital tourmalines (Morton, 1991).

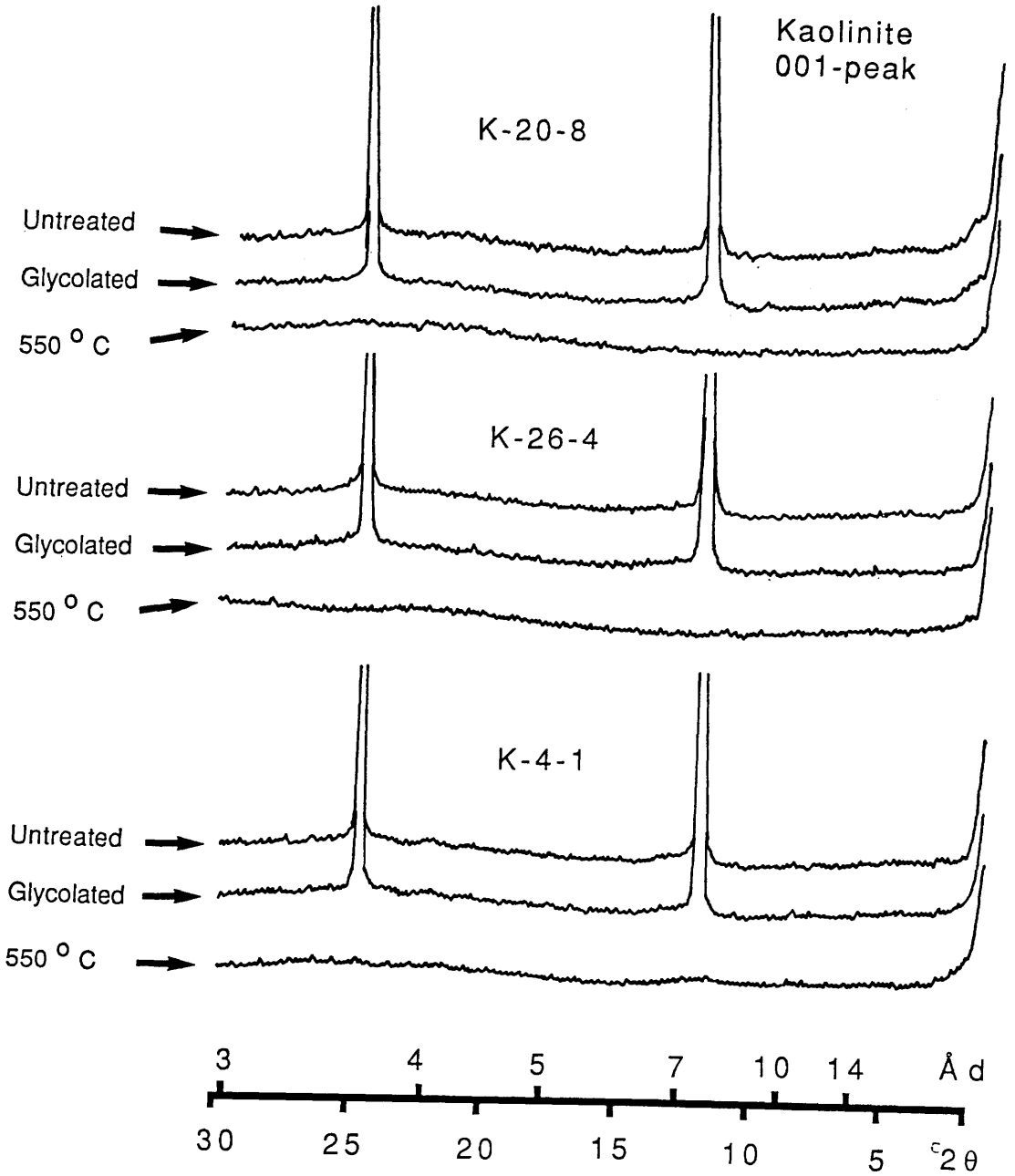


Fig. 3.12 X-ray diffractogram of oriented clay fractions ($< 2 \mu\text{m}$) - Lower Saq Sandstone.

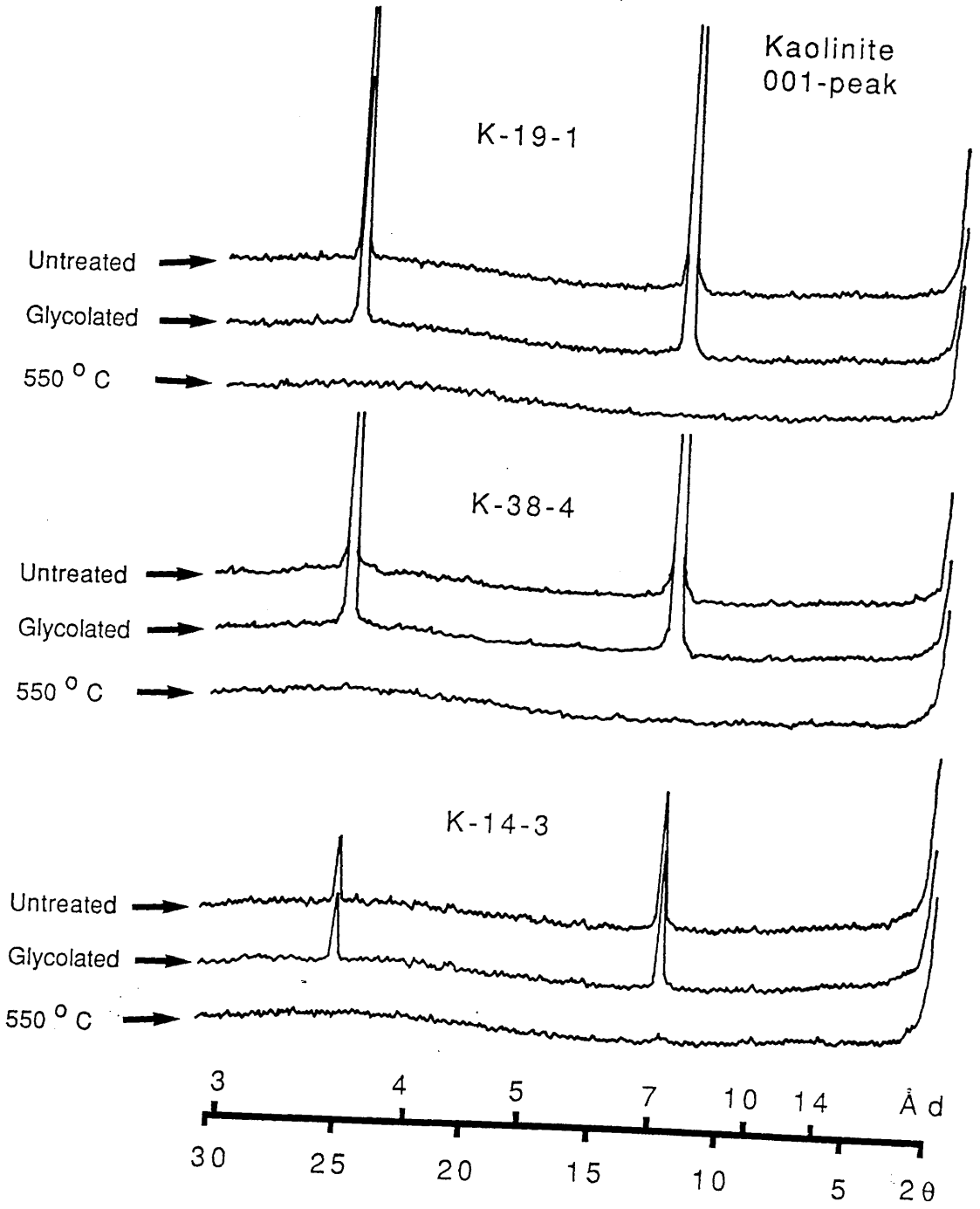


Fig. 3.13 X-ray diffractogram of oriented clay fractions ($< 2 \mu\text{m}$) - Middle Saq Sandstone.

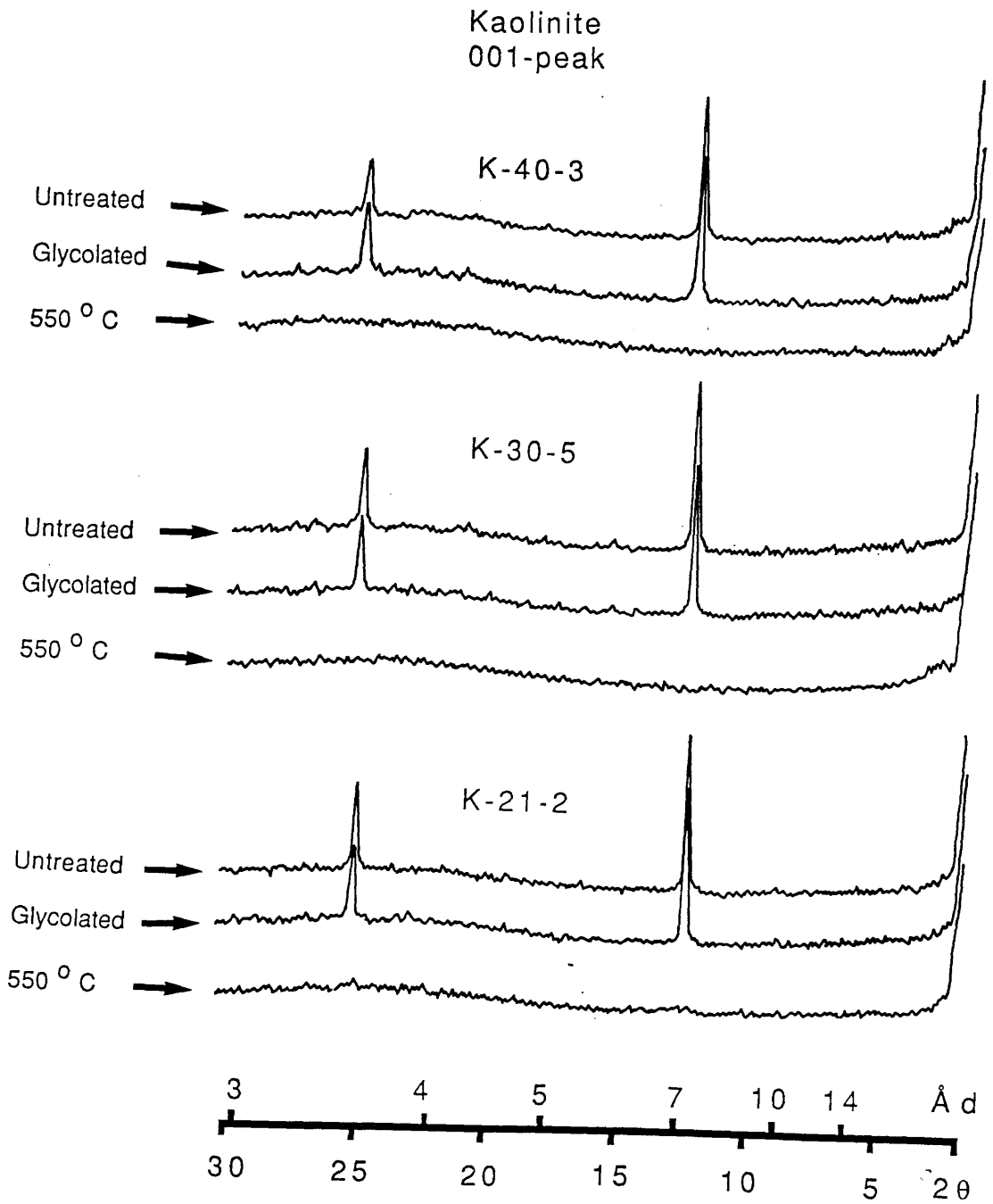


Fig. 3.14 X-ray diffractogram of oriented clay fractions ($< 2 \mu\text{m}$) - Uppert Saq Sandstone.

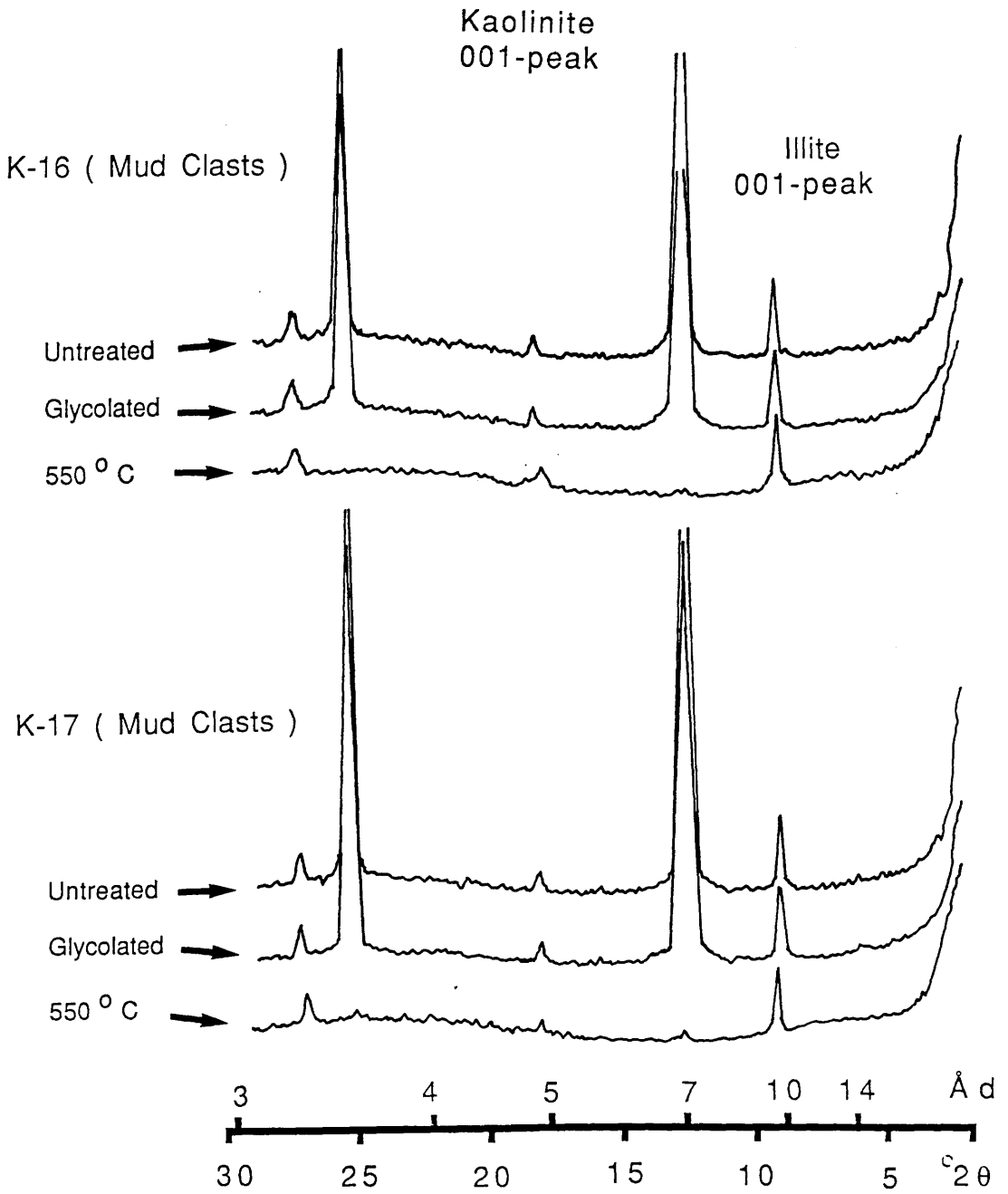
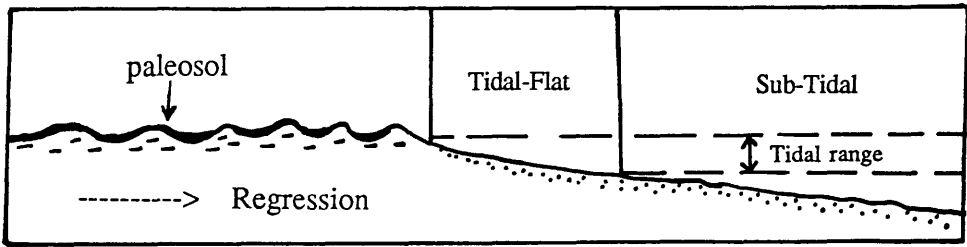


Fig. 3.15 X-ray diffractogram of oriented clay fractions ($< 2 \mu\text{m}$) - from mud-clasts of the Saq Sandstone.

Stage (A) Formation of paleosol



Stage (B) Reworking of paleosol (Ferricrete) by marine environment.

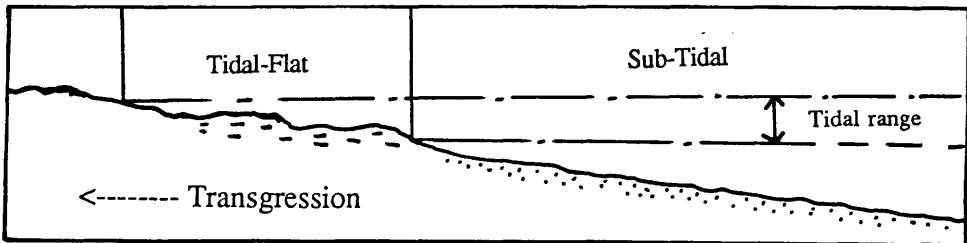


Fig. 3.16 Diagram showing stages of formation and reworking of ferricrete.

STAGE		TIME	
		Early	Late
Compaction		—————	
Cementation	Quartz Overgrowth	—————	
	Early Calcite	—————	
	Iron Oxide	—————	
	Secondary Calcite	—————	
	Kaolinite	—————	

Fig. 3.17 Diagrammatic model showing stages of diagenesis of the Saq Sandstone.

YEARS	PROCESS	RESULT
10^8	(4) Working of basement:	Immature sediments
10^7	(3) Reworking of older formations	Maturing of sediments (increase in angularity, abraded overgrowths)
10^6		
10^5	(2) Working of older sediments	Maturing of sediments (reworking iron cemented clasts)
10^4		
10^3	(1) Reworking on sediment surface	Rounding of grains & maturing of sediments
10^2		
10^0		
10^{-1}		

Fig. 3.18 Diagram showing the various processes which are thought to control the maturity of Saq Sandstone, (1) etc refer to processes which are referred to in Figs. 3.19 and 3.20).

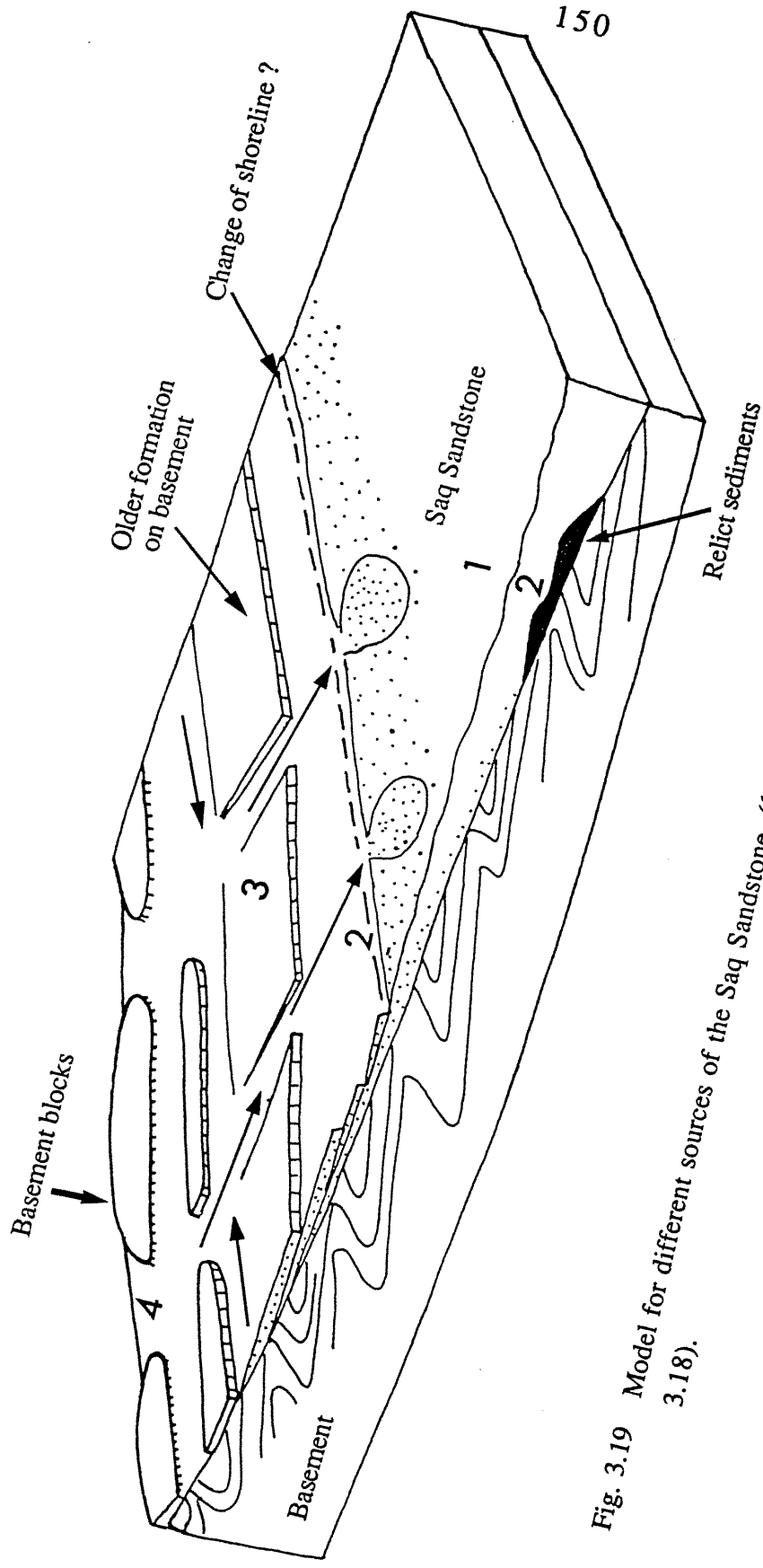


Fig. 3.19 Model for different sources of the Saq Sandstone, (1, 2, 3 and 4 see Fig. 3.18).

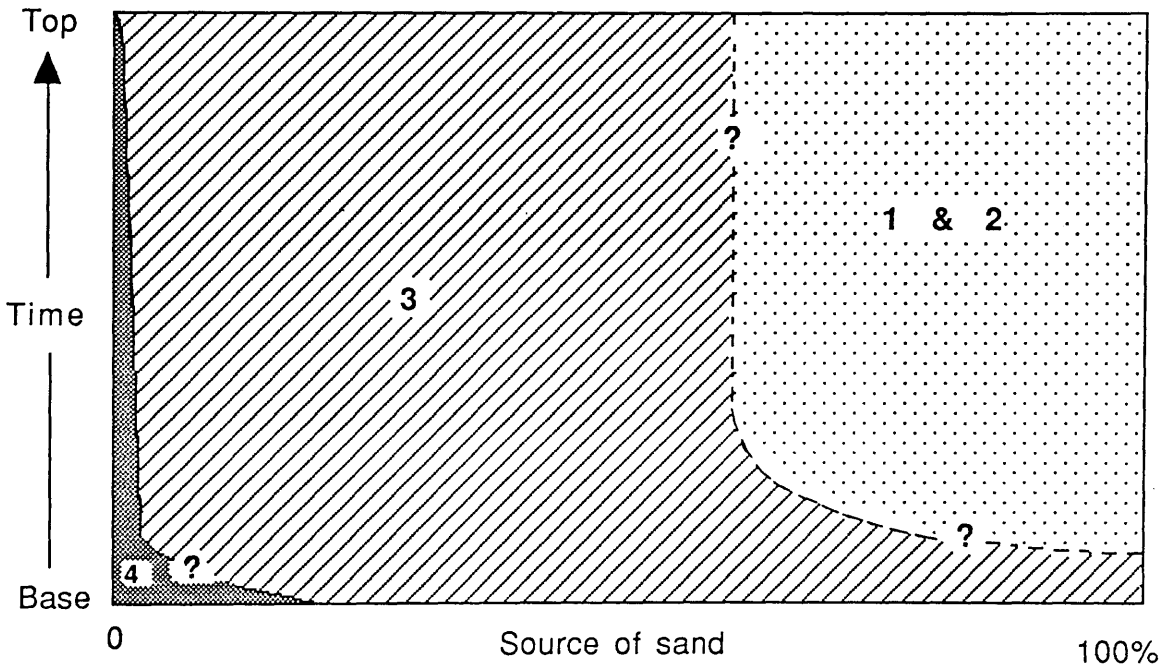


Fig. 3.20 Diagrammatic model showing the percentage input of each process of maturity of the Saq Sandstones, (1, 2, 3 and 4 see Fig. 3.18).



Plate 3.1 Photomicrograph showing two generations of quartz overgrowths - Lower Saq Sandstone, (X10)

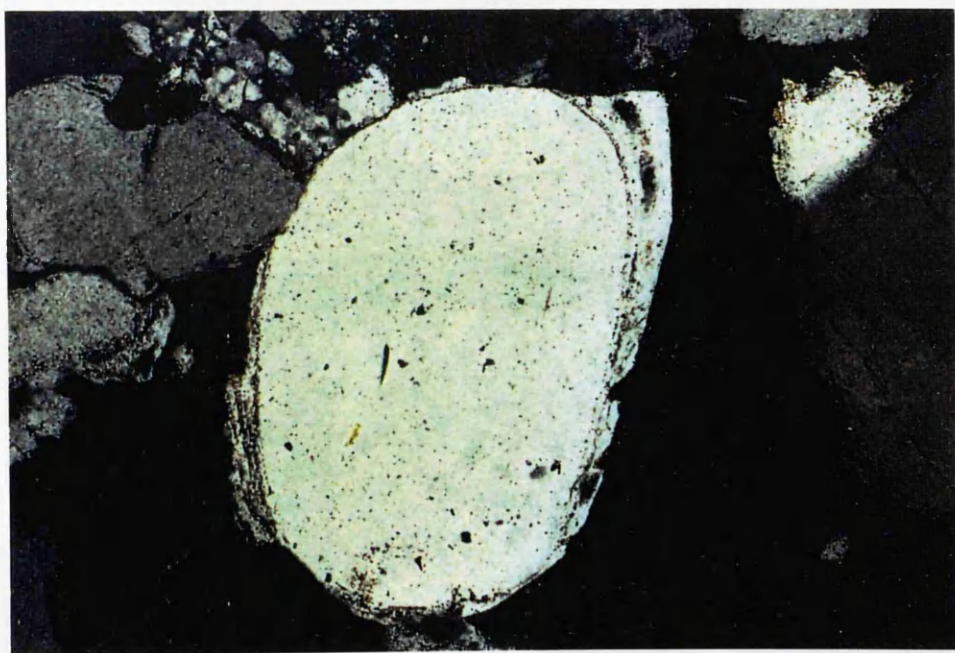


Plate 3.2 Photomicrograph showing more than three generations of quartz overgrowths and euhedral quartz overgrowth - Middle Saq Sandstone, (X10)

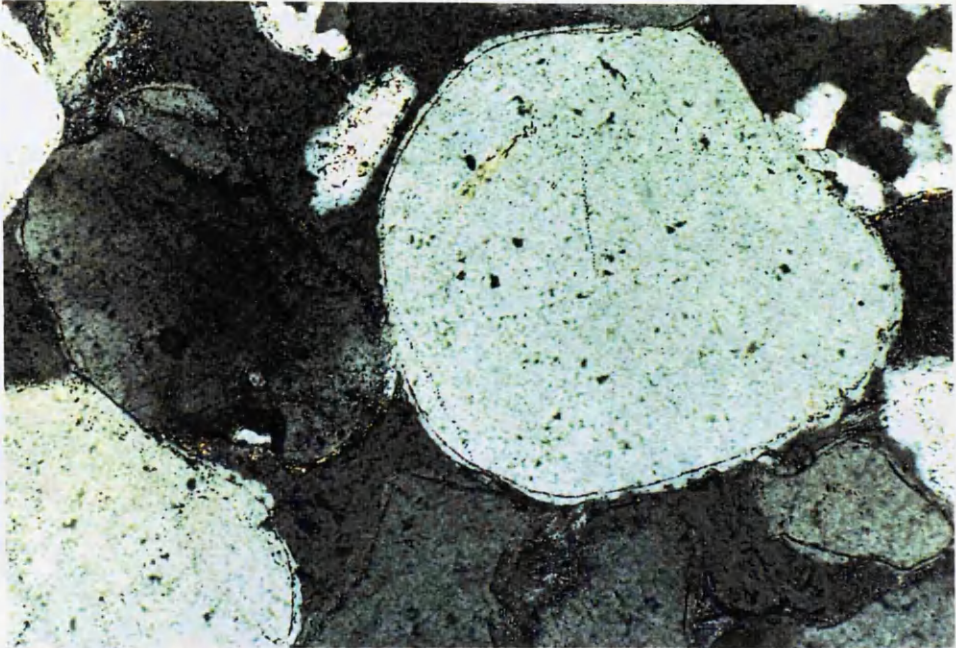


Plate 3.3 Photomicrograph showing inherited well rounded overgrowth - Middle Saq Sandstone, (X10)

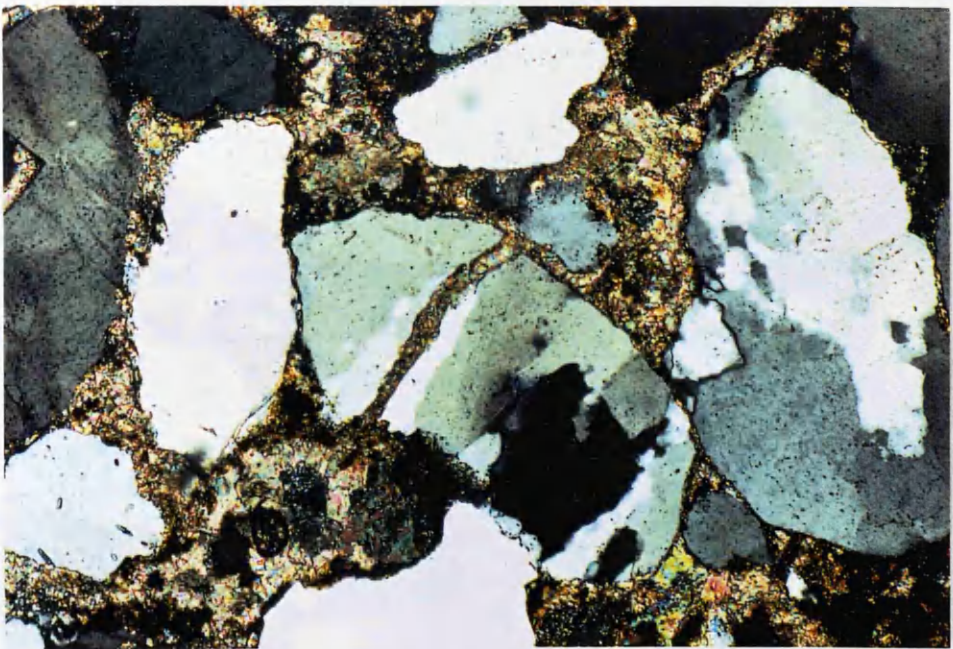


Plate 3.4 Photomicrograph showing undulose polycrystalline quartz grain breaking down to monocrystalline quartz - Lower Saq Sandstone, (X2.5).

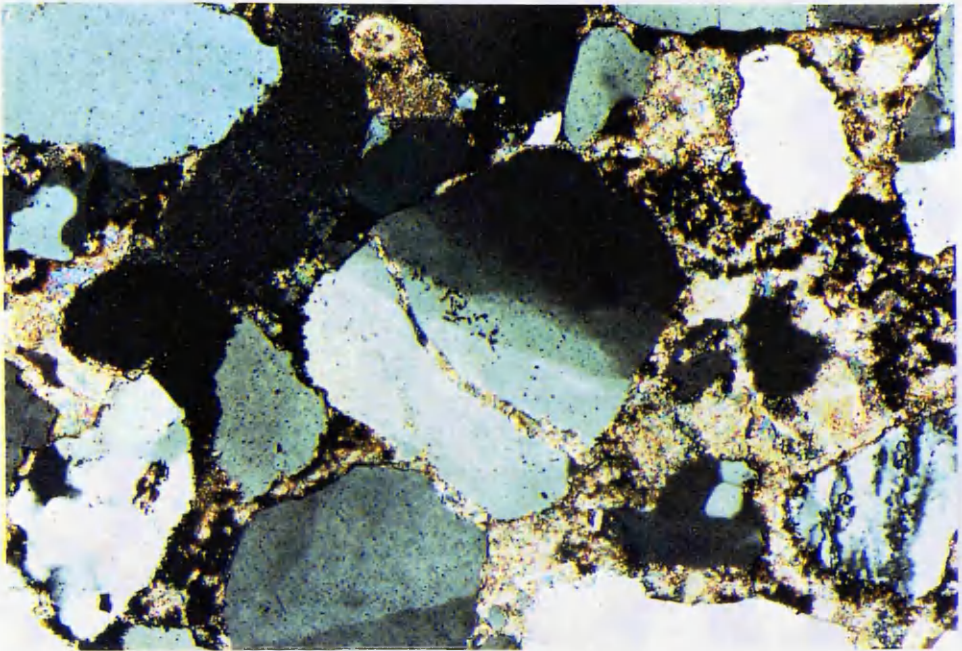


Plate 3.5 Photomicrograph showing undulose monocrystalline quartz grain breaking down to non-undulose monocrystalline grains - Lower Saq Sandstone, (X2.5)

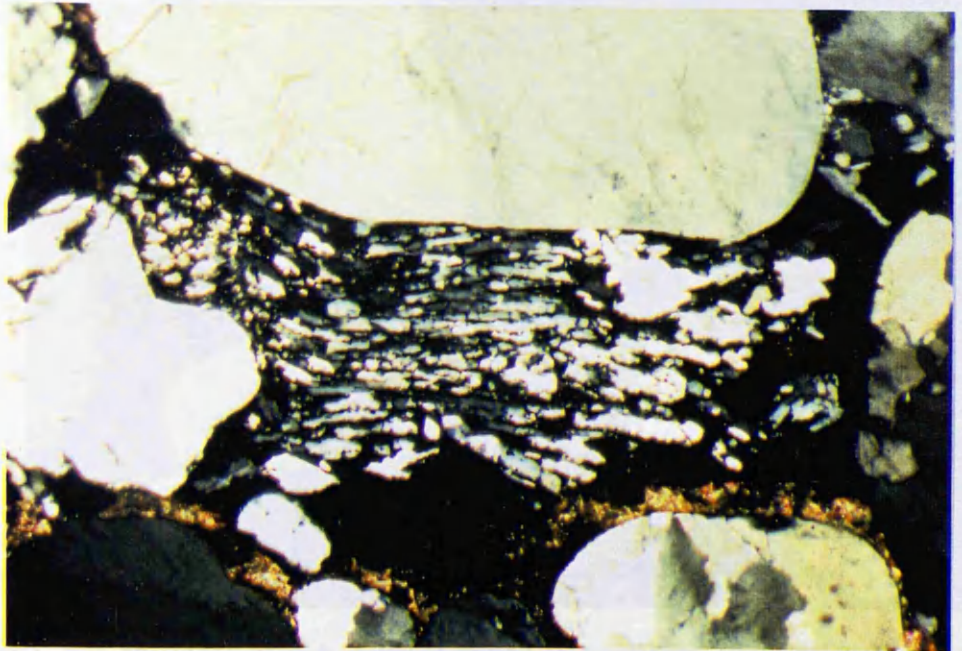


Plate 3.6 Photomicrograph showing metamorphic polycrystalline quartz rich rock fragment - Lower Saq Sandstone, (X2.5).

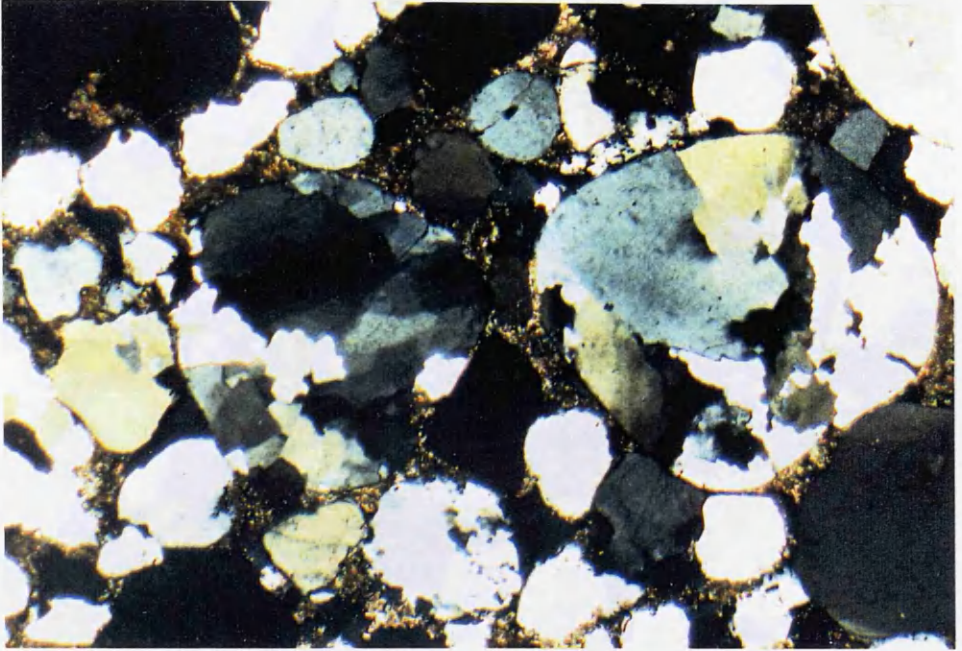


Plate 3.7 Photomicrograph showing well rounded polycrystalline quartz grain - Lower Saq Sandstone, (X10).



Plate 3.8 Photomicrograph showing altered feldspar grain - Lower Saq Sandstone, (X10).

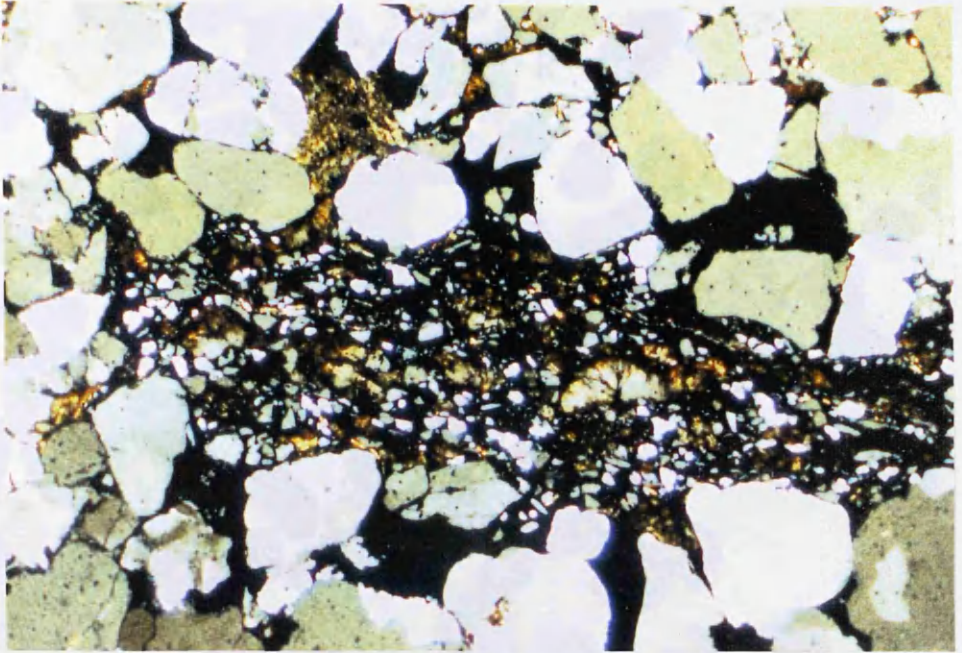


Plate 3.9 Photomicrograph showing Sedimentary rock fragment - Lower Saq Sandstone, (X2.5).



Plate 3.10 Photomicrograph showing sedimentary rock fragment (sandstone) - Lower Saq Sandstone, (X10)



Plate 3.11 Photomicrograph showing well rounded heavy minerals, (T= Tourmaline; R=Rutile; O=Opaque; Z=Zircon) - Upper Saq Sandstone, (X10)

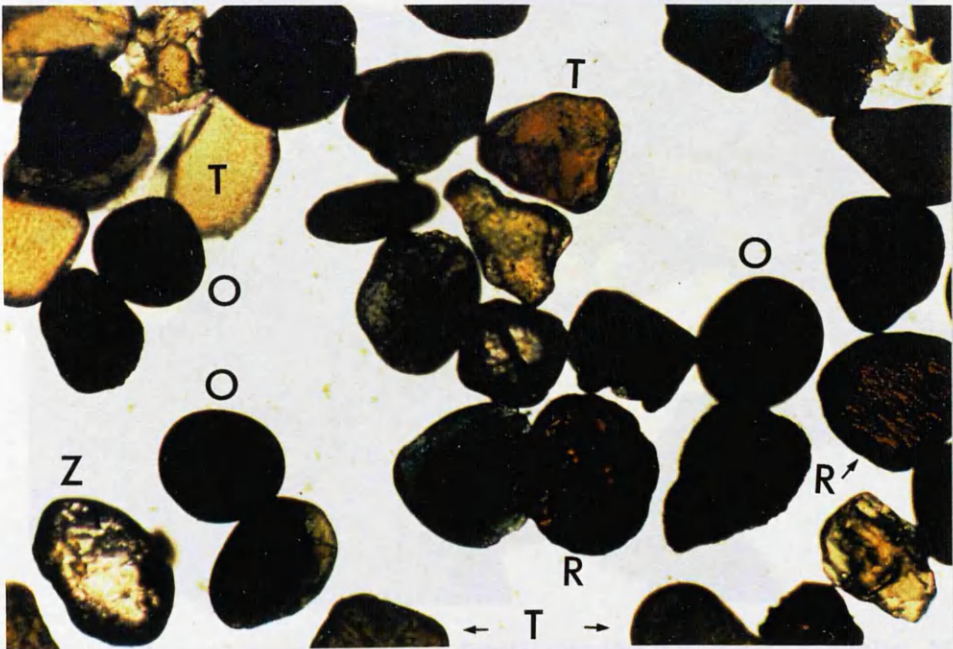


Plate 3.12 Photomicrograph showing heavy minerals, (T= Tourmaline; R=Rutile; O=Opaque; Z=Zircon) - Middle Saq Sandstone, (X10).

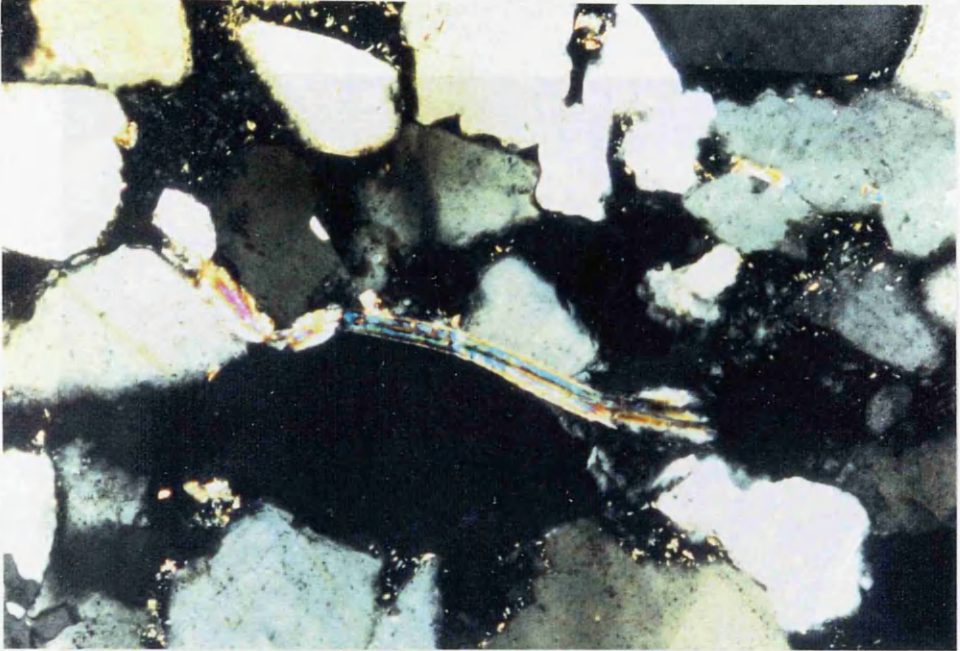


Plate 3.13 Photomicrograph showing the effect of mechanical deformation on the flake of muscovite - Lower Saq Sandstone, (X10).



Plate 3.14 Photomicrograph showing detrital muscovite altered to kaolinite - Middle Saq Sandstone, (X10).

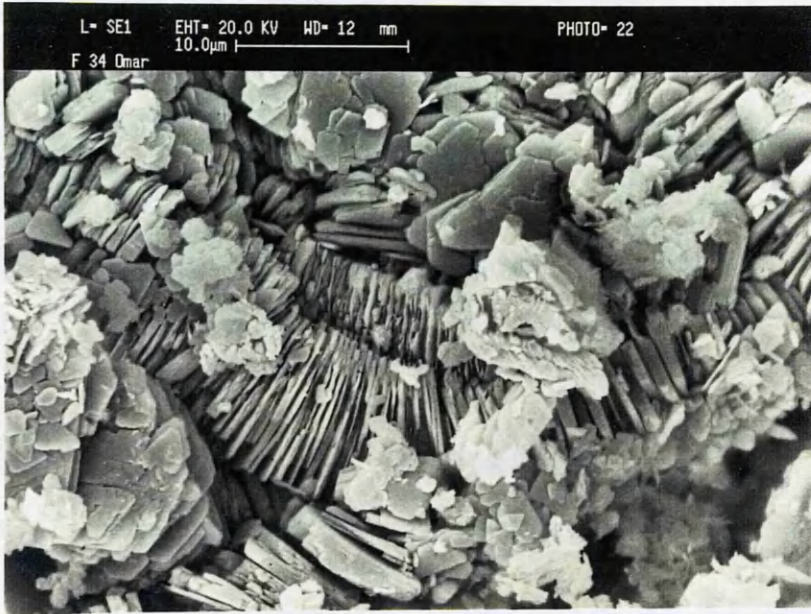


Plate 3.15 SEM photomicrograph showing authigenic kaolinite consisting of stacked pseudo-hexagonal platy crystals (books) - Middle Saq Sandstone.

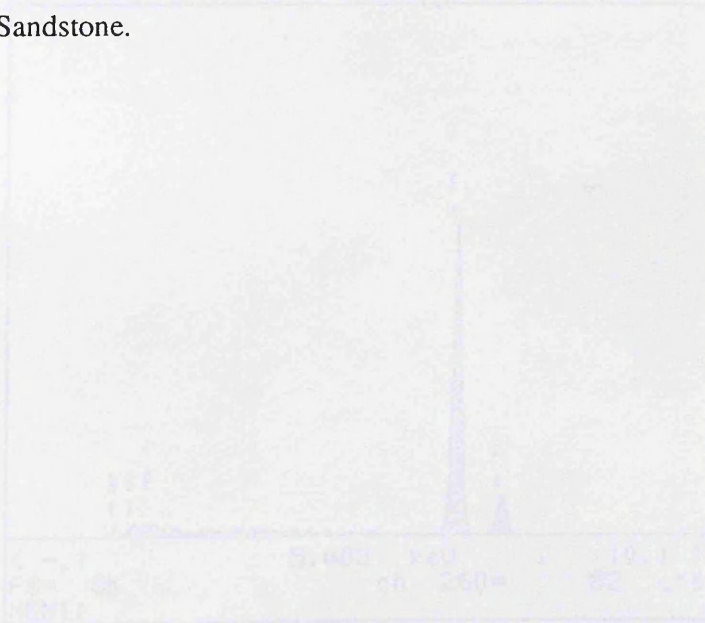


Fig. 3.21 Energy-dispersive spectrum of ferrite (Plate 3.16) - Upper Saq Sandstone.

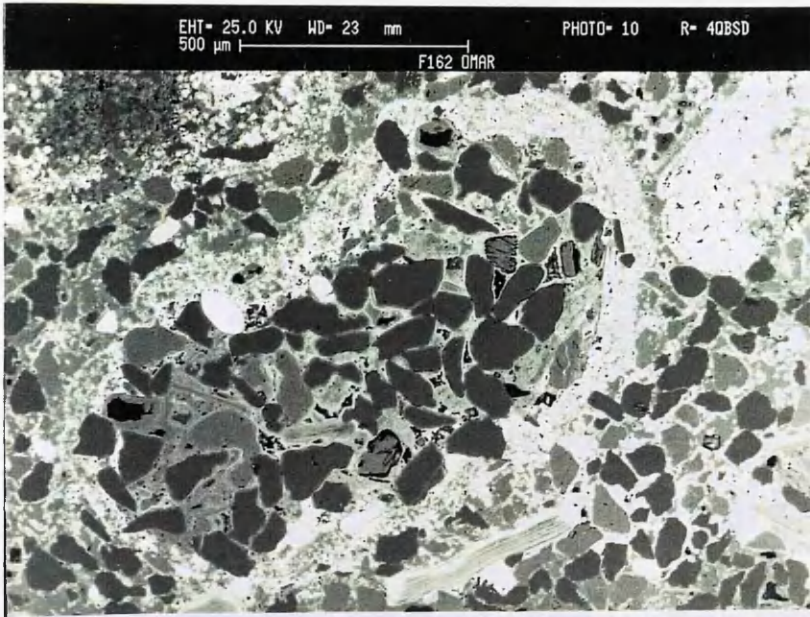


Plate 3.16 Back scattered electron image micrograph showing ferricrete coating quartz grains -Upper Saq Sandstone.

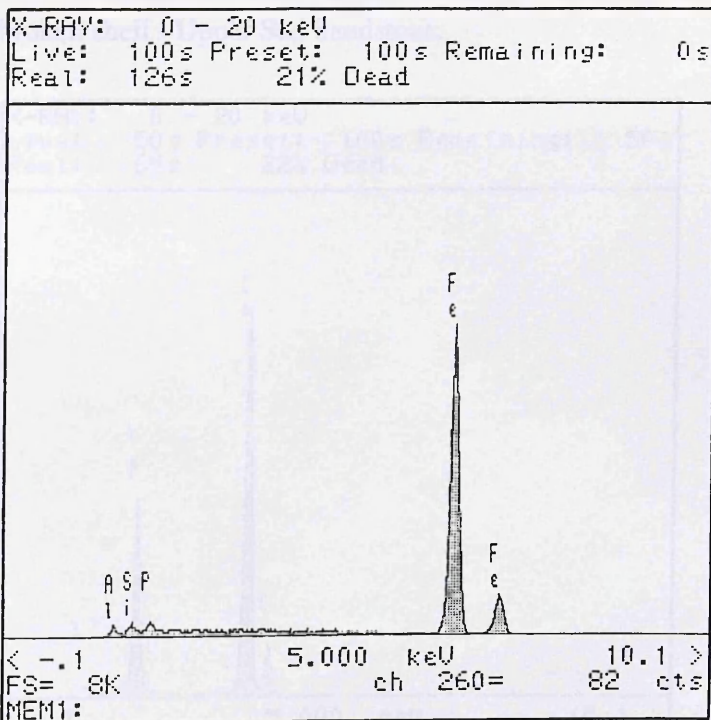


Fig. 3.21 Energy dispersive spectrum of ferricrete (Plate 3.16) - Upper Saq Sandstone.

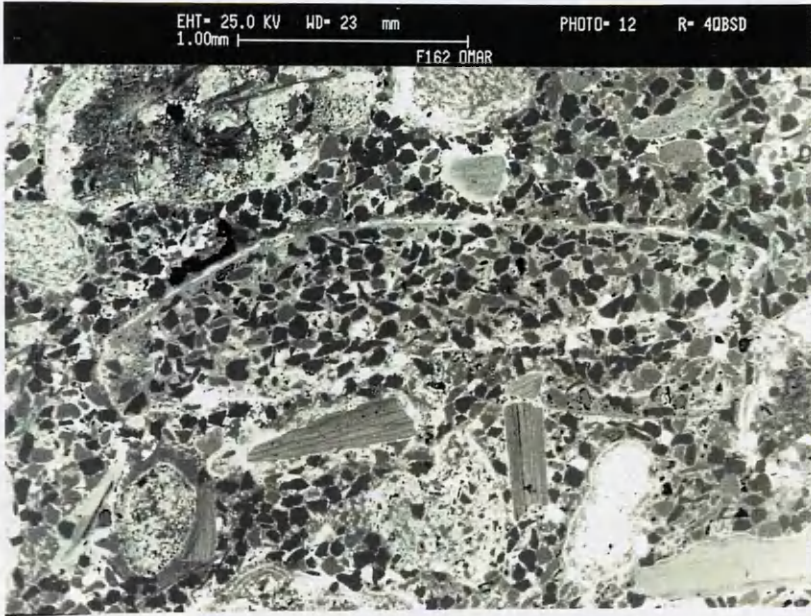


Plate 3.17 Back scattered electron image micrograph showing ferricrete coating broken shell - Upper Saq Sandstone.

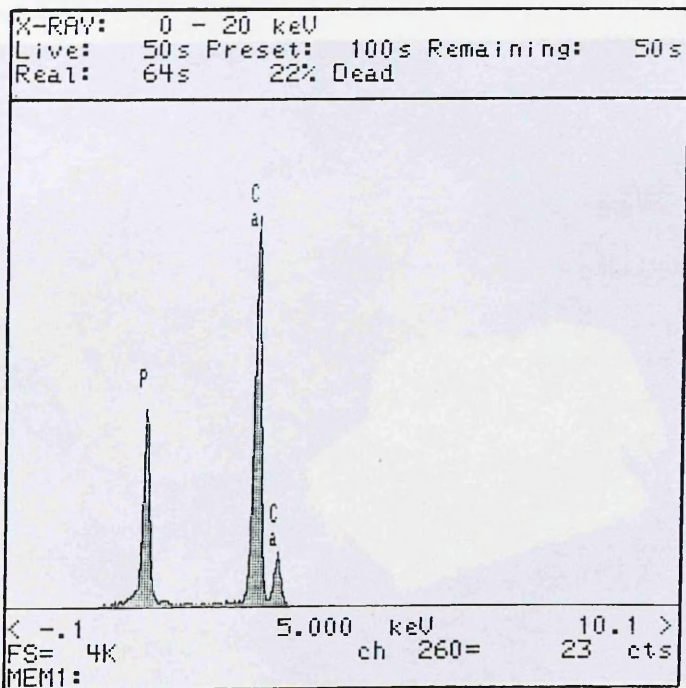


Fig. 3.22 Energy dispersive spectrum of brachiopod shell (Plate 3.17) - Upper Saq Sandstone.

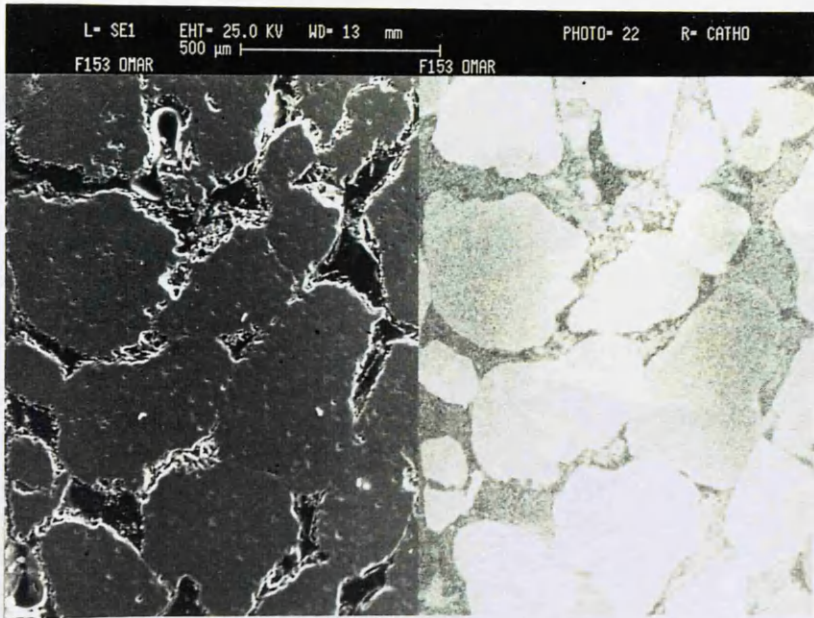


Plate 3.18 SEM micrograph (left) and SEM luminescence (right) showing the effect of quartz overgrowth on the nature of quartz grains - Middle Saq Sandstone.



Plate 3.19 Photomicrograph showing convex-concave contact between quartz grains as result of pressure dissolution - Middle Saq Sandstone, (X10).



Plate 3.20 Photomicrograph showing the different stage of cementation - Middle Saq Sandstone, (X2.5).

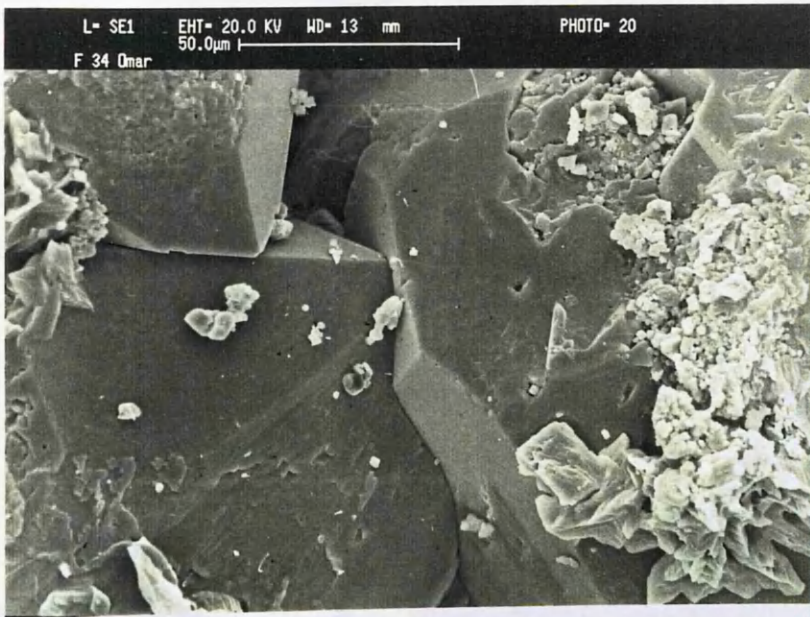


Plate 3.21 SEM micrograph showing euhedral quartz overgrowths - Middle Saq Sandstone.



Plate 3.22 Photomicrograph showing carbonate cement framing chert grain, (X40)



Plate 3.23 Photomicrograph showing hematite coating sand grain, note the hematite is present where grains are in contact - Lower Saq Sandstone, (X40).

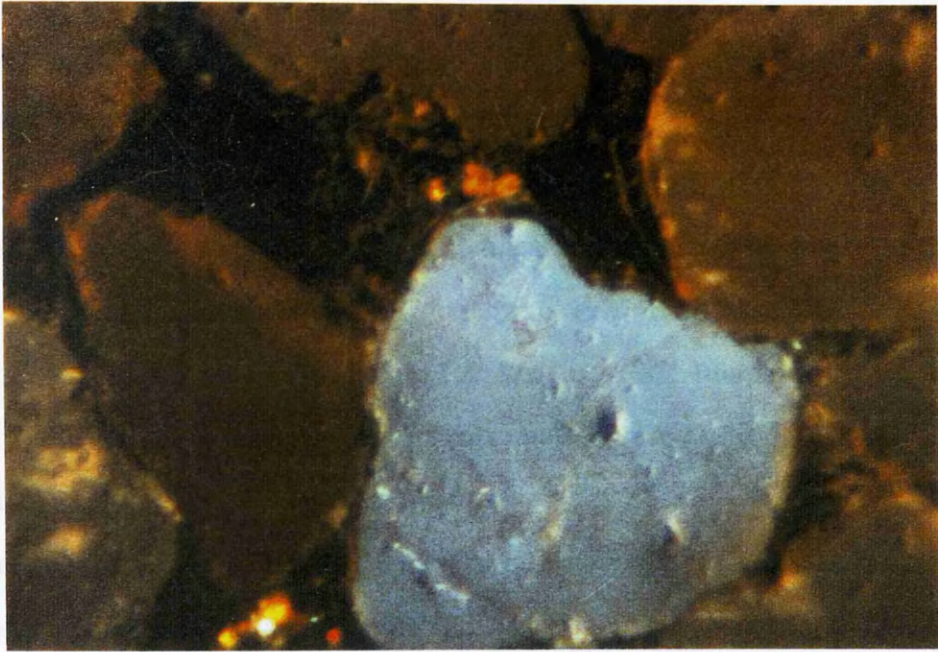


Plate 3.24 Photomicrograph showing luminescence of quartz (Blue, dull red and Black (overgrowth)); and also carbonate (Brilliant orange) - Lower Saq Sandstone, (X10).

CHAPTER FOUR

GEOCHEMISTRY OF THE SAQ SANDSTONE

4.1 Introduction

The composition of sedimentary rocks results from the type of source area, the intensity of weathering, transport distance, sorting and diagenetic history. The tectonic setting of the depositional sedimentary environment is the ultimate control on sediment composition (Pettijohn, 1963; Crook, 1974; Schwab, 1975; Dickinson & Suczek, 1979; Blatt *et al.*, 1980; Ronov, 1981; Hickman & Wright, 1983; Bhatia & Crook, 1986; Condie, 1986; Argast & Donnelly, 1987; Yamamoto, 1987; Denis & Dabard 1988; McCann, 1991).

The geochemistry of sedimentary rocks reflects predominantly the nature and proportion of their detrital components and hence their provenance. Even though diagenesis may alter original chemistry, diagenetic changes are themselves related to plate tectonic environments (Siever, 1979), and bulk composition should still reflect tectonic setting and so enable development of chemically-based discriminates to supplement the petrographic approach (Roser & Korsch, 1986).

Chemical variation in sedimentary rocks is dominated by two components. The first is SiO_2 which has abundance related to the presence of detrital quartz. The second is a group of compounds of which Al_2O_3 is the most abundant, corresponding to the presence of clay mineral components. The specific composition of any rock is largely determined by the relative amounts of these two components. This in turn is governed by the grain size of the original detritus, with coarse-grained materials composed predominantly of quartz (Wyborn & Chappell, 1983).

The purposes of the geochemical studies were: (1) To document the chemical composition of the Saq Sandstone. (2) To investigate any vertical or lateral changes in

composition which were not recorded in petrographic data, and (3) To try to deduce the provenance and tectonic setting of the Saq Sandstone.

4.2 Analytical methods

A total of 161 samples from Lower, Middle, and Upper Saq Sandstone covering an area of more than 8000 Km² were analysed for major and trace elements using an x-ray fluorescence spectrometer (XRF). FeO, CO₂, and H₂O were determined by wet chemical analysis. The chemical analyses are presented in Tables 4.1 to 4.3 (see appendix B), and the averages of major and trace elements in Tables 4.4 and 4.5. The Analytical methods are described briefly below:

4.2.1 X-Ray fluorescence spectrometry (XRF)

X-ray fluorescence spectrometry was used to determine 10 major oxides, SiO₂, TiO₂, Al₂O₃, Fe oxides (total), MnO, MgO, CaO, Na₂O, K₂O, and P₂O₅, and 16 trace elements, Rb, Zr, U, Sr, Pb, Th, Cu, Y, Zn, Ga, Ni, Cr, Co, Ce, La, and Ba. Following the method of Harvey *et al.*, (1973), major elements analyses were performed on fused glass beads made by fusing 0.375 gm of 100 mesh rock powder and 2.00 gm of flux (Lithium tetraborate).

Trace element compositions were determined on pressed pellets (Leake *et al.*, 1969) consisting of 6.0 gm of 250 mesh rock powder and 1.0 gm of thermal binder (Phenol formaldehyde).

All Major and trace element determinations were carried out using Phillips PW 1450/20 sequential automatic x-ray spectrometer.

4.2.2 Wet chemical analysis

Ferrous iron oxide (FeO), water (H₂O), and carbon dioxide (CO₂) contents were determined by the standard procedure of wet chemical analysis. FeO was determined by titration of a standard dichromate solution with a rock solution made by dissolving a

measured amount of whole rock powder in sulphuric and hydrofluoric acid. The FeO percentage, determined by titration, is used to calculate the amounts of Fe₂O₃ per cent using the following equation

$$\text{Fe}_2\text{O}_3 = \text{Fe}_2\text{O}_3 \text{ (XRF value)} - (1.112 \times \text{FeO (titration)})$$

Carbon dioxide (CO₂), and water (H₂O) were determined simultaneously. The rock powder (0.50 gm) was inserted in a combustion tube at 1100°C. The H₂O and CO₂ produced were removed with a current of nitrogen, absorbed and their quantities determined gravimetrically.

All analyses of samples for major elements were carried out in duplicate.

4.3 Niggli number

SiO₂ is generally the largest single constituent of rock chemical analyses, where any increases in SiO₂ are generally accompanied by decreases in other constituents. This inevitably arises from a combination of the constant summation effect of percentages, the predominance of SiO₂ in most rock compositions and the fact that quartz is nearly pure SiO₂. If the negative correlation imposed by varying quartz content, which is a predominant factor in many detrital sediments, is to be removed some procedure such as that introduced by Niggli, (1954) has to be adopted.

Niggli numbers are based on percentaging the sum of the molecular contents where $\text{al} (\text{Al}_2\text{O}_3) + \text{c} (\text{CaO}) + \text{fm} (\text{MgO} + \text{FeO} + \text{Fe}_2\text{O}_3 + \text{MnO}) + \text{alk} (\text{Na}_2\text{O} + \text{K}_2\text{O}) = 100$, while $\text{si} (\text{SiO}_2)$, $\text{p} (\text{P}_2\text{O}_5)$, and $\text{ti} (\text{TiO}_2)$ are calculated on the same basis as that used to reduce $\text{al} + \text{c} + \text{fm} + \text{alk}$ to 100. (Niggli, 1954; Van de Kamp & Leake, 1985).

Plotting different variables it is possible to use Niggli numbers of sediments to derive a good deal of information about the nature of constituent minerals. For example by plotting Niggli k versus al-alk we can distinguish between a source of K (Potassium) from K-Feldspar and one from sheet silicate minerals such as micas. By plotting of al-alk

versus trace elements it is possible to deduce which trace elements are dominantly in clay minerals and micas (Van de Kamp & Leake, 1985).

4.4 Geochemistry of major elements

Several recent studies (Loring, 1982; Bhatia, 1983; Van de Kamp & Leake, 1985; Roser & Korsch, 1986), have used major element geochemistry as an indication of differences in mineral composition, as a maturity index, and also as an indication of the provenance and geotectonic setting.

4.4.1 SiO₂

The Saq Sandstone show a high content of SiO₂ at the expense of other oxides, and the percentage shows an inverse relationship with other oxides. The average of SiO₂ in Lower, Middle, and Upper Saq Sandstones are 90.02%, 94.95%, and 92.95% respectively. Generally there is an increase in SiO₂ upward in the sequence and this is an indication of the increase in maturity of the Saq Sandstone with time. The Middle Saq Sandstone has a slightly higher SiO₂ than the Upper this could be due to the increased proportion of Al₂O₃ derived from micas which are more abundant in the Upper Saq Sandstone.

4.4.2 Al₂O₃

The abundance of Al₂O₃ in the Saq Sandstone may be related to the abundance of clay minerals and mica, with minor contributions from feldspar. The weak positive correlation between Al₂O₃ versus K₂O ($r=0.23$) indicates that most of the Al₂O₃ is from mica and clay minerals (Fig.4.2)

The average Al₂O₃ in Lower, Middle, and Upper Saq Sandstone is 3.8%, 2.27%, and 2.5% respectively, and shows an inverse relationship ($r=-0.52$) between Al₂O₃ and SiO₂ (Fig. 4.1). This could be an indication either of the upward change in maturity of

the Saq Sandstone, or due to the progressive concentration of micas in the Upper Saq Sandstone.

4.4.3 TiO₂

The average TiO₂ content of the Lower, Middle, and Upper Saq Sandstones are 0.27%, 0.24%, and 0.39% respectively. All the Saq Sandstone show an inverse relationship of TiO₂ with SiO₂ (Fig.4.3)

The main sources of TiO₂ in sediments are (1) residues of weathering in the form of chemically altered grains such as rutile or in the form of partly decomposed minerals like micas (2) new products of weathering such as anatase and clay minerals (3) diagenetic minerals such as rutile (Wedepohl, 1978).

A plot of al-alk versus TiO₂ (Fig. 4.4) shows no clear relationship. This suggests that the titanium may be present mainly in detrital minerals such as rutile and ilmenite, or to less extent be associated with clay minerals weak positive correlation.

4.4.4 FeO and Fe₂O₃

The averages of FeO in Lower, Middle, and Upper Saq Sandstones are 0.11%, 0.03%, and 0.05% respectively, and the averages of Fe₂O₃ content are 1.16%, 0.32%, and 0.65% in Lower, Middle, and Upper Saq Sandstone. All Saq Sandstone samples appear to have more Fe₂O₃ than FeO. The explanation of the high Fe₂O₃ in the Saq Sandstone could be either that the oxidation of ferrous minerals occurs during deposition, so the resulting sandstone has a higher Fe³⁺/Fe²⁺ ratio, or could be due to different amounts of Fe₂O₃ and FeO in the source area.

A plot of Al₂O₃ versus Fe₂*O₃ (total) shows a weak positive correlation (r=0.15) suggesting that the Fe₂O₃ content is associated with clay minerals and iron oxides.(Fig.4.5).

The high content of Fe₂O₃+FeO in the Saq Sandstone could also be interpreted as reflecting the presence of ferruginous cement.

4.4.5 CaO

The average contents of CaO in the Lower, Middle, and Upper Saq Sandstones are 1.66%, 1.09%, and 1.02% respectively

The negative correlation of CaO with SiO₂ ($r=-0.36$) and the positive correlation of CaO with CO₂ and P₂O₅ (Figs. 4.6 to 4.8) indicate that carbonate and apatite may be responsible for the abundance of CaO in the Saq Sandstone. The petrography study shows that the percentage of carbonate cement in Lower, Middle, and Upper Saq Sandstones are 1.81%, 1.16%, and 1.11% respectively.

However an additional reason for the high percentage of carbonate in the Saq Sandstone could carbonate replacement of some of the clay or even some micas, during diagenesis. It may also be due to an increase in the amount of carbonate available from pure fluids during diagenesis.

4.4.6 Na₂O

The average Na₂O contents of Lower, Middle and Upper Saq Sandstones are 0.09%, 0.09% and 0.14% respectively. Na-feldspar and clay minerals are the main sources of Na in sandstones (Wedepohl, 1978), but as the petrographic study of the Saq Sandstone does not show any Na-feldspar, the most source of Na could be clay minerals.

There is weak negative correlation between Na₂O and SiO₂ (Fig. 4.9).

4.4.7 K₂O

The average K₂O contents of Lower, Middle, and Upper Saq Sandstones are 0.04%, 0.04%, and 0.55% respectively. The K-content of sandstones is primarily from K-feldspar and K-mica (Wedepohl, 1978).

A plot of al-alk against Niggli k has been used to distinguish between K in feldspar and K in sheet silicates such as micas and clay minerals. High al-alk (>30) indicates clay-rich rocks (shale), where low al-alk (<30) indicates a high feldspar content, supported by negative correlation with Niggli k, if k was largely in potassium feldspar (K-feldspar

has $al-alk=0$, $k=1.0$) or positive correlation if K was largely sheet silicates. The absence of negative or positive correlation suggests that a mixture of the two minerals was present (Van de Kamp & Leake, 1985).

A plot of $al-alk$ against Niggli k in the Saq Sandstone (Fig. 4.10) shows a weak positive correlation, suggesting that the K in the Saq Sandstone is largely contributed from sheet silicate minerals such as micas. The majority of samples have $al-alk$ more than 30 which supports this conclusion .

4.5 Geochemistry of trace elements

Many studies have used trace elements to decipher the provenance of sediments or the environments of deposition (Van de Kamp *et al.*, 1976; Sinior & Leake, 1978; Hichma & Wright, 1983; Van de Kamp & Leake, 1985).

The elements La, Ce, Y, Th, Zr and Ti are the most suited for provenance and tectonic setting determinations because of their relatively low mobility during sedimentary processes and their low residence time in sea water (Holland, 1978). These elements are transported quantitatively into clastic sedimentary rocks during weathering and transportation and thus would reflect the signature of the parent material (McLennan *et al.*, 1983).

4.5.1 Niggli $al-alk$ versus trace elements

Van de Kamp & Leake, 1985 used the relationship between $al-alk$ (a parameter to measure the aluminium contained in clay minerals and micas rather than in the feldspar), and various trace elements to indicate which elements are related to sheet silicate and which elements are not.

Plots of trace elements against $al-alk$ were made and most give an undefined trend which suggests that these elements are neither concentrated mainly in feldspar nor in sheet silicates (Figs. 4.11 to 4.24).

4.5.2 K₂O versus trace elements

Trace elements like lead, barium and rubidium are frequently found in potassium-rich minerals because these elements have ionic radii close to that of potassium and may thus easily replace it (Krauskopf, 1983).

Most rubidium in sedimentary rocks resides in feldspar and sheet silicates (Wedepohl, 1978, Van de Kamp & Leake, 1985).

A plot of K₂O against rubidium, cerium and lanthanum in the Saq Sandstone shows a positive correlation, which suggests that these elements are concentrated in k-feldspar and/or sheet silicates (Figs.4.25 to 4.27). Where plots of other trace elements with K₂O do not show any clear trend it suggest that they are not concentrated in k-feldspar or sheet silicates.

4.5.3 Zr versus Th and U

Good positive correlations are present between zirconium and both thorium and uranium in the Saq Sandstone (Figs. 4.28 and 4.29). Zircon grains are almost certainly the major sources of Th and Zr in the Saq Sandstone.

4.5.4 Y+La+Ce versus Ni+Cr versus Sr

Hickman & Wright, (1983) during a study of the Appin Group slates, used the relationships between Y+La+Ce, Ni+Cr and Sr to decipher the provenances of these rocks. They pointed out that Ni and Cr indicate basic source regions, whilst Y, La and Ce indicate a granitic source whereas Sr indicates provenance containing the most sedimentary rocks. Accordingly, a triangular plot diagram for Y+La+Ce versus Ni+Cr versus Sr (Fig. 4.30) shows that the majority of the Saq Sandstone fall in the Sr sector, indicating that the Saq Sandstone were largely derived from a pre-existing sedimentary source.

4.6 Discrimination function analysis and tectonic setting

Several workers have used discrimination function analysis for sandstone geochemistry to decipher the tectonic setting (Davies & Ethridge, 1975; Blatt *et al.*, 1980; Ronov, 1981; Maynard *et al.*, 1982; Bhatia, 1983; Bhatia & Crook, 1986; Roser & Korsch, 1986).

The techniques of Bhatia, (1983), Bhatia & Crook, (1986), and Roser & Korsch, (1986) in discrimination function analysis have been applied here.

4.6.1 Bhatia (1983), Bhatia & Crook (1986) discrimination analysis

Bhatia, (1983) looked for geochemical discriminate functions which would enable the characterization of different tectonic settings based on a study of Palaeozoic turbidites from Australia. These tectonic settings include passive margins, active margins, continental island arcs, and oceanic island arcs.

The unstandardized discriminate function coefficients used by Bhatia, (1983) were used in this study to calculate discriminate scores for Lower, Middle, and Upper Saq sandstones are shown in Table 4.6 (Appendix B) and the results in Tables 4.7 to 4.9 (Appendix B) and plotted in Fig. 4.31.

All samples from the Saq Sandstone fall into the passive margin field which is characterized by mineralogically mature sediments deposited in plate interiors, at a stable continental margin or in intracratonic basins. Derived sediments are characterized by recycled quartz-rich sediments, originating in older adjacent continental terranes (Bhatia, 1983). Petrographic study indicates that most of the Saq Sandstones are derived from a stable craton, a continental block.

Bhatia, (1983) and Bhatia & Crook, (1986) used different relationships between major and trace elements of sandstones to differentiate them into different groups derived from different tectonic setting.

The most discriminate parameters are Al_2O_3/SiO_2 , K_2O/Na_2O , Fe_2O_3+MgO , $Al_2O_3/(CaO+Na_2O)$, and TiO_2 .

Bhatia, (1983) recognized four types of tectonic setting (1) Oceanic island arcs characterized by higher $\text{Fe}_2\text{O}_3+\text{FeO}+\text{MgO}$ and low $\text{K}_2\text{O}/\text{Na}_2\text{O}$ (2) Continental island arcs which have higher $\text{Fe}_2\text{O}_3+\text{FeO}+\text{MgO}$, higher TiO_2 , higher $\text{Al}_2\text{O}_3/\text{SiO}_2$, and lower $\text{K}_2\text{O}/\text{Na}_2\text{O}$; and (3) Active continental margins are characterized by lower $\text{Fe}_2\text{O}_3+\text{FeO}+\text{MgO}$, lower TiO_2 , lower $\text{Al}_2\text{O}_3/\text{SiO}_2$, (4) Passive margins are characterized by lower $\text{Fe}_2\text{O}_3+\text{FeO}+\text{MgO}$, $\text{Al}_2\text{O}_3/\text{SiO}_2$ and higher $\text{K}_2\text{O}/\text{Na}_2\text{O}$).

All these relationships have been applied to the Saq Sandstone, and none produced any meaningful results, (Figs 4.32 to 4.34).

The Saq Sandstone have low $\text{Fe}_2\text{O}_3+\text{MgO}$ and low $\text{Al}_2\text{O}_3/\text{SiO}_2$ which characterize passive margins but the majority of the samples fall outside of Bhatia's fields of different tectonic setting, so any results based on Bhatia's bivariate relationship would lead to a meaningless conclusion. The framework mineralogy suggests that the Saq Sandstone were derived from a stable craton of a continental block.

4.6.2 Roser & Korsch (1986) discrimination analysis

The geochemical characterization of clastic sediments is generally based on the variation of the $\text{SiO}_2/\text{Al}_2\text{O}_3$ and $\text{K}_2\text{O}/\text{Na}_2\text{O}$ ratios because these parameters reflect the relative abundance of stable constituents (quartz, mica, and k-feldspar) compared with unstable constituents (plagioclase and lithic fragments); this enables an estimate of the degree of maturity to be made.

Roser & Korsch, (1986) recognized three tectonic settings 1- passive continental margins (PM), 2- active continental margins, and 3- oceanic island arcs (ARC)

The major oxides have been recalculated to 100% volatile-free according to the Roser & Korsch, (1986) method.

A plot of $\text{K}_2\text{O}/\text{Na}_2\text{O}$ versus SiO_2 (Fig. 4.35) shows that all the samples from the Saq Sandstone fall in to the passive margin field, which is characterized by mineralogically mature sediments (quartz-rich) deposited in plate interiors at stable continental margins or in intracratonic basins.

4.7 Relation of grain-size and chemical composition

Grain size and chemical composition of clastic sediments are not independent variables. Grain size and sorting of the sediment particles were controlled by the hydraulics of the transporting medium and led to compositional fractionation because different size fractions possess different chemical compositions (Pettijohn, 1963; Roser & Korsch, 1985; Argast & Donnelly, 1987; Roser & Korsch, 1986; Okonkwo, 1989)

Grout, 1925 and Boswell, 1919 showed that silica content diminishes as grain size decreases, while K_2O and Al_2O_3 content rises with decreasing grain size. This could reflect the higher amount of SiO_2 in the Middle Saq and the higher amount of K_2O in the Upper Saq Sandstone.

The finer-grained samples (Upper Saq) have higher concentrations of K_2O and Al_2O_3 (0.55% and 2.5% respectively) while coarser-grained samples (Middle Saq) have slightly higher concentration of SiO_2 . This suggest that the finer-grained samples, at the time the sediment accumulated, contained more muscovite flakes which hydraulically would have had the same capability to be transported and deposited as the fine-grained sediments (Figs. 4.36 and 4.37).

4.8 Conclusion

1. The high amount of SiO_2 in most of the Saq Sandstone samples is considered to indicate a high degree of maturity, whilst some samples showing a low content of SiO_2 could reflect enrichment of the sediment with carbonate cement or clay minerals or the presence of detrital mica.
2. The high SiO_2/Al_2O_3 ratio of the Saq Sandstone precludes their derivation from any other than a pre-existing sedimentary source. This is because it is extremely doubtful that any single cycle of erosion could produce such mineralogically mature sediments.
3. The fine-grained Upper Saq Sandstone contains the higher concentrations of K_2O (average=0.55%) due to the sorting of muscovite with finer grains.

4. There is a weak relationship between grain size and chemical composition since coarser-grained sediments contained more silica than finer-grained sediments
5. The discriminate function analysis technique shows that the Saq Sandstone were derived from a passive continental margin
6. The high amount of CaO is related mainly to enrichment of sediments with carbonate cements.
7. The relationships between Y+La+Ce, Ni+Cr and Sr show that the Saq Sandstones were derived primarily from a pre-existing sedimentary source.
8. Bhatia's(1983) four bivariant relationships did not produced any meaningful result
9. The abundance of REE (La, Ce), highly charged cations (Th, U, Zr), and large cations(Rb and Pb) could be related to mica and heavy minerals, mainly tourmaline, zircon and rutile, suggesting a granitic or recycled detritus.
10. The Saq Sandstone geochemistry yields data which appear thoroughly consistent with results obtained by petrographic study.

Table 4.4 Average chemical composition of quartz arenites of the Saq Sandstone and other representative of quartz arenite (A, B and C from Pettijohn, 1963, Table 2).

Elements	Upper		Middle		Lower		A	B	C	D
	\bar{x}	S	\bar{x}	S	\bar{x}	S				
SiO ₂	92.45	3.30	94.53	4.04	89.83	6.06	93.45	83.79	99.54	86.50
TiO ₂	0.39	0.24	0.24	0.19	0.27	0.17	0.05	-	0.03	0.53
Al ₂ O ₃	2.50	1.33	2.27	2.09	3.80	2.43	0.73	0.48	0.35	5.71
Fe ₂ O ₃	0.65	0.68	0.32	0.74	1.16	1.14	0.63	0.06	0.09	2.69
FeO	0.05	0.06	0.03	0.04	0.11	0.14	0.14	-	-	-
MnO	0.02	0.03	0.02	0.01	0.03	0.01	0.01	-	-	0.02
MgO	0.10	0.08	0.10	0.07	0.10	0.08	0.01	0.05	0.06	0.69
CaO	1.02	0.90	1.09	1.21	1.66	2.03	0.04	8.81	0.19	0.05
Na ₂ O	0.14	0.13	0.09	0.12	0.09	0.15	0.08	-	-	0.02
K ₂ O	0.55	0.55	0.04	0.05	0.04	0.11	0.19	-	-	1.55
P ₂ O ₅	0.09	0.12	0.05	0.07	0.12	0.12	0.02	-	-	0.02
CO ₂	0.71	0.66	0.88	1.12	1.31	1.61	-	6.93	-	-
H ₂ O	0.99		1.02		1.55		0.68	-	0.25	-
Total	99.66		100.68		100.07		99.94	100.13	100.51	97.78

A: Lauhauuri Sandstone (Cambrian) Finland

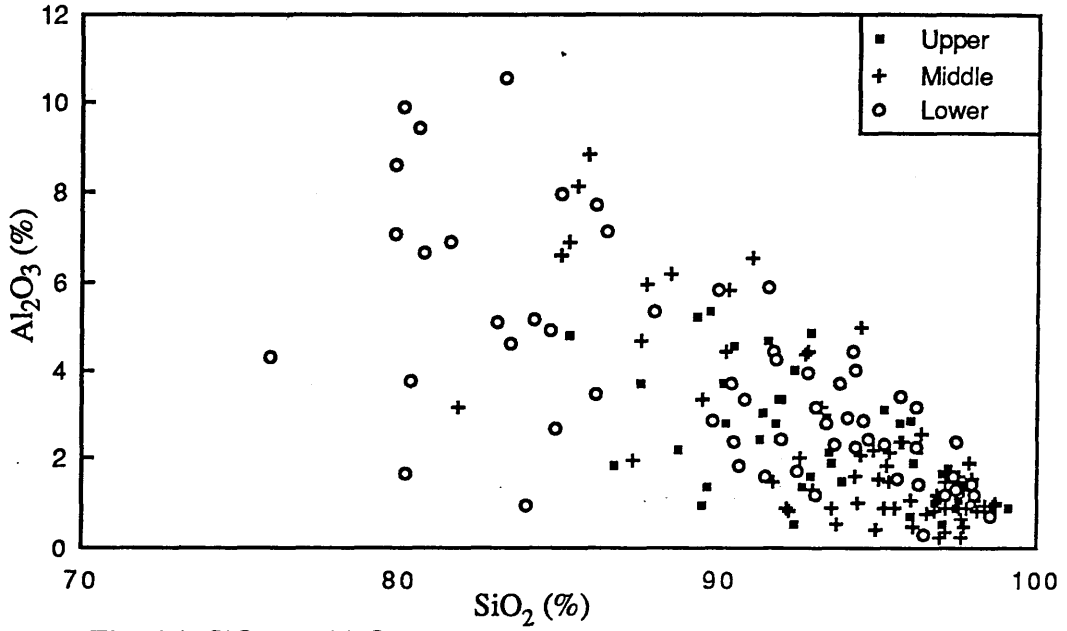
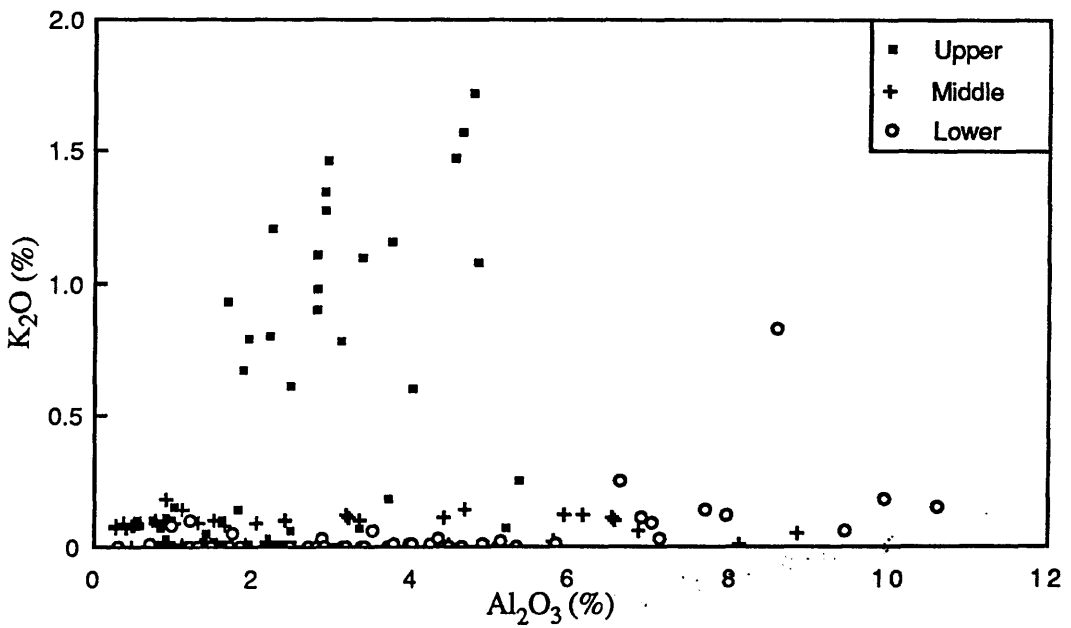
B: Simpson Sandstone (Ordovician) Cool Creek, Oklahoma

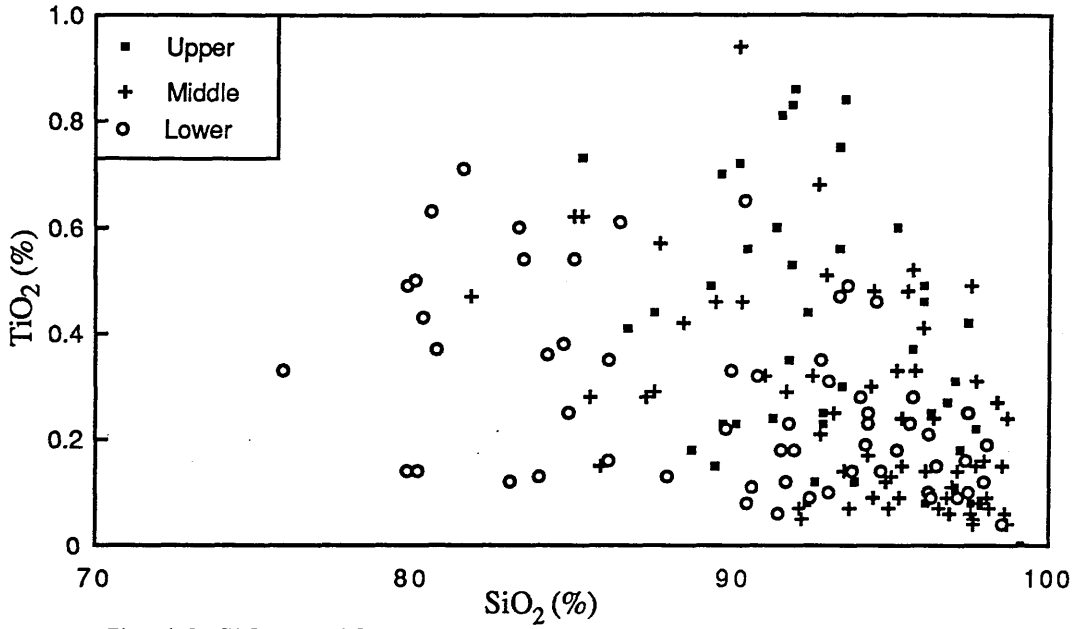
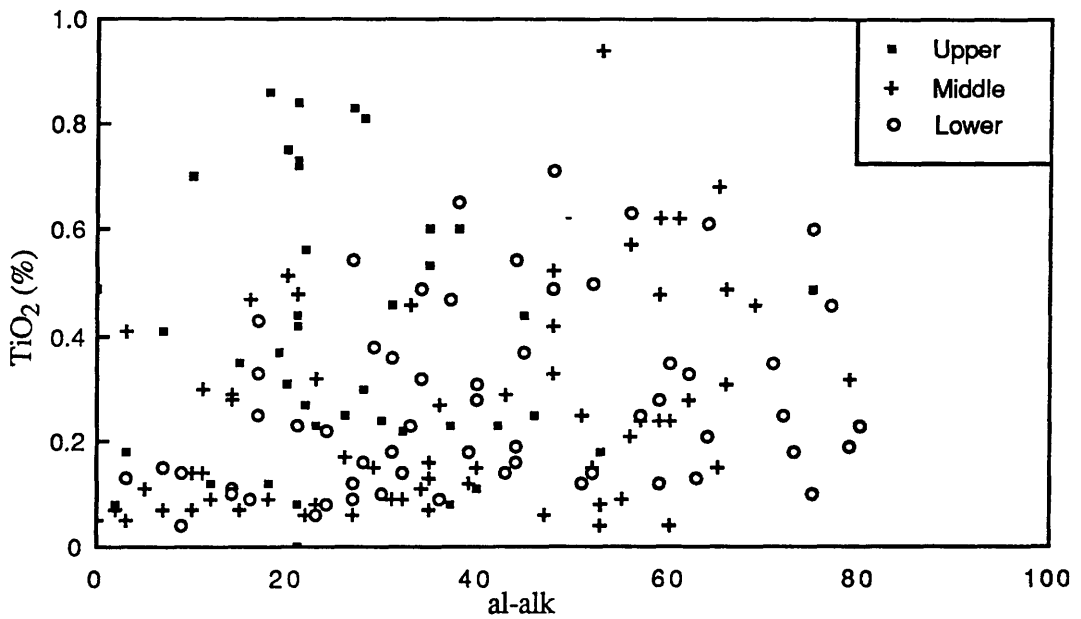
C: Tuscarora Quartzite (Silurian)

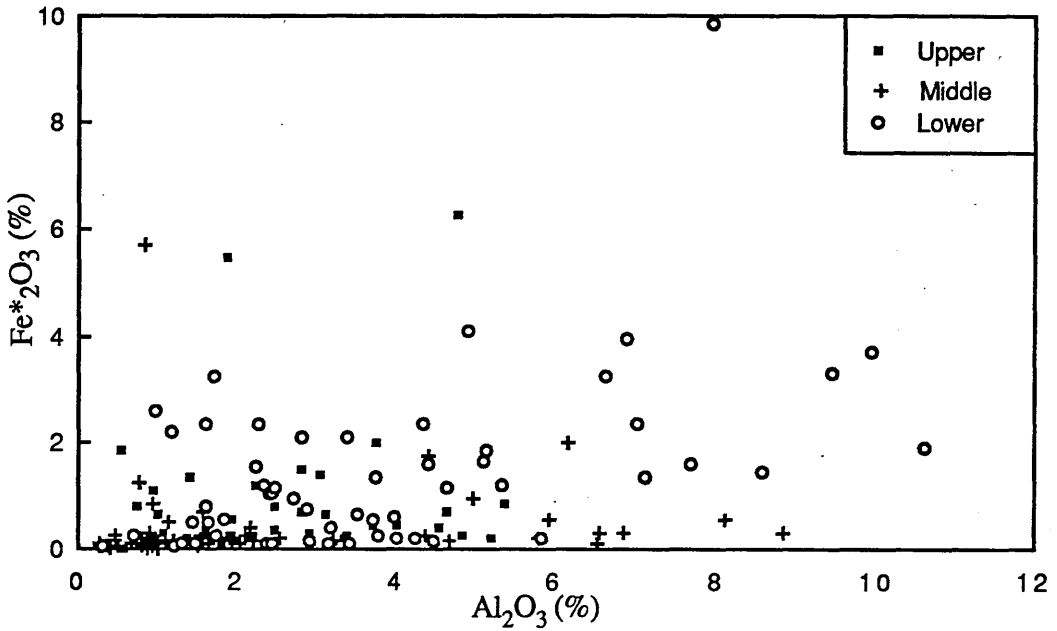
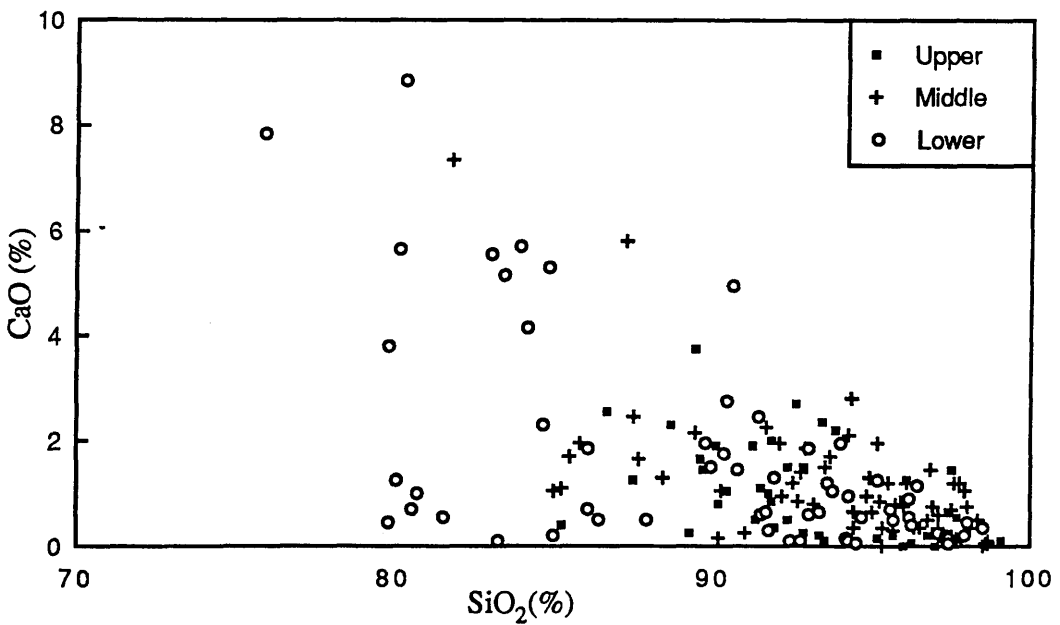
D: Shawangunk Quartzites-average of 11 samples (Argas & Donnelley, 1987)

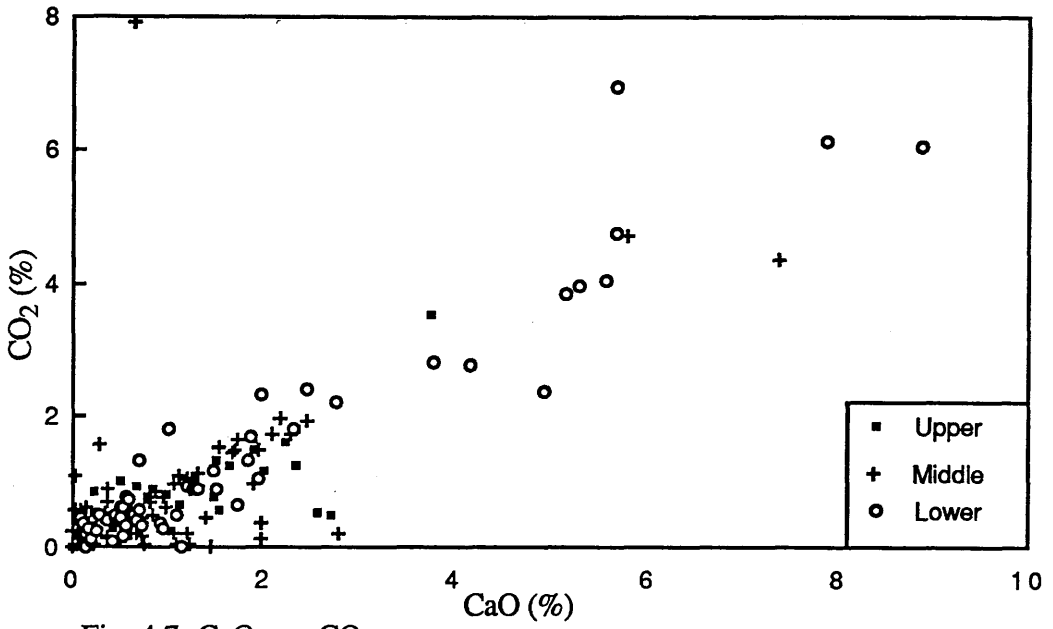
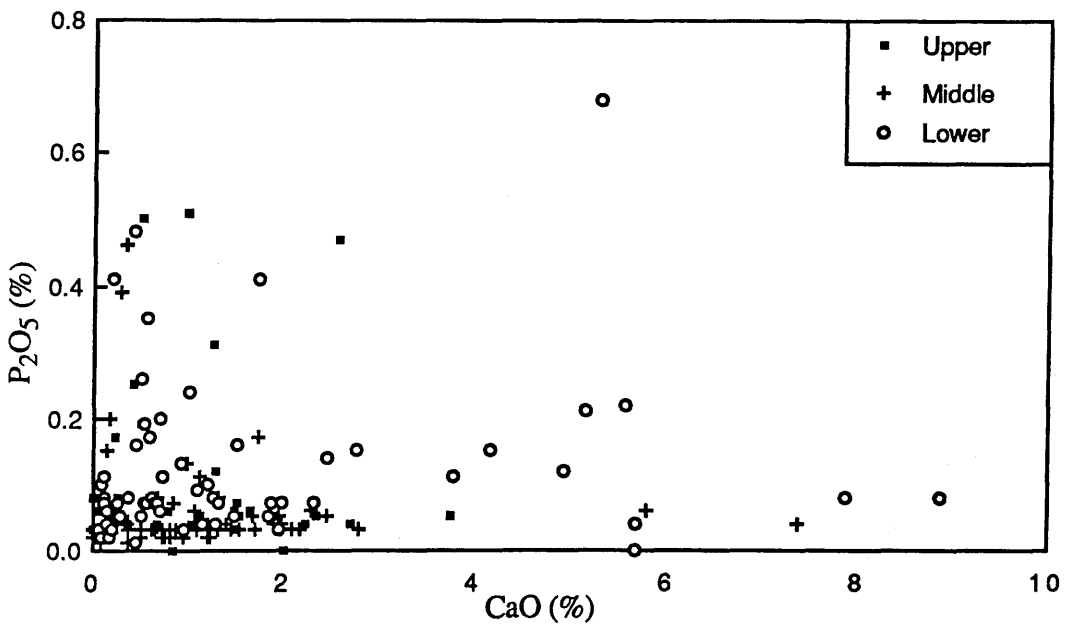
Table 4.5 Average of trace elements of the Saq Sandstones.

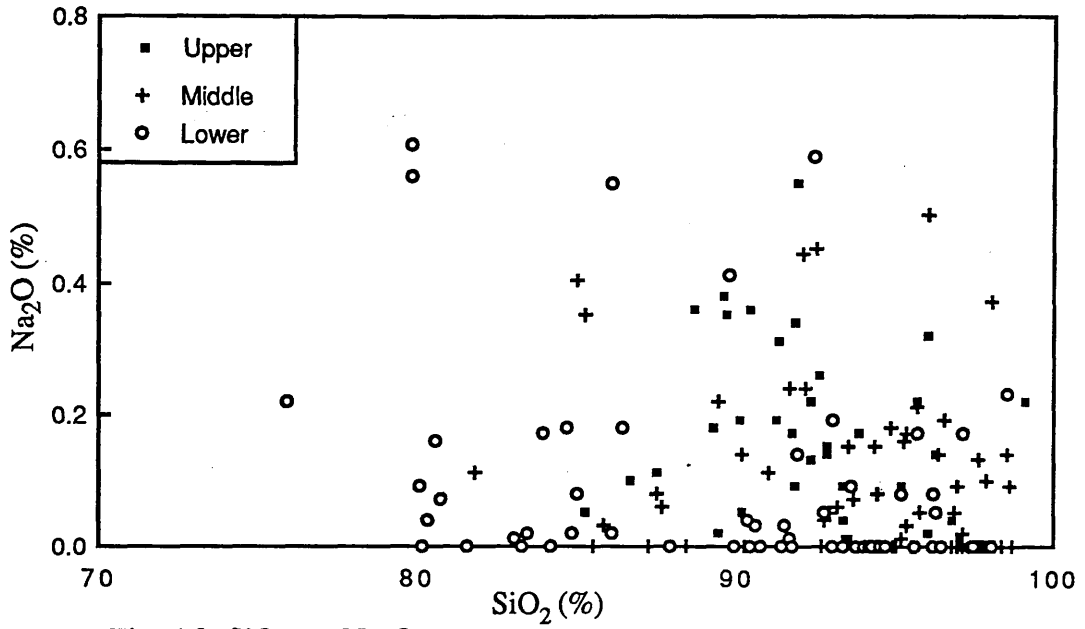
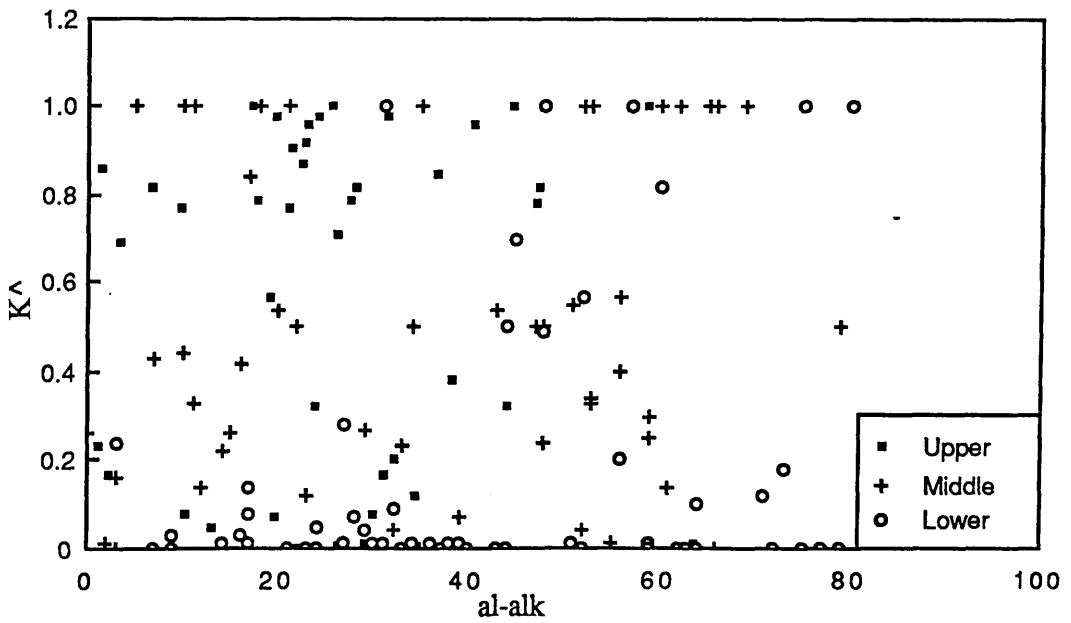
Elements	<u>Upper</u>		<u>Middle</u>		<u>Lower</u>	
	\bar{x}	s	\bar{x}	s	\bar{x}	s
Co	4.20	5.28	8.36	21.20	1.40	0.98
Cr	23.78	15.79	22.75	13.40	20.85	20.92
Ce	42.64	22.95	34.19	19.93	38.5	28.21
Ba	207	182.38	76.83	117.01	132.91	132.28
La	16.69	10.58	13.77	9.78	16.16	14.17
Zr	317.64	258.3	205	210.12	155.42	143.19
Y	16.85	16.06	14.47	10.08	15.17	13.54
Sr	46.66	47.06	72.73	44.40	153.44	99.05
U	2.13	1.13	1.93	1.17	2.14	0.71
Rb	14.46	17.88	2.52	10.19	2.33	7.08
Th	6.58	6.26	7.00	8.66	4.21	4.89
Pb	14.80	13.17	10.16	7.85	10.98	10.54
Ga	3.07	2.44	2.74	4.12	5.14	4.66
Zn	20.68	19.03	13.60	20.85	19.32	20.83
Cu	10.42	15.47	7.66	15.32	7.78	11.97
Ni	7.97	10.19	5.91	11.14	4.25	5.45

Fig. 4.1 SiO_2 vs Al_2O_3 Fig. 4.2 Al_2O_3 vs. K_2O

Fig. 4.3 SiO_2 vs TiO_2 Fig. 4.4 al-alk vs. TiO_2

Fig. 4.5 Plot of Al_2O_3 vs Fe^*O_3 Fig. 4.6 SiO_2 vs. CaO

Fig. 4.7 CaO vs. CO₂Fig. 4.8 CaO vs. P₂O₅

Fig. 4.9 SiO_2 vs. Na_2O Fig. 4.10 al-alk vs. K^\wedge

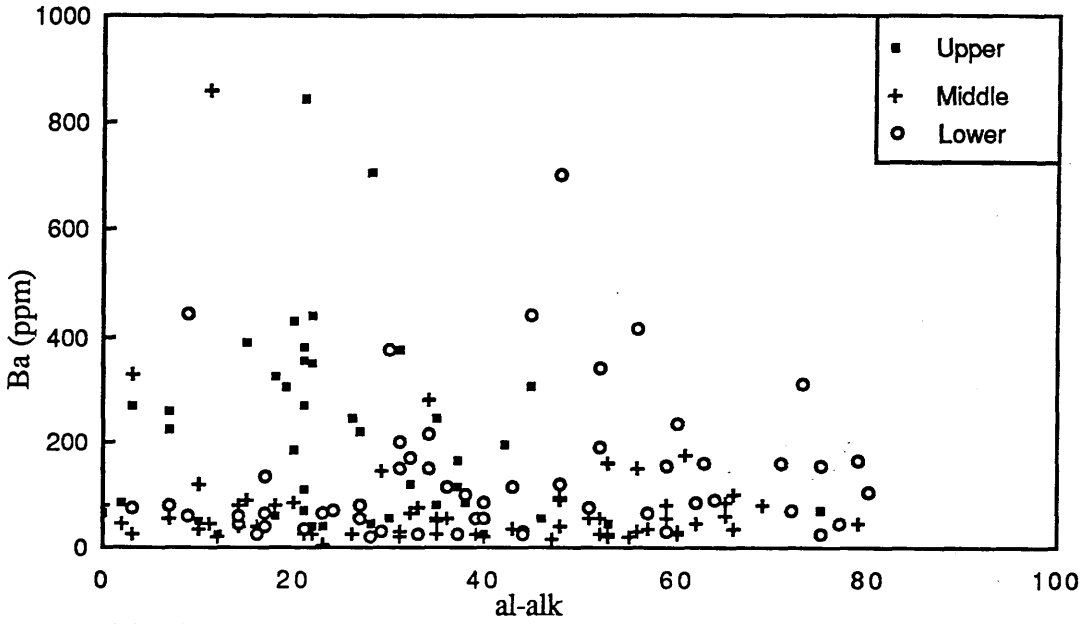


Fig. 4.11 al-alk vs. Ba

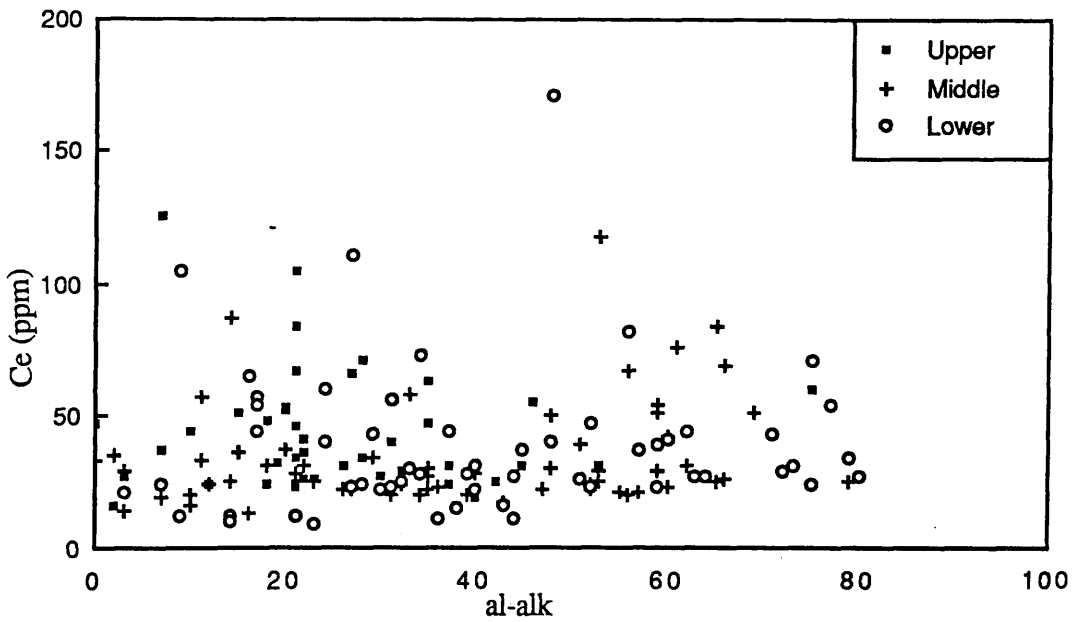


Fig. 4.12 al-alk vs. Ce

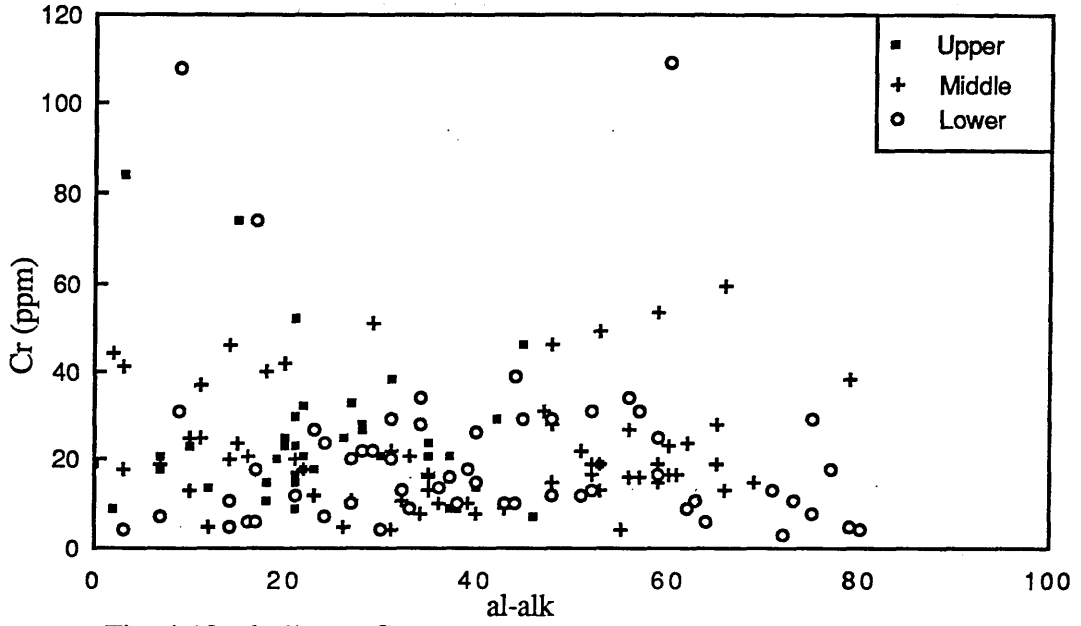


Fig. 4.13 al-alk vs. Cr

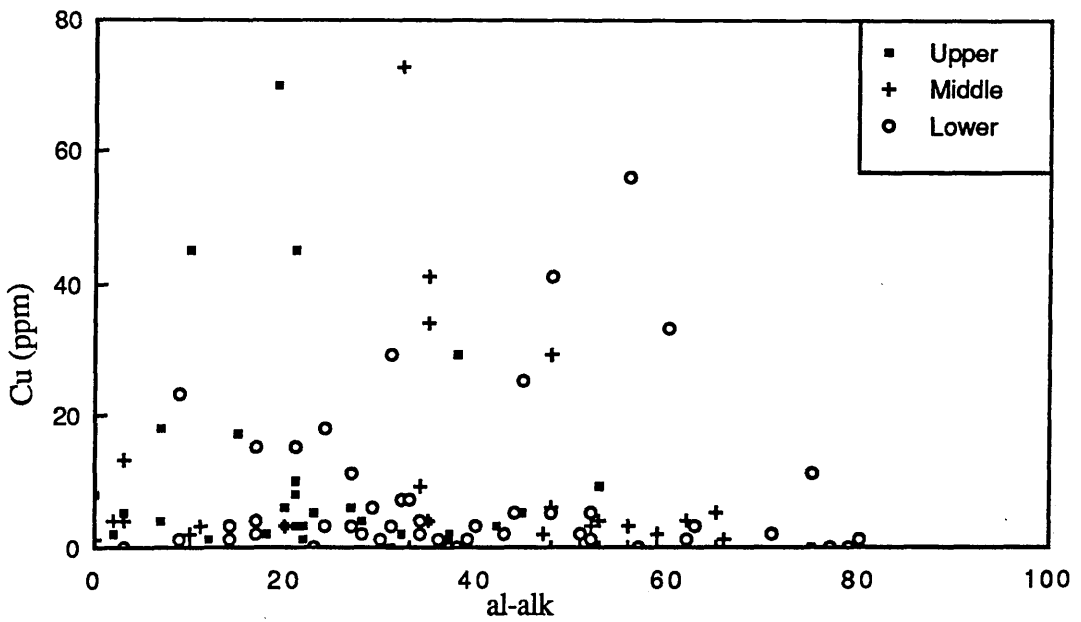


Fig. 4.14 al-alk vs. Cu

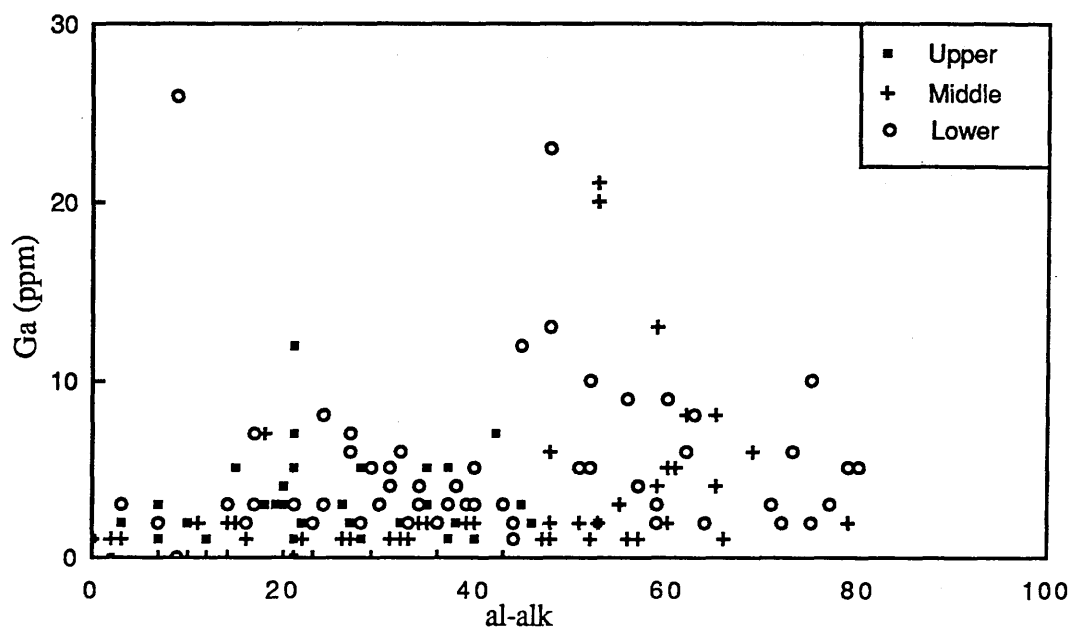


Fig. 4.15 al-alk vs. Ga

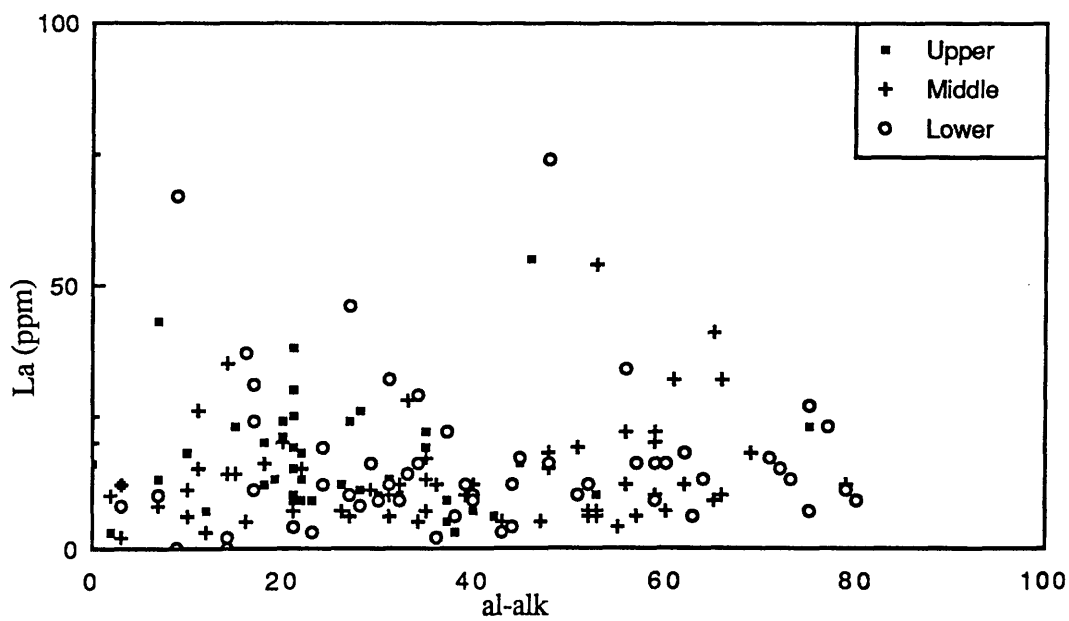


Fig. 4.16 al-alk vs. La

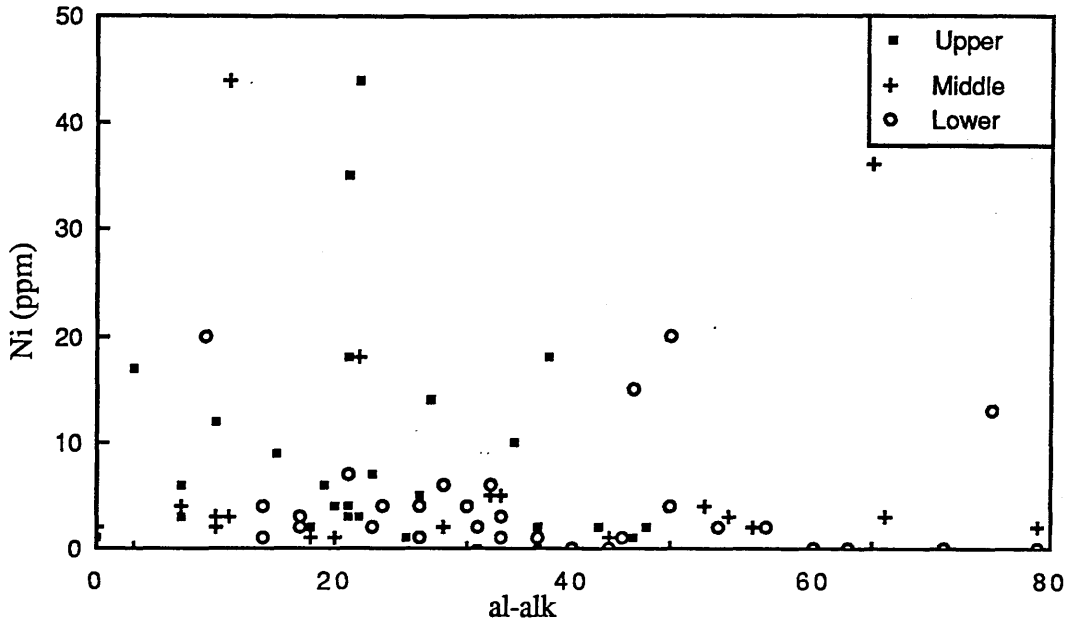


Fig. 4.17 al-alk vs. Ni

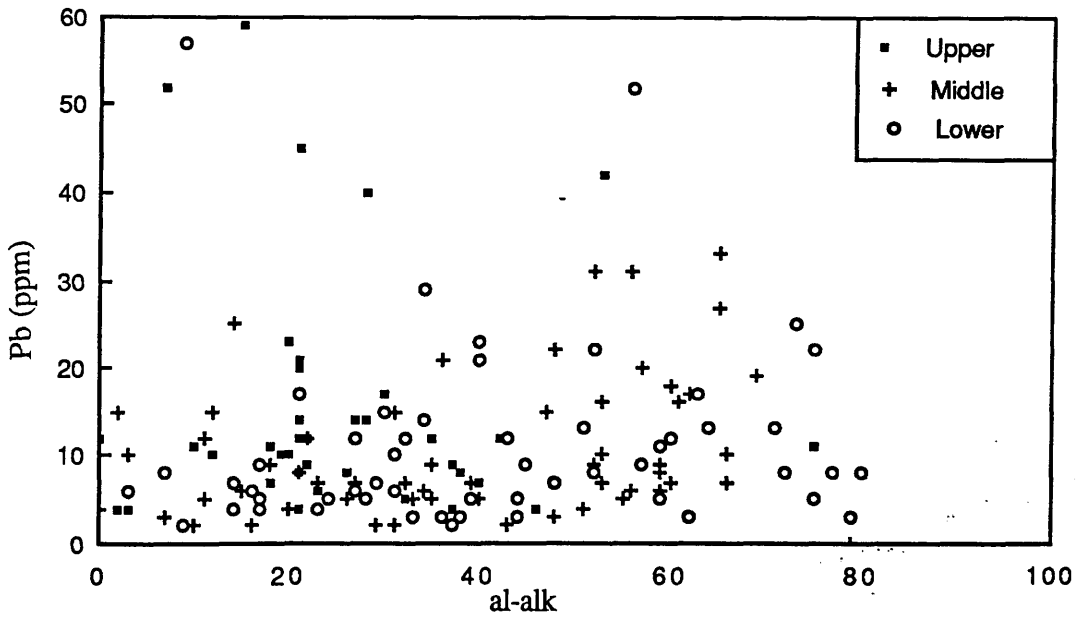


Fig. 4.18 al-alk vs. Pb

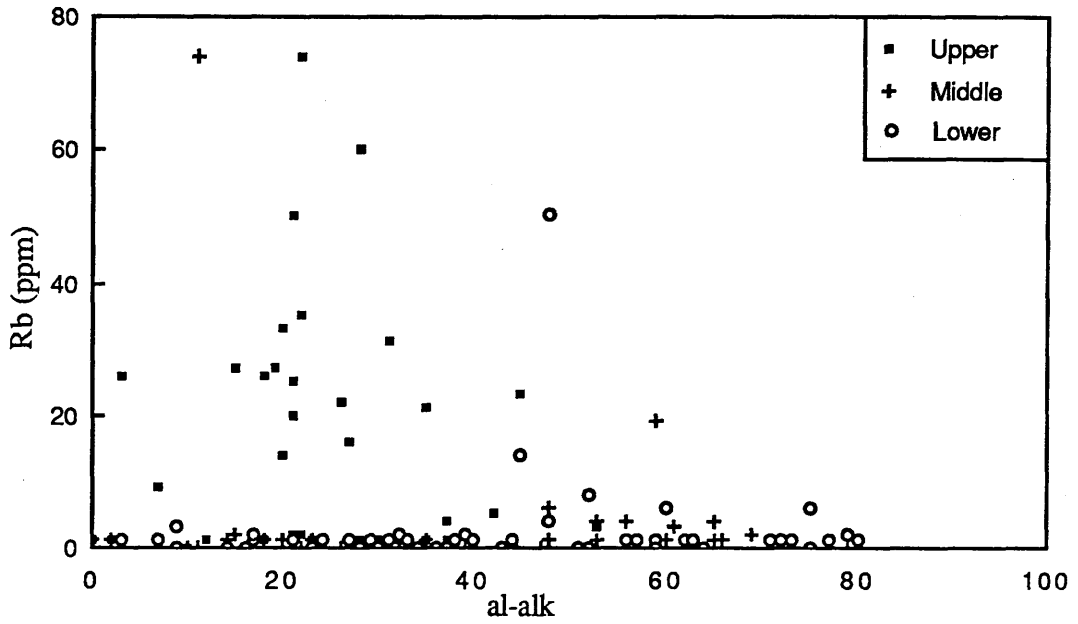


Fig. 4.19 al-alk vs. Rb

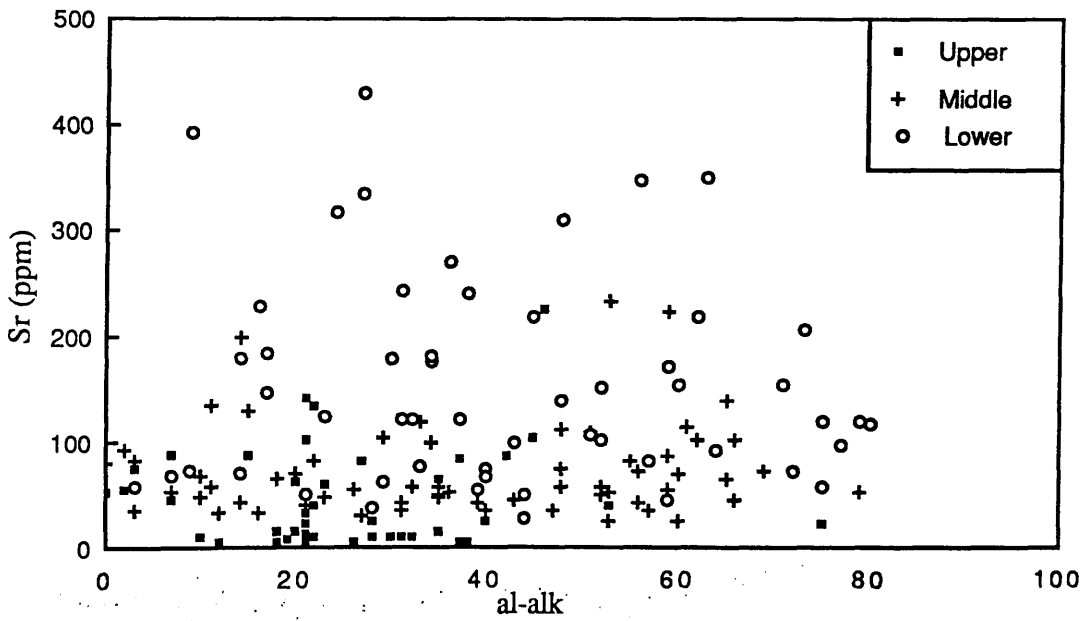


Fig. 4.20 al-alk vs. Sr

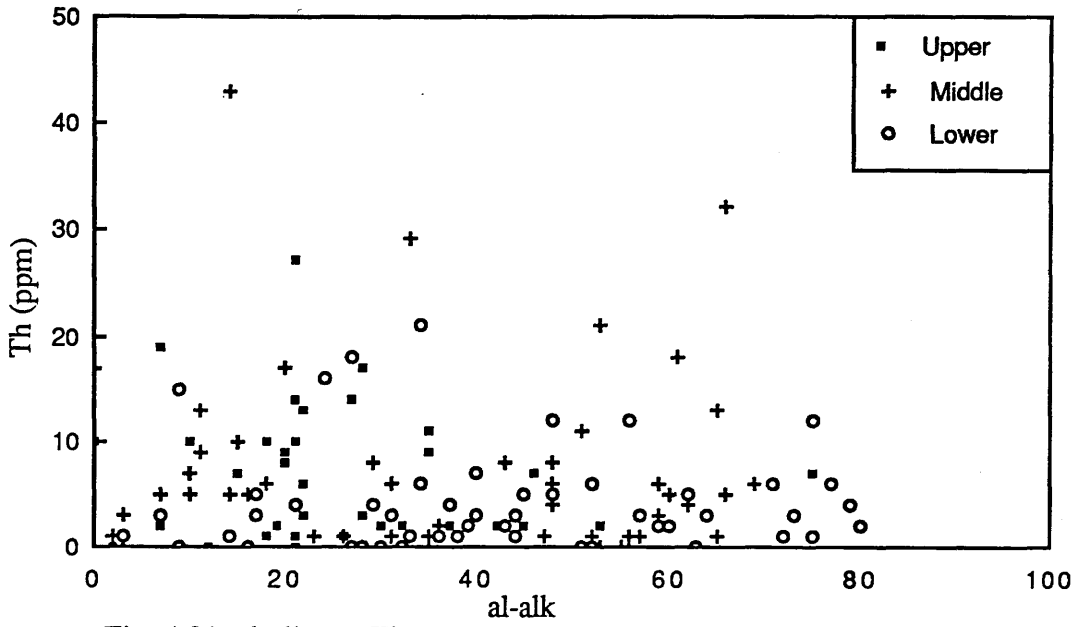


Fig. 4.21 al-alk vs. Th

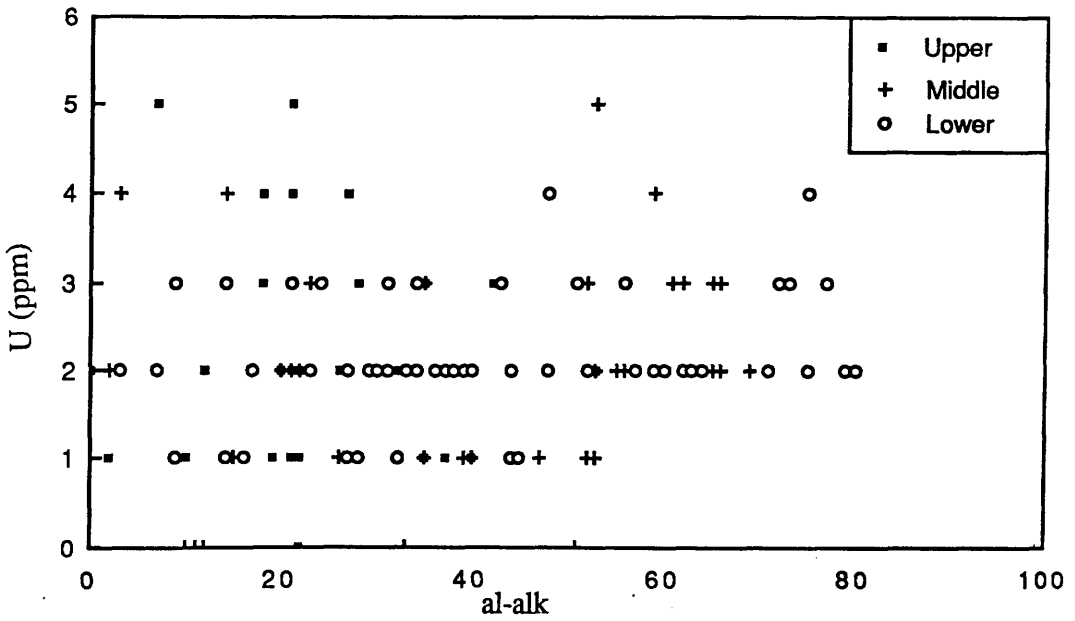


Fig. 4.22 al-alk vs. U

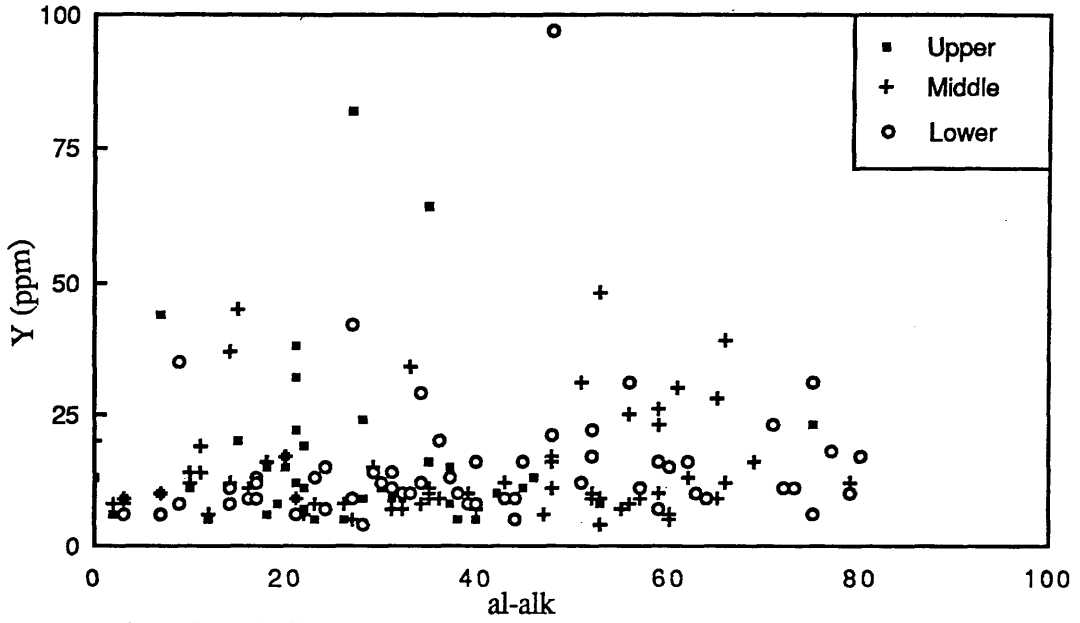


Fig. 4.23 al-alk vs. Y

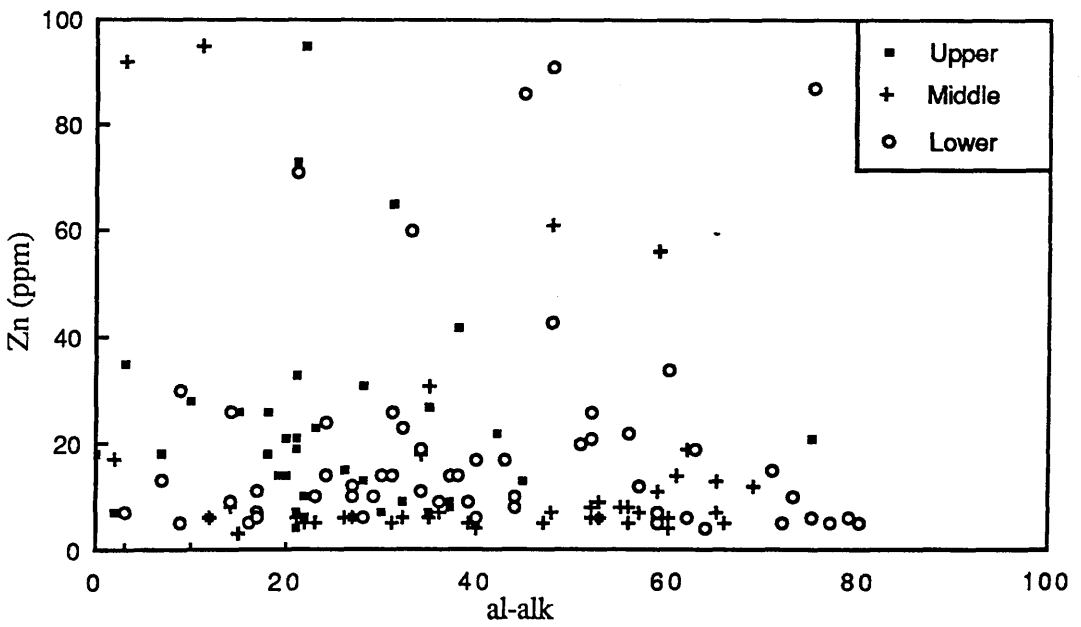
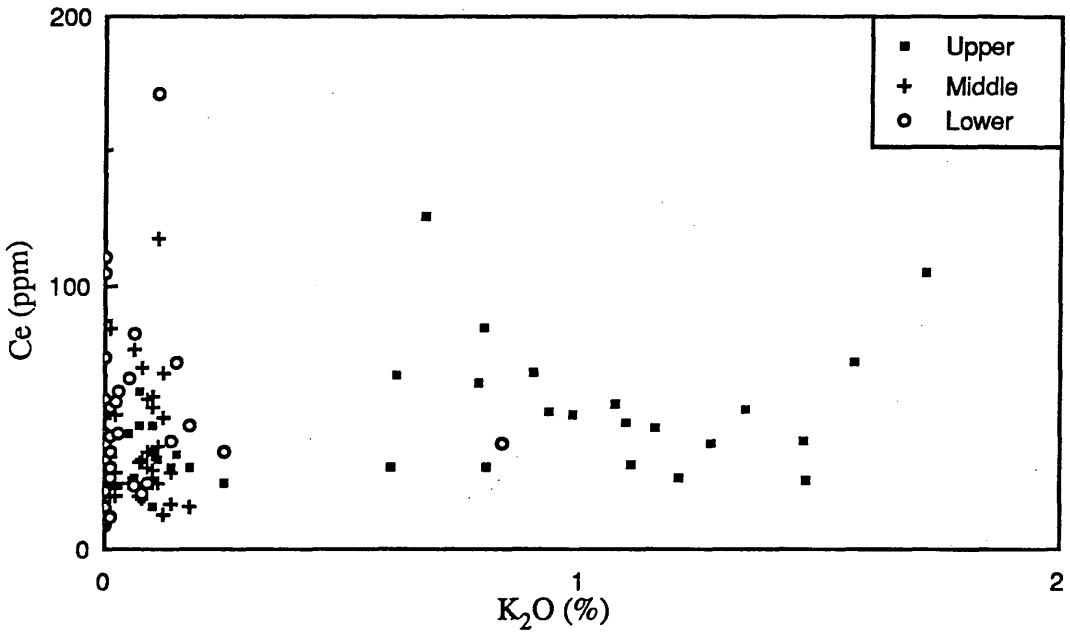
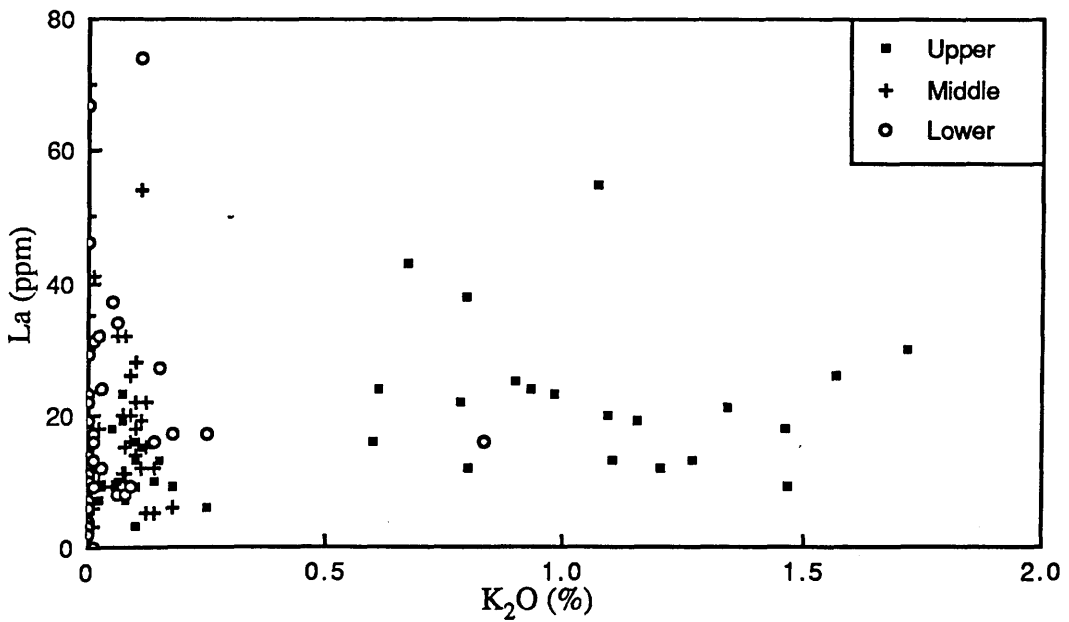


Fig. 4.24 al-alk vs. Zn

Fig. 4.25 K₂O vs. CeFig. 4.26 K₂O vs. La

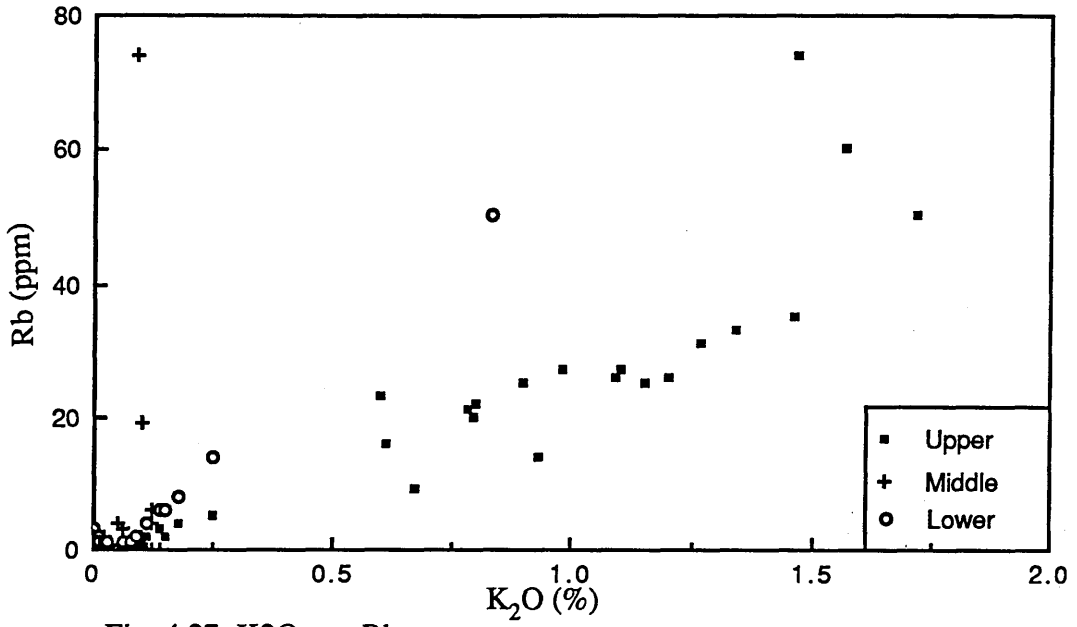
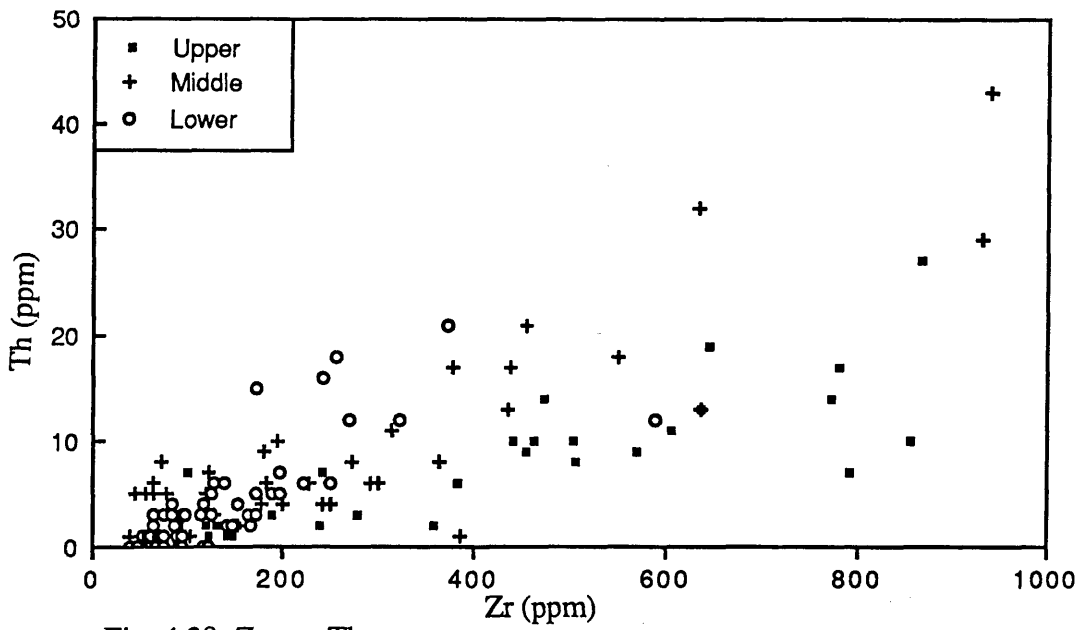
Fig. 4.27 K₂O vs. Rb

Fig. 4.28 Zr vs. Th

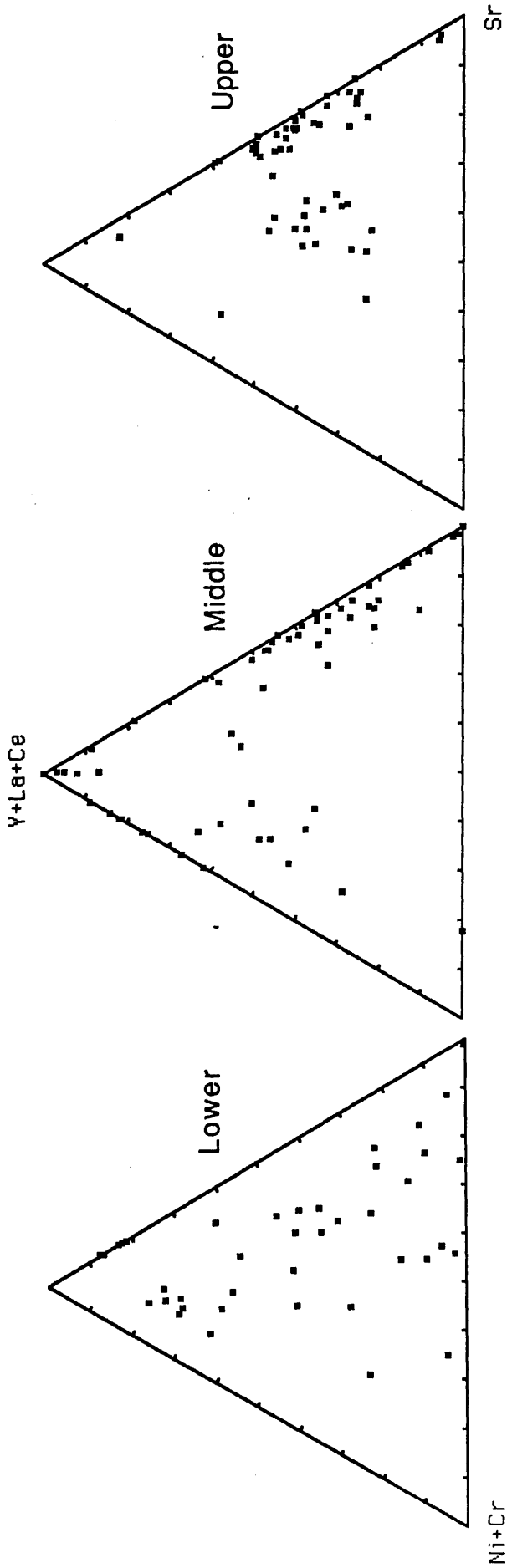


Fig. 4.30 Plot of Ni+Cr versus Y+La+Ce versus Sr to decipher the provenance of the Saq Sandstones (after Hickman & Wright, 1983).

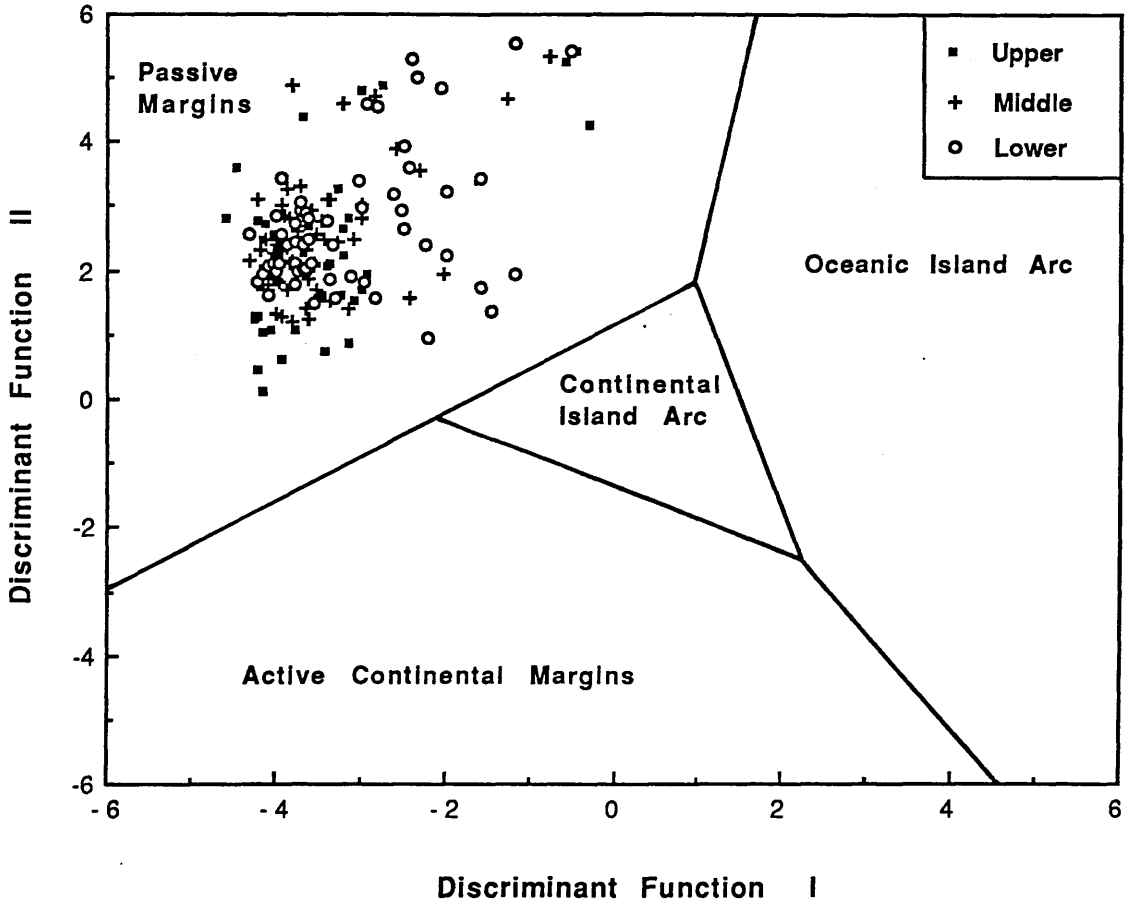


Fig. 4.31 Plot of Discriminate Function I versus Discriminate Function II to decipher the tectonic setting of the Saq Sandstones (after Bhatia, 1983).

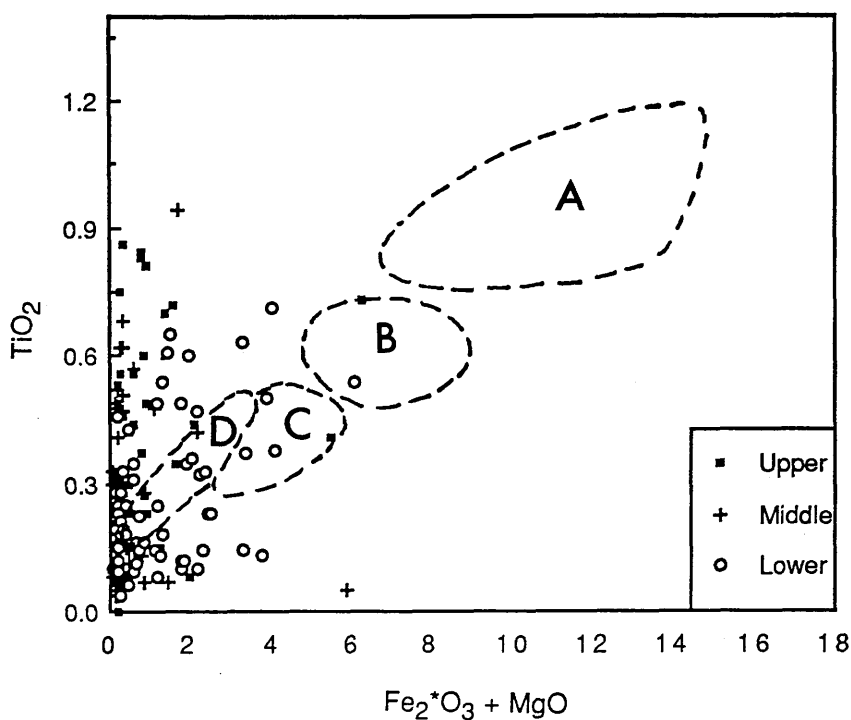


Fig. 4.32 Plot of $\text{Fe}_2^*\text{O}_3 + \text{MgO}$ versus TiO_2 to decipher the tectonic setting of the Saq Sandstones (after Bhatia, 1983): A = Oceanic island arcs; B = Continental island arcs; C = Active continental margins; D = Passive margins.

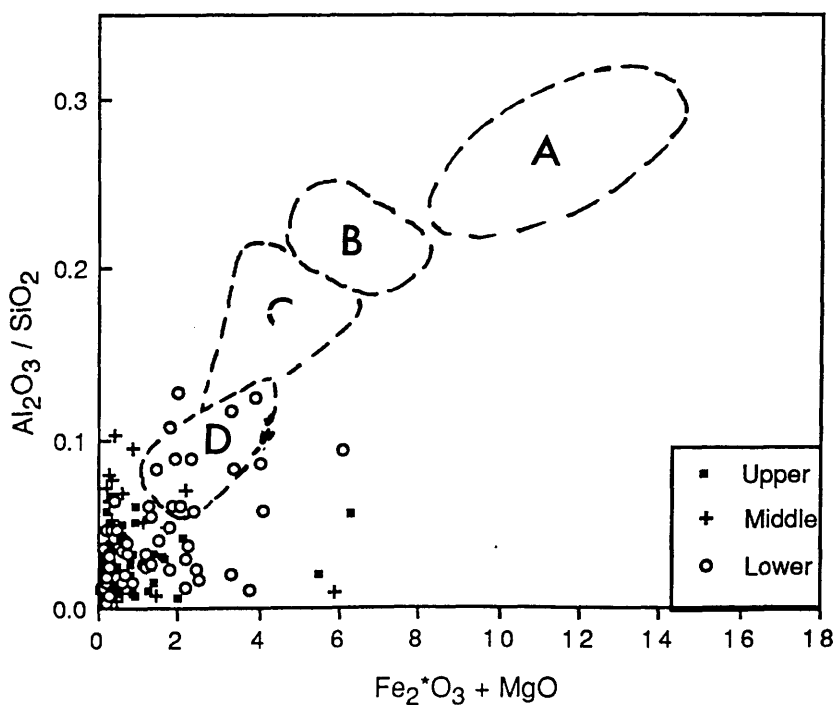


Fig. 4.33 Plot of $\text{Fe}_2^*\text{O}_3 + \text{MgO}$ versus $\text{Al}_2\text{O}_3 / \text{SiO}_2$ to decipher the tectonic setting of the Saq Sandstones (after Bhatia, 1983): A, B, C and D as in Fig. 3.32.

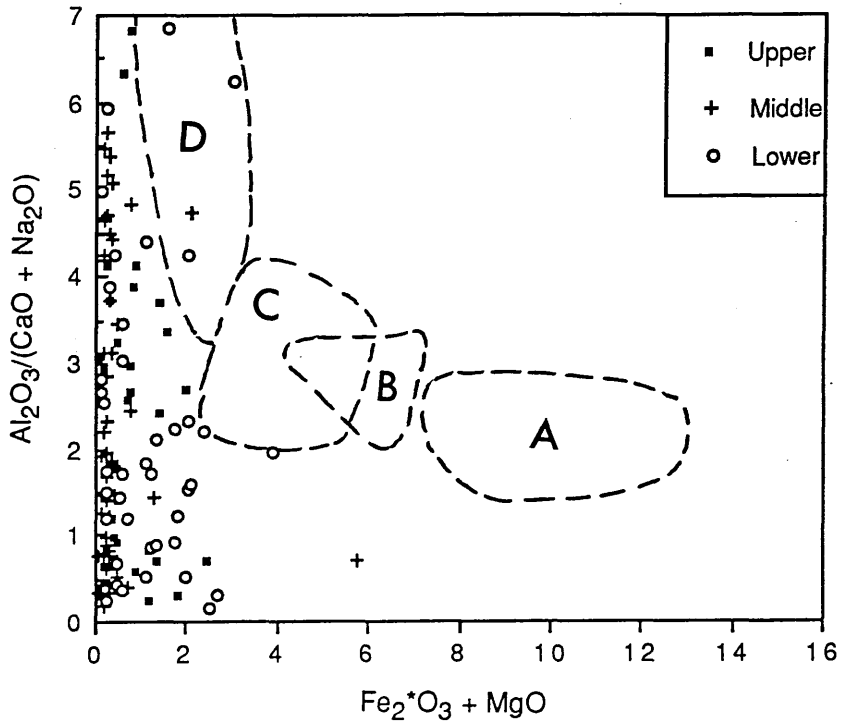


Fig. 4.34 Plot of $\text{Fe}_2^*\text{O}_3 + \text{MgO}$ versus Al_2O_3 ($\text{CaO} + \text{Na}_2\text{O}$) to decipher the tectonic setting of the Saq Sandstones (after Bhatia, 1983): A, B, C and D as in Fig. 3.32.

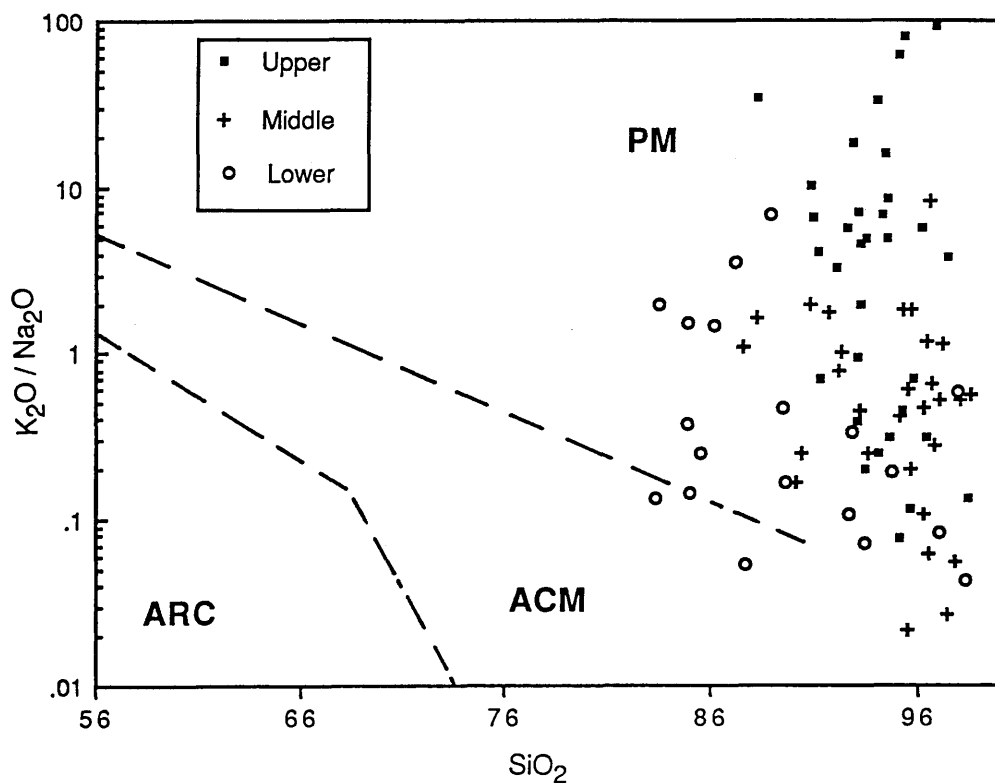
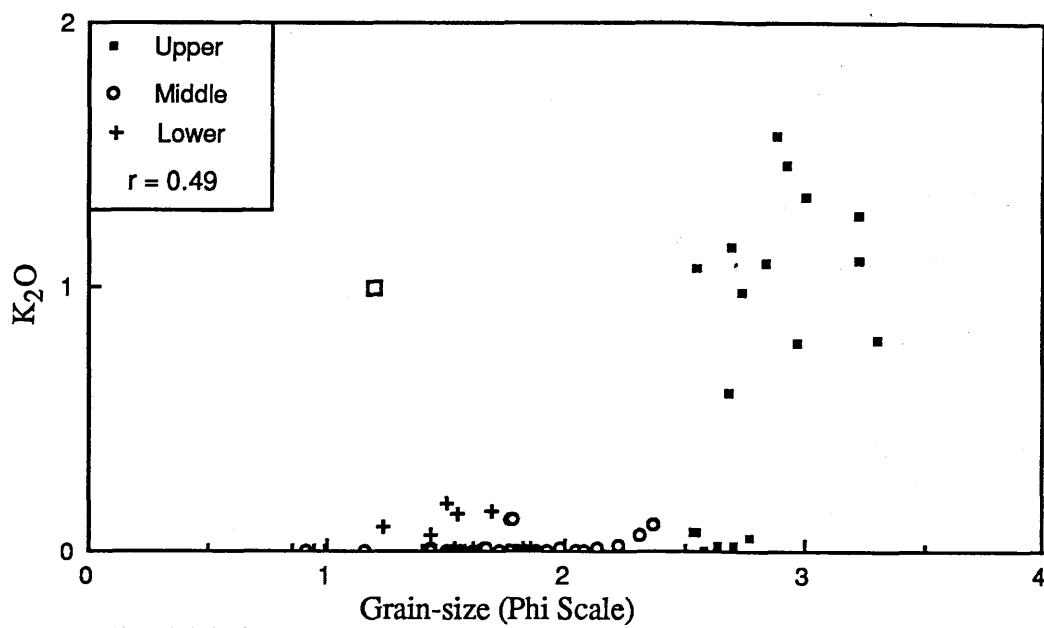
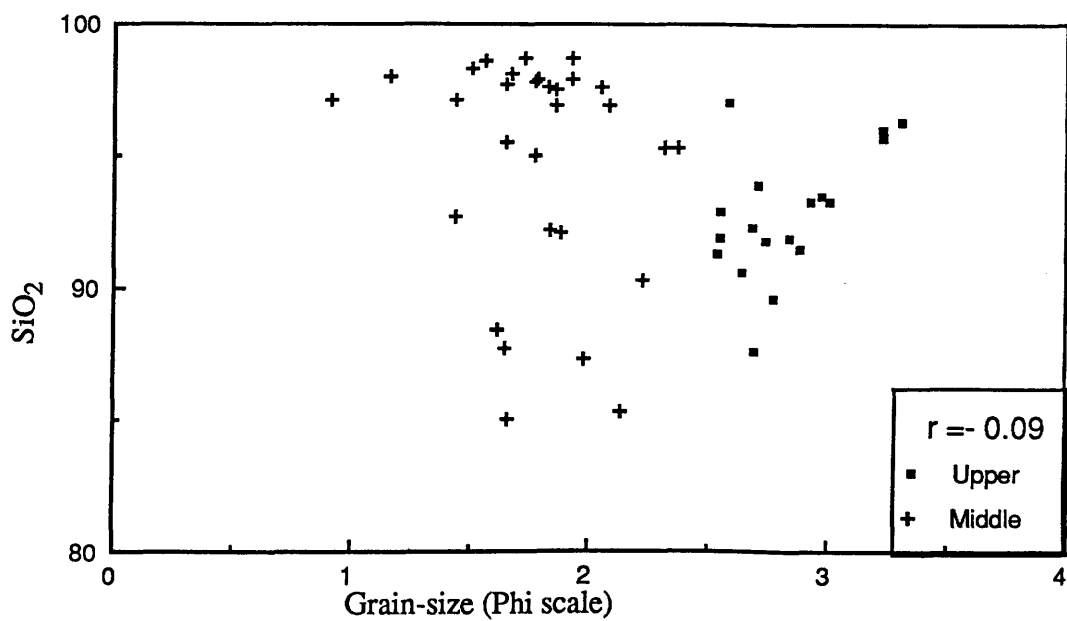


Fig. 4.35 Plot of SiO_2 versus K_2O/Na_2O to decipher the tectonic setting of the Saq Sandstones (after Roser & Korsch, 1986): PM= Passive margins; ACM= Active continental margins; ARC= Oceanic island margins.

Fig. 4.36 Grain-size vs. K_2O Fig. 4.37 Grain-size vs. SiO_2

CHAPTER FIVE

GRAIN-SIZE ANALYSES OF THE SAQ SANDSTONE

5.1 Introduction

The grain-size analysis of clastic rocks has consumed an enormous amount of research energy. The basic idea is that hydrodynamic sorting of a clastic sediment leaves an imprint on the grain size distribution which varies depending on the nature of the hydrodynamic process (Miall, 1984).

It has been used by geologists to characterize depositional environments of clastic sediments and also as an indication of the mechanism of sediment transport (Folk & Ward, 1957; Passega, 1964; Mason & Folk, 1958; Stewart, 1958; Friedman, 1961, 1967 and 1979; Sahu, 1964; Moiola & Weiser, 1968; Passega & Byramjee, 1969; Visher, 1969; Amaral & Prayor, 1977; Moshrif, 1980; 1983; Abu el-ella & Coleman, 1985; Darmonoian & Lindqvist, 1988; Zhenxia *et al.*, 1989; Dias & Neal, 1990).

The aims of the grain-size analysis were:

- (1) To obtain an overall view of the grain-size and the grain-size distribution of the Saq Sandstone.
- (2) To relate the grain-size frequency parameters to mode of transportation.
- (3) To relate the grain-size frequency distribution to the range of depositional environments.
- (4) To evaluate the degree to which the grain-size parameters can be used in differentiating the Saq Sandstones.

5.2 Method

The distribution of sedimentary particles with intermediate diameters ranging from 0.0625 mm to 16 mm (sand and fine conglomerate) is most commonly determined by sieving. The method used here was outlined by Folk, (1974).

Grain-size analyses were performed on more than 110 samples from the Saq Sandstone and carried out with a Ro-tap sieve shaker. A 0.5 ϕ interval was employed to provide maximum accuracy.

Grain-size parameters (graphic mean, inclusive graphic standard deviation, inclusive graphic skewness and kurtosis), as defined by Folk & Ward, (1957) were obtained from values intercepted at specific percentiles Tables 5.1 to 5.3 (Appendix C) on cumulative curves. Other grain-size parameters include median size (Md) and " C ", the first-percentile in the grain-size distribution (Passega, 1957). The grain-size parameters were then plotted on various bivariate diagrams.

5.3 Presentation of grain-size analyses data

There are several ways in which grain-size data can be plotted. The most common are cumulative curves and histograms :-

5.3.1 Cumulative curves

The data of grain-size analyses were plotted as cumulative curves on probability paper (Fig. 5.1 to 5.9) by plotting cumulative percentage versus grain-size in phi (ϕ) intervals to ensure maximum accuracy in determining grain-size parameters by graphic methods. One of the most striking observations is that most of these plots do not come out as one continuous straight line. In fact, commonly two or more straight line segments are present.

The interpretation of the shapes of cumulative grain-size distribution curves in terms of sedimentary response to hydraulic conditions, has attracted the attention of numerous geologists (Visher, 1969; Visher & Haward, 1974; Freeman & Visher, 1975; Sagoe & Visher, 1977). Visher and his co-workers proposed that each cumulative curve comprises a number of straight-line segments and divide each into three sectors, (Fig 5.10) which are associated with bed-load, saltation, and suspension transport.

However, there are a number of problems associated with simple interpretation of these probability curves.

- (1) When a sample of sandstone is taken it may contain many laminae, each of which is characterized by its own particle grain-size and grain-size characteristics. Laminae may be produced by different tractive events, occurring at different times. Some laminae may be produced by stronger, faster flows than others. On these cumulative curves all laminae are plotted as one sample, and these samples are often interpreted as if they were the result of single events, comprising tractive, saltation and suspend loads.
- (2) The fine segment of the cumulative curve is often seen to contain most of the heavy mineral population. As many of these minerals have a density greater than the density of quartz (2.71), they cannot readily be interpreted as part of the suspended load. With zircon having a density of 4.7, grains of would almost certainly have been part of the traction load.
- (3) Diagenetic modification after burial, either by the development of overgrowths or by grain-size reduction by pressure solution modifies apparent grain-size.
- (4) The individual grains of a given size may well travel in more than one transport mode depending on the weather (storm or not), Bridge, (1981).

The comparison of grain-size cumulative curves (Figs 5.1 to 5.9) and the interpretation of separate populations of grains in terms Visher's (1969) diagram leads to the following conclusions: (1) Most of the Saq Sandstones are unimodal; (2) Saltation is the main mechanism of transportation, the saltation population represent more than 90% of the distribution; (3) The Upper Saq Sandstone have mostly been transported by suspension with some saltation; (4) Saltation is the main mechanism for transportation of the Lower and Middle Saq Sandstones, bed-load transport was responsible for some of the movement.

In view of the criticisms levelled at the analysis of cumulative frequency distributions by the Visher methods, a more cautious view must now be taken of these data. It seems most unlikely that the Upper Saq Sandstones were deposited mainly by sediment transported in suspension. There are a variety of influences on the size-frequency distribution which may explain these distributions and these will be discussed later (paragraph 5.7)

5.3.2 Histogram

Histograms have been constructed from weight percentages where the class limits are defined according to Wentworth, (1922) phi scale. Most of the samples from the Saq Sandstone are showing asymmetrical unimodal distribution (Figs. 5.11 to 5.13), where the average grain-size for Lower Saq Sandstone is 1.65 ϕ (Medium sand). The average of Middle Saq Sandstone is 1.88 ϕ (Medium sand), and for the Upper Saq Sandstone is 2.76 ϕ (Fine sand).

It clear from the shapes of the histograms that there are vertical changes in grain-size distribution in the various part of the Saq Sandstone which could be attribute to changes in the energy of the transporting agents, relative distance from land, changes in environment and/or changes in the source of the sediments.

5.4 Grain-size parameters

The statistical parameters of grain-size, frequency distribution (median, graphic mean, inclusive graphic standard deviation, inclusive graphic skewness and kurtosis) have been employed as parameters for delineating the influences of depositional processes. In particular standard deviation and skewness are considered to be environmentally sensitive indicators while the mean size is a reflection of the overall competency of the transportational dynamic system (Folk & Ward, 1957; Friedman, 1961; Folk, 1974). Figure 5.14 shows the vertical variation in sequences of the Saq Sandstone, showing an upwards decrease in grain-size and an upwards increase in

sorting. Tables 5.4 to 5.6 (Appendix C) summarize the grain-size parameters, derived from Folk & Ward's, (1957) graphic measures.

5.4.1 Median (Md)

The median diameter corresponds to the grain-size of 50% of the sample on the cumulative curves, where half of the particles by weight are coarser than the median, and half are finer.

The average median diameters of the Lower, Middle, and Upper Saq Sandstones are 1.59 ϕ , 1.83 ϕ , and 2.74 ϕ respectively, which clearly separates the Upper from Middle and Lower Saq Sandstones.

5.4.2 Graphic mean-size (Mz)

The graphic mean-size is the best measure for determining the average grain-size, and is given by the formula (Folk, 1974)

$$Mz = \frac{\phi 16 + \phi 50 + \phi 84}{3}$$

According to Folk, (1974), the verbal limits of mean-size suggest the following

interpretation: Mz from	-1.0 to 0.0 ϕ	Very coarse sand
	0.0 to 1.0 ϕ	Coarse sand
	1.0 to 2.0 ϕ	Medium sand
	3.0 to 4.0 ϕ	Fine sand
	4.0 to 5.0 ϕ	Coarse silt

The average mean-sizes are 1.65 ϕ , 1.88 ϕ , and 2.76 ϕ for the Lower, Middle, and Upper Saq Sandstones respectively, which clearly separates the Upper From Lower and Middle Saq Sandstones. Mz values for the Lower Saq Sandstones range between 0.88 ϕ to 2.55 ϕ and for the Middle Saq Sandstones range between 0.91 ϕ to 2.67 ϕ , whilst those

of the Upper Saq Sandstones range between 1.79 ϕ to 3.30 ϕ . According to the nomenclature of Folk, (1974) the Upper Saq Sandstones are fine-grained and the Lower and Middle Saq Sandstones are medium-grained sandstone.

5.4.3 Inclusive graphic standard deviation (σ_I)

The inclusive graphic standard deviation is a measure of the sorting of the grain-size distribution and includes 90 percent of the size frequency distribution. Sorting is an expression of the constancy in the energy level of the depositing agent and thus reflects the presence or absence of coarse and (or) fine-grained fractions.

The inclusive graphic standard deviation (sorting) is given by the following formula (Folk, 1974) :-

$$\sigma_I = \frac{(\phi_{84} - \phi_{16})}{4} + \frac{(\phi_{95} - \phi_5)}{6.6}$$

The following is the classification scale for sorting

σ_I under	0.35 ϕ	Very well sorted
	0.35 to 0.50 ϕ	Well sorted
	0.50 to 0.71 ϕ	Moderately well sorted
	0.71 to 1.00 ϕ	Moderately sorted
	1.00 to 2.00 ϕ	Poorly sorted
	2.00 to 4.00 ϕ	Very poorly sorted
More than	4.00 ϕ	Extremely poorly sorted

The frequency distribution of the standard deviation (sorting) values for the Lower, Middle, and Upper Saq Sandstone is shown in figure 5.15. The Upper Saq Sandstone possesses better sorting than Lower and Middle Saq Sandstones. The Lower Saq Sandstone ranges between moderately sorted to moderately well sorted, with an average of 0.79 ϕ (moderately sorted), and Middle Saq Samples range between moderately well

sorted to will sorted, with average an 0.65ϕ (moderately will sorted). Most of the Upper Saq Sandstone is very well sorted to well sorted, with an average of 0.55ϕ (moderately well sorted)

The standard deviation values of the Saq Sandstone show considerable variation, especially between the Upper and both Lower and Middle Saq Sandstones.

5.4.4 Inclusive graphic skewness (SK_I)

Skewness is a measure of the symmetry of the grain-size distribution. A normal distribution, being symmetrical, has zero skewness. If the distribution possesses a coarse tail portion relative to the finer sizes, the skewness is negative; where as, if there is a tail portion in the fine sizes relative to the coarse sizes, the skewness is positive.

Inclusive Graphic Skewness is given by the following formula (Folk, 1974) :-

$$SK_I = \frac{\phi 16 + \phi 84 - 2\phi 50}{2(\phi 84 - \phi 16)} + \frac{\phi 5 + \phi 95 - 2\phi 50}{2(\phi 95 - \phi 5)}$$

According to Folk, (1974), the verbal limits of skewness suggest the following interpretation:-

SK_I from	+ 1.00 to + 0.30	Strongly fine skewed
	+ 0.30 to + 0.10	Fine skewed
	+ 0.10 to - 0.10	Near symmetrical
	- 0.10 to - 0.30	Coarse skewed
	- 0.30 to - 1.00	Strongly coarse skewed

The frequency distribution of skewness values for the Lower, Middle, and Upper Saq Sandstones are shown in figure 5.16. The skewness variation can be readily explained by the presence coarse and fine tails of the distribution. In the Upper Saq Sandstone, skewness ranges between fine skewed to near symmetrical with average of

0.09 (near symmetrical), most of the Upper Saq Sandstone is predominantly fine skewed, with some samples having coarse skewness, which can be attributed to the presence of coarse sands. In the Middle Saq Sandstone skewness ranges between fine skewed to near symmetrical with an average of 0.05 (near symmetrical). The Lower Saq Sandstone has an average of 0.07 (near symmetrical).

The distribution of skewness in the Saq Sandstone is significant where it increases from coarse skewed in the Lower and Middle units to fine skewed in the Upper Saq Sandstone. This could differentiate Upper from Lower and Middle Saq Sandstones.

5.4.5 Graphic kurtosis (k_G)

Kurtosis is used to describe departure from normality. It represents the ratio between sorting in the tail of the curve and sorting in the central portion. If the central portion is better sorted than the tails, the curve is said to be excessively peaked or leptokurtic; if the tails are better sorted than the central portion, the curve is flattened or platykurtic. Kurtosis may be measured by the following formula (Folk, 1974) :-

$$K_G = \frac{\phi_{95} - \phi_5}{2.44 (\phi_{75} - \phi_{25})}$$

The following verbal limits of kurtosis were suggested by Folk, (1974) :

k_G under	0.67	Very platykurtic
	0.67 to 0.90	Platykurtic
	0.90 to 1.11	Mesokurtic
	1.11 to 1.50	Leptokurtic
	1.50 to 3.00	Very leptokurtic
more than	3.00	Extremely leptokurtic

Kurtosis frequency distributions of the Lower, Middle, and Upper Saq Sandstones are shown in figure 5.17. The values of kurtosis fluctuate erratically around a central value of 1 with more than half of the samples having leptokurtic kurtosis. Friedman, (1961) pointed out that most sands are leptokurtic, interpreted by Mason & Folk, (1958) as resulting from mixing of the predominant population with very minor amounts of very coarse and fine gravel material.

The Upper Saq Sandstone ranges between leptokurtic and very leptokurtic with an average of 1.36 (leptokurtic), while the Lower and Middle Saq Sandstones range between mesokurtic to leptokurtic with averages of 1.58, 1.41 respectively, which according to Folk's classification is leptokurtic.

Kurtosis does not suggest any clear differentiation between the various part of the Saq Sandstone.

5.5 Multivariant test

For many years sedimentologists have been attempting to use grain-size analysis to deduce depositional environments. Bivariate plots between grain-size parameters and linear discriminate functions are some of the methods used for depositional environments discrimination.

5.5.1 Bivariate discriminate plots

Numerous bivariate analyses have been employed on recent and ancient sediments to differentiate between beach, fluvial, and eolian sediments (Friedman, 1961, 1967, 1979; Stewart, 1958; Folk & Ward, 1957; Passega, 1957, 1969; Amaral & Pryor, 1977; Moshrif, 1980; Abu el-ella & Coleman, 1985)

5.5.1.1 Median diameter vs Skewness & vs Standard deviation

The plots of median size verses skewness and standard deviation shown in figures 5.18 and 5.19 respectively have been used by Stewart (1958) to distinguish between wave action and river processes.

The interpretation rendered by discriminating fields (Stewart, 1958) indicate that wave action was the dominant process in the Upper Saq Sandstone, while river processes were dominant in the Lower and Middle Saq Sandstones.

5.5.1.2 Standard deviation vs. Mean-size

Mean-size plotted against standard deviation (Fig. 5.20) is considered to be an effective discriminator between river, dune, and beach sands (Friedman, 1961, 1967; Moiola & Weiser, 1968). Most of the Upper Saq Sandstone are beach deposits (Friedman, 1967) and the Lower and the Middle Saq Sandstones are mixed dune and river deposits (Friedman, 1961).

Most of the Saq Sandstone samples fall in the river field according to the diagram of Moiola & Weiser, (1968).

5.5.1.3 Mean-size vs. Skewness

Plots of mean-size versus skewness (Fig. 5.21) have been proposed as the most effective discriminator between beach and dune sands (Friedman, 1961; Moiola & Weiser, 1968). In Moiola and Weiser's diagram, (1968) all of the Upper Saq Sandstone samples fall in the dune field, and Lower and Middle Saq Sandstones samples are mixed dune and beach. In Friedman's (1961) diagram most of the Saq Sandstone reflect dune environments.

5.5.1.4 Standard deviation vs. skewness

Friedman, (1967) used standard deviation and skewness to discriminate between beach and river environments

A plot of standard deviation versus skewness (Fig. 5.22) shows that most of the Upper Saq Sandstone fall in the beach environment field and the Middle Saq Sandstone is mixed between beach and river environment fields. The Lower Saq Sandstone is river environment.

Methods of interpreting grain-size parameters tested here were not fully successful in disclosing the paleoenvironments of the Saq Sandstone. As pointed by Solohub & Klovan, (1970), the bivariate plots appear to be too simple to disentangle the complexity of factors affecting the grain-size distribution of sands and sandstones.

Zhenxia *et al.*, (1989) used grain-size parameters (standard deviation and skewness) in bivariate plots of tidal deposits. All tidal current sands fall in the river sand area, and they attributed this result to the fact that river sands and tidal current sands are transported and deposited by flows with restricted boundaries, so they fall in the same field.

5.5.2 Linear discrimination function

This method combines all the grain-size parameters into a single linear equation. Substituting size parameters of the unknown into the equation gives a value that can then be compared to values obtained from modern depositional environments (Amaral & Pryor, 1977).

The linear discriminate functions of Sahu, (1964) and Soven, (1966) were used here:-

5.5.2.1 The discrimination function of Sahu (1964)

Sahu, (1964) empirically established four discriminate functions based on the graphical parameters of Folk & Ward, (1957) to differentiate sedimentary environments.

The four discriminate functions are :-

- (1) Discriminate function Y1, to differentiate between eolian and beach environments, and calculated as

$$Y1 = 3.5688 Mz + 3.7016 \sigma_I^2 - 2.0766 SK_I + 3.1135 K_G$$

Where

Mz is the graphic mean

σ_I^2 is the variance

SK_I is the graphic skewness

K_G is the graphic kurtosis

A Y1 value less than (-2.7411) indicates an eolian environment ; one greater than (-2.7411) indicates a beach environment.

(2) Discriminate function Y2, is used to differentiate between shallow agitated marine environments and beach environments, and is calculated as

$$Y2 = 15.6534 Mz - 0.657091 \sigma_1^2 + 18.1071 SK_I + 18.5043 K_G$$

A Y2 value less than (65.3650) indicates a beach environment; one greater than (65.3650) indicates a shallow agitated marine environment

(3) Discriminate function Y3, is used to differentiate between a shallow agitated marine environment and a fluvial (deltaic) environment , and is calculated as

$$Y3 = 0.2852 Mz - 8.7604 \sigma_1^2 - 4.8932 SK_I + 0.0482 K_G$$

A Y3 value less than (-7.4190) indicates a fluvial (deltaic) environment; one greater than (-7.4190) indicates a shallow agitated marine environment

(4) Discriminate function Y4, is used to differentiate between turbidity current environments and fluvial (deltaic) environments, and is calculated as

$$Y4 = 0.7215 Mz - 0.4030 \sigma_1^2 + 6.7322 SK_I + 5.2927 K_G$$

A Y4 value is less than (9.8433) indicates a turbidity current environment; one greater than (9.8433) indicates a fluvial (deltaic) environment.

The Sahu parameters have been computed for the Lower, Middle and Upper Saq Sandstones and are summarized in Tables 5.7 to 5.9 (Appendix C), with averages in Table 5.10.

The Y1 indicates of beach environment for the Upper Saq Sandstone and an eolian environment for the Lower and Middle Saq Sandstones. The Y2 suggests a shallow agitated environment for the Lower and Upper Saq Sandstones, and a fluvial (deltaic) environment for the Middle Saq Sandstone. The Y3 value indicates a fluvial (deltaic) environment for all the Saq Sandstone. The Y4 value indicates a turbidity current environment for both Lower and Middle Saq Sandstones, and a fluvial (deltaic) environment for the Upper Saq Sandstone.

5.5.2.2 The discrimination function of Sevon (1966)

The linear discriminate functions of Sevon, (1966) have been computed for the Saq Sandstones to deduce the depositional environment. Sevon established three discriminate functions based on the graphical parameters of Folk & Ward, (1957). The three discriminate functions are:

- (1) Discriminate function R1, to differentiate between beach and dune environments, is calculated as follows

$$R1 = -0.0662 Mz + 0.02842 \sigma_1 - 0.0067 SK_I + 0.00399 K_G$$

If R1 is more than 0.025 it indicates beach environment, and if R1 is less than 0.025 it indicates a dune environment.

- (2) Discriminate function R2, is used to differentiate between beach and river environments, and is calculated as follows

$$R2 = 0.00152 Mz - 0.04371 \sigma_1 - 0.00624 SK_I + 0.00375 K_G$$

If R2 is more than 0.075 it indicates a beach environment, and if R2 is less than 0.075 it indicates a river environment.

- (3) Discriminate function R3, is used to differentiate between dune and river environments, and is calculated as follows

$$R3 = 0.04601 M_z - 0.049935 \sigma_1 + 0.00976 SK_1 + 0.01920 K_G$$

If R3 is more than 0.17 it indicates a dune environment, and if R3 is less than 0.14 it indicates a river environment. Values of R3 between 0.14 and 0.17 are in a field of overlap.

The results of these three tests for the Saq Sandstone are summarized in Tables 5.11 to 5.13 (Appendix C), and averages in Table 5.14. The R1 discriminate function indicates dune environments for all the Saq Sandstone and R2 and R3 discriminate functions indicate a river environment for the Saq Sandstone.

5.6 The grain-size image (CM Diagram)

Passega, (1957) proposed that the fine and coarse fractions of sediments often act independently of each other and hence should be treated separately. He interpreted the coarse fraction (characterized by C, the one-percentile particle diameter, measured in microns) as best representing the environment as a whole. Parameter M (the fifty-percentile particle diameter in microns) yields a measure of the sediments's average coarseness.

The CM diagram is constructed by plotting C versus M on logarithmic paper. Passega, (1957, 1964) interpreted the distribution of sample points on CM diagrams as reflecting the processes of sediment deposition.

Passega, (1964) subdivided the CM diagram in to five segments which correspond to particular sedimentation mechanisms (Fig. 5.23). These segments are (NO) rolling;

(OP) rolling and suspension; (PQ) suspension and rolling; (QR) graded suspension; (RS) uniform suspension, and (T) pelagic suspension, which represents the finest sediments (< 15 micron).

Passega & Byramjee, (1969) further subdivide the CM diagram into nine classes from I to IX (Fig. 5.23). Generally sediments of classes I, II, III and IX have values of C higher than 1 mm and these sediments have mainly been transported by a rolling mechanism, while sediments of classes IV, V, VI, VII, and VIII indicate grains have been transported by a suspension mechanism but include some sediments transported by rolling (These rolled sediments may have been transported long distances in suspension before being rolled and are therefore included in the classification with sediments deposited by the suspension mechanism), Passega & Byramjee, (1969). Line $M=100$ microns commonly divides uniform from graded suspension (saltation) sediments. Classes IV and V are generally graded suspension.

Figure 5.23 shows the distribution of the Saq Sandstone samples. All the Upper Saq Sandstone samples fall in class V, indicating that they were transported by a suspension mechanism. The majority of the Lower and Middle Saq Sandstone samples (> 75%) fall in classes IV and V, indicating that they were transported by a graded suspension (saltation) mechanism, and some of the samples (< 25) fall in class I, indicating that they were transported by rolling.

The averages of Upper (A), Middle (B), and Lower (C) Saq Sandstones are plotted in the CM diagram, Fig. 5.23, and all fall in classes IV and V, indicating that they were transported by a graded suspension (saltation) mechanism.

5.7 Discussion

- (1) There is clear upwards fining in the Saq Sandstone, with a sudden coarsening (medium-grained) toward the very top (where there are beaches). This fining can be produced by a number of factors:

- (a) Distance from source, if the Saq Sandstones are seen as a transgressive sheet, then the Upper Saq (with the exception of the very uppermost unit) may represent increasing distance from source (Fig. 5.24)
 - (b) The upwards fining may also be related to grain-size of the sediment entering the basin. During the interval from Lower to Upper Saq the basement may have been drained by a large river system which delivered progressively finer sediment load (Fig. 5.25).
 - (c) A change in environment. This is not thought to be significant as tidal bars are found throughout the sequence.
- (2) There is an overall increase in sorting toward the upper part of the sequence. This may be produced because coarse sizes were not available for the Upper Saq Sandstones. This view is supported by a slight upward change in skewness toward a more positive value. i.e. there is a long tail of fine sand in the Upper Saq as opposed to the Lower. This would suggest that factors 1 and 2 controlling grain-size are the significant controls on this whole frequency distribution.

Table 5.10 Summary of averages of Sahu s (1964) parameters of the Saq Sandstones.

Sahu Param. Saq	(Y1) Aeolian : Beach	(Y2) Beach : Shallow marine	(Y3) Shallow marine: Fluvial	(Y4) Fluvial : Turbidite
Upper	-5.2922 (Beach env.)	81.3848 (Shallow agitated env.)	-0.9060 (Fluvial"deltaic" env.)	10.2699 (Fluvial"deltaic" env.)
Middle	-1.3446 (Aeolian env.)	74.5270 (Shallow agitated env.)	-2.4094 (Fluvial"deltaic" envi.)	8.6215 (Turbidity env.)
Lower	-0.0950 (Aeolian env.)	84.0258 (Shallow Agitated env.)	-4.3436 (Fluvial"deltaic" env.)	8.3821 (Turbidity env.)

Table 5.14 Summary of averages of Sevons (1966) parameters of the Saq Sandstones

Sevon Parame. Saq	(R 1) Beach : Dune	(R 2) Beach : River	(R 3) Dune : River
Upper	-0.167 (Dune)	-0.0067 (River)	0.1378 (River)
Middle	-0.1008 (Dune)	-0.0155 (River)	0.0837 (River)
Lower	-0.083 (Dune)	-0.0231 (River)	0.066 (River)

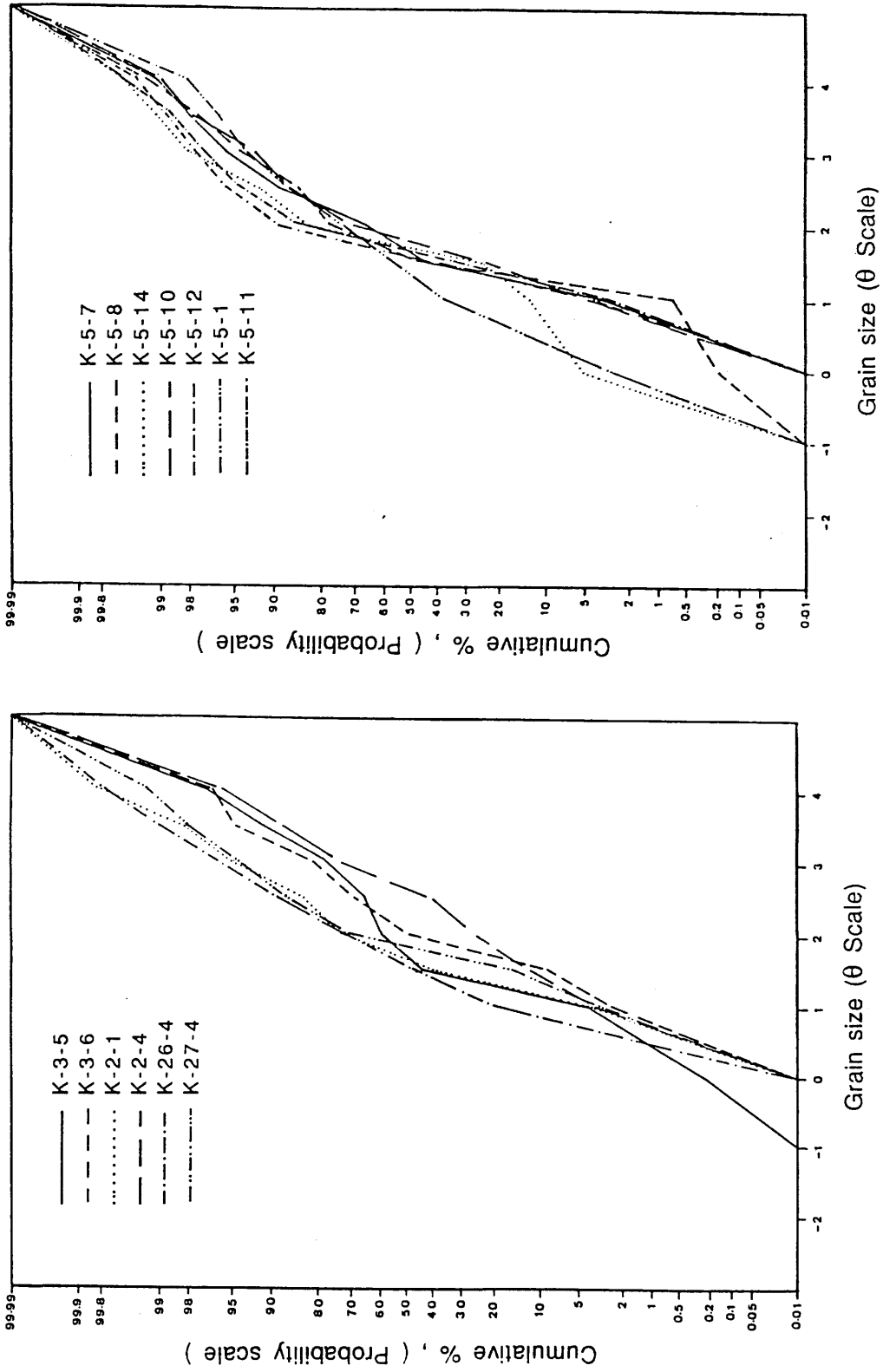


Fig. 5.1 Cumulative-frequency curves of grain-size of Lower Saq Sandstones.

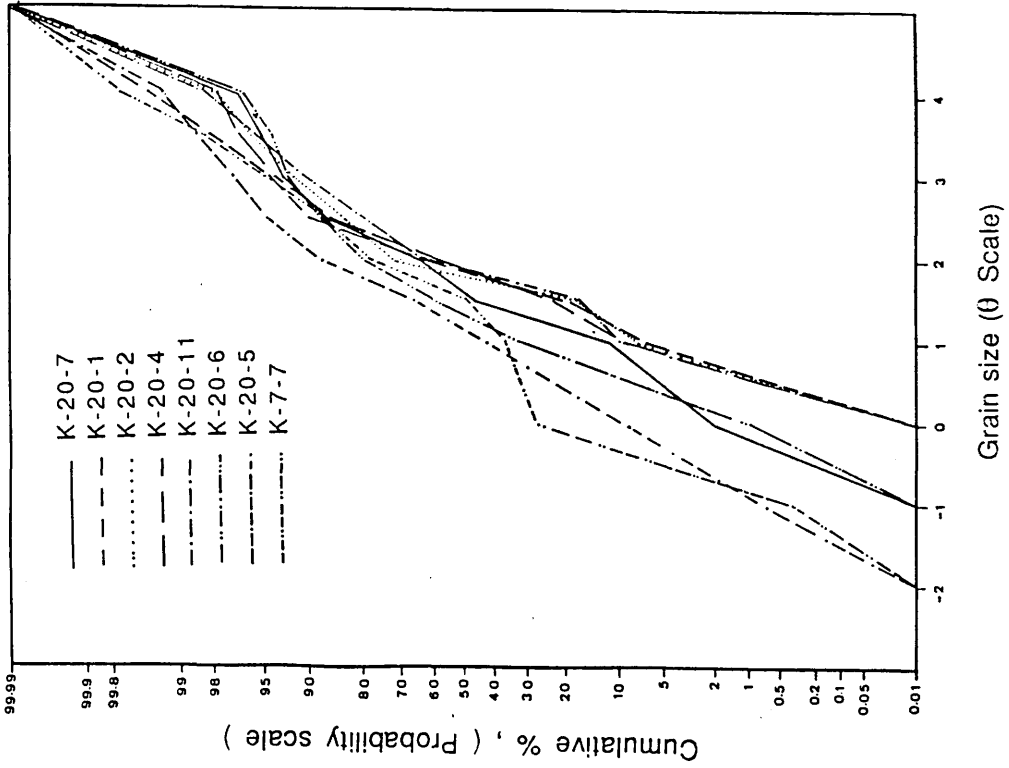
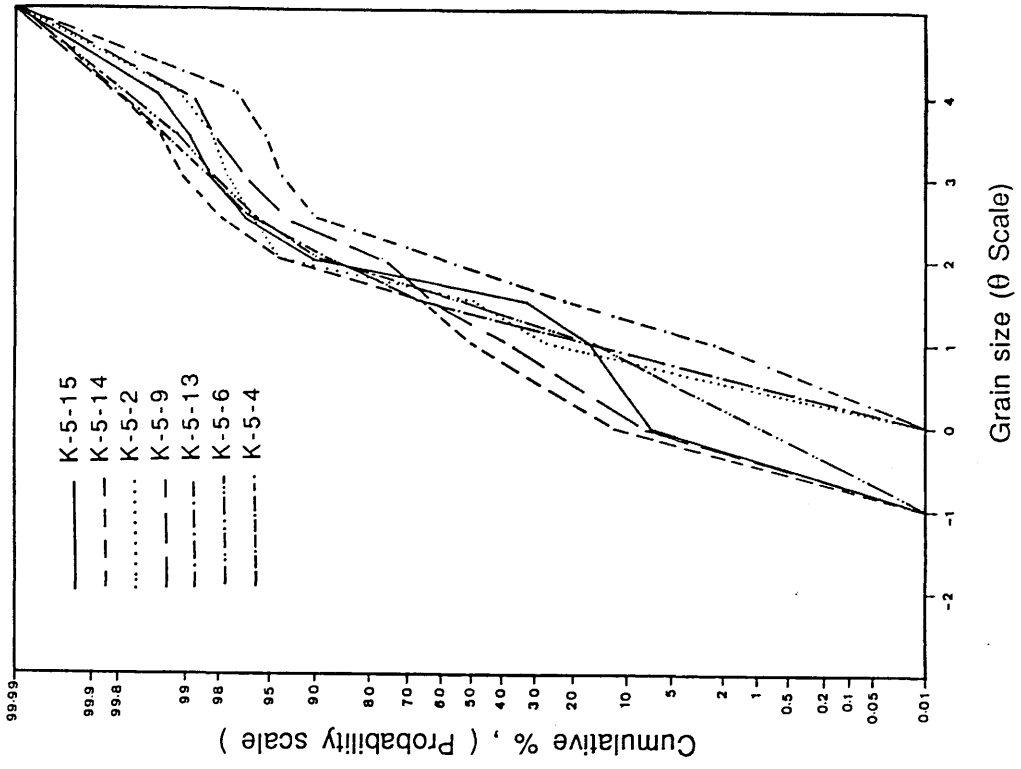


Fig. 5.2 Cumulative-frequency curves of grain-size of Lower Saq Sandstones.

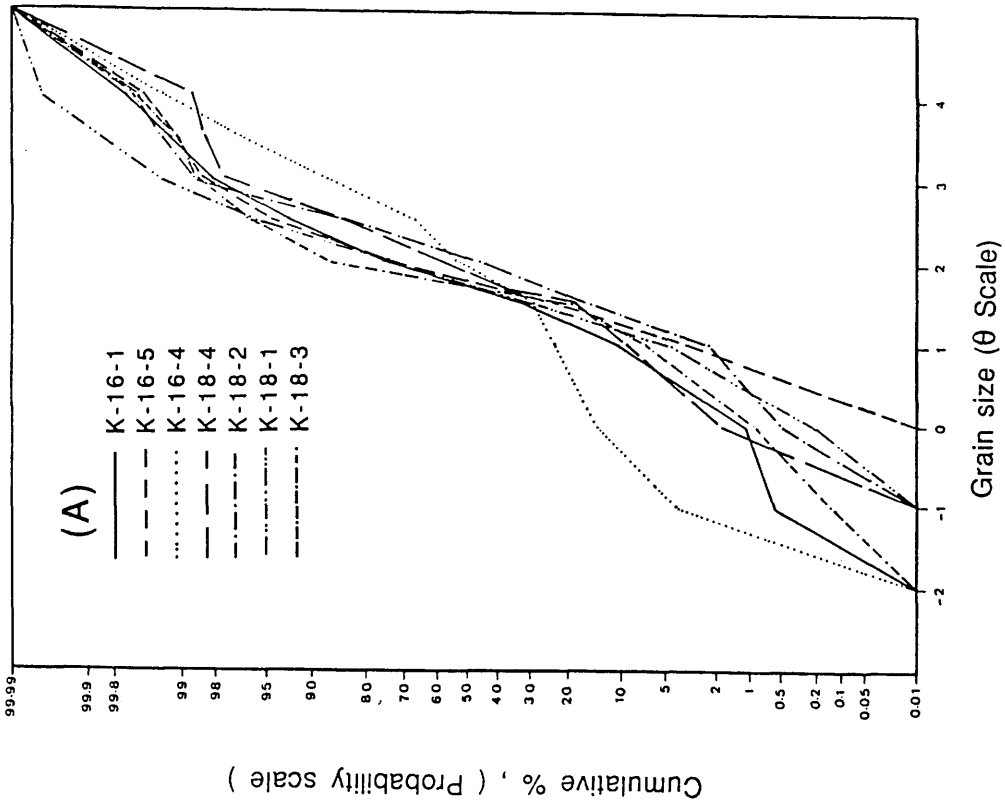
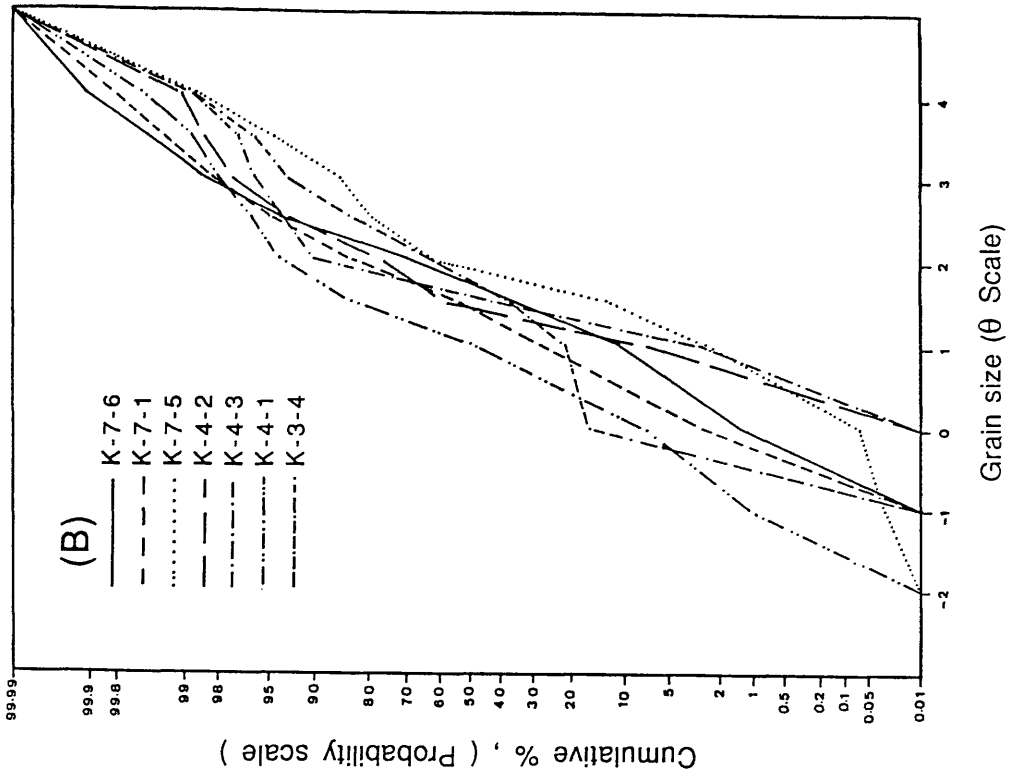


Fig. 5.3 Cumulative-frequency curves of grain-size of Middle (A) and Lower (B) Saq Sandstones.

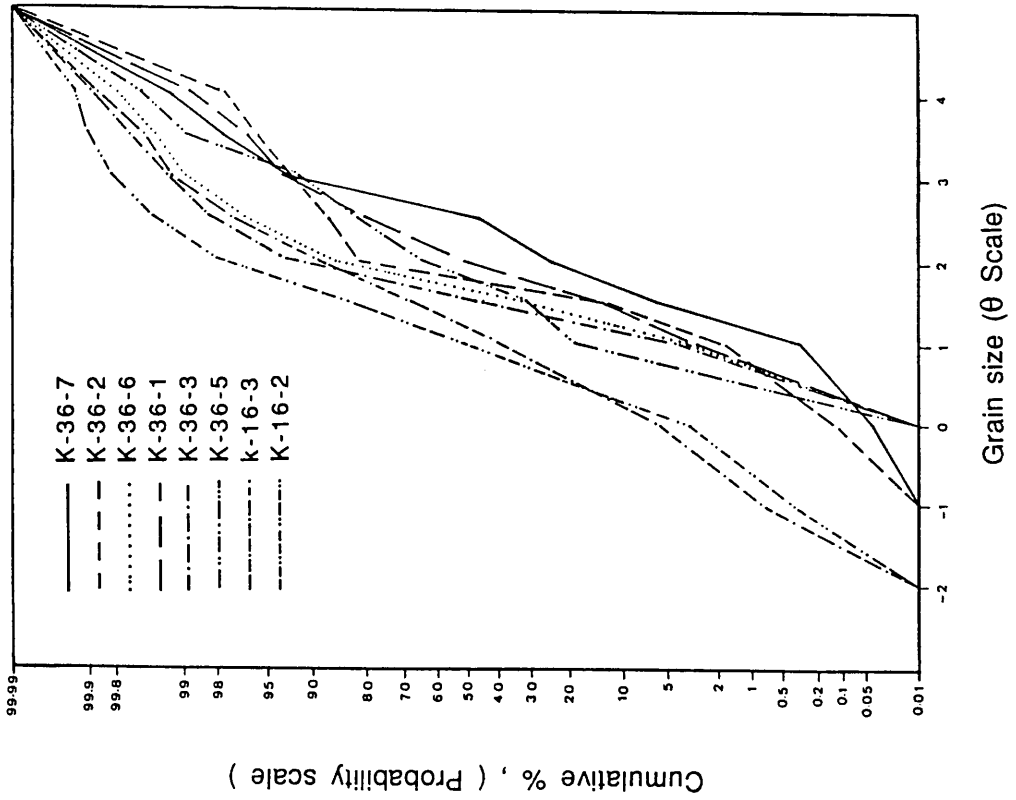
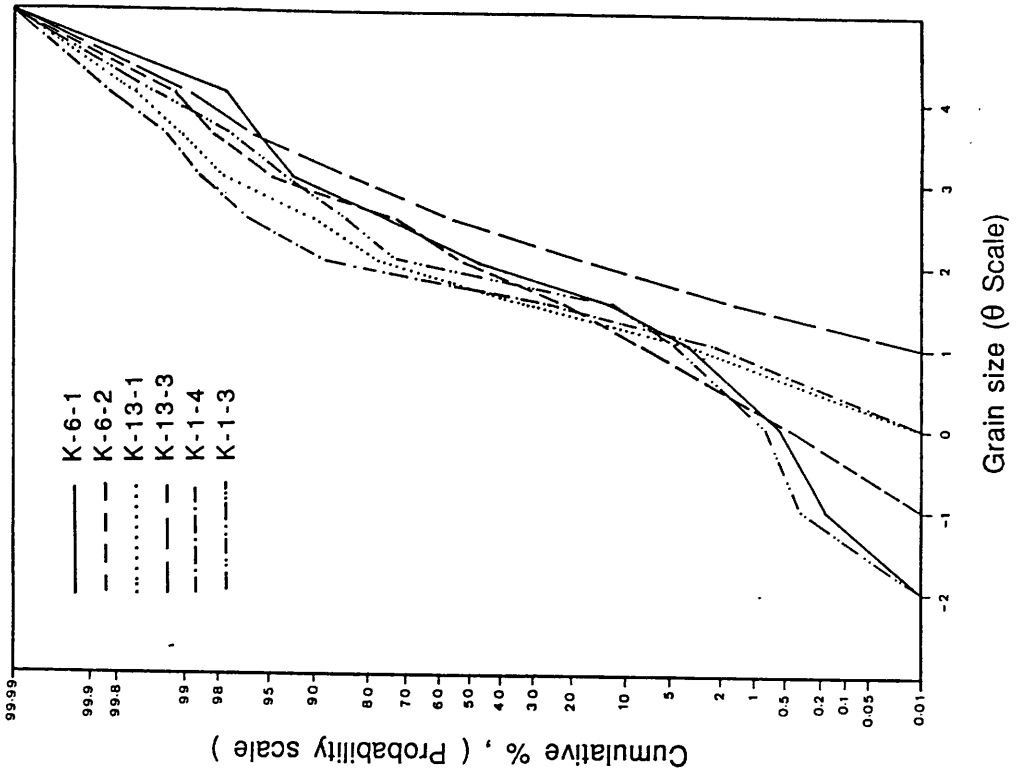


Fig. 5.4 Cumulative-frequency curves of grain-size of Middle Saq Sandstones.

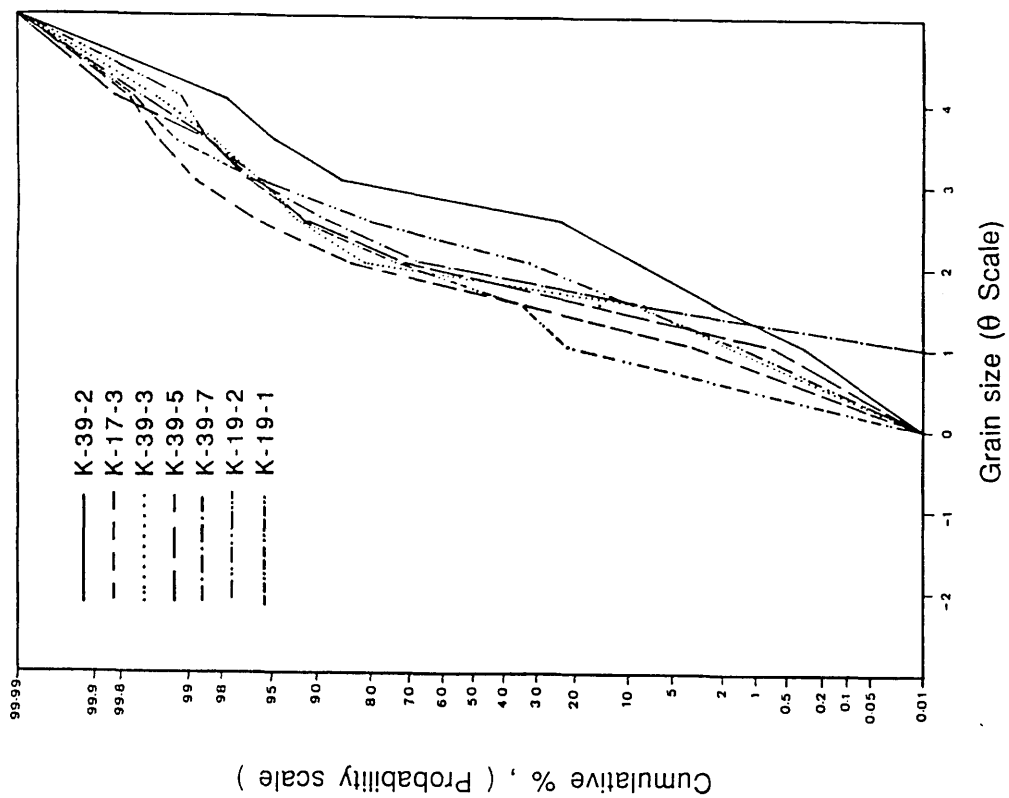
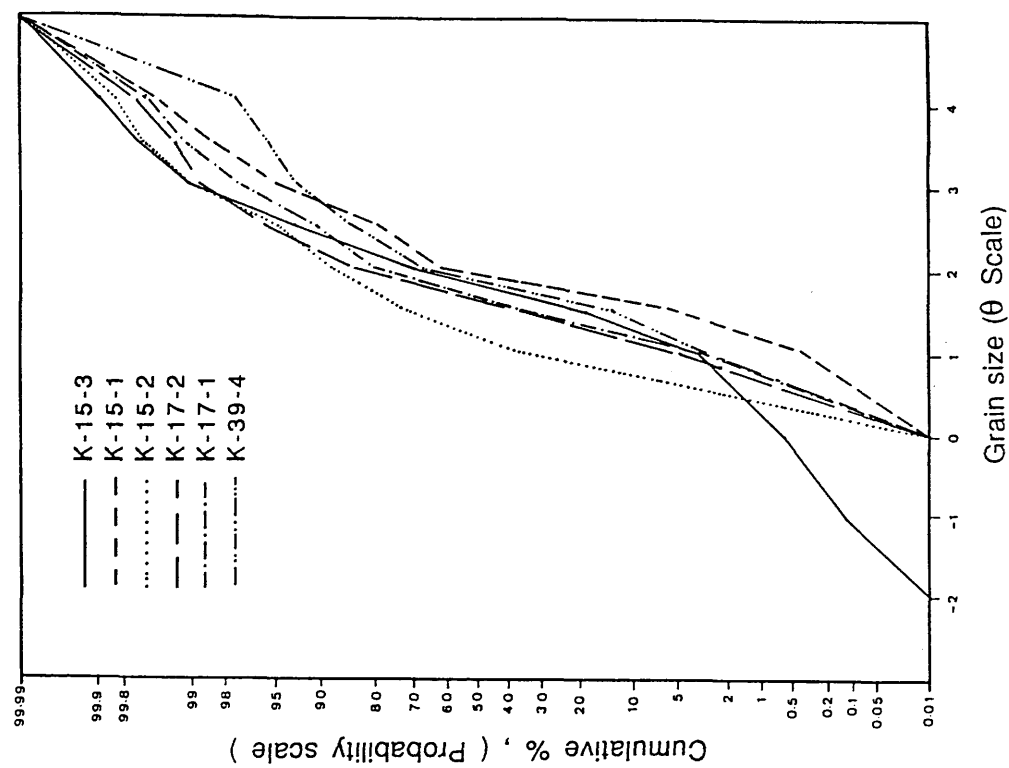


Fig. 5.5 Cumulative-frequency curves of grain-size of Middle Saq Sandstones.

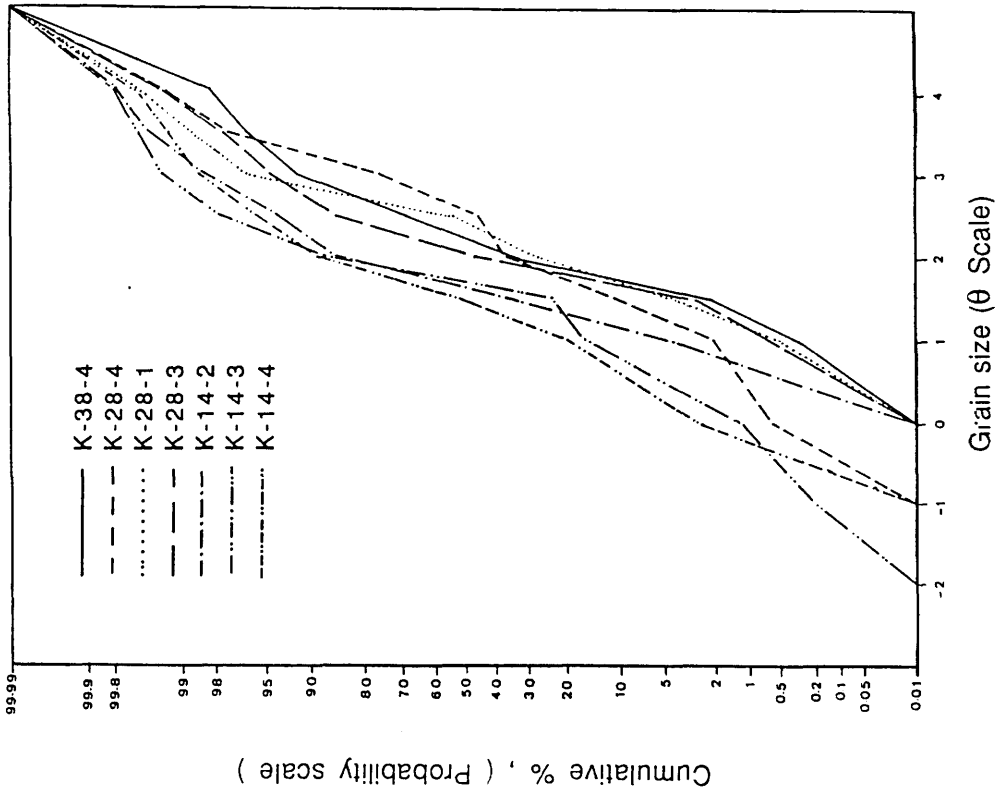
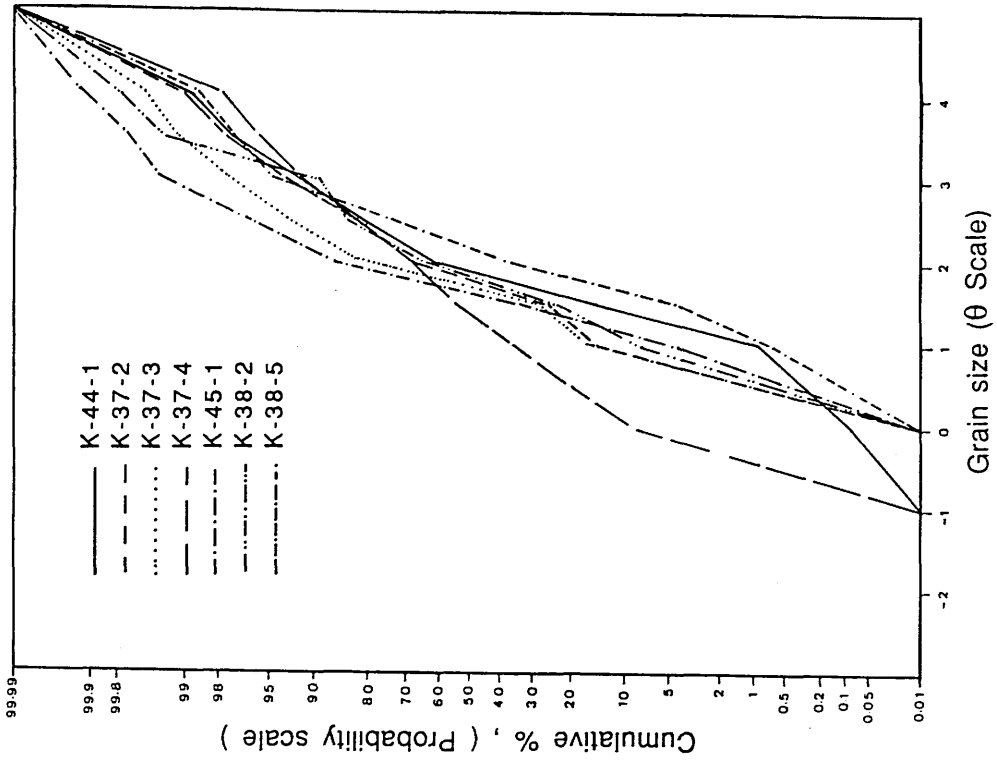


Fig. 5.6 Cumulative-frequency curves of grain-size of Middle Saq Sandstones.

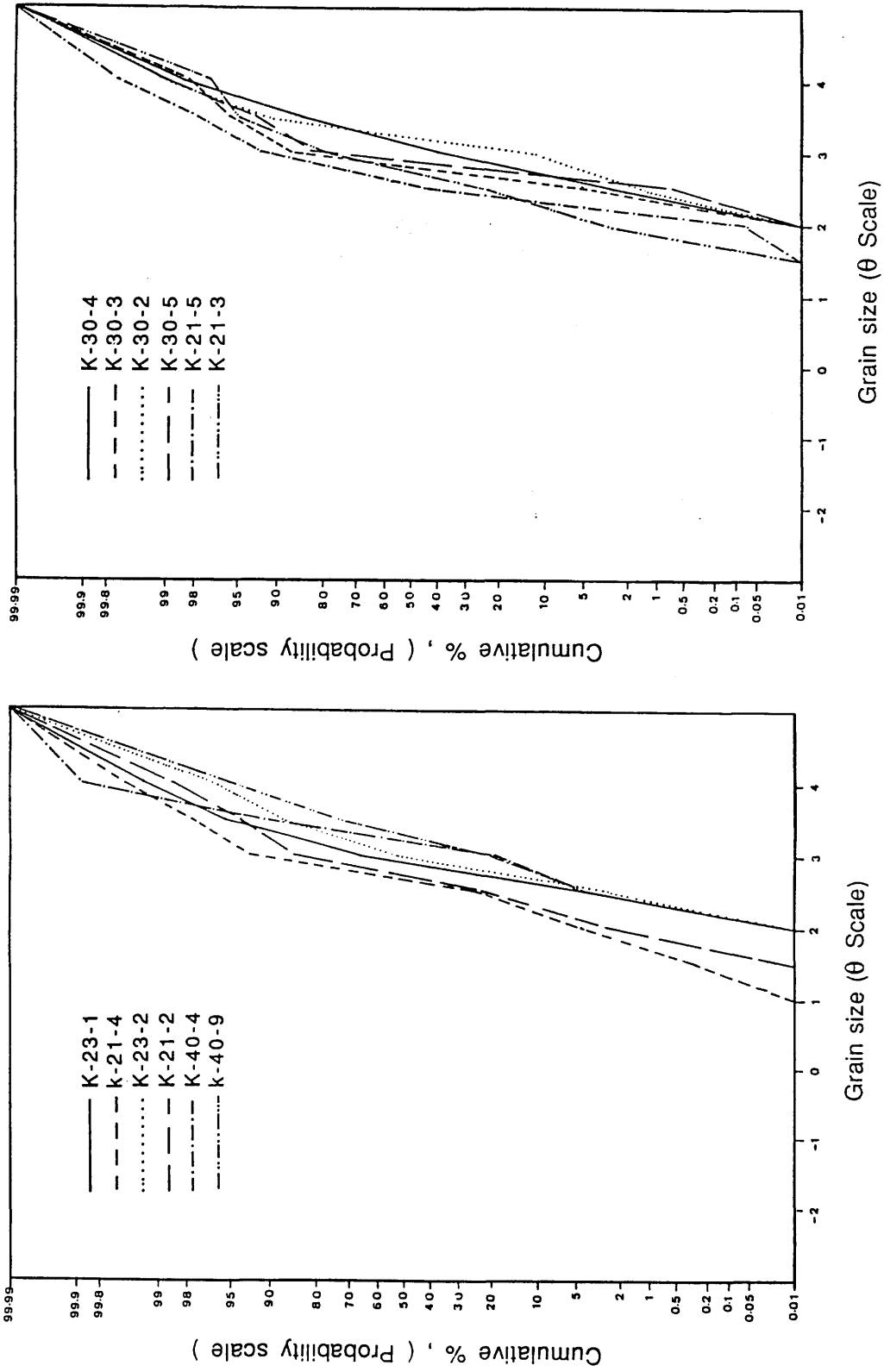


Fig. 5.7 Cumulative-frequency curves of grain-size of Upper Saq Sandstones.

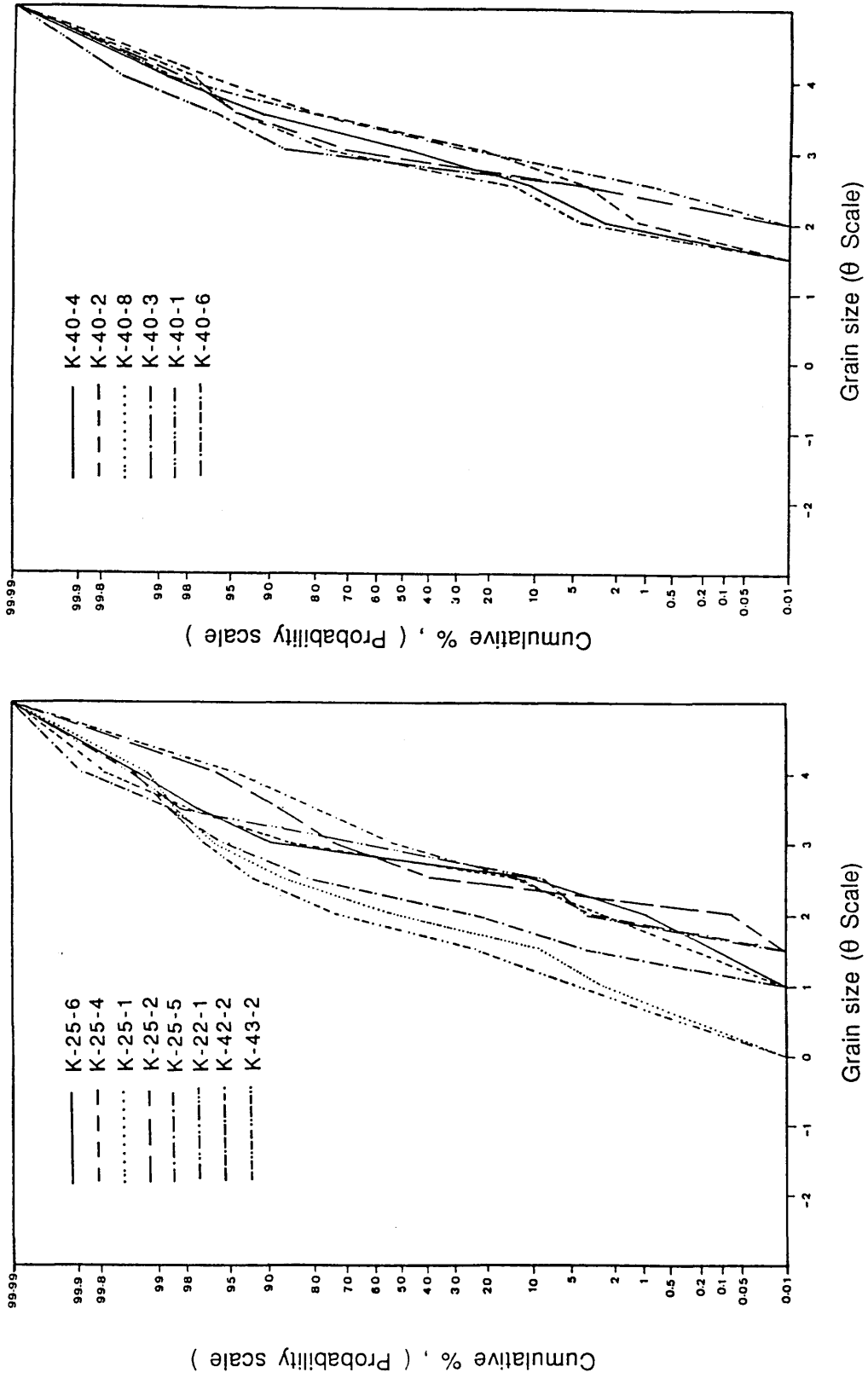


Fig. 5.8 - Cumulative-frequency curves of grain-size of Upper Saq Sandstones.

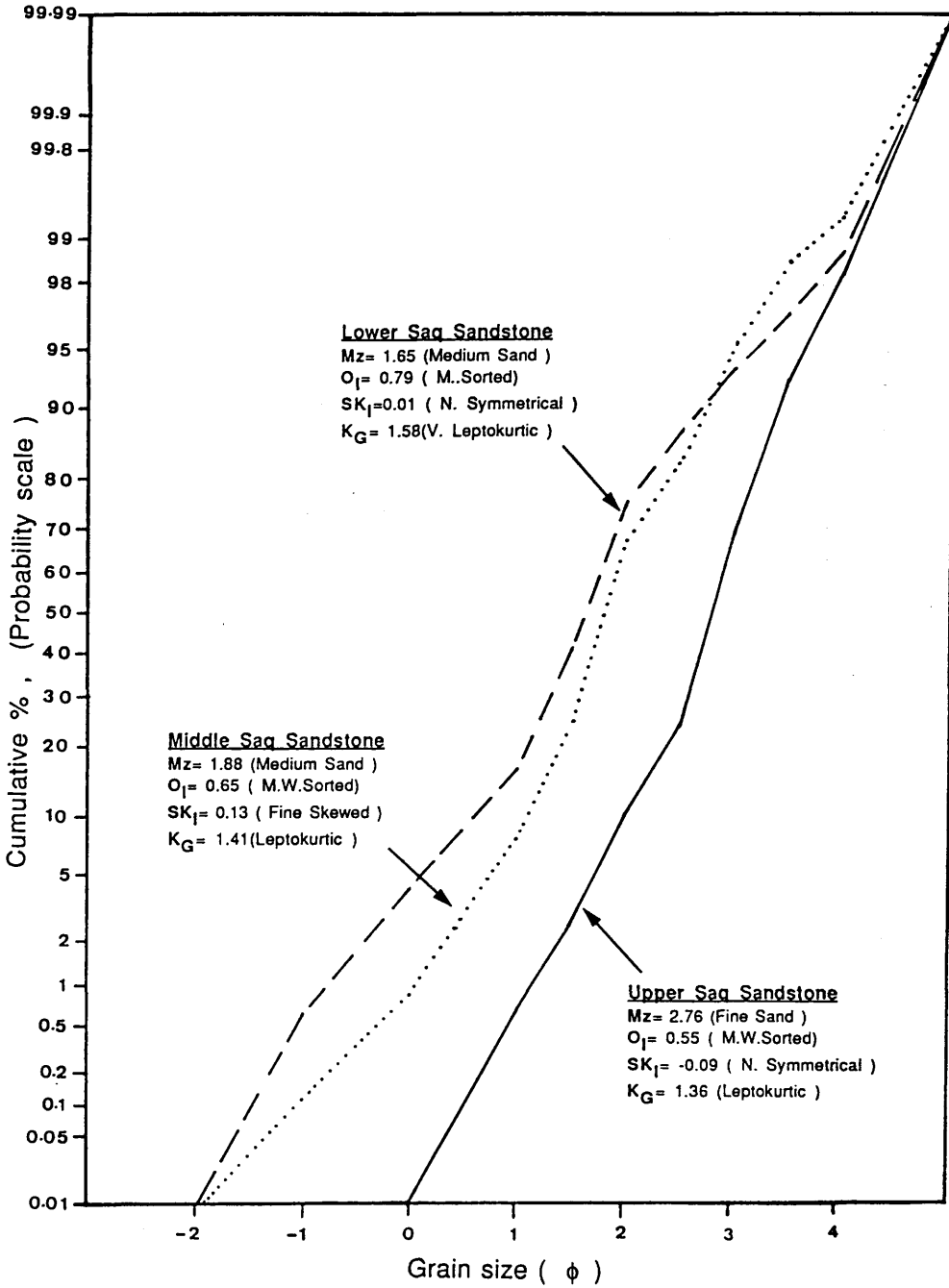


Fig. 5.9 Cumulative-frequency curves of grain-size of average Saq Sandstones.

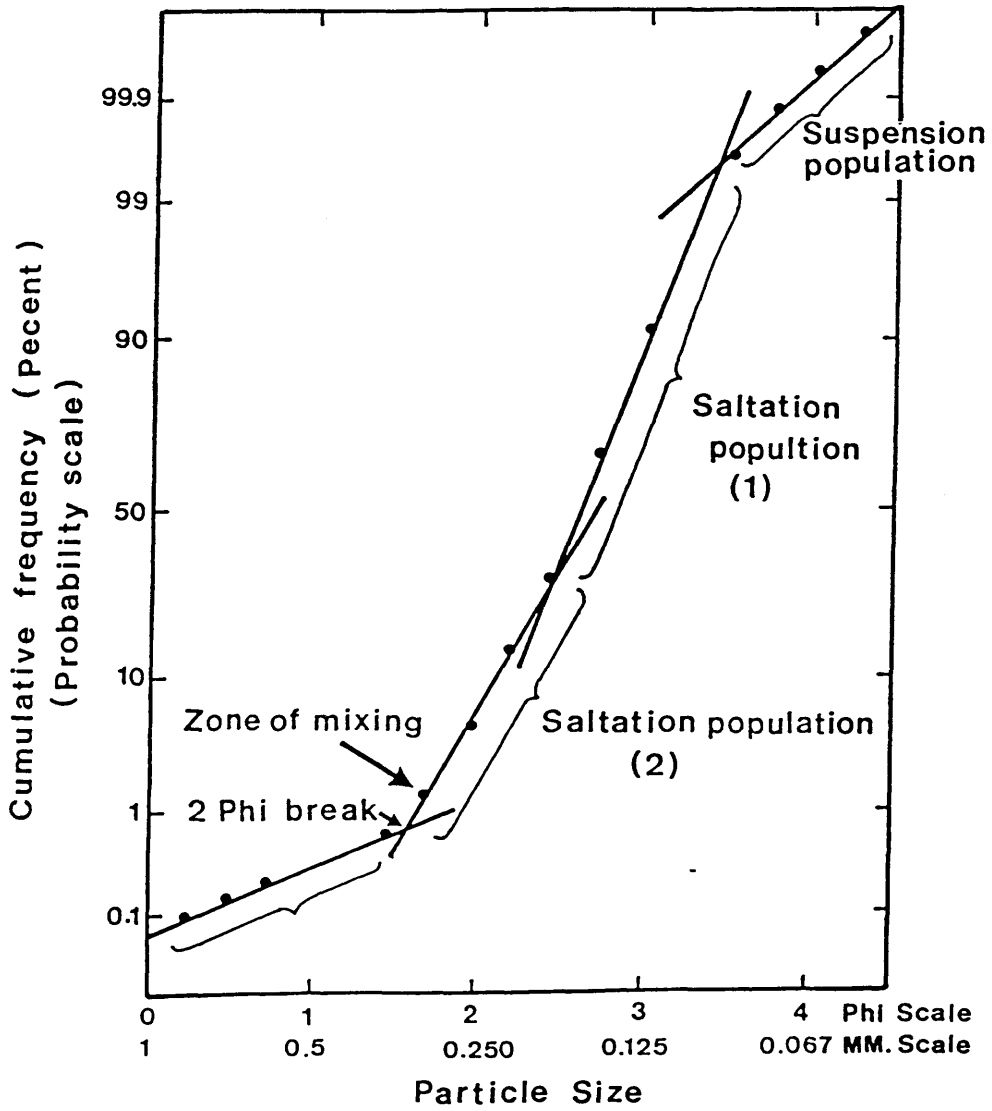


Fig. 5.10 Relation of sediment transport dynamics to populations and truncation points in grain-size distribution (after Visher, 1969).

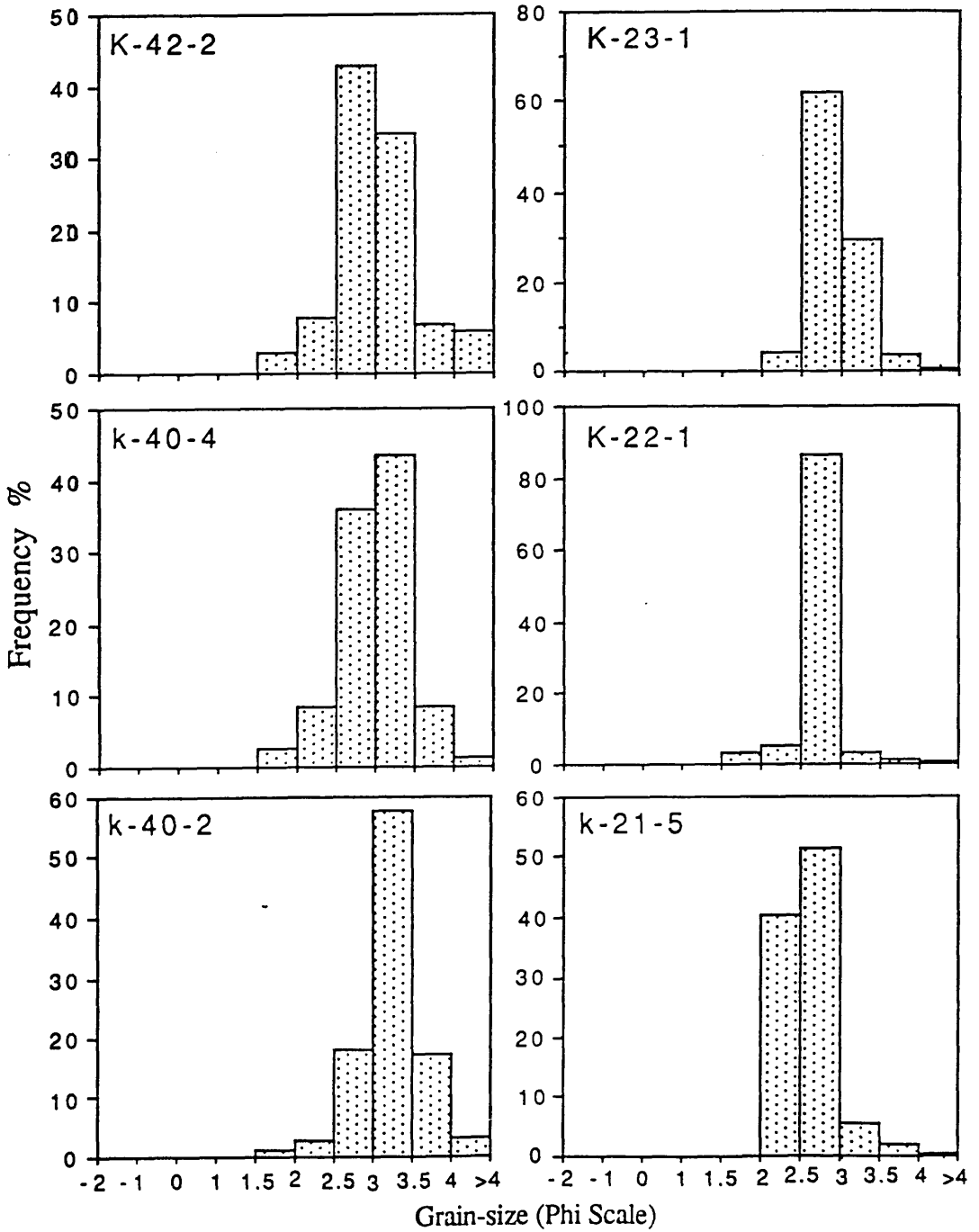


Fig. 5.11 Histograms, showing grain-size distribution of Upper Saq Sandstones.

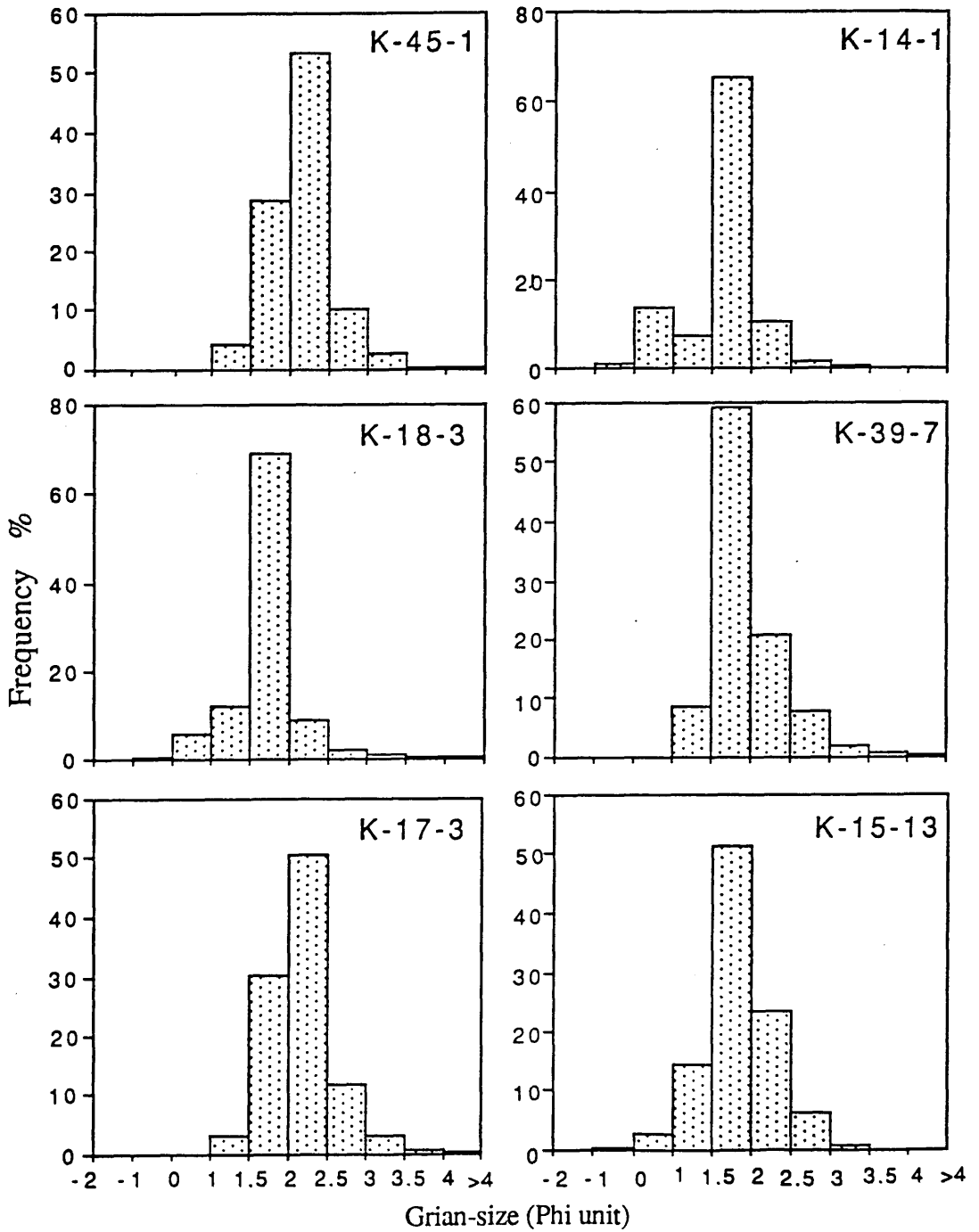


Fig. 5.12 Histograms, showing grain-size distribution of Middle Saq Sandstones.

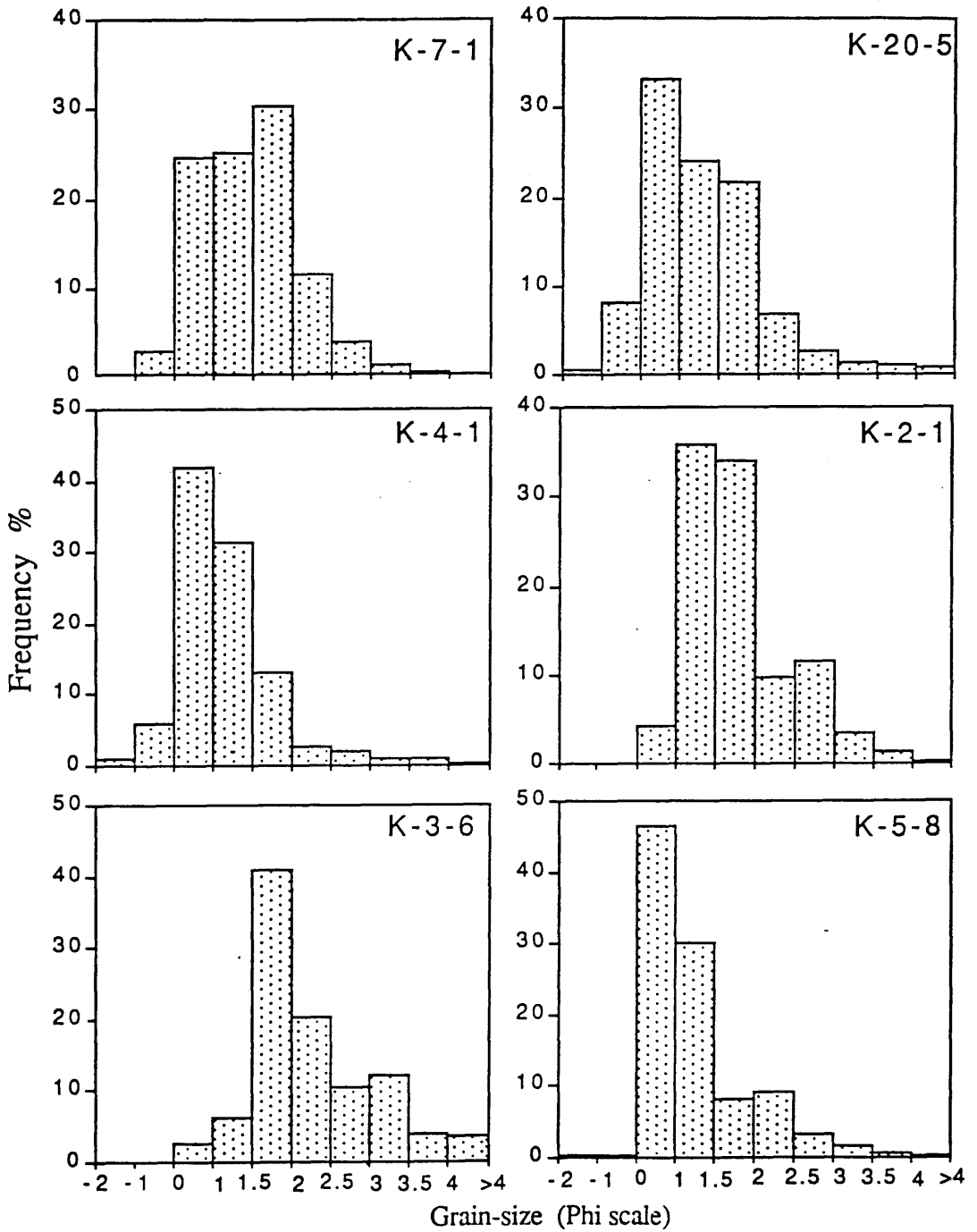


Fig. 5.13 Histograms, showing grain-size distribution of Lower Saq Sandstones.

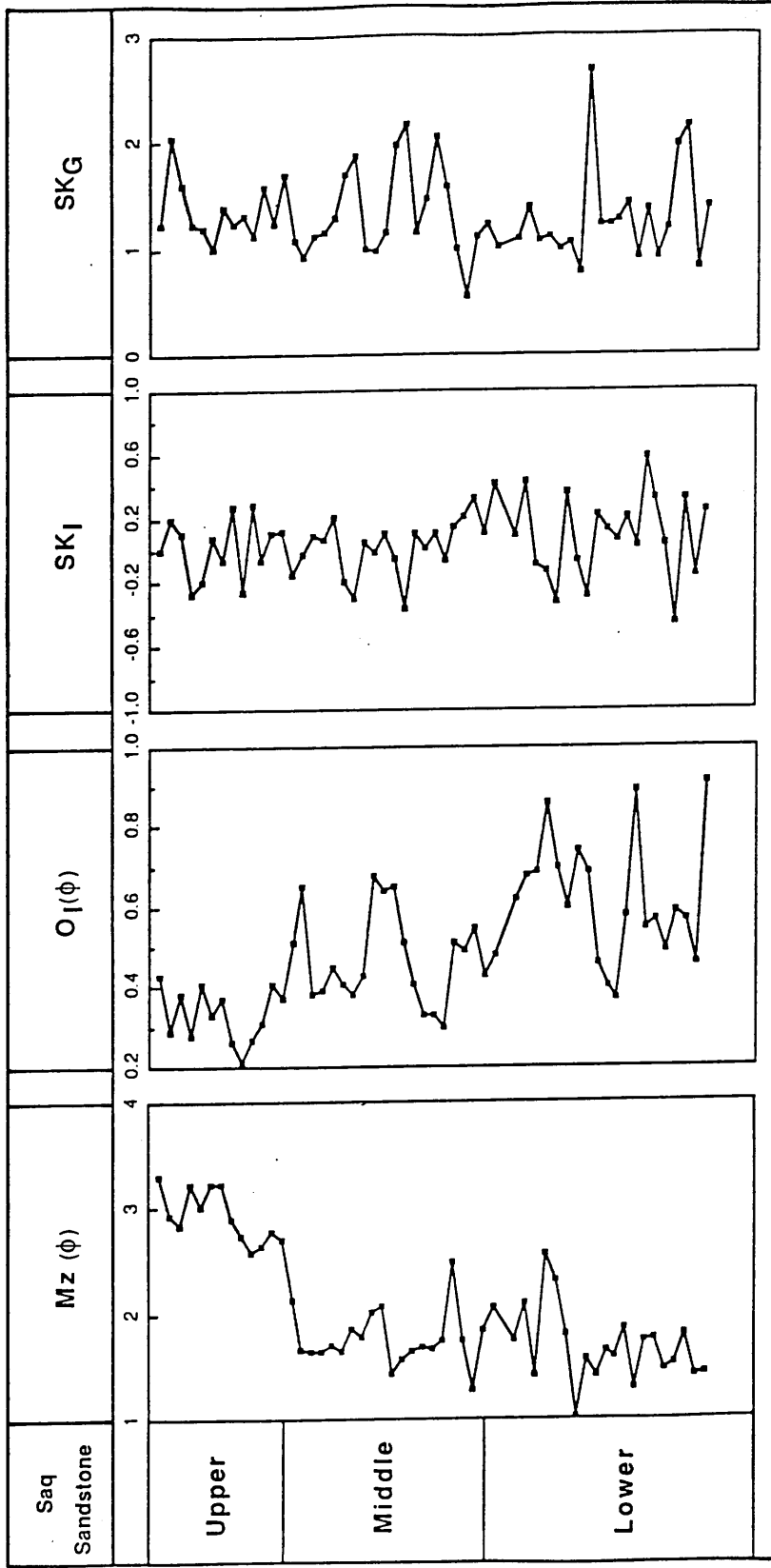


Fig. 5.14 Vertical variation of grain-size parameters in vertical sequence of Saq Sandstones.

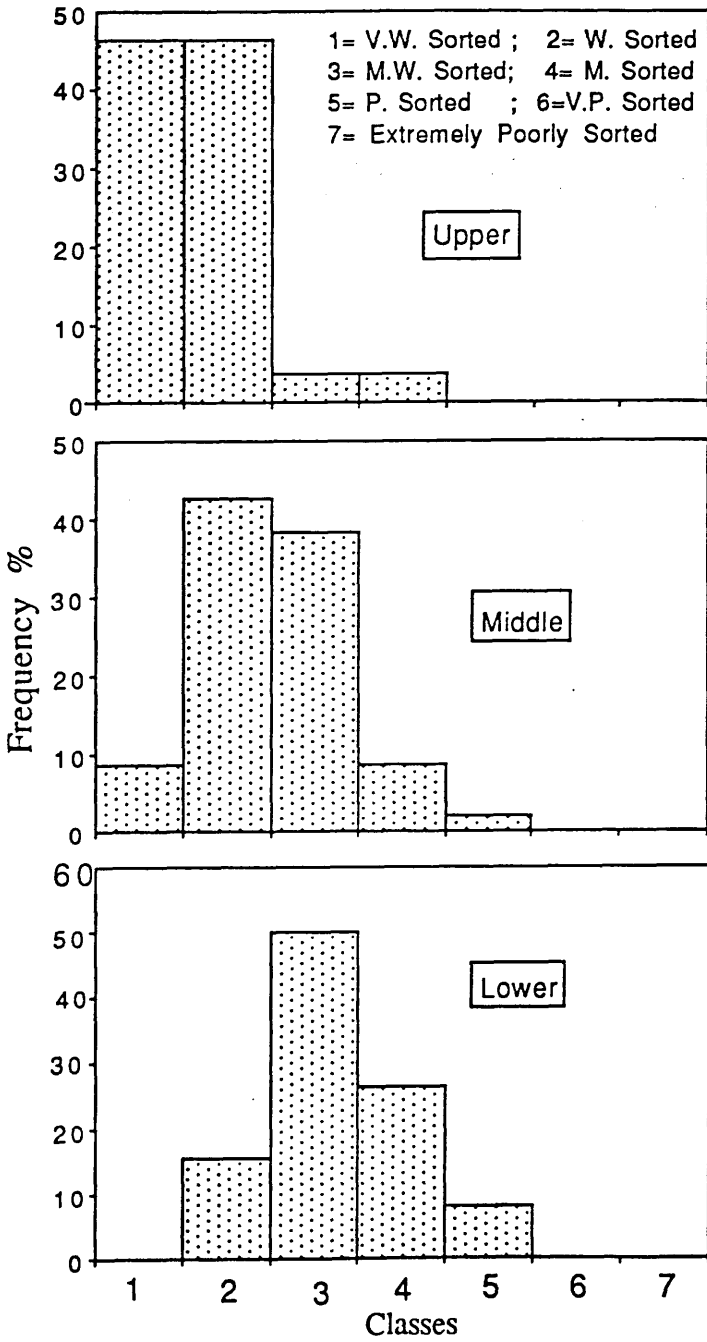


Fig. 5.15 Histograms, showing the average standard deviation (sorting) of Saq Sandstones.

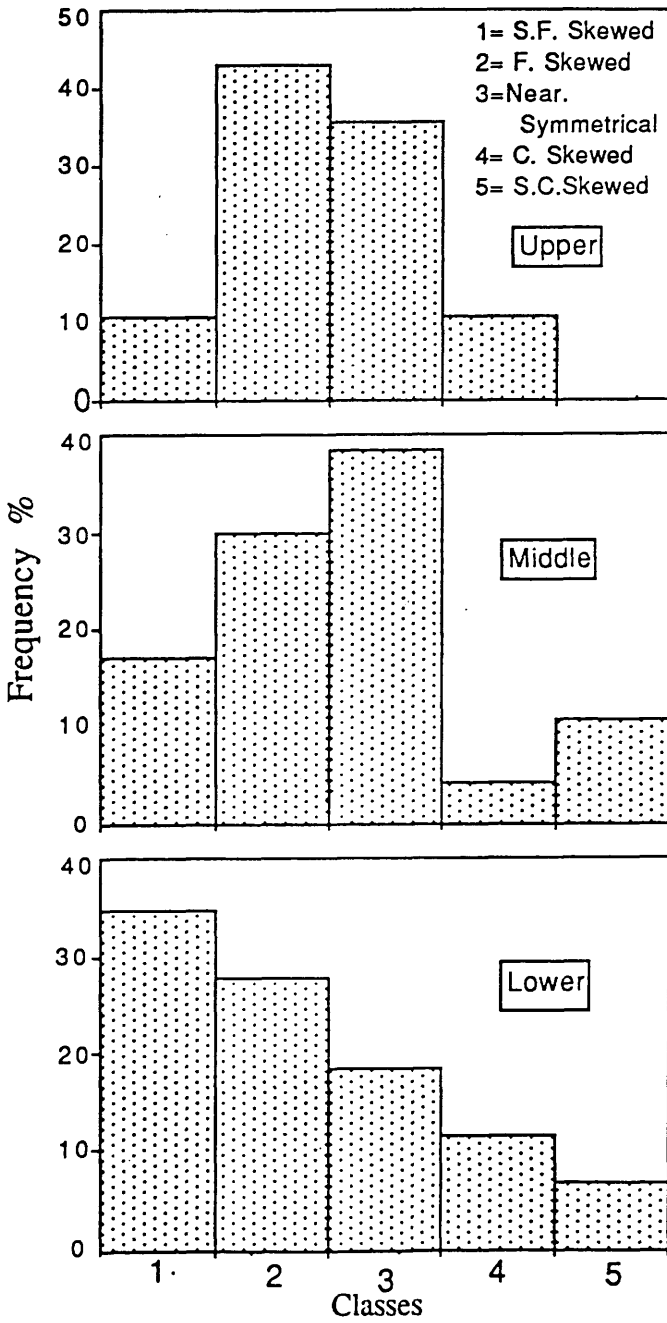


Fig. 5.16 Histograms, showing average skewness distribution of the Saq Sandstones.

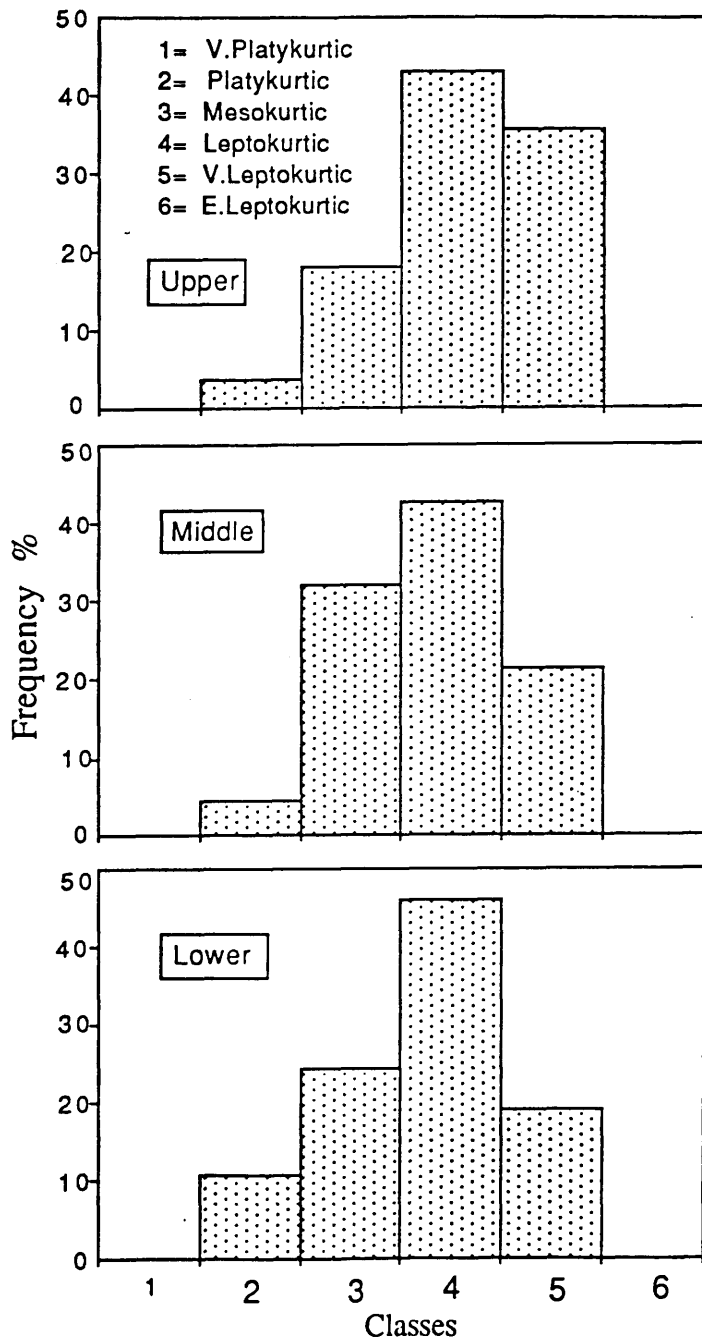


Fig. 5.17 Histograms, showing average Kurtosis distribution of the Saq Sandstones.

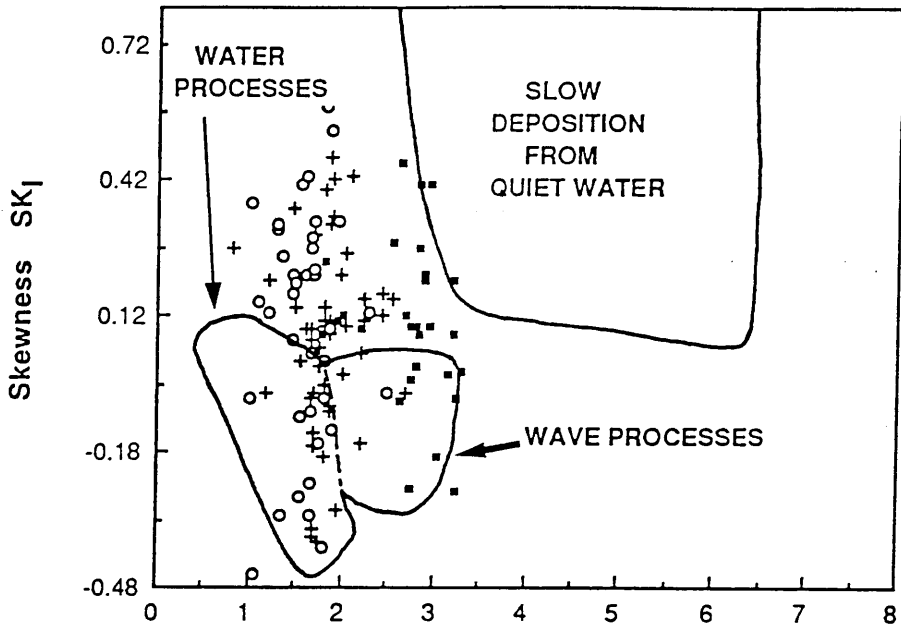


Fig. 5.18 Bivariant plot of median diameter vs. skewness (Stewart, 1958).

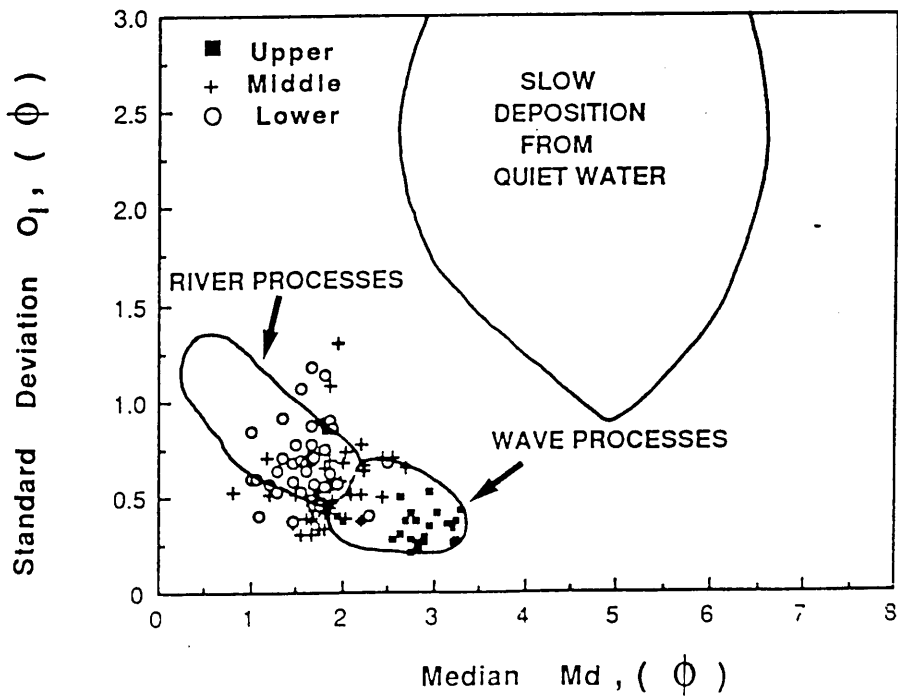


Fig. 5.19 Bivariant plot of median diameter vs. standard deviation (Stewart, 1958).

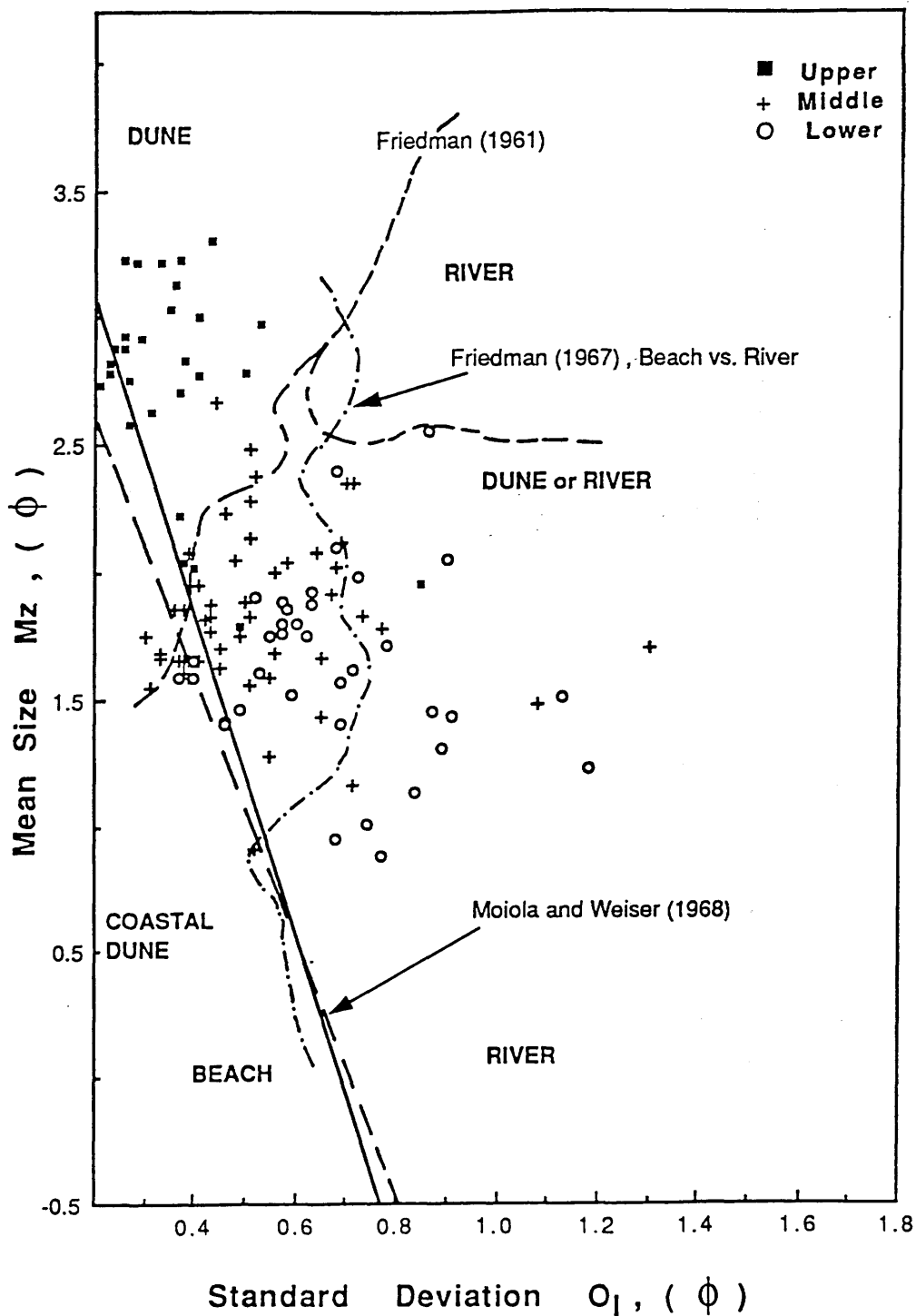


Fig. 5.20 Bivariate plot of mean-size vs. standard deviation, after Friedman (1961, 1967); Moiola & Weiser (1968) and Moshrif, (1980).

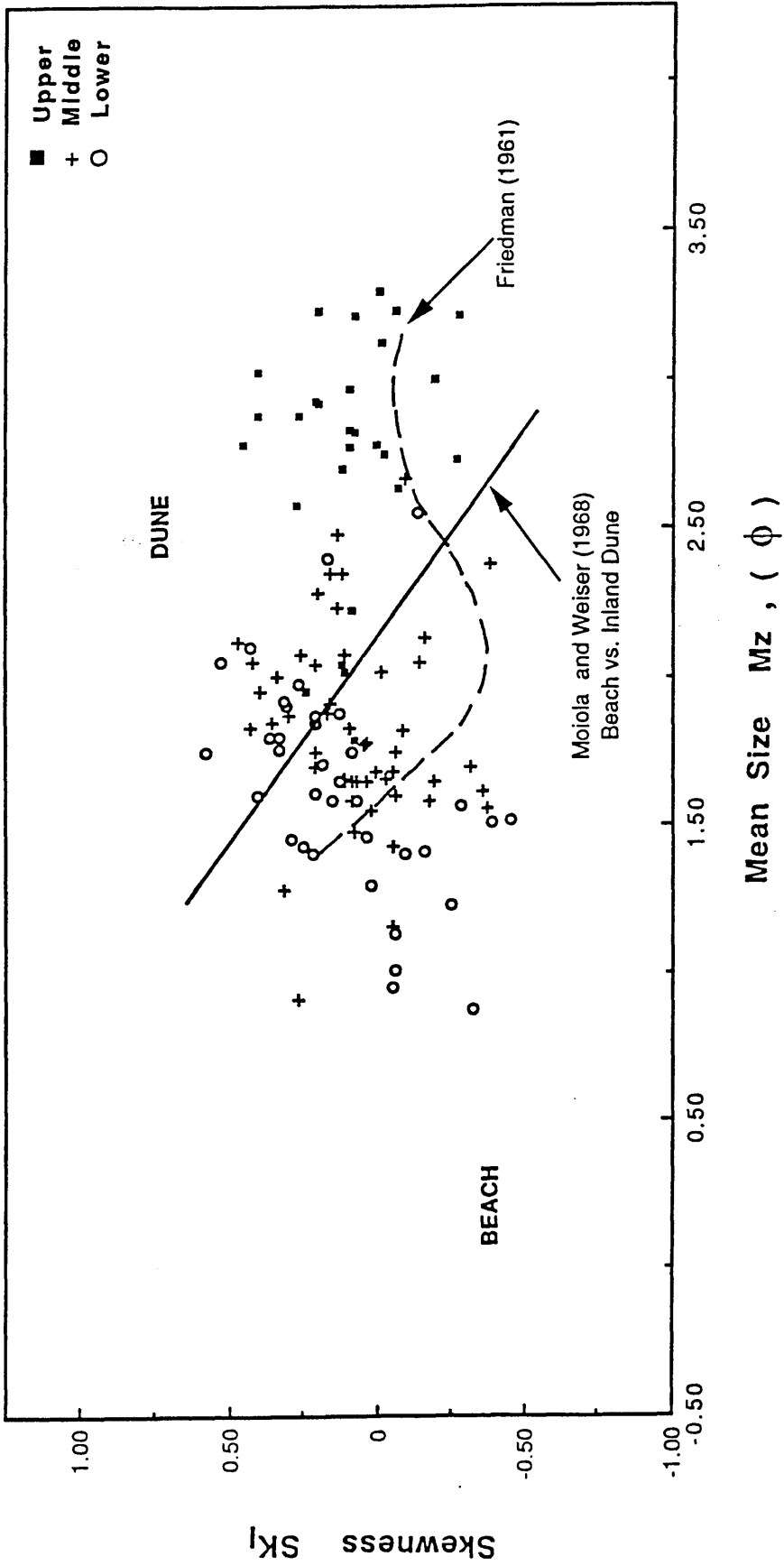


Fig. 5.21 Bivariate plot of mean-size vs. skewness, after Friedman (1961) and Moiola & Weiser, (1968).

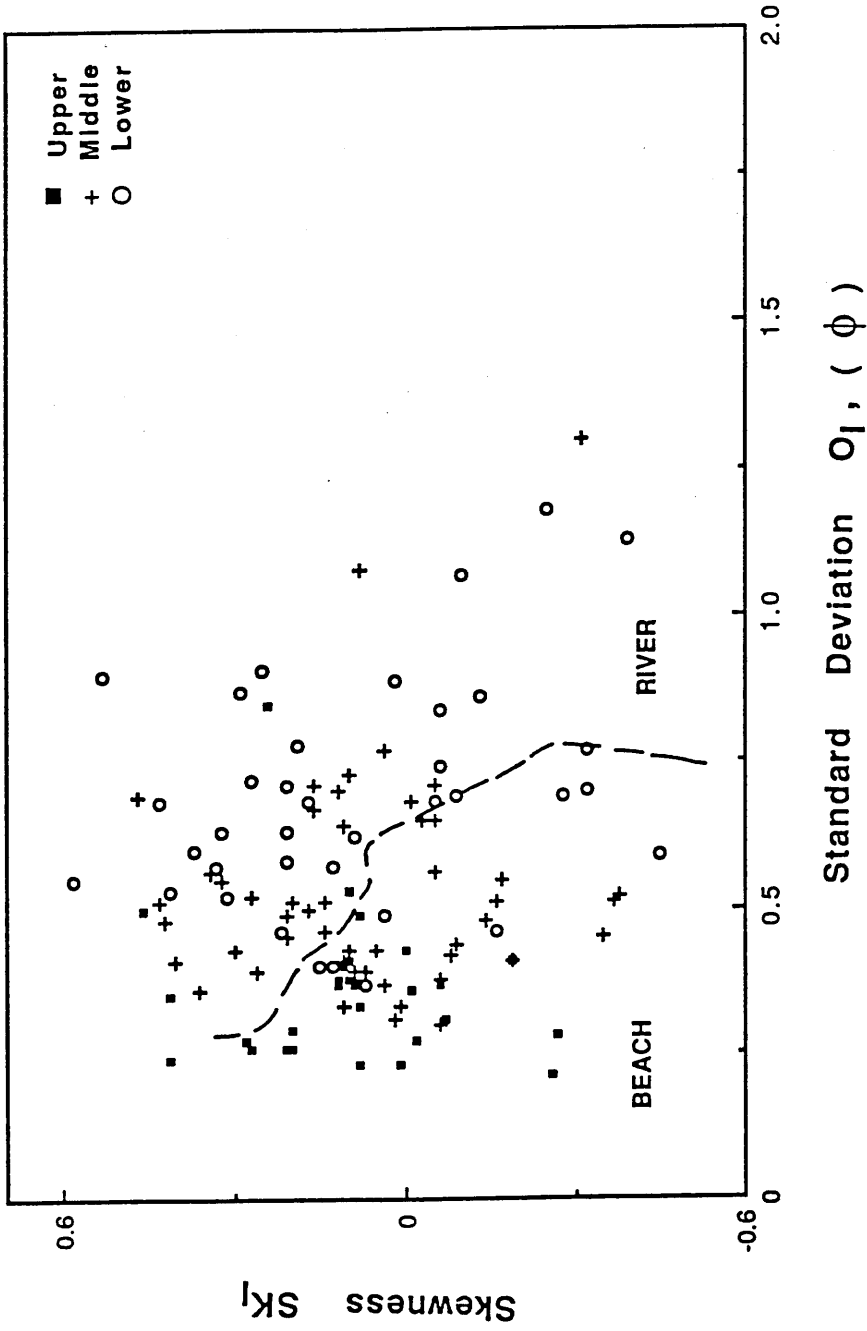


Fig. 5.22 Bivariate plot of standard deviation vs. skewness, after Friedman, (1967).

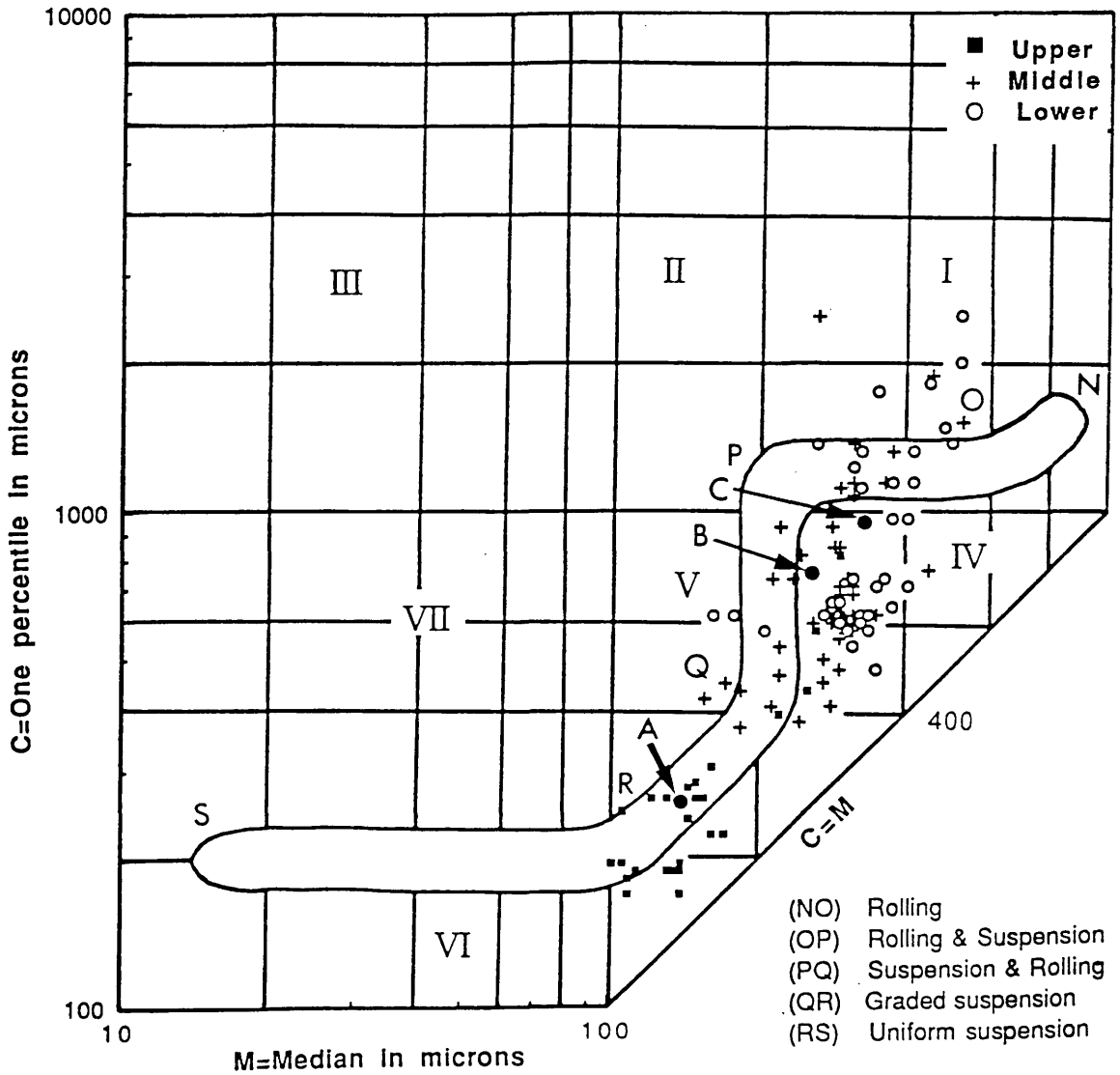


Fig. 5.23 Bivariate plot of C (1st phi percentile) vs. M (Median diameter), after Passega, 1957; Passega & Byramjee, 1969. A, B and C are the averages of Upper, Middle and Lower Saq Sandstone respectively.

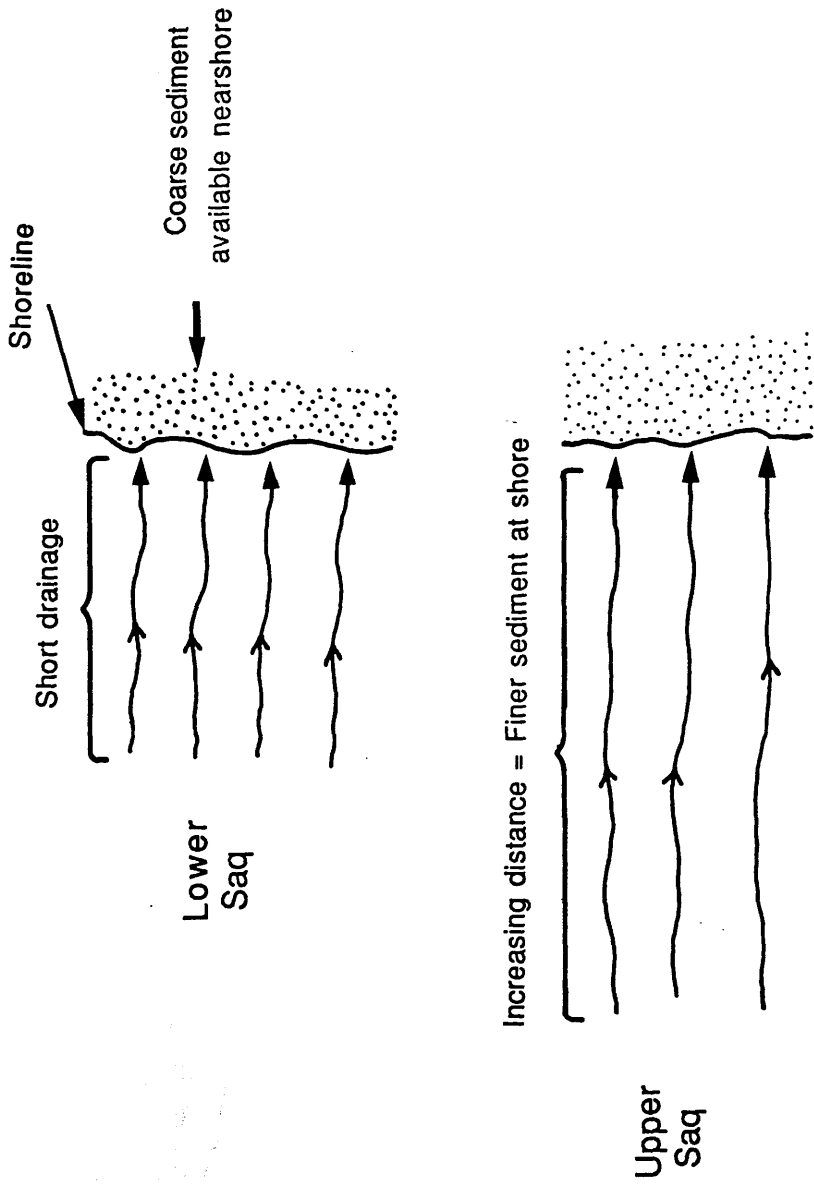


Fig. 5.24 Diagrammatic model showing the effect of the drainage distance on the grain-size.

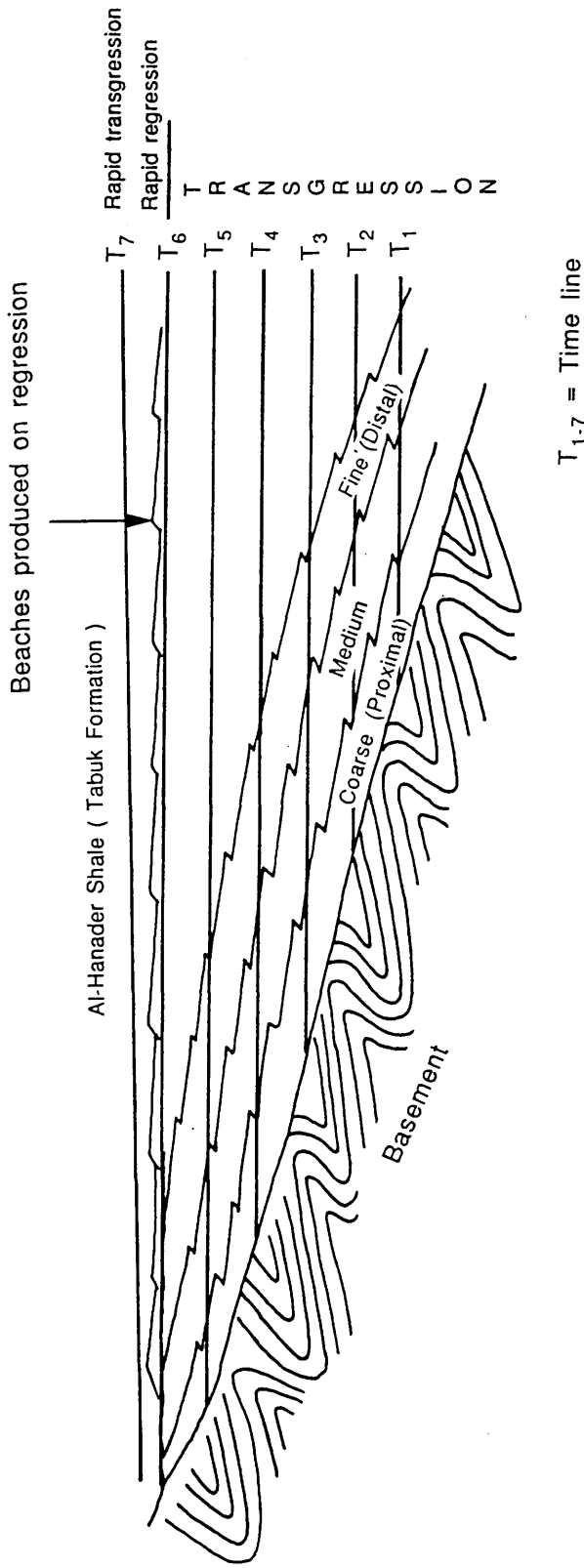


Fig. 5.25 Diagrammatic model showing the relation between grain-size and type of sediment source.

CHAPTER SIX

DEPOSITIONAL ENVIRONMENT AND PALAEOGEOGRAPHIC
SETTING OF THE SAQ SANDSTONE

6.1 Introduction

The Early Palaeozoic was a time of global sea-level rise, (Vail *et al.*, 1977; Matthews and Cowie, 1979; Ziegler *et al.*, 1979). Rocks recording this transgressive event are widespread throughout the world (Brasier, 1980; Dries *et al.*, 1981; Matthews & Cowie, 1979; Sloss, 1963, 1972; Williams, 1964, 1978; Hiscott, 1982; Hein, 1987; McKie, 1989, 1990).

Theoretical considerations of Early Cambrian configuration of continents, Earth-Moon separation, and palaeo-oceanographic conditions suggest that storms were not that important. The closer distance between the Moon and the Earth during the Early Cambrian, resulted in an increased speed and rotation of the Earth. This led to an increase in centrifugal force, with greater deflection of current during the Cambrian (Hein, 1987).

The effect of tides would have been much greater on many of the Cambrian continental shelf areas than on the shelves today for the following reasons: (1) the closer proximity of the Moon to the Earth would amplify the tidal forces; Also, (2) an increase in continental shelf width tends to further amplify the effect of semidiurnal tides (Klein & Ryer, 1978; Clarke & Battisti, 1981; Klein, 1982).

The resonant amplification of tides would have been facilitated because the transgression took place over a peneplained surface where relatively small changes in sea level would have profound effects on the shelf width (McKie, 1989).

6.2 Facies association and tidal current path

There are four main lithological facies associations in the Saq Sandstone which can now be interpreted in terms of tidal current path.

- (1) Granular conglomerates. These occur at intervals in the Saq Sandstone, mainly in alternation with sand sheets. They are thought to be the lag-sheets associated with scour surfaces in zones of bed load parting. They may represent the zone of gravel with sand ribbons described by Stride, (1963) and Kenyon, (1970).
- (2) Cross-stratified sand sheets. This association is dominant in the Saq Sandstone. It occurs between bars or as independent high topography. These sand sheets may be produced by migration of megaripples in response to asymmetrical tidal currents.
- (3) Bar fields. These formed by amalgamation of sand sheets, in areas of maximum thickness of the Middle Saq Sandstone.
- (4) Shales. These may have accumulated in down tidal current paths (Stride, 1963; McCave, 1971), where strong tidal currents are not present, or to the side of net sand transport paths (Stride *et al.*, 1982).

The possible integration of these association is illustrated in Figure 6.1, where they are compared with major sedimentary facies of the Jura Quartzite (Anderton, 1976) and Duolbasgaissa Formation (Banks, 1973).

This model of the Saq Sandstone tidal shelf sedimentation envisages a tidal transport path which is quite different from those described from situations existing in the present southern North Sea and the Celtic Sea (Stride, 1963; Veenstra, 1971; McCave, 1973; Belderson & Stride, 1966), where the directions of decreasing bed sediment size, maximum surface tidal current velocities, decreasing tidal current velocity (Fig. 6.2) and the bed-load sediment transport paths are all parallel. Although these modern shelf sediments are not fully in equilibrium with shelf processes as a result of the effects of the Holocene post glacial sea level rise, they provide a useful recent analogue (Anderton, 1976).

Belderson & Stride, (1966) also recognized a series of bed-form zones, roughly perpendicular to the bed-load sediment transport path, which they correlated with maximum surface current velocities.

6.3 Depositional history of the Saq Sandstone

It is now possible to integrate all the characteristics so far described and discussed (sedimentary facies, petrography, etc) into environmental models for the Lower, Middle and Upper Saq Sandstone. These characteristics lead to the deduction that the depositional environment was a tide-dominated shallow shelf.

Following the stabilization of the Arabian Shield, the maturely peneplained surface of the igneous and metamorphic rocks present supplied the pre-Saq basin with an influx of clastics that reflect a continental depositional environment (Idwah Formation).

The pre-Saq Idwah Formation was deposited in braided alluvial system, and was then reworked to varying degrees during subsequent marine transgressions, as the result of sea-level rising during Cambrian time (Vail *et al.*, 1977; Matthews & Cowie, 1979; Ziegler *et al.*, 1979).

Shelf processes (Tidal currents) began to sort and shape the residual sediments into migrating small bars and sand sheets during Lower Saq Sandstone deposition (Fig. 6.3). With further transgression, small bars and sand sheets amalgamated into the larger offshore bars of the Middle Saq Sandstone. Some of these larger bars eventually become isolated and then moribund because of deepening water or changing tidal flow paths (Fig. 6.4).

The transition from relatively small bars in the Lower Saq Sandstone to large scale bars in the Middle Saq Sandstone, could indicate an increase in water depth and strength of tidal currents which were capable of transporting large volumes of sand offshore. However, there are no clear facies or palaeocurrent changes from Lower to Middle Saq Sandstone.

Klein & Ryer, 1978; Clark & Battisti, 1981; Klien, 1982 reported that with increase in continental shelf width, tidal currents will be amplified. The Middle Saq Sandstone was deposited during a continuous transgression, therefore, the shelf was probably widening during this transgression (Makie, 1990).

The Upper Saq Sandstone was deposited during a time of shallowing of the shelf. The shoreline prograded over regions which had previously been occupied by deeper water tidal bars. Progradation could have been due to a large influx of sediment, uplift of the Saq basin, or a fall in sea-level (Figs. 6.5 and 6.6).

There is a general concensus that the early part of the Tremadoc (Early Ordovician) was a time of eustatic sea-level rise (Jaanusson, 1979; Ludvigsen *et al.*, 1988), but there is less agreement concerning the suggestions of some authors that this event was preceded by a sea-level fall. Fortey, (1984) proposed a single, eustatic lowering of sea-level at the boundary and this was elaborated upon by Miller, (1984) who recognized three short, closely spaced, falls of sea-level (Bryant & Smith, 1990).

So the Upper Saq Sandstone could have been deposited during the falling sea-level preceding the major transgression which deposited the Hanader Shale (Tabuk Formation).

Figure 6.7 summarizes the possible history of the evolution of the Saq Sandstone basin.

6.4 Palaeogeographic setting

The palaeogeography of the Arabian Peninsula was dominated by a positive and often emergent land-mass to the west (the Arabian-Nubian Shield), which was supplying sediments to shallow marine clastic deposition on the platform to the east and northeast. A broad and shallow epicontinental tidal sea with periodic transgressions and regressions accounts for the predominance of clastic sediments, but towards the east in Iran and the Arabian Gulf carbonates and evaporite deposits became an important part of the

geological record. To the north deeper water, with thick shale, sandstones and limestones occurred in Syria and Turkey.

Wolfart, (1981) summarized the paleogeography of the Middle East in general as following :

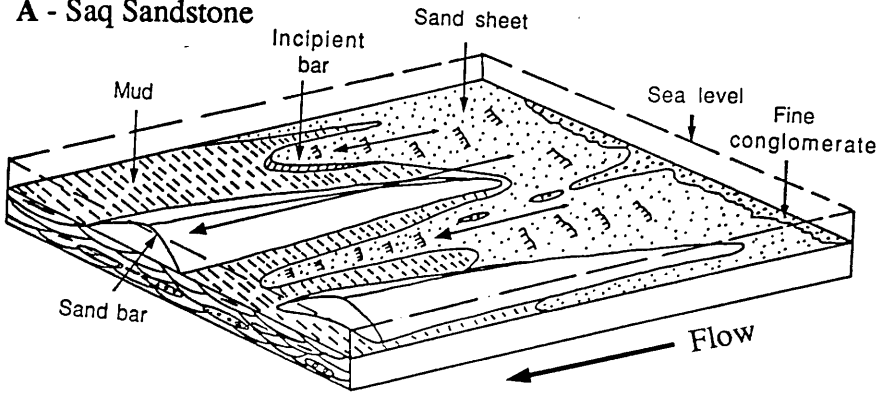
- (1) The oldest transgression is represented by the Infracambrian Hormuz Salt Formation and its carbonate equivalents in Oman, the Arabian Gulf and Iran. The presence of algal stromatolites and massive dolomites, relatively free of significant terrigenous detritus, strongly suggest a genesis in relatively shallow water. In the other areas of the Middle East, sedimentary rocks mainly of continental origin were formed during this time.
- (1) The next marine transgression was of middle (to Late) Early Cambrian age, as indicated by the faunal assemblage with redlichiid trilobites and *Cruziana* distributed all over Iran and as far to the west as Jordan. Intercalations of oolites indicate shallow water conditions. Contemporaneously in Arabia continental (to littoral) environments prevailed, and in Turkey non-fossiliferous carbonates and clastics were probably formed in marine environments.
- (3) The Middle Cambrian transgression mainly affected the southern part of Turkey and, perhaps temporarily, part of northern Iran. Middle Cambrian rocks have yielded the only marine fossils of the Turkish Cambrian. Dolomitic gypsiferous rocks with salt pseudomorphs, in northern and eastern Iran and perhaps, in Afghanistan, suggest that a temporarily lagoonal environment prevailed during the Middle Cambrian. Except for Oman, all over the Arabian Peninsula continental conditions continued.
- (4) The Late Cambrian transgression left fossiliferous carbonates, oolites, massive limestones and shale layers of shallow water origin in Iran and Afghanistan. In the Arabian Peninsula continental environments continued.

(5) The paleogeographical pattern of the Ordovician of the Middle East is very closely related to that of the Cambrian. The lithofacies of the stable shelf region around the Arabian craton are composed of only clastic, detrital material derived from the craton. In the mobile shelf region, particularly in Afghanistan, northern Iraq, and Turkey, thick sequences of conglomerates and quartzites yield abundant evidence of numerous swells which served as sources for the detrital sediments. In most parts of the mobile shelf region comprising Afghanistan, southern and northern Iran, north-eastern Syria, and southern Turkey, the Ordovician rocks are predominantly composed of grey-green or blue-grey, partly graptolitic shales, sandstones, and quartzites.

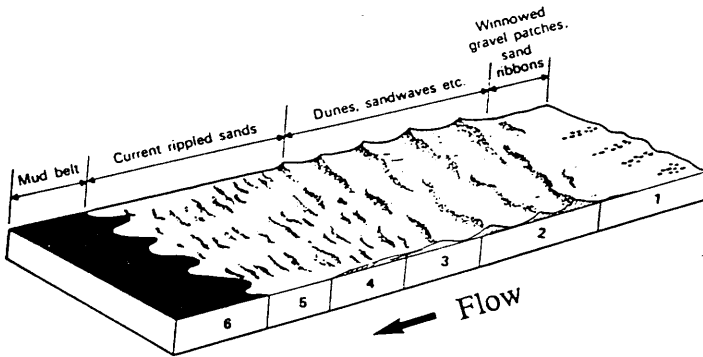
This study suggests modifications of the accepted palaeogeography of the Late Cambrian to Early Ordovician times - Saq Sandstone (Fig. 6.8):

(1) There is no evidence for the "continental - littoral" band of rocks belonging to the Saq Sandstone cycle illustrated in Figures 6.9 to 6.11. This has been re-interpreted as a band of littoral - tidal shelf deposits; (2) The "source area " has had to be moved further to the West and the Saq Sandstone is seen to be transgressive on to it; (3) The "source area " was probably not a source in the same sense as a mountain belt - but a broad plain or peneplain, over which the Cambrian sea transgressed. This source was peneplained in pre-Saq times and had lying on it sandstones of an older formation- the Idwah Formation; (4) There is no direct evidence for the age of the Saq Sandstone, so it may represent any interval or intervals from Middle Cambrian to Early Ordovician.

A - Saq Sandstone



B - Jura Quartzite (Anderton, 1976)



C - Duolbasgaissa Formation (Banks, 1973a)

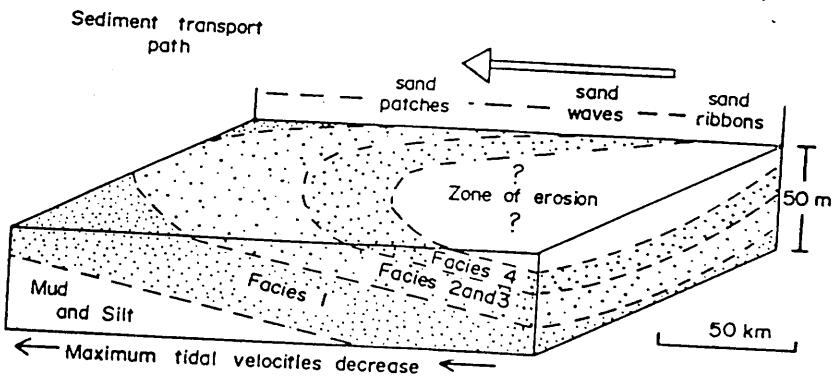


Fig. 6.1 Diagrammatic model illustrating major sedimentary facies of Saq Sandstone (A) compared with facies of Jura Quartzite (B) and Duolbasgaissa Formation (C).

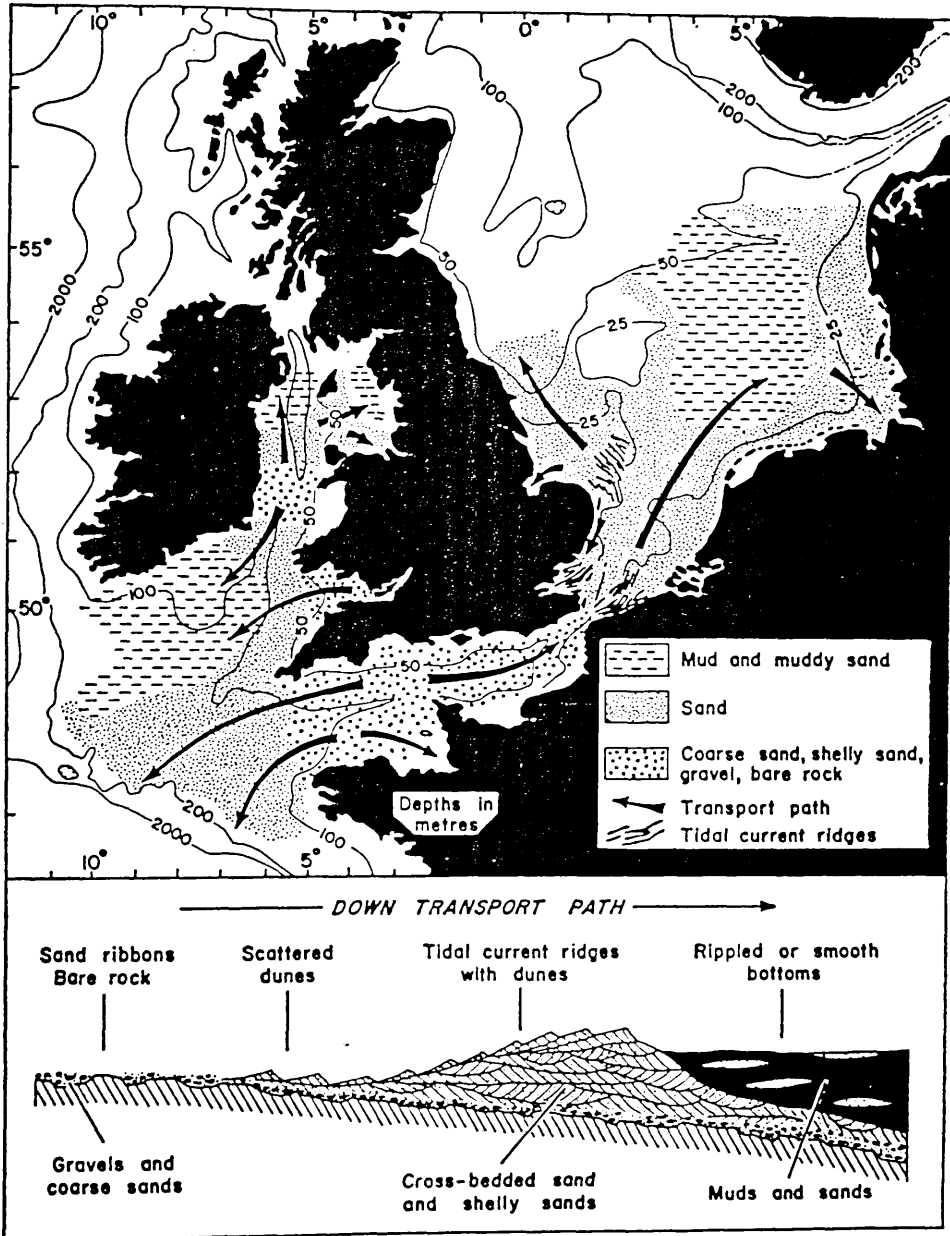


Fig. 6.2 Dispersal of sand around the British coast with sketch showing typical changes observed in a downcurrent direction (From Allen, 1970; Stride, 1963).

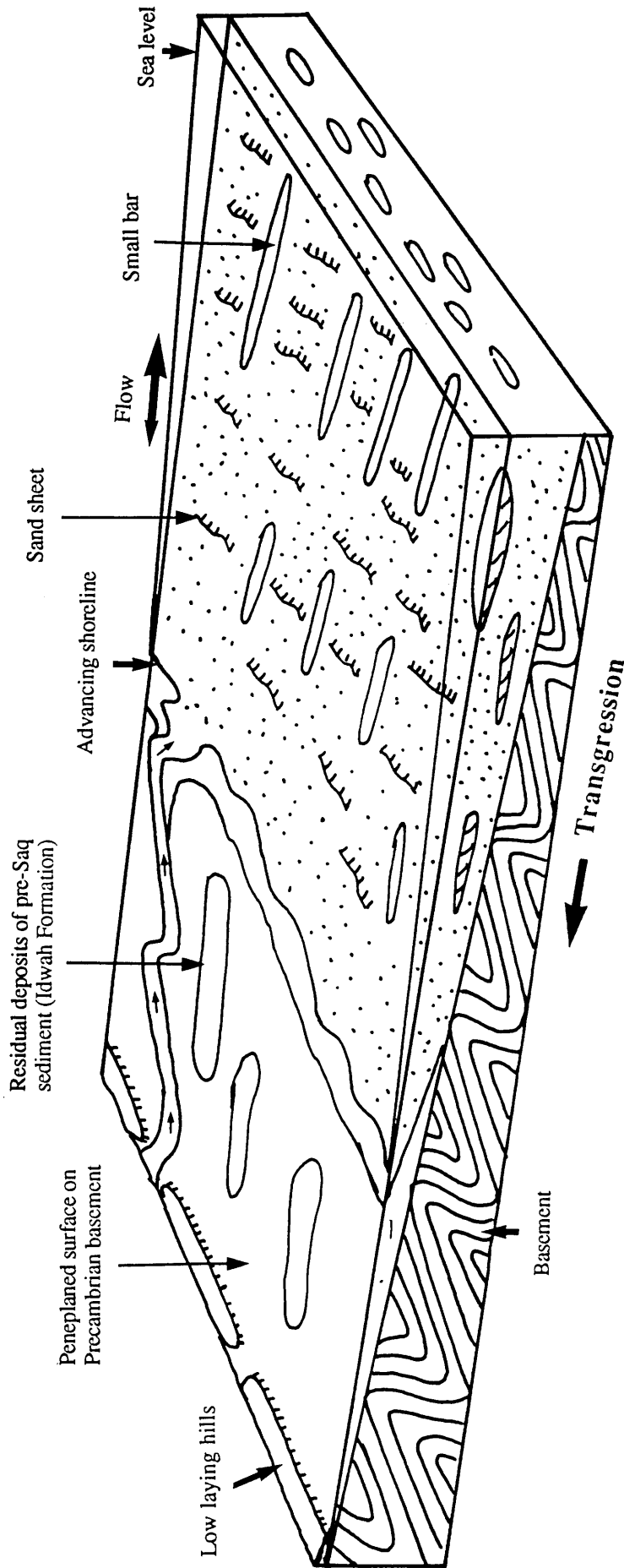


Fig. 6.3 Diagrammatic model of the Lower Saq Sandstone depositional environment

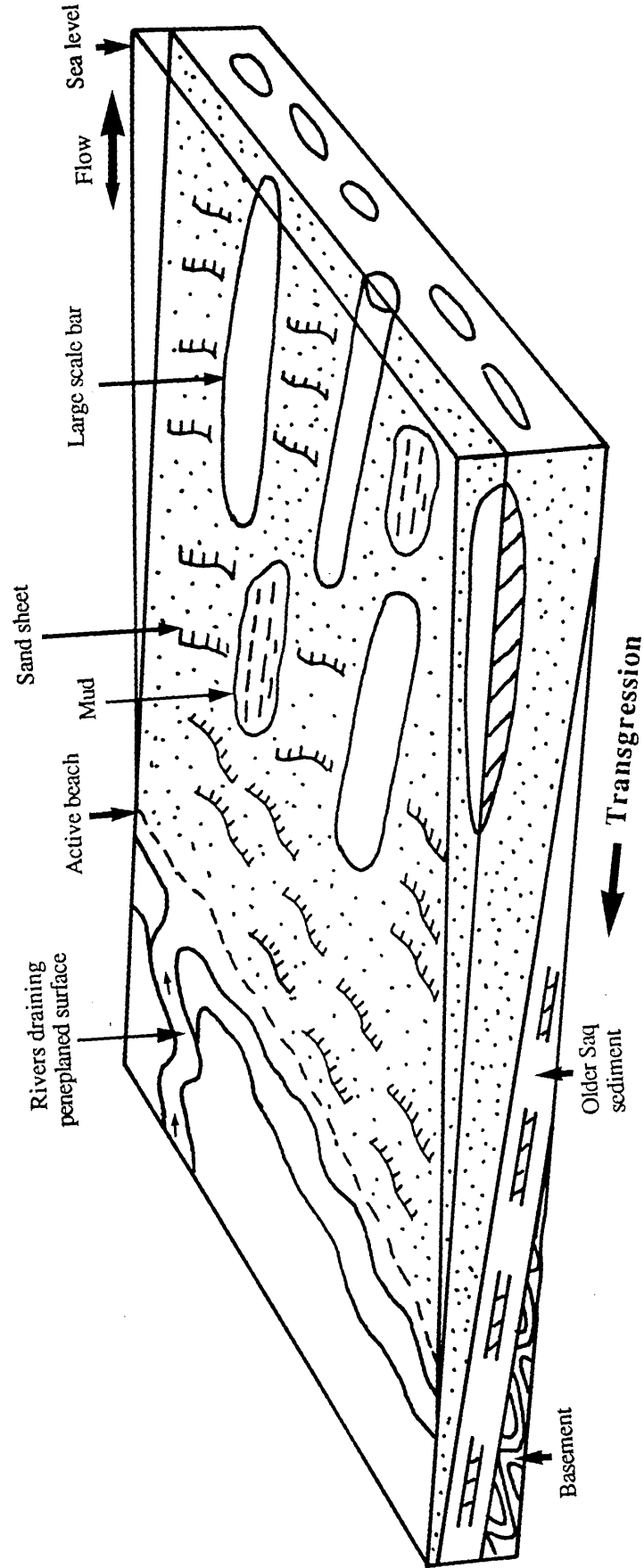


Fig.6.4 Diagrammatic model of the Middle Saq Sandstone depositional environment

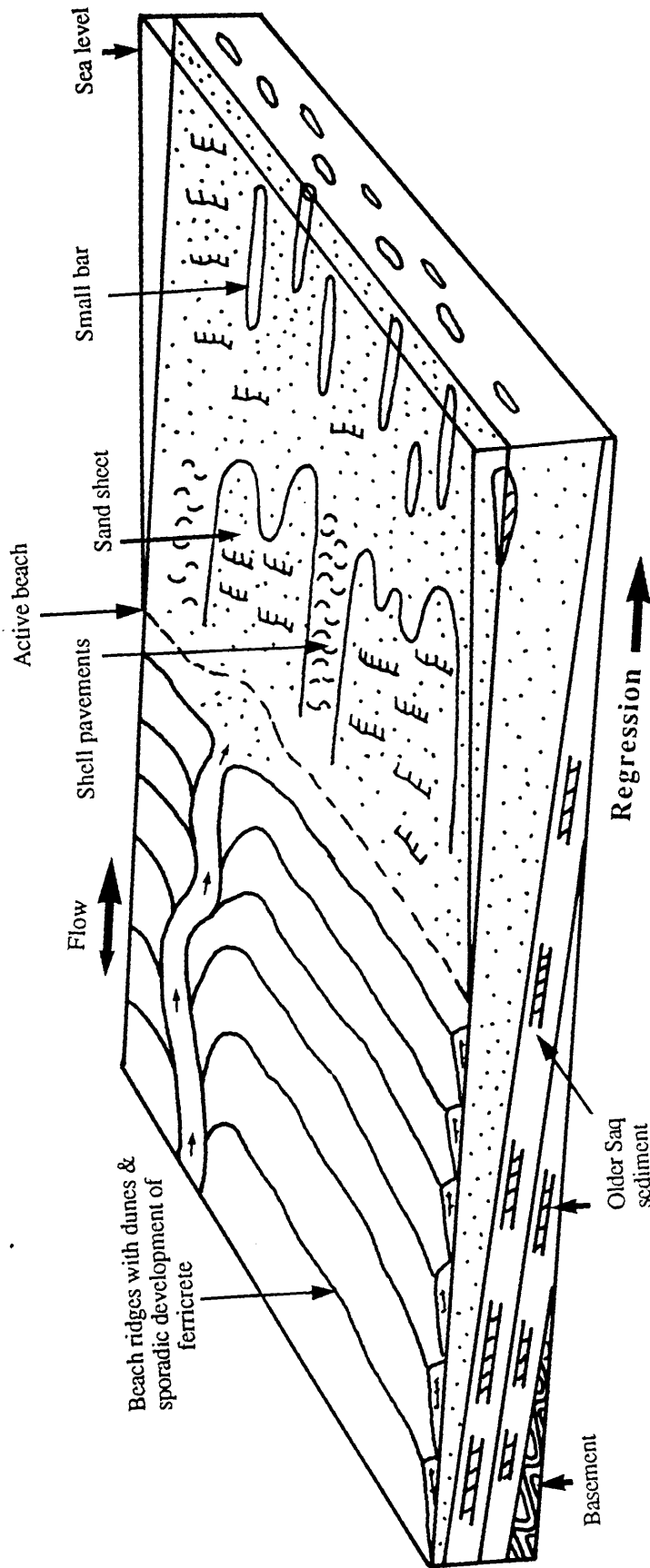


Fig. 6.5 Diagrammatic model of the Upper Saq Sandstone depositional environment

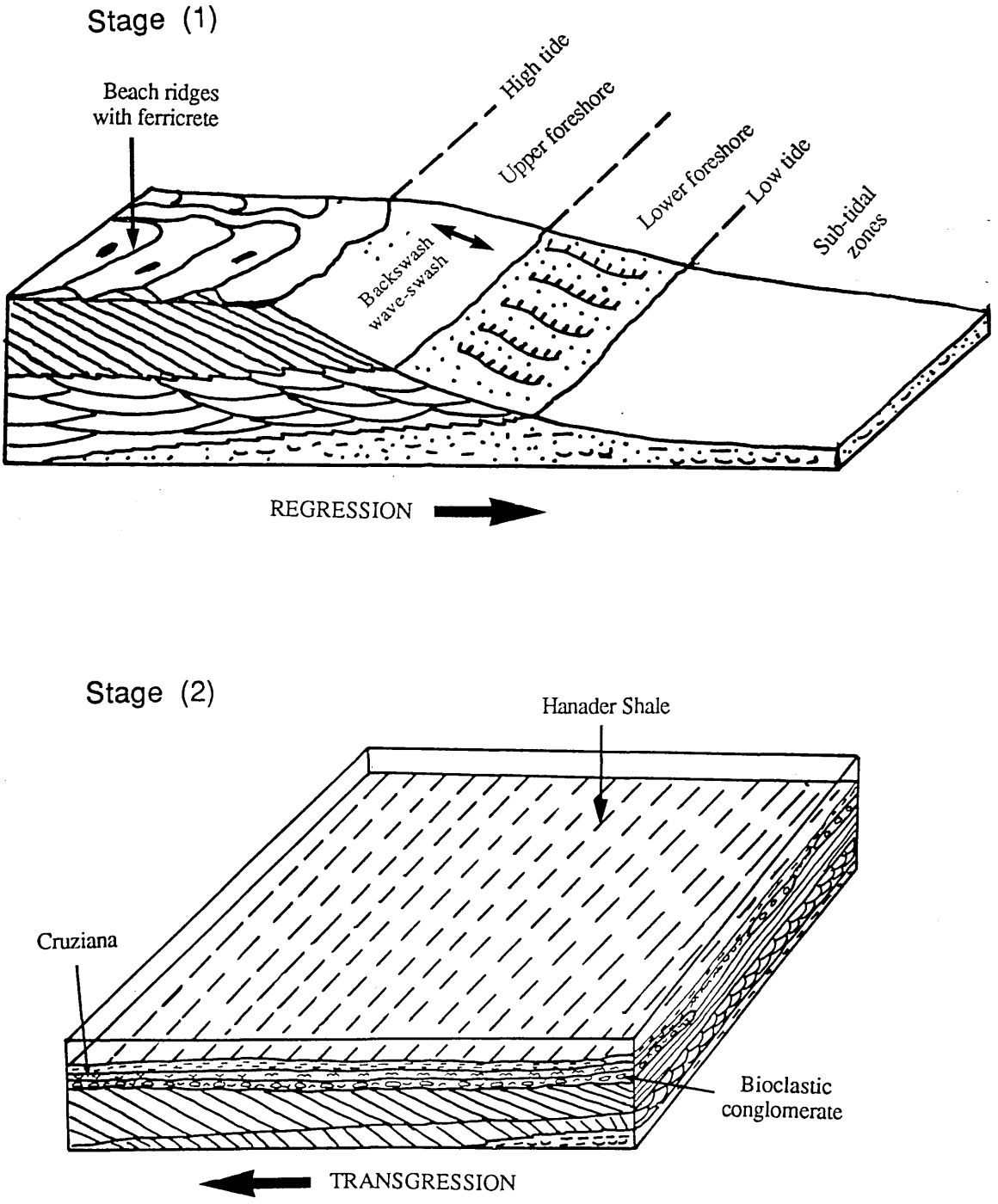


Fig.6.6 Diagrammatic model showing depositional environment of the most Upper Saq Sandstone

Fig. 6. Diagrammatic model showing the evolution of Saq Sandstone basin during Cambro-Ordovician time.

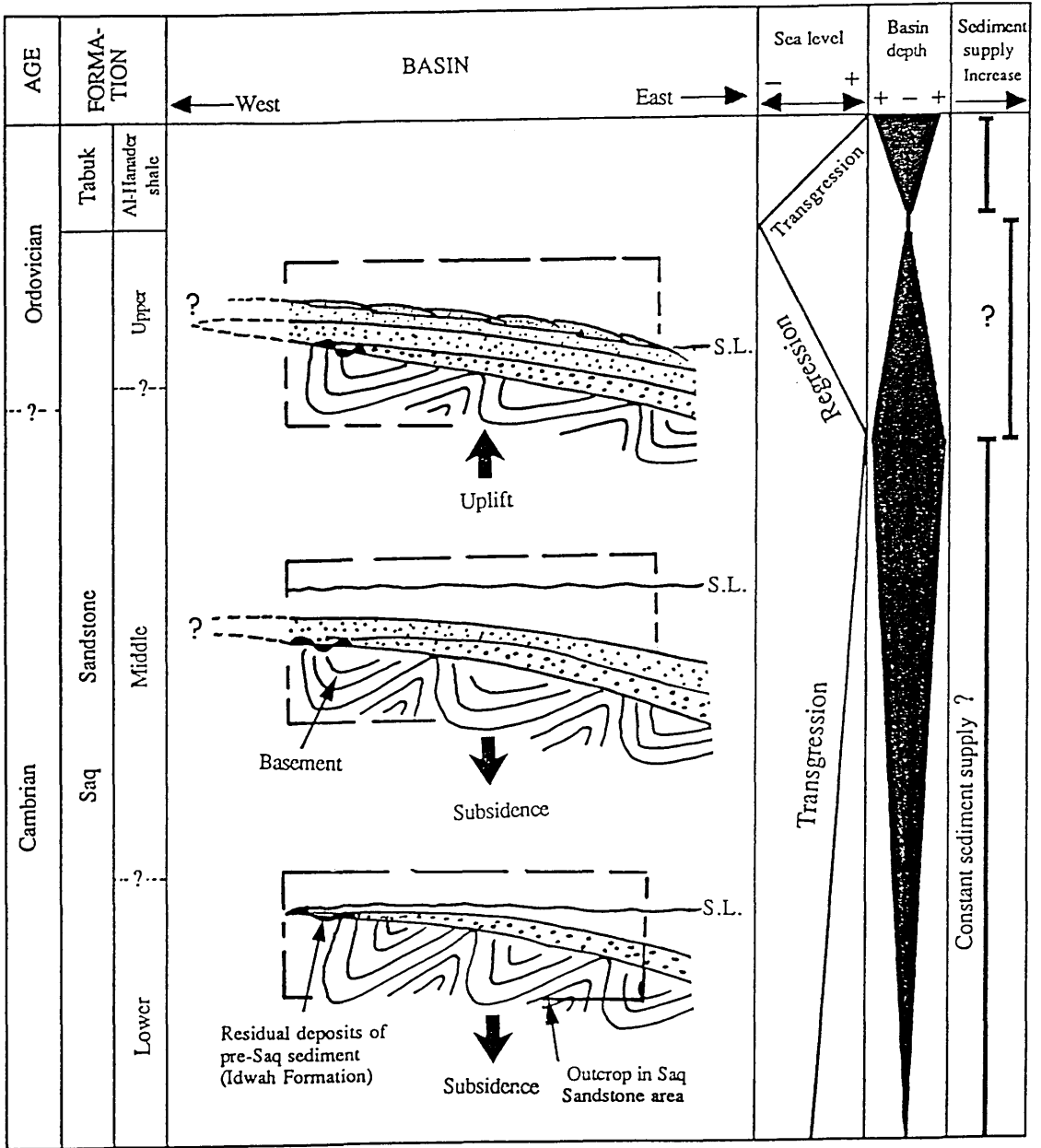


Fig. 6.7 Diagrammatic model showing the evolution of Saq Sandstone Basin throughout Cmbro-Ordovician time.

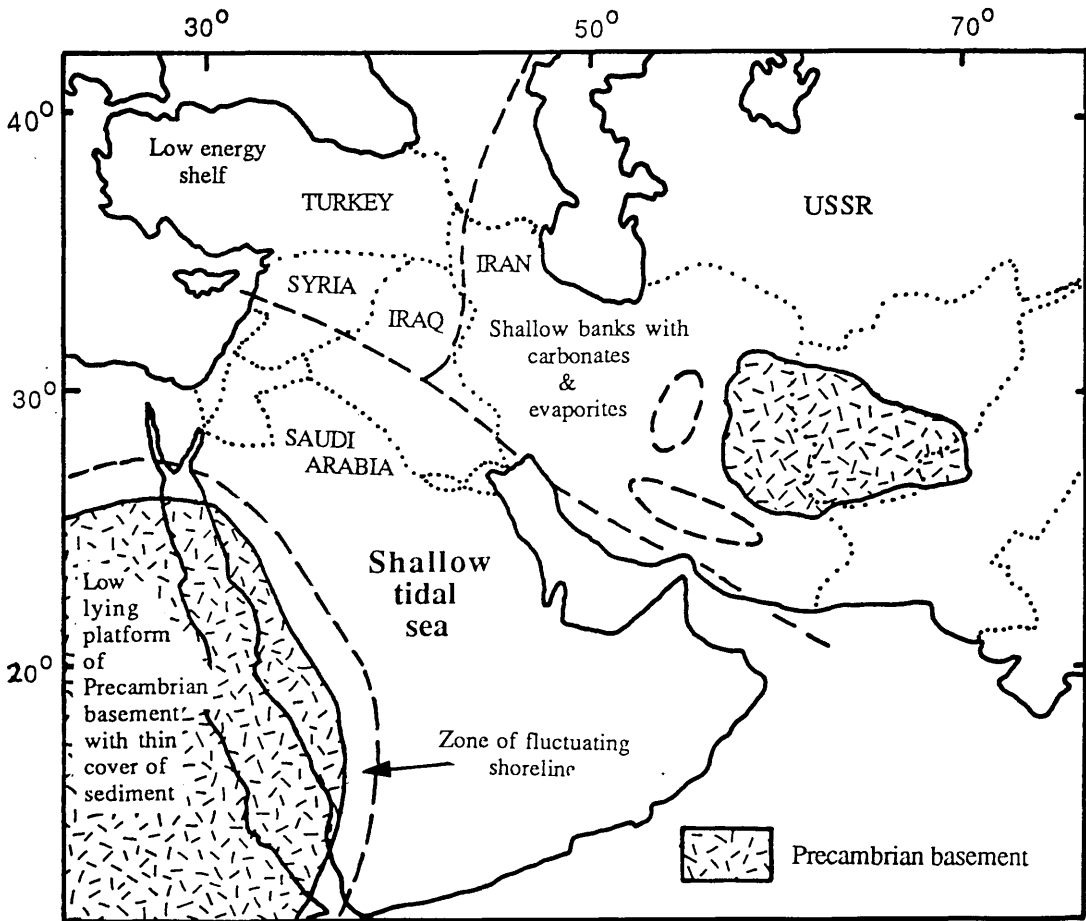


Fig. 6.8 Palaeogeographic reconstruction of tidal shelf environment during deposition of Cambro-Ordovician Saq Sandstone (adapted and modified from Walfort, 1981).

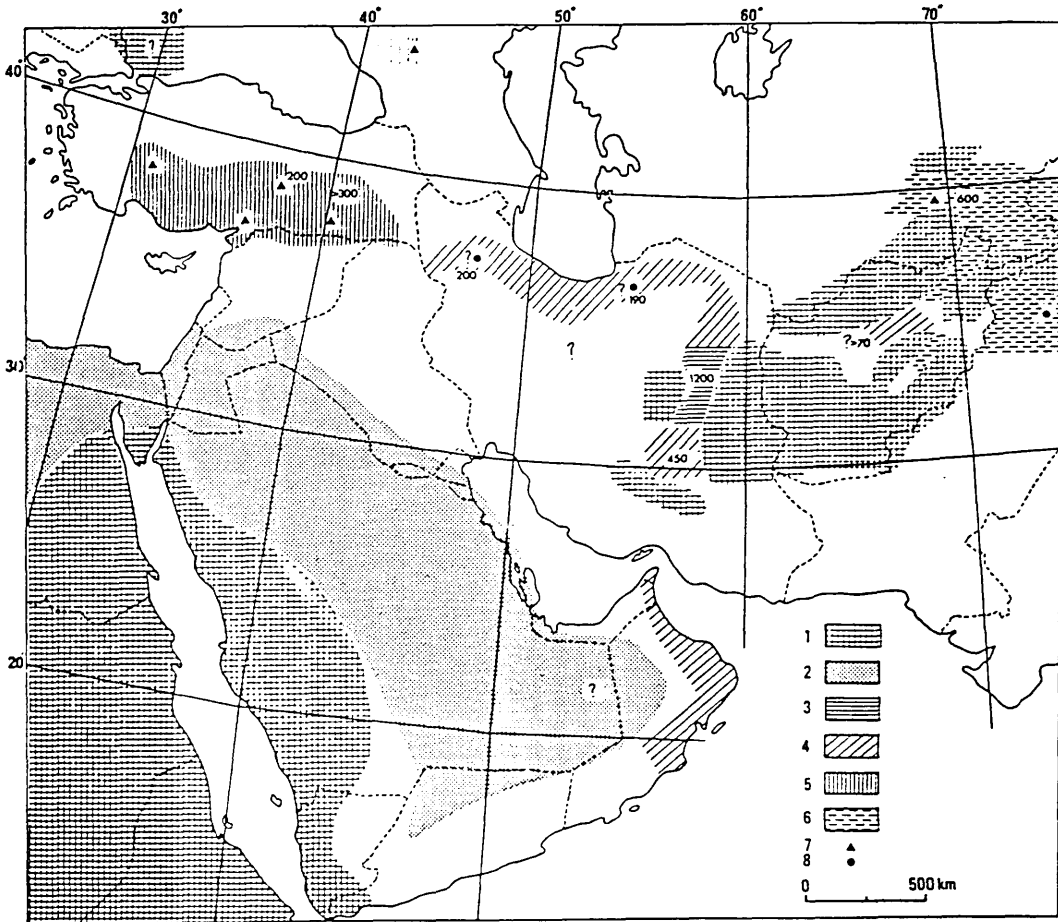


Fig. 6.9 Palaeogeography of Middle Cambrian. 1, Potential source area; 2, continental to littoral environment (sandstone, shale); 3, lagoonal to marine environment (dolomite, dolomitic marl, limestone); 4-6, marine environment; 4, dolomite, dolomitic maral with gypsum, limestone; 5, limestone, shale, sandstone; 6, shale with intercalations of limestone; 7, faunas mainly composed of Atlantic elements; 8, faunas composed of south Asiatic and Atlantic elements. Thickness in meters; (after Walfort, 1981).

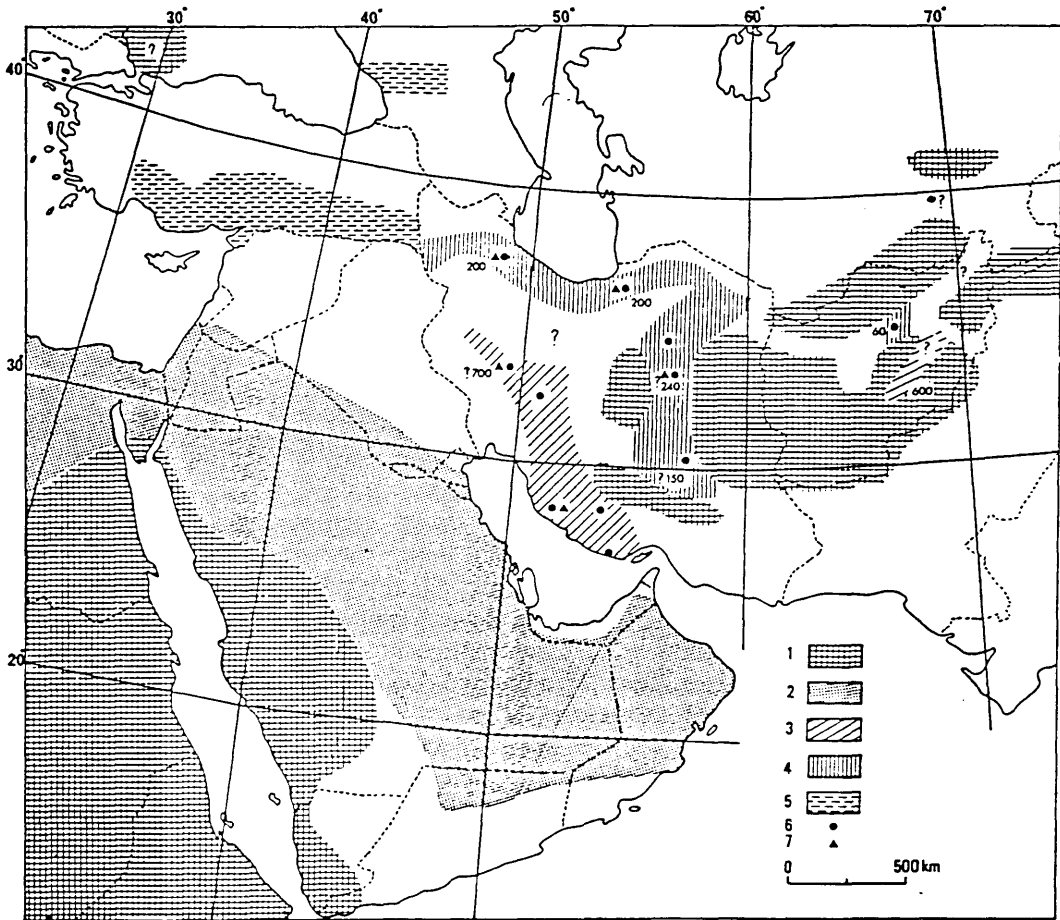


Fig. 6.10 Palaeogeography of Late Cambrian. 1, Potential source area; 2, continental to littoral environment (sandstone, shale); 3-5, marine environment, 3, sandstone, limestone, dolomite; 4, limestone, marl; 5, sandstone, shale; 6, early Late Cambrian faunas (Kushmanian); late Late Cambrian faunas (Changshanian to Daizanian). Thickness in meters, (after Walfort, 1981).

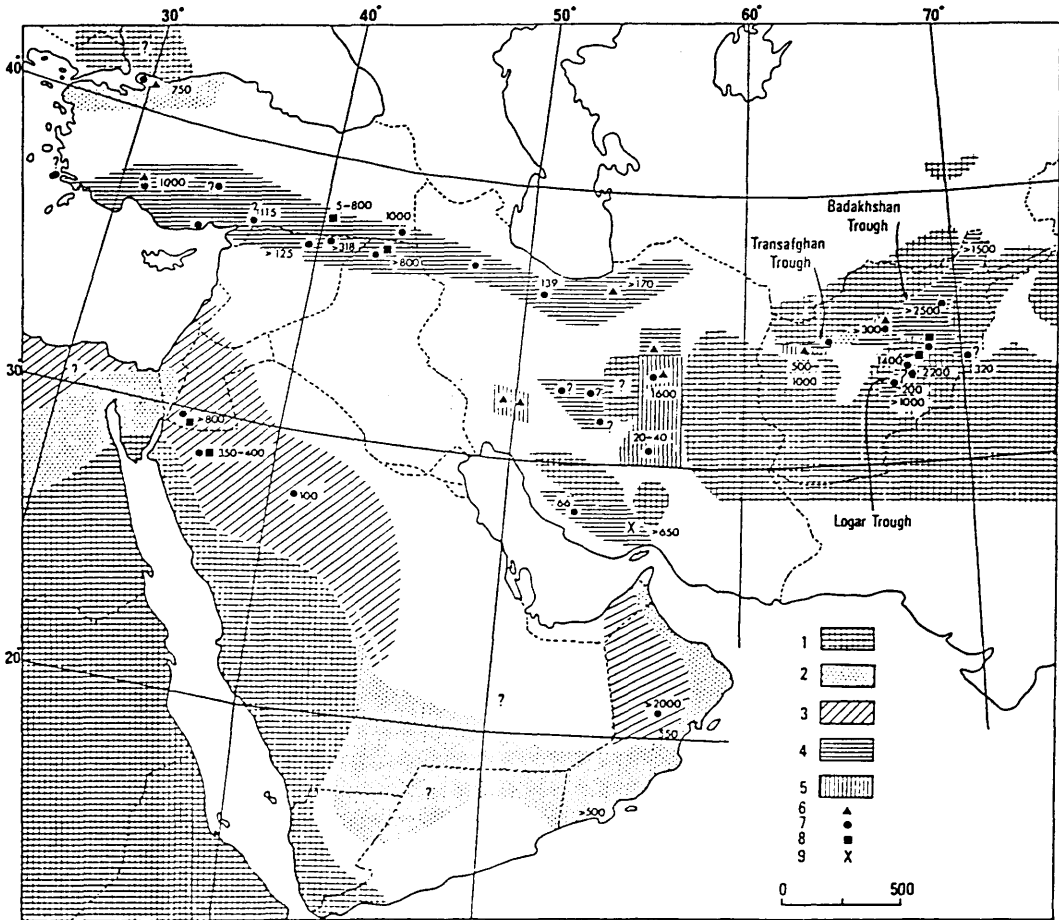


Fig. 6.11 Palaeogeography of Ordovician. 1, Potential source area; 2, continental to littoral environment (conglomerate, sandstone, shale); (3)-(5), marine environment; (3) sandstone, shale; (4) quartzite, sandstone, shale, sandy limestone; (5) predominantly maral and limestone; (6) Tremadoc funas; (7) Arenig to Llandeilo funas; (8) Caradoc to Ashgill faunas; (9) trace fossils. Total thickness in meters (after Walfort, 1981).

CHAPTER SEVEN

CONCLUSIONS

1. The Saq Sandstone is a 600m thick Middle Cambrian to Early Ordovician (?) sequence. It is a remarkably homogeneous unit consisting largely (>90%) of cross-stratified texturally and mineralogically mature fine to coarse quartz arenite, with subordinate shale, siltstone, breccia and conglomerate.
2. This study records a new pre-Saq formation (the Idwah Formation), composed of flat-stratified red sandstones and breccias of continental origin.
3. The Saq Sandstone is an upwards maturing sequence, in which monocrystalline quartz increases upwards from 82.51% in the Lower Saq to 92.48% in the Upper Saq Sandstone, and the geochemistry shows the upward increases SiO_2 .
4. The high maturity of the Saq Sandstones is attributed to four possible mechanisms: (1) reworking of sediments during deposition (ripples, megariipples etc.); (2) reworking of sediments belonging to an older phase of deposition; (3) reworking of sediments belonging to an older cycle (the Idwah Formation); (4) reworking directly from the basement in the present cycle.
5. The petrography and geochemistry indicate that the Saq Sandstone was derived largely from a craton interior possessing pre-existing and multi-cycle sedimentary rocks.
6. Cambro-Ordovician sandstones resembling the Saq Sandstone are found in Jordan (Quweria, Ram and Umm Sahm Formations); SW Sinai and Egypt (Sarbit, Abu Hamal, Nasib and Adedia Formations); Kufrah Basin, Libya (Hassaina and Memouniate Formations) and in Algeria (Ajjar Formation).
7. There is clear upwards fining in the Saq Sandstone, with an overall increase in sorting upwards in the sequence.

8. The erosion surface beneath the Saq Sandstone already existed, partly at least, when the Idwah Formation was laid down as this rests directly on the basement. This view is supported by : (1) the basal Saq conglomerates and breccias are very thin (usually <1m thick); (2) The quartz arenites of the Saq Sandstone rest directly on basic gneisses of the underlying Precambrian-Cambrian.
9. The last cooling event in the Precambrian-Cambrian basement was $530 \pm$ Ma (Greenwood et al., 1980), based on a whole-rock K-Ar dating. Neither the age of the Idwah Formation nor the age of the basal Saq Sandstone is known, but if a Middle Cambrian (\approx 540 Ma) - Early Ordovician (\approx 500 Ma ; Harland et al., 1989) is accepted for the Saq Sandstone then these leave little time to create the peneplaned surface upon which the Idwah and the Saq Formations were laid down.
10. Detailed facies analysis shows that the Saq Sandstone formed almost entirely in a marine environment. This environment was a tidally dominated shelf sea which initially drowned an old peneplaned surface cut into Precambrian-Cambrian rocks. This initially shallow sea deepened to generate large tidal sand bodies with associated sand sheets and areas of mud sedimentation. Finally the tidal shelf became shallow, and extensive beach deposits formed over the sequence during a period of major regression.
11. The Saq Sandstone was deposited initially during a transgression (Lower Saq) which then deepened (Middle Saq) and finally became a major regression (Upper Saq).
12. The palaeocurrent pattern throughout the Saq Sandstone is unimodal to the NE and this is attributed to a strong time-velocity asymmetry of tidal flow (Ebb-dominated). The consistency of palaeoflow orientation of an area more than 8000 Km² suggests a very uniform dispersing system, and/or a very extensive environment of which this is only a small part. The presence of strong tidal currents implies that the Saq basin was open to an ocean basin, probably to the NE during the deposition of the Saq Sandstone.

- 13 Three mechanisms have been recognized as important to the building up of marine tidal sand bars: (1) overtaking, (2) stacking of wedges and (3) scour and reactivation.

APPENDIX A

Table 3.1 Mineralogy of the Lower Saq Sandstone

Sample No.	Quartz		Feldspar	Lithic Fragments	Mica	Kaolinite	Cement		Silica	Heavy Minerals
	Mono.	Poly.					Carbonate	Iron		
K-2-1	82.50	7.25	0.75	0.50	0.25	1.25	1.25	3.50	0.00	0.75
K-2-2	76.25	6.25	0.50	0.25	0.00	4.50	4.25	6.25	0.00	0.50
K-2-4	84.00	3.25	0.50	0.00	0.75	1.75	4.75	3.75	0.25	0.00
K-3-2	80.25	6.50	0.25	0.25	0.25	0.75	6.75	3.25	0.00	0.00
K-3-4	77.25	8.50	0.25	0.50	0.00	1.00	4.25	6.75	0.00	0.75
K-3-5	81.25	7.00	0.25	0.00	0.25	0.50	5.25	3.50	0.00	0.50
K-3-6	77.75	8.75	0.50	0.25	0.75	0.75	3.50	5.00	0.00	1.00
K-4-1	71.75	10.25	0.25	0.50	0.00	4.75	5.75	3.50	0.00	0.50
K-4-2	78.50	9.75	0.25	0.25	0.75	2.00	2.00	4.25	0.25	0.00
K-4-3	77.50	11.0	0.75	0.50	0.25	1.75	1.00	5.00	0.00	0.00
K-5-1	72.00	8.00	0.75	0.25	0.50	5.75	1.25	8.75	0.00	0.00
K-5-2	77.50	7.75	1.25	1.00	0.25	1.25	1.75	5.75	0.00	0.25
K-5-4	79.00	8.00	0.75	0.75	0.00	1.00	1.25	7.50	0.00	0.00
K-5-6	79.50	8.25	0.50	0.25	0.50	1.75	1.75	5.75	0.00	0.25
K-5-5	75.50	10.00	0.75	1.00	0.75	2.00	1.75	4.75	0.00	0.75
K-5-7	73.00	12.25	0.50	0.75	0.50	2.75	2.50	5.75	0.00	0.00
K-5-8	81.50	10.50	0.25	0.50	0.00	1.75	2.75	0.00	0.00	0.00
K-5-9	77.50	8.50	1.25	1.00	0.75	2.00	0.25	5.00	0.25	0.00
K-5-10	78.75	7.75	1.00	0.75	0.50	3.25	0.75	4.75	0.00	0.25
K-5-11	82.00	6.75	0.25	0.50	0.00	1.75	1.00	5.75	0.00	0.50
K-5-12	82.00	7.25	0.75	0.50	0.25	2.75	1.50	3.25	0.00	0.75
K-5-13	81.25	9.50	0.00	0.00	0.00	3.25	0.75	2.50	0.75	0.75
K-5-14	82.50	8.00	0.50	0.50	0.25	1.25	0.75	4.25	0.50	0.50
K-5-15	74.25	8.50	0.75	1.00	0.00	2.75	5.25	4.50	0.00	0.25
K-7-1	94.00	3.00	0.25	0.00	0.75	0.50	0.25	0.50	0.00	0.00
K-7-5	86.50	6.25	1.00	1.25	0.00	1.25	0.25	0.50	0.25	0.75
K-7-6	86.75	8.50	0.75	0.00	0.75	0.25	0.50	0.00	0.25	0.75
K-7-7	81.50	11.50	1.00	0.75	0.00	0.75	2.00	0.00	0.00	0.25
K-7-8	80.50	9.75	0.50	0.75	0.00	2.75	1.25	1.75	0.00	0.00
K-7-9	80.75	7.25	1.00	1.75	0.00	2.50	0.00	3.75	0.50	0.50

Table 3.1 Continued

Sample No.	Quartz		Feldspar	Lithic Fragments	Mica	Kaolinite	Cement		Silica	Heavy Minerals
	Mono.	Poly.					Carbonate	Iron		
K-7-11	80.00	4.50	0.50	1.25	0.50	1.75	2.50	7.00	0.00	0.25
K-20-1	89.50	4.50	1.00	1.00	0.00	1.25	0.50	0.00	0.25	0.00
K-20-2	83.25	4.75	1.25	0.75	0.50	2.00	2.25	2.75	0.00	0.75
K-20-3	80.75	8.00	1.75	0.50	0.25	1.50	3.50	0.75	0.00	1.00
K-20-4	85.00	5.75	0.75	0.25	0.00	3.75	0.75	2.25	0.00	0.25
K-20-5	88.00	5.00	0.75	0.50	0.25	0.75	2.00	0.75	0.50	0.75
K-20-6	86.00	7.50	0.25	0.50	0.00	0.50	2.75	0.50	0.25	0.75
K-20-7	87.00	6.00	1.00	0.50	0.25	1.00	1.75	0.75	0.00	0.50
K-20-8	91.00	4.50	0.50	0.00	0.00	1.75	1.25	0.00	0.00	0.25
K-20-10	91.25	4.25	0.75	0.50	0.00	0.00	1.50	0.25	0.00	0.50
K-20-11	92.25	4.75	0.50	0.00	0.00	0.25	0.75	0.00	0.00	0.25
K-20-12	90.50	6.00	0.75	0.25	0.00	0.75	0.00	0.50	0.50	0.00
k-26-1	76.50	8.00	1.25	3.25	0.25	2.75	0.00	3.75	0.25	0.25
k-26-2	80.25	7.25	1.50	2.75	0.25	1.75	0.00	3.25	0.00	0.50
k-26-4	81.25	8.50	0.00	0.25	0.00	2.25	0.25	0.00	0.00	2.75
k-26-5	81.25	7.25	0.50	2.75	0.50	1.75	0.00	0.00	0.25	3.50
k-27-3	74.25	6.75	0.50	3.25	0.50	0.00	0.00	6.25	0.50	3.75
k-27-4	81.25	8.75	0.75	1.25	0.25	0.00	1.25	0.00	0.75	2.75

Table 3.2 Mineralogy of the Middle Saq Sandstone

Sample No.	Quartz		Chert	Feldspar	Lithic Fragments	Mica	Kaolinite	Cement		Silica	Heavy Minerals
	Mono.	Poly.						Carbonate	Iron		
K-1-1	81.00	7.75	4.00	1.25	0.50	0.00	2.50	2.50	0.25	0.00	0.25
K-1-3	78.75	6.00	1.00	0.75	2.25	0.00	4.00	3.75	3.50	0.00	0.00
K-1-4	84.75	5.25	1.25	0.50	0.50	1.00	4.50	1.25	0.50	0.00	0.50
K-1-5	85.00	5.75	1.50	0.50	0.00	0.75	4.75	0.50	1.25	0.00	0.00
K-1-7	88.50	6.50	1.25	0.75	0.25	0.50	0.75	1.25	0.00	0.25	0.00
K-6-1	90.00	6.25	1.00	0.25	0.50	0.00	0.75	0.50	0.25	0.00	0.50
K-6-2	82.25	7.25	1.75	0.50	0.75	0.00	2.00	0.50	4.75	0.00	0.25
K-6-4	83.25	9.50	1.50	0.50	0.25	0.00	0.75	0.25	3.25	0.00	0.75
K-6-6	80.50	6.25	2.50	0.75	1.25	0.25	2.75	0.75	4.75	0.00	0.25
K-36-1	87.00	6.75	1.75	0.75	0.50	0.00	0.00	2.75	0.00	0.50	0.00
K-36-2	89.75	4.50	2.00	0.50	1.25	0.50	0.25	0.50	0.00	0.75	0.00
K-36-3	93.25	2.50	1.25	0.25	0.75	0.75	0.50	0.25	0.00	0.50	0.00
K-36-4	90.25	6.25	0.50	0.75	0.50	0.00	1.25	0.00	0.00	0.25	0.25
K-36-5	87.00	7.00	2.00	0.25	1.25	0.25	0.50	0.75	0.00	0.25	0.75
K-36-6	87.25	6.00	2.00	0.75	0.50	0.00	0.50	1.25	0.25	1.00	0.50
K-36-7	88.00	4.25	1.50	0.25	1.25	0.00	1.00	2.50	0.00	0.75	0.50
K-36-8	86.75	7.25	1.25	0.25	0.50	0.25	1.25	2.25	0.00	0.00	0.25
K-36-9	83.75	6.50	2.50	0.75	1.50	0.75	2.25	0.00	2.00	0.00	.00
K-37-1	92.25	3.75	1.50	0.25	0.25	0.00	0.75	0.00	0.50	0.00	0.75
K-37-2	91.00	2.50	1.25	0.50	0.50	0.00	1.00	1.75	0.75	0.25	0.50
K-37-3	93.25	3.00	1.00	0.25	0.50	0.25	0.50	1.00	0.00	0.25	0.00
K-37-4	91.25	4.00	0.75	0.25	0.00	0.75	0.00	2.75	0.00	0.00	0.25
K-37-5	90.25	3.25	1.75	0.25	0.50	0.00	0.75	3.00	0.00	0.00	0.25
K-37-6	88.75	3.75	1.00	0.50	0.00	0.75	1.50	3.50	0.25	0.00	0.00
K-37-7	92.50	2.75	1.25	0.50	0.25	0.00	0.50	2.00	0.00	0.25	0.00
K-38-1	90.25	1.75	0.50	0.25	0.50	0.50	2.25	2.75	0.00	0.75	0.50
K-38-2	86.25	3.25	1.25	0.50	0.25	0.25	3.75	2.25	0.75	1.25	0.25
K-38-3	87.25	2.75	1.00	0.50	0.00	0.00	4.75	2.00	0.25	0.75	0.75
K-38-4	92.00	3.25	0.75	0.25	0.25	0.75	1.50	1.00	0.00	0.00	0.25
K-38-5	90.75	4.00	1.25	0.75	0.00	0.00	1.25	0.50	1.75	0.00	0.00

Table 3.2 Continued

Sample No.	Quartz		Feldspar	Lithic Fragments	Mica	Cement			Heavy Minerals	
	Mono.	Poly.				Chert	Kaolinite	Carbonate		Iron
K-38-6	92.00	3.50	0.25	0.00	0.50	1.00	0.50	0.00	0.25	0.00
K-38-7	93.25	3.50	0.50	0.25	0.00	0.75	0.75	0.00	0.00	0.25
K-18-1	92.00	3.25	0.50	0.25	0.25	0.75	0.00	0.00	1.75	0.75
K-18-2	93.75	3.25	0.50	0.00	0.50	0.25	1.25	0.00	0.00	0.25
K-18-3	95.00	1.75	0.25	0.25	0.00	0.25	0.50	0.00	0.75	0.50
K-18-4	93.75	2.50	0.75	0.50	0.25	0.00	0.75	0.00	0.50	0.75
K-39-1	90.00	4.25	0.25	0.00	0.25	0.75	2.00	0.00	0.75	0.75
K-39-2	91.75	5.75	0.50	0.00	0.00	0.25	1.00	0.00	0.00	0.00
K-39-3	88.00	5.50	0.75	0.50	0.50	1.00	1.25	0.00	0.25	0.25
K-39-4	94.75	2.00	0.00	0.25	0.00	0.25	0.50	0.00	0.75	1.00
K-39-5	94.00	2.75	0.50	0.25	0.25	0.50	0.25	0.75	0.00	0.00
K-39-6	95.25	3.50	0.00	0.00	0.00	0.00	0.50	0.00	0.25	0.00
K-39-7	94.75	1.00	0.50	0.00	0.25	0.50	1.25	0.00	0.25	0.25
K-39-8	93.50	1.25	0.25	0.00	0.25	3.00	0.50	0.00	0.25	0.25
K-39-9	92.00	3.25	0.75	0.50	0.00	0.75	1.25	0.00	0.50	0.50
K-13-1	89.75	5.00	0.25	0.50	0.75	0.50	1.50	0.00	0.25	0.75
K-13-2	94.00	3.50	0.00	0.25	0.00	0.25	1.00	0.00	0.25	0.00
K-13-3	90.25	2.25	1.00	0.25	0.00	0.00	0.50	4.50	0.00	0.00
K-13-4	85.00	4.00	0.50	0.50	0.25	0.25	0.50	7.25	0.00	0.75
K-14-1	92.75	2.25	0.50	0.25	0.00	1.50	1.25	0.00	0.25	0.25
K-14-2	95.25	1.50	0.50	0.25	0.25	0.75	0.00	0.00	.75	0.00
K-14-3	94.00	2.00	0.75	0.00	0.25	0.25	0.00	0.00	1.50	0.75
K-14-4	90.00	3.25	0.50	0.75	0.75	0.00	0.50	0.00	1.75	0.50
K-14-5	90.25	6.00	0.00	0.50	0.00	0.50	0.00	0.00	0.75	0.75
K-15-1	92.00	3.50	0.75	1.00	0.25	0.50	0.00	0.00	0.75	0.00
K-15-3	92.25	3.75	0.75	0.75	0.00	0.25	0.00	0.00	1.25	0.00
K-15-4	92.75	3.75	0.25	0.50	0.50	0.75	0.00	0.00	0.00	0.25
K-15-5	85.50	9.25	0.00	0.25	0.00	0.75	0.00	0.00	0.00	0.75
K-15-6	87.50	5.75	0.50	0.00	0.00	0.25	2.75	0.00	0.00	1.25
K-17-1	88.00	7.00	1.00	0.50	0.00	1.50	0.50	0.00	0.25	0.00

Table 3.2 Continued

Sample No.	Quartz		Feldspar	Lithic Fragments	Mica	Cement			Heavy Minerals	
	Mono.	Poly.				Chert	Kaolinite	Carbonate		Iron
K-17-2	93.00	3.50	0.50	0.00	0.75	0.75	0.50	0.00	0.25	0.25
K-17-3	94.75	3.00	0.25	0.00	0.50	0.25	0.25	0.00	0.00	0.25
K-17-4	85.00	5.75	1.00	0.75	0.50	2.75	1.25	0.75	0.00	0.50
K-17-6	86.75	3.50	0.75	0.25	0.00	1.25	3.75	2.00	0.00	0.50
K-19-1	89.25	6.00	0.50	0.75	0.50	0.75	0.50	0.00	0.75	0.00
K-19-2	92.75	4.50	0.50	0.00	0.00	0.75	0.75	0.00	0.00	0.00
K-19-3	87.50	3.25	0.75	0.00	0.50	3.50	1.75	0.75	0.00	0.75
K-19-4	88.25	3.50	0.50	0.25	0.50	3.75	1.25	0.25	0.00	0.75
K-43-1	92.00	2.75	0.25	0.50	0.00	1.00	2.00	0.00	0.50	0.50
K-43-2	90.75	3.25	0.75	0.50	0.75	1.00	1.25	0.00	0.25	0.75
K-43-3	89.75	4.75	0.25	0.75	0.50	0.25	0.50	2.50	0.00	0.25
K-43-4	91.75	4.25	0.50	0.50	0.25	0.75	1.00	0.25	0.00	0.00
K-43-5	93.50	3.75	0.25	0.25	0.00	0.50	0.75	0.25	0.00	0.25
K-43-6	90.00	5.00	0.25	0.75	0.75	0.75	1.00	0.50	0.00	0.50
K-44-1	88.50	4.00	1.00	0.50	1.50	1.00	2.00	0.75	0.25	0.00
K-44-2	89.25	4.75	1.25	1.00	0.25	0.50	0.75	0.25	0.25	0.75
K-44-3	91.50	3.50	0.75	0.25	0.50	0.25	1.75	0.00	0.00	1.00
K-44-4	91.25	3.75	0.50	0.00	0.00	0.50	2.25	1.25	0.00	0.00
K-44-5	87.25	5.00	0.75	0.25	0.75	0.00	4.75	0.75	0.00	0.00
K-45-1	89.50	4.50	0.50	0.00	0.25	0.50	3.50	0.00	0.25	0.25
K-45-2	91.50	3.75	0.25	0.75	0.00	0.75	1.75	0.50	0.00	0.25
K-45-3	91.00	4.75	0.50	0.00	0.75	0.50	0.75	0.25	0.00	0.50
K-45-4	92.00	3.50	0.75	0.75	0.50	0.25	0.00	1.00	0.00	0.75
K-28-1	90.75	4.25	0.50	0.25	0.00	1.25	1.25	0.00	0.00	1.00
K-28-2	89.75	3.25	0.75	0.50	0.00	2.25	1.25	0.00	0.75	0.25
K-28-3	88.75	3.75	1.00	0.50	0.00	2.75	1.00	1.25	0.00	0.25
K-28-4	91.25	3.00	0.75	0.25	0.25	1.25	1.25	0.00	0.50	0.50
K-28-5	89.75	3.25	0.50	0.00	0.25	2.00	1.75	0.75	0.25	0.75
K-16-1	93.50	2.00	0.75	0.50	0.25	0.50	0.00	0.00	0.75	0.50
K-16-2	91.00	5.50	1.00	0.50	0.00	0.50	0.00	0.00	1.25	0.00

Table 3.2 Continued

Sample No.	Quartz		Feldspar	Lithic Fragments	Mica	Cement			Heavy Minerals	
	Mono.	Poly.				Kaolinite	Carbonate	Iron		Silica
K-16-3	88.00	7.25	1.00	0.25	0.25	0.00	1.50	0.00	0.50	0.00
K-16-4	92.50	4.00	0.75	0.00	0.50	0.00	1.25	0.00	0.25	0.00
K-16-5	94.00	2.25	0.25	0.25	0.00	0.00	0.50	0.00	1.75	0.50
K-16-6	91.00	3.00	1.00	0.75	0.50	0.00	0.25	0.00	2.50	0.25

Table 3.3 Mineralogy of the Upper Saq Sandstone

Sample No.	Quartz		Feldspar	Lithic Fragments	Mica	Cement			Heavy Minerals	
	Mono.	Poly.				Kaolinite	Carbonate	Iron		Silica
K-21-1	91.00	2.50	1.00	0.00	0.75	1.00	2.25	0.00	0.25	0.25
K-21-2	95.00	2.50	0.25	0.00	0.00	0.50	0.75	0.00	0.00	0.50
K-21-3	92.50	2.50	0.75	0.00	0.50	0.50	2.00	0.00	0.00	0.75
K-21-4	87.00	5.25	0.25	0.50	0.25	0.75	3.00	1.75	0.00	0.25
K-21-5	90.50	3.75	0.75	0.25	0.00	1.00	1.25	0.00	0.00	1.25
K-42-1	90.75	3.00	0.50	0.75	0.75	0.75	2.00	0.25	0.00	0.00
K-42-2	90.50	2.75	1.25	1.00	0.25	0.50	1.75	0.50	0.00	0.50
K-42-3	91.75	2.00	0.75	0.50	0.75	1.75	1.00	0.25	0.00	0.75
K-42-4	93.00	2.00	0.50	0.25	0.75	0.50	1.50	0.25	0.50	0.25
K-42-5	91.00	3.50	0.75	0.25	1.00	0.75	1.25	0.50	0.00	0.00
K-22-1	94.00	2.00	0.75	0.25	1.00	0.75	0.00	0.00	0.50	0.25
K-22-2	94.25	1.25	0.75	0.00	1.75	1.25	0.00	0.00	0.00	0.50
K-22-3	91.25	2.00	1.50	0.25	1.50	0.75	0.00	1.75	0.00	0.75
K-22-4	94.75	1.00	1.25	0.00	1.00	0.50	0.00	0.00	0.75	0.50
K-22-5	91.25	1.75	1.25	0.50	0.75	0.75	2.00	1.25	0.00	0.25
K-23-1	92.25	3.25	1.00	0.25	0.25	1.50	0.00	0.00	0.25	0.50
K-23-2	90.75	2.25	0.75	0.75	0.00	0.75	2.75	1.00	0.00	0.75
K-40-2	93.50	2.75	0.75	0.25	0.75	0.75	0.50	0.00	0.00	0.75
K-40-3	94.00	3.25	0.75	0.25	0.25	0.00	0.25	0.00	0.50	0.25
K-40-4	94.00	2.25	1.25	0.50	0.75	0.25	0.25	0.00	0.25	0.00
K-40-5	91.50	2.75	2.00	0.75	0.25	0.50	1.25	0.00	0.00	0.25
K-40-6	93.00	3.50	1.50	0.25	0.25	0.00	0.75	0.00	0.00	0.50
K-40-8	95.25	2.25	0.75	0.50	0.75	0.25	0.00	0.00	0.25	0.00
K-40-9	92.25	2.75	1.00	0.25	1.00	0.75	1.50	0.00	0.00	0.00
K-41-1	95.00	2.00	0.50	0.00	0.25	0.50	0.75	0.00	0.00	0.25
K-41-2	95.50	1.75	0.25	0.25	0.00	0.25	0.00	0.00	0.75	0.50
K-41-3	95.25	1.75	0.50	0.00	0.25	0.50	0.50	0.00	0.00	0.75
K-41-4	92.00	2.00	0.75	0.50	0.75	0.25	1.25	0.25	0.00	1.25
K-41-5	95.25	1.50	0.25	0.25	0.25	0.75	0.00	0.00	0.75	0.25
K-25-1	94.25	2.50	0.50	0.25	0.25	0.00	1.25	0.00	0.25	0.00

Table 3.3 Continued

Sample No.	Quartz		Feldspar	Lithic Fragments	Mica	Kaolinite	Cement		Silica	Heavy Minerals
	Mono.	Poly.					Carbonate	Iron		
K-25-2	94.00	3.75	0.00	0.00	0.00	0.25	0.75	0.00	0.00	0.75
K-25-3	94.75	3.00	0.50	0.25	0.00	0.50	0.00	0.00	0.00	0.25
K-25-4	89.25	4.00	1.00	0.50	1.00	0.75	1.75	0.00	0.50	0.50
K-25-5	90.25	2.75	1.00	0.50	0.75	1.25	1.75	0.00	0.00	1.00
K-25-6	92.75	2.50	0.75	0.00	0.25	0.50	2.00	0.00	0.00	0.25
K-30-1	88.00	2.50	1.00	0.00	0.50	4.00	0.75	2.50	0.25	0.00
K-30-2	95.50	1.25	0.50	0.00	0.50	1.25	0.00	0.00	0.00	0.50
K-30-3	91.50	3.25	0.75	0.50	0.25	0.50	2.75	0.00	0.00	0.25
K-30-4	92.25	2.75	0.50	0.00	0.75	0.50	2.00	1.25	0.00	0.00
K-30-5	87.25	2.25	1.00	0.50	1.25	3.25	0.50	2.75	0.00	0.75
K-23-3	92.75	2.75	2.50	0.00	0.50	0.00	0.00	1.00	0.00	0.00
K-40-1	93.75	2.75	1.25	0.50	0.00	0.50	0.00	0.00	1.00	0.00

Table 3.5 Tourmaline analyses

Oxide	1	2	3	4	5	6	7	8	9	10	11	12
SiO ₂	35.84	37.31	36.50	36.42	35.65	35.77	35.42	34.47	37.26	36.08	37.40	35.53
TiO ₂	0.91	0.94	0.32	1.21	0.71	0.55	0.64	0.50	0.58	0.79	0.39	0.66
B ₂ O ₃	N.A.											
Al ₂ O ₃	34.25	34.10	33.96	34.53	34.01	34.39	33.56	35.23	34.88	34.03	35.31	34.22
FeO	6.64	3.41	7.96	6.72	7.70	7.17	7.83	5.92	3.76	6.67	0.51	8.05
MnO	0.00	0.09	0.00	0.00	0.04	0.06	0.07	0.10	0.00	0.15	0.04	0.00
MgO	5.54	7.74	5.35	5.38	5.56	5.99	5.62	6.62	7.56	5.91	9.46	5.42
CaO	0.81	1.34	0.35	0.19	0.76	0.85	1.20	1.28	0.92	0.36	1.84	0.41
Na ₂ O	1.86	1.04	1.51	1.52	1.52	1.07	1.57	1.79	0.93	1.85	1.53	1.67
K ₂ O	0.11	0.00	0.02	0.00	0.00	0.01	0.05	0.05	0.07	0.13	0.14	0.00
F	N.A.											
H ₂ O	N.A.											

N.A. = Not Analyzed

Table 3.5 Continued

Oxide	13	14	15	16	17	18	19	20	21	22	23	24
SiO ₂	34.73	36.71	35.27	34.40	34.27	35.58	36.06	35.18	34.14	34.38	35.17	33.60
TiO ₂	0.60	0.01	0.53	1.10	1.23	0.46	1.02	0.77	0.24	0.42	0.37	0.34
B ₂ O ₃	N.A.											
Al ₂ O ₃	33.41	32.15	32.27	33.57	30.41	34.44	31.77	34.39	34.54	33.85	34.11	35.07
FeO	13.71	8.83	9.92	8.48	10.78	6.96	5.62	8.78	13.68	15.01	11.10	11.59
MnO	0.03	0.00	0.04	0.20	0.00	0.00	0.11	0.11	0.01	0.15	0.02	0.04
MgO	2.09	5.52	5.60	5.75	5.94	5.64	8.29	4.90	1.47	0.92	3.73	3.18
CaO	0.28	0.32	0.80	1.30	1.24	0.43	2.20	0.32	0.11	0.18	0.13	0.07
Na ₂ O	1.09	2.33	1.52	1.16	2.06	2.29	0.86	1.40	1.69	1.06	1.32	2.02
K ₂ O	0.10	0.04	0.00	0.00	0.03	0.16	0.02	0.09	0.00	0.00	0.00	0.05
F	N.A.											
H ₂ O	N.A.											

N.A. = Not Analyzed

Table 3.5 Continued

Oxide	25	26	27	28	29	30	31	32	33	34	36	36
SiO ₂	35.69	33.47	36.61	36.78	35.27	34.17	33.63	33.63	34.55	34.66	34.96	35.4
TiO ₂	0.40	1.03	0.75	0.35	0.60	0.01	0.92	0.36	0.16	0.99	0.82	0.62
B ₂ O ₃	N.A.	N.A.										
Al ₂ O ₃	34.29	33.28	35.28	35.76	33.49	35.70	35.38	34.07	31.76	34.33	30.12	35.3
FeO	2.93	11.61	1.31	2.07	6.69	11.32	7.26	13.47	9.51	6.72	8.10	6.76
MnO	0.21	0.08	0.00	0.17	0.23	0.17	0.11	0.33	0.29	0.20	0.07	0.18
MgO	9.27	3.83	9.09	8.48	6.73	2.78	5.94	2.14	6.78	6.37	8.27	5.53
CaO	0.61	0.82	0.93	0.66	0.39	0.07	0.50	0.06	0.08	0.38	2.07	0.20
Na ₂ O	2.55	1.78	1.90	1.61	2.65	1.63	2.17	1.89	2.82	2.31	1.55	1.87
K ₂ O	0.01	0.06	0.08	0.01	0.00	0.05	0.05	0.00	0.02	0.00	0.01	0.03
F	N.A.	N.A.										
H ₂ O	N.A.	N.A.										

N.A. = Not Analyzed

Table 3.5 Continued

Oxide	37	38	39	40	41	42	43	44	45	46	47
SiO ₂	33.33	34.72	34.16	34.08	35.55	34.04	35.13	34.31	34.24	34.70	33.38
TiO ₂	0.55	0.28	0.33	0.52	0.00	0.25	0.33	0.72	1.39	1.01	0.55
B ₂ O ₃	N.A.										
Al ₂ O ₃	33.52	35.79	34.94	32.69	34.14	33.93	33.99	33.71	32.51	32.36	30.05
FeO	10.44	10.62	12.13	11.25	11.67	11.83	5.54	6.44	5.05	6.86	16.82
MnO	0.00	0.00	0.20	0.15	0.17	0.30	0.00	0.00	0.19	0.00	0.21
MgO	4.65	2.73	2.35	4.56	2.06	1.90	6.72	5.81	6.95	6.68	1.61
CaO	0.64	0.03	0.02	0.28	0.00	0.00	0.46	0.45	0.57	0.57	0.00
Na ₂ O	2.78	1.79	1.73	2.41	1.45	1.76	1.98	1.65	1.79	2.03	2.95
K ₂ O	0.05	0.00	0.10	0.02	0.00	0.00	0.00	0.00	0.00	0.00	0.00
F	N.A.										
H ₂ O	N.A.										

N.A. = Not Analyzed

Table 3.6 Muscovite analyses

Elements	(1)	(2)	(3)	(4)	(5)	(6)	(7)	(8)	(9)	(10)	(11)
SiO ₂	48.96	48.08	48.67	49.09	47.34	48.34	48.96	48.08	48.67	49.09	47.34
TiO ₂	0.88	0.92	1.24	0.98	0.91	0.64	0.88	0.92	1.24	0.98	0.91
Al ₂ O ₃	31.07	31.31	29.44	29.34	30.69	28.04	31.77	31.31	29.44	29.34	30.69
FeO(Tot.)	1.65	1.85	2.65	2.79	4.37	5.37	1.65	1.85	2.65	2.79	4.37
MnO	0.04	0.21	0.05	0.04	0.00	0.02	0.04	0.21	0.05	0.07	0.00
MgO	0.52	0.62	1.23	1.06	0.59	1.19	0.52	0.62	1.23	1.06	0.59
CaO	0.00	0.02	0.00	0.00	0.00	0.00	0.00	0.02	0.00	0.00	0.00
Na ₂ O	0.17	0.12	0.00	0.09	0.20	0.06	0.17	0.12	0.00	0.09	0.20
K ₂ O	11.54	11.28	11.93	11.83	10.53	11.87	10.54	11.28	11.93	11.21	10.77
F	N.A.										
H ₂ O	N.A.										
Total	94.83	94.41	95.10	95.22	94.63	95.53	94.53	94.41	95.21	94.63	94.87

N.A.= Not Analyzed

Table 3.6 Continued

Elements	(12)	(13)	(14)	(15)	(16)	(17)	(18)	(19)	(20)	(21)	(22)
SiO ₂	47.11	47.93	49.33	48.30	47.44	48.64	48.03	47.86	47.55	47.96	48.33
TiO ₂	0.77	0.75	0.45	1.07	0.73	0.86	0.11	0.88	0.97	0.81	0.94
Al ₂ O ₃	32.76	32.44	31.96	31.83	32.74	32.55	31.92	32.95	31.77	32.09	32.12
FeO(Tot.)	1.76	1.59	1.94	1.65	1.64	1.19	1.53	0.28	1.34	2.56	1.43
MnO	0.21	0.04	0.05	0.01	0.00	0.00	0.02	0.05	0.23	0.05	0.02
MgO	0.55	0.53	0.94	1.09	0.72	1.21	0.94	0.53	1.04	0.95	0.44
CaO	0.00	0.00	0.00	0.00	0.00	0.00	0.00	0.00	0.00	0.00	0.00
Na ₂ O	0.12	0.11	0.05	0.05	0.21	0.07	0.21	0.11	0.12	0.00	0.12
K ₂ O	11.35	11.54	11.17	10.53	10.98	10.95	11.59	11.96	11.74	10.95	10.95
F	N.A.										
H ₂ O	N.A.										
Total	94.63	94.90	95.89	94.53	94.46	95.47	94.35	94.62	94.76	95.40	94.35

N.A.= Not Analyzed

Table 3.6 continued

Elements	(23)	(24)	(25)	(26)	(27)	(28)	(30)	(A)	(B)	(C)	(D)
SiO ₂	47.95	48.53	49.80	49.88	47.65	48.03	49.01	45.24	48.42	45.72	47.39
TiO ₂	0.69	0.50	1.07	1.16	0.59	0.92	0.95	0.01	0.87	0.87	0.62
Al ₂ O ₃	31.40	32.80	31.29	31.45	32.80	33.30	31.73	36.85	27.16	32.43	36.70
FeO(Tot.)	1.91	1.52	1.73	1.47	1.61	1.10	1.45	0.19	7.38	3.92	0.99
MnO	0.09	0.19	0.00	0.07	0.07	0.05	0.00	0.12	0.00	0.04	0.00
MgO	0.19	0.35	1.11	0.83	0.49	0.30	0.89	0.08	trace.	0.73	0.52
CaO	0.00	0.05	0.02	0.00	0.00	0.02	0.03	0.00	trace.	0.04	0.01
Na ₂ O	0.08	0.06	0.26	0.29	0.05	0.07	0.09	0.64	0.35	0.58	1.56
K ₂ O	11.22	11.53	10.26	10.37	11.22	10.85	10.83	10.08	11.23	10.44	8.59
F	N.A.	0.91	trace.	0.36	0.03						
H ₂ O	N.A.	4.58	4.50	N.A.	4.60						
Total	94.53	95.53	94.54	94.76	94.38	94.44	94.98	98.70	99.91	95.43	101.01

N.A.= Not Analyzed

- (A) Rose-muscovite, pegmatite, New Mexico(Heinrich, E.W. & Levinson, A. A., Am. Min. 1953,38, p25)
 (B) Muscovite, Low grade psammitic schist, Inverness-shire (Lambert, r. st J., 1959, Trans. Roy. Soc. Edinburgh, 63, p553)
 (C) Plutonic Muscovite (Miller et al., 1981, Cana. Minera., 19, 25-34)
 (D) Sillimanite-muscovite schist (Pigage, 1982, Cana. Minera., 20, 349-378)

APPENDIX B

CONFIDENTIAL

Table 4.1 Chemical analysis (major & trace elements) of the Lower Saq Sandstone.

Sample No.	K-20-4	K-5-8	K-20-3	K-5-15	K-26-5	K-27-4	K-3-6	K-2-3	K-20-8	K-20-2	K-2-1	K-7-1
(Wt%)												
SiO ₂	83.04	93.75	87.96	97.37	92.47	86.10	75.93	80.14	89.98	83.46	95.72	97.44
TiO ₂	0.12	0.14	0.13	0.16	0.09	0.16	0.33	0.14	0.33	0.54	0.28	0.10
Al ₂ O ₃	5.10	3.69	5.33	1.59	2.72	3.48	4.31	1.69	5.82	4.62	3.38	1.29
Fe ₂ O ₃	1.54	0.45	1.09	0.61	0.20	0.52	1.96	2.70	0.18	1.13	0.07	0.09
FeO	0.10	0.11	0.10	0.09	0.03	0.13	0.36	0.51	0.00	0.02	0.02	0.00
MnO	0.02	0.04	0.04	0.02	0.01	0.00	0.02	0.02	0.03	0.00	0.04	0.01
MgO	0.22	0.13	0.07	0.13	0.00	0.00	0.00	0.00	0.13	0.19	0.05	0.00
CaO	5.56	1.07	0.60	0.19	0.19	1.86	7.87	6.67	1.50	5.15	0.51	0.45
Na ₂ O	0.01	0.00	0.00	0.00	0.59	0.55	0.22	0.00	0.00	0.02	0.17	0.00
K ₂ O	0.00	0.00	0.00	0.00	0.05	0.06	0.03	0.00	0.00	0.00	0.00	0.00
P ₂ O ₅	0.22	0.09	0.26	0.03	0.10	0.07	0.08	0.00	0.16	0.21	0.05	0.02
H ₂ O	1.98	0.37	3.64	0.23	3.43	5.35	2.19	3.10	0.92	1.67	0.59	0.43
CO ₂	3.13	0.48	0.50	0.09	0.09	1.67	6.11	5.95	0.88	3.83	0.43	0.07
Total	101.04	100.32	99.72	100.51	99.97	99.95	99.41	100.92	99.93	100.84	101.31	99.90
Fe* 2O ₃	1.65	0.57	1.20	0.71	0.23	0.66	2.36	3.27	0.18	1.15	0.09	0.09
(ppm)												
Co	2	nd	nd	nd	nd	nd	1	2	nd	3	nd	nd
Cr	10	13	11	39	6	22	74	108	9	20	25	8
Ce	23	23	27	11	65	24	44	66	44	80	39	24
Ba	80	336	161	28	24	18	133	443	85	53	156	26
La	10	12	6	4	37	8	24	67	18	46	16	7
Zr	117	61	123	53	93	46	125	172	171	256	165	70
Y	9	17	10	5	9	4	13	35	16	42	16	6
Sr	430	151	350	27	229	38	146	392	220	335	171	56
U	1	2	2	1	1	1	2	3	2	2	2	2
Rb	1	0	1	0	0	0	1	53	1	1	1	0
Th	0	0	0	1	0	0	5	15	5	18	2	1
Pb	12	8	17	3	6	5	5	57	3	6	11	5
Ca	7	5	8	2	2	2	3	26	6	6	3	2
Zn	12	26	19	10	5	6	7	30	6	10	7	6
Cu	11	1	3	5	nd	2	2	23	1	3	nd	nd
Ni	4	nd	0	1	nd	nd	2	20	nd	1	nd	nd

nd: Not detected

Table 4.1 Continued

Sample No.	K-2-2	K-5-13	K-7-5	K-3-2	K-7-4	K-4-1	K-7-8	K-20-6	K-5-14	K-20-5	K-27-3	K-26-7
(Wt%)												
SiO ₂	86.13	97.43	94.52	84.85	98.03	93.00	91.53	90.62	96.18	90.38	86.46	81.03
TiO ₂	0.35	0.25	0.46	0.25	0.19	0.31	0.18	0.11	0.21	0.65	0.61	0.54
Al ₂ O ₃	7.68	2.41	2.88	2.69	1.20	3.15	5.83	1.84	3.14	3.73	7.13	7.94
Fe ₂ O ₃	1.46	0.11	0.13	0.84	0.07	0.36	0.14	0.45	0.12	1.19	1.27	5.06
FeO	0.11	0.00	0.00	0.10	0.00	0.03	0.08	0.09	0.00	0.13	0.15	0.81
MnO	0.05	0.04	0.05	0.04	0.04	0.04	0.05	0.06	0.04	0.01	0.02	0.01
MgO	0.31	0.09	0.07	0.25	0.07	0.20	0.15	0.13	0.13	0.17	0.00	0.08
CaO	1.31	0.13	0.26	5.28	0.45	1.84	0.60	4.93	0.53	1.73	0.52	0.20
Na ₂ O	0.02	0.00	0.00	0.02	0.00	0.00	0.03	0.03	0.00	0.04	0.18	0.08
K ₂ O	0.14	0.00	0.00	0.00	0.00	0.00	0.01	0.00	0.00	0.00	0.03	0.12
P ₂ O ₅	0.06	0.04	0.03	0.68	0.01	0.05	0.08	0.12	0.07	0.41	0.19	0.41
H ₂ O	0.93	0.13	1.12	1.56	0.11	0.90	1.30	3.98	0.39	1.59	3.73	1.10
CO ₂	0.70	0.00	0.06	3.95	0.43	1.32	0.50	0.75	0.15	0.63	0.59	0.13
Total	99.22	100.63	99.58	100.51	100.60	101.20	100.48	98.93	100.96	100.66	100.88	100.51
Fe* ₂ O ₃	1.58	0.11	0.13	0.95	0.07	0.39	0.23	3.93	0.12	1.33	1.44	5.96
(ppm)												
Co	2	nd	nd	nd	nd	nd	nd	8	nd	1	nd	2
Cr	109	3	18	6	10	15	11	12	6	24	19	8
Ce	41	29	54	57	27	22	31	71	27	40	23	33
Ba	234	68	47	42	23	54	310	701	91	72	77	84
La	16	15	23	11	12	10	13	74	13	19	9	7
Zr	147	88	250	726	114	95	97	589	82	242	49	276
Y	15	11	18	9	9	8	11	97	9	15	4	13
Sr	153	72	98	139	49	75	206	310	93	318	39	53
U	2	3	3	nd	2	2	3	4	2	3	2	0
Rb	6	1	1	nd	1	1	1	4	0	1	0	nd
Th	2	1	6	nd	3	3	3	12	3	16	5	10
Pb	12	8	8	4	5	21	25	7	13	5	7	5
Ca	9	2	3	7	1	3	6	23	2	3	4	1
Zn	34	5	5	11	8	17	10	91	4	24	7	nd
Cu	33	nd	0	15	nd	3	nd	41	nd	3	1	nd
Ni	0	nd	nd	3	nd	0	nd	20	nd	4	nd	1

nd: Not detected

Table 4.1 Continued

Sample No.	K-4-2	K-5-5	K-7-7	K-20-7	K-4-3	K-5-12	K-5-11	K-5-3	K-5-6	K-20-1	K-7-10	K-7-6
(Wt%)												
SiO ₂	93.33	94.64	95.19	90.43	94.28	96.33	95.62	90.77	91.98	80.33	94.27	97.89
TiO ₂	0.47	0.14	0.18	0.08	0.23	0.15	0.23	0.32	0.18	0.43	0.25	0.12
Al ₂ O ₃	2.80	2.42	2.35	2.38	2.26	0.29	1.58	3.37	2.45	3.74	3.99	1.46
Fe ₂ O ₃	1.94	0.97	0.09	1.05	2.13	0.05	2.25	1.95	1.03	0.24	0.19	0.10
FeO	0.15	0.06	0.00	0.00	0.21	0.00	0.10	0.16	0.09	0.00	0.00	0.01
MnO	0.06	0.07	0.05	0.03	0.05	0.05	0.07	0.04	0.03	0.04	0.02	0.05
MgO	0.09	0.11	0.17	0.15	0.11	0.18	0.14	0.11	0.17	0.25	0.23	0.06
CaO	0.66	0.55	1.27	2.74	0.33	1.13	0.72	1.46	1.29	8.86	0.94	0.27
Na ₂ O	0.00	0.00	0.08	0.00	0.00	0.00	0.00	0.00	0.14	0.04	0.00	0.00
K ₂ O	0.00	0.00	0.00	0.00	0.00	0.00	0.00	0.00	0.00	0.01	0.01	0.00
P ₂ O ₅	0.07	0.07	0.04	0.15	0.11	0.04	0.11	0.05	0.07	0.08	0.03	0.02
H ₂ O	0.53	0.81	0.93	0.97	0.89	0.48	0.35	0.87	0.92	0.91	0.75	0.31
CO ₂	0.39	0.31	0.87	2.19	0.11	0.61	0.33	1.17	0.88	6.03	0.27	0.18
Total	100.49	100.15	101.22	100.17	100.71	99.31	101.50	100.27	99.23	100.96	100.95	100.47
Fe* 2O ₃	2.11	1.04	0.09	1.05	2.36	0.05	2.36	2.13	1.13	0.24	0.19	0.11
(ppm)												
Co	1	nd	nd	nd	1	nd	2	2	nd	nd	nd	nd
Cr	16	10	18	10	9	7	12	28	20	18	31	17
Ce	44	16	28	15	30	24	12	28	23	54	37	23
Ba	23	114	54	101	26	82	35	148	148	67	64	29
La	22	3	12	6	14	10	4	16	12	31	16	9
Zr	115	65	141	70	93	64	83	127	75	163	125	68
Y	13	9	8	10	10	6	6	12	11	12	11	7
Sr	122	100	54	241	76	67	49	176,	121	184	83	44
U	2	3	2	2	2	2	3	2	3	2	2	2
Rb	0	0	2	1	1	1	1	0	1	2	1	0
Th	4	2	2	1	1	3	4	6	3	3	3	nd
Pb	2	12	5	3	3	8	17	29	6	9	9	5
Ca	3	3	3	4	2	2	3	4	4	3	4	2
Zn	14	17	9	14	60	13	71	11	26	6	12	5
Cu	0	2	1	0	7	nd	15	2	3	4	0	nd
Ni	1	0	nd	nd	6	nd	7	1	nd	0	nd	nd

nd: Not detected

Table 4.1 Continued

Sample No.	K-7-9	K-7-2	K-26-4	K-5-2	K-2-4	K-5-9	K-20-10	K-5-10	K-20-9	K-5-1	K-20-11	K-3-5
(Wt%)												
SiO ₂	83.26	94.04	94.17	96.16	79.83	92.75	91.47	92.31	93.03	80.56	98.49	83.99
TiO ₂	0.60	0.28	0.19	0.10	0.14	0.35	0.06	0.23	0.10	0.63	0.04	0.13
Al ₂ O ₃	10.59	2.90	4.44	2.24	7.03	3.94	1.64	4.22	1.17	9.43	0.71	0.96
Fe ₂ O ₃	1.76	0.15	0.16	1.52	2.12	0.40	0.49	0.18	2.02	2.96	0.24	2.39
FeO	0.12	0.00	0.00	0.03	0.21	0.18	0.00	0.03	0.15	0.31	0.00	0.20
MnO	0.06	0.00	0.03	0.03	0.04	0.02	0.03	0.01	0.03	.040	0.00	0.07
MgO	0.09	0.11	0.17	0.21	0.00	0.00	0.00	0.00	0.00	0.00	0.00	0.13
CaO	0.14	1.95	0.19	0.92	3.78	0.34	2.45	0.49	0.72	0.46	0.37	5.69
Na ₂ O	0.00	0.00	0.00	0.08	0.61	0.05	0.00	0.00	0.19	0.16	0.22	0.17
K ₂ O	0.15	0.00	0.00	0.00	0.09	0.01	0.00	0.01	0.00	0.06	0.01	0.08
P ₂ O ₅	0.08	0.03	0.06	0.13	0.11	0.07	0.14	0.05	0.17	0.20	0.08	0.04
H ₂ O	3.82	0.74	0.71	0.19	2.68	2.31	0.79	1.56	0.93	4.27	0.14	1.91
CO ₂	0.10	1.02	0.15	0.37	2.80	0.11	2.39	0.22	0.58	0.17	0.40	4.75
Total	100.77	101.22	100.27	101.98	99.44	100.53	99.46	99.37	99.09	99.25	100.70	100.51
Fe* ₂ O ₃	1.89	0.15	0.16	1.55	2.3	0.60	0.49	0.21	2.19	3.30	0.24	3.61
(ppm)												
Co	2	1	nd	nd	1	nd	nd	nd	nd	3	nd	nd
Cr	29	26	5	4	13	13	27	4	5	34	31	4
Ce	71	31	34	22	25	43	9	27	10	82	12	21
Ba	155	85	166	371	167	160	63	104	60	411	60	73
La	27	9	11	9	9	17	3	9	0	34	0	8
Zr	320	197	84	58	74	139	43	87	59	269	39	60
Y	31	16	10	12	10	23	13	17	11	31	8	6
Sr	120	66	120	179	123	153	125	117	69	348	73	56
U	4	2	2	2	1	2	2	2	1	3	1	2
Rb	6	1	2	0	2	1	0	1	0	1	0	1
Th	12	7	4	0	0	6	nd	2	1	12	0	1
Pb	22	23	3	15	12	13	4	8	7	52	2	6
Ga	10	5	5	3	6	3	2	5	3	9	0	3
Zn	87	6	6	14	23	15	10	5	26	22	5	7
Cu	11	nd	nd	1	7	2	0	1	3	56	1	0
Ni	13	nd	nd	nd	2	nd	2	nd	1	2	nd	nd

nd: Not detected

Table 4.1 Continued

Sample No.	K-3-3	K-3-4	K-5-4	K-5-7	K-20-12	K-7-11	K-26-6
(Wt%)							
SiO ₂	89.74	84.70	93.59	91.69	96.27	80.06	97.12
TiO ₂	0.22	0.38	0.49	0.12	0.09	0.50	0.09
Al ₂ O ₃	2.86	4.87	2.33	4.39	1.42	9.93	1.21
Fe ₂ O ₃	0.69	3.88	1.11	1.42	0.47	3.48	0.05
FeO	0.04	0.19	0.10	0.17	0.02	0.21	0.00
MnO	0.00	0.02	0.02	0.04	0.02	0.04	0.06
MgO	0.00	0.00	0.0	0.17	0.11	0.19	0.08
CaO	2.31	2.30	1.19	0.63	0.42	1.25	0.26
Na ₂ O	0.41	0.18	0.09	0.01	0.05	0.09	0.17
K ₂ O	0.03	0.01	0.00	0.00	0.00	0.18	0.10
P ₂ O ₅	0.07	0.07	0.10	0.07	0.48	0.08	0.07
H ₂ O	1.38	1.84	0.75	1.68	0.91	3.33	0.39
CO ₂	1.97	1.78	0.93	0.46	0.09	0.89	0.25
Total	99.76	100.22	100.70	100.85	100.35	100.23	99.85
Fe* ₂ O ₃	0.73	4.09	1.22	1.61	0.49	3.71	0.05
(ppm)							
Co	nd	4	nd	nd	nd	2	nd
Cr	7	22	34	12	14	31	23
Ce	60	43	73	26	11	47	43
Ba	68	30	212	76	115	188	210
La	12	16	29	10	2	17	11
Zr	688	151	372	67	76	221	236
Y	7	14	29	12	20	22	13
Sr	198	61	181	106	270	101	68
U	nd	2	3	3	2	2	0
Rb	nd	1	nd	0	0	8	0
Th	nd	4	21	0	1	6	12
Pb	5	7	14	13	3	22	4
Ga	8	5	3	5	2	10	2
Zn	14	10	19	20	9	21	nd
Cu	18	6	4	2	1	5	nd
Ni	4	6	3	nd	0	2	nd

nd: Not detected

Table 4.2 Chemical analysis (major & trace elements) of the Middle Saq Sandstone

Sample No.	K-14-1	K-14-3	K-38-2	K-18--3	K-19--2	K-28--2	K-38-6	K-38-5	K-18-4	K-17-4	K-19-1	K-15-5
(Wt%)												
SiO ₂	92.69	98.30	85.58	97.49	95.30	90.17	94.84	95.37	97.64	87.69	95.83	92.07
TiO ₂	0.68	0.27	0.28	0.06	0.09	0.94	0.12	0.24	0.15	0.57	0.15	0.07
Al ₂ O ₃	4.34	0.98	8.11	0.88	1.88	4.39	2.19	2.15	0.46	5.93	1.52	0.92
Fe ₂ O ₃	0.17	0.13	0.44	0.15	0.17	1.67	0.13	0.31	0.16	0.47	0.16	0.70
FeO	0.08	0.03	0.09	0.00	0.02	0.07	0.00	0.09	0.00	0.10	0.02	0.14
MnO	0.02	0.03	0.01	0.06	0.01	0.01	0.00	0.01	0.01	0.03	0.01	0.04
MgO	0.09	0.13	0.32	0.15	0.17	0.00	0.00	0.00	0.00	0.00	0.00	0.00
CaO	0.84	0.50	1.68	0.72	0.87	0.32	0.95	0.69	0.23	1.65	0.00	1.94
Na ₂ O	0.00	0.00	0.00	0.00	0.16	0.14	0.18	0.03	0.00	0.06	0.17	0.44
K ₂ O	0.01	0.00	0.01	0.00	0.01	0.11	0.02	0.02	0.00	0.12	0.01	0.01
P ₂ O ₅	0.07	0.03	0.03	0.02	0.03	0.15	0.02	0.03	0.02	0.05	0.03	0.05
H ₂ O	1.20	0.06	2.23	0.46	0.82	2.31	1.33	0.79	0.45	1.50	1.53	2.99
CO ₂	0.49	0.07	1.48	0.34	0.84	0.14	0.77	0.37	0.11	1.42	0.00	1.49
Total	100.68	100.53	100.26	100.33	100.37	100.42	100.55	100.10	99.23	99.59	99.66	100.86
Fe ²⁺ O	0.26	0.16	0.54	0.15	0.19	1.75	0.13	0.41	0.16	0.58	0.18	0.86
(ppm)												
Co	nd	nd	nd	nd	nd	nd	nd	nd	nd	0	nd	nd
Cr	28	10	24	11	11	49	10	19	8	27	19	44
Ce	84	23	31	22	24	78	20	29	28	67	24	35
Ba	58	53	47	62	66	157	25	31	19	147	25	43
La	41	12	12	6	12	54	10	10	12	22	6	10
Zr	434	151	176	43	55	453	73	126	128	384	75	63
Y	28	9	13	5	7	48	10	10	7	25	9	8
Sr	140	51	102	29	56	235	42	55	34	72	50	92
U	3	2	3	2	1	5	1	2	1	3	3	2
Rb	1	0	1	1	0	4	0	1	0	4	0	1
Th	13	2	4	nd	nd	21	nd	3	3	8	0	1
Pb	33	21	17	7	7	16	7	8	5	16	5	15
Ga	4	0	8	1	1	20	2	2	2	5	2	1
Zn	7	7	19	6	6	9	5	6	4	23	6	17
Cu	nd	0	4	nd	73	4	nd	2	nd	46	34	4
Ni	nd	nd	5	nd	nd	2	nd	nd	nd	7	nd	2

nd: Not detected

Table 4.2 Continued

Sample No.	K-38-7	K-28-4	K-15-1	K-17-2	K-17-1	K-28-3	K-15-6	K-38-1	K-17-3	K-38-4	K-28-1	K-18-5
(Wt%)												
SiO ₂	94.29	94.47	87.31	97.79	97.39	94.47	92.21	92.75	97.65	95.80	96.34	95.03
TiO ₂	0.17	0.09	0.28	0.08	0.16	0.48	0.05	0.21	0.31	0.33	0.24	0.13
Al ₂ O ₃	1.64	2.09	1.96	0.92	1.56	4.95	0.83	4.44	1.33	2.41	2.54	1.57
Fe ₂ O ₃	0.20	0.20	0.20	0.05	0.09	0.91	5.55	0.11	0.09	0.12	0.12	0.61
FeO	0.04	0.06	0.01	0.00	0.00	0.04	0.15	0.01	0.02	0.00	0.08	0.80
MnO	0.01	0.02	0.04	0.02	0.05	0.04	0.01	0.03	0.00	0.05	0.02	0.05
MgO	0.00	0.00	0.07	0.03	0.09	0.19	0.19	0.07	0.00	0.13	0.21	0.13
CaO	2.09	0.43	5.80	1.21	1.07	0.67	0.96	1.38	0.59	0.80	0.36	0.64
Na ₂ O	0.00	0.08	0.00	0.00	0.00	0.00	0.00	0.01	0.00	0.00	0.00	0.00
K ₂ O	0.00	0.00	0.00	0.00	0.00	0.00	0.00	0.01	0.00	0.00	0.00	0.00
P ₂ O ₅	0.03	0.03	0.06	0.02	0.03	0.08	0.13	0.04	0.02	0.03	0.03	0.03
H ₂ O	0.69	1.64	0.31	0.32	0.79	0.09	0.74	0.25	0.69	0.65	0.35	0.47
CO ₂	1.73	0.37	4.69	0.88	0.03	0.21	0.60	0.45	0.15	0.69	0.17	0.59
Total	100.89	99.48	100.73	101.32	101.76	102.13	101.42	99.75	100.85	101.01	100.46	100.05
Fe* ₂ O ₃	0.24	0.27	0.21	0.05	0.09	0.95	5.72	0.12	0.11	0.12	0.21	1.50
(ppm)												
Co	nd	nd	nd	nd	nd	nd	19	nd	nd	nd	nd	nd
Cr	5	4	46	12	16	15	18	16	13	28	17	13
Ce	22	21	87	25	27	51	14	20	26	30	42	30
Ba	26	22	82	4	27	55	24	28	36	89	28	51
La	7	4	35	3	9	20	2	12	10	15	16	13
Zr	69	54	939	55	97	182	41	69	171	199	150	87
Y	8	7	37	8	11	23	8	8	12	11	6	9
Sr	54	82	199	47	50	225	34	42	46	74	69	47
U	1	2	4	3	1	4	4	2	2	2	2	3
Rb	0	0	1	1	0	1	1	1	0	1	1	1
Th	1	0	43	1	1	6	0	0	5	4	2	1
Pb	5	5	25	7	9	6	6	6	10	7	7	5
Ga	1	3	2	0	2	4	1	1	1	2	2	2
Zn	6	8	8	5	6	11	92	5	5	7	4	31
Cu	nd	0	3	0	41	0	13	0	nd	6	nd	4
Ni	1	0	nd	nd	nd	3	36	nd	nd	nd	nd	1

nd: Not detected

Table 4.2 Continued

Sample No.	K-16-6	K-16-2	K-18-1	K-14-2	K-16-5	K-16-1	K-16-3	K-17-6	K-38-3	K-15-3	K-15-4	K-16-4
(WT%)												
SiO ₂	96.93	97.57	98.70	98.56	97.05	98.65	98.06	88.43	85.87	96.88	97.86	97.97
TiO ₂	0.11	0.04	0.04	0.06	0.09	0.24	0.07	0.42	0.15	0.06	0.08	0.09
Al ₂ O ₃	1.12	0.67	0.93	0.98	0.89	0.99	0.81	6.15	8.85	1.21	1.94	1.10
Fe ₂ O ₃	0.37	0.10	0.09	0.10	0.14	0.16	0.15	1.85	0.22	0.13	0.13	0.11
FeO	0.12	0.00	0.00	0.01	0.02	0.00	0.03	0.12	0.08	0.03	0.01	0.00
MnO	0.01	0.01	0.01	0.02	0.02	0.03	0.02	0.09	0.05	0.03	0.02	0.02
MgO	0.00	0.00	0.13	0.11	0.11	0.07	0.11	0.22	0.11	0.15	0.17	0.13
CaO	0.27	0.08	0.14	0.03	0.53	0.04	0.35	1.30	1.96	1.44	0.13	0.75
Na ₂ O	0.09	0.00	0.00	0.09	0.00	0.00	0.00	0.00	0.03	0.05	0.10	0.37
K ₂ O	0.00	0.00	0.00	0.00	0.00	0.00	0.00	0.12	0.05	0.00	0.00	0.01
P ₂ O ₅	0.39	0.02	0.01	0.02	0.03	0.02	0.01	0.08	0.03	0.03	-0.03	0.02
H ₂ O	0.33	1.59	0.35	0.77	0.34	0.18	0.22	1.49	0.85	0.99	0.31	0.11
CO ₂	0.13	0.00	0.08	0.02	0.06	0.04	0.19	0.93	1.57	0.55	0.10	0.55
Total	99.87	100.08	100.48	100.77	99.28	100.42	100.02	99.71	99.79	101.55	100.88	101.23
Fe* 2O ₃	0.50	0.10	0.09	0.11	0.16	0.16	0.18	1.98	0.28	0.16	0.14	0.11
(ppm)												
Co	nd	5	nd	nd	nd	nd						
Cr	8	23	13	31	4	16	17	15	19	18	19	5
Ce	20	23	25	22	23	21	22	50	25	31	29	24
Ba	278	26	22	13	18	35	15	93	83	24	23	21
La	5	7	7	5	6	6	9	15	9	15	6	3
Zr	81	44	58	40	55	102	47	298	74	51	55	54
Y	8	5	4	6	7	9	6	17	9	6	9	6
Sr	99	25	25	35	34	35	33	112	64	83	52	33
U	2	2	2	1	2	2	2	2	2	2	1	0
Rb	0	1	1	0	1	1	1	6	4	0	0	nd
Th	nd	nd	0	1	1	1	0	6	1	nd	nd	nd
Pb	6	9	7	15	15	20	14	22	27	12	10	15
Ga	2	1	2	1	1	1	1	6	8	1	21	0
Zn	18	6	6	5	5	7	6	61	13	5	6	6
Cu	9	nd	nd	2	nd	nd	0	29	5	nd	0	nd
Ni	1	nd	nd	nd	nd	nd	nd	18	3	nd	nd	nd

nd: Not detected

Table 4.2 Continued

Sample No.	K-14-5	K-18-2	K-19-3	K-19-4	K-19-5	K-36-1	K-36-2	K-36-3	K-36-4	K-36-8	K-37-2	K-37-1
(Wt%)												
SiO ₂	97.11	95.52	90.29	85.30	85.03	94.32	91.03	97.06	96.05	98.54	91.65	95.64
TiO ₂	0.14	0.48	0.46	0.62	0.62	0.30	0.32	0.09	0.41	0.15	0.29	0.52
Al ₂ O ₃	1.49	0.91	5.79	6.84	6.56	1.01	6.52	0.35	1.09	0.79	1.50	2.38
Fe ₂ O ₃	0.11	0.07	0.10	0.22	0.27	0.02	0.12	0.06	0.15	0.04	0.07	0.10
FeO	0.00	0.01	0.09	0.07	0.03	0.00	0.00	0.00	0.00	0.00	0.00	0.00
MnO	0.04	0.06	0.04	0.01	0.01	0.02	0.01	0.00	0.00	0.03	0.00	0.01
MgO	0.09	0.13	0.00	0.00	0.00	0.05	0.09	0.10	0.08	0.18	0.16	0.10
CaO	0.33	1.21	1.06	1.10	1.06	2.08	0.27	0.37	0.73	0.00	2.26	0.44
Na ₂ O	0.02	0.00	0.00	0.35	0.40	0.15	0.11	0.00	0.50	0.14	0.24	0.21
K ₂ O	0.00	0.00	0.02	0.06	0.10	0.09	0.11	0.09	0.14	0.08	0.10	0.10
P ₂ O ₅	0.46	0.02	0.04	0.11	0.06	0.03	0.04	0.20	0.06	0.02	0.06	0.05
H ₂ O	0.32	0.87	2.46	3.97	4.35	1.52	1.11	1.31	0.34	0.06	1.95	0.24
CO ₂	0.21	1.07	0.86	1.07	0.95	0.91	0.25	0.16	0.15	0.00	1.72	0.30
Total	100.95	100.35	101.21	99.72	99.44	100.50	99.98	99.79	99.70	100.03	100.00	100.09
Fe* 2O ₃	0.12	0.08	0.20	0.30	0.30	0.02	0.12	0.06	0.15	0.04	0.07	0.10
(ppm)												
Co	nd	nd	nd	nd	6	70	1	0	nd	nd	nd	nd
Cr	17	20	15	17	53	25	38	40	41	51	20	46
Ce	22	28	51	76	54	57	25	31	29	34	25	30
Ba	54	27	81	172	81	860	47	81	326	142	39	41
La	7	7	18	32	22	26	12	16	12	11	14	18
Zr	85	250	291	552	622	638	242	226	65	362	119	271
Y	10	9	16	30	26	19	12	16	9	15	12	16
Sr	58	40	73	114	86	134	51	64	81	104	42	57
U	1	2	2	3	4	0	nd	nd	nd	nd	nd	nd
Rb	0	0	2	3	19	74	0	1	0	0	0	0
Th	1	4	6	18	13	13	4	6	3	8	5	8
Pb	31	8	19	16	9	12	0	9	10	2	7	3
Ga	1	0	6	5	13	2	2	7	1	0	0	1
Zn	8	6	12	14	56	95	nd	nd	0	nd	nd	nd
Cu	3	0	16	40	30	3	nd	nd	4	nd	nd	0
Ni	0	0	0	0	11	44	2	1	0	2	1	0

nd: Not detected

Table 4.2 Continued

Sample No.	K-39-1	K-36-6	K-36-7	K-36-5
(Wt%)				
SiO ₂	96.51	96.95	92.51	95.16
TiO ₂	0.07	0.11	0.32	0.33
Al ₂ O ₃	0.78	0.25	2.03	0.87
Fe ₂ O ₃	1.09	0.11	0.08	0.02
FeO	0.15	0.00	0.00	0.00
MnO	0.00	0.05	0.00	0.00
MgO	0.21	0.02	0.05	0.07
CaO	0.35	0.73	1.18	1.96*
Na ₂ O	0.19	0.00	0.45	0.01
K ₂ O	0.10	0.08	0.09	0.08
P ₂ O ₅	0.04	0.03	0.03	0.04
H ₂ O	0.31	0.42	0.80	1.37
CO ₂	0.11	0.42	0.91	0.35
Total	99.91	99.17	98.45	100.26
Fe* ₂ O ₃	1.26	0.11	0.00	0.02
(ppm)				
Co	nd	nd	0	1
Cr	24	20	14	11
Ce	36	45	23	33
Ba	90	75	83	88
La	14	12	11	9
Zr	195	235	89	90
Y	45	24	11	20
Sr	129	118	62	69
U	1	6	0	3
Rb	2	2	0	1
Th	10	17	7	9
Pb	6	3	5	2
Ga	2	9	0	0
Zn	3	56	nd	nd
Cu	nd	15	nd	nd
Ni	nd	15	1	2

nd: Not detected

Table 4.3 Continued

Sample No.	K-40-4	K-25-4	K-40-5	K-30--2	K-40--1	K-30--4	K-25--6	K-40-6	K-40-2	K-40-9	K-30-5	K-30-3
(Wt%)												
SiO ₂	95.98	91.25	93.33	95.20	96.29	90.16	93.47	95.68	93.35	91.54	86.69	91.84
TiO ₂	0.46	0.24	0.75	0.60	0.25	0.72	0.30	0.37	0.56	0.81	0.41	0.83
Al ₂ O ₃	2.89	2.47	2.88	3.09	2.18	2.80	2.15	2.79	2.91	4.63	1.85	2.46
Fe ₂ O ₃	0.31	0.36	0.24	0.63	0.24	1.45	0.23	0.65	0.10	0.70	2.45	0.78
FeO	0.02	0.00	0.04	0.05	0.00	0.13	0.00	0.12	0.06	0.03	0.15	0.09
MnO	0.01	0.00	0.01	0.02	0.03	0.02	0.02	0.03	0.04	0.02	0.03	0.01
MgO	0.00	0.00	0.00	0.21	0.11	0.13	0.24	0.09	0.11	0.18	0.00	0.00
CaO	0.00	1.89	0.91	0.20	0.06	0.78	2.34	0.19	0.82	1.12	2.55	0.83
Na ₂ O	0.02	0.19	0.04	0.09	0.14	0.05	0.01	0.22	0.09	0.00	0.10	0.09
K ₂ O	1.27	0.06	1.34	0.78	0.80	0.90	0.00	1.10	1.46	1.57	0.67	0.61
P ₂ O ₅	0.08	0.05	0.04	0.06	0.03	0.06	0.05	0.03	0.03	0.05	0.47	0.00
H ₂ O	0.00	0.96	0.00	0.37	0.08	2.67	0.49	0.11	0.14	0.37	2.44	0.80
CO ₂	0.00	1.48	0.66	0.13	0.00	0.77	1.79	0.07	0.21	0.63	0.51	0.86
Total	101.05	98.95	100.24	101.43	100.21	100.64	101.09	101.45	99.88	101.65	98.32	99.20
Fe* ₂ O ₃	0.33	0.36	0.28	0.69	0.24	1.59	0.23	0.78	0.17	0.73	2.62	0.88
(ppm)												
Co	nd	nd	nd	5	nd	2	nd	2	nd	3	7	14
Cr	38	21	23	24	25	23	28	20	21	27	21	33
Ce	40	27	53	63	31	67	34	32	41	71	25	66
Ba	373	57	426	245	242	352	45	302	436	705	259	219
La	13	10	21	22	12	25	11	13	18	26	43	24
Zr	276	92	570	607	142	857	189	239	383	781	646	774
Y	9	11	15	64	5	32	9	8	11	24	44	82
Sr	77	63	88	76	56	109	75	65	85	140	213	84
U	2	2	2	3	2	4	1	1	2	3	5	4
Rb	31	1	33	21	22	25	1	27	35	60	9	16
Th	3	2	9	11	1	10	3	2	6	17	19	14
Pb	10	17	10	12	8	21	40	10	12	14	52	14
Ga	4	3	3	3	3	3	1	3	2	2	2	2
Zn	13	7	14	27	15	73	6	26	14	5	6	4
Cu	0	nd	6	4	0	10	0	70	0	0	2	0
Ni	nd	nd	4	10	1	18	0	6	0	0	0	0

nd: Not detected

Table 4.3 Continued

Sample No.	K-21--6	K-22-1	K-22-3	K-22-5	K-22-2	K-23-1	K-23-2	K-23-3	K-41-1	K-41-2	K-41-3	K-41-4
(Wt%)												
SiO ₂	91.33	92.88	87.57	91.77	92.34	96.98	88.70	90.41	97.03	97.19	96.74	92.44
TiO ₂	0.60	0.25	0.44	0.35	0.44	0.31	0.18	0.56	0.11	0.18	0.27	0.08
Al ₂ O ₃	3.04	4.83	3.71	2.79	3.98	1.65	2.22	4.52	0.55	1.79	1.01	0.54
Fe ₂ O ₃	1.37	0.26	1.91	1.26	0.45	0.14	1.08	0.28	0.02	0.11	0.61	1.67
FeO	0.01	0.00	0.10	0.21	0.00	0.00	0.10	0.10	0.00	0.00	0.05	0.15
MnO	0.01	0.01	0.02	0.01	0.02	0.00	0.04	0.21	0.02	0.04	0.02	0.07
MgO	0.00	0.08	0.08	0.15	0.12	0.13	0.11	0.21	0.02	0.16	0.20	0.16
CaO	0.51	0.25	1.27	0.98	0.99	0.00	2.32	1.03	0.18	0.17	0.22	1.49
Na ₂ O	0.31	0.15	0.11	0.17	0.13	0.01	0.36	0.36	0.00	0.00	0.04	0.11
K ₂ O	0.00	1.07	1.15	0.98	0.60	0.93	1.20	1.47	0.08	0.14	0.15	0.10
P ₂ O ₅	0.19	0.08	0.12	0.51	0.50	0.03	0.05	0.04	0.02	0.03	0.05	0.07
H ₂ O	2.31	0.78	1.85	0.52	0.25	0.08	1.89	0.84	1.72	0.22	0.14	1.78
CO ₂	0.46	0.24	1.02	0.79	0.50	0.00	1.24	0.22	0.10	0.12	0.14	1.32
Total	99.14	100.87	99.23	100.28	100.32	100.26	99.49	100.25	99.85	100.15	99.64	99.95
Fe* ₂ O ₃	1.38	0.26	2.02	1.49	0.45	0.14	1.19	0.39	0.02	0.11	0.67	1.84
(ppm)												
Co	1	nd	nd	nd	nd	4	nd	5	nd	nd	nd	1
Cr	9	7	16	74	46	25	84	18	14	19	32	9
Ce	16	55	46	51	31	52	27	26	19	32	24	16
Ba	83	55	380	388	305	183	271	348	37	43	35	83
La	3	35	19	23	16	24	12	9	4	9	7	3
Zr	49	78	160	792	358	507	218	140	148	49	172	150
Y	5	8	38	20	11	17	9	9	9	5	7	8
Sr	40	54	102	87	104	61	57	74	51	45	43	40
U	2	2	nd	nd	nd	nd	nd	nd	2	2	1	2
Rb	1	0	25	27	23	14	20	26	2	1	2	3
Th	0	8	nd	7	2	8	2	nd	1	nd	3	2
Pb	8	4	12	59	9	23	3	4	8	8	9	42
Ga	2	1	7	5	3	4	2	2	1	2	2	2
Zn	42	nd	4	26	13	21	2	35	7	42	10	6
Cu	29	nd	nd	17	5	3	10	5	3	29	1	9
Ni	19	3	4	9	1	4	2	17	nd	18	3	nd

nd: Not detected

Table 4.3 Continued

Sample No.	K-41-5	K-42-1	K-42-2	K-42-3	K-42-4	K-42-5
(WT%)						
SiO ₂	96.04	97.41	90.10	89.71	92.86	89.48
TiO ₂	0.49	0.42	0.23	0.23	0.23	0.15
Al ₂ O ₃	0.73	0.91	3.68	5.34	1.61	0.94
Fe ₂ O ₃	0.69	0.19	0.41	0.68	0.34	0.99
FeO	0.10	0.00	0.05	0.15	0.00	0.10
MnO	0.02	0.01	0.02	0.01	0.01	0.00
MgO	0.16	0.26	0.04	0.10	0.08	0.19
CaO	0.91	0.65	1.89	1.46	1.52	3.75
Na ₂ O	0.32	0.00	0.19	0.35	0.14	0.02
K ₂ O	0.10	0.11	0.18	0.25	0.10	0.10
P ₂ O ₅	0.13	0.03	0.05	0.06	0.05	0.05
H ₂ O	0.54	0.12	1.72	1.28	2.40	0.62
CO ₂	0.29	0.35	1.62	1.20	0.54	3.51
Total	100.52	100.46	100.18	100.82	99.88	99.90
Fe* ₂ O ₃	0.80	0.19	0.47	0.85	0.34	1.10
(ppm)						
Co	nd	nd	nd	nd	nd	nd
Cr	19	15	21	29	18	18
Ce	47	34	31	25	26	37
Ba	64	69	114	192	40	223
La	16	15	9	6	9	13
Zr	440	148	131	120	67	153
Y	13	9	8	10	5	10
Sr	52	51	85	88	60	88
U	2	2	1	3	2	2
Rb	1	2	4	5	1	0
Th	10	1	2	2	nd	2
Pb	12	8	9	12	6	8
Ga	1	1	5	7	2	3
Zn	18	7	9	22	23	13
Cu	8	3	1	3	5	4
Ni	1	nd	2	2	7	3
nd: Not detected						

Table 4.6 Unstandardised discriminate function coefficient used to calculate discriminate scores for the Saq Sandstone

Elements	Discriminate Function I	Discriminate FunctionII
SiO ₂	-0.0447	-0.421
TiO ₂	-0.972	1.988
Al ₂ O ₃	0.008	-0.526
Fe ₂ O ₃	-0.267	-0.551
FeO	0.208	-1.610
MnO	-3.032	2.720
MgO	0.140	0.881
CaO	0.195	-0.907
Na ₂ O	0.719	-0.177
K ₂ O	-0.032	-1.840
P ₂ O ₅	7.510	7.244
Constant	0.303	43.570

Table 4.7 Discriminate scores of the Lower Saq Sandstone

Sample No.	DF I	DF II	Sample No.	DF I	DF II	Sample No.	DF I	DF II
K-20-4	-1.16	1.95	K-7-7	-3.66	1.97	K-5-7	-3.66	2.03
K-5-8	-3.13	1.92	K-20-7	-2.49	2.64	K-20-12	-0.52	5.42
K-20-3	-2.04	4.83	K-4-3	-3.93	2.56	K-7-11	-3.76	2.75
K-5-15	-4.10	1.63	K-5-12	-3.79	2.44			
K-26-5	-2.42	3.61	K-5-11	-3.99	1.99			
K-27-4	-2.50	3.93	K-5-3	-3.97	2.13			
K-3-6	-1.59	1.73	K-5-6	-3.41	2.76			
K-2-3	-2.97	1.82	K-20-1	-1.47	1.35			
K-20-8	-2.62	3.18	K-7-10	-3.79	1.78			
K-20-2	-1.59	3.44	K-7-6	-4.16	1.93			
K-2-1	-3.75	2.00	K-7-9	-3.92	3.43			
K-7-1	-4.03	2.13	K-7-2	-3.57	1.47			
K-27-3	-2.80	4.56	K-26-4	-3.69	2.41			
K-2-2	-3.71	2.93	K-5-2	-3.32	1.58			
K-5-13	-4.09	2.08	K-2-4	-1.99	2.24			
K-7-5	-3.99	2.87	K-26-7	-1.99	3.23			
K-3-2	2.15	6.77	K-5-9	-3.70	3.07			
K-7-4	-4.22	1.84	K-20-10	-2.53	2.92			
K-4-1	-3.58	2.11	K-5-10	-3.66	2.91			
K-7-8	-3.33	2.40	K-20-9	-3.02	3.38			
K-20-6	-2.22	0.95	K-5-1	-2.93	4.59			
K-3-5	-2.83	1.58	K-20-11	-3.36	1.86			
K-5-14	-3.68	2.03	K-3-3	-2.99	2.98			
K-20-5	-1.19	5.56	K-3-4	-3.77	2.09			
K-4-2	-4.31	2.58	K-5-4	-3.63	2.83			
K-5-5	-3.86	2.39	K-26-6	-3.61	2.49			

Table 4.8 Discriminate scores of the Middle Saq Sandstone

Sample No.	DF I	DF II	Sample No.	DF I	DF II	Sample No.	DF I	DF II
K-14-1	-3.86	3.25	K-16-5	-3.85	2.13	K-39-5	-3.94	2.15
K-14-3	-4.13	2.05	K-16-1	-4.30	2.16	K-39-6	-2.29	3.57
K-38-2	-3.26	2.43	K-16-3	-4.08	1.78	K-39-7	-3.44	2.50
K-18-3	-4.02	1.89	K-17-6	-3.87	2.35	K-39-8	-2.99	2.83
K-19-2	-3.57	2.07	K-38-3	-3.16	1.39	K-39-1	-3.80	1.77
K-28-2	-3.82	4.89	K-15-3	-3.63	1.26	K-36-6	-3.95	2.34
K-38-6	-3.61	1.87	K-15-4	-3.88	1.70	K-36-7	-3.37	3.09
K-38-5	-3.95	2.32	K-16-4	-3.66	1.41	K-36-5	-3.57	2.12
K-18-4	-4.11	2.50	K-14-5	-0.77	5.34	K-18-1	-4.09	1.70
K-17-4	-3.58	2.95	K-18-2	-4.22	3.10	K-14-2	-4.00	1.86
K-19-1	-3.84	2.80	K-19-3	-3.74	2.70	K-39-3	-3.80	2.15
K-15-5	-3.08	2.47	K-19-4	-2.85	4.71	K-39-4	-3.51	2.57
K-38-7	-3.51	1.52	K-19-5	-3.20	4.60			
K-28-4	-3.74	2.59	K-36-1	-3.38	1.52			
K-15-1	-2.44	1.56	K-36-2	-3.65	2.33			
K-17-2	-3.82	1.18	K-36-3	-2.59	3.90			
K-17-1	-3.94	1.27	K-36-4	-3.46	2.79			
K-28-3	-3.95	1.83	K-36-8	-4.07	2.16			
K-15-6	-3.98	1.33	K-37-2	-2.99	3.03			
K-38-1	-3.52	1.68	K-37-1	-3.92	3.01			
K-17-3	-4.19	2.30	K-37-3	-3.90	2.87			
K-38-4	-4.03	2.29	K-37-4	-3.70	3.33			
K-28-1	-3.96	2.08	K-37-7	-3.50	1.62			
K-18-5	-3.99	2.41	K-37-5	-2.03	1.96			
K-16-6	-1.28	4.67	K-37-6	-3.40	3.10			
K-16-2	-3.98	2.26	K-39-2	-3.70	2.44			

Table 4.9 Discriminate scores of the Upper Saq Sandstone

Sample No.	Disc. Func. I	Disc.Func.II	Sample No.	Disc. Func. I	Disc.Func.II
K-25-2	-3.67	2.21	K-22-1	-3.42	0.74
K-22-3	-3.36	2.11	K-25-3	-3.47	1.61
K-22-5	-0.31	4.26	K-25-5	-2.73	4.88
K-22-2	-0.46	5.43	K-21-5	-3.24	1.61
K-23-1	-4.14	1.03	K-30-1	-3.16	2.82
K-23-2	-3.15	0.85	K-40-4	-3.94	0.62
K-23-3	-4.21	1.27	K-25-4	-3.21	2.64
K-41-1	-4.02	2.55	K-40-5	-4.25	1.30
K-41-2	-4.08	2.06	K-30-2	-4.19	1.74
K-41-3	-4.02	2.54	K-40-1	-4.06	1.09
K-41-4	-3.61	2.67	K-30-4	-4.20	2.79
K-41-5	-3.28	3.25	K-40-6	-4.15	0.14
K-40-2	-4.23	1.23	K-40-8	-4.45	3.61
K-40-9	-4.21	0.44	k-21-3	-3.00	1.69
K-30-5	-0.59	5.25	K-21-4	-3.67	4.38
K-30-3	-4.60	2.82	K-21-1	-3.73	2.09
K-21-5	-2.98	4.82	K-25-6	-3.40	2.06
K-42-1	-4.15	2.49			
K-42-2	-3.20	2.23			
K-42-3	-3.08	1.54			
K-42-4	-3.40	2.77			
K-42-5	-2.93	1.94			
K-25-1	-1.60	3.41			
K-21-2	-3.76	1.06			
K-40-3	-4.12	2.75			

Table 5.1 Seven percentes of grain size analyses(Lower Saq Sandstone)

Sample No.	5Ø	16Ø	25Ø	50Ø	75Ø	84Ø	95Ø
k-5-5	-0.10	1.00	1.30	1.65	1.80	1.90	2.30
k-20-7	0.50	1.10	1.25	1.65	2.20	2.40	3.55
k-3-4	-0.20	0.10	1.15	1.95	2.35	2.50	3.30
k-5-15	-0.15	0.20	0.45	1.05	1.65	1.80	2.10
k-5-2	0.70	0.90	1.00	1.50	1.75	1.85	2.20
k-4-2	0.90	1.15	1.25	1.45	2.00	2.20	2.70
k-5-9	-0.10	0.40	0.70	1.30	2.00	2.20	2.80
k-5-13	0.75	1.00	1.10	1.35	1.65	1.85	2.40
k-20-10	-0.30	-0.10	0.00	1.10	1.55	1.65	1.90
k-20-1	0.95	1.40	1.60	1.85	2.20	2.40	3.10
k-20-2	0.95	1.45	1.60	1.80	2.15	2.50	3.40
k-20-4	0.90	1.35	1.60	1.80	2.15	2.45	3.25
k-20-11	0.85	1.40	1.55	1.85	2.35	2.70	3.45
k-5-6	0.55	1.05	1.60	1.45	1.75	1.90	2.40
k-5-4	1.15	1.40	1.15	1.75	2.00	2.25	3.50
k-7-7	-0.15	-0.20	1.55	1.55	1.95	2.35	3.10
k-3-5	1.05	1.25	-0.05	1.70	1.90	3.20	3.80
k-5-7	1.05	1.25	1.35	1.65	2.20	2.40	2.95
k-5-8	1.20	1.30	1.35	1.55	1.95	2.40	3.05
k-2-1	1.05	1.25	1.40	1.65	2.10	2.50	3.00
k-5-14	0.10	0.90	1.35	1.70	1.90	2.10	2.70
k-5-10	1.05	1.35	1.50	1.80	2.15	2.40	3.15
k27-4	1.10	1.50	1.55	1.80	2.15	2.40	3.05
k-2-2	1.10	1.50	1.60	2.50	2.80	2.90	3.40
k-4-3	1.10	1.25	1.85	1.60	1.80	1.90	2.70
k-7-6	0.60	1.15	1.35	1.70	2.10	2.40	2.60
k-3-6	1.25	1.80	2.00	2.30	2.70	3.10	3.60
k-26-5	-0.90	-0.20	0.30	1.00	1.65	1.95	2.60
k-20-6	0.40	0.70	0.90	1.35	1.90	2.30	3.50
k-7-1	0.20	0.70	0.95	1.45	1.85	2.05	2.55
k-4-1	-0.20	0.30	0.55	1.00	1.35	1.55	2.25
k-7-5	1.20	1.55	1.65	1.90	2.35	2.85	3.55
k-5-12	1.10	1.30	1.40	1.65	1.90	2.00	2.60
k-20-5	-0.25	0.30	0.60	1.20	1.70	1.90	2.65
k-5-1	0.20	0.60	0.80	1.30	1.70	2.40	3.25
k-5-11	1.05	1.25	1.35	1.60	1.80	1.90	2.45
k-2-4	1.10	1.65	2.00	2.65	3.05	3.35	3.95

Table 5.2 Seven percentes of grain-size analyses(Middle Saq Sandstone)

Sample No.	5Ø	16Ø	25Ø	50Ø	75Ø	84Ø	95Ø
k-37-7	0.50	1.20	1.50	1.70	1.90	1.95	2.25
k-18-4	0.60	1.40	1.55	1.80	2.00	2.45	2.80
k-28-1	1.55	1.85	1.95	2.45	2.65	2.75	2.90
k-28-4	1.25	1.65	1.85	2.25	3.00	3.15	3.50
k-36-7	1.45	1.80	2.00	2.55	2.65	2.80	3.20
k-36-2	1.25	1.50	1.60	1.75	1.90	2.25	3.40
k-18-2	1.20	1.55	1.65	2.10	2.20	2.50	2.80
k-1-4	1.15	1.40	1.50	1.70	1.85	1.95	2.40
k-1-1	1.10	1.50	1.60	1.75	1.90	2.00	2.25
k-36-6	1.05	1.20	1.40	1.65	1.85	1.95	2.35
k-44-1	1.30	1.50	1.65	1.90	2.35	2.60	3.20
k-16-3	-0.10	0.45	0.68	1.20	1.65	1.85	2.30
k-16-2	0.10	0.45	0.60	0.95	1.35	1.50	1.80
k-17-1	1.05	1.30	1.40	1.65	1.90	2.15	2.63
k-36-1	1.15	1.55	1.70	1.95	2.40	2.60	3.25
k-18-1	1.05	1.35	1.45	1.75	2.05	2.20	2.50
k-13-1	1.10	1.30	1.40	1.70	1.95	2.25	2.75
k-16-5	1.10	1.40	1.50	1.85	2.05	2.20	2.55
k-17-3	1.10	1.30	1.40	1.65	1.90	2.00	2.45
k-14-2	1.05	1.30	1.40	1.65	1.85	1.95	2.60
k-15-3	1.10	1.45	1.55	1.80	2.05	2.25	2.60
k-6-2	0.80	1.35	1.60	2.00	2.55	2.70	3.05
k-28-3	1.60	1.75	1.85	2.05	2.30	2.45	3.05
k-17-2	1.05	1.30	1.40	1.65	1.90	2.00	2.45
k-15-1	1.14	1.65	1.70	1.90	2.35	2.60	3.00
k-19-2	1.25	1.60	1.80	2.20	2.45	2.60	2.95
k-14-3	0.50	1.05	1.55	1.70	1.90	1.95	2.35
k-18-3	0.85	1.40	1.55	2.20	1.90	1.95	2.45
k-36-3	1.05	1.25	1.30	1.55	1.75	1.85	2.10
k-45-1	1.05	1.30	1.40	1.65	1.85	2.00	2.35
k-15-5	0.65	0.80	0.90	1.20	1.60	1.85	2.55
k-12-4	1.15	1.55	1.65	1.85	2.20	2.95	3.40
k-13-3	1.75	2.00	2.15	2.45	2.85	3.00	3.45
k-37-4	-0.10	0.40	0.70	1.45	2.25	2.60	3.40
k-36-5	0.75	0.95	1.25	1.80	2.30	2.60	3.15
k-37-2	0.80	1.10	1.50	1.80	2.30	2.60	3.15
k-14-4	0.30	0.90	1.25	1.50	1.80	1.90	2.95
k-38-2	0.90	1.30	1.55	1.85	2.30	2.60	3.20
k-19-1	0.70	0.95	1.20	1.70	2.10	2.35	2.70
k-38-5	1.55	1.80	1.90	2.20	2.55	2.70	3.10
k-39-2	1.80	2.30	2.55	2.70	2.90	3.00	3.55
k-38-4	1.65	1.80	1.95	2.25	2.26	2.80	3.35
k-39-3	1.40	1.60	1.65	1.80	1.95	2.15	2.85
k-39-5	1.30	1.50	1.60	1.80	2.10	2.30	2.85
k-39-7	1.45	1.60	1.70	1.85	2.15	2.40	2.85
k-1-3	1.10	1.40	1.60	1.85	2.15	2.50	3.15
k-16-1	1.10	1.50	1.70	2.05	2.50	2.70	3.35

Table 5.3 Seven percentes of grain-size analyses(Upper Saq Sandstone)

Sample No.	5Ø	16Ø	25Ø	50Ø	75Ø	84Ø	95Ø
k-25-6	2.40	2.60	2.70	2.80	2.90	2.95	3.75
k-25-4	2.15	2.55	2.60	2.75	2.90	2.95	3.30
k-21-4	2.05	2.35	2.50	2.65	2.80	2.90	3.20
k-21-2	2.15	2.40	2.55	2.70	2.90	3.00	3.60
k-30-2	2.75	3.05	3.10	3.20	3.35	3.45	3.60
k-30-5	2.65	2.70	2.80	2.85	2.95	3.10	3.60
k-40-9	2.55	2.90	3.05	3.30	3.55	3.70	4.05
k-40-5	2.55	2.95	3.05	3.25	3.40	3.45	3.60
k-40-6	2.05	2.55	2.60	2.80	3.00	3.15	3.60
k-30-3	2.50	2.60	2.70	2.85	2.90	3.00	3.70
k-30-4	2.60	2.75	2.85	3.15	3.40	3.50	3.75
k-40-1	2.55	2.65	2.70	2.85	3.00	3.15	3.45
k-42-2	2.15	2.50	2.70	2.95	3.15	3.45	4.05
k-40-3	2.70	2.90	3.00	3.20	3.45	3.55	3.80
k-22-1	2.20	2.55	2.60	2.75	2.85	2.90	3.00
k-40-8	2.55	2.65	2.75	2.90	2.95	3.20	3.55
k-41-1	1.42	1.65	1.80	2.00	2.30	2.45	2.70
k-40-2	2.55	2.90	3.05	3.25	3.45	2.55	3.90
k-40-4	2.20	2.60	2.75	3.05	3.25	3.35	3.65
k-23-1	2.55	2.70	2.80	2.90	3.10	3.20	3.45
k-21-3	2.10	2.40	2.50	2.75	3.00	3.15	3.60
k-23-2	2.60	2.75	2.80	2.95	3.25	3.40	3.85
k-25-1	1.25	1.65	1.75	1.95	2.30	2.45	2.60
k-41-2	0.75	1.15	1.35	1.80	2.55	2.90	3.45
k-21-5	2.25	2.35	2.40	2.55	2.75	2.85	3.20
k-25-2	2.25	2.35	2.40	2.65	3.05	3.35	3.90
k-25-5	1.60	1.90	2.00	2.20	2.45	2.55	2.95
k-25-3	1.00	1.35	1.55	1.75	2.05	2.25	2.75

Table 5.4 Summary of grain-size analyses of the Lower Saq Sandstones

Sample No.	Md (ϕ)	Mz (ϕ)	σ_1 (ϕ)	SK _J	KG
K-5-6	1.45	1.46(M.Sand)	0.49(W. Sorted)	0.04(N. Symmetrical)	1.18(Leptokurtic)
K-7-7	1.55	1.23(M.Sand)	1.18(P. Sorted)	-0.25(C. Skewed)	0.73(Platykurtic)
K-5-4	1.75	1.80(M.Sand)	0.57(M. W. Sorted)	0.33(S. F. Skewed)	2.14(V.Leptokurtic)
K-5-5	1.65	1.52(M.Sand)	0.59(M. W. Sorted)	-0.45(S. C. Skewed)	1.97(V.Leptokurtic)
K-20-7	1.65	1.71(M.Sand)	0.78(M. Sorted)	0.19(F. Skewed)	1.31(Leptokurtic)
K-5-14	1.70	1.57(M.Sand)	0.69(M. W. Sorted)	-0.28(C. Skewed)	2.66(V.Leptokurtic)
K-5-10	1.80	1.85(M.Sand)	0.58(M. W. Sorted)	0.21(F. Skewed)	1.43(Leptokurtic)
K-27-4	1.80	1.90(M.Sand)	0.52(M. W. Sorted)	0.31(S. F. Skewed)	1.45(Leptokurtic)
K-2-2	2.50	2.30(F.Sand)	0.70(M. W. Sorted)	-0.32(S. F. Skewed)	0.99(Mesokurtic)
K-4-3	1.60	1.58(M. Sand)	0.40(W. Sorted)	0.150(F. Skewed)	1.46(Leptokurtic)
K-7-6	1.70	1.75(M.Sand)	0.62(M. W. Sorted)	0.09(N. Symmetrical)	1.09(Mesokurtic)
K-3-4	1.95	1.51(M.Sand)	1.13(P. Sorted)	-0.39(S. C. Skewed)	1.19(Leptokurtic)
K-5-15	1.05	1.01(M.Sand)	0.74(M. Sorted)	-0.06(N. Symmetrical)	0.77(Platykurtic)
K-3-5	1.70	2.05(F.Sand)	0.90(M. Sorted)	0.53(S. F. Skewed)	2.04(V.Leptokurtic)
K-3-6	2.30	2.40(F.Sand)	0.68(M. W. Sorted)	0.17(F. Skewed)	1.38(Leptokurtic)
K-5-2	1.50	1.41(M.Sand)	0.46(W. Sorted)	-0.16(C. Skewed)	0.82(Platykurtic)
K-26-5	1.0	0.92(C.Sand)	1.07(P. Sorted)	-0.10(C. Skewed)	1.06(Mesokurtic)
K-20-6	1.35	1.45(M.Sand)	0.87(M. Sorted)	0.29(F. Skewed)	1.28(Leptokurtic)
K-4-2	1.45	1.60(M.Sand)	0.53(M. W. Sorted)	0.41(S. F. Skewed)	0.98(Mesokurtic)
K-7-1	1.45	1.40(M.Sand)	0.69(M. W. Sorted)	-0.09(N. Symmetrical)	1.07(Mesokurtic)
K-5-7	1.65	1.76(M.Sand)	0.57(M. W. Sorted)	0.33(S. F. Skewed)	0.91(Platykurtic)
K-5-9	1.30	1.30(M.Sand)	0.89(M. Sorted)	0.02(N. Symmetrical)	0.91(Mesokurtic)
K-5-8	1.55	1.75(M.Sand)	0.55(M. W. Sorted)	0.58(S. F. Skewed)	1.37(Leptokurtic)
K-4-1	1.00	0.95(C.Sand)	0.68(M. W. Sorted)	-0.05(N. Symmetrical)	1.25(Leptokurtic)
K-7-5	1.90	2.10(F.Sand)	0.68(M. W. Sorted)	0.43(S. F. Skewed)	1.38(Leptokurtic)
K-5-13	1.35	1.40(M.Sand)	0.46(W. Sorted)	0.22(F. Skewed)	1.22(Leptokurtic)
K-5-12	1.65	1.65(M.Sand)	0.40(W. Sorted)	0.13(F. Skewed)	1.23(Leptokurtic)
K-20-5	1.20	1.13(M.Sand)	0.84(M. Sorted)	-0.06(N. Symmetrical)	1.08(Mesokurtic)
K-5-1	1.30	1.43(M.Sand)	0.91(M. Sorted)	0.25(F. Skewed)	1.39(Leptokurtic)
K-5-11	1.60	1.58(M.Sand)	0.37(W. Sorted)	0.07(N. Symmetrical)	1.27(Leptokurtic)

Table 5.4 Continued

Sample No.	Md (σ)	Mz (σ)	σ_1 (σ)	SK ₁	K _G
K-2-1	1.65	1.80(M.Sand)	0.60(M. W. Sorted)	0.37(S. F. Skewed)	1.06(Mesokurtic)
K-2-4	2.65	2.55(M.Sand)	0.86(M. Sorted)	-0.13(C. Skewed)	1.11(Leptokurtic)
K-20-10	1.10	0.88(C.Sand)	0.77(M. Sorted)	-0.32(S. C. Skewed)	0.58(V.Platykurtic)
K-20-1	1.85	1.88(M.Sand)	0.57(M. W. Sorted)	0.13(F. Skewed)	1.46(Leptokurtic)
K-20-2	1.80	1.92(M.Sand)	0.63(M. W. Sorted)	0.32(S. F. Skewed)	1.82(V.Leptokurtic)
K-20-4	1.80	1.87(M.Sand)	0.63(M. W. Sorted)	0.21(F. Skewed)	1.61(V.Leptokurtic)
K-20-11	1.85	1.98(M.Sand)	0.72(M. Sorted)	0.27(F. Skewed)	1.42(Leptokurtic)

Table 5.5 Summary of grain-size analyses of the Middle Saq Sandstone

Sample No.	Md (ϕ)	Mz (ϕ)	σ_1 (ϕ)	SK ₁	KG
K-37-7	1.70	1.62(M.Sand)	0.45(W. Sorted)	-0.35(S. C. Skewed)	1.79(V.Leptokurtic)
K-18-4	1.80	1.65(M.Sand)	0.41(M. W. Sorted)	-0.19(N. Symmetrical)	1.69(V.Leptokurtic)
K-28-1	2.45	2.35(F.Sand)	0.70(W. Sorted)	0.12(S. C. Skewed)	0.76(Platykurtic)
K-28-4	2.25	2.35(F.Sand)	0.71(M. Sorted)	0.16(F. Skewed)	0.80(Platykurtic)
K-36-7	2.55	2.38(F.Sand)	0.52(M. W. Sorted)	-0.38(S. C. Skewed)	1.10(Mesokurtic)
K-36-2	1.75	1.83(M.Sand)	0.51(M. W. Sorted)	0.43(S. F. Skewed)	2.94(V.Leptokurtic)
K-18-2	2.10	2.05(F.Sand)	0.48(W. Sorted)	-0.14(C. Skewed)	1.19(Leptokurtic)
K-1-4	1.70	1.68(M.Sand)	0.33(V. W. Sorted)	0.01(N. Symmetrical)	1.46(Leptokurtic)
K-1-1	1.75	1.75(M.Sand)	0.30(V. W. Sorted)	-0.06(N. Symmetrical)	1.57(V.Leptokurtic)
K-36-6	1.65	1.60(M.Sand)	0.38(W. Sorted)	-0.06(N. Symmetrical)	1.18(Leptokurtic)
K-44-1	1.90	2.00(M.Sand)	0.56(M. W. Sorted)	0.34(S. F. Skewed)	1.08(Leptokurtic)
K-16-3	1.18	1.16(M.Sand)	0.71(M. Sorted)	-0.05(N. Symmetrical)	1.01(Mesokurtic)
K-16-2	0.97	0.91(C.Sand)	0.52(M. W. Sorted)	0.27(F. Skewed)	0.93(Mesokurtic)
K-17-1	1.65	1.70(M.Sand)	0.45(W. Sorted)	0.21(F. Skewed)	1.29(Leptokurtic)
K-36-1	1.97	2.04(F.Sand)	0.58(M. W. Sorted)	0.21(F. Skewed)	1.23(Leptokurtic)
K-18-1	1.75	1.77(M.Sand)	0.43(W. Sorted)	0.05(N. Symmetrical)	0.99(Mesokurtic)
K-13-1	1.70	1.75(M.Sand)	0.49(W. Sorted)	0.21(F. Skewed)	0.55(Leptokurtic)
K-16-5	1.85	1.82(M.Sand)	0.42(W. Sorted)	-0.08(N. Symmetrical)	1.08(Mesokurtic)
K-17-3	1.65	1.65(M.Sand)	0.38(W. Sorted)	0.09(N. Symmetrical)	1.11(Mesokurtic)
K-14-2	2.65	1.65(M.Sand)	0.41(W. Sorted)	0.11(F. Skewed)	1.15(Leptokurtic)
K-15-3	1.80	1.83(M.Sand)	0.43(W. Sorted)	0.10(N. Symmetrical)	1.23(Leptokurtic)
K-6-2	2.00	2.02(F.Sand)	0.68(M. W. Sorted)	-0.01(N. Symmetrical)	0.97(Mesokurtic)
K-28-3	2.05	2.08(F.Sand)	0.39(W. Sorted)	0.26(F. Skewed)	1.32(Leptokurtic)
K-17-2	1.65	1.65(M.Sand)	0.39(W. Sorted)	0.07(N. Symmetrical)	1.15(Leptokurtic)
K-15-1	1.90	2.05(F.Sand)	0.48(M. W. Sorted)	0.42(S. F. Skewed)	1.01(Leptokurtic)
K-19-2	2.20	2.13(M.Sand)	0.51(M. W. Sorted)	-0.16(C. Skewed)	1.07(Mesokurtic)
K-14-3	1.70	1.56(M.Sand)	0.51(M. W. Sorted)	-0.37(S. C. Skewed)	2.16(V.Leptokurtic)
K-18-3	2.20	1.85(M.Sand)	0.38(W. Sorted)	-1.30(S. C. Skewed)	1.87(V.Leptokurtic)
K-36-3	1.55	1.55(M.Sand)	0.31(V. W. Sorted)	0.02(N. Symmetrical)	0.96(Mesokurtic)
K-45-1	1.65	1.65(M.Sand)	0.37(W. Sorted)	0.04(N. Symmetrical)	1.18(Leptokurtic)

Table 5.5 Continued

Sample No.	Md (ϕ)	Mz (ϕ)	σ_1 (ϕ)	SK ₁	KG
K-15-5	1.20	1.28(M.Sand)	0.55(M. W. Sorted)	0.32(S. F. Skewed)	1.11(Leptokurtic)
K-39-4	1.85	2.12(F.Sand)	0.69(M. W. Sorted)	0.47(S. F. Skewed)	1.68(V.Leptokurtic)
K-13-3	2.45	2.48(F.Sand)	0.51(M. W. Sorted)	0.14(F. Skewed)	0.99(Mesokurtic)
K-37-4	1.45	1.48(M.Sand)	1.08(P. Sorted)	0.08(N. Symmetrical)	0.93(Mesokurtic)
K-36-5	1.80	1.78(M.Sand)	0.77(M. Sorted)	0.04(N. Symmetrical)	0.93(Mesokurtic)
K-37-2	1.80	1.83(M.Sand)	0.73(M. Sorted)	0.10(F. Skewed)	1.20(Leptokurtic)
K-14-4	1.50	1.43(M.Sand)	0.65(M. W. Sorted)	-0.05(N. Symmetrical)	1.97(V.Leptokurtic)
K-38-2	1.85	1.91(M.Sand)	0.67(M. W. Sorted)	0.16(F. Skewed)	1.25(Leptokurtic)
K-19-1	1.70	1.66(M.Sand)	0.65(M. W. Sorted)	-0.03(N. Symmetrical)	0.91(Mesokurtic)
K-38-5	2.20	2.23(F.Sand)	0.46(W. Sorted)	0.14(F. Skewed)	0.98(Mesokurtic)
K-39-2	2.70	2.67(F.Sand)	0.44(W. Sorted)	-0.09(N. Symmetrical)	2.04(Leptokurtic)
K-38-4	2.25	2.28(F.Sand)	0.51(M. W. Sorted)	0.20(F. Skewed)	1.07(Mesokurtic)
K-39-3	1.80	1.85(M.Sand)	0.36(W. Sorted)	0.36(S. F. Skewed)	1.98(V.Leptokurtic)
K-39-5	1.80	1.87(M.Sand)	0.43(W. Sorted)	0.30(S. F. Skewed)	1.27(Leptokurtic)
K-1-3	1.85	1.66(M.Sand)	0.33(V. W. Sorted)	0.11(F. Skewed)	2.04(V.Leptokurtic)
k-16-1	2.05	2.08(F.Sand)	0.64(M. W. Sorted)	0.11(F. Skewed)	1.15(Leptokurtic)
K-39-7	1.85	1.95(M.Sand)	0.41(W. Sorted)	0.40(S. F. Skewed)	1.27(Leptokurtic)

Table 5.6 Summary of grain-size analyses of the Upper Saq Sandstone

Sample No.	Md (ϕ)	Mz (ϕ)	σ_1 (ϕ)	SK ₁	KG
K-25-6	3.80	2.78(F. Sand)	0.23(V. W. Sorted)	0.01(F. Skewed)	2.76(V. Leptokurtic)
K-25-4	2.75	2.75(F. Sand)	0.27(V. W. Sorted)	-0.02(N. Symmetrical)	1.57(V. Leptokurtic)
K-21-4	2.65	2.63(F. Sand)	0.31(V. W. Sorted)	-0.07(N. Symmetrical)	1.57(V. Leptokurtic)
K-21-2	2.70	2.70(F. Sand)	0.37(W. Sorted)	0.12(F. Skewed)	1.70(V. Leptokurtic)
K-30-2	3.20	3.23(V. F. Sand)	0.26(V. W. Sorted)	0.20(F. Skewed)	1.72(V. Leptokurtic)
K-30-5	2.85	2.88(F. Sand)	0.24(V. W. Sorted)	0.41(S. F. Skewed)	2.60(V. Leptokurtic)
K-40-9	3.30	3.30(V. F. Sand)	0.43(W. Sorted)	0.00(N. Symmetrical)	1.23(Leptokurtic)
K-40-5	3.25	3.22(V. F. Sand)	0.28(V. W. Sorted)	-0.27(C. Skewed)	1.23(Leptokurtic)
K-40-6	2.80	2.83(F. Sand)	0.38(W. Sorted)	0.10(N. Symmetrical)	1.59(V. Leptokurtic)
K-30-3	2.85	2.82(F. Sand)	0.23(V. W. Sorted)	0.08(N. Symmetrical)	2.46(V. Leptokurtic)
K-30-4	3.15	3.13(V. F. Sand)	0.36(W. Sorted)	-0.01(N. Symmetrical)	0.86(Platykurtic)
K-40-1	2.85	2.88(F. Sand)	0.26(V. W. Sorted)	0.27(F. Skewed)	1.23(Leptokurtic)
K-42-2	2.95	2.97(F. Sand)	0.53(M. W. Sorted)	0.10(F. Skewed)	1.73(V. Leptokurtic)
K-40-3	3.2	3.22(V. F. Sand)	0.33(V. W. Sorted)	0.08(N. Symmetrical)	1.00(Mesokurtic)
K-22-1	2.75	2.73(F. Sand)	0.21(V. W. Sorted)	-0.26(C. Skewed)	1.31(Leptokurtic)
K-40-8	2.90	2.92(F. Sand)	0.29(V. W. Sorted)	0.20(F. Skewed)	2.05(V. Leptokurtic)
K-41-1	2.00	2.04(F. Sand)	0.38(W. Sorted)	0.12(F. Skewed)	1.03(Mesokurtic)
K-40-2	3.25	3.23(V. F. Sand)	0.37(W. Sorted)	-0.06(N. Symmetrical)	1.38(Leptokurtic)
K-40-4	3.05	3.00(F. Sand)	0.41(W. Sorted)	-0.19(C. Skewed)	1.19(Leptokurtic)
K-23-1	2.90	2.93(F. Sand)	0.26(V. W. Sorted)	0.21(F. Skewed)	1.23(Leptokurtic)
K-21-3	2.75	2.77(F. Sand)	0.41(W. Sorted)	0.10(F. Skewed)	1.23(Leptokurtic)
K-23-2	2.95	3.03(V.F.Sand)	0.35(W. Sorted)	0.41(S. F. Skewed)	1.14(Leptokurtic)
K-25-1	1.95	2.02(F. Sand)	0.40(W. Sorted)	0.11(F. Skewed)	1.00(Mesokurtic)
K-41-2	1.80	1.95(M. Sand)	0.85(M. Sorted)	0.24(F. Skewed)	0.92(Mesokurtic)
K-21-5	2.55	2.58(F. Sand)	0.27(V. W. Sorted)	0.28(F. Skewed)	1.11(Leptokurtic)
K-25-2	2.65	2.78(F. Sand)	0.50(W. Sorted)	0.46(S. F. Skewed)	1.04(Mesokurtic)
K-25-5	2.20	2.22(F. Sand)	0.37(W. Sorted)	0.09(N. Symmetrical)	1.23(Leptokurtic)
K-25-3	1.78	1.79(M. Sand)	0.49(W. Sorted)	0.08(N. Symmetrical)	1.43(Leptokurtic)

Table 5.7 Summary of Sahu's Parameters (1964) for the Lower Saq Sandstone

Sample No.	Y1(Eolian:Beach)	Y2(Shallow agitated:Beach)	Y3(Sh. agitated:Fluvial-deltaic)	Y4(Turbidity:Fluvial-deltaic)
K-5-6	-0.7308(Aeolian)	61.1900(Beach)	-1.8258(Fluvial-deltaic)	7.4712(Turbidity)
K-7-7	3.5564(Aeolian)	119.7284(Sh.agitated)	-10.5887(Sh.agitated)	2.5069(Turbidity)
K-5-4	0.7564(Aeolian)	95.0995(Sh.agitated)	-3.8445(Fluvial-deltaic)	14.7157(Fluvial-deltaic)
K-5-5	2.9320(Aeolian)	74.9717(Sh.agitated)	-0.3190(Fluvial-deltaic)	8.3536(Turbidity)
K-20-7	-0.1664(Aeolian)	94.4257(Sh.agitated)	-5.7087(Fluvial-deltaic)	9.2010(Turbidity)
K-5-14	5.0226(Aeolian)	100.0114(Sh.agitated)	-2.2247(Fluvial-deltaic)	13.1345(Fluvial-deltaic)
K-5-10	-1.3408(Aeolian)	81.3269(Sh.agitated)	-3.3780(Fluvial-deltaic)	10.1814(Fluvial-deltaic)
K-27-4	-1.9089(Aeolian)	79.9536(Sh.agitated)	-3.2739(Fluvial-deltaic)	11.0232(Fluvial-deltaic)
K-2-2	-2.6475(Aeolian)	80.7252(Sh.agitated)	-2.0230(Fluvial-deltaic)	4.5475(Turbidity)
K-4-3	-0.8122(Aeolian)	64.9781(Beach)	-1.6146(Sh.agitated)	9.8126(Turbidity)
K-7-6	-1.61564(Aeolian)	74.4500(Sh.agitated)	-3.2562(Fluvial-deltaic)	7.4826(Turbidity)
K-3-4	3.8526(Aeolian)	122.4989(Sh.agitated)	-8.7897(Sh.agitated)	4.2477(Turbidity)
K-5-15	0.9440(Aeolian)	64.9541(Beach)	-4.1784(Fluvial-deltaic)	4.1794(Turbidity)
K-3-5	0.9331(Aeolian)	132.6594(Sh.agitated)	-9.0063(Sh.agitated)	15.5177(Fluvial-deltaic)
K-3-6	-2.9098(Beach)	96.5661(Sh.agitated)	-4.1316(Fluvial-deltaic)	9.9936(Fluvial-deltaic)
K-5-2	-1.3634(Aeolian)	48.2517(Beach)	-0.6291(Fluvial-deltaic)	4.1949(Turbidity)
K-26-5	4.4626(Aeolian)	107.4353(Sh.agitated)	-9.2269(Sh.agitated)	5.1394(Turbidity)
K-20-6	1.0100(Aeolian)	101.3692(Sh.agitated)	-7.5745(Sh.agitated)	9.4680(Turbidity)
K-4-2	-2.4704(Aeolian)	69.0612(Sh.agitated)	-3.9634(Fluvial-deltaic)	8.9881(Turbidity)
K-7-1	0.0284(Aeolian)	71.3688(Sh.agitated)	-3.2795(Fluvial-deltaic)	5.8755(Turbidity)
K-5-7	-2.9304(Beach)	71.7131(Sh.agitated)	-3.9151(Fluvial-deltaic)	8.1768(Turbidity)
K-5-9	1.0843(Beach)	89.5986(Sh.agitated)	-6.6223(Fluvial-deltaic)	5.5697(Turbidity)
K-5-8	-2.0645(Aeolian)	83.1234(Sh.agitated)	-4.9229(Fluvial-deltaic)	12.2962(Fluvial-deltaic)
K-4-1	2.3169(Aeolian)	67.4796(Sh.agitated)	-3.4749(Turbidity)	6.7783(Turbidity)
K-7-5	-2.3791(Aeolian)	96.5780(Sh.agitated)	-5.4894(Fluvial-deltaic)	11.5274(Fluvial-deltaic)
K-5-13	-0.8714(Aeolian)	62.3776(Beach)	-2.4721(Fluvial-deltaic)	8.8629(Turbidity)
K-5-12	-1.7366(Aeolian)	61.4557(Beach)	-1.5079(Fluvial-deltaic)	8.8629(Turbidity)
K-20-5	2.0662(Aeolian)	82.9509(Sh.agitated)	-5.5134(Fluvial-deltaic)	5.8431(Turbidity)
K-5-1	1.7705(Aeolian)	107.0458(Sh.agitated)	-8.0029(Sh.agitated)	9.7378(Turbidity)
K-5-11	-1.3231(Aeolian)	58.4959(Beach)	-1.0299(Fluvial-deltaic)	8.2770(Turbidity)
K-2-1	-2.5592(Aeolian)	78.1455(Sh.agitated)	-4.3997(Fluvial-deltaic)	9.2547(Turbidity)

Table 5.7 Continued

Sample No.	Y1 (Eolian:Beach)	Y2 (Shallow agitated:Beach)	Y3 (Sh. agitated:Fluvial-deltaic)	Y4 (Turbidity:Fluvial-deltaic)
K-2-4	-2.6367(Aeolian)	106.7005(Sh.agitated)	-5.0623(Fluvial-deltaic)	6.5415(Turbidity)
K-20-10	1.5244(Aeolian)	57.6721(Beach)	-3.3492(Fluvial-deltaic)	1.3115(Turbidity)
K-20-1	-1.2309(Aeolian)	80.1474(Sh.agitated)	-2.8758(Fluvial-deltaic)	9.8279(Turbidity)
K-20-2	-0.3808(Aeolian)	95.6065(Sh.agitated)	-4.4075(Fluvial-deltaic)	13.0122(Fluvial-deltaic)
K-20-4	-0.6278(Aeolian)	88.9462(Sh.agitated)	-3.8936(Fluvial-deltaic)	11.1242(Fluvial-deltaic)
K-20-11	-1.2868(Aeolian)	96.2223(Sh.agitated)	-5.2294(Fluvial-deltaic)	10.5529(Fluvial-deltaic)

Table 5.8 Summary of Sahu's Parameters (1964) for the Middle Saq Sandstone

Sample No.	Y1(Eolian:Beach)	Y2(Shallow agitated:Beach)	Y3(Sh. agitated:Fluvial-deltaic)	Y4(Turbidity:Fluvial-deltaic)
k-37-7	1.2952(Aeolian)	65.5051(Sh.agitated)	0.4750(Fluvial-deltaic)	8.1876(Turbidity)
k-18-4	0.3900(Aeolian)	64.7057(Beach)	-0.0091(Fluvial-deltaic)	8.7883(Turbidity)
k-28-1	-1.4558(Beach)	85.2190(Sh.agitated)	-4.1729(Fluvial-deltaic)	6.3283(Turbidity)
k-28-4	-4.3621(Beach)	87.6100(Sh.agitated)	-4.4902(Fluvial-deltaic)	6.8036(Turbidity)
k-36-7	-3.2788(Beach)	98.4968(Sh.agitated)	0.2223(Fluvial-deltaic)	4.8720(Turbidity)
k-36-2	2.6926(Aeolian)	107.9254(Sh.agitated)	-3.7190(Fluvial-deltaic)	19.6708(Fluvial-deltaic)
k-18-2	-2.4674(Aeolian)	66.7139(Sh.agitated)	-0.6913(Fluvial-deltaic)	6.7420(Turbidity)
k-1-4	-1.0675(Aeolian)	60.6507(Beach)	-0.4534(Fluvial-deltaic)	8.9628(Turbidity)
k-1-1	-0.8994(Aeolian)	61.2725(Beach)	-0.0799(Sh.agitated)	9.1319(Turbidity)
k-36-6	-1.3770(Aeolian)	55.2824(Beach)	-0.4582(Fluvial-deltaic)	6.9376(Turbidity)
k-44-1	-3.3202(Beach)	78.0542(Sh.agitated)	-3.7884(Fluvial-deltaic)	9.3216(Turbidity)
k-16-3	-0.9970(Aeolian)	61.7072(Sh.agitated)	-1.2561(Fluvial-deltaic)	8.9355(Turbidity)
k-16-2	-0.0088(Aeolian)	54.1102(Beach)	-3.3856(Fluvial-deltaic)	7.2874(Turbidity)
k-17-1	-1.7370(Aeolian)	67.5899(Sh.agitated)	-2.2545(Fluvial-deltaic)	9.3862(Turbidity)
k-36-1	-2.6416(Aeolian)	80.6002(Sh.agitated)	-3.3856(Fluvial-deltaic)	9.2600(Turbidity)
k-18-1	-2.6538(Aeolian)	59.0807(Beach)	-1.3119(Fluvial-deltaic)	6.7780(Turbidity)
k-13-1	-4.0803(Beach)	57.1500(Beach)	-2.6053(Fluvial-deltaic)	5.4905(Turbidity)
k-16-5	-2.3135(Aeolian)	58.6163(Beach)	-0.5827(Fluvial-deltaic)	6.4195(Turbidity)
k-17-3	-2.0849(Aeolian)	57.4859(Beach)	-1.1813(Fluvial-deltaic)	7.6613(Turbidity)
k-14-2	-1.9141(Aeolian)	60.1455(Beach)	-1.4846(Fluvial-deltaic)	7.9498(Turbidity)
k-15-3	-2.2245(Aeolian)	65.3663(Sh.agitated)	-1.5279(Fluvial-deltaic)	8.4290(Turbidity)
k-6-2	-2.4564(Aeolian)	79.7718(Sh.agitated)	-3.3790(Fluvial-deltaic)	6.3376(Turbidity)
k-28-3	-3.2901(Beach)	71.6869(Sh.agitated)	-1.9479(Fluvial-deltaic)	10.1761(Fluvial-deltaic)
k-17-2	-1.8903(Aeolian)	58.3699(Beach)	-1.1489(Fluvial-deltaic)	7.6870(Turbidity)
k-15-1	-4.1907(Beach)	73.5231(Sh.agitated)	-3.4401(Fluvial-deltaic)	9.5592(Turbidity)
k-19-2	-2.9750(Beach)	67.3351(Sh.agitated)	-0.8366(Fluvial-deltaic)	6.0180(Turbidity)
k-14-3	2.8889(Aeolian)	74.7799(Sh.agitated)	0.0809(Fluvial-deltaic)	9.9621(Fluvial-deltaic)
k-18-3	2.2985(Aeolian)	46.7512(Beach)	6.0818(Fluvial-deltaic)	2.3920(Turbidity)
k-36-3	-2.2284(Aeolian)	48.7036(Beach)	-0.4514(Sh.agitated)	6.2952(Turbidity)
k-45-1	-1.7909(Aeolian)	57.3830(Beach)	-0.8675(Fluvial-deltaic)	7.6499(Turbidity)
k-15-5	-0.6568(Aeolian)	66.2474(Sh.agitated)	-3.7972(Fluvial-deltaic)	8.8307(Turbidity)

Table 5.8 Continued

Sample No.	Y1(Eolian:Beach)	Y2(Shallow agitated:Beach)	Y3(Sh. agitated:Fluvial-deltaic)	Y4(Turbidity:Fluvial-deltaic)
k-12-4	-1.5488(Aeolian)	104.0669(Sh.agitated)	-5.7850(Fluvial-deltaic)	13.3934(Fluvial-deltaic)
k-13-3	-5.0961(Beach)	76.7656(Sh.agitated)	-2.2086(Fluvial-deltaic)	7.8667(Turbidity)
k-37-4	1.7651(Aeolian)	118.4677(Sh.agitated)	-10.1427(Sh.agitated)	6.0583(Turbidity)
k-36-5	-1.3452(Aeolian)	84.7553(Sh.agitated)	-4.8372(Fluvial-deltaic)	6.2368(Turbidity)
k-37-2	-1.0297(Aeolian)	87.6779(Sh.agitated)	-4.5779(Fluvial-deltaic)	8.1300(Turbidity)
k-14-4	2.6979(Aeolian)	85.6945(Sh.agitated)	-2.9538(Fluvial-deltaic)	10.9515(Fluvial-deltaic)
k-38-2	-1.5951(Aeolian)	85.4223(Sh.agitated)	-4.1104(Fluvial-deltaic)	8.8901(Turbidity)
k-19-1	-1.4646(Aeolian)	70.0424(Sh.agitated)	-3.0371(Fluvial-deltaic)	5.6418(Turbidity)
k-38-5	-4.4146(Beach)	69.4803(Sh.agitated)	-1.8555(Fluvial-deltaic)	7.6529(Turbidity)
k-39-2	-2.2736(Aeolian)	90.6349(Sh.agitated)	-0.3958(Fluvial-deltaic)	12.0396(Fluvial-deltaic)
k-38-4	-4.2579(Beach)	76.2017(Sh.agitated)	-2.5553(Fluvial-deltaic)	8.5497(Turbidity)
k-39-3	-0.7053(Aeolian)	80.6317(Sh.agitated)	-2.2738(Fluvial-deltaic)	14.1856(Fluvial-deltaic)
k-39-5	-2.6580(Aeolian)	70.3540(Sh.agitated)	-2.4932(Fluvial-deltaic)	10.0160(Fluvial-deltaic)
k-39-7	-3.2134(Beach)	72.3131(Sh.agitated)	-2.8125(Fluvial-deltaic)	10.7537(Fluvial-deltaic)
k-1-3	0.6020(Aeolian)	72.8809(Sh.agitated)	-0.9204(Fluvial-deltaic)	12.6914(Fluvial-deltaic)
k-16-1	-2.5548(Aeolian)	82.7452(Sh.agitated)	-3.4778(Fluvial-deltaic)	8.1627(Turbidity)

Y1(Eolian:Beach) Y2(Shallow agitated:Beach) Y3(Sh. agitated:Fluvial-deltaic) Y4(Turbidity:Fluvial-deltaic)
 -1.5488(Aeolian) 104.0669(Sh.agitated) -5.7850(Fluvial-deltaic) 13.3934(Fluvial-deltaic)
 -5.0961(Beach) 76.7656(Sh.agitated) -2.2086(Fluvial-deltaic) 7.8667(Turbidity)
 1.7651(Aeolian) 118.4677(Sh.agitated) -10.1427(Sh.agitated) 6.0583(Turbidity)
 -1.3452(Aeolian) 84.7553(Sh.agitated) -4.8372(Fluvial-deltaic) 6.2368(Turbidity)
 -1.0297(Aeolian) 87.6779(Sh.agitated) -4.5779(Fluvial-deltaic) 8.1300(Turbidity)
 2.6979(Aeolian) 85.6945(Sh.agitated) -2.9538(Fluvial-deltaic) 10.9515(Fluvial-deltaic)
 -1.5951(Aeolian) 85.4223(Sh.agitated) -4.1104(Fluvial-deltaic) 8.8901(Turbidity)
 -1.4646(Aeolian) 70.0424(Sh.agitated) -3.0371(Fluvial-deltaic) 5.6418(Turbidity)
 -4.4146(Beach) 69.4803(Sh.agitated) -1.8555(Fluvial-deltaic) 7.6529(Turbidity)
 -2.2736(Aeolian) 90.6349(Sh.agitated) -0.3958(Fluvial-deltaic) 12.0396(Fluvial-deltaic)
 -4.2579(Beach) 76.2017(Sh.agitated) -2.5553(Fluvial-deltaic) 8.5497(Turbidity)
 -0.7053(Aeolian) 80.6317(Sh.agitated) -2.2738(Fluvial-deltaic) 14.1856(Fluvial-deltaic)
 -2.6580(Aeolian) 70.3540(Sh.agitated) -2.4932(Fluvial-deltaic) 10.0160(Fluvial-deltaic)
 -3.2134(Beach) 72.3131(Sh.agitated) -2.8125(Fluvial-deltaic) 10.7537(Fluvial-deltaic)
 0.6020(Aeolian) 72.8809(Sh.agitated) -0.9204(Fluvial-deltaic) 12.6914(Fluvial-deltaic)
 -2.5548(Aeolian) 82.7452(Sh.agitated) -3.4778(Fluvial-deltaic) 8.1627(Turbidity)

Table 5.9 Summary of Sahu's Parameters (1964) for the Upper Saq Sandstone

Sample No.	Y1(Eolian:Beach)	Y2(Shallow agitated: Beach)	Y3(Sh. agitated:Fluvial-deltaic)	Y4(Turbidity:Fluvial-deltaic)
K-25-5	-1.1529(Aeolian)	98.2454(Sh.agitated)	0.4135(Fluvial-deltaic)	16.6596(Fluvial-deltaic)
K-25-4	-4.6146(Beach)	76.5266(Sh.agitated)	0.3192(Fluvial-deltaic)	10.1296(Fluvial-deltaic)
K-21-4	-3.9966(Beach)	75.2673(Sh.agitated)	0.3263(Fluvial-deltaic)	9.6910(Turbidity)
K-21-2	-4.0956(Beach)	84.8149(Sh.agitated)	-0.9320(Fluvial-deltaic)	11.6825 (Fluvial-deltaic)
K-30-2	-6.3422(Beach)	90.3989(Sh.agitated)	-0.5437(Fluvial-deltaic)	12.7311(Fluvial-deltaic)
K-30-5	-2.8397(Beach)	104.4769(Sh.agitated)	-1.5966(Fluvial-deltaic)	18.5757(Fluvial-deltaic)
K-40-9	-7.2740(Beach)	86.3879(Sh.agitated)	-0.5968(Fluvial-deltaic)	8.8148(Turbidity)
K-40-5	-6.8021(Beach)	73.5767(Sh.agitated)	1.5716(Fluvial-deltaic)	7.0023(Turbidity)
K-40-6	-4.8268(Beach)	85.2210(Sh.agitated)	-0.8939(Fluvial-deltaic)	11.0589(Fluvial-deltaic)
K-30-3	-2.2717(Aeolian)	96.3363(Sh.agitated)	-0.1814(Fluvial-deltaic)	15.5810(Fluvial-deltaic)
K-30-4	-8.0094(Beach)	73.2352(Sh.agitated)	-0.1501(Fluvial-deltaic)	6.6604(Turbidity)
K-40-1	-6.7518(Beach)	77.1162(Sh.agitated)	-1.1077(Fluvial-deltaic)	10.3459(Fluvial-deltaic)
K-42-2	-4.3986(Beach)	98.4621(Sh.agitated)	-1.9989(Fluvial-deltaic)	11.8925(Fluvial-deltaic)
K-40-3	-8.1363(Beach)	77.5051(Sh.agitated)	-0.3931(Fluvial-deltaic)	8.1399(Turbidity)
K-22-1	-4.9747(Beach)	65.2302(Beach)	1.7235(Fluvial-deltaic)	7.1561(Turbidity)
K-40-8	-4.1014(Beach)	92.4856(Sh.agitated)	-0.7571(Fluvial-deltaic)	14.2233 (Fluvial-deltaic)
K-41-1	-3.6893(Beach)	63.1475(Beach)	-1.2373(Fluvial-deltaic)	7.6903(Turbidity)
K-40-2	-6.6152(Beach)	84.0188(Sh.agitated)	-0.0287(Fluvial-deltaic)	9.2150(Turbidity)
K-40-4	-6.0081(Beach)	76.4600(Sh.agitated)	0.3718(Fluvial-deltaic)	7.1333(Turbidity)
K-23-1	-6.8268(Beach)	76.9499(Sh.agitated)	-0.7335(Fluvial-deltaic)	10.0138(Fluvial-deltaic)
K-21-3	-5.6164(Beach)	79.1213(Sh.agitated)	-1.1426(Fluvial-deltaic)	9.1071(Turbidity)
K-23-2	-7.6698(Beach)	84.0432(Sh.agitated)	-2.1762(Fluvial-deltaic)	10.9331(Fluvial-deltaic)
K-25-1	-3.6794(Beach)	62.8517(Beach)	-1.3284(Sh.agitated)	7.4266(Turbidity)
K-41-2	-1.9355(Aeolian)	98.9417(Sh.agitated)	-6.8388(Fluvial-deltaic)	7.6073(Turbidity)
K-21-5	-6.0673(Beach)	70.8562(Sh.agitated)	-1.2336(Fluvial-deltaic)	9.6297(Turbidity)
K-25-2	-6.7078(Beach)	87.4721(Sh.agitated)	-3.5857(Fluvial-deltaic)	10.4893(Fluvial-deltaic)
K-25-5	-3.7770(Sh.agitated)	67.9913(Sh.agitated)	-0.9486(Fluvial-deltaic)	8.6847(Turbidity)
K-25-3	-1.2049(Aeolian)	71.6336(Sh.agitated)	-1.8958(Fluvial-deltaic)	9.2749(Turbidity)

Table 5.11 Summary of Sevon's Parameters (1966) for the Lower Saq Sandstone

Sample No.	R1 (Beach:Dune)	R2 (Beach:River)	R3 (Dune:River)
K-5-6	-0.078 (Dune)	-0.015 (River)	0.065 (River)
K-7-7	-0.043 (Dune)	-0.045 (River)	0.009 (River)
K-5-4	-0.096 (Dune)	-0.016 (River)	0.098 (River)
K-5-5	-0.072 (Dune)	-0.013 (River)	0.073 (River)
K-20-7	-0.087 (Dune)	-0.027 (River)	0.066 (River)
K-5-14	-0.071 (Dune)	-0.016 (River)	0.086 (River)
K-5-10	-0.101 (Dune)	-0.018 (River)	0.085 (River)
K-27-4	-0.107 (Dune)	-0.016 (River)	0.092 (River)
K-2-2	-0.126 (Dune)	-0.021 (River)	0.086 (River)
K-4-3	-0.088 (Dune)	-0.010 (River)	0.082 (River)
K-7-6	-0.094 (Dune)	-0.020 (River)	0.071 (River)
K-3-4	-0.060 (Dune)	-0.040 (River)	0.032 (River)
K-5-15	-0.042 (Dune)	-0.027 (River)	0.023 (River)
K-3-5	-0.105 (Dune)	-0.031 (River)	0.093 (River)
K-3-6	-0.135 (Dune)	-0.021 (River)	0.104 (River)
K-5-2	-0.075 (Dune)	-0.013 (River)	0.056 (River)
K-26-5	-0.025 (Dune)	-0.040 (River)	0.008 (River)
K-20-6	-0.068 (Dune)	-0.032 (River)	0.050 (River)
K-4-2	-0.089 (Dune)	-0.019 (River)	0.069 (River)
K-7-1	-0.068 (Dune)	-0.023 (River)	0.049 (River)
K-5-7	-0.098 (Dune)	-0.020 (River)	0.073 (River)
K-5-9	-0.057 (Dune)	-0.033 (River)	0.033 (River)
K-5-8	-0.098 (Dune)	-0.019 (River)	0.085 (River)
K-4-1	-0.038 (Dune)	-0.023 (River)	0.033 (River)
K-7-5	-0.117 (Dune)	-0.024 (River)	0.093 (River)
K-5-13	-0.076 (Dune)	-0.014 (River)	0.067 (River)
K-5-12	-0.093 (Dune)	-0.011 (River)	0.080 (River)
K-20-5	-0.046 (Dune)	-0.030 (River)	0.030 (River)
K-5-1	-0.064 (Dune)	-0.033 (River)	0.049 (River)
K-5-11	-0.089 (Dune)	-0.009 (River)	0.079 (River)
K-2-1	-0.100 (Dune)	-0.021 (River)	0.076 (River)
K-2-4	-0.139 (Dune)	-0.028 (River)	0.094 (River)
K-20-10	-0.031 (Dune)	-0.028 (River)	0.010 (River)
K-20-1	-0.103 (Dune)	-0.017 (River)	0.087 (River)
K-20-2	-0.104 (Dune)	-0.019 (River)	0.094 (River)
K-20-4	-0.100 (Dune)	-0.019 (River)	0.087 (River)
K-20-11	0.085 (River)	-0.106 (Dune)	-0.024 (River)

Table 5.12 Summary of Sevon's Parameters (1966) for the Middle Saq Sandstone

Sample No.	R1 (Beach:Dune)	R2 (Beach:River)	R3 (Dune:River)
K-37-7	-0.084 (Dune)	-0.008 (River)	0.082 (River)
K-18-4	-0.089 (Dune)	-0.007 (River)	0.086 (River)
K-28-1	-0.133 (Dune)	-0.024 (River)	0.088 (River)
K-28-4	-0.133 (Dune)	-0.025 (River)	0.089 (River)
K-36-7	-0.135 (Dune)	-0.012 (River)	0.100 (River)
K-36-2	-0.097 (Dune)	-0.011 (River)	0.119 (River)
K-1-4	-0.960 (Dune)	-0.006 (River)	0.088 (River)
K-1-1	-0.100 (Dune)	-0.004 (River)	0.095 (River)
K-36-6	-0.090 (Dune)	-0.009 (River)	0.076 (River)
K-44-1	-0.114 (Dune)	-0.019 (River)	0.088 (River)
K-16-3	-0.052 (Dune)	-0.025 (River)	0.036 (River)
K-16-2	-0.043 (Dune)	-0.019 (River)	0.036 (River)
K-17-1	-0.096 (Dune)	-0.013 (River)	0.082 (River)
K-36-1	-0.115 (Dune)	-0.018 (River)	0.090 (River)
K-18-1	-0.101 (Dune)	-0.012 (River)	0.079 (River)
K-13-1	-0.101 (Dune)	-0.018 (River)	0.068 (River)
K-16-5	-0.103 (Dune)	-0.011 (River)	0.082 (River)
K-17-3	-0.094 (Dune)	-0.010 (River)	0.079 (River)
K-14-2	-0.093 (Dune)	-0.011 (River)	0.078 (River)
K-15-3	-0.104 (Dune)	-0.012 (River)	0.087 (River)
K-6-2	-0.110 (Dune)	-0.022 (River)	0.077 (River)
K-28-3	-0.123 (Dune)	-0.010 (River)	0.104 (River)
K-17-2	-0.094 (Dune)	-0.010 (River)	0.079 (River)
K-15-1	-0.120 (Dune)	-0.016 (River)	0.093 (River)
K-19-2	-0.121 (Dune)	-0.014 (River)	0.091 (River)
K-14-3	-0.077 (Dune)	-0.009 (River)	0.084 (River)
K-18-3	-0.097 (Dune)	0.003 (River)	0.092 (River)
K-36-3	-0.090 (Dune)	-0.007 (River)	0.074 (River)
K-45-1	-0.094 (Dune)	-0.009 (River)	0.080 (River)
K-15-5	-0.066 (Dune)	-0.019 (River)	0.055 (River)
K-39-4	-0.117 (Dune)	-0.023 (River)	0.099 (River)
K-13-3	-0.146 (Dune)	-0.015 (River)	0.109 (River)
K-37-4	-0.064 (Dune)	-0.041 (River)	0.032 (River)
K-36-5	-0.092 (Dune)	-0.027 (River)	0.061 (River)
K-37-2	-0.096 (Dune)	-0.025 (River)	0.071 (River)
K-14-4	-0.067 (Dune)	-0.018 (River)	0.070 (River)
K-38-2	-0.103 (Dune)	-0.022 (River)	0.079 (River)
K-19-1	-0.087 (Dune)	-0.022 (River)	0.061 (River)
K-38-5	-0.131 (Dune)	-0.013 (River)	0.099 (River)
K-39-2	-0.155 (Dune)	-0.006 (River)	0.139 (River)
K-38-4	-0.135 (Dune)	-0.016 (River)	0.101 (River)
K-39-3	-0.106 (Dune)	-0.007 (River)	0.108 (River)
K-39-5	-0.108 (Dune)	-0.013 (River)	0.091 (River)
K-39-7	-0.115 (Dune)	-0.012 (River)	0.097 (River)
K-1-3	-0.093 (Dune)	-0.004 (River)	0.100 (River)
K-16-1	-0.115 (Dune)	-0.021 (River)	0.086 (River)
k-18-2	-0.116 (Dune)	-0.012 (River)	0.091 (River)

Table 5.13 Summary of Sevon's Parameters (1966) for Upper Saq Sandstone

Sample No.	R1 (Beach:Dune)	R2 (Beach:River)	R3 (Dune:River)
K-25-5	-0.166 (Dune)	0.004 (River)	0.169 (None)
K-25-4	-0.167 (Dune)	-0.002 (River)	0.142 (None)
K-21-4	-0.158 (Dune)	-0.003 (River)	0.134 (River)
K-21-2	-0.162 (Dune)	-0.006 (River)	0.139 (River)
K-30-2	-0.201 (Dune)	-0.001 (River)	0.170 (Dune)
K-30-5	-0.176 (Dune)	0.001 (River)	0.174 (Dune)
K-40-9	-0.201 (Dune)	-0.009 (River)	0.154 (None)
K-40-5	-0.198 (Dune)	-0.001 (River)	0.154 (None)
K-40-6	-0.170 (Dune)	-0.007 (River)	0.142 (None)
K-30-3	-0.196 (Dune)	0.001 (River)	0.163 (None)
K-30-4	-0.193 (Dune)	-0.007 (River)	0.142 (None)
K-40-1	-0.180 (Dune)	0.007 (River)	0.145 (None)
K-42-2	-0.175 (Dune)	-0.012 (River)	0.144 (None)
K-40-3	-0.200 (Dune)	-0.006 (River)	0.151 (None)
K-22-1	-0.168 (Dune)	0.002 (River)	0.137 (River)
K-40-8	-0.177 (Dune)	-0.002 (River)	0.160 (None)
K-41-1	-0.120 (Dune)	-0.010 (River)	0.095 (River)
K-40-2	-0.197 (Dune)	-0.005 (River)	0.156 (None)
K-40-4	-0.181 (Dune)	-0.007 (River)	0.138 (River)
K-23-1	-0.183 (Dune)	-0.003 (River)	0.147 (None)
K-21-3	-0.167 (Dune)	-0.009 (River)	0.131 (River)
K-23-2	-0.188 (Dune)	-0.009 (River)	0.147 (None)
K-25-1	-0.118 (Dune)	-0.011 (River)	0.092 (River)
K-41-2	-0.102 (Dune)	-0.032 (River)	0.067 (River)
K-21-5	-0.160 (Dune)	-0.005 (River)	0.129 (River)
K-25-2	-0.168 (Dune)	-0.016 (River)	0.127 (River)
K-25-5	-0.131 (Dune)	-0.008 (River)	0.108 (River)
K-25-3	-0.099 (Dune)	-0.013 (River)	0.086 (River)

REFERENCES

- AALTO, K. R. 1989. Petrology and tectonostratigraphic terranes of the northwest California and southwest Oregon Coast Ranges: **J. Sediment. Petrol.**, 59, 561-571.
- ABU EL-LA, R. AND COLEMAN, J. M. 1985. Discrimination between depositional environments using grain-size analysis: **Sedimentology**, 32, 743 - 748.
- AGAR, R. A. 1985. Stratigraphy and palaeogeography of the Siham group: direct evidence for a late Proterozoic continental microplate and active continental margin in Saudi Arabia Shield: **Jour. Geol. Soc. London**, 142, 1205-1220.
- AL-LABOUN, A. A. 1982. The subsurface stratigraphy of pre-Khuff Formations in central and northwestern Arabia, Jeddah, Saudi Arabia, King Abdulaziz University: **unpublished Ph.D. thesis**, 102p.
- _____ 1986. Stratigraphy and hydrocarbon potential of the Paleozoic succession in both Tabuk and Widyan basins, Arabia, in Future petroleum provinces of the world(ed) by M. T. HALBUTY: **Am Assoc. Petroleum Geologists Memoir**, 40, 373-397.
- ALLEN, J. R. L. 1968. Current Ripples: Their relation to patterns of water and sediment motion, **North-Holland publishing company**, Amsterdam, 433p.
- _____ 1970. Physical processes of sedimentation, New York, **American Elsevier**, 248p.
- _____ 1980. Sand waves: a model of origin and internal structure: **J. Sediment. Petrol.**, 26, 281-328.
- _____ AND BANKS, N. L. 1972. An interpretation and analysis of recumbent folded deformed cross-bedding: **Sedimentology**, 19, 257-283.
- ALLEN, P. A. AND HOMEWOOD, P. 1984. Evolution and mechanics of a Miocene tidal sandwave: **Sedimentology**, 31, 63-81.
- AMARAL, E.J. AND PRYOR, W. A. 1977. Depositional environment of the St Peter Sandstone deduced by textural analysis: **J. Sediment. Petrol.**, 47, 151-180.
- ANDERTON, R. 1976. Tidal shelf sedimentation: an example from the Scottish Dalradian: **Sedimentology**, 23, 429-459.
- ARGAST, S. AND DONNELLY, T. W. 1987. The chemical discrimination of clastic sedimentary components: **Jour. Sediment. Petrol.**, 57, 813-823.
- ARKELL, W. J. 1952. Jurassic ammonites from Jebel Tuwaiq, Central Arabia: **Phil. Trans. R. Soc. London**, series B, 236, 241-313.

- BAHAFZALLAH, A., JUX, A. AND OMARA, S. 1981. Stratigraphy and facies of Devonian Jauf Formation Saudi Arabia: **Neues Jahrbuch fur Geologie und Palaontologie Monatshefte**, 1, 1-18, Stuttgart.
- BANERJEE, I. 1980. A subtidal bar model for the Eze-Aku sandstones, Nigeria: **Sediment. Geol.**, 25, 291-309.
- BANKS, N.L. 1973. Tide-dominated offshore sedimentation, lower Cambrian, North Norway: **Sedimentology**, 29, 213-228
- BARWIS, J. H. AND MAKURATH, J. H. 1978. Recognition of ancient tidal inlet sequences: an example from the Upper Silurian Keyser Limestone in Virginia: **Sedimentology**, 25, 61 - 82.
- BASAHHEL, A. N. et al. 1984. Early Cambrian platform of the Arabian Shield: **Neues Jahrbuch fur Geologie und Palaontologie Monatshefte**, H.2, 113-128.
- BASU, A. YOUNG, S.W., SUTTER, L. J., GALUIN, J. W. AND MACK, G.H. 1975. Re-evaluation of the use of undulatory extinction and polycrystallinity in detrital quartz for provenance interpretation: **J. Sediment. Petrol.**, 45, 873-882.
- BELDERSON, R. H. , JOHNSON, M. A. AND KENYON, N. H. 1982. Bedforms. In A. H. Stride (eds), **Offshore Tidal Sands: Chapman & Hall, London**, 27-57.
- _____ AND STRIDE, A. H. 1966. Tidal current fashioning of a basal bed: **Mar. Geol.**, 4, 237-257.
- _____ AND STRIDE, A. H. 1969. Tidal currents and sandwave profiles in the northeastern Irish Sea: **Nature**, 222, 74.
- BELLINI, E. AND MASSA, D. 1980. A stratigraphic contribution to the Paleozoic of the Southern basins of Libya, In **The geology of Libya (ed)**, by SALEM, M. J. and BUSEREWIL, M. T. , 1-56, London: **Academic Press**.
- BENDER, F. 1975. Jordan, In: **Geology of the Arabian Peninsula: U. S. Geol. Surv. Prof. Paper**, 560 I, 36p.
- BENNACEF, A., BEUF, S., BIJU-DUVAL, B., DeCHARPAL, O., GARIEL, O. AND ROGNON, P. 1971. Example of cratonic sedimentation: Lower Paleozoic of Algerian Sahara: **Am. Assoc. Petrol. Geol. Bull.**, 55, 2225-2245.
- BENTOR, Y. K. 1985. The crustal evolution of the Arabian-Nubian massif with special reference to the Sinai Peninsula: **Precambrian Research**, 28, 1-74.
- BERG, R./R. 1975. Depositional environment of Upper Cretaceous Sussex sandstone, House Creek Field Wyoming: **Am. Asso. Petrol. Geol. Bull**, 59, 2099-2110.

- BEYDOUN, Z. R. 1988. The Middle East: Regional geology and petroleum resources: **Scientific Press, U. K.**, 269p.
- BHATIA, M. R. AND CROOK, K. A. W. 1986. Trace element characteristics of graywackes and tectonic setting discrimination of sedimentary basins: **Contrib. Mineral. Petrol.**, 92, 181-193.
- _____ 1983. Plate tectonics and geochemical composition of sandstone: **J. Geol.**, 91, 611-627.
- BIGOT, M. 1970. Geology of the Tabuk and Jauf Formations in the Wadi Al-Fajr area: **Bureau de Recherches Geologiques et Minieres**, 70, Jed. n 28; Jeddah.
- _____ AND LAFOY, C. 1970. The Paleozoic series in Tabuk basin: **Bureau de Recherches Geologiques et Minieres**, 70 Jed. n 11; Jeddah.
- BLACKENHORN, M. 1914. Syrien Arabian Und Mesopotamien: **Handbuch der regionalen geologic, Heidelberg**, 5, Abt. 4, H. 17.
- BLAKEY, R. C. 1984. Marine sand-wave complex in the Permian of central Arizona: **J. Sediment. Petrol.**, 54, 29-51.
- BLATT, H., MIDDLETON, G. AND MURRAY, R. 1980. Origin of sedimentary rocks: **Prentice-Hall, Englewood Cliffs, N. J.**, 634p.
- _____ AND CHRISTIE, J. M. 1963. Undulatory extinction in quartz of igneous and metamorphic rocks and its significance in provenance of sedimentary rocks: **J. Sediment. Petrol.**, 33, 559-579.
- _____ 1967. Origin characteristic of clastic quartz grains: **J. Sediment. Petrol**, 37, 401-424.
- BLUCK, B. J. 1971. Sedimentation in the meandering river Endrick: **Scott. J. Geol.**, 7, 93-138.
- _____ 1979. Structure of coarse grained braided stream alluvium: **Trans. R. Soc. Edinburgh**, 70, 181-221.
- BOERSMA, J. R. AND H. J. TERWINDT. 1981. Neap-spring tide sequences of intertidal shoal deposits in a mesotidal estuary: **Sedimentology**, 28, 151-170.
- BOKMAN, J. 1952. Clastic quartz particles as indices of provenance: **J. Sediment. Petrol.**, 22, 14-17.
- BOSWELL, P. G. H. 1919. Sands; considered geologically and inustrially under war conditions: **Univ. Liverpool, Inaugurat Lectures**, 38p.
- BOYLES, J. M. AND SCOTT, A. J. 1982. A model for migrating shelf-bar sandstone in Upper Mancos Shale (Campanian), Northwestern Colorado: **Bull. Am. Assoc. Petrol. Geol.**, 66, 491-508.
- BRAMKAMP, R. A. AND RAMIREZ, L. F. 1958. Geologic map of Northern Tuwayq Quadrangle, Kingdom of Saudi Arabia: **U. S. Geol. Surv. Miscellaneous Geologic Investigation**, map 1-207 A.

- _____, RAMIRES, L. F., BROWN, G. F. AND POCOCK, A. E. 1963. Geology of the Wadi Ar Rimah quadrangle Kingdom of Saudi Arabia: **U. S. Geol. Surv. Miscellaneous Geologic Investigation**, Map 1-206A.
- BRASIER, M. D. 1980. The lower Cambrian transgression and glauconite-phosphate facies in western Europe: **J. Geol. Soc. London**, 137, 695-703.
- BRENNER, R. L. AND DAVIES, D. K. 1973. Storm generated coquina sandstone: genesis of high energy marine sediments from the Upper Jurassic of Wyoming and Montana: **Bull. Geol. Soc. Am.**, 84, 1685-1698.
- _____, AND MARTINSEN, J. 1990. The Fossil Sandstone - a shallow marine sand wave complex in the Namurian of Cumbria and north Yorkshire, England: **Proc. Yorkshire Geol. Soc.**, 48, 149-162.
- BRIDGE, J. S. 1981. Hydraulic interpretation of grain size distribution, using physical model for bedload transport: **J. Sediment. Petrol.**, 51, 1109-1124.
- BROWN, G. F. 1970. Eastern margin of the Red Sea and the coastal structures in Saudi Arabia: **Phil. Trans. R. Soc. London**, 267A, 75-87.
- _____, AND JACKSON, R. O. 1960. The Arabian Shield: **International Geological Congress, Copenhagen**, 21, 9: 69-77.
- BRYANT, I. D. AND SMITH, M. P. 1990. A composite tectonic-tectonic origin for shelf sandstone at the Cambrian-Ordovician boundary in North Greenland: **J. Geol. Soc. London**, 147, 795-809.
- BUCKE, D. P. AND MANKIN, C. J. 1971. Clay mineral diagenesis within inter-laminated shales and sandstone: **J. Sediment. Petrol.**, 41, 971.
- CARROLL, D. 1970. Clay minerals: A guide to their X-ray identification: **Geol. Soc. Am. Spec. Pap.**, 126, 75p
- CARVER, R. E. 1971. Procedures in sedimentary petrography: **Wiley Interscience**, 653p.
- CARRIGY, M. A. AND MELLON, G. B. 1964. Authigenic clay minerals cements in Cretaceous and Tertiary sandstones of Alberta: **J. Sediment. Petrol.**, 34, 461-472.
- CASTON, V. N. D. 1972. Linear sand banks in southern North Sea: **Sedimentology**, 18, 63-78.
- CAVAZZA, W. 1989. Detrital modes and provenance of the Stilo-Capo d'Orlando (Miocene), southern Italy: **Sedimentology**, 36, 1077-1090.
- CHANDLER, F. W. 1988. Quartz arenites: review and interpretation: **Sediment. Geol.**, 58, 105-126.
- CHEN, D. 1977. Table of key lines X-ray powder diffraction patterns of minerals in clay and associated rocks: **Dept. Nat. Resources. Indiana State Surv. Spec. Pap.**, 21, 67p.

- CLARK-LOWES, D. D. 1980. Sedimentology and mineralization potential of Saq and Tabuk Formation: Qassim district: **Imperial College, Open-File Report CRC/1C-7.**
- CLARKE, A. J. AND BATTISTI, D. S. 1981. The effect of continental shelves on tides: **Deep-Sea Res.**, 28A, 665-682.
- CLIFTON, H. E. , HUNTER, R. E. AND PHILLIPS, R. L. 1971. Depositional structures and processes in the non-barred high energy nearshore: **J. Sediment. Petrol.**, 41, 651-670.
- _____ 1969. Beach lamination: Nature and origin: **Mar. Geol.**, 7, 553-559.
- _____ 1975. Recognition of ancient beaches and beach environments(abs): **Bull. Am Assoc. Petrol. Geol. Ann. Mtg. Abs.**, 2, p12.
- _____ 1981. Progradational sequences in Miocene shoreline deposits, southeastern Caliente Range, California: **J. Sediment. Petrol.**, 51, 165-184.
- CLOUD, P. , AWRAMIK, S. M. AND HADLEY, D. G. 1979. Earliest Phanerozoic or latest Proterozoic fossils from the Arabian Shield: **Directorate General of Mineral Resources, Saudi Arabia, Proj. Rep. 260:** 1-39, Jeddah.
- CONDIE, K. C. 1986. Geochemistry and tectonic setting of Early Proterozoic supracrustal rocks in the southwestern United States.: **J. Geol.**, 94, 845-864.
- CROOK, K. A. 1974. Lithogenesis and geotectonics: The significance of compositional variation of flysch arenites (graywackes), in Dott, R. H., Jr and Shaver, R. H. eds., Modern and Ancient Geosynclinal Sedimentation: Soc. Econ. Paleontologists Mineralogist Spec. Publ. 19, 304-310.
- DALRYMPLE, R. W. , KNIGHT, R. J. AND LAMBLASE, J. J. 1978. Bedforms and their hydraulic stability relationship in a tidal environment, Bay of Fundy, Canada: **Nature**, 275, 100 - 104.
- _____ 1984. Morphology and internal structure of sandwaves in the Bay of Fundy: **Sedimentology**, 31, 365-382.
- DAPPLES, E. C. 1971. Physical classification of carbonate cement in quartzose sandstone: **J. Sediment. Petrol**, 41, 196-205.
- DARMOIAN, S. A. AND LINDQVIST, K. 1988. Sediments in the estuarine environments of Tigirs/Euphrates delta, Iraq, Arabian Gulf: **Geol. J.**, 23, 15-37.
- DAVIES, D. K. AND ETHRIDGE, F. G. 1975. Sandstone composition and depositional environments: **Bull. Am. Assoc. Petrol. Geol.**, 59, 239-264.
- DEER, W. A., HOWIE, R. A. AND ZUSSMAN, J. 1983. An introduction to the rock-forming minerals: **Longman, London**, 528p.

- DELFOUR, J. 1967. Report on the mineral resources and geology of the Hulayfah-Musayna'ah region: **Bureau de Recherches Geologiques et Minieres**, open-file report 66-A-8, 139p.
- _____. 1970. The J'Balah group, a new unit of the Arabian Shield: **Bureau de Recherches Geologiques et Minieres**, report 70-JED-4.
- _____. 1982. Geology and mineral resources of the northern Arabian shield, a synopsis of Bureau de Recherches Geologiques et Minieres investigation 1965-1975: Open-file report: **Bureau de Recherches Geologiques et Minieres**, -OF-02-30.
- _____, DHELLEMMES, R. , ELASASS, P. VASLET, D. BROSSE, J. M. , Le NINDRE, Y-M , AND DOTTIN, O. 1982. Geological map of the ad Dawadimi quadrangle, sheet 24G, Kingdom of Saudi Arabia (with explanatory notes): **Saudi Arabian Deputy Ministry for Minerals Resources**, Geologic Map GM-60C, scale 1:250 000.
- DENIS, E. AND DABARD, M. P. 1988. Sandstone petrography and geochemistry of Late Proterozoic sediments of the Armorican Massif (France) - A key to basin development during the Cadomian orogeny: **Precamb. Res.**, 42, 198-206.
- DIAS, J. M. A AND NEAL, W. J. 1990. Modal size classification of sands: An example from the northern Portugal continental shelf: **J. Sediment. Petrol.**, 60, 426-437.
- DICKINSON, W. R. 1970. Interpreting detrital modes of graywacke and arkose: **J. Sediment. Petrol.**, 40, 695-707.
- _____. AND SUCZEK, C. A. 1979. Plate tectonic and sandstone composition: **Am. Assoc. Petrol. Geol. Bull.**, 63, 2164-2182.
- _____. AND VALLONI, R. 1980. Plate setting and provenance of sands in modern ocean basins: **Geology**, 8, 82-86.
- _____, KLUTE, M. A., HAYES, M.J., JANECKE, S.U., LUNDIN, E.R., MCKITTRICK, M.A., AND OLIVARES, M.D.. 1988. Paleogeographic and paleotectonic setting of Laramide sedimentary basin in the central Rocky Mountain region: **Geol. Soc. Am. Bull.**, 100, 1023-1039.
- _____, BEARD, L.S., BRACKENRIDGE, G.R., ERJAVEC, J.L., FERGUSON, R.C., INMAN, K.F., KNEPP, LINFBERG. F.A. AND PYBERG, P.T. 1983. Provenance of North American Phanerozoic sandstone in relation to tectonic setting: **Geol. Soc. Am. Bull.**, 94, 222 - 235.
- DORSEY, R. J. 1988. Provenance evolution and unroofing history of a modern arc-continent collision: Evidence from petrography of Plio-Pleistocene sandstones, Eastern Taiwan: **J. Sediment. Petrol.**, 58, 208-218.

- DOTT, R. H. AND BATTEN, R. L. 1971. *Evolution of the Earth: McGraw-Hill, New York, 649pp.*
- DRIESE, S.G., BYERS, C.W., DOTT, R.H. JR. 1981. Tidal deposition in the basal upper Cambrian Mt. Simon Formation in Wisconsin: *J. Sediment. Petrol.* 51, 367-381.
- DUNBAR, C. O. AND RODGERS, J. 1957. *Principles of stratigraphy: John Wiley and Sons, Inc. New York, 366p.*
- DUTTA, P. K. 1987. Origin and rarity of first-cycle quartz arenite (abs.): *Bull. Am. Assoc. Petrol. Geol.* , 71, 551.
- EL-KHAYAL, A. A. AND ROMANO, M. 1988. A revision of the upper part of the Saq Formation and Hanadir Shale (Lower Ordovician) of Saudi Arabia: *Geol. Mag.*, 125, 161-174.
- _____, CHALONER, W. G. AND HILL, C. R. 1980. Paleozoic plants from Saudi Arabia: *Nature*, 285, 33-34.
- ELSTON, D. P. AND SCOTT, G. R. 1976. Unconformity at the Cardenas-Nankowep contact (Precambrian), Grand Canyon Supergroup, northern Arizona: *Geol. Soc. Amer. Bull.*, 87, 1763-1772.
- FLECK, R. J., GREENWOOD, W. R., HADLY, D. G., ANDERSON, R.E. AND SCHMIDT, D. L. 1980. Rubidium-strontium geochronology and plate-tectonic evolution of the southern part of the Arabian Shield: *U. S. Geol. Surv. Prof. Paper.* 1131.
- FOLK, R. L. 1974. *Petrology of sedimentary rocks: Hemphill Publishing Company, Austin, Texas. 182p.*
- _____, AND WARD, W. C. 1957. Brazos Rivers bar: A study in the significance of grain size parameters: *J. Sediment. Petrol.*, 27, 3-27.
- FON, N. A. 1981. Offshore bar deposits of Semilla Sandstone Member of Mancos Shale (Upper Cretaceous), San Juan Basin, New Mexico: *Bull. Am Assoc. Petrol. Geol.*, 65, 706-721.
- FORTEY, R. A. 1984. Global earlier Ordovician transgressions and regressions and their biological implications. In BURUTON, D. L. (eds.) *Aspect of the Ordovician System: Universitetsforlaget, Oslo, 37-50.*
- FRANZINELLI, E. AND POTTER, P. E. 1983. Petrology, chemistry and texture of modern river sands, Amazon river system : *J. Geol.*, 91, 23-39.
- FREEMAN, W. E. AND VISHER, G.S. 1975. Stratigraphic analysis of the Navajo Sandstone: *J. Sediment. Petrol.*, 45, 651-668.
- FRIEDMAN, G. M. 1961. Distinction between dune, beach and river sand from the textural characteristics: *J. Sediment. Petrol.*, 31, 514-529.

- _____ 1967. Dynamic processes and statistical parameters compared for size frequency distribution of beach and river sands: **J. Sediment. Petrol.**, 37, 327-354.
- _____ 1979. Differences in size distributions of populations of particles among sands of various origins: **Sedimentology**, 26, 3-32.
- FRUTT, D. J. AND ELMORE, R. D. 1988. Tide and storm-dominated ridges on a muddy shelf: Cottage Grove Sandstone (Upper Pennsylvanian), Northwestern Oklahoma: **Bull. Am. Assoc. Petrol. Geol.**, 72, 1200-1211.
- FUCHTBAUER, H. 1967. Influence of different types of diagenesis on sandstone porosity: **Proceed, 7th World Petrol. Congress**, 2, 353-369.
- GALEHOUSE, J.S. 1971. Point counting. In Carver(ed) Procedures in sedimentary rocks: **Wily Interscience**, New York, 385-407.
- GARRELS, R. M. AND CHRIST, C. L. 1965. Solutions, minerals and equilibria: 2ed : **Freeman, Cooper and Co., San Francisco**, 450p.
- GASS, I. G. 1977. The evolution of the Pan-African crystalline basement in NE Africa and Arabia: **J. Geol. Soc. London**, 134, 129-138.
- GETTINGS, M. E. AND STOESER, D. B. 1981. A tabulation of radiometric age determinations for the Kingdom of Saudi Arabia: **D. G. M. R. Misc., doc.**, 20, 1-52. Jeddah.
- GLENNIE, K. W. 1970. Desert sedimentary environments: **Elsevier, Amsterdam**, 222p.
- GOLDRING, R. 1985. The formation of trace fossils (*Cruziana*): **Geol. Mag.**, 122, 1, 65-72.
- GOOLD, D. K. 1986. The composition of coarse sediment in Basal Upper Old Red Sandstone alluvial fan conglomerate of the Northwest Midland Valley, Scotland: A provenance study, Unpublished M.Sc. thesis: **Glasgow University**.
- GRAHAM, S. A., INGERSOLL, R. U. AND DICKINSON, W.R. 1976. Common provenance for lithic grains in Carboniferous from Ouachita Mountains and Black Warrior Basin: **J. Sediment. Petrol.**, 46, 620-632.
- GREENWOOD, W. R. , HADLEY, D. G., ANDERSON, R. E. , FLECK, R. J. AND SCHMIDT, D. L. 1976. Late Proterozoic cratonization in southwestern Saudi Arabia: **Phil. Trans. R. Soc. London**, 280A, 517-527.
- _____, HADLY, D. G. , ANDERSON, R. E. FLECK, R. J. AND ROBERTS, R. J. 1980. Precambrian geologic history and plate tectonic evolution of the Arabian Shield: **Saudi Arabia Dir. Gen. Miner. Resources Bull.**, 24, 35p.
- GRIM, R. E. 1962. Applied clay mineralogy: **McGraw Hill, London**, 422p.

- _____ AND JOHNS, W. D. 1954. Clay minerals investigation of sediments in the northern Gulf of Mexico: **Clays and Clay Minerals Proc. 2nd Int. Conf.**, 81-103.
- GROUT, F. F. 1925. The relation of texture and composition of clays: **Geol. Soc. Am. Bull.**, 36, 393-415.
- HADELY, D. G. AND SCHMIDT, D. B. 1980. Proterozoic sedimentary rocks and basins of the Arabian Shield and their evolution: **Dir. Gen. Min. Res. Saudi Arabia Proj. Rep.**, 242, 1-41, Jeddah.
- _____ 1973. Geology of the Sahl-al-Matran quadrangle northwestern Hijaz, Saudi Arabia: **Dir. Gen. Min. Res. Geol.**, Map GM-6 scale 1:100,000.
- _____ 1975. Geology of the Qal'at as-Sawarah quadrangle: **U. S. Geol. Surv.**, Map, GM-24.
- HARLAND, W. B. , ARMSTRONG, R. L., COX, A. V. , CRAIG, L. E. , SMITH, A. G. AND SMITH, D. G. 1989. A geologic time scale 1989: **Cambridge University Press**, 263p.
- HARRIS, C. W. AND ERIKSSON, K. A. 1990. Allogenic controls on the evolution of storm to tidal shelf sequences in the Early Proterozoic Uncompahgre Group, southwest Colorado, USA: **Sedimentology**, 37, 189-213.
- HARRIS, P. T. 1988. Large-scale bedforms as indicators of mutually evasive sand transport and the sequential infilling of wide-mouthed estuaries: **Sediment. Geol.** , 57, 273-298.
- HARVEY P. K., TAYLOR, D. M., HENDRY, R. D. AND BANCROFT, F. 1973. An accurate fusion method for the analysis of rocks and chemically related materials by X-ray fluorescence spectrometry: **X-ray Spectrometry**, 2, 33-44.
- HARWOOD, G. 1988. Microscopic techniques: II. Principles of sedimentary petrography, In Techniques in sedimentology (ed), by M. Tucker, 108-173: **Blackwell Scientific Publications**, Oxford.
- HAYES, J. 1970. Polytypism of chlorite in sedimentary rocks: **Clays and Clay Minerals**, 18, 285-306.
- HEIN, F.H. 1987. Tidal/littoral offshore shelf deposits- Lower Cambrian Gog group, southern Rocky Mountains, Canada: **Sediment. Geol.**, 52, 155-182.
- HELAL, A. H. 1964a. On the occurrence of lower Paleozoic rocks in Tabuk area, Saudi Arabia: **Neues Jahrbuch fur Geologie und Palaontologie Monatshefte**, 7, 391-414, Stuttgart.
- _____ 1964b. On the occurrence and stratigraphic position of Permo-Carboniferous tillites in Saudi Arabia: **Geologisches Rundschau**, 54, 193-207, Stuttgart.

- _____ 1965. General geology and lithostratigraphic subdivision of the Devonian rocks of the Jauf area, Saudi Arabia: **Neues Jahrbuch fur Geologie und Palaontologie Monatshefte**, 9, 527-551, Stuttgart.
- _____ 1968. Stratigraphy of outcropping Paleozoic rocks around the northern edge of the Arabian Shield: **Z. Dt. Geol. Ges.**, 117, 506-543, Hannover.
- HEMER, D. O. 1965. Application of Palynological in Saudi Arabia: **Fifth Arab Petroleum Congress**, Cairo.
- _____ AND NYGREEN, P. W. 1967a. Algal, acritarchs and other microfossils incertae sedie from the Lower Carboniferous of Saudi Arabia: **Micropaleontology**, 13, 183-194.
- _____ AND NYGREEN, P. W. 1967b. Devonian palynology of Saudi Arabia: **Review of Palaeobotany and Palynology**, 5, 51-61, Amsterdam.
- HENSON, F. R. 1951. Observation on the geology and petroleum occurrences of the Middle East: **3rd World Petroleum Congress**, 1, 118-140.
- HEREFORD, R. 1977. Deposition of the Tapeats Sandstone (Cambrian) in central Arizona: **Geol. Soc. Am. Bull.**, 88, 199-211.
- HICKMAN, A. H. AND WRIGHT, A. E. 1983. Geochemistry and chemostratigraphical correlation of slates, marbles and quartz and quartzites of the Appin Group, Argyle, Scotland: **Trans. Roy. Soc. Edinburgh, Earth Sciences**, 73, 251-278.
- HISCOTT, R.N. 1982. Tidal deposits of the Lower Cambrian Random Formation, eastern Newfoundland: facies and paleoenvironments: **Bull. Can. Petrol. Geol.** 19, 2028-2042.
- HOBDAY, D. K. AND TANKARD, A. J. 1978. Transgressive-barrier and shallow-shelf interpretation of the Lower Peninsula Formation, South Africa: **Geol. Soc. Am. Bull.**, 89, 1733-1744.
- HOBSON, J. P. JR. , FOWLER, M. L. AND BEAUMONT, E. A. 1982. Depositional and statistical exploration models Upper Cretaceous offshore sandstone complex, Sussex Member, Hous Creek Field, Wyoming: **Bull. Am. Assoc. Petrol. Geol.** , 66, 689 - 707.
- HOLLAND, H. D. 1978. The geochemistry of the atmosphere and oceans: **Wiley, New York**, p 387.
- HOOKE, R. LeB., 1968. Laboratory studies of the influence of granules on flow over a sand bed: **Geol. Soc. Am. Bull.**, 65, 2534-2545.
- HOUBOLT, J. J. H. C. 1968. Recent sediments of southern Bight of the North Sea: **Geol. Mijnb.**, 47, 245-273.

- _____ 1982. A comparison of recent shallow marine tidal sand ridges with Miocene sand ridges in Belgium, In The Ocean Floor by R.A Scrutton and M. Talwani, (eds), 69-80: **John Wiley and Sons Ltd.**
- HOUSEKNECHT, D. W. 1988. Intergranular pressure solution in four quartzose sandstones: **J. Sediment. Petrol.**, 58, 228-246.
- HOUTHUYS, R. AND GULLENTOPS, H. 1988. Tidal transverse bars building up a longitudinal sand body (Middle Eocene, Belgium). In Tide-influenced sedimentary environments and facies , P. I. de Boer ., Gelder, A. van and Nio, S. D., (eds), 153-166: **D. Reidel Publishing Company, Dordrecht, Holland.**
- HUNTER, R. E. 1977. Basic types of stratification in small aeolian dunes: **Sedimentology**, 24, 361-388.
- _____ 1981. Stratification style in eolian sandstone: some Pennsylvanian to Jurassic examples from Western Interior U.S.A., in Ethridge, F. G. and Flores, R. M. (eds) Recent and ancient nonmarine depositional environments: Models for exploration: **Soc. Econ. Paleon. Mineral. Spec. Pub.**, 31, 315-329.
- HUSSEINI, M. I. 1991. Tectonic and depositional model of the Arabian and adjoining plates during the Silurian - Devonian: **Bull. Am. Assoc. Petrol. Geol.**, 75, 108-120.
- INGERSOLL, R.V. AND SUCZEK, C.A. 1979. Petrology and provenance of Neogene sand from Nicobar fans DSDP sites 211 and 218: **J. Sediment. Petrol.**, 39, 1217-1228.
- JAANUSSON, V. 1979. Ordovician. In ROBINSON, R. A. AND TEICHERT, C. (eds.) treatise on Invertebrate Palaeontology. Part A, Introduction, **Geol. Soc. Am.**, Lawrence, Kansas, 136-166.
- JETT, G.A. AND HELLER, P.L. 1988. Tectonic significance of polymodal compositions in Melange Sandstones, western Melange Belt, North Cascade Range, Washington: **J. Sediment. Petrol.**, 58, 52-61.
- JOHNSON, H. D. 1977. Shallow marine sequences: an example from the Precambrian of North Norway: **Sedimentology**, 24, 245-270.
- _____ AND BALDWIN, C. T. 1986. Shallow siliciclastic seas, In Sedimentary Environments and facies (eds), by H. R. Reading, 229-282: **Blackwell Scientific Publication** (2ed eds), Oxford.
- JOHNSON, M. A. AND BELDERSON, R.H. 1969. The tidal origin of some vertical sedimentary changes in epicontinental seas: **Jour. Geol.**, 77, 353-357.
- JOHNSON, M. J. , STALLARD, R. F. and MEADE, R. H. 1988. First-cycle quartz arenite in the Orinoco river basin, Venezuela and Columbia: **Jour. Geol.**, 96, 263-277.

- _____1990. Tectonic versus chemical-weathering controls on the composition of fluvial sands in tropical environments: **Sedimentology**, 37, 713-726.
- KANTOROWICZ, J. 1984. The nature, origin and distribution of authigenic clay minerals from middle Jurassic Ravenscar and Brent group sandstones: **Clays and Clay Mine.**, 19, 359-375.
- KARPOFF, R. 1957a. Esquisse geologique de L'Arabie Seoudite: **Bull. Soc. Geol. France**, 7, 653-697.
- _____1957b. Sur L'existence du Maestrichtien au de Djeddah(Arabie Seoudite): **C. R. Acad. France**, 245,1322-1324.
- _____1960. L'Antecambrien de la peninsula Arabique: **24th Internat. Congr. Report**, 9, 78-94.
- KENYON, N. H AND STRIDE, A. H. 1970. The tide swept sediments between the Shetland Isles and France: **Sedimentology**, 14, 159-173.
- _____1970. Sand ribbons of European tidal seas: **Mari. Geol.**, 9, 25-39.
- KLEIN, G. de V. 1970. Deposition and dispersal dynamics of intertidal sand bodies: **J. Sediment. Petrol.**, 40, 1095-1127.
- _____1977Clastic tidal facies: **Continuing Education Publication Company**, Champaign, Illinois. 149p.
- _____1982. Probable sequential arrangement of depositional systems on cratons: **Geology**,10, 17-22.
- _____AND RYER, T. A. 1978. Tidal circulation patterns in Precambrian, Paleozoic and Cretaceous epeiric and mioclinal shelf seas: **Geol. Soc Am. Bull.**, 89, 1050-1058.
- KOCUREK, G. 1981. Significance of interdune deposits and bounding surfaces in aeolian dune sand: **Sedimentology**, 28, 753-780.
- KORA, M. 1984. The Paleozoic outcrops of Um Bugma area, Sinai, unpublished: **Ph.D Thesis**, Mansoura, Egypt.
- KORSCH, R.J. 1984. Sandstone compositions from the New England, Eastern Australia: Implication for tectonic setting: **J. Sediment. Petrol.**, 54, 192-211.
- KRAUSKOPF, K. B. 1983. Introduction to geochemistry, (2nd ed.). The Earth and Planetary Sciences, international series: **Mc Graw Co., New York**, 617pp.
- KRYNINE, P. D. 1941. Paleogeographic and tectonic significance of sedimentary quartzites(abstract): **Geol. Soc. Am. Bull.**, 52, 1915-1916.
- _____1942. Differential sedimentation and its products during one complete geosynclinal cycle: **Annales Congreso Panamerican Ingeneria de Minas Y Geologia, Geology-Part 1, 2**, p537-561.

- KUMAR, N. AND SANERS, J. E. 1974. Inlet sequence: a vertical succession of sedimentary structures and textures created by the lateral migration of tidal inlets: **Sedimentology**, 21, 491-532.
- LASH, G. G. 1986. Anatomy of an early Paleozoic subduction complex in the central Appalachian orogen: **Sediment. Geol.**, 51, 75-96.
- LEAKE, B. E., HENDRY, G. L., KEMP, A., PLANT, A. G., HARREY, P. K., WILSON, J. R., COATS, J. C., AUCOTT, J. W., LUNEL, T. AND HOWART, R. J. 1969. The chemical analysis of rock powders by automatic X-ray fluorescence: **Chem. Geol.**, 5, 7-86.
- LEVELL, B. K. 1980. Evidence for currents and associated waves in Late Precambrian shelf deposits from Finnmark, North Norway: **Sedimentology**, 27, 153-166.
- LORING, D. H. 1982. Geochemical factors controlling the accumulation and dispersal of heavy metals in the Bay of Fundy sediments: **Can. Jour. Earth Sci.**, 19, 930-944.
- LUDVIGSEN, R., PRATT, B. R. AND WESTROP, S. R. 1983. The myth of a eustatic sea level drop near the base of the Ibexian Series: **Bull. of New York State Museum**, 462, 65-70.
- MacCARTHY, I. A. J. 1987. Transgressive facies in the South Munster Basin, Ireland: **Sedimentology**, 34, 238-422.
- MACK, G.H., JAMES, C. AND THOMAS, W.A. 1981. Orogenic provenance of Mississippian sandstone associated with Southern Appalachian-Ouachita Orogen: **Bull. Am. Assoc. Petrol. Geol.**, 65, 1444-1456.
- _____, THOMAS, W. A. AND HORSELY, C. A. 1983. Composition of Carboniferous Sandstones and tectonic framework of Southern Appalachian-Ouachita Orogen: **J. Sediment. Petrol.**, 53, 931-946.
- _____. 1984. Exceptions to the relationship between plate tectonics and sandstone composition: **J. Sediment. Petrol.**, 54, 212-220.
- MASON, C. C. AND FOLK, R. L. 1958. Differentiation of beach, dune, and aeolian flat environments by size analysis, Mustsang Island: **J. Sediment. Petrol.**, 28, 211-226.
- MATTHEWS, S. C. AND COWIE, J. W. 1979. Early Cambrian transgression: **J. Geol. Soc. London**, 136, 133-135.
- MAYNARD, J. B., VALLONI, R. AND YU, H. -S., 1982. Composition of modern deep-sea sands from arc-related basins: in LEGGETT, J. K., ed., Trench-forearc geology: sedimentation and tectonics on modern and ancient active plate margins: **Geol. Soc. London Spec. Pub.**, 10, 551-561.
- McBRIDE, E. F. 1963. A classification of common sandstones: **J. Sediment. Petrol.**, 33, 664-669.

- _____. 1974. Significance of color in red, green, purple, olive, brown, and gray beds of Difunta Group, Northeastern Mexico: **J. Sediment. Petrol.**, 44, 760-773.
- _____. 1985. Diagenetic processes that affect provenance determination in sandstone, in Zuffa, G. G. (ed), Provenance of Arenites: NATO ASI series C, v. 148, 95-113.
- McCABE, P. J. AND JONES, C. M. 1977. The formation of reactivation surfaces within superimposed deltas and bedforms: **J. Sediment. Petrol.**, 47, 707-715.
- McCANN, T. 1991. Petrological and geochemical determination of provenance in the southern Welsh Basin. In Developments in sedimentary provenance studies, by Morton, A. C, Todd, S. P. and Haughton, P. D. W, (eds): **Geol. Soc. Spec. Pub.**, No. 57, 215-230.
- McCAVE, I. N. 1971. Sand waves in the North Sea off the coast of Holland: **Mar. Geol.**, 10, 199-225.
- _____. 1973. The sedimentology of a transgression: Portland Point and Cooksburg Members (Middle Devonian), New York State: **J. Sediment. Petrol.**, 43, 484-504.
- McCIURE, H. A.. 1978. Early Paleozoic glaciation in Arabia: **Palaeogeography Palaeoclimatology, Palaeoecology**, 25, 315-326.
- McKIE, T. 1989. Barrier island to tidal shelf transition in the Early Cambrian Eriboll Sandstone: **Scott. J. Geol.**, 25, 273-293.
- _____. 1990. Tidal and storm influenced sedimentation from a Cambrian transgressive passive margin sequence: **J. Geol. Soc. London**, 147, 785-794.
- McLENNAN, S. M., TAYLOR, S. R. AND ERIKSSON, K. A. 1983. Geochemistry of Archean shales from the Pilbara supergroup, Western Australia: **Geochim. Cosmochim. Acta**, 74, 1211-1222.
- MEYER, R. 1976. Continental sedimentation, soil genesis and marine transgression in the basal beds of the Cretaceous in the east of the Paris Basin: **Sedimentology**, 23, 235-253.
- MIALL, A. D. 1984. Principles of sedimentary basin analysis. (eds): **Springer-Verlag**, 490p.
- MILLER, C.F., STODDARD, E.F., BRADFISH, T.J. AND DOLLASE, W.A. 1981. Composition of plutonic muscovite: genetic implication: **Canadian Mineralogist**, 19, 25-34.
- MILLER, J. F. 1984. Cambrian and earliest Ordovician condont evolution, biofacies and provincialism, **Spec. Paper Geol. Soc. Am.**, 196, 43-68
- MOFJELD, H. 1976. Tidal currents. In Marine sediment-transport and environmental management, Stanley, D.J. and Swift, D. J. P. (eds), 53-64: **John Wiley & Sons**, New York.

- MOIOLA, R. J. AND WEISER, D. 1968. Textural parameters: An evaluation: **J. Sediment. Petrol.**, 38, 45-53.
- MOORE, G. F. 1979. Petrography of subduction zone sandstones from Nias Island, Indonesia: **J. Sediment. Petrol.**, 49, 71-84.
- MORTON, A. C. 1985. Heavy mineral provenance studies, in Zuffa, G. G. (ed), Provenance of Arenites: NATO ASI series C, v. 148, 249-277.
- _____. 1991. Geochemical studies of detrital heavy minerals in their application to provenance research. In Developments in sedimentary provenance studies, by Morton, A. C, Todd, S. P. and Haughton, P. D. W, (eds): **Geol. Soc. Soc. Spec. Pub.**, No. 57, 31-44.
- MOSHRIF, M. A. 1980. Recognition of fluvial environments in the Biyadh-Wasia Sandstones (Lower-Middle Cretaceous) as revealed by textural analysis: **J. Sediment. Petrol.**, 50, 603-612.
- MOWBRAY, T. DE AND VISSER, M. J. 1984. Reactivation surface in subtidal channel deposits, Oosterschelde, Southwest Netherland: **J. Sediment. Petrol.**, 54, 811-824.
- MURRIS, R. J. 1980. Middle East: stratigraphic evolution and oil habitat: **Bull. Am. Assoc. Petrol. Geol.** , 64, 597-618.
- NARAYAN, J. 1971. Sedimentary structure in the Lower Greensand of the Weald, England and the Bas-Boulonnais, France: **Sediment. Geol.**, 6, 73-109.
- NASSIEF, M. O., MACDONALD, R AND GASS, I. G. 1984. The Jebel Thurwah upper Proterozoic ophiolite complex, western Saudi Arabia: **Jour. Geol. Soc. London**, 141, 537-546.
- NIGGLI, P. 1954. Rocks and mineral deposits: **Freeman, San Francisco**, 559p
- NIO, S.-D. 1976. Marine transgressions as a factor in the formation of sandwave complexes: **Geol. Mijnb.**, 55, 18-40.
- _____, SIEGENTHALER, C. AND YANG, C. S. 1983. Megaripple cross-bedding as a toll for the reconstruction of the paleo-hydrolics in A Holocene subtidal environment, S.W.Netherlands: **Geol. Mijnb.**, 62, 499-508.
- OKONKWO, C. T. G. 1989. Geochemistry and sedimentology of Grampian metasedimentary rocks, Upper Strathspey: **Scott. J. Geol.**, 3, 239-248.
- PASSEGA, R. 1957. Texture as characteristic of clastic deposition: **Bull. Am. Assoc. Petrol. Geol.**, 41, 1952-1984.
- _____, AND BYRAMJEE, R. 1969. Grain-size image of clastic deposits: **Sedimentology**, 13, 233-252.
- _____. 1964. Grain size representation by CM patterns, a geological tool: **J. Sediment. Petrol.**, 34, 830-847.

- PETTIJOHN, F. J. 1941. Persistence of heavy minerals and geologic age: **J. Geol.**, 49, 610-625.
- _____. 1963. Data of geochemistry. Chapter 5. Chemical composition of sandstones-excluding carbonates and volcanic sands: **U.S. Geol. Surv. Prof. Pap.**, 440-S.
- _____. 1975. Sedimentary rocks, (3rd ed): **Harper and Row**, New York, 628p.
- _____, POTTER, P. E. AND SIEVER, R. 1984. Sand and sandstone: **Springer-Verlag**, New York, 618p
- PHILLIPS, W.E. AND GRIFFEN, D.T. 1981. Optical mineralogy: The nonopaque minerals: **W.H. Freeman and Company**, San Francisco, 677p.
- PIGAGE, L. C. 1982. Linear regression analysis of Sillimanite-Forming reactions at Azure Lake: **Canadian Mineralogist**, 20, 349-378.
- PITTMAN, E. D. 1974. Origin of clay in sandstone - evidence from scanning electron microscopy: **Amer. Assoc. Miner. Ann. Mtgs.**, Abstracts, 1, San Antonio, Texas, p71.
- POSTMA, A.H. 1967. Sediment transport and sedimentation in the estuarine environment. In **Estuaries**, Lauff, G.H. (eds), 158-179: **Am. Assoc. Adv. Sci.**, Washington D.C.
- POWERS, R. W. 1968. Saudi Arabia. in: **Asie: lexique Stratigraphique International**, V.3, Fascicula 10,b.1 (edited by Dubertret, I) Centre National de la Recherche Scientifique, Paris.
- _____, RAMIREZ, L. F., REDMOND, C. D. AND ELBERG, E. L. Jr. 1966. Geology of the Arabian Peninsula-Sedimentary geology of Saudi Arabia: **U. S. Geol. Surv. Prof. Paper**, 650-D.
- PRYOR, W.A., AMARAL, E.J., 1971. Large-scale cross-stratification in the St. Peter Sandstone: **Geol Soc. Am. Bull**, 82, 239-244.
- QUENNEL, A. M. 1951. The geology and mineral resources of (former) Transjordan: **Colonial Geology and Mineral resources**, 2, 85-115.
- RAMSEYER, K., BANMANN, J., MATTER, A. AND MULLIS, J. 1988. Cathodoluminescence colours of alpha-quartz: **Mineral. Mag.**, 52, 669-677.
- REINECK, H. E. AND SINGH, I. B. 1973. Depositional sedimentary environment-with reference to terrigenous clastics, 439pp: **Springer-Verlag**, Berlin.
- RICHARDS, M. T. 1986. Tidal bed form migration in shallow marine environments: Evidence from the Lower Triassic, Western Alps, France. In KNIGHT, R. J. ANF McLEAN, J. R. (eds.), shelf sand and sandstones, **Canad. Soc. Petrol. Geol.**, Memoir 11, 257-276.
- RONOV, A. B. 1981. Composition and evolution of the sediments in major continental structural zones: **Geochem. Inter.**, 6, 13-23.

- ROSER, B. P. AND KORSCH, R. J. 1986. Determination of tectonic setting of sandstone-mudstone suites using SiO₂ content and Na₂O.K₂O ratio: **J. Geol.**, 94, 635-650.
- RUST, I. C. 1977. Evidence of shallow marine and tidal sedimentation in the Ordovician Graafwater Formation, Cape province, South Africa: **Sediment. Geol.**, 18, 123-133.
- SAGOE, K. O. AND VISHER, G.S. 1977. Population breaks in grain size distribution of sand- a theoretical model: **J. Sediment. Petrol.**, 47, 285-310.
- SAHU, B.K. 1964. Depositional mechanisms from the size analysis of clastic sediments: **J. Sediment. Petrol.**, 34, 73-83.
- SAINT-MARC, P. 1978. Arabian Peninsula, in The Phanerozoic geology of the world : part II, the Mesozoic, Amsterdam: Elsevier, p.435-462.
- SANTISTEBAN, C. AND TABERNER, C. 1988. Geometry, structure and geodynamics of a sand wave complex in the southeast margin of the Eocen Catalan Basin Spain. In Tide-influenced sedimentary environments and facies, P. L. de Boer, Gelder, A. van and Nio, S. D..(ed): **D Reidel Publishing Company**- Dordrecht, 123-138.
- SAXENA, S.K. 1966. Evolution of zircon in sedimentary and metamorphic rocks: **Sedimentology**, 6, 1
- SCHIEBER, J. 1989. The origin of the Neihart quartzite, a basal deposits of the Mid-Proterozoic Belt supergroup, Montana, U.S.A.: **Geol. Mag.**,126, 271-281.
- SCHMIDT, G. F., HADLEY, D. G., GREENWOOD, W. R., GONZALES, L., COLEMAN, R. G. and BROWN, G. F. 1973. Stratigraphy and tectonism of the southern part of the Precambrian Shield of Saudi Arabia, Saudi Arabia: **Gen. Dir. Miner. Resour. Bull.** , 8, 13p.
- SCHWAB, F. L. 1975. Framework mineralogy and chemical composition of continental margin-type sandstone: **Geology**, 3, 487-490.
- _____1981. Evolution of the western continental margin, French-Italian Alps: sandstone mineralogy as an index of plate-tectonic setting: **J. Geol.**, 89, 349-368.
- SCIELACHER, A. 1970. Cruziana stratigraphy of non-fossiliferous, Paleozoic sandstone. In: Trace fossils. T.P. Crimes and Harper, L.C. (eds): **Seel House Press**, Liverpool, 447-476.
- SELLEY, R. C. 1970. Ichnology of Paleozoic sandstones in southern desert of Jordan; a study of trace fossils in their sedimentologic context;, in Trace Fossils: Geological Jour., Special Issue No. 3, 477-488.
- _____1972. Diagnosis of marine and non-marine environments from the Cambro-Ordovician sandstone of Jordan: **Q J. Geol. Soc. London**, 128, 135-150.

- SENIOR, A. AND LEAKE, B. E. 1978. Regional metesomatism and the geochemistry of the Dalradian metasediments of Connemara, western Ireland: **Jour. Sediment. Petrol.**, 19, 585-625.
- SEVON, W. D. 1966. Distinction of New Zealand beach, dune and river sands by their grain-size distribution characteristics: **N. Zealand J. Geol. Geophys.**, 9, 212-223.
- SEYMOUR, R. J. 1980. Longshore sediment transport by tidal currents: **J. Geophys. Res.**, 85, 1899-1904.
- SHARIEF, F. A. 1982. Lithofacies distribution of the Permian-Triassic rocks in the Middle East: **J. Petrol. Geol.**, 4, 3.
- SHELTON, J.W. 1964. Authigenic kaolinite in sandstone: **J. Sediment. Petrol.**, 34, 102-111.
- SIBLEY, D. F. AND BLATT, H. 1976. Intergranular pressure solution and cementation of Tuscarora orthoquartzite: **J. Sediment. Petrol.**, 46, 881-896.
- SIEVER, R. 1962. Silica solubility, 0^o-200^oC, and the diagenesis of siliceous sediments: **J. Geol.**, 70, 127-150.
- _____. 1979. Plate-tectonic controls on diagenesis: **J. Geol.**, 87, 127-155.
- SIPPLE, P. F. 1968. Sandstone petrology evidence from luminescence petrography: **J. Sediment. Petrol.**, 38, 530-554.
- SLOSS, L. L. 1963. Sequences in the cratonic interior of the North America: **Geol. Soc. Am. Bull.**, 74, 93-111.
- _____. 1972. Synchrony of Phanerozoic sedimentary-tectonic events of the North American craton and the Russian Platform: **24th Internat. Geol. Cong.**, Section 6, Montreal, P.Q., 24-32.
- SMITH, J. V. AND STENSTROM, R. C. 1965. Electron excited luminescence as a petrology tool: **J. Sediment. Petrol.**, 73, 627-635.
- SMITH, N. D. 1972. Some sedimentological aspects of planar cross-stratification in sandy braided river: **J. Sediment. Petrol.**, 42, 624-634.
- SMITH, A. M. AND TAVENER-SMITH, R. 1988. Early Permian giant cross-beds near Nqutu, South Africa, interpreted as part of a shoreface ridge: **Sediment. Geol.**, 57, 41-58.
- SOEGARRRD, K. AND ERIKSSON, K.A. 1989. Origin of thick, first-cycle quartz arenite successions: evidence from the 1.7 Ga Ortega, north New Mexico: **Precamb. Res.**, 43, 129-141.
- SPEARING, D. R. 1976. Upper Cretaceous Shannon sandstone an offshore shallow marine sand body, 28th Ann. Field Conf., 1976, **Wyo. Geol. Soc. Gdbk.**, 65-72.

- STACEY, J. C. and HEDGE, C. E. 1984. Geochronologic and isotopic evidence for early Proterozoic continental crust in the eastern Arabian Shield: **Geology**, 12, 340-343.
- STEINEKE, M. , BRAMKAMP, R. A. AND SANDER, N. J. 1958. Stratigraphic relation of Arabian Jurassic oil in, L. G. WEEKS, (ed): **Habitat of oil**, Am. Assoc. Petroleum Geologists, Tulsa, Oklahoma, 1384p.
- STEWART, H. B. Jr. 1958. Sedimentary reflection of depositional environment in San Miguel lagoon, Baja California, Mexico: **Bull. Am. Assoc. Petrol. Geol.**, 42, 2567-2618.
- STOESER, D. B. and CAMP, V. E. 1985. Pan-African microplate accretion of the Arabian Shield: **Geol. Soc. Am. Bull.**, 96, 817-826.
- STRIDE, A. H. 1963. Current-swept sea floors near the southern half of Great Britain: **Q. J. Geol. Soc. London**, 119,175-199.
- _____ BELDERSON, R. H., KENYON, N. H. AND JOHNSON, M. A. 1982. Offshore tidal deposits: sand sheet and sand banks facies. In *Offshore Tidal Sands: Process and Deposits*, pp213: **Chapman and Hall**, London.
- _____ AND CHESTEMAN, W. D. 1973. Sedimentation by non-tidal current around northern Denamark: **Marine Geology**, 15, M53-M58.
- SUCZEK, C. A. AND INGERSOLL, R. V. 1985. Petrology and provenance of Cenozoic sand from the Indus Cone and Arabian Basin DSDP sites 221,222 and 224: **J. Sediment. Petrol.**, 55, 340-346.
- SUTTINER, L. J., BASU, A. AND MACK, G.H. 1981. Climate and the origin of quartz arenites: **J. Sediment. Petrol.**,51, 1235-1246.
- _____ 1974. Sedimentary petrographic province: an evaluation in ROSS C.A. (ed), *Paleogeographic provinces and provinciality*: **Soc. Eco. Spec.Publ. No.**, 21, 75-84.
- _____ AND DUTTA, P.K., 1986. Alluvial sandstone composition and paleoclimate, I. Framework mineralogy: **J. Sediment. Petrol.**, 56, 329-345.
- SWEET, K., KLEIN, G. D. AND SMIT, D. E. 1971. A Cambrian tidal sand body - the Eriboll Sandstone of northwest Scotland: An ancient-recent analog: **J. Geol.**,49,400-415.
- _____ AND SMIT, D.E. 1972. Paleogeography and depositional environments of the Cambro-Ordovician shallow-marine facies of the North Atlantic: **Geol. Soc. Am. Bull.**, 83, 3223-3248.
- SWIFT, D. J. P, HUDELSON, P. M. BRENNER, P. L. AND THOMPSON, P. 1987. Shelf construction in a foreland basin: storm beds, shelf sandbodies and shelf-slope depositional sequences in the Upper Cretaceous Mesaverde Group, Book Cliffs, Utah: **Sedimentolgy**, 34, 423-457.

- THOMPSON, W. O. 1937. Original structure of beaches bars and dunes: **Geol. Soc. Am. Bull.**, 45, 723-752.
- TORTOSA, A., PALOMARES, M. AND ARRIBAS, J. 1991. Quartz grain types in Holocene deposits from the Spanish Central System: some problems in provenance analysis. In Developments in sedimentary provenance studies, by Morton, A. C, Todd, S. P. and Haughton, P. D. W, (eds): **Geol. Soc. Soc. Spec. Pub.**, No. 57, 47-54.
- TREWINDT, J. H. J. 1971. Sandwaves in the southern Bight of the North Sea: **Mar. Geol.**,10, 51-67.
- VAIL, P.R., MITCHUM, R.M.,JR.,AND S. THOMPSON III. 1977. Seismic stratigraphy and global changes of sea level, part 4: Global cycles of relative changes of sea level. In Seismic stratigraphy- application to hydrocarbon exploration, C.E.Payton (ed.): **Am. Assoc. Petrol. Geol. Memoir**, 26.
- VALLONI, R. AND MAYNARD, J. B. 1981. Detrital modes of recent deep-sea sands and their relation to tectonic setting : a first approximation: **Sedimentology**, 28. 75-83.
- _____AND MEZZADRI, G. 1984. Compositional suites of terrigenous deep-sea sands of the present continental margins: **Sedimentology**, 31, 353-364.
- VAN ANDEL, T. H. 1959. Reflection on the interpretation of heavy minerals analysis: **J. Sediment. Petrol.**, 29, 153-163.
- VAN de KAMP, P. C. , LEAKE, B. E. AND SENIOR, A. 1976. The petrography and geochemistry of some California arkoses with application to identifying gneisses of metasedimentary origin: **J. Geol.**, 84, 195-212.
- _____AND LEAKE, B. E. 1985. Petrography and geochemistry of feldspathic and mafic sediments of the northeastern Pacific margin: **Trans. Roy. Soc. Edinburgh, Earth Sciences**, 76, 411-449.
- VAN HOUTEN, F. B. 1961. Climatic significance of red beds In NAIRN, A. E. M. (ed), Descriptive Paleoclimatology: **Interscience Publication**, New York, 89-139.
- _____1964. Origin of red beds-some unsolved problems: In NAIRN, A. E. M. (ed), Problems in Paleoclimatology: Proceeding of NATO paleoclimates conference, 647-661.
- _____1973. Origin of red beds, a review 1961-1972: **Annual Review of Earth and Planetary science**.1, 39-61.
- _____1968. Iron oxides in red beds: **Geol. Soc. Am. Bull.**, 79, 399-416.
- VASLET, D. BEURRIER, M. VILLEY, M. , MANIVIX, J. Le STRAT, P. ,Le NINRE, Y-M, BERTHIAUX, A. BROSSE, J-M AND FOURNIGUET, J. 1985. Geoligical map of the AL FAYDAH QUADRANGLE, SHEET 25G,

- Kingdom of Saudi Arabia (with explanatory notes): **Saudi Arabian Deputy Ministry for Minerals Resources**, Geologic Map GM-102C, scale 1:250 000.
- _____, BROSSE, J. M. and Le NINDRE, Y. M. 1982. Geology of Phanerozoic of the ad-Dawadimi quadrangle, Sheet 24G: **Bureau de Recherches Geologiques et Minières-OF-01-29**.
- VEEN, J. VAN 1935. Sand waves in the southern North Sea: **Int. Hydrograph. Rev.**, 12, 21-29.
- VELBEL, M. A. 1985. Mineralogically mature sandstones in accretionary prisms: **J. Sediment. Petrol.**, 55, 685-690.
- VISHER, G. S. 1969. Grain size distribution and depositional process: **J. Sediment. Petrol.**, 39, 1074-1106.
- _____, AND HAWARD, J. D. 1974. Dynamic relationship between hydraulics and sedimentation in the Altamaha Estuary: **J. Sediment. Petrol.**, 44, 502-521.
- WARE, M. J. AND HISCOOT, R. N. 1985. Sedimentology of Proterozoic cratonic sheet sandstones of the eastern Canadian Shield: Sims Formation, Labrador, Canada: **Precamb. Resear.**, 30, 1-26.
- WEDEPOHL, K. H. (ed) 1978. Handbook of geochemistry, II: **Springer-Verlag Berlin**.
- WENTWORTH, C. K. 1922. A scale of grade and class terms for clastic sediments: **J. Geol.**, 30, 377-392.
- WHITE, D. L. 1985. The significance of continental derivation of the Proterozoic Manahid Formation, southeastern Arabian Shield: **J. Geol. Soc. London**, 142, 1235-1238.
- WILLIAMS, G. E. 1989. Precambrian tidal sedimentary cycles and earth's paleorotation: **Eos**, January, 33.
- WILLIAMS, H. 1964. The Appalachians in northeastern Newfoundland - a two-sided symmetrical system: **Am. J. Sci.**, 262, 1137-1158.
- _____, 1978. Geological development of the northern Appalachians: its bearing on the evolution of the British Isles. In Crust evolution in northwestern Britain and adjacent region, D. R. Bowes and B. L. Leake, (ed.): **Geological J.**, Spec. Issue No. 10 seel House Press, Liverpool, England, pp. 1-22.
- WILLIAMS, P. L , VASLET, D. , JOHNSON, P. R. , BERTHIAUX, A. LESTRAT, P. AND FOURNIGUCT, J. 1986. Geolgical map of the Jabal Habashi quadrangle, sheet 26F, Kingdom of Saudi Arabia (with explanatory notes): **Saudi Arabian Deputy Ministry for Minerals Resources**, Geologic Map GM-98C, scale 1:250 000.

- WILSON, M.D. AND PITTMAN, E.D. 1977. Authigenic clays in sandstone: recognition and influence on reservoir properties and paleoenvironmental analysis: **J. Sediment. Petrol.**, 47, 3-31.
- WOLFART, R. 1981. Lower Palaeozoic rocks of the Middle East. In: Lower Palaeozoic of the Middle East, Eastern and Southern Africa and Antarctica: John Wiley & Son, New York, pp5-130.
- WRIGHT, L. D. 1981. Nearsore tidal currents and sand transport in a macrotidal environment: **Geo-Marine Lett.**, 1, 173-179.
- WYBORN, L. A. I. AND CHAPPELL. B. W. 1983. Chemistry of the Ordovician and Silurian greywackes of the Snowy Mountains, southern Australia: An example of chemical evolution of sediments with time: **Chemical Geol.**, 39, 81-92.
- YAMAMOTO, K. 1987. Geochemical characteristics and depositional environments of cherts and associated rocks in the Franciscan and Shimanto terranes: **Sediment. Geol.**, 52, 65-108.
- YOUNG, S.W. 1976. Petrographic texture of detrital polycrystalline quartz as an aid to interpreting crystalline source: **J. Sediment. Petrol.**, 46, 595-603.
- ZHENXIA, L., YICHANG, H. AND QINIAN, Z. 1989. Tidal current ridges in the Southwestern Yellow sea: **J. Sediment. Petrol.**, 59, 432-437.
- ZIEGLER, A. M. SCOTese, C. R. McKERROW, M. E. AND BAMBACH, R. K. 1979. Palaeozoic paleogeography: **Ann. Rev. Earth Planet. Sci.**, 7, 473-502.
- ZINKERNAGEL, U. 1978. Cathodoluminescence of quartz and its application to sandstone petrology: **Contrib. Sedimentol.**, 18, 69p

